



**LIBRARY**  
**New Delhi**

II No. \_\_\_\_\_  
xc. No. 19405 \_\_\_\_\_

This book can be issued on or after \_\_\_\_\_

Return Date

Return Date

---

1. Books are issued for 14 days, beyond  
it for next 7 days a fine of 15 paisa  
@ afterwards 25 paisa per day shall  
be charged.
2. Books may be renewed at the discre-  
tion of the head Library Services.
3. Dog-earing of pages of a book,  
marking or writing there in with ink  
or pencil, tearing or taking out its  
pages or otherwise damaging it will  
constitute an injury to a book.
4. Unless a borrower points out the  
injury at the time of borrowing the  
book, he shall be required to replace  
the book or pay its price. If detected  
at the time of return,

**TRY TO KEEP THIS BOOK  
FRESH AND CLEAN**



**PROCEEDINGS  
OF THE  
INDIAN ACADEMY OF SCIENCES**

**VOL. XIX**

**SECTION A**

**BANGALORE CITY  
PRINTED AT THE BANGALORE PRESS, MYSORE ROAD  
1944**



## CONTENTS

### SECTION A—VOL. XIX

No. 1—January, 1944

PAGE

The Oil of <i>Mimusops elangii</i> (Linn.) . . . . .	A. R. SUKUMARAN KARTHA AND K. N. MENON	1
Synthetic Experiments in the Benzo-Pyrone Series. Part VIII. Some Transformations of 5-Hydroxy-Coumarin Derivatives. . . . .	B. KRISHNASWAMY, K. RANGANADHA RAO AND T. R. SESHADRI	5
Azo Dye Formation in 5-Hydroxycoumarins . . . . .	S. RANGASWAMI AND K. RANGANADHA RAO	14
Raman Effect and Hydrogen Bonds. Part IX. Solutions of Salicylic Acid and Aspirin . . . . G. V. L. N. MURTY AND T. R. SESHADRI		17
Alkaloids. Part I. The Oxidation of Papaverine to Papaveraldine (Xanthaline) by Selenium Dioxide . . . . .	K. N. MENON	21
Note on the Separation of the Electronic and Non-Electronic Components of Cosmic Radiation . . . . .	H. J. BHABHA	23
The Method of Shower Anti-Coincidences for Measuring the Meson Component of Cosmic Radiation . . . . .	VIKRAM SARABhai	37
Study of the Optical Properties of Gels. Part I. Thorium Molybdate Gels . . . . .	MATA PRASAD AND S. GURUSWAMY	47
Study of the Optical Properties of Gels. Part II. Thorium Arsenate Gels . . . . .	MATA PRASAD AND S. GURUSWAMY	66
Study of the Optical Properties of Gels. Part III. Silicic Acid Gels . . . . .	MATA PRASAD AND S. GURUSWAMY	77
Synthesis of Hibiscetin . . . . .	P. RAMACHANDRA RAO, P. SURYAPRAKASA RAO AND T. R. SESHADRI	88

No. 2—February, 1944

Raman Effect in Relation to Crystal Structure: Sodium Nitrate . . . . .	B. SUNDARA RAMA RAO	93
An Electrical Method of Studying the Movement of Water and Salts in Soil: Part I. A Sensitive A. C. Bridge with an Electronic Null-Point Indicator . . . . .	A. U. MOMIN	100
Scattering of Light in Single Crystals: Intensity Measurements . . . . .	S. BHAGAVANTAM AND K. VENKATESWARLU	108

<b>Effect of Temperature on the Intensities of Raman Lines: Part III.</b>	
Liquids . . . . .	K. VENKATESWARLU 111

<b>The New Light-Effect in Chlorine under Electrical Discharge:</b>	
Part I. Influence of Different Irradiations on the Production of the Phenomenon under Constant Electrical Conditions	P. G. DEO 117

No. 3—March, 1944

Diffraction Coronæ due to Non-Spherical Particles . . . . .	G. N. RAMACHANDRAN 123
<b>The Lunar Atmospheric Tide at Bangalore (1895-1904)</b> . . . . .	C. SESHACHAR AND V. R. THIRUVENKATACHAR 131
Fluorescence Spectrum of Uranyl Fluoride . . . . .	D. D. PANT AND N. D. SAKHWALKAR 135
5-Hydroxy and Methoxy Flavylium Salts . . . . .	L. RAMACHANDRA ROW AND T. R. SESHADRI 141
Congruence Properties of Ramanujan's Function $\tau(n)$ . . . . .	K. G. RAMANATHAN 146
<b>The Measurement of Surface Tension by Means of Sessile Drops</b> . . . . .	H. J. TAYLOR AND J. ALEXANDER 149

No. 4—April, 1944

Influence of Temperature on the Quenching of Active Nitrogen at Various Pressures . . . . .	S. S. JOSHI AND A. PURUSHOTHAM 159
Chemical Examination of the Roots of <i>Centaurea Behen</i> Linn. Isolation of Behnin . . . . .	PRITHVI NATH BHARGAVA AND SIKHIBHUSHAN DUTT 163
On the Existence of a Metric for Higher Path-Spaces . . . . .	V. SEETHARAMAN 167
Separation of Electronic and Non-Electronic Components of Cosmic Radiation by Bhabha's Method . . . . .	S. V. CHANDRASHEKHAR AIYA 177
<b>The Evaluation of the Specific Heat of Rock-Salt by the New Crystal Dynamics</b> . . . . .	BISHESHWAR DAYAL 182

No. 5—May, 1944

<b>The Crystal Symmetry and Structure of Diamond.</b> SIR C. V. RAMAN 189	
<b>The Nature and Origin of the Luminescence of Diamond</b> . . . . .	SIR C. V. RAMAN 199
<b>The Raman Spectrum of Diamond</b> . . . . .	R. S. KRISHNAN 216

## PAGE

The Lattice Spectrum and Specific Heat of Diamond . . . . .	BISHESHWAR DAYAL	224
The Fluorescence and Absorption Spectra of Diamond in the Visible Region . . . . .	ANNA MANI	231
The Ultra-Violet Absorption Spectrum of Diamond . . . . .	K. SUNANDA BAI	253
Intensity of X-Ray Reflection by Diamond . . . . P. S. HARIHARAN	261	
Birefringence Patterns in Diamond . . . . .	SIR C. V. RAMAN AND G. R. RENDALL	265
Luminescence Patterns in Diamond . . . . K. SUNANDA BAI	274	
X-Ray Topographs of Diamond . . . . G. N. RAMACHANDRAN	280	
Ultra-Violet Transparency Patterns in Diamond . G. R. RENDALL	293	
Experimental Evidence for the Existence of the Four Possible Structures of Diamond . . . . . R. S. KRISHNAN	298	
X-Ray Reflection and the Structure of Diamond . . . . .	G. N. RAMACHANDRAN	304
Magnetic Susceptibility of Diamond . . . . . A. SIGAMONY	310	
The Photo-Conductivity of Diamond. Part I. Experimental Results . . . . .	DEVI DATT PANT	315
The Photo-Conductivity of Diamond. Part II. Theoretical Con- siderations . . . . . DEVI DATT PANT	325	
The Crystal Forms of the Panna Diamonds . . . . S. RAMASESHAN	334	

No. 6—June, 1944

Bacterial Chemotherapy. IV. Synthesis of N <sup>4</sup> , N <sup>1</sup> -Diacyl Sulphanil- amides . . . . .	S. RAJAGOPALAN	343
Bacterial Chemotherapy. V. Synthesis of Phenolic Azo-dyes derived from the Sulphonamides . . . . .	S. RAJAGOPALAN	351
Calculation of the Elastic Constants of Quartz at Room Tempera- ture from the Raman Effect Data . . . . .	BISHAMBHAR DAYAL SAKSENA	357
Chemistry of Gossypol. Part IV. Behaviour of Gossypol as an Ortho-Hydroxy Aldehyde: Formation of <i>a</i> -Pyrones and Flavy- lium Salts . . . . . B. KRISHNASWAMY, K. SATYANARAYANA MURTY AND T. R. SESHA DRI	370	
The Magnetic Susceptibility and Anisotropy of Carborundum . . . . .	A. SIGAMONY	377

Synthesis of Compounds Related to Santonin . . . . .	PAGE
(MISS) K. D. PARANJAPE, N. L. PHALNIKAR, B. V. BHIDE AND K. S. NARGUND	381
Synthesis of Cantharidine and Desoxycantharidine . . . . .	
(MISS) K. D. PARANJAPE, N. L. PHALNIKAR, B. V. BHIDE AND K. S. NARGUND	385
Opacity Changes during the Coagulation of Sols by Electrolytes MATA PRASAD, S. GURUSWAMY AND N. A. PADWAL	389
Fluorescence Reactions with Boric Acid and O-Hydroxy-Carbonyl Compounds, and their Application in Analytical Chemistry. Part III. Effect of Bromination of the O-Hydroxy-Carbonyl Molecule on the Appearance of Fluorescence Effects with Boric Acid . . . . . K. NEELAKANTAM AND V. VENKATESWARLU	401
Effect of Electric Field on Tyndall Scattering . . . . .	
R. S. SUBRAHMANYA, K. S. GURURAJA DOSS AND BASRUR SANJIVA RAO	405
Kombur Sesha Iyengar Kuppuswamy Iyengar—In Memoriam . . . . .	
B. S. MADHAVA RAO	414

disaturated glycerides is also high. It has been recently shown<sup>4</sup> (1943) that oxidation of 80.0 g. of oil yielded 22.8 g. of an azelaoglyceride mixture containing 10.53 g. of mono-azelao-glycerides corresponding to 14.34% of disaturated glycerides in the oil. This is not the first time that a seed fat with less than 33% of saturated acids has been found to contain a large percentage of disaturated glycerides. Neem oil containing only 30% of saturated acids has been shown by Hilditch and Murthi<sup>5</sup> (1939) to contain 1.7% of disaturated glycerides, but the present investigation seems to be the first instance when the occurrence of linolic disaturated glycerides in a seed fat is definitely indicated. Elangi oil yielded, after three crystallisations from acetone 25% of a sparingly soluble portion which contained 25% of linolic acid. In the case of neem oil (*loc. cit.*) the sparingly soluble portion contained less than 4% of linolic acid. It is probable that the linolic acid glycerides in Elangi oil have been rendered comparatively sparingly soluble by the associated high saturated acid content. The fact that no portion of the fat showed an iodine value of more than 86 shows that probably there is no linoleo-diolein or more unsaturated glyceride molecule in the fat, the linolic acid being combined at least with one saturated acid radical in building up the glyceride molecule.

### *Experimental*

150 g. of sun-dried, crushed seed kernel gave on extraction with benzene 37.6 g. of oil (25.07% yield). 374 g. of the oil was saponified, the soap ether extracted and then the free acids liberated, yielding 349 g. of water insoluble fatty acids corresponding to 93.28%.

*Constants of Mixed Acids.*—Titre—24.2°; Refractive Index—1.4578; Mean Molecular Weight—278.0; Iodine Value—86.6.

309.3 g. of the mixed acids gave 65.45 g. of solid acids and 243.85 g. of liquid acids corresponding to 21.16% and 78.84% respectively.

*Solid Acids.*—Mean Molecular Weight—296.6; Iodine Value—0.90; Titre—48.4°; Refractive Index—1.4434.

*Liquid Acids.*—Mean Molecular Weight—281.1; Iodine Value—106.5; Refractive Index—1.4625.

On analysing the methyl esters of the acids separately by the ester fractionation method, the solid acids were found to consist of 49.4% palmitic, 47.74% stearic, 2.16% behenic and 0.79% unsaturated acids; while the liquid acids were found to consist of 0.69% palmitic, 81.10% oleic and 18.21% linolic acids. Thus composition of total acids is found to be

palmitic 10·97%, stearic 10·10%, behenic 0·46%, oleic 63·98%, and linolic 14·49%.

80·8 g. of the dry, purified, neutral oil was oxidised giving 3·4 g. of a residue of completely saturated glycerides corresponding to 4·25% by weight.

### Summary

The constants, acid composition and trisaturated glyceride content of Elangi oil are reported.

### REFERENCES

1. Kesava Menon .. *J. Soc. Chem. Ind.*, 1910, **28**, 1430.
2. Rau and Simonsen .. *Indian Forest Records*, 1922, **9**, 95.
3. Bushell and Hilditch .. *J. Soc. Chem. Ind.*, 1938, **57**, 48.
4. Kartha and Menon .. *Proc. Ind. Acad. Sci.*, 1943, A **17**, 114.
5. Hilditch and Murthi .. *J. Soc. Chem. Ind.*, 1939, **58**, 310.

## SYNTHETIC EXPERIMENTS IN THE BENZO-PYRONE SERIES

Part VIII. Some Transformations of 5-Hydroxy-Coumarin Derivatives

BY B. KRISHNASWAMY, K. RANGANADHA RAO  
AND  
T. R. SESHADRI

(From the Department of Chemistry, Andhra University, Waltair, now at Madras)

Received December 10, 1943

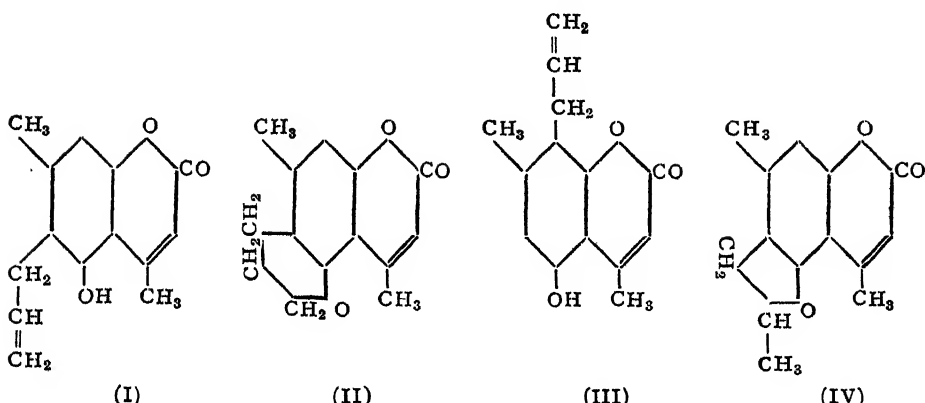
Of the two types, 7-hydroxy- and 5-hydroxy-coumarins, the former have been more fully examined in the past obviously due to their common occurrence in nature and the greater ease with which they can be prepared by synthetic methods. In connection with our work on insecticides more information was required about 5-hydroxy-coumarin derivatives and the results presented in this paper were obtained in that connection. There is considerable difference between the two types of compounds and their derivatives. The 7-hydroxy-compounds exhibit marked fluorescence in solution whereas the 5-hydroxy-compounds are entirely devoid of this characteristic. They also differ in their solubility in mild alkalies, the 5-hydroxy-compounds being less soluble.

The Claisen and Fries transformations of 7-hydroxy-coumarin derivatives have been investigated in detail in the past. The allyl ethers do not readily undergo transformation below 200° and the best yields are obtained by heating between 210–240°. In general they rarely exceed 30%, due to the formation of considerable amounts of resins. Of the two alternative ortho-positions (6 and 8) available for the migration, the 8-position seems to be almost exclusively involved, since only 8-allyl-7-hydroxy-coumarins have so far been obtained.<sup>1</sup> On the other hand when the acetate is subjected to Fries migration a small amount of the 6-acetyl-derivative is also obtained though the main bulk of the product is the 8-substituted compound.<sup>2</sup> In regard to the 5-hydroxy-coumarins the positions that could be involved in the above transformations are 6 and 8, the former being ortho and the latter para to the original hydroxyl group. The transformation of the allyl ethers in this type of compounds has not so far been described. Fries migration has been studied by Shah<sup>3</sup> and by Limaye<sup>4</sup> in the case of the acetate of 4-methyl-

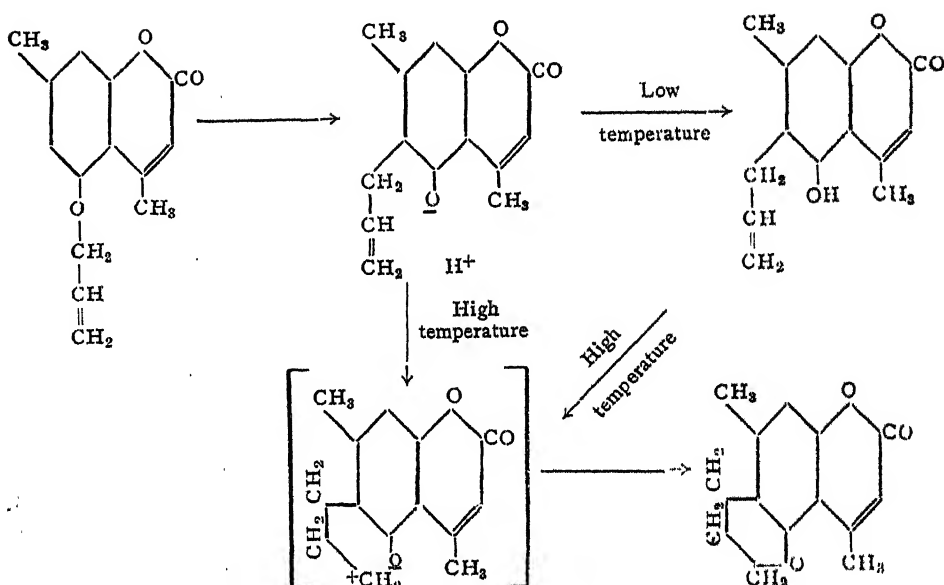
5-hydroxy coumarin and they have been able to obtain only the 6-acetyl-derivative. This is rather extraordinary since it is generally considered that in the Fries transformation para migration takes place more easily than the ortho.

As a typical example of 5-hydroxy-coumarins, 5-hydroxy-4:7-dimethyl-coumarin has now been chosen since it is readily made from orcinol and ethylacetacetate by the well-known Pechmann condensation. It was originally prepared by Pechmann and Cohen<sup>5</sup> who thought it was a 7-hydroxy-compound in analogy with 4-methyl umbelliferone obtained from resorcinol. It however does not give the characteristic fluorescence of umbelliferone derivatives. Its correct constitution as a 5-hydroxy-compound was later established by Dey.<sup>6</sup> Its allyl ether gives rise to different products depending upon the temperature employed for the migration. When heated at 160–5° C. (lower temperature) for about 2 hours it forms in a very high yield an alkali-soluble product (I) having all the properties of an allyl phenol and a melting point of 178–9°. But if the migration is carried out at a higher temperature (195–200°) at atmospheric pressure or *in vacuo* an alkali insoluble substance (II) is formed as the entire product and it melts at 164–5°. When the experiment is carried out at 225–30° two products are obtained the alkali-insoluble substance (II) which is the major component and an alkali-soluble substance (III) melting at 239–40°. All the three are isomeric and from their reactions and properties it could be concluded that compound (I) is 6-allyl-5-hydroxy-4:7-dimethyl-coumarin, compound (II) has a ring structure produced by interaction between the hydroxyl and the ethylene double-bond and compound (III) is the para isomer of (I), that is 8 allyl-5-hydroxy-4:7-dimethyl-coumarin. In support of this idea it has been found by heating (I) again at 215–20°, a substance identical with (II) could be obtained. It could therefore be concluded that when higher temperatures are employed for migration both the 6-(I) and 8-allyl (III) compounds are formed, the former immediately undergoing cyclisation to yield (II); this change is not possible with the 8-allyl compound.

The alkali-insoluble substance appears to be a single entity since repeated recrystallisation and fractionation has given rise to only one product with a constant melting point. There are two possible structures for this compound the chroman (II) and the methyl-coumaran (IV). In order to settle this point the methyl-coumaran has been prepared from (I) by adopting the procedure of Adams *et al.*<sup>7</sup> (using mercuric chloride) as modified in a recent publication by Krishnaswamy and Seshadri.<sup>8</sup> Since it is quite different from the alkali-insoluble product obtained by Claisen transformation the latter has been assigned the chroman structure (II).



The above results are interesting in many respects. While carrying out the pyrolytic rearrangement of phenylallyl ether into *o*-allyl-phenol, Claisen<sup>7a</sup> observed that a small amount of 2-methylcoumaran was formed. The yield of this could be raised to 60% by employing acids or salts as catalysts. In connection with synthetic work relating to vitamin E,<sup>9</sup> it was found that ring closure of ortho-allylphenols derived from  $\psi$ -cumoquinol in the presence of catalysts is dependent on the nature of the side-chain. With a simple allyl group methyl-coumaran was produced, whereas with dimethyl-allyl and phytetyl groups the chroman was formed. The crotyl group was an intermediate case giving rise to a mixture of both. Subsequently Hurd and Hoffmann<sup>9a</sup> showed that with the simpler phenols having allyl and crotyl groups it is possible to get either the coumaran or the chroman ring by suitably adjusting the conditions. In the absence of peroxides the coumarans were produced and in their presence chromans were formed. With dimethyl-allyl group the chroman was produced even without a peroxide. The results reported in the present paper indicate the existence of another possibility where even the simple allyl group can give rise to a chroman in the absence of peroxide or catalyst probably due to the influence of the 5-hydroxycoumarin structure already present. Obviously in these reactions the nature of the product is dependent on a number of factors (1) the structure of the original phenolic body, (2) the nature of the allyl side chain and (3) the presence or absence of peroxides. It should be mentioned here that almost quantitative yields of the coumarino-chroman are obtained when it is directly made from the allyl ether as contrasted with the partial transformation of the 6-allyl-5-hydroxy coumarin (yield 30%). Obviously the 6-allyl compound is not an intermediate stage between the allyl ether and the chroman in the direct process. The following mechanism could probably represent the changes correctly.

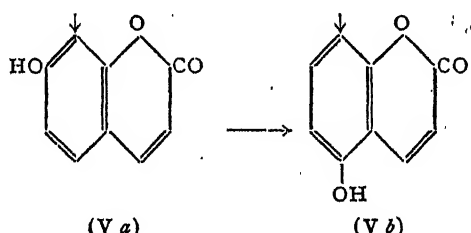


In order to ascertain whether the peculiarities mentioned above are innate characteristics of the 5-hydroxy-compound or are due to the effect of the methyl group coming from the orcinol part, the Claisen migration of the allyl ether of 7-hydroxy-5-methyl-coumarin, a condensation product of orcinol and malic acid,<sup>5a</sup> has also been studied. The results are quite analogous to those of umbelliferone derivatives and the methyl group of the orcinol nucleus has no special effect. The migration does not take place at a lower temperature ( $170^\circ$ ) and at a higher temperature ( $200^\circ$ ) only 8-allyl-7-hydroxy-5-methyl-coumarin is obtained in comparatively small yields. There is thus marked difference between 7-hydroxy and 5-hydroxy-coumarins in the nature of the claisen migration of the corresponding allyl ethers. The former undergo change only at a higher temperature and the yields of the allyl phenols are poor, probably due to polymerisation taking place side by side yielding resins. The latter undergo the migration easily and give good yields of products, the nature of which depend upon the temperature employed.

The Fries migration of 5-acetoxy-4:7-dimethyl coumarin has also been examined now. The product yields only one crystalline compound whose properties and reactions indicate that it is the 6-acetyl derivative; migration to the 8-position does not seem to have taken place to any appreciable extent and in this there is agreement with the behaviour of 5-acetoxy-4-methyl coumarin. The exclusive formation of the 6-acetyl-compound as the result of Fries reaction of 5-hydroxy-coumarin-acetates may probably

be attributed to the high temperature that has necessarily to be employed in the case of these compounds in order to get them fused with aluminium chloride. High temperature has been found to favour in other cases also ortho migration in preference to the para<sup>10</sup>.

The difference in the behaviour of 7-hydroxy and 5-hydroxy coumarin derivatives in Claisen and Fries migrations may be partly due to the fact that in the former only ortho positions are available for reaction and in the latter an ortho and a para position. Similar differences exist in nitration also. In 7-hydroxy-coumarin the 8th position is consistently very highly reactive as compared with the feeble reactivity of position 6 in all reactions. This was attributed by Rangaswamy and Seshadri<sup>11</sup> to the preferential orientation of a double-bond between the 7th and 8th positions (formula V). In 5-hydroxy coumarins position 6 (ortho) has been shown to be reactive in Claisen and Fries migrations. Working with 5-hydroxy-4-methyl-coumarin Parekh and Shah<sup>12</sup> found that nitration at 0° C. gave the 8-nitro compound (*p*-nitration) whereas at the room temperature 6 : 8-dinitro compound was produced. Obviously ortho or para reactivity in 5-hydroxy coumarins is controlled by the nature of the entering group and the conditions. The formula (V) satisfactorily explains all the properties of 5-hydroxy coumarins also. A para position can be activated in any disposition of the double bonds in the benzene ring. Hence in studying the possible fixation of double bonds two rival ortho positions alone seem to offer possibilities of correct comparison and not an ortho and a para combination; 5-hydroxy coumarins do not seem to be, therefore, suitable for this study.



### Experimental

**5-Hydroxy-4:7-dimethyl-coumarin.**—This compound was obtained in very good yields by keeping overnight a mixture of equimolecular proportions of orcinol and ethylacetacetate and twice their combined weight of concentrated sulphuric acid and working it up the following day (2.8 g. of coumarin from 2.0 g. of orcinol).

It could also be obtained in equally good yields by heating the mixture in the above proportions in a boiling water-bath for 1 hour.

Appel's method using anhydrous alcoholic solution and saturating it with dry hydrogen chloride gave the product in good yields but the method is not very convenient.

**5-Allyloxy-4 : 7-dimethyl-coumarin.**—5-Hydroxy-4 : 7-dimethyl-coumarin (9.5 g.) and allyl bromide (6.0 g.) were dissolved in anhydrous acetone (400 c.c.), anhydrous potassium carbonate (20 g.) added and the mixture boiled under reflux on a water-bath for about 6 hours. The acetone was then removed by distillation and water added to the residue. The insoluble solid was filtered and recrystallised from alcohol; the allyl ether was thus obtained as rectangular plates melting at 127–8°; yield almost quantitative. (Found: C, 73.3; H, 6.4;  $C_{14}H_{14}O_3$  requires C, 73.0; H, 6.1%).

**Claisen migration:** (i) **6-Allyl-5-hydroxy-4 : 7-dimethyl-coumarin.**—The allyl ether (2 g.) was heated for 2 hours in a paraffin-bath, the temperature of which was maintained at 160–5°. The product was then mostly soluble in aqueous sodium hydroxide. The alkali solution on acidifying yielded a precipitate, which on recrystallisation from alcohol, was obtained as colourless elongated rhombohedral crystals, melting at 178–9°. The substance gave no prominent colour with ferric chloride; yield 1.5 g. (Found: C, 73.2; H, 6.4;  $C_{14}H_{14}O_3$  requires C, 73.0; H, 6.1%).

(ii) a. **4 : 7-Dimethyl-coumarino-5 : 6-chroman.**—The allyl ether (5 g.) was heated in a paraffin-bath at 225–30° for 2 hours. The final product was separated into an alkali-soluble fraction and an alkali-insoluble fraction. The latter on recrystallisation from alcohol gave rectangular plates, melting at 164–5°; yield 4.0 g. (Found: C, 73.1; H, 6.4;  $C_{14}H_{14}O_3$  requires C, 73.0; H, 6.1%).

b. **8-Allyl-5-hydroxy-4 : 7-dimethylcoumarin.**—The alkali-soluble fraction obtained in the above experiment was liberated by acidifying the alkaline solution. The precipitate thus obtained on recrystallisation from alcohol yielded colourless rectangular plates and prisms, melting at 239–40°; yield 0.2 g. (Found: C, 72.7; H, 6.5;  $C_{14}H_{14}O_3$  requires C, 73.0; H, 6.1%).

The above chroman could also be obtained in almost quantitative yields by heating the allyl ether (2 g.) at 195–200° either at atmospheric pressure or in an evacuated system (water-pump) but no 8-allyl-compound could be isolated in these cases.

(iii) The 6-allyl compound obtained in (I) (1 g.) was heated at 215–20° in a paraffin-bath for 2 hours. It was then separated into an alkali-soluble fraction and an alkali-insoluble fraction. The alkali-soluble portion after

repeated purification was found to be identical with the original 6-allyl-compound (melting at 178–9°). The alkali-insoluble portion on recrystallisation from alcohol was obtained as rectangular plates, melting at 163–4°; (yield 0·3 g.); the mixed melting-point with chroman obtained in (ii a) was undepressed.

*Mercuric chloride addition compound of 6-allyl-5-hydroxy-4: 7-dimethyl coumarin.*—To a solution of 6-allyl-5-hydroxy-4: 7-dimethyl-coumarin (2 g.) in methyl alcohol (20 c.c.), a solution of mercuric chloride (2·5 g.) in the same solvent (20 c.c.) was added and the mixture left overnight. The mercuric chloride addition product crystallised out in rectangular rods. The pure sample obtained by washing the precipitate with a little alcohol melted at 228–9°; yield 3·5 g. (Found: Cl, 14·0;  $C_{14}H_{14}O_3$ ,  $HgCl_2$  requires Cl, 14·2%).

*4: 7-Dimethyl coumarino-a-iodomethyl-dihydro-5: 6-furan.*—The mercuric chloride addition compound (3 g.), was ground up with excess of a solution of iodine in potassium iodide solution; the reaction was facilitated by warming the mixture on a water-bath for about an hour. The precipitate was then filtered and recrystallised from alcohol. It was then obtained as rectangular prisms, melting at 166–7°; yield almost quantitative. (Found: I, 35·1;  $C_{14}H_{13}O_3$  I requires I, 35·7%).

*4: 7-Dimethyl-coumarino-a-methyl-dihydro-5: 6-furan.*—The iodine compound (2·5 g.) was suspended in alcohol (50 c.c.) and small pieces of sodium metal were pressed to the bottom of the container by means of a glass rod. The addition of sodium was continued till the reaction became very slack. The solution was then diluted with water and acidified. On standing, a precipitate was obtained, which on recrystallisation yielded colourless rectangular plates melting at 205–6°; yield 0·2 g. The substance is insoluble in hot dilute sodium hydroxide. (Found: C, 73·3; H, 6·4;  $C_{14}H_{14}O_3$  requires C, 73·0; H, 6·1%).

*7-Allyloxy-5-methyl coumarin.*—7-Hydroxy-5-methyl coumarin<sup>22</sup> was allylated as in the previous case using allyl-bromide and anhydrous potassium carbonate in acetone medium. The allyl ether crystallised out from alcohol in rectangular plates, melting at 78–9°; yield quantitative. (Found: C, 72·4; H, 5·8;  $C_{13}H_{12}O_3$  requires C, 72·2; H, 5·6%).

*8-Allyl-7-hydroxy-5-methyl-coumarin.*—The above compound (2 g.) was heated in an oil-bath at 200–5° for about 2 hours. The product thus obtained was found to be almost completely soluble in aqueous sodium hydroxide. The clear solution was acidified and the precipitate obtained therefrom repeatedly recrystallised from alcohol. The allyl phenol was

thus obtained in rectangular plates, melting at 174–5°; yield 0·6 g. (Found: C, 71·8; H, 5·2;  $C_{13}H_{12}O_3$  requires C, 72·2; H, 5·6%).

The Claisen migration was also carried out at a higher temperature (230–40°). The yield of the allyl phenol was considerably lower than in the previous case due to greater resinification but no chroman could be isolated.

**4:7-Dimethyl-5-acetoxy-coumarin.**—It was prepared by heating together a mixture of 5-hydroxy-4:7-dimethyl-coumarin, acetic anhydride and anhydrous sodium acetate. On recrystallisation from alcohol the acetate was obtained as rectangular plates, melting at 199–200° (*cf.* Pechmann<sup>3</sup>, 195°).

**Fries migration of the acetate: preparation of 6-acetyl-5-hydroxy-4:7-dimethyl coumarin.**—The acetate (3 g.) and anhydrous aluminium chloride (6 g.) were powdered together and heated in an oil-bath at 130° at first and the temperature was slowly raised to 170° during the course of half-an-hour. The heating was continued at this temperature for an hour more. The material was then cooled and aluminium chloride was dissolved out using dilute hydrochloric acid. The solid left behind was filtered and recrystallised from glacial acetic acid. 6-Acetyl-5-hydroxy-4:7-dimethyl-coumarin was thus obtained as rectangular plates, melting at 177–8°. By repeated crystallisation and fractionation no change was effected in the melting point and no other product could be isolated. This substance gives a marked brown colour with ferric chloride indicating the presence of an ortho-hydroxy-carbonyl grouping in it. Yield 1·0 g. (Found: C, 67·6; H, 5·4;  $C_{13}H_{12}O_4$  requires C, 67·2; H, 5·2%).

### Summary

Claisen migrations of the allyl ether of 4:7-dimethyl-5-hydroxy-coumarin gives rise to three isomeric compounds depending upon the conditions, (I) 6-allyl-5-hydroxy-4:7-dimethyl coumarin (high yield), (II) the corresponding chroman (high yield), and (III) 8-allyl-5-hydroxy-4:7-dimethyl coumarin (low yield). (II) has been shown to be a chroman by comparison with the corresponding methyl coumaran obtained by authentic methods from (I). The acetate of the above coumarin undergoes Fries reaction to give the 6-acetyl compound. Claisen migrations of the allyl ether of 7-hydroxy-5-methyl-coumarin yields only the 8-allyl-derivative. The difference in the behaviour of the derivatives of 5- and 7-hydroxy coumarins and the special conditions of the chroman and coumaran ring closure of *o*-allyl phenols are discussed.

## REFERENCES

1. Baker and (Miss) Lothian     *J. C. S.*, 1935, 628.
2. Limaye                        .. *Ber.*, 1932, 375.
3. Shah *et al.*               .. *J. C. S.*, 1938, 228.
4. Limaye *et al.*              .. *Rasayanam*, 1938, 153.
5. Pechmann and Cohen        .. *Ber.*, 1884, 17, 2188.
- 5a. ——— and Welsh          .. *Ibid.*, 1884, 17, 1649.  
Rao and Seshadri             .. *Proc. Ind. Acad. Sci., A*, 1941, 13, 255.
6. Dey                           .. *J. C. S.*, 1915, 1614.
7. Adams *et al.*              .. *J. A. C. S.*, 1922, 1781..
- 7a. Claisen *et al.*          .. *Ann. der chemie*, 1913, 401, 21.
8. Krishnaswamy and Seshadri *Proc. Ind. Acad. Sci., A*, 1941, 13, 43.
9. Karrer *et al.*              .. *Helv. Chim. Acta*, 1939, 1287.
- 9a. Hurd and Hoffman        .. *J. Org. Chem.*, 1940, 5, 212.
10. Blatt                       .. *Chem. Rev.*, 1940, 27, 417.
11. Rangaswami and Seshadri *Proc. Ind. Acad. Sci., A*, 1937, 6, 122.
12. Parekh and Shah          .. *J. I. C. S.*, 1942, 335.

# AZO DYE FORMATION IN 5-HYDROXYCOUMARINS

BY S. RANGASWAMI

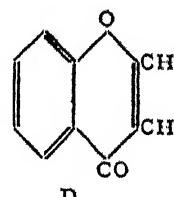
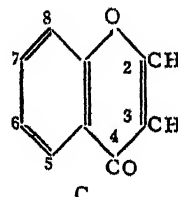
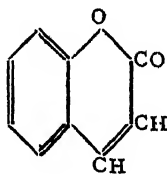
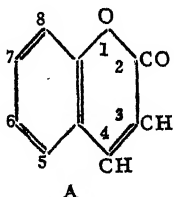
AND

K. RANGANADHA RAO

(From the Department of Chemistry, Andhra University, Waltair, now at Madras)

Received December 10, 1943

FROM a study of the reactivity of 7-hydroxy-coumarins<sup>1</sup> and -chromones<sup>2</sup> it was concluded that though these compounds normally exhibited great reactivity in position 8 indicating that a double bond was fixed between the 7 and 8 positions as in (A) and (C), reactivity in the alternative structures (B) and (D) was not altogether precluded. The coupling of phenolic compounds with diazonium salts to form azo dyes is a very facile reaction taking place energetically even at low temperatures, and even feeble reactivity of a nuclear position would suffice to direct a diazo group to that position. Hence in order to get more information on the subject of bond fixation, the behaviour of certain 7-hydroxy-chromones and -coumarins towards diazotised *p*-nitroaniline was studied in detail.<sup>3</sup> The results indicated that the factors controlling the composition of the azo dye are rather complex and that, whether a mono- or a bis-azo dye is formed may depend not only on the disposition of aromatic double bonds and the quantity of the reagent employed, but on various other factors such as the solubility of the mono-azo dye that may be produced first, and its capacity to react further to form the bis-azo dye.



With a view to see how far the above conclusion regarding the factors that control azo dye formation is valid, the reactivity of 5-hydroxy-7-methylcoumarin<sup>4</sup> (I) and 5-hydroxy-4:7-dimethyl-coumarin<sup>5</sup> (II) has now been investigated. In these two compounds the question of bond fixation does not come in as in the case of 7-hydroxy-coumarins, and both the 6 and 8 positions, which are respectively ortho and para to the 5-hydroxy, may be expected to react, resulting in the formation of bis-azo dyes, provided of course, there are no other interfering factors. The reactivity of 7-hydroxy-5-methylcoumarin<sup>6,7</sup> (III) has also been studied for purposes of comparison.

with 5-hydroxy-7-methylcoumarin, and also with the object of seeing if the introduction of an alkyl substituent in the benzene part of the coumarin ring system has any influence on azo dye formation.

The diazo-coupling reactions were carried out in a manner essentially the same as that employed for the chromones and coumarins previously studied.<sup>3</sup> In the case of (III) the reaction was carried out in sodium carbonate medium but this could not be done with (I) and (II) as these 5-hydroxycoumarins were very sparingly soluble in sodium carbonate. The use of sodium hydroxide was also precluded as this would result in the possible opening of the  $\alpha$ -pyrone ring. Hence dilute ammonium hydroxide was employed in conjunction with alcohol to get them into solution. The diazonium salt solution was prepared by diazoising *p*-nitraniline and making up the solution to known volume, the temperature being kept near 0° throughout the process. Calculated quantities of this solution were added to the ice-cold solutions of the coumarins to give just one molecular proportion of the reagent in one set of experiments and slightly more than two molecular proportions in another set. After allowing the mixture to stand in the refrigerator for two days, the dye was filtered, crystallised from glacial acetic acid and washed with a large volume of water and then with a little alcohol. The air-dry dye was then examined for its composition by analysing for nitrogen.

	Phenolic compound	Medium employed	No. of molecular proportions of diazoised <i>p</i> -nitraniline	% N found in dye	% N calculated for		Colour of dye
					Mono-azo dye	Bis-azo dye	
I	5-Hydroxy-7-methylcoumarin	Ammonia and alcohol	1 >2	12.5 14.7	12.9	17.7	Brown Dark brown
I	5-Hydroxy-4 : 7-dimethylcoumarin	Ammonia and alcohol	1 >2	12.1 13.6	12.4	17.2	Red Dark brown
II	7-Hydroxy-5-methylcoumarin	Sodium carbonate	1 >2	12.7 15.7	12.9	17.7	Red brown Red brown

The results recorded in the above table show that in all the three cases only mono-azo dyes were formed when one molecular proportion of the diazonium salt was employed, and a mixture of the mono- and bis-azo dyes with more than two molecular proportions of the reagent. In the case of the 5-hydroxy-coumarins, though both the ortho and para (6 and 8) positions are free and may be expected to react with the diazonium salt to give bis-azo dyes, this has not happened even when excess of the reagent

was available. The present findings thus confirm the opinion already expressed<sup>32</sup> that bis-azo dye formation is not controlled only by the disposition of nuclear double bonds and the reactivity of positions in the original compound, but is subject to various other factors, such as solubility related to the mono-azo dye and its reactivity.

The results obtained with 7-hydroxy-5-methylcoumarin were not very different from those with 7-hydroxycoumarin, thus showing that the introduction of an alkyl substituent in the benzene part has not changed the reactivity of 7-hydroxycoumarin to any degree.

### *Summary*

The 5-hydroxycoumarins behave very similar to 7-hydroxycoumarins in regard to azo-dye formation with one and more than two molecular proportions of diazotised *p*-nitraniline. The significance of these results is discussed.

The authors desire to express their grateful thanks to Prof. T. R. Seshadri for his kind interest in this work.

### **REFERENCES**

1. Rangaswami and Seshadri .. *Proc. Ind. Acad. Sci., A*, 1938, **7**, 8.
2. \_\_\_\_\_ .. *Ibid.*, A, 1939, **9**, 1.
3. \_\_\_\_\_ .. *Ibid.*, A, 1939, **9**, 526.
- 3a. \_\_\_\_\_ .. *Ibid.*, A, 1941, **14**, 565.
4. Sastry and Seshadri .. *Ibid.*, A, 1940, **12**, 498.
5. Dey .. *J. C. S.*, 1915, 1614.
6. Pechmann and Welsh .. *Ber.*, 1884, **17**, 1649.
7. Rao and Seshadri .. *Proc. Ind. Acad. Sci., A*, 1941, **13**, 255.

*A Correction.*—In the paper entitled “Fixation of Aromatic Double Bonds” by Rangaswami and Seshadri (*Proc. Ind. Acad. Sci., A*, 1941, **14**, 547–71), the inclusion of the word “7-hydroxy-4-methylcoumarin” in the first line on page 565 is a mistake. This compound gives a bis-azo dye with one molecular proportion of diazonium salt, only in sodium hydroxide medium (*vide* reference 3 in the present paper) and under these circumstances there is the possibility of the pyrone ring opening out.

# RAMAN EFFECT AND HYDROGEN BONDS

## Part IX. Solutions of Salicylic Acid and Aspirin

BY G. V. L. N. MURTY\* AND T. R. SESHADRI

(From the Department of Chemistry, Andhra University, Waltair, now at Madras)

Received December 10, 1943

IN previous publications of this series<sup>1</sup> the Raman spectra of some typical carboxylic acids and their solutions in various solvents were described and the phenomenon of association through hydrogen bonds discussed. Acetic and propionic acids represent normal aliphatic acids, formic acid is exceptional and exhibits greater complexity, and benzoic and cinnamic acids form a third type. Salicylic acid has now been taken up for study as a further interesting case since in it should exist two opposing influences, (1) formation of intermolecular hydrogen bonds leading to association and (2) formation of intramolecular hydrogen bonds (chelation) hindering association.

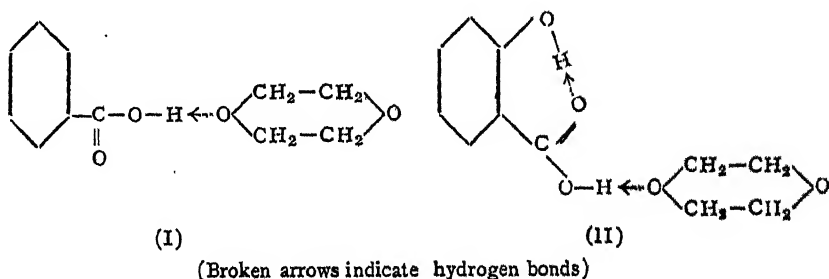
The Raman spectrum of salicylic acid does not seem to have been investigated completely before. The only reference to this substance relates to the low frequency Raman lines in the crystalline state by Venkateswaran.<sup>2</sup> The C=O frequencies have not so far been recorded. Since the present investigation deals mainly with these frequencies, Raman spectra of the solutions of the substance in dioxan and in benzene are now described. Due to the existence of fluorescence there was difficulty in recording the entire spectrum and hence the frequencies given below are not exhaustive. The picture obtained with the dioxan solution was bright and quite clear particularly in the C=O region.

*Raman spectrum of salicylic acid in dioxan solution.*—440 (1) 565 (5)  
816 (3) 1036 (9) 1137 (1) 1156 (2) 1253 (10) 1328 (6) 1400 (1) 1465 (6) 1586 (2)  
1670 (6).

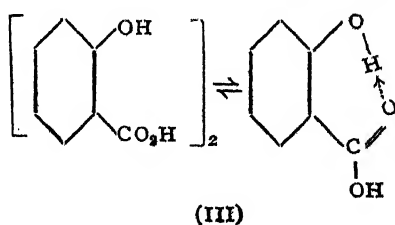
There is only one line in the C=O region and it is bright; the frequency corresponds to that of the bright C=O line of the esters of salicylic acid attributable to the chelate form. It could therefore be inferred that in dioxan solution salicylic acid has the chelate structure. Since it has already been shown in the case of benzoic acid that the dimers break down in

\* Now working in the Research Laboratory, Tata Iron and Steel Works, Jamshedpur.

dioxan solution into monomer solvent associates (formula I), a similar condition may be expected to prevail in regard to salicylic acid solution also, with the difference that chelation takes place in this acid due to the presence of the phenolic hydroxyl in the ortho position (formula II). It may be recalled here that dioxan does not disrupt the chelate ring form in the esters of salicylic acid.



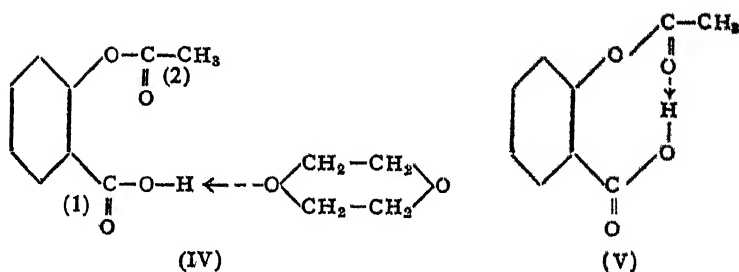
The spectrum of salicylic acid in benzene solution was not bright mainly due to low solubility at room temperature. But all the frequencies mentioned above could be found in it. There was however one marked difference; two C=O frequencies were present, a feeble one at 1670 cm.<sup>-1</sup> and a brighter one at 1700 cm.<sup>-1</sup> The state of the acid molecules in benzene solution therefore seems to be complex. The feeble line at 1670 cm.<sup>-1</sup> could reasonably be attributed as before to chelate structures which are present to an appreciable extent. These most probably consist of the monomolecular form of the acid. Though molecular weight determinations in this solvent give values almost double that required for the ordinary formula, experiments carried out by Hendrixson<sup>8</sup> on the partition of the acid between benzene and water indicate the existence of appreciable amounts of the monomeric form. In his partition experiments the effect of water present in the benzene solution may be expected to cause some discrepancy favouring the monomolecular form. However, the difference between benzoic acid and salicylic acid is quite marked even in these experiments. In the case of the latter the monomeric form is present in far greater amounts. This seems to be obviously due to the influence of the phenolic hydroxyl leading to increased stability of the monomers by chelation.



The brighter line at  $1700 \text{ cm}^{-1}$  should then be attributed to the dimers of the acid. It is difficult to say at present what exact structure these have. The ring form similar to that of benzoic acid dimers seems to be precluded since such a structure may be expected to have a much lower  $\text{C}=\text{O}$  frequency (about  $1650 \text{ cm}^{-1}$  as in benzoic acid). Some type of open structure is therefore indicated.

More light could be expected to be thrown on this subject by a detailed study of salicylic acid in other solvents and also of some of its derivatives. This study could not at present be made due to dislocation caused by the global war now raging. However, the result obtained in a preliminary study of acetyl salicylic acid (aspirin) in dioxan solution may be here recorded since it is somewhat remarkable and interesting. The picture showed some continuous spectrum, but the  $\text{C}=\text{O}$  region was clear. There was only one intense and broad line at  $1726 \text{ cm}^{-1}$ . This corresponds to the  $\text{C}=\text{O}$  frequency of ethyl benzoate ( $1720 \text{ cm}^{-1}$ ) and the new faint line of salicylates attributable to the unchelated  $\text{C}=\text{O}$  bonds. The dioxan solution of benzoic acid has also a  $\text{C}=\text{O}$  line in this region.

In dioxan solution the monomeric form of aspirin could be expected to be produced just as in the case of benzoic acid and associated with the solvent by means of hydrogen bonds as represented by formula (IV). This contains two  $\text{C}=\text{O}$  groups. The existence of  $\text{C}=\text{O}$  (1) can account for the frequency at  $1726 \text{ cm}^{-1}$  satisfactorily based on analogies quoted in the previous paragraph. But  $\text{C}=\text{O}$  (2) corresponds to the carbonyl present in phenyl acetate and may be expected to give a strong line at about  $1766 \text{ cm}^{-1}$ . This is definitely absent in the spectrum. Formula (IV) may not therefore represent the correct position, and it is possible that  $\text{C}=\text{O}$  (2) is involved in hydrogen bond formation. A ring structure as in (V) appears to be more satisfactory; it involves the existence of a chelate hydrogen bond between the carbonyl of the acetate group and the hydrogen atom of the carboxyl group. This formulation not only locates the frequency of  $\text{C}=\text{O}$  (1) at about  $1726 \text{ cm}^{-1}$  but further suggests that the frequency of  $\text{C}=\text{O}$  (2) should be lowered as the result of chelation by about 40 wave numbers to almost the same value as  $\text{C}=\text{O}$  (1), namely  $1726 \text{ cm}^{-1}$ . The observed line is rather broad and it may be due to the juxtaposition of the two  $\text{C}=\text{O}$  lines merging into one. In support of this idea could be stated that  $\text{C}=\text{O}$  (2) corresponds to the carbonyl group in phenyl esters and is a powerful donor and that the H atom of the carboxyl is a strong acceptor, and hence these could form intramolecular hydrogen bonds with facility. Further support could probably be obtained from a study of related compounds and derivatives which could not be undertaken now.



## *Summary*

The Raman spectrum of salicylic acid has been studied for the first time in dioxan and benzene solutions. In the former monomolecular chelate structures associated with the solvent predominate; in the latter some chelate monomers exist, but the major portion consists of dimers whose structure is not quite clear. The spectrum of acetyl salicylic acid (aspirin) in dioxan seems to indicate that it has a chelate structure.

## REFERENCES

1. Murty and Seshadri .. *Proc. Ind. Acad. Sci. A*, 1942, **15**, 230,  
238; 1942, **16**, 50, 264.
2. Venkateswaran .. *Ibid.*, A, 1939, **8**, 448.
3. Hendrixson .. *Zeit. Anorg. Chemie*, 1897, **13**, 73.

# ALKALOIDS

## Part I. The Oxidation of Papaverine to Papaveraldine (Xanthaline) by Selenium Dioxide

BY K. N. MENON  
(*Maharaja's College, Ernakulam*)

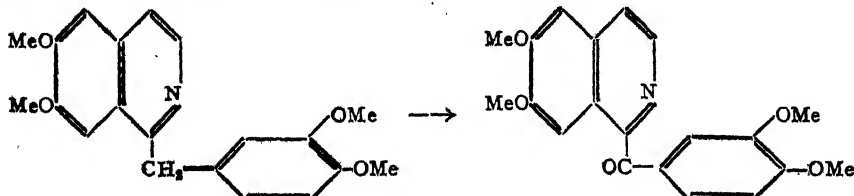
Received December 2, 1943

ONE of the most successful methods for elucidating the constitution of alkaloids is the examination of the behaviour of the alkaloids towards oxidising agents. Very often the initial products of the oxidation are further attacked by the oxidising agent resulting in degradation products of comparatively small molecular weight and often much oxalic acid. It is mainly for this reason that it has frequently been found difficult to isolate the initial product of the oxidation and that, in its place, a variety of degradation products derived from one or the other half of its molecule are the only substances that can be discovered. This leads to difficulties in rigidly fixing the constitution of the substance.

In the course of some investigations it became evident that the oxidative methods commonly employed are not helpful in deciding alternative possibilities of ring structure. It was found that selenium dioxide oxidation was useful in getting workable quantities of the primary oxidation products, but interpretation of the results became difficult due to the lack of specific knowledge concerning the action of selenium dioxide on condensed polynuclear heterocyclic structures. In order to gain insight in this direction it was decided to examine the behaviour of selenium dioxide towards alkaloids of known constitution.

Riley<sup>1</sup> gives an excellent review of the use of selenium dioxide as an oxidising agent and a perusal of the literature shows that the outstanding feature is the highly specific nature of the oxidising action of selenium dioxide. Although selenium dioxide is undoubtedly a relatively vigorous oxidising agent, its action stops at specific stages even though the compound produced is unstable towards oxidising agents and highly reactive, as in the case of mesoxalic ester,<sup>2</sup> ketohydroxysuccinic ester,<sup>3</sup> pyridine and quinoline aldehydes<sup>4</sup>, etc. Hence the hope is entertained that selenium dioxide oxidation would prove a very useful tool in alkaloid chemistry.

When papaverine, in acetic acid solution, is oxidised with selenium dioxide it is converted into papaveraldine (xanthaline).



This result is in conformity with the observation that an aryl group can activate the adjacent methylene group and render it susceptible to attack by selenium dioxide<sup>5</sup>. The quantitative yield of papaveraldine and the absence of other degradation products is specially noteworthy.

Papaveraldine, first isolated by Smith<sup>6</sup> from opium in which it occurs only in minute quantities, was examined by Dobson and Perkin<sup>7</sup> and proved to be identical with the product<sup>8</sup> obtained by the oxidation of papaverine, dissolved in sufficient dilute sulphuric acid to form the acid salt, with cold 2% potassium permanganate solution. The identity of the selenium dioxide oxidation product was established by a comparison of the melting points of the alkaloid, its methiodide and picrate.

### *Experimental*

To papaverine (10 g.) dissolved in acetic acid (100 c.c.) was added pure selenium dioxide (4 g.) and the mixture heated on the water-bath for 1½ hrs. and then refluxed for the same period. After oxidation the acetic acid solution was filtered and the filtrate evaporated to dryness on the water-bath. The residue was ground up with 100 c.c. of 50% hydrochloric acid when the product went into solution and after a short time the hydrochloride separated out. 400 c.c. of water was added and the mixture heated on the water-bath. The solution was filtered from a small quantity of insoluble impurity and allowed to cool when the hydrochloride (m.p. 200°) separated out. This was decomposed with ammonia and the free base crystallised from methylethyl ketone yielding plate-like crystals melting at 209–211° (Literature<sup>7</sup>–210°). The methosulphate was converted into methiodide and crystallised from dilute methyl alcohol in orange yellow crystals melting at 133–135° (Literature<sup>7,9</sup>–132 and 135°). The picrate crystallised in fine yellow needles melting at 208–209° (Literature<sup>9</sup>–208–209°). The platinic chloride analysed for the formula  $(C_{20}H_{19}O_5N.HCl)_2 \cdot PtCl_4 \cdot H_2O$ .

### *Summary*

The selenium dioxide oxidation of papaverine yields papaveraldine.

### REFERENCES

1. *Journal of the Royal College of Science*, 1935, 5, 7.
2. Müller, *Ber.*, 1933, 66, 1668.
3. Astin and Riley, *J. C. S.*, 1934, 844.
4. Henze, *Ber.*, 1934, 67, 750.
5. I. G. Farb., A. G., B. P., 1931, 347, 743; Fisher, *J. A. C. S.*, 1934, 56, 2056; Chakravarthi and Swaminathan, *J. Indian Chem. Soc.*, 1934, 11, 715.
6. *Pharm. J.*, 1893, 793.
7. *J. C. S.*, 1911, 99, 135.
8. Goldschmidt, *Monatsh.*, 1885, 6, 956.
9. \_\_\_\_\_, *Ibid.*, 1886, 7, 485; see also Kabachnik and Zitser, *J. Gen. Chem. (U.S.S.R.)*, 1937, 7, 162.

# NOTE ON THE SEPARATION OF THE ELECTRONIC AND NON-ELECTRONIC COMPONENTS OF COSMIC RADIATION

BY H. J. BHABHA, F.R.S.

(*Cosmic Ray Research Unit, Indian Institute of Science, Bangalore*)

Received December 14, 1943

COSMIC radiation is known to be composed of two main components which differ greatly in their behaviour. One component consists of electrons, positrons and gamma-rays and is called the soft component. The other, called the hard component, consists of mesons of positive and negative charge, and probably also of neutral mesons. The words soft and hard are used in this paper only in the sense defined above, and carry with them no indication of the energy or penetrating power of the individual particles. There may also exist a certain number of very high energy protons which we will consider here with the hard component. There is in addition a certain number of neutrons, low energy protons and fragments of disintegrated nuclei which do not need to be considered in this paper. The behaviour of the soft component is accurately described by the quantum theory and in particular the cascade theory, while the behaviour of the penetrating component is known both theoretically and experimentally to a much lesser extent. In studying the behaviour of the hard component experimentally, various devices have been used by different authors for excluding the effects of the soft component. The degree of accuracy of the experiments and even the interpretation of some of them depend on the extent to which these devices discriminate against the soft component. The most commonly used method of discriminating between the soft and hard components is to observe or measure their penetration through plates or blocks of different thicknesses of some dense material such as lead. The heavy material then serves either for excluding the soft component due to its greater absorability, or, as is usual in experiments with a Wilson chamber, as a medium in which the electrons produce showers and can thus be distinguished from the particles of the hard component. We shall show that great caution is required in interpreting the results, and that in many cases the exclusion of the soft component by these methods is much less than has been supposed. Finally we shall describe a new experimental arrangement which makes the maximum use of the shower producing property of the soft component for distinguishing it from the hard component.

### 1. Theoretical Results on the End of a Shower

We begin by considering the behaviour, as described by the cascade theory, of the soft component in passing through a slab of some heavy material. We take as the basis of our further calculations the results of Bhabha and Chakrabarty (1942, 1943 referred to in this paper as B and A respectively) who have taken collision loss into account accurately in the calculation of the cascade process. Even for particles whose energy is much below the critical energy their figures are accurate to within thirty per cent. and for higher energies the accuracy is much greater. It has been shown in the papers mentioned above that the accuracy of other calculations of the cascade process is much less than this. As usual, the calculations can be applied to all substances if lengths in the substance are measured in terms of radiation units, and energies are measured in terms of the critical energy. The critical energy is the mean energy lost by an electron by collision alone in travelling a distance of one radiation unit. It is denoted by  $\beta$ . The figures to be taken for the units of length and the critical energies in different substances are given in Table I of A. In lead, for example, the unit of length is 0.525 cm., and the critical energy is 6.93 MeV. In air the critical energy is 103 MeV.

Consider a block of some substance, say lead, of thickness  $t$  measured in terms of the radiation unit. Then an electron of energy  $E = \epsilon \beta$  entering the block vertically from above, say, produces on the average  $N(\epsilon, t)$  particles which emerge from the bottom face of the block.  $N(\epsilon, t)$  includes particles both above and below the critical energy, and its values are given in Table III of B. We shall particularly require the values of  $N$ , on the one hand at the end of a shower, that is at thicknesses so large that the cascade has been practically absorbed so that  $N$  is less than or of the order one, and on the other hand at thicknesses of 2 to 4 units where  $N$  is a maximum. It was shown in B that

$$N(\epsilon, t) = \frac{1}{\sqrt{2\pi}} e^{(s-1)y - \lambda t + \phi(s, t)} \{ -\lambda''t + \phi''(s, t) \}^{-\frac{1}{2}} \quad (1)$$

where

$$\phi(s, t) = \log \frac{D - \lambda}{\mu - \lambda} - \log(s - 1) - (s - 1) G, \quad (2)$$

$$y = \log \epsilon,$$

$$G = \log g(s, t).$$

$D$  is constant and  $\lambda$  and  $\mu$  are functions of  $s$  only while  $g$  and hence  $\phi$  are functions of only  $s$  and  $t$ . These functions are defined and tabulated in A. A dash denotes differentiation with respect to  $s$ . For any given values of  $y$  and  $t$  the value of  $s$  has to be taken at the saddle point

defined by

$$y - \lambda' t + \frac{d}{ds} \log \frac{D - \lambda}{\mu - \lambda} - \frac{1}{s - 1} - G - (s - 1) G' = 0 \quad (3)$$

$s$  is therefore a slowly varying function of  $y$  and  $t$ . Further

$$-\lambda'' t + \phi''(s, t) = -\lambda'' t + \frac{d^2}{ds^2} \log \frac{D - \lambda}{\mu - \lambda} + \frac{1}{(s - 1)^2} - (s - 1) G'' - 2 G' \quad (4)$$

and is only a function of  $s$  and  $t$ . The energy  $\epsilon$  of the shower producing electron only appears in these expressions in the first terms on the right-hand sides of (1) and (3). (4) is independent of  $y$  or  $\epsilon$ .

We now investigate the value of  $\epsilon$  or  $y$  which produces at a given thickness  $t$  a given number of particles  $N'$ , say. By (1) we must have

$$y - \frac{\lambda}{s - 1} t + \frac{1}{s - 1} \phi(s, t) - \frac{1}{2(s - 1)} \log 2\pi \{-\lambda'' t + \phi''(s, t)\} - \frac{\log N'}{s - 1} = 0. \quad (5)$$

In addition there is the usual relation (3) between  $y$ ,  $t$  and  $s$  which must always be satisfied. Subtracting (5) from (3) we get

$$\left( \frac{\lambda}{s - 1} - \lambda' \right) t + \frac{d}{ds} \log \frac{D - \lambda}{\mu - \lambda} - \frac{1}{s - 1} \log \frac{D - \lambda}{\mu - \lambda} + \frac{\log(s - 1) - 1}{s - 1} - (s - 1) G' + \frac{1}{2(s - 1)} \log 2\pi \{-\lambda'' t + \phi''(s, t)\} + \frac{\log N'}{s - 1} = 0 \quad (6)$$

This equation does not contain  $y$ , and determines the value of  $s$  as a function of  $t$  which satisfies the required condition. On substituting this value of  $s$  into either (3) or (5) we get the required value of  $y$  which produces  $N'$  particles on the average at a thickness  $t$ . The equation (6) can be solved quite easily numerically by using the tables given in A. It appears that the value of  $s$  varies very slowly as a function of  $t$ , and for all  $t$  between 4 and 30 it has roughly the fairly constant value 2.90 for  $N$  between 1 and 1/10, and the value 3.30 for  $N$  between 1/10 and 1/100. (See note added in proof.)

In particular, it is of importance to know the values of  $\epsilon$  such that the number of particles is just 1, or conversely, the depth  $t$  at which the number of particles  $N$  falls to 1 for a given  $\epsilon$ . This depth  $t$  may be called the penetration range of a shower produced by an electron of energy  $\epsilon$ . Putting  $N' = 1$  in (5) we get

$$\log \epsilon = \frac{\lambda}{s - 1} t - \frac{1}{s - 1} \phi(s, t) + \frac{1}{2(s - 1)} \log 2\pi \{-\lambda'' t + \phi''(s, t)\} \quad (7)$$

$\phi$  and the last term of (7) vary slowly with  $t$ , so that the main variation with  $t$  is determined by the first term on the right of (7). For  $s = 2.80$  the value of  $\lambda/(s - 1)$  is 0.265. Actually, the calculations which were carried out in B show that for all  $t$  between 4 and 30  $N = 1$  when

$$\log \epsilon = 0.283 t + 1.94, \quad (8)$$

this formula being far more accurate (to within 2%) than the degree of accuracy of the cascade calculations. This shows that the last two terms in (7) in effect change the coefficient of  $t$  from 0.265 to 0.283. Formula (8) expresses to a high degree of accuracy the penetration range of a shower produced by an electron of energy  $\epsilon$ . The values of  $\epsilon$  for different values of  $t$  calculated from formula (8) are given in the second row of Table I. The corresponding values of  $E$  in lead are given by the third row.

TABLE I

$t$	4	10	15	20	30
$E$ in MeV. $\therefore$	21.51 $1.50 \times 10^3$	117.9 $8.24 \times 10^3$	192.7 $3.40 \times 10^3$	1998 $1.40 \times 10^4$	$3.39 \times 10^4$ $2.36 \times 10^5$
$\left(\frac{\beta_{air}}{\beta_{pb}}\right)^{1.00}$	0.50	0.020	0.0013	0.00009	

On comparing (7) with (8) we see that to a good approximation we can write (1) in the form

$$N(\epsilon, t) = (f\epsilon)^r \quad (9)$$

for  $N \lesssim 1$ , where

$$f = e^{-0.283 t - 1.94} = 10^{-0.123 t - 0.80} \quad (10)$$

and  $r = s - 1$ . The remarks we have made above show that we can take  $r = 1.8$  with considerable accuracy for  $N$  lying between 1 and  $1/10$  and  $r = 2.00$  for  $N$  between  $1/10$  and  $1/100$ .

In applying the theory to the interpretation of experiments it is essential to take fluctuations into account. It has been shown by Euler (1938) that at the end of a shower and at the maximum the fluctuations are given by a Poisson distribution as originally assumed by Bhabha and Heitler (1937). The probability that in any given case  $n$  particles appear from the bottom of the lead block when the mean number is  $N$  is

$$e^{-N} \frac{N^n}{n!}. \quad (11)$$

The sum of this expression over all integral values of  $n$  from 0 to  $\infty$  is 1 as it should be. The probability that by a fluctuation no particle appears from

the bottom of the plate is therefore  $e^{-N}$ , and the probability that one or more particles appear is

$$1 - e^{-N}. \quad (12)$$

Electrons of different energies fall on top of the plate, and we assume that the number whose energy is greater than  $E$  is given by

$$J \left( \frac{k}{E} \right)^\alpha, \quad (13)$$

where  $J$  and  $k$  are constants, whose values do not concern us here. For the soft component produced by cascade processes in the atmosphere directly connected with the primary radiation incident at the top  $\alpha = 1.90$  according to Euler and Heisenberg (1938) or 1.87 according to Blackett while for the soft component in air at sea level, which is mainly due to the decay of mesons, the coefficient  $\alpha$  is roughly 2.9 according to Euler and Heisenberg. If there is only air above the plate, then the spectrum (13) would hold down to particles of the critical energy in air, i.e., 103 MeV. Below this critical energy the spectrum would be flatter and reach some finite value as  $E \rightarrow 0$ . It has been shown in B that at the maximum of the cascade the ratio of the number above the critical energy to the total number is 0.8/1.8, while at greater thicknesses this number is somewhat less. Our results do not depend critically on the value of  $\alpha$ .

The number of electrons of energy greater than  $E$  which impinges vertically on the plate and produces one or more particles at the bottom is then, according to (12) and (13),

$$J \alpha k^\alpha \int_E^\infty \left( 1 - e^{-N} \left( \frac{E'}{\beta}, t \right) \right) \frac{dE'}{E'^{\alpha+1}}. \quad (14)$$

This would be the contribution of the particles of the soft component with energies greater than  $E$  to coincidences in a vertical counter telescope with an absorber of thickness  $t$  between the counters. Since for large  $N$  the second factor in (14) is in any case negligibly small, we can with quite sufficient accuracy introduce (9) in (14). We then get

$$\begin{aligned} J \alpha \left( \frac{k}{\beta} \right)^\alpha \int_e^\infty & \left( 1 - e^{-(f_e)^r} \right) \frac{d\epsilon}{\epsilon^{\alpha+1}} \\ &= J \left( \frac{fk}{\beta} \right)^\alpha \frac{\alpha}{r} \int_{(f_e)^r}^\infty (1 - e^{-x}) \frac{dx}{x^{\frac{\alpha}{r}+1}} \end{aligned} \quad (15)$$

Dividing this by (13) we get  $p(E, t)$  the fraction of the number of electrons of energy greater than  $E$  which produces a coincidence through a slab of thickness  $t$ , namely

$$p(E, t) = \frac{a}{r} (f\epsilon)^a \int_{(f\epsilon)^r}^{\infty} (1 - e^{-x}) \frac{dx}{x^{\frac{a}{r}+1}} \quad (16)$$

On integrating by parts twice we get, for  $a \neq r$

$$\begin{aligned} p(E, t) &= 1 - e^{-(f\epsilon)^r} \left\{ 1 - \frac{r}{a-r} (f\epsilon)^r \right\} \\ &\quad - (f\epsilon)^a \frac{r}{a-r} \Gamma\left(2 - \frac{a}{r}\right) \left\{ 1 - W\left(2 - \frac{a}{r}, (f\epsilon)^r\right) \right\} \end{aligned} \quad (17a)$$

where  $W$  is the incomplete gamma function defined by

$$W\left(2 - \frac{a}{r}, (f\epsilon)^r\right) = \frac{1}{\Gamma\left(2 - \frac{a}{r}\right)} \int_0^{(f\epsilon)^r} e^{-x} x^{1 - \frac{a}{r}} dx \quad (18)$$

and is tabulated.\* For  $a = r$  we get for (15)

$$p(E, t) = 1 - e^{-(f\epsilon)^r} + (f\epsilon)^r \int_{(f\epsilon)^r}^{\infty} e^{-x} \frac{dx}{x}. \quad (17b)$$

The integral in the last term is just the logarithmic integral  $-Ei(- (f\epsilon)^r)$ , which has also been tabulated. For  $(f\epsilon)^r \ll 1$  (17a) and (17b) reduce to

$$\frac{a}{a-r} (f\epsilon)^r - \frac{r}{a-r} (f\epsilon)^a \Gamma\left(2 - \frac{a}{r}\right) + \frac{a}{2(2r-a)} (f\epsilon)^{2r} + 0 (f\epsilon)^{3r} \quad (19a)$$

and

$$(f\epsilon)^r \{1 - \log \gamma (f\epsilon)^r\} + \sum_{n=2}^{\infty} (-1)^n \frac{1}{(n-1) \cdot n!} (f\epsilon)^{nr} \quad (19b)$$

respectively.  $\gamma$  is the Euler-Mascheroni constant so that  $\log \gamma = 0.577$ . In deducing (19b) from (17b) use has been made of the well-known relation

$$\log \gamma = \int_0^1 \frac{1 - e^{-x}}{x} dx - \int_1^{\infty} \frac{e^{-x}}{x} dx \quad (20)$$

(19b) is of course the limiting form of (19a) when  $r \rightarrow a$ . The figures for  $p(E, t)$  for different values of  $(f\epsilon)^r$  are given in the second and third rows of Table II for  $r = a = 1.90$  and  $r = 1.90, a = 2.90$  as an indication.

---

\* See for example, Jahnke-Emde, *Tables of Functions*.

The probability that one electron should emerge from the bottom of a plate when the average number is  $N$  is  $Ne^{-N}$  according to (11). The fraction of the number of electrons with energy greater than  $E$  which produces only one particle in passing through a plate of thickness  $t$  is got by replacing  $1 - e^{-N}$  by  $Ne^{-N}$  in (15) and is

$$p_1(E, t) = \frac{a}{r} (f\epsilon)^a \int_{(f\epsilon)^r}^{\infty} e^{-x} \frac{dx}{x^{\frac{a}{r}}} \quad (21)$$

This gives just

$$p_1(E, t) = \frac{a}{a-r} (f\epsilon)^r e^{-(f\epsilon)^r} - \frac{a}{a-r} (f\epsilon)^a \Gamma\left(2 - \frac{a}{r}\right) \left\{1 - W\left(2 - \frac{a}{r}, (f\epsilon)^r\right)\right\} \quad (22a)$$

for  $r \neq a$  and

$$p_1(E, t) = (f\epsilon)^r \int_{(f\epsilon)^r}^{\infty} e^{-x} \frac{dx}{x} = -(f\epsilon)^r Ei(-(f\epsilon)^r) \quad (22b)$$

for  $r = a$ . In the case  $(f\epsilon)^r \ll 1$  (22a) and (22b) reduce to

$$\frac{a}{a-r} \left\{ (f\epsilon)^r - (f\epsilon)^a \Gamma\left(2 - \frac{a}{r}\right) \right\} + \frac{a}{2r-a} (f\epsilon)^{2r} + \dots \quad (23a)$$

and

$$- (f\epsilon)^r \log \gamma (f\epsilon)^r + \sum_{n=2}^{\infty} (-1)^n \frac{(f\epsilon)^{nr}}{(n-1)(n-1)!} \quad (23b)$$

respectively. The figures for  $p_1(E, t)$  are given in the fourth and fifth rows of Table II for different values of  $(f\epsilon)^r$  and  $r = a = 1.9$  and  $r = 1.90$ ,  $a = 2.90$  respectively.

The probabilities that two or more particles are produced under the same conditions are got by subtracting the figures of the fourth row from those of the second.

In applying the formulae developed above to the total soft component, we may take  $E = 103$  MeV, the critical energy in air below which the spectrum (13) gets flattened out due to the collision loss suffered by the electrons in air. It has been shown in B that the number of electrons above the critical energy due to the cascade process is roughly half the total number of electrons. Thus to get the fraction of the total number of electrons which behave in the particular manner under considerations one has to divide the figures of Table II by roughly two. For  $E = 103$  MeV,  $\epsilon = 14.9$ , and the first four values of  $(f\epsilon)^r$  given in Table I correspond to  $t = 20, 15, 10$  and  $4$  respectively. Thus, the percentage of the total soft component

at the maximum of the atmospheric absorption curve which produces a coincidence in a vertical counter telescope through 10.5, 7.9, 5.3 and 2.1 cm. of lead is approximately .05, 0.5, 5 and 36 respectively. Since the total intensity of the electronic component is four times the intensity of the hard component at the maximum of the atmospheric absorption curve, the errors in the count where the different thickness of lead absorbed mentioned above are used for cutting out the soft component are 0.2, 2, 20 and 144 per cent. respectively.

TABLE II

$(f_e)^r$	.. ..	0.00011	0.0016	0.024	0.59	1.0
$p(e, t)$ for $\alpha=r$	.. ..	0.001	0.011	0.1	0.72	0.85
$p(e, t)$ for $\alpha=2.9, r=1.9$	.. ..	0.0003	0.004	0.06	0.66	0.81
$p_1(e, t)$ for $\alpha=r$	.. ..	0.001	0.009	0.08	0.27	0.22
$p_1(e, t)$ for $\alpha=2.9, r=1.9$	.. ..	0.00031	0.0044	0.053	0.12	0.11

At sea level most of the soft component in air is due to the decay of mesons, and its spectrum is then of the form (13) with  $\alpha \approx 2.9$ , as mentioned above. The figures for the corresponding processes at sea level are then given by the third and fifth rows of Table II.

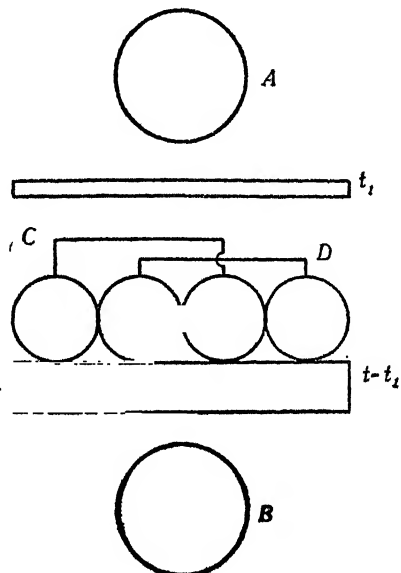
If fluctuations were negligible then the fraction of the number of electrons with energy greater than 103 MeV, which impinge vertically on a lead plate of thickness  $t$  and produce a coincidence would be just  $(\beta_{air}/\beta_{pb}e)^\alpha$  with  $e$  given by the second row of Table I for an incident spectrum of the form (13). The corresponding figures are given in the fourth row of Table I for  $\alpha = 1.90$ . These figures are to be compared with the first four figures in the second row of Table II. We see that the effect of fluctuations increases the number of electrons which apparently penetrate a given absorber ten fold for the larger thicknesses.

## 2. A New Experimental Arrangement for Excluding the Electronic Component

In this section we shall describe an arrangement which makes a much more effective use of cascade multiplication for excluding the electronic component. This arrangement was devised especially for measuring the penetrating component in stratospheric balloon flights, where it is necessary to cut down the weight of the absorber to a minimum. It is also particularly useful in all those experiments in which it is desired to exclude high energy electrons.

The essence of the method consists in splitting a given thickness  $t$  of absorber into two parts, of thicknesses  $t_1$  and  $t - t_1$ , respectively, and

introducing a set of counters in anticoincidence between the two. The arrangement is indicated in Fig. 1. A represents schematically either a single counter or a set of counters in parallel. So does B. Between the two plates a number of counters are put side by side and connected alternately in parallel to form two independent counter trays C and D. It will



be shown now that if the sets A, B and C or A, B and D are put in coincidence with C and D always in anticoincidence then the soft component is cut out to a high degree and we get a measurement of the penetrating component. The size of the counters in the trays C and D and the geometry of the whole arrangement, as for example, the distance of these trays from the upper absorber  $t_1$  is determined by the condition that any shower produced in  $t_1$  by an electron travelling in the direction AB shall have the maximum chance of operating both the sets C and D, *i.e.*, that at least one particle of the shower shall pass through one of the counters of the set C, and at least one other through one of the counters of the set at D. This condition operates as follows. The particles in a shower emanating from the plate  $t_1$  whose axis lies in the direction AB lie mainly within a cone whose half angle is of the order of  $40^\circ$  as estimated by Bhabha and Heitler, and within this cone the shower particles are scattered roughly at random, with some concentration towards the middle. This cone cuts the plane in which the counters of the sets C, D lie in approximately a circle. Then the required condition is satisfied if, first, the area of this circle is completely covered by

counters of the sets C and D, and secondly half the area is covered by counters of the set C and the other half by counters of the set D. In these circumstances the probability that a shower of  $n$  particles should have all its particles pass through counters of one of the sets C or D, but none through any counter of the other set is approximately  $(\frac{1}{2})^{n-1}$ . This is the probability that a shower of  $n$  particles does *not* produce a coincidence between C and D.

Now consider an electron of energy  $E = \beta \epsilon$  which operates the counter A and impinges on the plate  $t_1$ . It produces on the average a shower of  $N(\epsilon, t_1)$  particles at the bottom of the plate. The probability that in any given case the shower contains  $n$  particles is given by (11), and the probability that this shower does not produce a coincidence is got by multiplying this by  $2^{-n+1}$ . Hence, the total probability that the particle which enters the top of the plate  $t_1$  actuates at least one of the set of counters C or D, but not both is  $Q(N(t_1))$  where

$$Q(N(t_1)) = \sum_{n=1}^{\infty} e^{-N(t_1)} \frac{N(t_1)^n}{n!} \frac{1}{2^{n-1}} = 2 (e^{-\frac{1}{2} N(t_1)} - e^{-N(t_1)}). \quad (24)$$

This expression is small compared with 1 for large  $N$ , and has the maximum value  $\frac{1}{2}$  for  $N = \log_2 4$ . This same particle of energy  $E$  produces at the bottom of the second plate on the average,  $N(\epsilon, t)$  particles, and the probability that one or more particles should appear at the bottom is given by (12). Hence, the total probability  $P(\epsilon)$  that an electron of energy  $E$  passing through the counter A should produce a coincidence in the counters AB and actuate only one of the sets C or D is got by multiplying (12) by (24) and is

$$P(\epsilon) = 2 (e^{-\frac{1}{2} N(E, t_1)} - e^{-N(E, t_1)}) (1 - e^{-N(E, t)}). \quad (25)$$

The expression (25) is the probability for an electron of energy  $E$  being counted as a hard particle. For a given total thickness  $t$  of absorber,  $t_1$  must be chosen so as to make (25) a minimum particularly for the low values of  $\epsilon$  which are just sufficient to produce a coincidence through the total thickness  $t$  of absorber. As shown in B (eq. 30), for a given value of  $\epsilon$  the maximum number of particles occurs at a thickness  $t_m$  given by

$$t_m = 1.01 \log \epsilon - 1.92. \quad (26)$$

Comparing this with the thickness given by (8) at which the average number of particles falls to one, we see that  $t_1$  must be about a quarter of  $t$ . In Table III we give the figures for  $t = 10$  and two values of  $t_1$  equal to 2 and 4 respectively. The values of  $N(\epsilon, t)$  in the fourth and seventh columns of

the table have been obtained from the figures given in Table III of B by graphical interpolation. It is clear that the smaller value of  $t_1$  is more effective in cutting out the soft component since at the smaller thickness the lower energies produce more particles and  $Q(N(t_1))$  is thus smaller. For higher energies the values of  $N(t_1)$  are so large for either thickness that the soft component is cut out to a high degree in both cases. For  $t_1 = 2$ ,

TABLE III

E in $10^8$ e.V.			$t_1 = 2$			$t_1 = 4$			Incident spectrum (13) $(k/E)^{-2.9}$
	$N(\epsilon, t=10)$	$1-e^{-N(t=10)}$	$N(\epsilon, t_1)$	$Q(N(2))$	$P(\epsilon)$	$N(\epsilon, t_1)$	$Q(N(4))$	$P(\epsilon)$	
1	$\lesssim 0.03$	.03	2.3	.43	.013	.	.	.	1
2	$\sim 0.08$	.08	4	.23	.018	2	.44	.034	.13
3.6	$\sim 0.3$	.28	6	.095	.027	4.6	.18	.05	.024
8	1	.63	9	.022	.014	10	.013	.008	.0024
20	$\sim 5$	1.00	15	.0011	.0011	$\sim 26$	0	0	.00017

the figures in the sixth column show that the maximum value of  $P$  is less than .03, so that whatever the form of the spectrum the percentage of the electronic component which could at most be counted as hard particle is 3%, while for  $t_1 = 4$  it could at most be 5% as shown by the figures in the ninth column. The actual fraction of electrons of energy above  $E$  in an incident spectrum of the type (13) which pass for hard particles is

$$\alpha (E_0)^\alpha \int_{E_0} P(\epsilon) \frac{dE}{E^{\alpha+1}}. \quad (27)$$

This expression cannot be evaluated analytically since there is no simple analytic expression for  $N(\epsilon, t_1)$  like the one given in (9) for  $N(\epsilon, t)$ . However, it can be evaluated numerically without much difficulty. The form of the incident differential spectrum is given for  $\alpha = 1.9$  in the last column of Table III normalised to unity for  $E = 10^8$  e.V. We find that for  $t_1 = 2$  the fraction of the number of particles above  $10^8$  e.V. which is recorded as a penetrating particle is about 2%. This figure is to be compared with the figure of 10% given in Table II for the same thickness, of lead, namely 5 cm., but without the anticoincidence device.

For greater thicknesses of absorber, say  $t = 15$  or 20, the effectiveness of the anti-coincidence arrangement is enormously increased, for then the number of particles produced at the thickness  $t_1$  by a primary electron whose energy is high enough for the cascade initiated by it to penetrate the thickness  $t$  is much larger, and consequently  $Q(N(t_1))$  is very much smaller. Our method differs from previous arrangements in the anti-

coincidence device being put *not* at the bottom of the whole absorber, but after that fraction of it at which the number of particles in the cascade is a maximum.

In stratosphere balloon flights for measuring the vertical intensity of the hard component it is necessary to increase the effective area of a counter set without increasing the solid angle. In this case each of the counters denoted symbolically by A and B in Fig. 1 usually consist of a number of counters in parallel having a total area ' $a$ ' say. The counter sets C and D with counters of each set alternating as in Fig. 1 can then be made to cover the same area ' $a$ ' together, each set covering an area  $a/2$ . Since a triple coincidence arrangement is much better in minimising the effect of side showers, while at the same time it is not desirable to halve the total number of counts by putting one of the sets C or D always in coincidence with A and B, the other set being always in anticoincidences, the following arrangement makes the most effective use of the absorber sent up for excluding the soft component. The circuits are wired to record coincidences in the sets A, B and C or A, B and D, but not those in which C and D both register a count simultaneously. The details of the experimental arrangements and the circuits will be communicated by my collaborators in another paper.

Mesons also produce electron showers either by the knock-on-process or by the emission of a quantum of radiation. None of these processes depends critically on the energy of the meson. There are also processes in which a meson can produce several energetic mesons in one act. A meson which is accompanied by any of these processes would of course be eliminated by the anticoincidence arrangement. But since the probability of a meson being accompanied by a number of charged particles in the neighbourhood of the anticoincidence counters is very much smaller than the chance of an electron producing a cascade, their effect is only to make the count of the penetrating particles by the above method a few per cent. less than the actual number.

There is however one important application of the experimental arrangement described above to the study of mesons. Since a meson is an unstable particle, every meson which comes near the end of its range must either decay or be absorbed by a nucleus. In the former case the decay electron produces a cascade. In the latter case the nucleus is excited by an amount of energy approximately equal to the rest energy of the meson, leading to processes in which several high energy electrons, protons or heavier fragments may be emitted. The result is that every meson which comes to the end of its

range produces in general several high energy charged particles, and the effect of these is to smear the apparent range of a meson as measured by absorption in heavy material with counters in coincidence. For example, even if a mono-energetic band of mesons existed, then there would not be a sharp drop in the coincidence count after an absorber thickness equivalent to their range had been added, due to the effects mentioned above. If, however, the anticoincidence arrangement described above is used then these effects are cut out and it would be possible to study much more accurately the range spectrum of cosmic ray mesons.

### *Summary*

A formula for the depth of the penetration of a cascade as a function of the energy of the primary electron is given based on the calculations of Bhabha and Chakrabarty. A simple formula for the end of a shower is also given. It is shown that fluctuation plays an important part in determining the ability of an electron to operate two counters separated by a given thickness of absorber and increases the number of such electrons ten-fold for thick absorbers. Formulae are given for the number of electrons which enter an absorber of thickness  $t$  and result in one or more particles emerging from the other side of the absorber.

A new experimental arrangement is described which makes a much more effective use of the cascade process for separating the electrons from the penetrating particles. This arrangement is suitable for measuring the penetrating component in high altitude balloon flights, and for studying the range spectrum of cosmic ray mesons.

### **REFERENCES**

Bhabha and Chakrabarty .. *Proc. Roy. Soc., A*, 1943, **181**, 267-303 referred to in this paper as A.  
——— .. *Proc. Ind. Acad. Sci., A*, 1942, **15**, 464-76 referred to in this paper as B.  
——— and Heitler .. *Proc. Roy. Soc., A*, 1937, **159**, 432-58.  
Euler .. *Naturwiss.*, 1938, **26**, 382.  
Euler and Hesienberg .. *Ergebnisse der Exakten Naturwissenschaften*, 1938, 1-69.  
*Zs. f. Phys.*, 1938.

*Note added in proof.*—At my request Mr. S. K. Chakrabarty has calculated more accurately the values of  $s$  satisfying equation (6) for given values of  $N$  and  $t$  on the basis of the tables given in A. His results are given in the following table :—

*Values of s satisfying equation (6)*

(Calculated by Chakrabarty)

$N \backslash t$	2	4	10	20	30
1	3.44	3.05	2.92	2.92	2.92
0.1			3.36	3.11	3.04
0.01				3.33	3.18

We see that for  $N \approx 1$   $s$  has the almost constant value 2.9 for  $t$  lying between 4 and 30. For  $N$  lying between 0.1 and 0.01 the values of  $s$  lie between 3.0 and 3.4 for  $t$  between 10 and 30.

# THE METHOD OF SHOWER ANTI-COINCIDENCES FOR MEASURING THE MESON COMPONENT OF COSMIC RADIATION

BY VIKRAM SARABHAI

(*Department of Physics, Indian Institute of Science, Bangalore*)

Received December 14, 1943

(Communicated by Sir C. V. Raman, Kt., F.R.S., N.L.)

## 1. Introduction

IT is comparatively simple enough to distinguish between ionising particles of electronic and of heavier mass in the Wilson Chamber as long as the energy of the particles is not too high. In experiments with Geiger counters however, there is no direct and simple way for identification of the type of the particles, and so far the criterion of penetrability has been the one most widely used for differentiation of the two main components of cosmic radiation. Bhabha<sup>1</sup> has however pointed out how it is necessary to use 7.9 cm. of lead in order that all but 2% of the electronic component can be stopped. This naturally puts a limit to the minimum energy of the meson component that is measured. When therefore we try to measure the meson component by filtering out the soft electronic component with 7.9 cm. of lead, we measure in fact only mesons with energy greater than  $1.3 \times 10^8$  e.v. It is known however that there are mesons of less energy in the cosmic ray spectrum. According to Blackett,<sup>2</sup> all particles with energy less than  $2 \times 10^8$  e.v. behave like electrons in their energy loss, but Anderson and Neddermeyer<sup>3</sup> find penetrating particles with less energy and have pointed out that Blackett's figure should be actually only  $1.1 \times 10^8$  e.v. Williams<sup>4</sup> has investigated the low energy spectrum, but has not made observations on the energy loss, and takes Blackett's observations to conclude that all the particles that he investigated in the low energy region were of electronic mass. More recently Bostick<sup>5</sup> has found evidence for slow mesons in a Wilson Chamber at 14,000 ft., and it is becoming increasingly clear that slow mesons are present in the cosmic ray spectrum. Rossi and Griesen<sup>6</sup> estimate that the slow mesons which get absorbed by 15 cm. of lead form 7% of the total meson intensity at an altitude of 850 ft., but may be as high as 27% at 14,100 ft. The results of Schein *et al.*<sup>7</sup> also point to the fact that the intensity of slow mesons increases rapidly with altitude.

Of late, the problem of knowing the correct proportion of electrons and mesons in the atmosphere at various altitudes has attracted a great

deal of attention. Auger<sup>8</sup> and Griesen<sup>9</sup> have utilised accurate absorption experiments with lead and iron absorbers in order to get an estimate of not only the electron (soft) component, but also the meson (hard) component. In order to arrive at the slow meson component which he finds to be about 8%, Griesen has to make correction for what he calls the "Collision and Shower Effects". The estimation of the latter is perhaps the only weak link in an otherwise beautiful analysis. Stimulated by the idea of Bhabha to utilise the generation of secondaries of the soft component in order to exclude it, the author has tried out a new experimental arrangement for obtaining the intensity of slow mesons. The importance of this method lies not so much in reducing the weight of lead for measuring the meson intensity in balloon experiments, or in the exclusion of high energy electrons as in bringing for the first time the slow mesons in the field of direct experimental measurements.

## *2. Method of Shower Anti-coincidences*

It has been found experimentally that a good proportion of the electrons measured by a cosmic ray telescope are already associated in the atmosphere with other ionising particles. The number so associated can be increased by placing in the apparatus a block of lead of thickness corresponding to the observed maximum of the Rossi curve. In order to exclude the

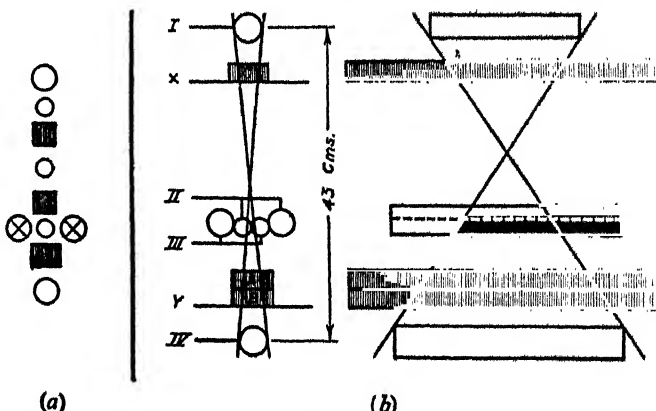


FIG. 1. (a) Showing the arrangement of Jesse *et al.*

(b) Showing the experimental arrangement used for measuring shower anti-coincidences.

electrons, we can then devise an arrangement whereby the arrival of the associated particle can be cancelled by an anti-coincidence arrangement, and keep just so much additional lead underneath to absorb low energy electrons which might emerge from the top lead unaccompanied by other shower particles. In fact Schien, Jesse and Wollan<sup>10</sup> have utilised the phenomenon of shower

production for making sure that the electron component was not greatly affecting the meson intensity that they measured in their balloon experiments with varying amounts of lead used to filter out the soft component. They measured events in which counters on the sides registered a particle associated with the penetrating particle in the main cone, as shown in Fig. 1 (*a*). Such an arrangement with the side counters working in anti-coincidence was initially suggested by Bhabha, but while on the basis of Auger's results, the atmospheric showers on account of their large spread will be probably quite well detected by this arrangement, the showers generated in the lead above may not be registered equally well on account of their small spread. In order to increase the efficiency of detection of both the atmospheric showers and those generated in the lead, it is desirable not to exclude the area of the main cone of measured radiation for the registering of the showers. This, however, cannot be accomplished by the use of the usual anti-coincidence arrangement, and a circuit is now devised whereby it is possible to tackle the main cone by placing two sets of counters in and adjoining the cone of the measured radiation (Fig. 1 *b*) and arranging matters so that only a coincidence between these two sets will cancel the event. This arrangement is simpler than the one now mentioned by Bhabha<sup>1</sup> and when used with quadruple coincidences would ensure that side showers do not vitiate the result. The circuit used for measuring the shower anti-coincidences is shown in Fig. 2. The two sets of anti-counters are connected in a Rossi coincidence arrangement with their mixer tube serving the dual role of a shower discriminator and a pulse reverser feeding the shower anti-pulse to the main coincidence circuit. Even though this means that the anti-pulse is fed through two stages as against the one stage for the main coincidence pulse, it is possible to attain an efficiency of 100% in the registration of shower anti-coincidences. The efficiency was measured in the following way:

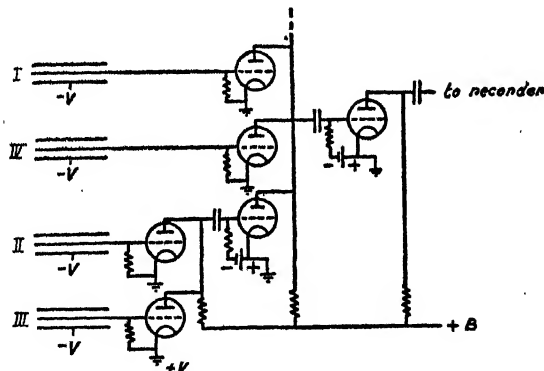


FIG. 2. Basic circuit used for measuring shower anti-coincidences. All tubes are Marconi Z21 and details are omitted.

An array of 4 counters A, B, C, D comprised a vertical telescope. The two end counters A, D were smaller both in length and diameter than the two middle counters B, C of the telescope. This ensures that every particle coming in the main cone determined by A, B will pass through the sensitive volumes of counters B, C. The double coincidences AD and the quadruple coincidences ABCD were measured. The difference in these two rates should be due to the effect of side showers and the inefficiency of counters B and C. This should equal the shower anti-coincidence rate AD-(BC) where the two centre counters are connected individually to the shower anti-coincidence tubes. The agreement of these counting rates was within a statistical accuracy of 1%. In order to see whether the feeding of one anti-pulse had any effect on the efficiency of registration of the main anti-coincidence rate AD, it was compared with the counting rate AD-(C) and the rate AD-(B) wherein the anti-pulse was fed to only one of the shower coincidence tubes. No effect falling outside the statistical accuracy of the measurements was found.

The circuit for the measurement of shower anti-coincidences is now being utilised for an accurate study of the intensity of slow mesons, and the results will be communicated later. However, a preliminary test has been made at various altitudes in Kashmere during August and September 1943, and the results of this preliminary survey are presented below.

### *3. Preliminary Survey of Meson Intensity at Various Altitudes in Kashmere*

In August 1943, an expedition was undertaken to Kashmere in order to find suitable locations where high altitude cosmic ray experiments could be performed. Though at that time the work on the experiment for measuring the slow meson intensity by the method of shower anti-coincidences had not progressed very far, it was decided to conduct that experiment at various altitudes in Kashmere to give a preliminary idea of both the working of the method of shower anti-coincidences and of the experimental technique involved in carrying out experiments on high peaks of the Himalayas. The most suitable period during which ascents can be undertaken to altitudes higher than 12,000 feet is from the middle of August to the middle of September. This consideration made it imperative to undertake the expedition in spite of the fact that the ideal experimental conditions for the method of shower anti-coincidences had not then been fully worked out.

A completely battery operated unit for registering fourfold coincidences along with shower anti-coincidences was set up. Marconi Z21 tubes were used for the amplifier on account of their low filament current

drain, and the mechanical recorder was operated by a type 31 tube in the final stage. The B supply was furnished by a Stabilovolt regulator tube fed from a Vibrapack operated from one of two 6 volt accumulators taken with the expedition. The accumulators were charged at the location of the experiment by means of a petrol generator set which was carried to all altitudes except the highest. The high voltage for the counters was obtained from a small unit of dry cells made up of Eveready type 712 cells connected in series. The counters were operated 50 volts above threshold potential and were all well within the flat portion of their plateau. The counters were mounted on a portable wooden stand, and the exact geometrical arrangement is shown in Fig. 1 (b). It was found that within the main cone the efficiency of registering showers was greater with narrow counters than with counters of large diameter, but that outside the main cone the larger the sensitive volume used, the larger was the measured shower effect. The counters comprising the shower detecting tray were therefore of two diameters. The top counter I of the telescope measuring the vertical intensity was of smaller length than the others in order to ensure that the area of the block C included in the main cone was smaller than the area of the shower detecting tray. Electrons arriving along the boundary of the main cone will thus have a greater chance of being cut out by the showers they would generate in C.

The experiment was attempted at 5 different altitudes in Kashmere. It was first tried near Gangabal at Tronkhal (11,000 ft.) and then at Cosmic Ray point (13,900 ft.). Good consistent results were obtained at both these locations. It was then attempted at Srinagar (5,200 ft.) and, in order to obtain a check on the Gangabal results, at Gulmarg (8,900 ft.) and near Alpathar (12,800 ft.). Unfortunately, the Srinagar results were not satisfactory, and it was not possible to repeat them for want of time. At Alpathar, the shower anti-coincidence arrangement did not work on account of what was later detected to be the failure of one of the Z21 tubes. However, the total cosmic ray intensity was measured and has been used as a check on the other points. While all the experiments at Kashmere were carried out at geo-magnetic latitude 25° N., the experiment has been repeated at Bangalore (3,000 ft.) at geo-magnetic latitude 3° N. The latitude effect does not permit us to compare directly the results at Bangalore with those of Kashmere, but the Bangalore results serve to illustrate the working of the method of shower anti-coincidences.

At each location, the following counting rates were measured. Double coincidences I IV and shower anti-coincidences I IV-(II III) were measured with (1) no lead, (2) lead block  $C_x$  (27.7 gm./cm.<sup>2</sup>) placed above the shower detecting counters at X, (3) lead block  $C_x$  at X and lead

block  $B_y$  ( $27 \cdot 4$  gm./cm. $^2$ ) under the shower detecting counters at Y and (4) lead block  $C_x$  at X and lead blocks  $B_y$  and  $A_y$  ( $26 \cdot 5$  gm./cm. $^2$ ) at Y. The double coincidence rate II III was also measured without any lead in the apparatus to register the intensity of atmospheric showers. The object of placing C at X was to increase the showers associated with the soft component, and varying amount of lead was placed at Y in order to investigate the absorption of the total intensity as measured by coincidences I IV and the meson intensity as measured by coincidences I IV-(II III). The experimental values of the intensity determined with the various arrangements at different altitudes are given in Table I.

TABLE I

Coincidence Counting Rates per minute	I IV	I IV-(II III)	II III Atmospheric showers						
Lead Blocks	..	..	$C_x$	$C_x$	$C_x+B_y$	$C_x+B_y$	$C_x+B_y+A_y$	$C_x+B_y+A_y$	..
Bangalore 3,000 ft.	$2 \cdot 876$ $\pm 0 \cdot 035$	$2 \cdot 738$ $\pm 0 \cdot 037$	$2 \cdot 526$ $\pm 0 \cdot 031$	$2 \cdot 341$ $\pm 0 \cdot 029$	$2 \cdot 282$ $\pm 0 \cdot 089$	$2 \cdot 168$ $\pm 0 \cdot 043$	$2 \cdot 129$ $\pm 0 \cdot 033$	$2 \cdot 074$ $\pm 0 \cdot 035$	$29 \cdot 05$ $\pm 4 \cdot 47$
Gulmarg 8,900 ft.	$4 \cdot 61$ $\pm 1 \cdot 10$	$4 \cdot 03$ $\pm 1 \cdot 17$	$3 \cdot 65$ $\pm 1 \cdot 17$	$2 \cdot 93$ $\pm 1 \cdot 16$	$3 \cdot 01$ $\pm 1 \cdot 15$	$2 \cdot 74$ $\pm 1 \cdot 11$	$2 \cdot 66$ $\pm 1 \cdot 10$	$2 \cdot 39$ $\pm 0 \cdot 06$	$52 \cdot 40$ $\pm 1 \cdot 54$
Tronkhali 11,000 ft.	$5 \cdot 24$ $\pm 1 \cdot 14$	..	$4 \cdot 40$ $\pm 1 \cdot 15$	$4 \cdot 00$ $\pm 1 \cdot 15$	$3 \cdot 89$ $\pm 1 \cdot 18$	$3 \cdot 66$ $\pm 1 \cdot 18$	$3 \cdot 69$ $\pm 1 \cdot 10$	$3 \cdot 28$ $\pm 0 \cdot 08$	$66 \cdot 6$ $\pm 1 \cdot 2$
Alpathar 12,800 ft.	$5 \cdot 93$ $\pm 1 \cdot 16$	..	..	..	..	..	..	..	..
Cosmic Ray Point 13,900 ft.	$6 \cdot 54$ $\pm 2 \cdot 20$	..	$5 \cdot 82$ $\pm 2 \cdot 24$	$4 \cdot 58$ $\pm 1 \cdot 18$	$5 \cdot 03$ $\pm 2 \cdot 20$	$4 \cdot 41$ $\pm 1 \cdot 18$	$4 \cdot 10$ $\pm 1 \cdot 17$	$4 \cdot 02$ $\pm 1 \cdot 17$	$78 \cdot 4$ $\pm 2 \cdot 7$
	..	..	..	..	..	..	..	..	..

The absorption curves are shown in Fig. 3 for the different altitudes. These curves clearly exhibit that as the electron intensity gets absorbed with increasing lead, the difference between the rates I IV and I IV-(II III) steadily diminishes. The forms of the two curves are also different; for while the slope of the curve I IV appears to increase with diminishing thickness of lead, the slope of the curve I IV-(II III) seems to vary in the opposite direction. On theoretical grounds of decay the curve for the meson intensity should become horizontal for zero thickness of lead absorber, and we have here a striking demonstration of the fact that the intensity measured by shower anti-coincidences refers mainly to mesons only. While we are not justified in taking the value I IV-(II III) without lead as giving the meson intensity for no lead, because the efficiency of excluding electrons by their

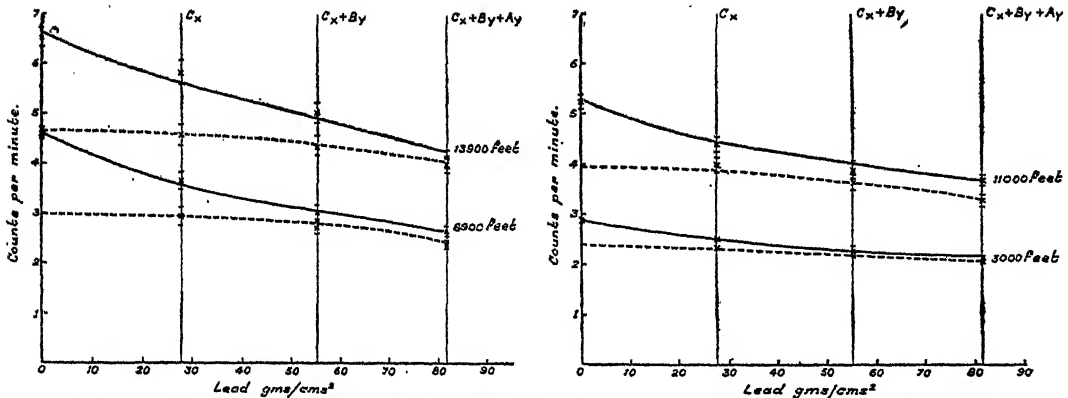


FIG. 3. Graphs showing for various altitudes the absorption by lead of the total intensity given by the counting rates I IV (continuous curves) and the meson intensity given by the counting rates I IV-(II III).

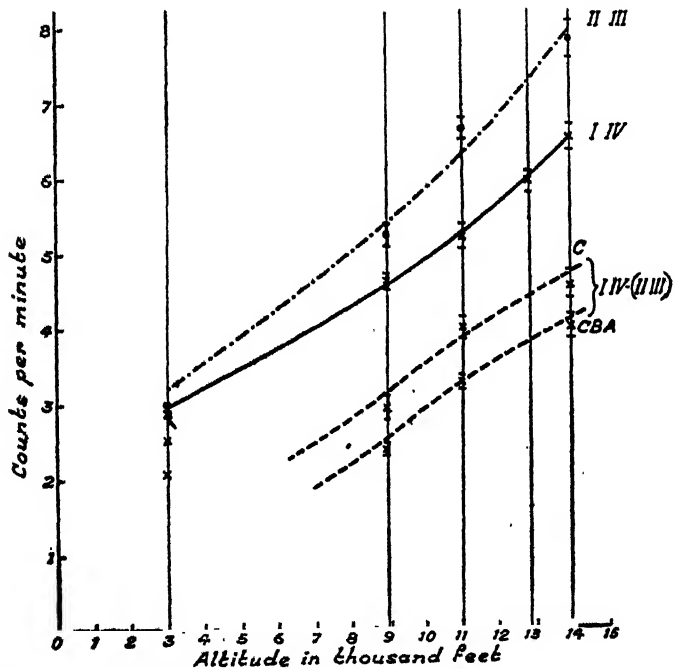


FIG. 4. Graphs showing intensity altitude curves for  
 (1) Atmospheric shower rate II III,  
 (2) Total intensity I IV, and  
 (3) Meson intensity as measured by I IV-(II III) with lead  $C_x$  and  $C_x + B_y + A_y$ .  
 The Bangalore results have been plotted but are not directly comparable.

Showers might be low without the lead block C, we can roughly extrapolate the shower anti-coincidence curve to zero thickness. It is then found that the percentage of mesons in the total cosmic ray intensity diminishes from

79% at 3,000 ft. to a value of 64% at 13,900 ft; but large error may be involved in both these estimates. At the same time however, the percentage of slow mesons in the total meson intensity appears to increase from 11% to about 18%.

The variation of the various counting rates with altitude is plotted in Fig. 4. The variation of the atmospheric shower rate is also given for comparison on the same graph. It is seen that while the total intensity I IV varies in a manner similar to the variation of the atmospheric shower intensity, the meson intensity as measured by the shower anti-coincidences has a flatter slope. The accuracy of the results is not such as to definitely conclude that the variation of the hard and soft components is very different in the region of the atmosphere investigated, but there seems to be little doubt that above 10,000 ft. the total intensity starts to rise more rapidly than the meson intensity. This is indeed in agreement with the results of Jesse *et al.*

#### 4. Discussion

Judged by the preliminary results obtained at Kashmere, the method of shower anti-coincidences appears to be fairly satisfactory in giving the meson intensity. The Kashmere readings however suffered from one serious drawback in that only double coincidences were measured with and without shower anti-coincidences. The contribution of side showers to double coincidences can be quite appreciable, as demonstrated by Greisen and Nereson.<sup>11</sup> This contribution would depend among other things on the separation of the two counters measuring the double coincidence rate. In the experiment performed at Bangalore for determining the efficiency of registering shower anti-coincidences, the maximum contribution due to side showers came to 13% of the double coincidence rate assuming 100% efficiency for the two middle counters. The separation of the counters A and D was in that experiment only 14 cm., while the separation of counters I and IV in the Kashmere and Bangalore series was 43. cm. Another point which should be considered before judging the accuracy of the Kashmere results is that while the Kashmere results were obtained with the apparatus in a small tent, the Bangalore experiment was performed in a tiled roof building where the ceiling was about 30 ft. above the apparatus. Taking all these into account, it appears that the contribution of side showers could not be greater than 10% of the double coincidence rate I IV without lead absorbers. The effect of side showers would be independent of the amount of lead placed within the apparatus, and would therefore adversely affect the operation of the shower anti-coincidence arrangement in detecting mesons. This is because the percentage increase due to side showers in the meson intensity

would be greater than in the total intensity and this would tend to increase the proportion of mesons.

The Kashmere results can be improved upon by placing a lesser thickness of lead at X than was actually used. The thickness of lead necessary for the maximum of the Rossi curve obtained from triple coincidences I II III would obviously be the ideal thickness to use. It comes to about 1.5 cm. Apart from being most effective in cutting out showers, it will also lower the low energy limit for the measurement of mesons. A further point that emerges is to test the absorption of the meson intensity as measured by shower anti-coincidences in the region of smaller thicknesses of lead absorber in the position Y. An accurate experiment is now in progress where quadruple coincidences are measured along with shower anti-coincidences and a much greater statistical accuracy is aimed at. The results will be shortly published in another communication.

The main defect of the method of shower anti-coincidences for measuring the meson intensity lies in the fact that multiple penetrating particles that are sometimes observed in a Wilson Chamber are also liable to be cut out. In addition, it is possible that knock-on electrons accompanying the mesons might prevent them from being measured. Both these effects would be more pronounced for high energy mesons and may not affect appreciably the intensity of slow mesons. The result of this might be to increase the measured proportion of slow mesons to the total number of mesons. The last and the most obvious possibility of error arises from electrons which may not produce large enough showers so as to be cut out by the shower anti-coincidence arrangement. With the help of a more accurate determination of the meson absorption curve, it is hoped that it would be possible to estimate the errors due to these causes.

One point that emerges from a comparison of the results at Bangalore and Kashmere is that at Bangalore there is a considerable hardening of the radiation. This is clearly seen in Fig. 4 showing the variation of the intensity with altitude, where the Bangalore values are also plotted. Probably the hardening is due to the latitude effect, but some of it might be attributed to causes connected with the different experimental environment at Bangalore. This hardening if confirmed by subsequent more accurate experiments would throw light on interesting questions regarding the origin of the meson component; but it would be too premature to draw any conclusions at present. Another point of interest in the altitude intensity curves is the tendency of the meson intensity curves to become flat with increasing altitude. Here too, little weight can be attached on account of the fact that there are

only three points from which the shape of the curve can be judged. However, all these questions indicate the necessity of performing the experiment with greater accuracy and under more rigorous conditions at various altitudes and at different latitudes. This will be shortly undertaken.

It is a pleasure to acknowledge the support and assistance of Prof. Sir C. V. Raman and helpful discussions with Prof. Bhabha. The Kashmere expedition would not have been possible but for the willing help given by the State Officials and friends, and in particular the Prime Minister Sir Haksar, The Governor Pandit Dar, Col. Sir R. N. Chopra, and Maj. Haddow. I am grateful to Mrinalini Sarabhai, Gira Sarabhai, Gautam Sarabhai, Pandit Tikkalal, Dr. Dayal Singh and B. V. A. Iyer who helped during the expedition at Kashmere.

### 5. Summary

A new method of measuring the meson intensity by registering shower anti-coincidences is described. Its special merit lies in bringing for the first time under the field of direct experimental measurements, the slow mesons which are usually cut out in experiments where lead absorbers are used to filter out the soft electron component. The preliminary results obtained with this arrangement at altitudes up to 13,900 ft. in Kashmere are reported. Absorption curves for the meson and the total intensity at various altitudes as well as the altitude intensity curves for the total and the meson component have been given. Improvements in the technique by using fourfold instead of twofold coincidences for measuring the vertical intensity, and the use of optimum thickness of lead for generating the maximum number of showers are suggested.

Some special points of interest which emerge from the altitude intensity curves for mesons have been pointed out, and the need for more accurate measurement is indicated to decide the issues.

### BIBLIOGRAPHY

1. Bhabha .. *Proc. Ind. Acad. Sci. (A)*, In print.
2. Blackett .. *P. R. S. (A)*, 1938, 165, 11.
3. Anderson and Neddermeyer *Phy. Rev.*, 1937, 51, 884; 1938, 54, 88.
4. Williams .. *P. R. S. (A)*, 1939, 172, 194.
5. Bostick .. *Phy. Rev.*, 1942, 61, 557.
6. Rossi and Griesen .. *Ibid.*, 1942, 61, 121.
7. Schien, Wollan and Groetzinger .. *Ibid.*, 1940, 58, 1027.
8. Auger .. *Ibid.*, 1942, 61, 684.
9. Greisen .. *Ibid.*, 1943, 63, 323.
10. Schein, Jesse and Wollan .. *Ibid.*, 1941, 59, 615.
11. Greisen and Neresen .. *Ibid.*, 1942, 62, 316.

# STUDY OF THE OPTICAL PROPERTIES OF GELS

## Part I. Thorium Molybdate Gels

BY MATA PRASAD AND S. GURUSWAMY

(*From the Chemical Laboratories, Royal Institute of Science, Bombay*)

Received August 17, 1943

TYNDALL<sup>1</sup> seems to have been the first to take note of the blue colour and the polarised character of the light scattered by gold sol. Lord Rayleigh<sup>2</sup> developed the theory of the scattering of light by colloidal solutions and his equation is of considerable importance for the study of colloidal particles. Mardles<sup>3</sup> has studied the changes with temperature of the Tyndall-number (*i.e.*, the ratio of the intensity of the light scattered by sols and gels to that of some standard) of sols and gels of cellulose acetate in benzyl alcohol during the reversible sol-gel transformation by visual photometry. His results show that the Tyndall-number depends on the mechanical treatment and the rate of gelation. Further it varies with temperature and the concentration of cellulose acetate. The Tyndall-number—temperature curves reveal the existence of a maximum which decreases with the rise of temperature.

Kraemer and co-workers<sup>4</sup> made a detailed quantitative study of the Tyndall intensity of gelatin solutions and found that the intensity of scattered light increased enormously within a narrow range of pH near the isolectric point. The influence of pH on the intensity of the light scattered by casein solutions has been studied by Holweda<sup>5</sup>.

Krishnamurthi<sup>6</sup> has measured the intensity and depolarisation of the scattered light during the sol-gel transition of agar-agar and gelatin, using unpolarised incident light. His results point to the existence of a maximum gelation temperature. Further he finds that there is practically no change in Tyndall-number with time at or above 40° C., but at or below 35° C., it increases with time until a constant value is reached, and that the particles in the gel state are bigger and/or greater than in the sol state. It has been remarked in his paper that the variations in the intensity of scattered light are due to changes in the particle size and number alone, while the changes in the depolarisation factors are due to changes in the shape of the particles. He has not made any calculations from the observed total intensity of scattering, the scattering due to anisotropy, size and number separately.

D. S. Subba Ramiah<sup>7</sup> and R. S. Krishnan<sup>8</sup> have shown that in order to obtain information regarding the size and shape of the particles in the colloidal state it is not sufficient to measure the intensity and depolarisation of the scattered light, using unpolarised light alone. They suggest that it is necessary to obtain the values of depolarisation factors for the light scattered transversely by a colloidal system with incident light unpolarised, ( $\rho_u$ ) vertically polarised ( $\rho_v$ ), and horizontally polarised ( $\rho_h$ ).

Accordingly D. S. Subba Ramiah<sup>7</sup> has measured the values of  $\rho_v$ ,  $\rho_h$ , and  $\rho_u$  for (1) sulphur suspensions in water, (2) castor oil emulsions in water, (3) arsenic sulphide sol in water, and (4) casein solutions in water, at various pH values, and has shown how the inter-comparison of the values of these three quantities furnishes more information regarding the size and anisotropy of shape and/or structure of the particles than the measurement of only one of the three quantities.

The application of the measurements of  $\rho_v$ ,  $\rho_h$  and  $\rho_u$  has been extended by K. Subba Ramiah<sup>9</sup> to the study of protein solutions. He has also studied the changes in intensity and  $\rho_v$ ,  $\rho_h$  and  $\rho_u$  during the setting of silicic acid, stearic acid and sodium stearate gels.<sup>10</sup> He finds that in the case of silicic acid gels (1) there is a continuous increase in the micellar size during gelation and this increase continues even after the gel has set, though at a small rate; (2) the micelles have almost complete spherical symmetry at a stage prior to gel-formation; and (3) in the case of rapidly setting systems the micelles show greater departure from sphericity. As judged from the high polarisation of the transversely scattered light when the electric vector of the incident polarised light is along the direction of propagation of the incident light, the particles in these gels have a large size even at the earliest stage of formation. This result makes the correlation of the scattering data obtained by him with the particle constants, in the course of gel-formation, very complicated.

Recently Prasad and Gogate<sup>11</sup> have investigated the opacity changes during the setting of inorganic gels by an improved apparatus designed by them. Desai and Guruswamy<sup>12</sup> have continued this investigation to more inorganic gels using Prasad and Gogate's apparatus. It has been pointed out by the above-mentioned authors that the changes in number, size, distribution, arrangement, etc., of the micelles of the gel, contribute to the observed changes in opacity. In the present investigation, the intensity and depolarisation factors ( $\rho_v$ ,  $\rho_h$  and  $\rho_u$ ) of the light scattered transversely by thorium molybdate gels have been studied and an attempt has been made to separate the scattering due to anisotropy and size.

### Experimental

#### 1. Intensity measurements

The intensity of light scattered transversely by the gel-forming mixture was studied by allowing the scattered light to fall on a photocell. The current from the photocell was amplified by a valve bridge circuit and measured by a suitably shunted Moll galvanometer. The circuit employed for amplification is essentially the same as that developed by Ananthakrishnan.<sup>13</sup> The principle of working consists in bringing the bridge to balance with the photocell in the dark. When light falls on the photocell, the photoelectric current flowing across the grid leak produces a small change in the grid potential of one valve and the balance is disturbed. The resultant current is a measure of the light falling on the photocell.

*Testing the linearity of the photocell unit.*—To test the linearity of the photocell unit the following method was employed. The photocell was completely covered with a black paper and a slit ( $8 \times 8$  mm.) was cut on the paper in front of the vane of the photocell. A Hefner's standard lamp was placed at different distances ( $d$ ) from the photocell and the corresponding deflections of the galvanometer ( $D$ ) were noted. Care was taken to place the lamp such that the slit on the photocell and the flame were in the horizontal plane and the rays falling on the photocell were normal to its surface. The results obtained are shown in Table I. The constant value of  $D \times d^2$  excepting at higher intensities shows that the response by the photocell unit is linear within the range of intensity of scattering investigated. Even the deviations from linearity at higher intensities are not great and a correction has been applied to the deflections obtained at these intensities from the  $D - 1/d^2$  graph.

TABLE I

Distance of the lamp from the photocell ( $d$ )	Deflections of the galvanometer ( $D$ )	$D \times d^2$
cm.		
100	4.3	$4.30 \times 10^4$
90	5.5	$4.45 \times 10^4$
80	6.9	$4.42 \times 10^4$
70	8.7	$4.26 \times 10^4$
60	12.0	$4.32 \times 10^4$
50	16.7	$4.17 \times 10^4$
40	23.6	$3.78 \times 10^4$

*The optical arrangement.*—Light from a pointolite lamp A (Fig. 1) was condensed on the gel-forming mixture contained in a rectangular glass cell C ( $4'' \times 2.5'' \times 0.9''$ ) by means of a long focal length lens L ( $f = 30$  cm.).

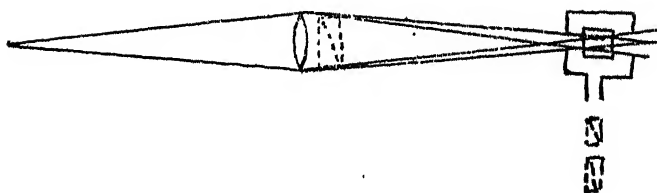


FIG. 1

The track of the beam of light in the glass cell was very nearly parallel in the neighbourhood of the focus, to which of course, the observations were confined.

Precautions were taken to reduce the effect of secondary scattering to a minimum by using as thin an incident beam as possible (a few mm.) and also by measuring the intensity of the scattered light near the place where the incident beam entered and without too long a passage through the scattering medium. In the present experiment the observation slit was  $7 \times 4$  mm., and it was 7 and 3 mm. away from the place where the incident beam entered the glass cell.

The glass cell C was kept in a hollow wooden box painted black with a groove cut for the glass cell C. The glass cell was painted black except for three openings two for the entry and exit of the incident beam of light and a third for the admission of the scattered light into the photocell. This latter aperture was rectangular ( $7 \times 4$  mm.) and was exactly opposite to the focus of the track in the gel-forming mixture. The wooden box with the glass cell was fixed in another big box, which was painted black inside. Light entered the second box through a slit in one of its sides.

The photocell unit was placed at a distance of 6 cm. from the centre of the focus of the incident beam. The divergent nature of the scattered light has been pointed out by Ananthakrishnan.<sup>13</sup> To eliminate errors due to this and to measure the intensity of scattering exactly at right angles to the incident track, a slit having the same width as the observation slit of the glass cell C was permanently fixed between the photocell and the scattering window.

When there was no glass cell in the wooden box, the galvanometer showed zero deflection with or without the incident light, showing thereby that the galvanometer deflections are exclusively due to the light scattered by the gel-forming mixture with time.

*Estimate of the absolute intensity of light scattered by gels.*—The intensity of scattered light has been expressed in arbitrary units, namely, in terms

of the deflections of the galvanometer in cm. A rough estimate of this arbitrary unit has been made. It has been found that 1 cm. of the galvanometer deflection is approximately equal to five times the intensity of scattering in benzene under the conditions of the experiment.

## 2. Depolarisation measurements

The depolarisation factor of the light scattered transversely by the gel-forming mixture was determined by the well-known Cornu's method. The experimental arrangement was as follows. The light from a carbon arc was condensed by a long focal length lens ( $f = 30$  cms.) on a rectangular glass cell ( $4'' \times 2.5'' \times 0.9''$ ) containing the gel-forming mixture. A mounted Nicol Prism served to get plane polarised light, polarised in any desired plane. The cell was painted black excepting for three slits, two for the incident light to pass through and a third for observation. Precautions were taken to eliminate parasitic light. The depolarisation factor is expressed as percentage and is  $= \tan^2 \theta \times 100$  where  $2\theta$  is the angle between the two positions of the Nicol for which there is equality of illumination. The aperture of the lens was reduced when  $\rho_u$  measurements were taken.

R. S. Krishnan<sup>14</sup> has pointed out that in emulsions and protein solutions in which the scattering is very intense, the secondary scattering has a marked influence on the depolarisation factors. The values of  $\rho_v$ ,  $\rho_h$  and  $\rho_u$  in general, are enhanced due to the presence of secondary scattering in solutions. He has also pointed out that the effect of secondary scattering could be eliminated by illuminating the colloidal solutions by means of a very narrow pencil of light and measuring the depolarisation factors by the Cornu's method. Although the scattering of the gels investigated, excepting in the initial stages, is not so intense as in emulsions and protein solutions, a pencil of light as thin as possible (a few mm.) was employed.

R. S. Krishnan has studied the dispersion of depolarisation as well as the extinction coefficient of a number of colloids for incident light of different wavelengths. In a series of papers entitled 'dispersion of depolarisation of light scattering in colloids'<sup>21</sup> he has shown the importance of making comparative studies of  $\rho_v$ ,  $\rho_h$  and  $\rho_u$  at different wavelengths. In the case of the gels studied in this investigation the size of the particles, as shown later, is less than the wavelength of light and hence the depolarisation of the light scattered transversely will not show any marked dependence upon the wavelength of the incident light. This has been of great advantage in the present measurements since white light could be used as the source, for which

the intensity of scattering is large and hence the accuracy of measurements is greater.

*Convergence error.*—There has been considerable divergence of views regarding the existence of this error. The convergence error is of very great importance only when we are dealing with depolarisation factors which are relatively small as are met with in gases (*cf.* Ananthakrishnan<sup>15</sup>).

### 3. Preparation of gels

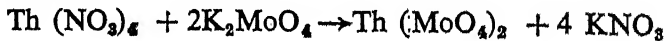
Thorium molybdate gels were prepared by the method of Prakash and Dhar,<sup>16</sup> and the following solutions were employed:—(1) 6% solution of thorium nitrate  $\text{Th}(\text{NO}_3)_4 \cdot 4\text{H}_2\text{O}$ . (A); (2) 10% solution of potassium molybdate (B). It was found that if the two solutions were mixed a precipitate is obtained which disappears in a few seconds and results in an opaque mixture which clears up during setting and after some time sets to a nearly transparent gel.

In order to prepare the gels different volumes of (A) and (B) were taken in two different test-tubes and the volume in each of the test-tubes was made to 25 c.c. by the addition of distilled water; thus the total volume of the gel-forming mixture was 50 c.c. The two solutions were mixed and the changes in the intensity and depolarisation factors with time were measured.

The course of gelation is greatly modified by the presence of non-electrolytes (*cf.* Prasad, Mehta and Desai).<sup>17</sup> Hence the influence of the non-electrolytes on gelation was also investigated.

### 4. Results

The results obtained with gels prepared by mixing different amounts of A and B are shown in Tables II to VIII, in which T represents the time in minutes. The amount of thorium molybdate in the gel has been calculated from the equation:



and is given on the top of the tables. The amount of thorium nitrate remaining unreacted is shown as excess of thorium nitrate in the tables.

TABLE II

A = 25 c.c. = 1·21 g. of thorium nitrate

B = 5 c.c. = 0·5 g. of potassium molybdate

The amount of thorium molybdate formed = 0·58 g.

The excess of thorium nitrate present = 0·71 g.

T	Observations	$\rho_v$	$\rho_h$	$\rho_u$	I in cm.
1	An opaque sol. The scattered light is red in colour ..	..	..	..	26·5
2		..	..	..	25·0
3	Opacity decreases ..	84·0	..	84·0	23·5
4		..	..	..	22·0
5		..	89	..	17·2
6	Scattered light is white in colour ..	76·0	..	..	12·4
7		..	..	78·0	9·5
8		66·0	..	..	7·3
10		32·0	73	63·0	6·4
12		..	..	..	6·0
15	Viscous ..	28·3	..	52·8	5·9
20	Nearly set ..	25·9	67	52·8	5·9
30	Set to a gel ..	25·9	67	52·8	5·9

TABLE III

A = 25 c.c. = 1·21 g. of thorium nitrate

B = 4 c.c. = 0·4 g. of potassium molybdate

The amount of thorium molybdate formed = 0·52 g.

The excess of thorium nitrate present = 0·76 g.

T	Observations	$\rho_v$	$\rho_h$	$\rho_u$	I in cm.
1		..	..	..	21·5
2	An opaque sol ..	74·0	..	..	18·9
3		..	..	..	15·6
4		..	..	73·0	9·8
5		..	89	..	4·8
6		..	..	..	3·6
7		33·3	..	49·0	3·4
8		..	..	..	3·2
10		18·9	78	33·3	2·9
15		12·6	..	..	2·8
20		..	..	29·5	2·7
30	Very viscous ..	11·9	..	29·5	2·6
45	Set to a gel ..	11·9	78	29·5	2·6

TABLE IV

A = 25 c.c. = 1.21 g. of thorium nitrate

B = 3 c.c. = 0.3 g. of potassium molybdate

The amount of thorium molybdate formed = 0.35 g.

The excess of thorium nitrate present = 0.91 g.

T	Observations	$\rho_v$	$\rho_h$	$\rho_u$	I in cm.
1	Opaque sol .. ..	..	..	..	17.3
2		..	..	..	14.4
3		66.0	..	..	7.4
4		..	..	30.7	2.9
5		23.8	90	..	2.2
6		..	..	18.0	2.0
8		10.6	..	..	1.9
10		8.2	..	16.3	1.8
15		7.2	80	14.7	1.8
40		7.2	80	14.0	1.8
90	Set to a gel .. ..	7.2	70	14.0	1.8

TABLE V

A = 20 c.c. = 0.91 g. of thorium nitrate

B = 3 c.c. = 0.3 g. of potassium molybdate

The amount of thorium molybdate formed = 0.35 g.

The excess of thorium nitrate present = 0.61 g.

T	Observations	$\rho_v$	$\rho_h$	$\rho_u$	I in cm.
1	An opaque sol .. ..	..	..	..	17.7
2		..	..	..	15.5
3		68.0	..	..	14.5
4		..	..	..	13.0
5		61.0	87	..	10.8
6		..	..	..	7.0
7		40.6	..	76.0	3.3
8		..	..	..	2.0
10		19.6	79	49.0	1.8
15		..	..	..	1.8
20	Viscous .. ..	10.6	..	20.8	1.8
90	The gel sets in about three hours .. ..	9.9	..	20.8	1.8
		9.9	67	20.8	1.8
		..	67..	20.8	1.8

TABLE VI

A = 25 c.c. = 1·21 g. of thorium nitrate	
B = 5 c.c. = 0·5 g. of potassium molybdate	
HCl (1N) = 1·0 c.c.	
The amount of thorium molybdate formed (assuming that HCl exercises no solvent action)	= 0·58 g.
The excess of thorium nitrate present	= 0·71 g.

T	Observations	$\rho_v$	$\rho_h$	$\rho_u$	I in cm.
1	An opaque sol . . .	..	..	..	17·4
2		..	..	..	9·9
3	Opacity decreases . .	51·0	..	68·0	6·7
4		30·7	..	58·9	5·6
5		..	85	..	5·2
6		23·8	..	49·0	4·7
8		..	..	..	4·4
10		20·8	..	45·5	4·2
15	Set to a gel . . .	19·8	..	40·6	4·0
20		19·8	..	37·6	3·5
30		19·8	70	37·6	3·5

TABLE VII

A = 25 c.c. = 1·21 g. of thorium nitrate	
B = 5 c.c. = 0·5 g. of potassium molybdate	
HCl (1 N) = 3·0 c.c.	
The amount of thorium molybdate formed (assuming that HCl exercises no solvent action)	= 0·58 g.
The excess of thorium nitrate present	= 0·71 g.

T	Observations	$\rho_v$	$\rho_h$	$\rho_u$	I in cm.
1	An opaque sol. The opacity decreases rapidly . . .	..	..	..	1·7
3		23·8	..	45·5	0·9
5		12·5	85	30·7	0·8
7	Set to a gel . . .	9·9	..	23·8	..
10		9·3	..	21·8	..
15		9·3	..	20·8	0·7
30		9·3	78	20·8	0·7

TABLE VIII

A = 25 c.c. = 1.21 g. of thorium nitrate

B = 3 c.c. = 0.3 g. of potassium molybdate

Ethyl alcohol = 10.0 c.c.

The amount of thorium molybdate formed = 0.35 g.

The excess of thorium nitrate present = 0.91 g.

T	Observations	$\rho_v$	$\rho_h$	$\rho_u$	I in cm.
1	Opaque sol	..	..	..	14.8
2	Opacity decreases ..	..	..	..	13.0
3		51.0	..	49.0	10.2
4		..	..	..	6.6
5		18.9	89	29.5	3.7
7		..	..	..	2.4
8		13.3	..	13.3	1.9
10		12.5	..	11.2	1.5
20	The sol is viscous ..	11.9	..	9.9	1.4
45	Nearly set	..	11.9	70	9.9
90	Set to a gel	..	11.9	..	9.9

*Discussion of the Results**1. Changes of the intensity and the depolarisation factors during setting*

It will be seen from Tables II to VIII that the values of  $\rho_v$  are very high and they decrease during setting and then reach a constant value ; in some cases these values are very small (*cf.* Table IV). Any deviation from zero value of  $\rho_v$  shows that the particles are anisotropic. Since the values of  $\rho_v$  are very high it shows that the particles are highly anisotropic in shape or/and structure. During gel-formation the anisotropy in shape or/and structure decreases and the gel becomes less and less anisotropic.

The values of  $\rho_h$  are also very high. They decrease during gelation and reach a constant value when the gel sets. The high value of  $\rho_h$  indicates that the particles are not very large in comparison with the wavelength of light and a decrease in its value shows that the particles grow in size during gel-formation. Since the values of  $\rho_h$  are very high they could not be accurately determined by Cornu's method.

The values of  $\rho_u$  also decrease during the formation of gels.  $\rho_u$  is related to  $\rho_v$  and  $\rho_h$  by the relation  $\rho_u = (1 + \frac{1}{\rho_h}) / (1 + \frac{1}{\rho_v})$ . (R. S. Krishnan.<sup>8</sup>)

The decrease in the value of  $\rho_u$  is due to the decrease in the value of  $\rho_v$ .

The intensity of scattered light decreases rapidly during gel-formation, and reaches a constant value after some time. It is interesting to note that

the values of I and the depolarisation factors reach a constant value much before the gels set. For example, in the case of the gel prepared by mixing 20 c.c. of thorium nitrate and 3 c.c. of potassium molybdate (Table V) the values of I and depolarisation factors reach a constant value in about 20 minutes, whereas the gel sets in about three hours.

*2. The effect of different constituents of the gel-forming mixture on the rate of change of intensity and on the values of  $\rho_v$*

The effect of thorium nitrate on the formation of the gel can be seen from Tables II, III and IV. Increasing amounts of thorium nitrate increase the rate of change of the intensity of scattering and make the gel more transparent and less anisotropic. The time of setting is also increased by the addition of increasing amounts of thorium nitrate to the gel-forming mixture. Increasing amounts of HCl make the gel more transparent and less anisotropic, cause it to set earlier, and increase the rate of change of intensity of scattered light (Tables II, VI and VII). The gel formed in the presence of ethyl alcohol is more transparent and anisotropic (*cf.* Tables IV and VIII).

*3. Size of the particles*

The very high values of  $\rho_v$  in the initial stages of gel-formation suggest that at this stage the particles are highly anisotropic. Therefore an attempt was made to separate the density and orientation scatterings and to study their changes during gel-formation. In order to do that it is essential to get an idea of the magnitude of the size of the gel-particles.

The high values of  $\rho_v$  indicate that the particles are not very large compared to the wavelength of light. An approximate idea of the magnitude of the size of the particles was obtained by comparing the scatterings in the forward and backward directions. The intensity of light scattered at  $45^\circ$  and  $135^\circ$  to the incident beam by the least anisotropic thorium molybdate gel (*cf.* Table IV,  $\rho_v = 7.2$ ) was compared. The following apparatus was employed for this purpose. The gel was prepared in a cylinder of diameter 2.5 cm. A thin beam of light was admitted through the centre of the cylinder. The whole cylinder was blackened excepting for 4 slits, two for the incident light to pass through, one at  $45^\circ$  and another  $135^\circ$  to the track of light. The slits at  $45^\circ$  and  $135^\circ$  were equal in area ( $8 \times 4$  mm.). The cylinder was kept in a small rectangular tank containing water to avoid errors due to the spherical nature of the cylinder. The tank was suitably blackened so that the track at  $45^\circ$  and  $135^\circ$  could be clearly observed without parasitic light. There was not much deviation of the track. The other experimental details were the same as those employed for the measurement

of the intensity of light scattered transversely. Visual measurements showed that there was no great difference in the intensity of the two scattered beams. A quantitative measurement of the intensity was then made by keeping the photocell unit at equal distances from the two slits. All parasitic lights were cut off by suitable screening. A number of readings were taken and it was found that the ratio of the intensities of scattering at  $135^\circ$  and at  $45^\circ$  was not greater than 1.5.

If the scattering particles are very small compared with the wavelength of light, the scattered energy is distributed symmetrically around the scattering particle, and it is represented by Rayleigh's formula. Shoulejkin<sup>18</sup> has calculated the intensity of scattered light for particles of size comparable with the wavelength of light and his results show that if the diameter of the particle exceeds  $1/3 \lambda$ , the distribution of the scattered light is no longer symmetrical. At  $2\rho \approx \lambda/3$ , one notices a definite asymmetry of scattering, the brightness of the scattered light in the direction of the incident rays being 2.5 times greater than in the opposite direction (the relative value of  $m'$ , that is, relative refractive index of the particles to that of the medium, used for calculation was 1.32).

Blumer<sup>19</sup> has studied theoretically the intensity of scattered light at different angles to the incident light, by particles of different sizes having different relative refractive indices. In the following table (Table IX) is given the intensities of scattered light ( $i_1 + i_2$ ) at  $45^\circ$  and  $135^\circ$  by particles of different sizes. These values have been taken from his paper,<sup>19</sup> for the relative refractive index of the particles and the medium equal to 1.25, which probably corresponds to the case of gels under investigation. The values of  $I_{135}/I_{45}$  are given in the last column of Table IX.

TABLE IX

$\alpha = \frac{2\pi p}{\lambda}$	$(i_1 + i_2)$ for $45^\circ$ ( $I_1$ )	$(i_1 + i_2)$ for $135^\circ$ ( $I_2$ )	$I_2/I_1$
0.01	$.3769 \times 10^{-13}$	$.3769 \times 10^{-13}$	1.00
0.1	$.3730 \times 10^{-7}$	$.3749 \times 10^{-7}$	1.00
0.2	$.2400 \times 10^{-5}$	$.2400 \times 10^{-5}$	1.00
0.3	$.2727 \times 10^{-4}$	$.2727 \times 10^{-4}$	1.00
0.5	$.6460 \times 10^{-3}$	$.9010 \times 10^{-3}$	1.39
0.6	$.1900 \times 10^{-2}$	$.2704 \times 10^{-2}$	1.42
1.0	.022	.1177	5.10
1.2	.0373	.2763	7.4
2.0	.0100	1.9874	198.00

It will be seen from the above table that the value of the intensity at  $135^\circ$ /the intensity at  $45^\circ$  is one for the particles whose value of  $\alpha$  does not

exceed  $0 \cdot 3$ , that is, the diameter of the particles is not greater than about  $\cdot 3/\pi\lambda = 0 \cdot 1\lambda$ . If the diameter of the particles is greater than this, a definite asymmetry of scattering sets in, and  $I_{135}$  becomes many times greater than  $I_{45}$ . The values of  $I_{135}/I_{45}$  obtained in this experiment was not greater than  $1 \cdot 5$ . It has to be remembered that no special precautions were taken to remove dust particles, etc., from the different solutions used and so this may contribute to more backward scattering. Even if the value of  $I_{135}/I_{45}$  for this gel is taken as  $1 \cdot 5$ , it can be seen from Table IX that the diameter of the particles is much less than  $\cdot 8/\pi\lambda$ , that is, about  $\frac{1}{4}\lambda$ . The gel particles are highly hydrated and therefore the actual size of the particles may be greater than  $\frac{1}{4}\lambda$ . But this increase in size cannot be determined by the above method as hydration cannot produce any direct change in the intensity of scattered light because there is no difference in refractive index between the water that is attached to the micelles and the "free" water.

Thus it will appear both from the values of  $\rho_h$  and from the comparison of intensities in the backward and forward directions that the size of the particles even after the gel has set is less than the wavelength of light.

Another evidence for the smallness of the size of the particles is obtained from the microscopic examination of the gel. The smallest particles that can be seen through a microscope<sup>22</sup> at its best magnification have a diameter of about  $1/2000$  mm. or  $5000 \times 10^{-8}$  cm. Since the microscopic examination does not reveal the identity of individual gel particles, this can be taken as a further evidence to show that the diameter of the gel particles is less than the wavelength of light.

For the purpose of discussion of results it has been presumed that all the gel particles are of the same size and shape.

#### 4. Separation of the density scattering and orientation scattering

The total intensity of light scattered by a transparent "homogeneous" medium consisting of optically anisotropic particles whose linear dimensions are small in comparison with the wavelength of light is the sum of two types of scattering, namely, (i) density scattering  $I_D$  and (ii) Orientation or anisotropy scattering  $I_A$ .

The density scattering  $I_D$  is due to local inhomogeneities that are produced in the medium by the thermal agitation of the particles in it. It will be greater, the larger the compressibility of the medium and can therefore assume very large values in the neighbourhood of the critical temperature where the compressibility becomes very large.

The anisotropy or orientation scattering  $I_A$  arises from the fact that the moment induced by the incident electric vector in an anisotropic particle is not in general parallel to the direction of the electric vector. Detailed calculations have been made by Cabannes<sup>20</sup> and Ramanathan<sup>21</sup> on the intensity of scattering due to orientation of anisotropic particles in homogeneous transparent media and they find that the effect of fluctuations in orientation would be to increase the total scattering to  $\frac{6 + 6\rho}{6 - 7\rho}$  times the density scattering alone. In this expression  $\rho$  denotes the ratio of the weak component to the strong component in the partially polarized light that would be scattered in a direction transverse to the direction of propagation of the incident light in the medium, the incident light being unpolarised.

The foregoing discussions refer to a stationary medium at constant temperature. In the case of gels the number, size and shape of the particles vary with time during the process of gel-formation. Therefore a detailed study of the orientation and density scattering at various stages of gel-formation will enable one to follow closely the progressive changes in the number, size and shape of the particles.

From the measurement of the total intensity and depolarisation factor of the scattered light using unpolarised incident light, the component of scattering due to fluctuations in density and that due to fluctuations in the orientation of the scattering particles can be separately calculated as follows:

Let  $I$  be the total scattering observed. It is equal to  $I_D + I_A$  where  $I_D$  is given by the relation  $I_D = I / \frac{6 + 6\rho}{6 - 7\rho}$  or  $I \times \frac{6 - 7\rho}{6 + 6\rho}$ .

$$\text{Hence, } I_A = I - \left( I \times \frac{6 - 7\rho}{6 + 6\rho} \right) = I \times \frac{13\rho}{6 + 6\rho}.$$

The changes in the orientation scattering indicate the changes in the shape and structure of the particles taking place during gelation.

The density scattering is directly proportional to the number of particles and the square of the volume of the particles, provided the size of the particles is less than the wavelength of light (Rayleigh<sup>2</sup>). Under standard and fixed conditions  $I_D$  is given by

$$I_D = K N V^2 \dots \dots \dots (i) \text{ where all the constants are included in } K.$$

If  $C$  is the amount of matter in the colloidal state, then  $C = N V \sigma$  where  $\sigma$  is the density of the substance in the colloidal state and is a constant.

Eliminating  $N$  between the two equations, we obtain

$$I_D = K C V / \sigma \dots \dots \dots (ii)$$

Therefore if the changes in  $I_D$  are measured in the case of a system undergoing gelation, they would represent the changes in the volume of the individual particles taking place during this process, provided the condition regarding the size of the particles in the Rayleigh's equation is satisfied by the system at all stages of gel-formation. It has been established already that the size of the particles even after the gel has set, is less than the wavelength of light.

On eliminating  $V$  between the first two equations we obtain:

$$I_D = C^2 K / N \sigma^2 \dots \dots \quad (iii)$$

Therefore the reciprocal of the changes in the value of  $I_D$  during gelation would represent the changes in the number of the scattering particles taking place during gel-formation.

The values of  $I_D$  were calculated in the case of a gel system containing  $A = 25$  and  $B = 5.0$  (cf. Table II). This choice was made because, in this case, the rate of change of  $I$  with time is the slowest. This would avoid any errors creeping in on account of the rapid changes of  $I$  with time. Further for the sake of accuracy the values of  $I$  and  $\frac{6 + 6\rho}{6 - 7\rho}$  have not been taken from the data in Table II but from the smoothed curve drawn between  $I$  and  $\frac{6 + 6\rho}{6 - 7\rho}$  against time; the values of these factors are given in Table X. The calculated values of  $I_D = I \times \frac{6 - 7\rho}{6 + 6\rho}$  and  $I_A = I \times \frac{13\rho}{6 + 6\rho}$  are shown in columns 4 and 5 of Table X.

TABLE X

Time in minutes	$\frac{6 + 6\rho}{6 - 7\rho}$	$I$ in cm.	Density scattering $I_D$	Anisotropy scattering $I_A$	Volume of the particles in relation to the volume after gelation
3	92.0	23.5	0.26	23.2	0.18
4	50.0	22.0	0.44	21.6	0.30
5	32.0	17.2	0.54	16.7	0.37
7	13.7	9.5	0.69	8.8	0.47
10	6.2	6.4	1.03	5.4	0.70
12	5.0	6.0	1.20	4.8	0.81
15	4.0	5.9	1.48	4.4	1.00
20	4.0	5.9	1.48	4.4	1.00

(a) *Changes in the anisotropy scattering during gelation.*—It will be seen from Table X that in the early stages of gel-formation  $I_A$  predominates over

$I_D$ . The anisotropy scattering decreases rapidly during gelation and it is this scattering that decides the final observed changes of the total intensity of scattering which also decreases during gel-formation.

(b) *Changes in the density scattering during gelation.*—It is very interesting to note that although the total scattering decreases during gelation, the density scattering  $I_D$  increases during gel-formation. The increase of  $I_D$  during gelation points out that an increase in volume and a decrease in the number of particles take place during gel-formation. This is analogous to coagulation. Hence this gives an independent evidence to support the view that gelation is a special type of coagulation.

(c) *Changes in the volume of the individual particles during gel-formation.*—If  $I_f$  is the density scattering at the final stage of gelation and  $I_D$  at any other stage, then from equation (ii)  $I_D/I_f = V/V_f$ , where  $V$  and  $V_f$  are the corresponding volumes at the two stages. If  $V_f$  is assumed to be unity then  $V = I_D/I_f$ .

These values of  $V$  at different stages of gelation have been calculated in the case of gels corresponding to Table II and the data obtained are shown in the last column of Table X. It will be seen that the volume of the individual particles increases during gelation and reaches a constant value when the gel is set. The volume of the particles in the gel state is about six times of that at the commencement of the gelation process.

(d) *Comparative volume of the gel particles, in gels under different conditions of formation.*—An attempt has been made to compare the final volume of the gel particles, in the gels formed under different conditions. The results are shown in Table XI. The third column gives the concentration of the gel (the amount of thorium molybdate per litre) corresponding

TABLE XI

Gel corresponding to table No.	Amount of thorium molybdate formed	Concentration of thorium molybdate	Final values of $I_D$	Relative volume of the particles	The amount of excess of thorium nitrate
II	0.58	11.6	1.48	1.00	0.71
III	0.52	10.4	1.32	1.00	0.76
IV	0.35	7.0	1.32	1.48	0.91
V	0.35	7.0	1.13	1.26	0.61

to table numbers given in column 1 of Table XI. The final values of the density scattering which is proportional to CV is shown in column 4.

The numbers in column 5 is a measure of the comparative volume of the particles obtained by dividing the numbers in column 4 by the concentration of thorium molybdate expressed in grams per litre and expressing these values relative to the volume of the particles of the gel corresponding to Table II. In the last column is given the excess of thorium nitrate, etc., present which may exert an influence on the volume of the particles.

The results show that there are only little changes in the final volumes of the particles in the gels formed under different conditions. The relation between size and the excess of thorium nitrate present are not marked, due probably to other factors like the amount of potassium nitrate, etc., present in the gel-forming system.

(e) *The mechanism of the formation of the gel.*—From the results obtained the following can be inferred regarding the process of the formation of thorium molybdate gel. When thorium nitrate and potassium molybdate solutions are mixed, a precipitate of thorium molybdate is formed which is peptised in a few seconds by thorium nitrate (an excess of thorium nitrate is always necessary for gel-formation in this case) to a highly anisotropic (high  $\rho_v$ ) opaque thorium molybdate sol. This opaque sol can be prepared if necessary by diluting the product obtained by mixing the two solutions. The high value of  $\rho_v$  and  $\rho_u$  may be due to the high anisotropy in shape or/and structure of the sol particles. The sol then gets coagulated and so there is an increase in the volume and a decrease in the number of scattering particles during gel-formation. The volume of the coagulated particles is less than the wavelength of light. During gelation the anisotropy scattering decreases and this is due to the decrease in shape or/and structure of the particles taking place during the formation of the gel. The gel is not set when the coagulation is complete, that is, when the values of I become constant. The coagulum now takes up plenty of water and the gel particles become heavily hydrated. This process does not produce any change in the intensity of scattered light for reasons explained before. Probably at this stage great changes in viscosity take place and after a time the whole system sets to a gel.

### 5. *Applicability of the relation* $\rho_u = \left(1 + \frac{1}{\rho_h}\right) / \left(1 + \frac{1}{\rho_v}\right)$

The applicability of the relation connecting  $\rho_v$ ,  $\rho_h$  and  $\rho_u$  theoretically deduced by R. S. Krishnan<sup>8</sup> has been examined in the case of the gels studied in this investigation by comparing the observed values of  $\rho_u$  with those calculated from the above relation using the final values of  $\rho_v$  and  $\rho_h$ , that is, the values at the completion of the gelation process. The results are given in Table XII.

TABLE XII

Gel corresponding to table No.	Final observed values of			
	$\rho_h$	$\rho_v$	$\rho_u$ (obs.)	$\rho_u$ (cal.)
II	67	25.9	52.8	51.2
III	78	11.9	29.5	24.3
IV	70	7.2	14.0	16.3
V	67	9.9	20.8	22.5
VI	70	19.8	37.6	40.1
VII	78	9.3	20.8	19.4

Considering the difficulties in the accurate determination of the high values of  $\rho_h$  by Cornu's method, it can be inferred that Krishnan's relation holds good for the gel investigated.

#### Summary and Conclusions

The changes in the intensity and depolarisation factors of the light transversely scattered by thorium molybdate gels have been investigated. The intensity of scattered light has been measured by a photoelectric arrangement with an amplifying unit. The depolarisation factors ( $\rho_v$ ,  $\rho_h$  and  $\rho_u$ ) have been measured by the well-known Cornu's method using a double image prism and Nicol.

It has been shown from the measurements of  $\rho_h$  and a comparison of the backward and forward scatterings that the size of the particles even after the gel has set is smaller than the wavelength of light. An approximate estimate of the size of the particles of thorium molybdate gels has been made by comparing the light scattered at  $45^\circ$  and  $135^\circ$  to the direction of the incident light. It has been shown that the size of the particles is about  $\frac{1}{4} \lambda$ . It has been pointed out that hydration produces no change in scattering and so the actual size of the gel particles may be greater than  $\frac{1}{4} \lambda$ .

Since the size of the particles is smaller than the wavelength of light, the density scattering  $I_D$  and the anisotropy scattering  $I_A$  have been separately calculated from the total intensity of scattering and their changes during gelation studied. It has been found that the density scattering increases during gel-formation. This increase is due to an increase in the volume and a decrease in the number of particles during gel-formation. This is analogous to coagulation. It has therefore been inferred that gelation is a coagulation and hydration phenomenon.

The study of the anisotropy scattering has led to interesting results. In the early stages of gel-formation, the anisotropy scattering is very many times greater than the density scattering, in other words, it dominates over the

density scattering. The anisotropy scattering decreases rapidly during gelation and it is this scattering that decides the final observed changes in the intensity of scattered light. Thus the total intensity of scattered light decreases although the density scattering increases during the formation of the gel.

A comparison of the final volume of the gel particles of the same gel formed by mixing different amounts of the gel-forming constituents shows that there are no great changes in the final volumes of the gel particles in the gels formed under different conditions of gel-formation.

It has been found that the relation connecting  $\rho_y$ ,  $\rho_h$  and  $\rho_u$  theoretically deduced by R. S. Krishnan holds good for the gel investigated.

The process of formation and the effect of different constituents of the gel-forming mixture on the course of gel-formation have been discussed in detail.

One of the authors (S. G.) is grateful to Pioneer Magnesia Works for awarding him a scholarship during the progress of this work. Our best thanks are due to Dr. K. R. Ramanathan, M.A., D.Sc., for the loan of a double image prism and Nicol used in this investigation and to Mr. D. H. Marathe, I.E.E., Gr.I.E.E. (London), M.I.R.E., for his help in building the photoelectric unit.

#### REFERENCES

1. Tyndall .. *Phil. Mag.*, 1869, **37**, 384.
2. Lord Rayleigh .. *Ibid.*, 1899, **47**, 375.
3. Mardles .. *Trans. Farad. Soc.*, 1923, **18**, 318.
4. Kraemer and Fanselow .. *J. Phys. Chem.*, 1925, **29**, 1169.
- and Dexter .. *Ibid.*, 1927, **31**, 764.
5. Holweda .. *Rec. Trav. Chim.*, 1931, **50**, 601.
6. Krishnamurthi .. *Proc. Roy. Soc. (A)*, 1929, **122**, 77; 1930, **129**, 490.
7. D. S. Subba Ramiah .. *Proc. Ind. Acad. Sci.*, 1934, **1**, 709.
8. R. S. Krishnan .. *Ibid.*, 1934, **1**, 717 and 782.
9. K. Subba Ramiah .. *Ibid.*, 1937, **5**, 128.
10. .. *Ibid.*, 1937, **5**, 138; **6**, 499.
11. Prasad and Gogate .. *Ibid.*, 1943, **17**, 161.
12. Desai and Guruswamy .. *Ibid.*, 1943, **18**, 31.
13. Ananthakrishnan .. *Ibid.*, 1934, **1**, 201.
14. R. S. Krishnan .. *Ibid.*, 1939, **9**, 303.
15. Ananthakrishnan .. *Ibid.*, 1935, **2**, 133.
16. Prakash and Dhar .. *J. Indian Chem. Soc.*, 1929, **6**, 587.
17. Prasad, Mehta and Desai *J. Phys. Chem.*, 1932, **36**, 1324.
18. Shoulejkin .. *Phil. Mag.*, 1924, **48**, 307.
19. Cabannes .. *Ann. d. Phys.*, 1921, **5**, 15.
20. Ramanathan .. *Proc. Ind. Assn. Cultn. Sc.*, 1923, **8**, 1-22 and 181-98.
21. R. S. Krishnan .. *Proc. Ind. Aca. Sci.*, 1937, **5**, 94, 305, 407, 499 and 551.
22. Freundlich .. *The Elements of Colloid Chemistry*, p. 7.

# STUDY OF THE OPTICAL PROPERTIES OF GELS

## Part II. Thorium Arsenate Gels

BY MATA PRASAD AND S. GURUSWAMY

(From the Chemical Laboratories, Royal Institute of Science, Bombay)

Received August 17, 1943

IN a previous paper Prasad and Guruswamy<sup>1</sup> have investigated the changes in the intensity and depolarisation of the light transversely scattered by thorium molybdate gels during setting. In the present communication the intensity and depolarisation of the light transversely scattered by thorium arsenate gels during and after their formation have been studied. As in the case of thorium molybdate gels the density scattering and anisotropy scattering have been separately calculated from the total observed scattering and interpreted.

### Experimental

The gels were prepared by the method of Prasad and Desai<sup>2</sup> by mixing solutions of thorium nitrate and pyro-arsenic acid of suitable concentrations. The following solutions were employed for the preparation of the gels.

(A) *Thorium nitrate Th (NO<sub>3</sub>)<sub>4</sub>H<sub>2</sub>O 6% and (B) Pyro-arsenic acid 10%*. Different volumes of (A) diluted to 25 c.c. were taken in one test-tube and in another were taken different volumes of (B) together with HCl or alcohol diluted to 25 c.c. The two solutions were mixed and the values of the intensity of scattered light and depolarisation factors were measured during the process of gel-formation, by the arrangement as described in the previous paper. The results obtained with gels prepared with different amounts of (A) and (B) are given in Tables I to VII in which T represents time in minutes. The amount of thorium arsenate in the gel has been calculated from the equation:



and given on the top of the Tables. The amount of thorium nitrate remaining unreacted is shown as excess of thorium nitrate in the Tables.

<sup>1</sup> Proc. Ind. Acad. Sci., 1944, 19, 47.

<sup>2</sup> J. Univ. Bom., 1938, 7, 132.

TABLE I

 $A = 25 \text{ c.c.} = 1\cdot21 \text{ g. of thorium nitrate}$  $B = 5 \text{ c.c.} = 0\cdot5 \text{ g. of pyro-arsenic acid}$ 

The amount of thorium arsenate formed = 1·03 g.

The excess of pyro-arsenic acid present = 0·06 g.

T	Observations	$\rho_a$	$\rho_b$	$\rho_u$	I in cm.
1	Opaque viscous sol ..	..	..	11·0	1·4
2	Set to a gel ..	10·0	..	17·2	3·2
3	Opacity increases ..	13·2	..	23·6	4·2
4		17·5	..	29·5	4·8
5		19·8	89	33·0	5·0
6		..	..	35·5	5·2
8		23·0	..	40·0	5·4
10		..	81	43·8	5·5
12		26·5	..	47·2	5·7
15		28·3	70	49·1	5·8
20		30·7	70	49·1	5·8

TABLE II

 $A = 25 \text{ c.c.} = 1\cdot21 \text{ g. of thorium nitrate}$  $B = 3\cdot5 \text{ c.c.} = 0\cdot35 \text{ g. of pyro-arsenic acid}$ 

The amount of thorium arsenate formed = 0·83 g.

The excess of thorium nitrate present = 0·26 g.

T	Observations	$\rho_a$	$\rho_b$	$\rho_u$	I in cm.
1		..	..	12·8	0·5
2	Opacity increases ..	5·8	..	16·3	1·4
3		..	..	18·0	2·2
4		..	89	20·2	2·9
5	Viscous ..	10·5	..	21·8	3·3
6		..	..	24·5	3·5
8	Set to a gel ..	12·5	76	30·7	3·8
12		..	..	33·3	4·1
15		16·3	..	36·1	4·2
20		17·5	76	36·1	4·2

TABLE III

**A = 25 c.c. = 1·21 g. of thorium nitrate**

**B = 3 c.c. = 0·3 g. of pyro-arsenic acid**

The amount of thorium arsenate formed = 0·71 g.

The excess of thorium nitrate present = 0·40 g.

T	Observations	$\rho_v$	$\rho_h$	$\rho_u$	I in cm.
2		7·2	..	13·2	0·3
3		8·8	..	15·0	0·6
5		..	90	17·2	1·0
7		..	..	21·6	1·5
8	Viscous .. ..	11·9	..	23·8	1·8
10		..	..	27·0	2·1
12	Nearly set .. ..	13·2	..	29·5	2·4
15	Set to a gel .. ..	..	..	33·3	2·8
20		..	..	..	3·2
25	The gel is opaque and firm	14·7	81	38·0	3·3
30		14·7	81	38·0	3·4

TABLE IV

**A = 25 c.c. = 1·21 g. of thorium nitrate**

**B = 2·5 c.c. = 0·25 g. of pyro-arsenic acid.**

The amount of thorium arsenate formed = 0·59 g.

The excess of thorium nitrate present = 0·48 g.

T	Observations	$\rho_v$	$\rho_h$	$\rho_u$	I in cm.
2		..	..	7·0	0·1
5	Viscous .. ..	..	..	..	0·3
8	Opacity increases .. ..	..	..	9·0	0·5
15		5·8	..	10·6	1·0
20		7·2	85	11·5	1·6
25		9·9	..	12·5	2·3
30		12·5	..	14·0	2·8
35	Very viscous .. ..	13·2	..	16·3	3·1
40	Set to a gel .. ..	14·0	..	18·9	3·4
60		14·0	70	19·8	3·8

TABLE V

 $A = 20 \text{ c.c.} = 0.91 \text{ g. of thorium nitrate}$  $B = 3 \text{ c.c.} = 0.3 \text{ g. of pyro-arsenic acid}$ 

The amount of thorium arsenate formed = 0.71 g.

The excess of thorium nitrate present = 0.10 g.

T	Observations	$\rho_v$	$\rho_h$	$\rho_u$	I in cm.
2		..	..	4.5	0.3
5	Opacity increases ..	4.5	..	6.7	0.7
8		..	..	8.8	0.9
10		5.3	89	10.5	1.1
12	Very viscous ..	..	..	11.9	1.2
15	Nearly set ..	7.2	..	13.2	1.6
20	Set to a gel ..	9.3	..	14.0	2.0
25		10.5	..	14.7	2.4
30		10.5	..	15.5	2.8
40		10.5	75	15.5	3.0

TABLE VI

 $A = 25 \text{ c.c.} = 1.21 \text{ g. of thorium nitrate}$  $B = 5 \text{ c.c.} = 0.5 \text{ g. of pyro-arsenic acid}$  $HCl (1 N) = 2.0 \text{ c.c.}$ The amount of thorium arsenate formed (assuming  
that HCl exercises no solvent action) = 1.03 g.

The excess of pyro-arsenic acid present = 0.06 g.

T	Observations	$\rho_v$	$\rho_h$	$\rho_u$	I in cm.
1		..	..	..	0.3
2		..	..	7.0	0.8
3	Opacity increases ..	7.7	..	8.5	1.8
4		..	..	9.0	2.8
5		9.3	89	10.5	3.5
6		..	..	12.0	4.1
7		..	..	..	4.4
8	Viscous ..	11.9	..	13.5	4.7
10	Very viscous ..	..	..	18.0	5.0
12	Nearly set ..	14.7	..	..	5.2
15	Set to a gel ..	16.3	75	22.8	5.5
20		..	..	25.9	5.8
30		22.8	..	29.5	6.0
45		22.8	70	29.5	6.0

TABLE VII

 $A = 25 \text{ c.c.} = 1.21 \text{ g. of thorium nitrate}$  $B = 5 \text{ c.c.} = 0.5 \text{ g. of pyro-arsenic acid}$ 

Ethyl alcohol = 5.0 c.c.

The amount of thorium arsenate formed = 1.03 g.

The excess of pyro-arsenic acid present = 0.06 g.

T	Observations	$\rho_v$	$\rho_h$	$\rho_u$	I in cm.
1					0.5
2					0.8
3	Opacity increases ..	5.8	..	4.5	1.1
4		..	..		1.5
5	Viscous	7.9	87	9.3	2.2
6		..	..	..	2.7
7		..	..	..	3.2
8		11.9	..	..	3.6
10	Nearly set	..	..	14.7	4.7
12		19.8	..		5.6
15	Set to a gel	23.8	75	21.8	6.8
20		27.1	..	32.0	8.6
25		29.5		40.6	10.0
45		30.7	68	45.5	..

*Discussion of the Results*1. *Changes in the intensity and depolarisation of the scattered light during setting*

The changes in the values of I and depolarisation factors during the gelation of thorium arsenate gels are shown in Tables I to VII. The values of  $\rho_v$  increase during gelation. This is contrary to what happens in the case of thorium molybdate gels. The values of  $\rho_v$  are very small when the solutions are mixed showing that the particles in the initial stages are nearly spherical. An increase in the value of  $\rho_v$  shows that during gelation they become anisotropic in shape or/and structure.

$\rho_h$  as in the case of thorium molybdate gels has a very high value in the beginning and it decreases during gelation. This shows that the particles grow in size during gel-formation. Further the high value of  $\rho_h$  shows that the size of the particles is not very large in comparison with the wavelength of light.

The values of  $\rho_u$  increase during the formation of the gel. This is due to an increase in the value of  $\rho_v$  and a decrease in the value of  $\rho_h$ .

The intensity of scattered light also increases during gelation. As observed in the case of thorium molybdate gels, the final values of I and

depolarisation factors in gels formed by mixing different amounts of A and B are different.

Unlike thorium molybdate gels, the values of I,  $\rho_v$ ,  $\rho_h$  and  $\rho_u$  reach a constant value after or when the gel has set. In some cases, there are great changes in the values of I and depolarisation factors even after the gel has set. For example, the gel corresponding to Table I sets in about 2 minutes but large changes in the values of I and depolarisation factors continue to take place for about 20 mts.

## 2. *The effect of different constituents of the gel-forming mixture on the rate of change of intensity and on the values of $\rho_v$ .*

It will be seen from Tables II, III and IV that the time of setting is increased by the presence of increasing amounts of thorium nitrate in the gel-forming mixture. Further, the rate of change of intensity of scattered light is decreased and the gel becomes more transparent, as the amount of thorium nitrate in the gel is increased. Increasing amounts of HCl also increase the time of setting. The gel particles formed in the presence of HCl are less anisotropic (*cf.* Tables I and VI). The opacity of the gels formed in the presence and absence of HCl is nearly the same. Thus the action of HCl on the formation of this gel appears to be different from that on thorium molybdate gel. The gel formed in the presence of alcohol is very firm. The addition of alcohol to the gel-forming mixture increases the time of setting (*cf.* Tables I and VII). Further, such an addition increases the final values of I,  $\rho_v$  and  $\rho_u$ . The high final values of I,  $\rho_v$  and  $\rho_u$  may be due to the unavoidable appearance of tiny air bubbles formed probably on account of the evaporation of alcohol.

## 3. *The size of the particles*

The high value of  $\rho_h$  during and after gel formation indicates that the gel particles are not very large in comparison with the wavelength of light.

An approximate idea of the magnitude of the size of scattering particles in this gel has been obtained by comparing the intensity of scattered light in the directions  $45^\circ$  and  $135^\circ$  to the direction of the incident light, for the least anisotropic thorium arsenate gel (gel corresponding to Table V,  $\rho_v = 10.5$ ). The experimental arrangement employed for this purpose was the same as that used in the study of thorium molybdate gel. The results show that  $I_{135}/I_{45}$  is not greater than 1.5. So, the size of the particles even after the gel has set is not greater than  $\frac{1}{4}\lambda$  (*cf.* Prasad and Guruswamy, *loc. cit.*). The particles of the gel are highly hydrated and so their actual size may be greater than  $\frac{1}{4}\lambda$ . This increase could not be measured by this method as

hydration cannot produce any direct change in the intensity of scattered light.

#### 4. Separation of the density scattering and anisotropy scattering

The separation of the density and anisotropy scattering from the total scattering observed has been done for the gel setting in a long time (gel corresponding to Table IV) by the same method as employed in the case of thorium molybdate gel (Prasad and Guruswamy, *loc. cit.*). The results obtained are shown in Table VIII.

TABLE VIII

Time in minutes	$\frac{6 + 6\rho}{6 - 7\rho}$	I in cm.	Density scattering	Anisotropy scattering	Volume of the particles in relation to the final volume
2	1.17	0.1	0.09	0.01	0.04
5	1.20	0.3	0.25	0.05	0.10
8	1.22	0.5	0.41	0.09	0.17
10	1.23	0.6	0.49	0.11	0.20
15	1.26	1.0	0.79	0.21	0.32
20	1.29	1.6	1.24	0.36	0.51
25	1.32	2.3	1.74	0.56	0.71
30	1.36	2.8	2.06	0.74	0.84
35	1.44	3.1	2.15	0.95	0.88
40	1.53	3.4	2.22	1.18	0.91
60	1.56	3.8	2.44	1.36	1.00

The gel corresponding to Table I is very interesting. This gel is prepared by mixing 25 c.c. of thorium nitrate and 5 c.c. of pyro-arsenic acid diluted to 25 c.c. It sets in about 2 minutes and there are great changes in the values of I and depolarisation factors after it has set and these changes continue for about 20 minutes. Therefore, for this gel also the intensities of scattering due to density and anisotropy have been separately calculated and shown in Table IX.

TABLE IX

Time in minutes	$\frac{6 + 6\rho}{6 - 7\rho}$	I in cm.	Density scattering	Anisotropy Scattering
1	1.27	1.4	1.10	0.30
2	1.47	3.2	2.18	1.02
3	1.73	4.2	2.43	1.77
4	1.97	4.8	2.43	2.37
5	2.16	5.0	2.31	2.69
6	2.31	5.2	2.25	2.95
7	2.35	5.3	2.25	3.05
8	2.62	5.4	2.06	3.34
10	2.94	5.5	1.87	3.63
12	3.28	5.7	1.74	3.96
15	3.49	5.8	1.66	4.14
20	3.49	5.8	1.66	4.14

(a) *Variation of the anisotropy scattering during gelation.*—Unlike the case of thorium molybdate gel, the scattering due to anisotropy in this case increases during gel-formation. In the initial stages of gel-formation the anisotropy scattering is small compared with the density scattering. During the process of gel-formation it increases and at the final stage of gel-formation it contributes in comparable measure to the total observed scattering. This shows that the particles in the early stages of gel-formation are nearly spherical and they become more anisotropic in shape or/and structure as gelation proceeds.

The density scattering for the gel corresponding to Table I is fairly constant soon after it sets. Later on, it decreases steadily by a small amount. The anisotropic scattering for this gel is less than the density scattering in the beginning. Later on it increases enormously after the gel has set and becomes about 2·5 times the density scattering, when the total intensity reaches a constant value. The enormous changes in the total scattering taking place after the gel has set are therefore due to the changes in anisotropy of shape or/and structure of the particles.

(b) *Variation of the density scattering during gelation.*—As in the case of thorium molybdate gels, the density scattering increases during gel-formation (*cf.* Table VIII, column 4). This behaviour points out to an increase in the volume and a decrease in the number of particles taking place during gelation, thus showing that gelation is analogous to coagulation.

(c) *Changes in the volume of the individual particles during gelation.*—As in the case of thorium molybdate gels, the values of  $V = I_D/I_F$ , that is, the volume of the particles during gelation in relation to the final volume are calculated and shown in the last column of Table VIII. It will be seen that the volume of the particles increases during gelation and reaches a constant value when the gel is set. The volume of the particles in the gel state is about 25 times of that at the commencement of gel-formation.

(d) *Comparison of the final volume of the gel particles.*—The comparative volumes of the particles in gels formed by mixing different amounts of (A) and (B) are shown in column 5, Table X. These data have been obtained by dividing the final values of the density scattering  $I_D$  by the concentration of thorium arsenate in grams per litre (column 3, Table X) and expressing these values relative to the volume of the particles of the gel corresponding to Table III.

TABLE X

Gel corresponding to Table No.	Amount of thorium arsenate formed	Concentration of thorium arsenate	Final value of density scattering	Relative volumes of the gel particles	Excess of thorium nitrate
II	g. 0.83	16.6	1.79	1.11	g. 0.26
III	0.71	14.2	1.37	1.00	0.40
IV	0.59	11.8	2.44	2.14	0.48
V	0.71	14.2	2.11	1.55	0.10

It will be seen from the above table that the final volumes of the particles in the gel state change with a change in the values of (A) and (B), but the changes are not very great. The excess of thorium nitrate present which may contribute to changes in the volume of the particles is given in the last column of Table X. The effect of the presence of excess of thorium nitrate on the size is not very clear.

(e) *The mechanism of the formation of the gel.*—From the results obtained the following can be inferred as to the process of the formation of the gel. When the solutions of thorium nitrate and arsenic acid are mixed, a colloidal solution of thorium arsenate is immediately formed. The particles in the sol are nearly spherical (low value of  $\rho_s$ ). Later on, the sol gets coagulated; this is inferred from the increase in the size of the particles and a decrease in the number of particles during gelation. Unlike the behaviour of thorium molybdate gels, hydration also probably accompanies coagulation and the whole system sets to a gel by about the time taken for I and depolarisation factors to reach a constant value. The hydration of the particles cannot produce any change in the intensity of scattered light as there is no difference in refractive index between the water that is attached to the micelles and the "free" water. As the particles coagulate, they become more and more anisotropic (increase of anisotropic scattering during gelation). In this respect this gel is different from thorium molybdate, in which case, the anisotropy of the particles was found to decrease during gelation. From the above it can be seen that the time of setting is the time required for the coagulation of the sol of the gel-forming substance and the subsequent hydration of the gel particles. This time is increased by the presence of increasing amounts of thorium nitrate, HCl, and alcohol. This means that thorium nitrate, HCl and alcohol act as peptising agents hindering the coagulation and hydration.

5. Applicability of the relation  $\rho_u = \left(1 + \frac{1}{\rho_h}\right) / \left(1 + \frac{1}{\rho_0}\right)$

The applicability of the relation theoretically deduced by R. S. Krishnan<sup>3</sup> has been examined for this gel by comparing the observed values of  $\rho_u$  with those calculated from the final observed values of  $\rho_h$  and  $\rho_0$  obtained at the completion of the gelation process. The results are shown in Table XI.

TABLE XI

Gel corresponding to Table No.	Final observed values of			$\rho_u$ (cal.)
	$\rho_h$	$\rho_0$	$\rho_u$ (obs.)	
I	72	30.7	49.1	56.1
II	76	17.5	36.1	34.4
III	81	14.7	38.0	28.7
IV	70	14.0	19.8	30.1
V	75	10.5	15.5	22.2

Considering the difficulties in the accurate determination of the high values of  $\rho_h$  by Cornu's method it can be inferred that Krishnan's relation holds good for the gel investigated, though the agreement between the calculated and the observed values is not so good as in the case of thorium molybdate gels. This point is being separately investigated.

#### Summary and Conclusions

The changes in the intensity and depolarisation of the light transversely scattered by gel-forming mixtures of thorium arsenate gels during and after setting have been investigated. The intensity of scattered light has been measured by a photoelectric arrangement and the depolarisation factors by the well-known Cornu's method.

It has been shown from the measurements of the value of and a comparison of the backward and forward scatterings that the size of the gel particles is less than the wavelength of light. An approximate estimate of the size of the particles has been obtained by comparing the intensity of scattered light at  $45^\circ$  and  $135^\circ$  to the incident light. It has been shown that the size of the particles is about  $\frac{1}{4} \lambda$ . It has been pointed out that hydration produces no change in scattering and so the actual size of the particles may be greater than  $\frac{1}{4} \lambda$ .

Since the size of the particles is smaller than the wavelength of light the density scattering and anisotropy scattering have been separately calculated

<sup>3</sup> Proc. Ind. Acad. Sci., 1935, 1, 717, 782.

from the total observed scattering and their changes during gelation studied. It has been found that the density scattering increases during gel-formation, showing thereby that gelation is analogous to coagulation.

Further, it has been found that the anisotropy scattering increases during gel-formation and it is smaller than the density scattering. In one case of thorium arsenate gel, the intensity of scattered light and the values of  $\rho_u$  and  $\rho_v$  increase enormously even after the gel has set. In this case also the density and the anisotropy scatterings have been separated. The results show that there are great changes in the anisotropy scattering after the gel has set and it is this scattering that contributes to the changes in the total intensity of scattered light taking place after the gel has set.

The volume of the gel-particles at different intervals of time during gelation has been expressed in relation to the final volume of the particles. The results show that the particles increase by about 25 times during gel-formation.

A comparison of the final volume of the gel-particles of the same gel by mixing different amounts of the gel-forming constituents shows that there are no great changes in the final volume of the gel particles in the gels formed under different conditions of gel-formation.

The applicability of the relation  $\rho_u = \left(1 + \frac{1}{\rho_h}\right) / \left(1 + \frac{1}{\rho_v}\right)$  has been examined for this gel. It has been inferred by comparing the final observed and calculated values of  $\rho_u$  that the above-mentioned equation is applicable to this gel to a fair extent.

The process of formation and the effect of different constituents of the gel-forming mixture on the course of formation of the gel has been discussed in detail.

One of the authors (S.G.) is grateful to Pioneer Magnesia Works for awarding him a scholarship during the progress of this work. Our best thanks are due to Dr. K. R. Ramanathan, M.A., D.Sc., for the loan of a double-image prism and nicol used in this investigation and to Mr. D. H. Marathe, I.E.E., G.R.I.E.E. (London), M.I.R.E., for his help in building the photoelectric unit.

# STUDY OF THE OPTICAL PROPERTIES OF GELS

## Part III. Silicic Acid Gels

BY MATA PRASAD AND S. GURUSWAMY

(From the Chemical Laboratories, Royal Institute of Science, Bombay)

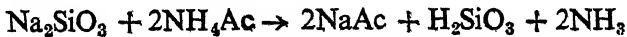
Received August 17, 1943

IN previous communications Prasad and Guruswamy<sup>1</sup> have studied the changes in the intensity and depolarization of the light scattered transversely by thorium molybdate and thorium arsenate gels during and after setting. The present communication deals with the study of the intensity and depolarization of light transversely scattered by silicic acid gels during and after their formation. The effects of the constituents of the gel-forming mixture and of the addition of HCl and ethyl alcohol on these factors have also been studied.

### Experimental

Silicic acid gel is the earliest known inorganic gel and this has been prepared by several workers usually by the action of acids, organic and inorganic, upon sodium silicate solutions. In the present investigation these gels were prepared by the method of Bhatnagar and Mathur<sup>2</sup> by mixing solutions of sodium silicate and ammonium acetate of suitable concentrations. The following solutions were used:

(A) Sodium silicate solution 6% and (B) Ammonium acetate 20%.—Different volumes of (A) diluted to 25 c.c. were taken in one test-tube. In another were taken different volumes of (B) together with HCl, alcohol, etc., diluted to 25 c.c. The two solutions were mixed and the intensity and depolarization factors were measured at different intervals of time during and after setting. The experimental arrangements were the same as that described in earlier publications. The results are given in Tables I to IX in which T represents time in minutes. The amount of silicic acid in the gel has been calculated from the equation:



and is given on the top of the tables. The amount of sodium silicate remaining unreacted is shown as excess of sodium silicate in the tables.

<sup>1</sup> Proc. Ind. Acad. Sci., 1944, 19, Parts I and II.

<sup>2</sup> Koll. Zeit., 1922, 30, 368.

TABLE I

A = 25 c.c. = 1.5 g. of sodium silicate

B = 5 c.c. = 1.0 g. of ammonium acetate

The amount of silicic acid formed = 0.51 g.

The excess of sodium silicate present = 0.71 g.

T	Observations	$\rho_v$	$\rho_h$	$\rho_u$	I in cm.
1					0.5
2	Opacity increases ..	2.5	81	2.2	1.1
3		..	..	..	2.1
4				2.8	3.1
5		3.4	76	3.8	4.1
6		..	..	5.8	4.6
7			..	..	5.2
8	Set to a gel ..	5.8	..	13.3	5.6
9					5.8
10		7.2	71	14.7	6.0
15			68	15.5	6.3
20		8.2	..	15.5	6.3

TABLE II

A = 25 c.c. = 1.5 g. of sodium silicate

B = 4.5 c.c. = 0.9 g. of ammonium acetate

The amount of silicic acid formed = 0.46 g.

The excess of sodium silicate present = 0.79 g.

T	Observations	$\rho_v$	$\rho_h$	$\rho_u$	I in cm.
1					0.2
2		2.0	..	3.1	0.8
3		..	..	..	1.1
4	Opacity increases ..	2.5	..	1.5	1.4
5		2.5	84	1.6	2.1
6	Viscosity increases ..	..	..	..	2.6
7		..	..	..	3.0
8				4.1	3.3
10		4.1	81	4.9	4.0
12					4.6
15	Set to a gel ..	6.2	76	9.3	5.3
20		7.7	..	11.9	5.9
25		8.3	..	13.3	6.1
35		8.4	70	15.5	6.2

TABLE III

 $A = 25 \text{ c.c.} = 1\cdot5 \text{ g. of sodium silicate}$  $B = 4 \text{ c.c.} = 0\cdot8 \text{ g. of ammonium acetate}$ The amount of silicic acid formed =  $0\cdot41 \text{ g.}$ The excess of sodium silicate present =  $0\cdot87 \text{ g.}$ 

T	Observations	$\rho_o$	$\rho_h$	$\rho_u$	I in cm.
3	Opacity increases ..	0·8	..	4·9	0·3
8		1·4	..	2·9	1·0
10		1·6	80	2·0	1·6
15		2·2	..	3·1	2·4
20	Viscous ..	3·5	..	4·1	3·0
25	Nearly set ..	4·9	70	5·3	3·6
30	Set to a gel ..	5·9	..	7·0	4·2
35		6·7	..	7·5	4·6
60		8·2	70	13·3	5·2

TABLE IV

 $A = 20 \text{ c.c.} = 1\cdot2 \text{ g. of sodium silicate}$  $B = 4 \text{ c.c.} = 0\cdot8 \text{ g. of ammonium acetate}$ The amount of silicic acid formed =  $0\cdot41 \text{ g.}$ The excess of sodium silicate present =  $0\cdot57 \text{ g.}$ 

T	Observations	$\rho_o$	$\rho_h$	$\rho_u$	I in cm.
1		..	..	..	0·6
2		..	..	..	0·9
5	Opacity increases ..	2·0	90	2·0	1·1
8		..	..	1·7	1·3
10		2·5	..	2·5	1·7
15		3·8	..	4·7	2·9
18		..	..	..	3·4
20		4·9	..	6·2	3·8
25	Nearly set ..	6·2	87	7·2	4·1
30	Set to a gel ..	..	..	8·2	4·5
45		..	..	..	4·9
60		8·2	..	12·5	4·9
180		8·3	78	14·7	..

TABLE V

 $A = 15 \text{ c.c.} = 0.9 \text{ g. of sodium silicate}$  $B = 4 \text{ c.c.} = 0.8 \text{ g. of ammonium acetate}$ 

The amount of silicic acid formed = 0.41 g.

The excess of sodium silicate present = 0.27 g.

T	Observations	$\rho_v$	$\rho_h$	$\rho_u$	I in cm.
2		..	..	..	0.6
3		..	..	..	0.9
5	Opacity increases ..	2.8	90	2.0	1.0
7		..	..	..	1.5
8		3.2	..	2.2	1.8
10		3.5	..	3.8	2.1
12		..	..	..	2.5
15	Viscous	4.5	..	5.8	3.3
18		..	..	..	3.6
20	Nearly set	5.8	75	7.7	3.8
30	Set to a gel	8.2	..	11.2	3.9
45		9.3	..	13.3	4.1
70		9.3	66	14.7	..

TABLE VI

 $A = 25 \text{ c.c.} = 1.5 \text{ g. of sodium silicate}$  $B = 4 \text{ c.c.} = 0.8 \text{ g. of ammonium acetate}$  $HCl (1 N) = 1.0 \text{ c.c.}$ 

The amount of silicic acid formed = 0.41 g.

The excess of sodium silicate present = 0.87 g.

T	Observations	$\rho_v$	$\rho_h$	$\rho_u$	I in cm.
2		2.0	..	2.6	1.0
3		..	..	..	1.2
5	Opacity increases ..	2.8	90	2.2	1.6
6		..	..	..	2.0
8	Viscous	3.4	..	3.4	2.9
10		4.5	..	4.1	3.6
12	Nearly set	5.3	..	4.9	4.0
15	Set to a gel	6.7	..	7.7	4.6
18		..	..	..	5.0
20		7.7	..	11.9	5.2
25		8.2	75	13.2	..
30		..	..	..	5.4
45		8.2	70	14.3	5.5

TABLE VII

A = 25 c.c. = 1.5 g. of sodium silicate

B = 4 c.c. = 0.8 g. of ammonium acetate

HCl (1 N) = 2.0 c.c.

The amount of silicic acid formed = 0.41 g.

The excess of sodium silicate present = 0.87 g.

T	Observations	$\rho_v$	$\rho_h$	$\rho_u$	I in cm.
1		..	..	..	1.0
2		2.2	..	3.4	1.5
3		..	..	..	2.3
4		..	..	..	3.1
5	Opacity increases ..	4.1	90	4.9	3.7
6		..	..	..	4.4
8	Viscous	6.2	..	9.6	5.0
10	Nearly set	..	..	..	5.4
12	Set to a gel	8.2	..	..	5.7
15		8.8	80	13.3	5.8
20		9.3	..	14.7	5.9
40		9.6	70	15.5	5.9

TABLE VIII

A = 25 c.c. = 1.5 g. of sodium silicate

B = 4 c.c. = 0.8 g. of ammonium acetate

Ethyl alcohol = 2.0 c.c.

The amount of silicic acid formed = 0.41 g.

The excess of sodium silicate present = 0.87 g.

T	Observations	$\rho_v$	$\rho_h$	$\rho_u$	I in cm.
2		..	..	..	0.2
3		2.8	..	4.5	0.4
4		..	..	..	0.6
5	Opacity increases ..	..	90	5.3	1.0
6		3.1	..	..	1.5
7		..	..	..	2.0
8		4.4	..	6.2	2.4
9		..	..	..	2.9
10	Viscous	..	..	7.2	3.3
12		5.3	..	8.8	4.2
15	Set to a gel	6.7	..	10.6	4.7
20		8.8	..	13.3	5.6
25		9.4	..	14.7	5.9
30		9.4	74	15.5	6.0

TABLE IX

 $A = 25 \text{ c.c.} = 1.5 \text{ g. of sodium silicate}$  $B = 4 \text{ c.c.} = 0.8 \text{ g. of ammonium acetate}$ 

Ethyl alcohol = 5.0 c.c.

The amount of silicic acid formed = 0.81 g.

The excess of sodium silicate present = 0.23 g.

T	Observations	$\rho_v$	$\rho_h$	$\rho_u$	I in cm.
2					2.2
3	Opacity increases ..	2.8	90	4.5	3.5
4		..	..	..	4.5
5		..	..	5.3	5.1
6		3.1	..	..	5.5
8		4.4	..	6.2	5.8
10	Viscous	..	..	7.2	6.0
12	Nearly set	5.3	..	8.8	..
15	Set to a gel	6.7	75	10.6	6.2
20		8.8	..	13.3	6.4
30		9.3	..	16.3	..
40		9.3	65	16.3	6.4

*Discussion of the Results**1. Changes in the intensity and depolarization factors during gel-formation*

The changes in the values of I and depolarization factors with time are shown in Tables I to IX. The values of  $\rho_v$  are very small in the beginning, that is when the solutions are mixed, showing the nearly spherical nature of the micelles in the initial stages of gel-formation. During gelation, these values increase indicating that the particles become more and more anisotropic in shape or/and structure.

$\rho_h$  has a very high value. It decreases during gelation showing thereby that particles grow in size with time. High values of  $\rho_h$  indicate that the particles are not very large in comparison with the wavelength of light.

The changes in the value of  $\rho_u$  with time are interesting. It increases during gel-formation at first slowly and afterwards rapidly and reaches a constant value. In the case of the gel which sets in a comparatively long time,  $\rho_u$  has a high value in the beginning; later on, it decreases at first, passes through a minimum and then increases to a constant value (Table II). The changes in the value of  $\rho_u$  may be due to the increase in the value of  $\rho_v$  and a decrease in the value of  $\rho_h$ .

The intensity of scattered light also increases during setting. Further, it has been observed that the values of I and depolarization factors increase

even after the gel has set. This observation is similar to the one made in the case of thorium arsenate gels (Prasad and Guruswamy, *loc. cit.*). The silicic acid prepared by Subba Ramiah<sup>8</sup> by mixing an acid and sodium silicate solutions seem to contain particles of size much greater (a comparatively low value of  $\rho_h$ ) than the gels prepared by mixing sodium silicate and ammonium acetate solutions. The gels prepared by mixing an acid and sodium silicate solutions take a long time to set, whereas, the gels prepared by the method used in this investigation, set in a very much shorter time.

## 2. The effect of different constituents of the gel-forming mixture on the rate of change of intensity of scattered light and on the values of $\rho_v$

Increasing amounts of sodium silicate in the gel-forming mixture increase the time of setting and decrease the rate of change of intensity of scattered light (*cf.* Tables I, II and III). On the other hand, increasing amounts of HCl decrease the time of setting and increase the rate of change of scattered light (*cf.* Tables III, VI and VII). Ethyl alcohol acts as a coagulating agent, for in the presence of ethyl alcohol, the gel is formed in a much shorter time (*cf.* Tables III and IX). It is interesting to note that the anisotropy of the gel particles in the various gels prepared from different amounts of the gel-forming constituents, is nearly the same as shown by the nearly same values of  $\rho_v$ .

## 3. Size of the Particles

The high value of  $\rho_h$  during and after gel-formation indicates that the size of the particles is small in comparison with the wavelength of light. As in the case of other gels an approximate idea of the magnitude of the size of the particles of silicic acid gels has been obtained by comparing the intensity of light scattered in the directions  $45^\circ$  and  $135^\circ$  to the incident light for the least anisotropic gel (gel corresponding to Table I,  $\rho_v=8.2$ ). The results show that  $I_{135}/I_{45}$  is not greater than 1.5 and therefore the size of the particles is not greater than  $\frac{1}{4} \lambda$  (*cf.* Prasad and Guruswamy, *loc. cit.*).

## 4. Separation of the density and anisotropy scattering

As in the case of thorium molybdate and thorium arsenate gels (Prasad and Guruswamy, *loc. cit.*) the density and anisotropy scatterings have been separately calculated from the total scattering and the results obtained are shown in Table X, in the case of the gel corresponding to Table III. The volume of the particles has been expressed in relation to the final volume of the

<sup>8</sup> Proc. Ind. Acad. Sci., 1937, 5, 138.

particles when the gelation is complete and the results are given in the last column of Table X.

TABLE X

Time in minutes	$\frac{6 + 6\rho}{6 - 7\rho}$	I in cm.	Density scattering	Anisotropy scattering	Volume of the particles in relation to the final volume
3	1.11	0.3	0.27	0.03	0.07
8	1.06	1.0	0.94	0.06	0.24
10	1.05	1.6	1.53	0.07	0.39
15	1.07	2.4	2.25	0.15	0.58
20	1.09	3.0	2.75	0.25	0.64
25	1.12	3.6	3.22	0.38	0.83
30	1.17	4.2	3.60	0.60	0.92
35	1.18	4.6	3.90	0.70	1.00
60	1.34	5.2	3.90	1.30	1.00

(a) *Changes in the anisotropy scattering during gelation.*—The contribution of the anisotropy scattering to the total scattering for silicic acid gels is comparatively smaller than those in gels of thorium molybdate and arsenate. As in the case of thorium arsenate gels, the anisotropy scattering increases during gel-formation. This shows that the particles become more anisotropic during gelation. In the earlier stages of gel-formation the anisotropy scattering is very small, showing that the particles are nearly spherical.

(b) *Changes in the density scattering during gelation.*—As in the case of other gels, the density scattering increases with time. This increase in the density scattering points to the increase in the volume and a decrease in the number of particles during gelation. Thus gelation is a coagulation process.

(c) *Changes in the volume of the individual particles during gelation.*—The volume of the individual particles at different intervals of time during gelation in relation to the final volume increases during gelation (column 4, Table X). The final volume of the gel particles is about 15 times of that at the commencement of the gelation process.

(d) *Comparison of the final volumes of the gel particles.*—A relative value of the volume of the particles in the gels prepared by mixing different amounts of A and B is shown in Table XI. These values have been obtained by dividing the final values of the density scattering  $I_D$  by the concentration of silicic acid in grams per litre (given in column 3) and expressing these values relative to the volume of the particles of the gel corresponding to Table V. The excess of sodium silicate which may exert an influence on the final volume of the gel particles is given in the last column of the table.

TABLE XI

Gel corresponding to table No.	Amount of silicic acid formed	Concentration of silicic acid	Final value of density scattering	Relative volumes of the particles	Excess of sodium silicate present
I	0.51 g.	10.2	4.47	1.17	0.71
II	0.46	9.2	4.39	1.28	0.79
III	0.41	8.2	3.90	1.27	0.87
IV	0.41	8.2	3.54	1.15	0.57
V	0.41	8.2	3.07	1.00	0.27
VI	0.41	8.2	4.01	1.31	0.87 & HCl

It will be seen that there are very little changes in the volume of the particles in the gels formed by mixing different amounts of (A) and (B).

(e) *The mechanism of the formation of the gel.*—From the results obtained, the following can be inferred regarding the process of formation of silicic acid gels. When the two solutions of sodium silicate and ammonium acetate are mixed, a colloidal solution of silicic acid is formed. The colloidal silicic acid coagulates and the particles also get hydrated, the two processes running concurrently. After some time the whole mass sets to a gel. During gelation, in addition to the increase in size, there is also an increase in anisotropy in shape or/and structure of the coagulum resulting in an increase in the value of  $\rho_u$ , and the anisotropy scattering  $I_A$ .

##### 5. The applicability of the relation connecting $\rho_v$ , $\rho_h$ and $\rho_u$

The applicability of the relation  $\rho_u = \left(1 + \frac{1}{\rho_h}\right) / \left(1 + \frac{1}{\rho_v}\right)$  connecting  $\rho_v$ ,  $\rho_h$  and  $\rho_u$  theoretically deduced by R. S. Krishnan has been examined in the case of silicic acid gels by comparing the observed values of  $\rho_u$  with those calculated from the above relation using the final observed values of  $\rho_v$  and  $\rho_h$ , that is, the values at the completion of the gelation process. The results obtained are shown in Table XII.

TABLE XII

Gel corresponding to table No.	Final observed values of			
	$\rho_h$	$\rho_v$	$\rho_u$ (obs.)	$\rho_u$ (cal.)
I	68	8.2	15.5	18.7
II	70	8.4	15.5	18.8
III	70	8.2	13.3	18.4
IV	78	8.3	14.7	17.5
VI	70	8.2	14.3	18.4

The observed and calculated values of  $\rho_u$  fairly agree with each other. It can be therefore inferred that Krishnan's relation holds good fairly for the gels investigated.

### *Summary and Conclusions*

The changes in the intensity and depolarization of the light transversely scattered by silicic acid gels during and after their formation have been investigated.

It has been shown from the measurements of  $\rho_h$  and a comparison of the backward and forward scatterings that the size of the particles is less than the wavelength of light. An approximate estimate of the size of the particles has been made by comparing the intensities of light scattered at  $45^\circ$  and  $135^\circ$  to the incident light. It has been found that the size of the particles is about  $\frac{1}{4}\lambda$ . It has been pointed out that hydration can produce no change in the intensity of scattering and so the actual size of the gel particles may be greater than  $\frac{1}{4}\lambda$ .

Since the size of the particles is less than the wavelength of light the density and anisotropy scatterings have been separately calculated from the observed total scattering, and their changes during gelation investigated. As in the case of other gels, the density scattering increases during gel-formation thereby showing that gelation is analogous to coagulation.

The anisotropy scattering is small compared with the density scattering in the early stages of gel-formation (about 1/9th). It increases during gel-formation and becomes about a third of the density scattering. The increase in the anisotropy scattering shows that the gel particles become more anisotropic during gelation.

The volume of the gel-particles at different intervals of time during gelation has been expressed in relation to the final volume of the gel-particles. The results show that the particles increase by about 15 times during gel-formation.

A comparison of the final volume of the gel particles of the same gel formed by mixing different amounts of the gel-forming constituents shows that there are no great changes in the final volume of the particles in the gels formed under different conditions of gel-formation.

It has been inferred by comparing the observed and calculated values of  $\rho_u$  that the relation  $\rho_u = \left(1 + \frac{1}{\rho_h}\right) / \left(1 + \frac{1}{\rho_v}\right)$  holds good fairly in the case of silicic acid gels.

The process of formation and the effect of different amounts of the gel-forming constituents on the formation of silicic acid gels as revealed by this investigation have been discussed in detail.

One of the authors (S.G.) is grateful to Pioneer Magnesia Works for awarding him a scholarship during the progress of this work. Our best thanks are due to Dr. K. R. Ramanathan, M.A., D.Sc., for the loan of a double-image prism and Nicol used in this investigation and to Mr. Marathe, L.E.E., Gr.I.E.E. (London), M.I.R.E., for his help in building the photoelectric unit.

## SYNTHESIS OF HIBISCETIN

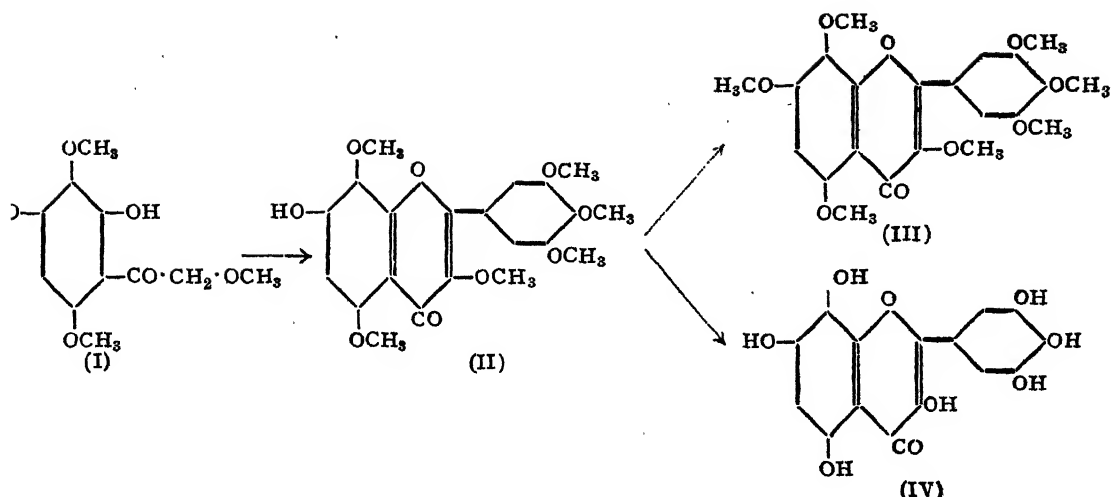
BY P. RAMACHANDRA RAO, P. SURYAPRAKASA RAO  
AND  
T. R. SESHA DRI

(From the Department of Chemistry, Andhra University, Waltair, now at Madras)

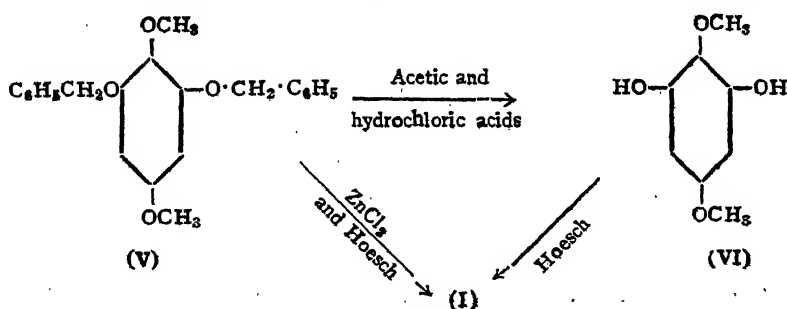
Received December 17, 1943

IT has recently been shown that the glucoside, Hibiscitrin is the main pigment component of the flower petals of *Hibiscus sabdariffa*, gossypitrin and sabdaritri being present in minor quantities.<sup>1</sup> The aglucone, hibiscetin has the formula C<sub>15</sub>H<sub>10</sub>O<sub>9</sub> and has seven hydroxyl groups thereby forming heptamethyl and hepta-acetyl derivatives. It is therefore one of the most highly hydroxylated compounds among flavones and flavonols. It gets readily oxidised in alkaline solutions. When its heptamethyl ether is decomposed with alcoholic potash, trimethyl gallic acid is formed as one of the products. In its reactions with alkaline buffer solutions and with *p*-benzoquinone it closely resembles herbacetin and gossypetin. Based on these results Rao and Seshadri proposed for it the constitution of 3:5:7:8:3':4':5'-heptahydroxy flavone.<sup>2</sup> It is thus the highest member of the herbacetin series of flavonols and carries three hydroxyl groups in the side phenyl nucleus.

The above constitution of hibiscetin has now been confirmed by synthesis. The method adopted is very similar to that employed by Baker, Nödzu and Robinson for the synthesis of gossypetin.<sup>3</sup> 2:4-Dihydroxy- $\omega$ :3:6-trimethoxy-acetophenone (I) is condensed with the sodium salt and anhydride of trimethyl gallic acid. The product is 7-hydroxy-3:5:8:3':4':5'-hexamethoxy flavone (II) which when methylated, readily yields the heptamethyl ether (III) melting at 194-96°. Its identity with hibiscetin heptamethyl ether has been established by a mixed melting-point determination. A preliminary report on this identity has been made by Rao<sup>4</sup> in *Current Science*. Demethylation of (II) using hydriodic acid gives rise to 3:5:7:8:3':4':5'-heptahydroxyflavone (IV) melting with decomposition at about 350°. A mixture of this with hibiscetin obtained from the flowers of *Hibiscus sabdariffa* behaves similarly. Further comparison of the composition melting points and the colour reactions (using dilute alkali, ferric chloride and alkaline buffer solutions) of the synthetic and natural samples has confirmed complete identity.<sup>2</sup>



For the preparation of the ketone (I) the original method of Baker *et al.*<sup>a</sup> involved the following stages. The tribenzyl ether of pyrogallol was oxidised by means of nitric acid to 2:6-dibenzyl-2,6-dimethoxy-p-benzoquinone. This was reduced to the corresponding quinol and methylated leading to the formation of 2:6-dibenzyl-1:4-dimethoxybenzene (V). Since benzyl ethers are much more readily hydrolysed than methyl ethers, debenzylation of (V) could be effected by the action of a mixture of hydrochloric and acetic acids at 65° and 2:5-dimethoxy resorcinol (VI) was obtained. This was subsequently converted to the ketone (I) by the application of Hoesch reaction using methoxy acetonitrile. The above method of debenzylation is not convenient and considerable drop in yield is sustained during the operation. The preparation of the ketone has now been rendered simpler and the yield considerably improved by a modification in the above procedure. When compound (V) is treated with methoxy acetonitrile and dry hydrogen chloride



in ethereal solution in the presence of anhydrous zinc chloride the ketimine hydrochloride corresponding to (I) is formed. Obviously debenzylation

and Hoesch condensation have taken place together. The presence of zinc chloride is quite necessary as otherwise no reaction takes place. Since (VI) undergoes Hoesch condensation in the absence of zinc chloride it could be inferred that this salt (in conjunction with hydrogen chloride) is responsible for the debenylation which seems to be a necessary preliminary to the subsequent Hoesch condensation.

### *Experimental*

**2: 4-Dihydroxy- $\omega$ : 3: 6-trimethoxy acetophenone.**—2: 6-dibenzylxy-1: 4 dimethoxy benzene (7 g.) prepared from pyrogallol according to the procedure adopted by Baker, Nodzu and Robinson<sup>3</sup> was dissolved in dry ether (75 c.c.) and methoxy-acetonitrile (3·5 g.) added. After the addition of anhydrous zinc chloride (3 g.), the mixture was saturated with dry hydrogen chloride at 0°, and the current of gas passed further for nearly four hours. The flask was then corked tightly, sealed with wax and left overnight in a refrigerator. The ketimine hydrochloride was formed as a dark brown semi-solid with a pale yellow incrustation. Further quantity was precipitated by the addition of dry ether. It was separated, and washed with more of ether. The original ether solution and the washings contained mainly benzyl chloride. The ketimine hydrochloride was dissolved in water (50 c.c.), and the solution (A) extracted with ether to remove impurities. The ether extract, which was slightly turbid, yielded on evaporation a sticky substance. When purified by crystallisation from alcohol using a little animal charcoal it was obtained as a colourless crystalline solid melting at 110°–12°. It gave a light violet colour with ferric chloride. The yield of this by-product was very variable and it went up to a maximum of 0·5 g. in one experiment. Its nature is still under investigation.

When the ketimine hydrochloride solution (A) was heated on the water-bath for an hour and cooled, the crude ketone crystallised out. Further quantities could be obtained by the concentration of the mother-liquor and extraction with ether. The crude compound was easily soluble in sodium carbonate solution, while the accompanying impurities were not. This property was made use of in the preliminary purification of the compound. It was finally crystallised from hot water, when it came out as long colourless needles melting at 150–51°. With ferric chloride an alcoholic solution of the substance gave a bluish violet colouration. The yield of the pure product was 3 g.

**7-Hydroxy-3: 5: 8: 3': 4': 5'-hexamethoxy flavone (hexamethyl hibiscetin).**—2: 4-Dihydroxy- $\omega$ : 3: 6-trimethoxy acetophenone (2 g.), sodium trimethyl gallate (8 g.) and trimethyl gallic anhydride (20 g.) were intimately

mixed together and heated under reduced pressure for four hours in an oil-bath at 175–80°. During heating there was some resinification of the material. The reaction product was dissolved in boiling alcohol (150 c.c.) and treated with 40% potassium hydroxide (20 c.c.) in small quantities during the course of 20 minutes. The mixture was then boiled under reflux for half an hour. The solvent was subsequently removed under reduced pressure, the residue dissolved in water (100 c.c.) and the solution saturated with carbon dioxide. As no flavonol separated out at this stage, the clear alkaline solution was treated with hydrochloric acid till the reaction was just acid and the precipitated trimethyl gallic acid rapidly filtered under suction. When the filtrate was extracted with ether and the solution evaporated, a pale yellow substance was obtained. It was washed with cold dilute sodium carbonate in order to remove the last traces of trimethyl gallic acid and was finally crystallised from dilute acetic acid. It was thus obtained as light yellow needles and rectangular plates melting at 238–40°. The yield was 0·5 g. [Found in air-dried material: C, 59·7; H, 5·7;  $C_{16}H_8O_2(OH)(OCH_3)_6$  requires: C, 60·3; and H, 5·3%.] The substance dissolved in alkali to form a yellow solution and developed no characteristic colour with ferric chloride.

3:5:7:8:3':4':5'-*Heptamethoxy flavone (heptamethyl hibiscetin)*.—The hexamethyl hibiscetin (0·2 g.) was dissolved in 20% sodium hydroxide (5 c.c.) and treated with dimethyl sulphate (0·5 c.c.) in drops with vigorous shaking. During the operation, the methylated product began to separate out, but the reaction was brought to completion by heating the mixture on a water-bath for half an hour. On cooling, the methyl ether precipitated out completely. It crystallised from dilute acetic acid as shining colourless needles and narrow rectangular plates melting at 194–96°. Mixed melting point with heptamethyl hibiscetin, prepared by the methylation of hibiscetin, was undepressed.

3:5:7:8:3':4':5'-*Heptahydroxy flavone (hibiscetin)*.—The hexamethyl hibiscetin obtained above (0·2 g.) was dissolved in acetic anhydride (0·5 c.c.) and treated with hydriodic acid (5 c.c.) of 1·7 density. The mixture was boiled under reflux for 3 hours. After dilution with an equal amount of water, sulphur dioxide was passed through the solution in order to remove iodine. A yellow solid was then found to have separated out. It was insoluble in all the ordinary organic solvents except dilute pyridine from which it crystallised as deep yellow shining rectangular plates and prisms melting at about 350° with decomposition. It dissolved, like the natural hibiscetin, in dilute alkali producing a red solution which rapidly changed to brown. With neutral lead acetate it gave a deep red

precipitate in alcoholic solution and with ferric chloride an olive brown colour. With alkaline buffer solutions its colour changes were exactly similar to those produced with the natural pigment; the initial deep yellow solution rapidly changed to green and then to blue; this colour quickly faded to brown and was pale yellow after 24 hours. [Found: C, 50.6; H, 3.8;  $C_{15}H_{10}O_9$ ,  $H_2O$  requires C, 51.1; H, 3.4.]

### Summary

A convenient method of preparing 2:4-dihydroxy- $\omega$ :3:6-trimethoxyacetophenone (I) directly from 2:6-dibenzylxyloxy-1:4-dimethoxybenzene is described. By the condensation of (I) with the sodium salt and anhydride of trimethylgallic acid, 7-hydroxy-3:5:8:3':4':5'-hexamethoxyflavone (II) is obtained. Methylation of (II) yields a heptamethyl ether (III) identical with heptamethyl hibiscetin. Demethylation of (II) gives rise to a heptahydroxy flavone (IV) which is found to be identical with hibiscetin in all its properties and reactions. The constitution of hibiscetin is therefore confirmed by synthesis as 3:5:7:8:3':4':5'-heptahydroxy flavone.

### REFERENCES

1. Rao and Seshadri .. *Proc. Ind. Acad. Sci., A*, 1942, **16**, 323.
2. \_\_\_\_\_ .. *Ibid.*, 1942, **15**, 148.
3. Baker, Nodzu and Robinson *J. C. S.*, 1929, 74.
4. Rao .. *Current Science*, 1942, **11**, 360.

# RAMAN EFFECT IN RELATION TO CRYSTAL STRUCTURE: SODIUM NITRATE

BY B. SUNDARA RAMA RAO

(*From the Department of Physics, Andhra University, Guntur*)

Received December 13, 1943

(Communicated by Professor S. Bhagavantam, F.A.Sc.)

## 1. Introduction

VERY few systematic attempts have so far been made to explain the observed striking differences, in respect of the Raman and infra-red spectra, between a free ion and the crystal of which it forms a part. Bhagavantam and Venkatarayudu\* have tackled this problem and indicated the general lines along which modifications are to be expected. According to these authors, the Raman spectrum of a crystal need not be identical with that obtained either in the molten or the dissolved states of the same substance although there may be similarities in several respects. Firstly, the values of the frequencies of particular oscillations may change on account of the existence of inter-ionic forces. Secondly, some of the lines may split into close components, the selection rules for the various components being entirely different among themselves and from those of the ion. Finally, some new lines may appear or some of those already existing in the ion may disappear in the crystal. This last result is of importance in connection with the origin of low-frequency Raman lines in crystals. Bhagavantam and Venkatarayudu have shown, in their paper already referred to, that the so-called lattice oscillations are simply the internal oscillations of the structure and that no special mechanism need be postulated for explaining their origin.

## 2. The Case of Sodium Nitrate

To illustrate these conclusions, the cases of sodium nitrate and calcite amongst other crystals, had been dealt with by them in a general manner.

The character table for the free  $\text{NO}_3^-$  ion (Table I) shows that there should be two single ( $\nu_1$  and  $\nu_2$ ) and two doubly degenerate ( $\nu_3$  and  $\nu_4$ ) internal normal modes.  $\nu_1$  represents the total symmetric oscillation and is Raman active and infra-red inactive.  $\nu_2$  represents the mode in which the central

\* *Proc. Ind. Acad. Sci.*, 1939, 9, 224.

TABLE I  
*Normal Modes of the Nitrate and Carbonate Ions*

$D_{3h}$	E	$2C^1$	$3C_2$	$\sigma_h$	$2S^1$	$3\sigma_g$	$n_i$	R & T	$n'_i$	Raman	Infra-red
$A_1'$	..	1	1	1	1	1	1	.	1	p	f
$A_2'$	..	1	1	-1	1	1	1	i	0	..	$M \perp \neq 0$
$E_1'$	..	2	-1	0	2	-1	3	1	2	D	..
$A_1''$	..	1	1	1	-1	-1	0	.	0	..	$M_s \perp \neq 0$
$A_2''$	..	1	1	-1	-1	-1	2	i	1	f	..
$E_2''$	..	2	-1	0	-2	1	1	1	0	..	..
$U_R$	..	4	1	2	4	1	2				
$h_j \cdot x_j'$	..	12	0	-6	4	-4	6				
$h_j \cdot \psi_j'$	..	6	0	0	4	-4	6				

atom moves along the trigonal axis and is Raman inactive and infra-red active.  $\nu_3$  and  $\nu_4$  are active in both Raman effect and infra-red absorption.

On the other hand, the character table for the  $\text{NaNO}_3$  crystal (Table II) shows that there should be nine single and nine degenerate normal modes.

TABLE II  
*Normal Modes of the Sodium Nitrate and Calcite Structures*

$D_{3d}^*$	E	$2S^{\frac{1}{2}}$	$2C^1$	i	$3\sigma_g$	$3C_2$	$n_i$	External T L	$n'_i$	Raman	Infra-red
$A_1$	..	1	1	1	1	1	1	0	0	1	f
$A_2$	..	1	1	1	1	-1	3	0	2	1	f
$B_1$	..	1	-1	1	-1	1	4	1	2	1	p
$B_2$	..	1	-1	1	-1	-1	2	0	1	1	f
$E_1$	..	2	1	-1	-2	0	6	1	3	2	f
$E_2$	..	2	-1	-1	2	0	4	0	2	2	p
$U_R$	..	10	2	4	2	0	4				
$h_j \cdot x_j'$	..	30	0	0	-6	0	-12				

The Raman active and infra-red inactive total symmetric oscillation of the  $\text{NO}_3^-$  ion splits into two modes, one of which comes under  $A_1$  (Raman active and infra-red inactive) and the other under  $B_2$  (inactive in both). The second non-degenerate mode of the free ion which is inactive in the Raman effect and active in the infra-red splits into two which come under  $A_2$  (inactive in both) and  $B_1$  (Raman inactive and infra-red active). The two doubly degenerate oscillations of the free ion, however, undergo a marked modification in the crystal. Both of these, in the case of the free ion, are active in the Raman effect as well as infra-red absorption. In the crystal, they continue to be degenerate but split into four modes and come under the representations  $E_1$  and  $E_2$  with altered selection rules.  $E_1$  is active in the

infra-red but inactive in the Raman effect while  $E_2$  is Raman active and infra-red inactive. As a consequence of this, we should expect absence of exact coincidence between the Raman and the infra-red frequencies in the  $\text{NaNO}_3$  crystal, whereas in the case of the free ion, the Raman effect frequencies coincide exactly with those obtained from measurements in infra-red absorption.

In addition to the four doubly degenerate and four single frequencies accounted for above, we should also expect five doubly degenerate and five single frequencies entirely characteristic of the crystal and which may be termed the lattice oscillations.

That all these features are exhibited in the Raman and infra-red spectra of calcite and sodium nitrate has been pointed out before. It is intended in this paper to make a quantitative study of the changes that are to be expected in the exact frequencies of the free ion and of the actual values in respect of the new oscillations that arise in the sodium nitrate crystal by postulating suitable crystalline forces.

The force-constants relevant to the case of the free ion can be calculated from the frequencies observed in solution and with the help of the following set of equations.

$$\lambda_1 = \frac{k + 3K_1}{m}; \quad \lambda_2 = K_3 \cdot \frac{M + 3m}{3mM};$$

$$\lambda_3 + \lambda_4 = \frac{2M + 3m}{2mM} (K + 3K_2) + \frac{3K_1}{2m};$$

$$\lambda_3 \lambda_4 = \frac{3(M + 3m)}{4m^2M} \times (KK_1 + 4KK_2 + 3K_1K_2).$$

The  $\lambda$ 's are related to the corresponding  $\nu$ 's by the equation  $\lambda^2 = 4\pi^2\nu^2$ . Identifying  $\nu_1$ ,  $\nu_2$ ,  $\nu_3$ ,  $\nu_4$  with 1048, 830, 725 and 1361 respectively,\* the following values are obtained.

$$K = 5.42 \times 10^5, \quad K_1 = 1.65 \times 10^5, \quad K_2 = 0.64 \times 10^5 \text{ and } K_3 = 4.40 \times 10^5.$$

Here  $K$  and  $K_1$  represent respectively the forces between nitrogen-oxygen and oxygen-oxygen atoms in the  $\text{NO}_3$  ion.  $K_2$  relates to a variation in the angle between any two N—O bonds and  $K_3$  arises when the nitrogen atom moves out of the plane of oxygens.

\* These values have been obtained in sodium nitrate solution and are taken from Hibben, *Raman Effect and its Chemical Applications* (1939).

*3. Normal Co-ordinates and Normal Frequencies of the  
Sodium Nitrate Structure*

The normal co-ordinates in respect of the various representations have already been worked out by Bhagavantam and Venkatarayudu and given in an earlier paper already referred to. Some of these, which have been erroneously entered, have to be corrected as below:—

$$Q_2' (L) = (Z_3 - Z_4) + (Z_5 + Z_6 + Z_7 - Z_8 - Z_9 - Z_{10})$$

$$Q_3' (i) = 3m_3 (Z_3 - Z_4) - m_2 (Z_5 + Z_6 + Z_7 - Z_8 - Z_9 - Z_{10})$$

$$Q'_{17a} (L) = (x_3 - x_4) + (x_5 - x_8 + x_7 - x_{10} + x_6 - x_9)$$

$$Q'_{18a} (i) = 3m_3 (x_3 - x_4) - m_2 (x_5 + x_6 + x_7 - x_8 - x_9 - x_{10})$$

$Q'_{17b}$  and  $Q'_{18b}$  are similar to  $Q'_{17a}$  and  $Q'_{18a}$  and must be corrected accordingly.

In order to calculate the frequencies in the case of the crystal, three additional force-constants have been introduced into the potential energy function.\* These are:

$K_4$ : force brought into play when the angle at any atom on the trigonal axis changes by one unit. This axis is a unique direction in the structure and in the static condition, all the atoms on it are collinear and hence every one of the angles is  $180^\circ$ .

$K_5$ : force brought into play when the distance between a sodium and the nearest oxygen atoms changes by one unit.

$K_6$ : force brought into play when a twist of one unit in the trigonal axis is produced by the bodily rotation of the individual  $\text{NO}_3$  groups.

With the foregoing notation of force-constants, the frequencies coming under the various irreducible representations (Table II) can be written down as follows. Details of calculation are omitted.

In the following equations,

$$r = \frac{b^2}{4a^2 + b^2}; s = \frac{ab}{4a^2 + b^2}; t = \frac{a^2}{4a^2 + b^2}$$

$a$  = distance between two nearest nitrogen and oxygen atoms

\* It must be mentioned here that the choice of these is somewhat arbitrary. The actual state of affairs in a crystal is obviously much more complicated and these force constants and the values that will be ascribed to them in the course of the paper can at best be regarded as representing, in effect, the sum total of all the possible types of crystalline forces. The description given cannot be interpreted as literally corresponding to what exists in the crystal.

$b$  = distance between two nearest nitrogen atoms.

$$p = M + 3m$$

$$\text{and } p_1 = M + 3m + M'$$

$M'$ ,  $M$  and  $m$  are respectively the masses of sodium, nitrogen and oxygen atoms.

$$A_1: \lambda = \frac{K + 3K_1 + 8t K_5}{m}$$

$A_2$ :  $\lambda$ 's are the roots of:

$$\begin{vmatrix} 12K_5r - 2p\lambda & -12K_5rM & 0 \\ -12K_5rM & 12K_5rM^2 + 2K_3p^2 - 6mMp\lambda & 0 \\ 0 & 0 & -24m\lambda \end{vmatrix} = 0$$

$B_1$ :  $\lambda$ 's are the roots of:

$$\begin{vmatrix} 16K_6 - 24m\lambda & 0 & 0 \\ 0 & 12K_5rM^2 + 2p^2K_3 - 6mMp\lambda & 12K_5Mrp_1 \\ 0 & 12K_5Mrp_1 & 12K_5p_1^2r - 2M'pp_1\lambda \end{vmatrix} = 0$$

$B_2$ :  $\lambda$ 's are the roots of:

$$\begin{vmatrix} K + 3K_1 + 8tK_5 - m\lambda & 2sK_5 \\ 48sK_5 & 12rK_5 - 2M'\lambda \end{vmatrix} = 0$$

$E_1$ :  $\lambda$ 's are the roots of:

$$\begin{vmatrix} 24K_5r - 12m\lambda & -48sK_5 & 24sK_5 & 24MsK_5 & 24p_1sK_5 \\ -48sK_5 & 12K_1 + 36K_2 + 36K_3 - 48K_5t - 6pK + 18pK_2 & -48p_1tK_5 \\ 24sK_5 & + 96K_5t - 24m\lambda & -48MtK_5 \\ 24MsK_5 & - 6pK + 18pK_2 & 24MtK_5 & 24p_1tK_5 + 8p_1K_4 \\ & - 48MtK_5 & - 24mK_4 & - 24mK_4 \\ & & + 24M^2tK_5 & + 144m^2K_4 \\ & & - 6mMp\lambda & - 6mMp\lambda \\ 24p_1sK_5 & - 48p_1tK_5 & 24p_1tK_5 + 8p_1K_4 & 24Mp_1tK_5 & 24p_1^2tK_5 \\ & & 24Mp_1tK_5 & + 16p_1^2K_4 & + 16p_1^2K_4 \\ & & 8mp_1K_4 & - 2M^2pp_1\lambda & - 2M^2pp_1\lambda \end{vmatrix} = 0$$

$E_2$ :  $\lambda$ 's are the roots of:

$$\begin{array}{cccc}
 12K + 36K_1 + 36K_2 & 48tK_5 & -6pK + 18pK_2 - 48MtK_5 & -48sK_5 \\
 + 96tK_5 - 24m\lambda & & & \\
 48tK_5 & 24tK_5 + 8K_4 & -24MtK_5 + 24mK_4 & -24sK_5 \\
 - 2p\lambda & & & \\
 -6pK + 18pK_2 & -24MtK_5 & 3p^2K + 9p^2K_2 + 24M^2tK_5 & 24MsK_5 \\
 -48MtK_5 & + 24mK_4 & + 72m^2K_4 - 6mMp\lambda & \\
 -48sK_5 & -24sK_5 & 24MsK_5 & 24K_5r - 12m\lambda
 \end{array} = 0$$

#### 4. Numerical Values of the Force-Constants and of the Frequencies in the Crystal

The total number of force-constants introduced in the case of the crystal is thus seven. The numerical values assumed for them are:

$$K = 5.42 \times 10^5; K_1 = 1.78 \times 10^5; K_2 = 0.64 \times 10^5;$$

$$K_3 = 4.40 \times 10^5 \text{ and } K_4 = 0.03 \times 10^5; K_5 = 0.35 \times 10^5;$$

$$K_6 = 0.07 \times 10^5.$$

$K_1$ ,  $K_2$  and  $K_3$  are the same as those calculated for the free ion.  $K_1$  is here  $1.78 \times 10^5$  whereas it was  $1.65 \times 10^5$  in the free ion. This increase is effected as each oxygen atom in a crystal will be under the force-field of a large number of other oxygens whereas in the ion we need consider only the influence of its two nearest neighbours. The values of  $K_4$ ,  $K_5$  and  $K_6$  have been chosen to give a reasonably good fit with the experimentally observed values of the crystalline frequencies.

Taking the above values of the force-constants, the frequencies that are attributed to the case of the  $\text{NaNO}_3$  crystal can be evaluated. The actual values obtained under each representation along with the activity rule are given below.

$A_1$  (Raman active, infra-red inactive): 1069.

$A_2$  (Inactive in both): 840, 229, 0.

$B_1$  (Infra-red active, Raman inactive): 843, 439, 71.

$B_2$  (Inactive in both): 1069, 380.

$E_1$  (Infra-red active, Raman inactive): 1411, 716, 292, 157, 60.

$E_2$  (Raman active and infra-red inactive): 1362, 766, 190, 87.

The results thus obtained have been summarised and compared with the experimental observations in Table III.

TABLE III

Raman	Calc. Obs.	..	87, 94,	190, 185,	766, 718,	1069, 1068,	1362 1382			
Infra-red*	Calc. Obs.	..	60, 71,	71, 133,	157, 217,	292, 217,	439, 692,	716, 831,	843, 1405	1411

\* The values of the observed infra-red frequencies are quoted from Schaefer and Matossi's book *Das Ultra Rote Spectrum*, 1930.

### 5. Discussion of Results

The following important conclusions can be drawn from the foregoing results.

The frequency of the total symmetric oscillation which is 1048 in the free ion should increase to 1069 in the crystal. This is confirmed by experiment.

The two doubly degenerate oscillations of the free ion remain doubly degenerate but split into four modes, two of which come under  $E_1$  and two under  $E_2$ .  $E_1$  is infra-red active but Raman inactive while  $E_2$  is Raman active but infra-red inactive. Hence, there should be no exact coincidence between the observed Raman and infra-red frequencies and this is confirmed by experiment.

The Raman spectrum of the  $\text{NaNO}_3$  crystal should exhibit two low-frequency lines at 190 and 87 which may be termed the lattice lines. This is confirmed by experiment and two lines having frequency shifts of 185 and 94 at the room temperature have actually been recorded in its Raman spectrum.

Similarly the infra-red spectrum should contain five different frequency shifts. Three for one orientation and two for another with values in qualitative agreement with those calculated have actually been observed in the infra-red absorption. It may, however, be remarked that the force-system postulated cannot be too much relied upon as it is only tentative and is capable of variation. The figures, nevertheless, represent correctly the order of magnitude.

### 6. Summary

By adopting a set of seven constants, four of which pertain to the forces in the free ion and the remaining three to the inter-ionic forces in the crystal, the observed Raman and infra-red spectra of  $\text{NaNO}_3$  crystal have been satisfactorily explained.

The author wishes to record here his grateful thanks to Prof. S. Bhagavantam for his helpful guidance during the progress of this work,

# AN ELECTRICAL METHOD OF STUDYING THE MOVEMENT OF WATER AND SALTS IN SOIL

## Part I. A Sensitive A. C. Bridge with an Electronic Null-Point Indicator

By A. U. MOMIN

(*Agricultural Meteorology Section, Meteorological Office, Poona*)

Received January 10, 1944

(Communicated by Dr. L. A. Ramdas)

### 1. Introduction

THE A. C. bridge method, first used by Kohlrausch for measuring the electrical conductivity of solutions, has been employed with numerous modifications by several workers in soil physics<sup>1,2,3</sup> for measuring the electrical conductivity of soils and soil extracts. In the original method of Kohlrausch a buzzer provided the alternating e.m.f. for the bridge and a telephone was used for detecting the null-point. Later workers have introduced modifications and refinements to reduce the errors produced by any lack of balance of out of phase voltages and to obtain a silent null-point.

The difficulties due to phase-angle differences, which in resistance bridges are due mainly to stray capacities in the connecting wires, the electrode system and the balancing resistances, have been overcome by first balancing out these out-of-phase components with a variable capacity connected across the adjustable arm of the bridge. The problem of obtaining a sharp and silent null-point has been only partially solved by making use of thermionic amplification and in some cases, where the telephone is directly connected to the bridge, by making use of grounding circuits<sup>1</sup> for maintaining the telephone circuit at zero potential throughout each cycle of the A. C.

All these methods developed by earlier workers are satisfactory only if the resistances to be measured are fairly low and a very high degree of precision is not aimed at, but if accurate and quick measurements of very high and rapidly changing resistances are to be made these methods have certain limitations.

In the present paper is described an electronic apparatus which has been designed for measuring the rapidly changing resistance of a soil column

between two grid electrodes when water is allowed to rise in the soil column by capillary action. The method described here was found to be quick and accurate and was successfully used in investigating the structure of the water front in an ascending column of moisture in soil, the adsorption of water vapour by air-dry soil and the movement of salts associated with the movement of water in soil. The results of this investigation will be described in the second part of this series.

## *2. Disadvantages of the Telephone as a Null-Point Indicator*

Although the telephone, when used in conjunction with an amplifier, is quite satisfactory for the measurement of low resistances, it has certain limitations if the resistances to be measured are very high and a high degree of precision is desired. The main disadvantages of the telephone as null-point indicator are as follows:—

(i) *Background noise*:—If an amplifier with a high voltage gain is used in conjunction with a telephone, there is always a certain amount of direct pick up from the source of alternating e.m.f. for the bridge which after amplification appears as a constant background noise. This makes it difficult to fix the exact position of the null-point on the scale of the bridge. Electro-static shielding is impracticable as it would be very difficult to shield adequately the input circuit of the amplifier from the wires feeding the alternating e.m.f. and other parts of the bridge.

(ii) *Logarithmic response of the human ear*:—This is another factor which introduces a certain amount of uncertainty in finding the exact position of the null-point. The insensitivity of the ear to changes in sound level of less than 2 or 3 decibels is responsible for the apparent flatness of the null-point. This defect is especially marked if the resistances to be measured are of the order of megohms.

(iii) *Limited range of frequencies that can be used*:—When the telephone is used the frequency of the applied e.m.f. must necessarily lie within a limited portion of the audible range, i.e., from about 50 to about 8,000 cycles per second. In addition, the response of the ordinary diaphragm type of telephone is not linear but has got a peak in the region of 1000–1500 c/s, and therefore it can be used successfully only within the above narrow band of frequencies.

(iv) *The telephone is not phase-selective*, thus its use necessitates a separate balancing of out-of-phase e.m.f.'s.

To overcome these difficulties it was decided to use some type of visual balance indicator.

### 3. Visual Balance Indicators in A.C. Bridges

Visual balance indicators in A.C. bridges may be classified under the following two main heads: (i) those using Meters, and (ii) those using Electronic devices.

(i) *Meters*:—For the detection of the conditions of balance, using a meter, the output of the bridge is either directly fed to a suitable type of a.c. galvanometer (vibration type, etc.) or it is first rectified by thermionic or copper oxide rectifiers and then fed to an ordinary galvanometer or a sensitive micro-ammeter.

(ii) *Electronic devices*:—Under this head come the numerous developments of the cathode-ray tube and also the electron-ray indicator tubes commonly used in radio receivers as tuning indicators.

As the apparatus making use of sensitive meters require frequent and critical adjustments and as our purpose was to develop an instrument which would be sensitive as well as robust and suitable for use under actual field conditions, the use of a meter was ruled out.

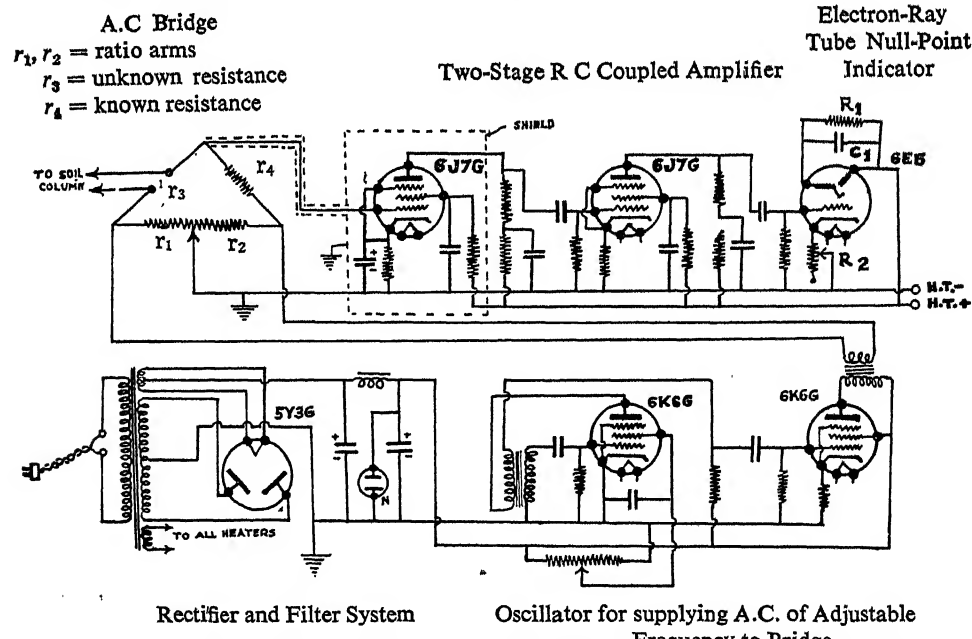


FIG. 1. Schematic circuit diagram of electron-ray tube null-point indicator for A.C. Bridge

The cathode-ray tube, although superior in many ways to all other types of indicators, was not suitable for our purpose as its operating voltages are very high and not easily obtainable under field conditions. It was therefore

decided to use an electron-ray tube which appeared to be the most suitable and promising from the point of view of portability, robustness and also sensitivity. This tube worked satisfactorily on voltages as low as 70 or 80 volts on the target. In addition, it had one useful feature which permitted the compensation for any direct pick-up or lack of balance due to out-of-phase voltages, by suitably adjusting the negative grid bias on the tube.

#### 4. *The Electron-Ray Tube*

The idea of using the electron-ray tube as a detector of balance in A.C. bridges is not new. It appears to have been first suggested by Ulrey.<sup>4</sup> Later Breazeale, Garman and Koelher have described<sup>5, 6, 7</sup> various arrangements suitable for different types of measurements. The apparatus designed by the present writer which is described in the following pages incorporates some of the desirable features of the apparatus designed by the above authors, with some new modifications to suit the present investigation. A schematic circuit diagram of the complete apparatus including the oscillator, rectifier and filter system is given in Fig. 1.

A type 6 E 5 electron-ray indicator tube has been used for the detection of the condition of balance in this apparatus. This tube has an indirectly heated cathode and the emission is focussed in the form of a beam on a fluorescent target which is maintained at a high positive potential. It has also an anode and two grids, one of which functions as a normal control grid in a triode and controls the anode current of the tube, and the other which is connected to the anode inside the tube and is directly in the path of the electron beam, is known as the ray-control grid. This ray-control grid casts a fan-shaped shadow on the fluorescent target and the angular width of this shadow is determined by the potential difference between the ray-control grid and the target, which is obtained by the flow of the anode current across a high resistance,  $R_1$ , connected between the anode and the target. The anode current is, of course, dependent on the negative bias on the control grid. Thus, by changing the value of this negative bias on the tube it is possible to change the angular width of the shadow on the target, the variation in the grid voltage for changing the shadow angle from 100° to 0° being about 3 or 4 volts. The anode current is almost cut off by a grid bias of about 4 volts and therefore there is no appreciable potential difference between the anode (to which is connected the shadow-forming grid) and the target. The electrons, therefore, take a straight path to the fluorescent target casting a fine crack-like shadow of the ray-control grid. Now if this bias on the control grid is made less negative by some means the anode current increases producing a potential difference across the load resistance,

$R_1$ , connected between the anode and the target. Since the shadow-forming grid is now at a negative potential with respect to the target, the electron beam is repelled by its field and the shadow opens out reaching a maximum angular width of  $100^\circ$  when the bias is 0 volts or slightly positive.

In the present apparatus this bias is obtained by rectifying and suitably filtering the amplified output of the A.C. bridge. The process of rectification is, however, performed in the electron-ray tube itself by the well-known anode-bend method which is usually employed in wireless receivers for demodulating the radio frequency signal. We need not go into the details of the rectifying action of this method as it is treated in great detail in many text-books on wireless communication. The circuit is arranged in such a way that an increase in the A.C. signal input to the grid of the 6 E 5 tube makes the bias less negative, thus increasing the anode current of the tube which consequently results in the opening of the shadow. Now if the A.C. bridge is adjusted to a condition of balance, the A.C. output should be a minimum; therefore, there is little decrease in the negative bias of the 6 E 5 tube and the anode current being almost negligible the angle of the shadow on the target is also a minimum. By suitably adjusting a variable resistance,  $R_2$ , in the cathode circuit it is possible to adjust the bias in such a way that when the bridge is correctly balanced the shadow will close down to a fine crack. Any movement of the slider contact of the bridge away from the null-point tends to open the shadow. With a two-stage high gain thermionic amplifier behind the 6 E 5, a movement of the slider as small as 1 millimetre away from the null-point can easily be detected. This means that a change of resistance of one part in a thousand can easily be detected by this instrument.

### 5. *The Amplifier*

As the successful operation and sensitivity of this null-point indicator greatly depend on the gain and stability of the amplifier which precedes it, care has been taken in designing the amplifier to ensure that the requisite sensitivity consistent with stability was obtained. The amplifier makes use of two type 6 J 7 pentodes with resistance capacity coupling in both the stages. By omitting the cathode by-pass condensers in the second valve and the 6 E 5 tube, a certain amount of degeneration is introduced into the circuit which not only increases its stability but also reduces distortion of the signal by making the response more linear. Special care has also been taken to provide adequate interstage shielding to reduce the tendency to oscillate which is common to all amplifiers with high voltage gain. The total gain of

this particular amplifier has not been measured, but by making use of the equation

$$\text{Voltage gain} = \frac{\mu R_L}{R_P + R_L}$$

where  $\mu$  = amplification factor of the valve

$R_L$  = load resistance, and

$R_P$  = anode-slope resistance of the valve;

it works out to be about 5,000 which appears to be reasonable and consistent with the sensitivity obtained in the instrument.

### 6. *The Source of Alternating e.m.f.*

In the early stages of this investigation the 50 c/s A.C. mains were used as the source of alternating e.m.f. for the bridge, an ordinary bell transformer being used for stepping down the mains voltage of 230 to about 6 volts. The results obtained with this arrangement were quite satisfactory, as far as sensitivity was concerned, but later on, it was desired also to study whether the frequency of the alternating e.m.f. applied to the bridge had any effect on the position of the null-point and also to see if any polarisation effects were produced at low frequencies. It was, therefore, decided to build a thermionic audio-frequency oscillator, with the desired frequency range. First a single valve oscillator making use of a type 6K6G power pentode and whose frequency was controlled by varying the screen-grid voltage of the pentode valve was built. Although the desired frequency range was obtained, the results obtained with this oscillator were not quite satisfactory as the output was very low. A power stage using another 6K6G tube was then added and the oscillator was found to give an output of approximately 4.5 watts with 300 volts on the plate and it had a frequency range of 25 to 600 cycles per second. The output was, however, not constant throughout the above range of frequencies, the maximum being somewhere at about 400 c/s. The problem of building an oscillator with a constant output should not be a difficult one, but since the variations in the output with frequency neither changed the position of the null-point appreciably nor greatly affected the sensitivity of the apparatus, no attempt has been made in that direction. The coupling between the oscillator and the bridge was effected by using a step-down transformer of the type commonly used in the output stages of radio receivers for matching the plate impedance of the power valve with that of the speech coil of the loudspeaker. The primary impedance of this transformer was about 6000 ohms and that of the secondary was about 2 ohms which was approximately the same as that of the slide

wire of the bridge. The high tension voltages and the heater current for the oscillator were obtained from a neon-tube stabilised rectifier unit delivering about 130 milliamperes at 350 volts. Since another small high tension unit was available, it was used for the amplifier and the electron-ray tube; but there is no reason why the same power pack should not be used both for the oscillator as well as for the electron-ray tube and amplifier, provided sufficient care is taken to introduce adequate decoupling between the two units.

Making use of the values given by Koehler for  $R_1$  and  $C_1$  it was found that the response of the electron-ray tube became sluggish which was undesirable for our investigation, where very rapidly changing resistances were to be measured. As will be seen from the circuit diagram,  $R_1$  and  $C_1$  form a circuit with a time constant; and with a resistance of 1 megohm and a capacity of  $1\mu fd$ , this constant will be one second. This means that it will take one second for the shadow to become steady after an adjustment of the slider of the bridge has been made. This was found to be rather slow for our purpose. A value of 300,000 ohms was therefore chosen for  $R_1$  which, with a capacity  $1\mu fd$ , was found to have a sufficiently quick response. Any reduction in the value of  $R_1$  will, of course, reduce the sensitivity of the circuit, although it will also make the response of the tube faster. The value of  $R_1$  chosen is therefore a compromise.

### *7. Method of Making Measurements*

With the oscillator switched off, *i.e.*, no e.m.f. applied to the bridge, the variable resistance,  $R_2$ , in the cathode circuit of the electron-ray tube is adjusted until the shadow just closes. The tube is now operating on the lower bend of the anode current—grid voltage characteristic of the tube and there is no appreciable anode current flowing. If the oscillator is now switched on and the bridge adjusted, it will be found that the shadow again closes when the bridge is exactly balanced. If there is any residual opening of the shadow due to direct pick-up, etc., it may be made to close again by a slight adjustment of  $R_2$ .

### *8. Conclusion*

The electron-ray tube apparatus described above has been used for measurements of the variations in electrical conductivity of Poona black cotton and the Punjab 'normal' soils with approaching moisture from below. It has also been used for studying the adsorption of water vapour by air-dry and heated Poona black cotton soil exposed to saturated air. The results of this investigation will be described in Part II of this paper. The

apparatus is also being used in other investigations where the measurement of electrical conductivity is involved, *viz.*, in studying the effect of transpiration on the electrical conductivity of the sap in growing plants and plant cuttings.

The following features of the present apparatus may be regarded as improvements on the arrangements used by previous workers:

(i) The response of the apparatus is much faster than that described by Koehler.

(ii) The present apparatus makes use of a high gain amplifier, which has been stabilised by introducing degeneration into the circuit. Consequently a higher sensitivity has been obtained without sacrificing stability which does not appear to have been done in the previous instruments.

(iii) The earthing and shielding arrangement in the circuit makes it non-susceptible to outside electrical disturbances. This is difficult with Garman's apparatus where a direct coupled amplifier is used.

(iv) The apparatus makes use of an audio-frequency power oscillator with variable frequency.

In conclusion, the writer wishes to express his gratitude to Dr. L. A. Ramdas, Agricultural Meteorologist, for suggesting the problem, for guidance and encouragement during the course of the investigation and for providing the necessary facilities for the work.

#### REFERENCES

1. Cashen, G. H. .. *Jour. Agri. Sci.*, January 1932.
2. Sen, Ashutosh .. *Ibid.*, January 1932.
3. Atkins, W. R. G. .. *Ibid.*, 1924.
4. Ulrey .. *Physics*, 1936, 7, 97.
5. Breazeale .. *R. S. I.*, 1937, 7, 250.
6. Garman .. *Ibid.*, 1937, 8, 327.
7. Koehler .. *Ibid.*, 1937, 8, 450.

# SCATTERING OF LIGHT IN SINGLE CRYSTALS

## Intensity Measurements

BY S. BHAGAVANTAM AND K. VENKATESWARLU

(*From the Department of Physics, Andhra University, Guntur*)

Received January 11, 1944

### 1. Introduction

EXPERIMENTAL observations regarding the relative intensities of the Rayleigh and Raman scattering in gases have so far been very meagre. Bhagavantam<sup>1</sup> showed that the intensity of the Rayleigh line in most typical gases is a few thousand times that of the vibrational Raman line. The cases of hydrogen and deuterium constitute an exception as the exciting line in them is only a few hundred times stronger than the Raman line. On the other hand, several authors<sup>2-6</sup> have determined the ratio of the intensity of the Rayleigh line to that of some of the prominent Raman lines in liquids like benzene, carbon tetrachloride, chloroform, etc. The results obtained by them differ to some extent amongst themselves but the general conclusion that the intensity of the Rayleigh line in liquids is a few hundred times that of the Raman lines is confirmed by all the workers. No work has at all been done so far in this direction with crystals. It will be of great interest to know the ratio of intensity of Rayleigh to that of the Raman scattering in the case of solids because such results can confidently be expected to throw light on the fundamental problem regarding the nature of the Raman scattering in solids. There are several experimental difficulties in the way of obtaining accurate results but an attempt is now made to develop a suitable technique for solving the problem.

Two typical crystals, calcite and quartz, which are available in this laboratory in the form of perfectly transparent and flawless one inch cubes with all their faces polished have been used in the present investigation. The results obtained are of great interest and are accordingly reported in this paper.

### 2. Experimental Details and Results

It is difficult to obtain the ratio of the relative intensities of Rayleigh and Raman scattering in crystals directly by photographic methods, because with the Rayleigh scattering is usually mixed up a large amount of spurious or parasitic light. As such, a special method has been adopted here to obtain an estimate of this ratio. This will be clear from Tables I and II.

The Raman spectra of the crystal (one inch cube) and a chosen liquid\* contained in a glass cell of exactly the same dimensions as the crystal are obtained under identical conditions on the same plate. Great care has been taken to see that the time of exposure, the intensity of the lamp and conditions of illumination remained the same in both cases. A set of intensity marks is given on each plate by the method of varying slit widths using a quartz globe tungsten ribbon lamp as the source. The intensities of the 1085 line in calcite and of the 465 line in quartz are compared in turn with that of the 460 line in carbon tetrachloride. The results obtained are given in column 4 of each of the tables given below.

TABLE I. Calcite

Optic axis parallel to	I Rayleigh (liquid)	I Rayleigh (liquid)	I Raman (crystal)	I Rayleigh (crystal)
	I Rayleigh (crystal)	I Raman (liquid)	I Raman (liquid)	I Raman (crystal)
OX	73			1.45
OY	83			2.20
OZ	65	400	0.87	3.8 2.2 7.1

TABLE II. Quartz

Optic axis parallel to	I Rayleigh (liquid)	I Rayleigh (liquid)	I Raman (crystal)	I Rayleigh (crystal)
	I Rayleigh (crystal)	I Raman (liquid)	I Raman (liquid)	I Raman (crystal)
OX	77			0.96
OY	93			1.22
OZ	103	400	0.55	5.4 3.5 7.1

OX, OY and OZ represent respectively the direction of incidence, of scattering and the vertical. In column 2 of each of the tables are given figures obtained by Bhagavantam and Narayana when they compared the intensities of Rayleigh scattering in calcite and quartz with that in air by employing intermediate liquid standards. These figures may be seen to agree with those given in their paper already referred to if the conversion factor  $I \text{ Rayleigh (liquid } CCl_4)/I \text{ Rayleigh (air)}^* = 918$  adopted by them is taken into account. In column 3 of each of the tables is given the ratio of the Rayleigh line to that of the 460 Raman line in  $CCl_4$  as determined by Veerabhadra Rao in this laboratory. It is easily seen that the figure given in the last column is obtained by dividing 400 with the product of columns 2 and 4 in each case and this represents the desired ratio.

\* In this paper, results obtained when the chosen liquid is carbon tetrachloride only are given. Benzene as a standard has also been experimented upon but the results are more difficult to interpret because of the large rotational wing that accompanies the Rayleigh scattering. This complication is practically absent in carbon tetrachloride.

### 3. Discussion of Results

The ratio of the intensities of Rayleigh and Raman scattering in a gas, a liquid and a crystal for one orientation are given in Table III for comparison.

TABLE III

Substance	Frequency of the Raman line		$\frac{I_{\text{Rayleigh}}}{I_{\text{Raman}}}$
Oxygen	..	1560	3330
Carbon tetrachloride	..	460	400
Calcite	..	1085	3.8

Comparatively low ratios obtained and reported in this paper for calcite and quartz are very significant. Since the intensity of Raman scattering in crystals is found to be of the same order as that observed in liquids, when equal volumes are illuminated by beams of the same intensity, we have to conclude that the Rayleigh scattering, mass per mass, has become very faint in the case of crystals whereas Raman scattering has retained its strength. This suggests that while Rayleigh scattering continues to be coherent, Raman scattering continues to be incoherent. The exact significance of such statements in relation to the mechanism of scattering in crystals is not clear and a discussion of the same will not be attempted now. The state of polarisation of the aggregate scattered light in crystals obtained by visual determinations cannot be taken as representing the character of Rayleigh scattering even approximately. Such results will be greatly influenced by the presence of depolarised Raman scattering because in the case of crystals the latter, if present, has an intensity comparable to that of the Rayleigh scattering. Only a spectroscopic investigation can lead to reliable values.

### 4. Summary

Employing carbon tetrachloride as an intermediate standard, the relative intensities of Rayleigh and Raman lines in specially cut crystals of calcite and quartz have been determined for different orientations. The Rayleigh line, in different instances, is found to possess an intensity which is only about two to seven times that of the principal Raman line.

### REFERENCES

1. Bhagavantam .. *Ind. Jour. Phys.*, 1931, 6, 319.
2. Daure .. *Ann. d. Phys.*, 1929, 12, 375.
3. Carrelli and Went .. *Z. f. Phys.*, 1932, 76, 236.
4. Dhar .. *Ind. Jour. Phys.*, 1934, 9, 189.
5. Veerabhadra Rao .. *Z. f. Phys.*, 1935, 97, 154.
6. Poornachandra Rao .. *Proc. Ind. Acad. Sci.*, 1940, 11, 1.

# EFFECT OF TEMPERATURE ON THE INTENSITIES OF RAMAN LINES

## Part III. Liquids

BY K. VENKATESWARLU

(From the Department of Physics, Andhra University, Guntur)

Received January 11, 1944

(Communicated by Prof. S. Bhagavantam)

PLACZEK's theory indicates that both the Stokes and the anti-Stokes Raman lines should increase in intensity with increase of temperature. The expressions for the intensities of the Stokes and the anti-Stokes lines as a function of temperature are given by (1) and (2).

$$I_{(\nu - \nu_i)} \propto (\nu - \nu_i)^4 \frac{1}{1 - e^{-\frac{hv_i}{kT}}} \quad (1) \qquad I_{(\nu + \nu_i)} \propto (\nu + \nu_i)^4 \frac{1}{e^{\frac{hv_i}{kT}} - 1} \quad (2)$$

Not much work has been done as regards the effect of temperature on the intensities of the Raman lines either in solids or in liquids. The early work of Landsberg and Mandelstamm<sup>1</sup> in the case of quartz, shows that the intensity of Stokes lines increases with temperature while the more recent work of Ornstein and Went<sup>2</sup> in the case of calcite and quartz, on the other hand, shows a marked decrease of intensity with increase of temperature. In two previous communications,<sup>3, 4</sup> the author has published some results in the case of a few typical crystals. The following are the main features observed by the author in the cases he has studied. The Stokes lines decrease in intensity with increase of temperature. The anti-Stokes lines generally increase in intensity with increase of temperature but not to the expected extent. The ratio of the intensities of the Stokes and the anti-Stokes lines in all cases is in conformity with the theoretically expected results. Some special features observed in the case of calcite are that the low frequency lines decrease in intensity more rapidly than the others and that the anti-Stokes lines show slight decrease in intensity. Small shifts of the low frequency lines towards the exciting line have also been noticed.

As regards liquids, Krishnan<sup>5</sup> pointed out that in the Raman spectrum of liquid carbon tetrachloride, the Stokes lines become weaker and the anti-Stokes lines stronger in intensity with increase of temperature. Ananthakrishnan<sup>6, 7</sup> concluded from the spectrograms he has obtained in the case of liquid  $CCl_4$  over an interval of temperature extending from 25° C. to 200° C. that the integrated intensities of the Stokes lines do not increase with increasing temperature and also that the anti-Stokes lines increase in intensity but not to such an extent as is required by Placzek's theory.

The work so far done in the case of liquids is very meagre and purely qualitative. As such and to fall in a line with the previous work done by

the author in the solids, the present investigation regarding the effect of temperature on the intensities of Raman lines in some typical liquids like carbon tetrachloride, benzene, chlorobenzene, etc., has been taken up.

## 2. Experimental

The experimental arrangements are the same as those described by the author in the previous communications. Light from a 6-inch quartz mercury arc lamp condensed by an 8-inch condenser is allowed to fall on the slit of the Raman tube containing the liquid under investigation. The scattered light coming out from the window of the tube is focussed on to the slit of a Fuess spectrograph. The Raman tube containing the liquid is heated by a specially made electric heater and a thermometer placed in contact with the tube indicated the temperature with an accuracy of  $\pm 2^\circ \text{C}$ . Intense and clear spectrograms are obtained in a very short time. The intensity of the source and the time of exposure are kept constant while obtaining the spectra at different temperatures. The Raman spectra at various temperatures along with a set of intensity marks given by the method of varying slit widths using the standard quartz globe tungsten ribbon lamp as the source are recorded on the same plate. The intensities of the various lines are computed in the usual way. As the lines did not show any appreciable broadening in the temperature region studied, only peak intensities have been compared.

## 3. Results and Discussion

Tables I, II, III and IV contain the results regarding the effect of temperature on the intensities of the Stokes Raman lines in liquid carbon tetrachloride, benzene, normal butyl alcohol and chlorobenzene respectively.

TABLE I. *Carbon Tetrachloride*

Frequency cm. <sup>-1</sup>	Temperature °K.	$\frac{I_R}{I_{305}}$ obs.	$\frac{I_R}{I_{305}}$ calc.	Quotient
215	305	1.00	1.00	1.00
	340	1.05	1.07	1.02
315	305	1.00	1.00	1.00
	340	0.94	1.05	1.12
460	305	1.00	1.00	1.00
	340	0.90	1.04	1.16
760	305	1.00	1.00	1.00
	340	0.84	1.01	1.20
790	305	1.00	1.00	1.00
	340	0.84	1.01	1.20

TABLE II. Benzene

Frequency cm. <sup>-1</sup>	Temperature °K.	$\frac{I_T}{I_{305}}$ obs.	$\frac{I_T}{I_{305}}$ calc.	Quotient
605	305	1.00	1.00	1.00
	345	0.89	1.03	1.16
850	305	1.00	1.00	1.00
	345	0.93	1.01	1.09
990	305	1.00	1.00	1.00
	345	0.97	1.01	1.04
1180	305	1.00	1.00	1.00
	345	0.90	1.01	1.12
1585	305	1.00	1.00	1.00
	345	0.89	1.00	1.12
1605	305	1.00	1.00	1.00
	345	0.91	1.00	1.10
3055	305	1.00	1.00	1.00
	345	0.97	1.00	1.03

TABLE III. Normal Butyl Alcohol

Frequency cm. <sup>-1</sup>	Temperature °K.	$\frac{I_T}{I_{305}}$ obs.	$\frac{I_T}{I_{305}}$ calc.	Quotient
825	305	1.00	1.00	1.00
	373	0.60	1.02	1.70
960	305	1.00	1.00	1.00
	373	0.72	1.02	1.42
1300	305	1.00	1.00	1.00
	373	0.76	1.01	1.33
1450	305	1.00	1.00	1.00
	373	0.75	1.00	1.33
2865	305	1.00	1.00	1.00
	373	0.76	1.00	1.32
2910	305	1.00	1.00	1.00
	373	0.80	1.00	1.25
2935	305	1.00	1.00	1.00
	373	0.82	1.00	1.22
2960	305	1.00	1.00	1.00
	373	0.82	1.00	1.22

TABLE IV. *Chlorobenzene*

Frequency cm. <sup>-1</sup>	Temperature °K.	$\frac{I_r}{I_{805}}$ obs.	$\frac{I_r}{I_{805}}$ calc.	Quotient
200	305	1.00	1.00	1.00
	358	0.88	1.10	1.25
	395	0.73	1.18	1.62
420	305	1.00	1.00	1.00
	358	0.87	1.06	1.22
	395	0.74	1.10	1.49
700	305	1.00	1.00	1.00
	358	0.92	1.02	1.11
	395	0.85	1.05	1.24
1000	305	1.00	1.00	1.00
	358	0.90	1.01	1.12
	395	0.78	1.02	1.31
1020	305	1.00	1.00	1.00
	358	0.91	1.01	1.11
	395	0.82	1.02	1.24
1080	305	1.00	1.00	1.00
	358	0.88	1.01	1.15
	395	0.75	1.02	1.36
1580	305	1.00	1.00	1.00
	358	0.92	1.00	1.09
	395	0.85	1.00	1.18
3065	305	1.00	1.00	1.00
	358	0.87	1.00	1.15
	395	0.73	1.00	1.37

Tables V and VI contain the results regarding the effect of temperature on the intensities of the anti-Stokes Raman lines in carbon tetrachloride and chlorobenzene respectively.

TABLE V. Carbon Tetrachloride

Frequency cm. <sup>-1</sup>	Temperature °K.	$\frac{I_T}{I_{305}}$ obs.	$\frac{I_T}{I_{305}}$ calc.	Quotient
-215	305	1.00	1.00	1.00
	340	1.12	1.19	1.06
-315	305	1.00	1.00	1.00
	340	1.18	1.24	1.05
-460	305	1.00	1.00	1.00
	340	1.22	1.31	1.07

TABLE VI. Chlorobenzene

Frequency cm. <sup>-1</sup>	Temperature °K.	$\frac{I_T}{I_{305}}$ obs.	$\frac{I_T}{I_{305}}$ calc.	Quotient
-200	305	1.00	1.00	1.00
	358	1.18	1.27	1.08
	395	1.25	1.45	1.16

Tables VII and VIII contain results regarding the effect of temperature on the ratio of the intensities of the Stokes and the anti-Stokes Raman lines in carbon tetrachloride and chlorobenzene respectively.

TABLE VII. Carbon Tetrachloride

Frequency cm. <sup>-1</sup>	Temperature °K.	$\frac{h\nu_j}{e^{kT}}$	$\left(\frac{\nu - \nu_j}{\nu + \nu_j}\right)^4 \frac{h\nu_j}{e^{kT}}$	$\frac{I_S}{I_{AS}}$ obs.
215	305	2.75	2.55	2.50
	340	2.48	2.30	2.34
315	305	4.40	3.95	4.08
	340	3.78	3.39	3.26
460	305	8.71	7.41	7.52
	340	6.97	5.93	5.60

TABLE VIII. Chlorobenzene

Frequency cm. <sup>-1</sup>	Temperature °K.	$\frac{h\nu_j}{e^{kT}}$	$\left(\frac{\nu - \nu_j}{\nu + \nu_j}\right)^4 \frac{h\nu_j}{e^{kT}}$	$\frac{I_S}{I_{AS}}$ obs.
200	305	2.56	2.39	2.53
	358	2.23	2.08	1.89
	395	2.07	1.93	1.48

From the results given above, the following conclusions may be drawn:—

(1) The Stokes lines decrease in intensity with increase of temperature excepting the line at  $215 \text{ cm}^{-1}$  in  $\text{CCl}_4$ .

(2) The anti-Stokes lines increase in intensity with increase of temperature but not to the expected extent.

(3) The ratio of the intensities of the Stokes and the anti-Stokes lines at various temperatures is in good agreement with the expected results.

In liquids, the large expansion at high temperatures causes a diminution in the density of the scattering medium and to that extent there will be a decrease in the number of effective scattering centres per unit volume. The effect of taking density into consideration is to increase the observed intensities of the Stokes lines. But in the cases studied in the present paper it can easily be seen that the intensities even after applying the correction for density, taking that the number of effective scattering centres per unit volume is inversely proportional to the density, are not equal to the calculated values.

A detailed explanation of the results obtained by the author both in solids and liquids will be dealt with in a separate communication.

#### 4. Summary

The effect of temperature on the intensities of the Raman lines in some typical liquids like carbon tetrachloride, benzene, normal butyl alcohol and chlorobenzene has been studied. It has been found that the Stokes lines in all the cases studied, excepting the line at  $215 \text{ cm}^{-1}$  in  $\text{CCl}_4$ , decrease in intensity with increase of temperature whereas the anti-Stokes lines increase in intensity but not to the expected extent. The ratio of the intensities of the Stokes and anti-Stokes lines, however, is in good agreement with the calculated value. The intensities of the Stokes lines, even after applying the correction for the change in density on the assumption that the number of effective scattering centres will be inversely proportional to the density, are not equal to the calculated values.

In conclusion, the author desires to express his grateful thanks to Prof. S. Bhagavantam, HON.D.Sc., for his kind interest in the work.

#### REFERENCES

1. Landsberg and Mandelstamm *Z. f. Phys.*, 1930, **60**, 364.
2. Ornstein and Went .. *Physica*, 1935, **2**, 503.
3. Venkateswarlu .. *Proc. Ind. Acad. Sci.*, 1941, **14**, 529.
4. \_\_\_\_\_ .. *Ibid.*, 1942, **16**, 45.
5. Krishnan .. *Nature*, 1928, **122**, 650.
6. Ananthakrishnan .. *Curr. Sci.*, 1936, **4**, 868.
7. \_\_\_\_\_ .. *Proc. Ind. Acad. Sci.*, 1937, **7**, 196.

# THE NEW LIGHT-EFFECT IN CHLORINE UNDER ELECTRICAL DISCHARGE

Part I. Influence of Different Irradiations on the Production of the Phenomenon under Constant Electrical Conditions

BY P. G. DEO, M.Sc.

(Research Scholar, College of Science, Benares Hindu University)

Received January 3, 1944

(Communicated by Prof. S. S. Joshi, D.Sc., F.A.Sc.)

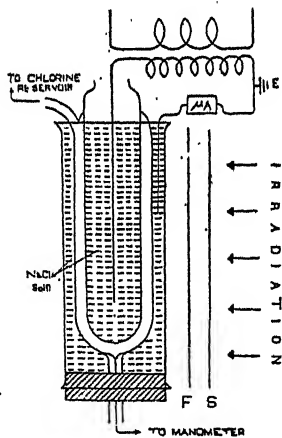
THAT the *new light-effect*<sup>1,2,3</sup> is markedly sensitive to but small variations in the magnitude of the numerous factors characteristic of an electrical discharge has been emphasized previously.<sup>4,5,6,8</sup> In the work now to be reported, as far as practicable, all these factors, such as the gas pressure (11 cm. Hg), applied potential (about 9400 volts r.m.s.), the temperature (23° C.), the frequency of the A.C. supply (50 cycles per second), 'ageing' of the system under the discharge, etc., have been kept constant. The only principal factor which has been allowed to vary is the nature of the light-source. These results (which are essentially an extension of earlier, preliminary ones,<sup>2,3,6</sup> were possible due to the loan of a Cambridge A.C. microammeter) reveal a new type of a *light-effect*, in which *i* the current produced under an electrical discharge in chlorine and other gases, is *diminished* on exposure to light. This diminution is instantaneous and also reversible, i.e., *i* under light is restored fully to the initial value on shutting off the light.<sup>5</sup>

The electrical discharge was produced in the annular space of a Siemens' type, soft glass ozoniser A (Fig. 1) filled at 11 cm. pressure with chlorine which was purified over liquid air. The ozoniser terminals, represented by a moderately concentrated saline solution inside the inner tube and in the bath surrounding the outer tube of the ozoniser, were connected to the secondaries of a high tension transformer. Its voltage was kept constant at the above-mentioned value by hand regulation of a variable rheostat introduced in the primary of the transformer. The discharge current *i* flowing through the ozoniser at the above potential was observed with an A.C. microammeter ( $\mu$ A in Fig. 1) connected between the earth and one of the ozoniser terminals. The microammeter was shunted with a *non-inductive* resistance varied in the range 100 to 700 ohms.

Five principal series of experiments were carried out using (a) 200 watt, 220 volt incandescent bulb, (b) copper arc, (c) iron arc, (d) carbon arc and (e) mercury vapour lamp. Employing each of these light-sources, four sets of observations were carried out for the *light-effect*, i.e., the diminution of  $i$  produced, when (i) the ozoniser was irradiated directly, and when each of *a*, *b*, *c*, *d* and *e* was screened successively with (ii) the red, (iii) green and (iv) violet filters kept at F in Fig. 1. For this purpose, long strips of carefully selected coloured glass were employed. The transmission-limits of each of the filters were observed with a Hilger's constant deviation glass spectrograph (Table I).

The ozoniser A was enclosed in an opaque box with a window in one side which could be closed with the desired light-filter, F. A shutter (S, in Fig. 1) next to the light-filter and worked by a pulley arrangement allowed light from any of the sources, to irradiate the ozoniser after passing through the filter F. The current in the dark was measured *with the light-source on*,

FIG. 1 (OZONISER A)  
EFFECT OF LIGHT ON ELECTRICAL DISCHARGE  
IN CHLORINE.



and the shutter S in position, so as to cover the filter F (Fig. 1); on moving the shutter, the ozoniser current diminished immediately due to light. These results are shown in Table I, in four vertical columns. Thus, for example, using (unfiltered) white light from the 200 watt incandescent bulb, results under the first column show the microammeter readings taken with a series of shunt resistances for  $i$  the current in the dark; the corresponding values on irradiation are shown in the next column. The difference is a measure of  $\Delta i$  the *light-effect*; this diminution is shown in the next column as a percentage of  $i$  the original current, in dark. These results show clearly

TABLE I (OZONISER A)  
Light-Effect under different kinds of Irradiation

Microammeter shunt	Filters											
	(i) White (7800-3700 Å)			(ii) Red (7070-6070 Å)			(iii) Green (5775-5070 Å)			(iv) Violet (4750-4000 Å)		
	<i>i</i>	In dark	Photo diminution %	<i>i</i>	In light	Photo diminution %	<i>i</i>	In dark	Photo diminution %	<i>i</i>	dark	Photo diminution %
Primary potential ..	..	..	35 volts (r.m.s.)							Transformer ratio ..	..	267
" current ..	..	..	About 0.25 amp.							Secondary potential ..	..	About 9400 volts (r.m.s.)
Frequency of the A.C. supply ..	..	..	50 cycles/sec.							Ozoniser A, PCl <sub>2</sub> ..	..	.., 11 cm.Hg (28 C.)
(a) Source of Irradiation : 200 watt bulb												
100	21	14	7	33	21	0.5	2	21.5	21	2	21	16
200	30	23	7	23	33	32.5	2	32	31.5	2	32	26
300	41	32	9	22	44	43	1	41	40.5	1	42	35
400	53	43	10	19	55	54	1	53	52.5	0.5	1	54
500	66	46.5	9.5	14	67	66	1	66	65	1	2	67
600	79	69.5	9.5	12	81	80	1	81	80	1	1	79
700	91	81.5	9.5	10	93	92	1	93	92	1	1	92
(b) Source of Irradiation : Copper arc												
100	22	17	5	22	22.5	22.5	0	0	22	21.5	2	21
200	32	26	6	19	33	33	0	0	32	31.5	1	31
300	42	34	8	19	43.5	43.5	0	0	43	42.5	1	42
400	53	54	9	17	55	55	0	0	54	53.5	1	54
500	66	57	9	14	67.5	67.5	0	0	66	65.5	1	67
600	80	70.5	9.5	11	80	80	0	0	78	77.5	1	80
700	91	82	9	10	91	91	0	0	91	90.5	1	92

TABLE—I (*Con'd*).

the general occurrence of the new effect, namely a photo-reduction of the conductivity under electrical discharge, a possibility which has been hitherto practically ignored in the now extensive literature on the electrical discharge phenomenon. The effect is seen to be as high as about 33%, 22%, 57%, 52% and 52% on direct irradiation from an incandescent bulb, copper arc, iron arc, carbon arc and mercury vapour lamp respectively. The interposition of a violet filter reduces the *light-effect* in all cases, to a value which at its maximum varies in the range 45 to 52%. The substitution of the green and red filters reduces markedly the corresponding *light-effect*. These results suggest that the effect varies in the order, white > violet > green, red.<sup>5,6,7,8</sup> The light-intensity is also a determining factor.<sup>5,6,7,8</sup> The much greater effect both under direct and violet filtered radiations, using both an iron arc and mercury vapour lamp, compared with that due to a 200 watt bulb is to be attributed to the fact that the short wave region is more intense in the former than in the latter.<sup>6,7,8</sup> An examination of the light intensities for *a*, *b*, *c*, *d* and *e* using the above filters with a P/1200 Kodak, super-panchromatic plate, a photoelectric cell and a thermopile has shown that the above quantity was lowest in green, the relative order being white (*i.e.*, unfiltered) > red > violet > green. That  $\Delta i$  the *light-effect* under green should be more than comparable with that due to red (Table I), despite the greater intensity available in the latter shows that intensity is the less predominant factor than frequency in determining the magnitude of this phenomenon, a deduction made previously from independent data.<sup>5,6,7,8</sup> In agreement with earlier results it is also seen that the *light-effect* under the direct (that is, unfiltered) radiations from any of the five light-sources employed is comparable with that due to the filtered violet.<sup>5,6,7,8</sup>

As has been suggested earlier,<sup>6,7,8</sup> a possible explanation of the fact that this *light-effect* is markedly greater under violet than under either green or red may be that the violet lies within the absorption spectrum of chlorine.<sup>9,10</sup> It is necessary, however, to draw attention to the considerations adduced by Joshi suggesting that the phenomenon might occur independently of the 'characteristic' light-absorption of chlorine.<sup>5,11</sup>

It is seen from Table I, say, in the case of *a*, the unfiltered white from the 200 watt bulb, that a change of the shunt resistance from 100 to 700 ohms has increased the microammeter deflection from 21 to 91 units for the discharge current in dark. It is remarkable, however, to see in all the cases that although  $\Delta i$  has increased from 7 to 9.5 units, the corresponding percentage photo-diminution has *decreased* from 33 to 10. Since no change in the main electrical constants of the discharge circuit has

been made with the exception of the microammeter shunt, it is to be anticipated on general grounds that the percentage photo-diminution would be sensibly constant. Work is in progress to investigate in some detail this apparent anomaly, as also the nature of other determinants for the production of this phenomenon.

Grateful thanks of the author are due to Dr. S. S. Joshi, D.Sc. (Lond.), F.A.Sc., Head of the Chemistry Department, for suggesting the problem and for valuable guidance during the work.

### *Summary*

Detailed results are given for the production of a *new light-effect in chlorine*. It is that the conductivity under an electrical discharge is reduced instantaneously and reversibly on irradiation. This effect increases by increasing the frequency and the intensity of light and that the former is the more important factor.

### REFERENCES

1. Joshi .. *Curr. Sci.*, 1939, 8, 548.
2. —— and Narasimhan .. *Ibid.*, 1940, 9, 536.
3. —— and Deshmukh .. *Nature*, 1941, 147, 806.
4. —— and co-workers .. *Proc. Indian Sci. Cong.*, 1940, Part III, Phys. Sec., Abst. 17; 1941, Part III, Chem. Sec., Abst. 34, 35; 1942, Part III, Phys. Sec., Abst. 36, 38; 1942, Part III, Chem. Sec., Abst. 50, 51, 55-70.
5. Joshi .. *Ibid.*, Presidential Address, Chem. Sec., pp. 70-75.
6. —— and Deo .. *Nature*, 1943, 151, 561.
7. —— .. *Curr. Sci.*, 1943, 11, 306.
8. Deo .. *Sci. & Cult.*, 1943, 9, 252.
9. Halban and Siedentoff .. *Z. Phys. Chem.*, 1922, 103, 71.
10. Elliott .. *Proc. Roy. Soc.*, 1929, A 123, 629.
11. Joshi .. *B. H. U. Journ.*, 1943, 8, 99-104.

# DIFFRACTION CORONÆ DUE TO NON-SPHERICAL PARTICLES

BY G. N. RAMACHANDRAN

(*From the Department of Physics, Indian Institute of Science, Bangalore*)

Received February 7, 1944

(Communicated by Sir C. V. Raman, Kt., F.R.S., N.L.)

## 1. Introduction

It is well known that if a number of opaque spherical particles are interposed in the path of a beam of light, they will give a corona consisting of bright and dark rings. To illustrate the formation of such coronæ, it is usual to employ lycopodium powder dusted on a glass plate which produces two or three bright rings. If, however, the lycopodium spores are observed under a microscope, it is found that their shape is not at all spherical. The shape can best be described as a tetrahedron with a spherical cap. In spite of this deviation from sphericity, it is remarkable that the lycopodium particles can give clear rings, the sizes of which can be verified to obey the circular disk formulæ fairly well.

It is commonly supposed that the formation of the rings is a sort of average effect and that different portions of the particles give rise to different sizes for the rings. Thus, if the shape of the particles does not differ from a sphere by a large amount, then these rings will be of nearly the same size, so that they can be observed. That this explanation is not correct will be seen from the following experiment.

Spores of "*pinus longifolia*" give a corona consisting of at least two bright rings. A photograph of the corona, together with a microphotograph of the spores, magnified about a hundred times, are reproduced in Fig. 4, Plate I. It will be seen from the photomicrograph that the shape of these spores does not at all approach that of a sphere. In fact, their maximum dimension is about double the minimum. Hence, if the formation of the corona is just an average effect, then no ring system must be visible. Actually, rings are visible, although they are not very clear on account of a large background intensity. It is therefore of interest to examine under what conditions a non-spherical particle can give rise to a visible ring system.

## 2. Diffraction Pattern of a Non-spherical Particle

In order to discuss the above problem, one has to consider somewhat in detail, the formation of a Fraunhofer diffraction pattern. Considering an aperture of arbitrary shape, and neglecting, as is generally done for small angle diffraction, the obliquity factor, it can be shown that the effect of the entire aperture at any point, other than the exact focus, reduces to that of a line distribution of light sources along its edge. This has been discussed by Rubinowicz (1917, 1924) and Laue (1936). But the result can be derived in a simple manner, and the simple derivation is given here for the sake of completeness.

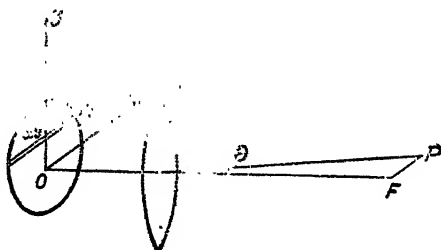


FIG. 1

Suppose that F is the focus of the lens (Fig. 1) and that it is required to find the intensity at a point P in the focal plane, at which the waves diffracted in a direction making an angle  $\theta$  with that of the incident wave are brought to a focus. Take a set of rectangular axes Ox and Oy in the aperture, so that the x-axis is parallel to FP. If the incident wave is represented by  $\sin Z$  (amplitude unity), then the amplitude at the point P is

$$\frac{1}{\lambda f} \iint \sin(Z - 2\pi x \sin \theta / \lambda) dx dy,$$

where the integration is performed over the whole aperture. Now, divide the aperture into a number of strips by means of lines parallel to the x-axis, the width of each strip being equal to  $dy$ . Integrating the above expression between the limits  $x_1$  and  $x_2$  which correspond to the extremities of one of these strips, the integral becomes

$$\frac{1}{2\pi f \sin \theta} \int [\cos(Z - 2\pi x \sin \theta / \lambda)]_{x_1}^{x_2} dy.$$

Now, calling the portion of the boundary intercepted by this strip as  $ds$ ,  $dy = ds \sin \phi$ , where  $\phi$  is the angle made by  $ds$  with the plane of diffraction, i.e., with the x-axis. Since the integral of  $dy$  vanishes when one makes a complete circuit round the edge, i.e.,  $\oint dy = \oint ds \sin \phi = 0$ ,  $\sin \phi$  must

be considered positive at one end of the strip, and negative at the other end. Hence, the effect of the entire aperture in the direction  $\theta$  may be written as

$$\frac{1}{2\pi f \sin \theta} \oint \cos(Z - 2\pi x \sin \theta/\lambda) \sin \phi \, ds.$$

This line integral is taken round the boundary of the aperture, and in it  $x$  and  $\sin \phi$  are to be regarded as functions of  $s$ . Hence, the resultant intensity is

$$I = (P^2 + Q^2)/4\pi^2 f^2 \sin^2 \theta, \text{ where}$$

$$P = \oint \cos(2\pi x \sin \theta/\lambda) \sin \phi \, ds \text{ and}$$

$$Q = \oint \sin(2\pi x \sin \theta/\lambda) \sin \phi \, ds.$$

Now, it is seen from the above formulæ that the parts of the edge for which  $\phi$  is zero, that is those which run parallel to the  $x$ -axis do not contribute anything to the intensity at the chosen point of observation,  $P$ . Indeed, we may go further, and state that the only sensible contributions are those made by parts of the edge running approximately parallel to the  $y$ -axis, for which  $\phi$  is nearly a right angle. For, the co-ordinate  $x$ , and therefore also the phase of the radiations, are stationary for these points, which may be designated as the ‘poles’ of the point of observation. Thus, in any case in which the aperture has a curved boundary without singularities, the line integral may be replaced by point sources placed at such poles, of which naturally there must be at least two. The diffraction pattern would then be regarded as the interferences of the radiation from these point sources. Geometrically, the positions of these sources are such that the tangents to the boundary at them are parallel, and are all perpendicular to the plane of diffraction. Such points may be said to be “opposed”, and they are responsible for the diffracted intensity in the direction considered. The existence of these poles has been observed experimentally by Banerjee (1919) and by Mitra (1919, 1920).

The problem thus reduces to finding such opposed points for a non-spherical particle. Then, the diffraction pattern will approximate to that given by a circular aperture, whose diameter is equal to the distance between these opposed points. It must be noted that when the diffraction corona is given by a large number of particles, the particles themselves are oriented in all directions, so that the pattern will always be circular. Hence, if the distance between the opposed points is a constant over a small region of the boundary, then the rings corresponding to this distance will stand out from the background intensity, the clarity of the rings being greater, the larger the region over which this distance is a constant. If, however, the shape of

the particle is completely arbitrary, and the distance is not a constant even for a small region, then no rings will be visible. Thus, the condition for the formation of a ring system is that the distance between the opposed points is a constant over an appreciable region of the boundary.

### 3. The Case of *Pinus longifolia*

The above criterion for the formation of a ring system by non-spherical particles directly explains why spores of *Pinus longifolia* must give rise to visible rings. The shape of this particle, as already mentioned, deviates very much from a sphere, the maximum and minimum dimensions being about  $55\ \mu$  and  $30\ \mu$ , so that if the corona is a sort of average effect, then one should expect no rings at all. However, on the idea of opposed point sources, the formation of the rings is easily understood.

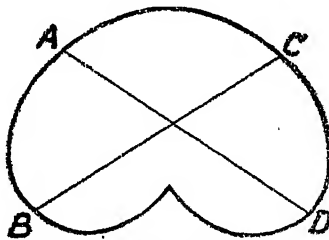


FIG. 2. Shape of *Pinus longifolia*

If one examines the shape of the particle as presented to the beam of light, it is found that it is mostly as shown in Fig. 2. In this cross-section, there is an appreciable portion of the boundary (AB and CD) over which the distance between the two opposed points is very nearly a constant. This, together with the fact that the particles are all orientated at random, is the reason why a visible system of rings is produced. Since the effective width varies rapidly in the other portions of the particle, the background intensity is quite large.

That this explanation of the formation of the rings is correct was verified by measurement. The diameters of the various rings were measured, and knowing the focal length, their angular radii were calculated. The distance AD or BC was determined from the microphotograph, as an average of a large number of measurements. This was found to be  $55\ \mu$ . Taking this value to be the diameter of a circular aperture, the angular radii of the rings in its diffraction pattern were calculated. These are tabulated in Table I below, and it will be seen from it that the agreement between the value calculated from the diameter, and the one measured is quite close,

showing that the rings correspond to the distance AD (or BC), as is to be expected from the theory.

TABLE I

Ring	Angular radius $\theta$		
	Calculated		Measured
1st Min.	..	..	0.0124
1st Max.	..	..	0.0169
2nd Min.	..	..	0.0221
2nd Max.	..	..	0.0274

#### 4. Coronae Produced by Lycopodium

As already stated, another typical example of a non-spherical particle is *Lycopodium*. The shape of a *Lycopodium* spore can best be described as a tetrahedron with a spherical cap. It is bounded by four sides, three of which are triangular planes while the fourth is spherical and convex. Hence, the cross-section presented by the *Lycopodium* spore to the incident beam of light may be approximately a circle, when the convex face is towards it, or a sector of circle, when one of the plane sides faces the beam. The latter (Fig. 3) is of more frequent occurrence, since the spore can rest on one of its plane sides. In fact, if the microphotograph is examined, it will be found that the circular shape is only of rare occurrence, while the commonest shape for the cross-section is that shown in Fig. 3. Intermediate shapes may also occur, but they resemble Fig. 3 in having a segment of a circle AB, and two lines OA and OB, which may be unequal.

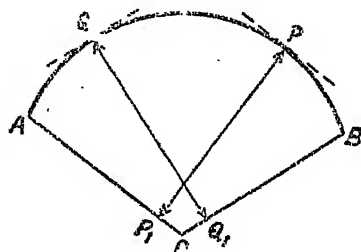


FIG. 3 Cross-Section of Lycopodium Spore

Let us therefore consider what the positions of the opposed points are for the shape shown in Fig. 3. The angle AOB is invariably greater than a right angle, so that there are points P and Q in the segment AB at which the tangents are parallel to OA and OB respectively. Hence, the opposed

sources are P and the whole line OA, and Q and the line OB. The distance between these are PP' and QQ', which are generally very nearly equal to each other. Hence the distance between the opposed sources is PP' or QQ'. Obviously, these opposed sources cover a very large portion of the boundary, so that the general background intensity given by the rest of the boundary is quite small. This is why the patterns with *Lycopodium* are much clearer than with *Pinus longifolia*.

There are, of course, variations in the size of the spores. These will give rise to a background intensity, which is discussed in the next section.

Thus, the ring system will correspond to the distance PP', (or QQ') i.e., the average value of PP' for all the particles. That this explanation of the formation of the rings is correct was verified as follows. The distances PP' and QQ' were actually measured from the microphotograph my means of a travelling microscope. The negative was rotated so as to bring OA (or OB) parallel to the vertical cross-wire, and the microscope was adjusted so that the cross-wire coincided with it. The microscope was then moved until the cross-wire was tangential to the curved boundary AB. The distance moved by the microscope gave a measure of PP', and since the magnification was known, the actual distance could be calculated. Both PP' and QQ' were measured for a large number of spores (both when they were nearly equal, and otherwise), and the average was determined.

This procedure was employed for two types of *Lycopodium*, *Lycopodium clavatum* and *Lycopodium bisdepuratum*, supplied by Merck, which were available in the laboratory. The values obtained were, for the *bisdepuratum* 33.1  $\mu$  and for the *clavatum* 34.4  $\mu$ . Taking this to be the diameter of the equivalent circular disk, the theoretical angular radii of the rings in

TABLE II

Ring	<i>Bisdepuratum</i>		Ring	<i>Clavatum</i>		
	Angular radius			Angular radius		
	Theoretical	Experimental		Theoretical	Experimental	
1st Min.	..	0.0206	0.0202	1st Min.	..	0.0194
1st Max.	..	0.0277	0.0280	1st Max.	..	0.0260
2nd Min.	..	0.0378	0.0361	2nd Min.	..	0.0355
2nd Max.	..	0.0454	0.0451	2nd Max.	..	0.0426
3rd Min.	..	0.0548	0.0533			0.0436
3rd Max.	..	0.0626	0.0615			

the corona were computed. The actual coronæ were also photographed, and the experimental values of these were calculated knowing the focal length of the lens. Enlarged pictures of the corona and also the microphotographs (magnification 94) are reproduced in Fig. 5, Plate I. The theoretical and experimental values of the angular radii are tabulated in Table II below. The agreement between the two is satisfactory, showing that the idea of the opposed points is true for *Lycopodium* also.

### 5. Coronæ due to Particles of Variable Size

It was mentioned in the previous section that variations in the size of the particles will affect the background intensity. The explanation of this is as follows. If there are a large number of spherical particles, whose size is not a constant, but varies slightly, then, the rings given by the different particles will not all be of the same size, but will be different. Consequently, the rings will not be perfectly bright and dark, but there will be some intensity in the dark portions also. This lack of darkness of the dark rings will be greater, the larger the variation in the size of the particles. If the variation is very large, the rings will be blotted out, and there will only be a continuous decrease of the intensity from the centre outwards.

It is also obvious that if the variation in the size of the particles is small then the position of the rings will very nearly correspond to those in the corona due to a sphere of the average size, but their intensities will differ from those in it.

The above results find a confirmation if one studies the coronæ given by the two types of *Lycopodium*. The most striking thing that is observed on looking at the photographs in Fig. 5 is the greater clarity and contrast of the rings given by the *bisdepuratum*. In fact, under identical conditions, three bright rings were visible in the negative of the corona of the *bisdepuratum*, while only two were seen in that of the *clavatum*. Also, the dark rings are darker, and the ring system clearer with the *bisdepuratum* as can be seen from Fig. 5.

The cause for this was investigated. A study of the microphotographs and a large number of observations under the microscope showed that the difference cannot be attributed to any difference in the shape of the particles, for they were both very nearly of the same shape. It was finally found that it must be ascribed to the difference in the range of particle-sizes in the two types. A large number of measurements of the size of the spores showed that the variation in the size was comparatively smaller for the *bisdepuratum* than for the other type. For the former, the size varied mostly between  $30 \mu$  and  $35 \mu$ , with only very few outside these limits. On the other hand,

for the latter, the variation was from  $30\ \mu$  to  $40\ \mu$ . This will be clear from the study of the following typical set of readings for the distance between the opposed points.

*Clavatum*.—Size in  $\mu$  32, 34, 31, 37, 37, 32, 33, 33, 30, 34,  
37, 33, 34, 34, 35, 36, 37, 39, 36, 37.

*Bisdepuratum*.—Size in  $\mu$  33, 34, 32, 31, 35, 34, 32, 34, 35, 34,  
31, 34, 33, 33, 30, 33, 33, 32, 33, 34.

The greater range of variation in the size of the *clavatum* spores clearly explains why the corona is less distinct with it than with the *bisdepuratum*.

The second result, namely that the radii of the rings correspond to a size which is the average has already been verified in the last section.

My best thanks are due to Prof. Sir C. V. Raman for the suggestion of the problem and for the kind guidance he gave me during the investigation.

#### Summary

It is pointed out that the Fraunhofer diffraction due to an obstacle of arbitrary shape can be replaced by that given by a linear distribution of sources along its boundary. Most of the intensity at any point in the pattern can again be supposed to originate from a finite number (usually two) of point sources, called "opposed points" or "poles", situated on the boundary. In this way, if there are a large number of non-spherical particles distributed at random, then a ring system will be formed whose size will correspond to the distance between the opposed points. If this distance is a constant over an appreciable region of the boundary, then the rings will stand out from the background intensity. This explanation of the formation of the rings, has been verified using spores of *Pinus longifolia* and of *Lycopodium*. It is also shown that variations in the size of the particles affect the clarity of the rings detrimentally, the rings becoming less and less clear as the range of particle sizes increases. This is also verified by using two types of *Lycopodium*.

#### REFERENCES

1. Banerjee, S. . . *Phil. Mag.*, 1919, **37**, 112.
2. Mitra, S. K. . . *Ibid.*, 1919, **38**, 289.
3. \_\_\_\_\_ . . . *Proc. Ind. Assoc. Cult. Sci.*, 1920, **6**, 1.
4. Laue, M. von . . . *Sitzungsber. Preuss. Akad. (Phys. Math. Klasse)*, 1936, 89.
5. Rubinowicz, A. . . *Ann. d. Physik*, 1917, **57**, 257.
6. \_\_\_\_\_ . . . *Ibid.*, 1924, **73**, 339.

# THE LUNAR ATMOSPHERIC TIDE AT BANGALORE (1895-1904)

BY C. SESHACHAR

(*Retired Meteorologist to Government, Bangalore*)

AND

V. R. THIRUVENKATACHAR

(*Department of Mathematics, Central College, Bangalore*)

Received February 18, 1944

(Communicated by Prof. B. S. Madhava Rao, D.Sc., F.A.Sc.)

## 1. *Introduction*

THE lunar atmospheric tide has been determined for a number of stations by Chapman and others. For stations in India the determinations have been made for Madras by Chapman,<sup>1</sup> for Bombay by Pramanik,<sup>2</sup> and for Kodaikanal and Periyakulam by Pramanik, Chatterjee and Joshi.<sup>3</sup> Since Kodaikanal is a high level station (7,480 ft.) and Periyakulam is at low-level (944 ft.), the latitudes for the two stations being nearly the same, it was expected that the investigation of the lunar tide at these two stations would throw some light on the influence of the altitude of the station on the lunar tide. As a result of their analysis Pramanik, Chatterjee and Joshi concluded that the amplitude of the semi-diurnal component of the lunar tide does not vary with the height of the station above sea-level. It was thought desirable to check this conclusion by an independent determination of the lunar tide at another high level station. With this object in view, the determination of the lunar atmospheric tide at Bangalore was undertaken and the results of the analysis of the data for Bangalore for the period 1895-1904 are presented in this paper. The determinations of Chapman include those for two other high level stations, *viz.*, Kimberley<sup>4</sup> and Mexico<sup>5</sup>; a comparison and discussion of these results is given in para 5 below.

## 2. *The Data*

Bangalore is situated in South India, its approximate geographical co-ordinates being: latitude  $12^{\circ} 58' N.$ , longitude  $77^{\circ} 35' E.$  The height of the barometer cistern above sea-level is 3,021 feet. The hourly values of the barometric pressure used in this paper were obtained from the tabulations of a Kew pattern photographically recording barograph. The readings were made at exact hours of local mean time and compared with those of a standard barometer.

### 3. General Plan of the Reductions

The method of reduction adopted was similar to that used by Chapman in his determinations. The solar diurnal variation was removed before the hourly values were retabulated according to lunar time. In this paper data have been used to the nearest .01 inch, and days of range greater than or equal to .07 inch after the removal of the solar diurnal variation have been excluded. The lunar day was treated as having a duration of 25 solar hours but 26 hourly entries were made in order to allow for non-cyclic variation. Greenwich times of lunar transit at Greenwich (as given in the Nautical Almanac) were used instead of the local times of local lunar transit. On this account a phase-correction of  $-5^{\circ} 21'$  was applied to the calculated phase angle  $\theta_2$ .

The material was subdivided, according to season, into three parts as follows :—

J = June Solstice = May, June, July and August.

E = Equinox = March, April, September and October.

D = Winter = November, December, January and February.

In addition, the lunar days were grouped according to lunar distance and separate inequalities were formed for groups of days centred at apogee and perigee. The period of 10 years was divided into two five-year groups and each set of data was independently reduced. The various sets of lunar hourly inequalities were then harmonically analysed and the semidiurnal component was derived in the form  $C_2 \sin(2t + \theta_2)$ , where  $t$  denotes time reckoned from lunar transit.

### 4. The Results

The following are the results for the seasonal and annual mean lunar tide at Bangalore. ( $N$  = number of days in the group.) The unit of pressure is 1 microbar.

Period	J = Summer			E = Equinox			D = Winter			Year			
	N	C <sub>2</sub>	$\theta_2$	N	C <sub>2</sub>	$\theta_2$	N	C <sub>2</sub>	$\theta_2$	N	C <sub>2</sub>	$\theta_2$	
1895-1899 ..	..	514	50	95°	543	52	100°	557	34	59°	1614	46	86°
1900-1904 ..	..	513	55	90°	557	45	92°	553	44	59°	1623	45	81°
1895-1904 ..	..	1027	50	90°	1100	49	97°	1110	41	57°	3237	46	84°

The accordance of the figures for the two groups of years is not quite good for the seasonal tide but the figures for the annual tide for the two

groups of years are in excellent accord. The results for the groups of days centred at apogee and perigee are as follow:—

	A			P		
	N	C <sub>2</sub>	θ <sub>2</sub>	N	C <sub>2</sub>	θ <sub>2</sub>
1895-1899 .. ..	391	35	88°	375	61	97°
1900-1904 .. ..	379	46	92°	386	47	90°
1895-1904 .. ..	770	41	90°	761	55	93°

### 5. Discussion

The seasonal variations in the amplitude and phase are similar to those at Madras and most other stations, the phase and amplitude being less in winter than at the other two seasons. The June-value of the amplitude is greater than the equinoctial value but the reverse is the case for the phase.

The amplitude is also greater at perigee than at apogee thus showing the expected type of variation with lunar distance. The effect is however more marked for the first group of years than for the second.

It has been mentioned in para 1 above that on the basis of the results for Periyakulam and Kodaikanal, Pramanik, Chatterjee and Joshi came to the conclusion that the amplitude of the lunar tide does not vary with the altitude of the station. With a view to discussing this question we collect below the results for some stations of increasing height above sea-level and in neighbouring latitudes, for which determinations of the lunar tide are available:—

Station	Latitude	Altitude (in feet)	C <sub>2</sub>
Madras .. .. ..	13° 01' N.	..	53
Bombay .. .. ..	18° 54' N.	..	49
Periyakulam .. .. ..	10° 09' N.	944	52
Bangalore .. .. ..	12° 58' N.	3,021	46
Kimberley .. .. ..	28° 42' S.	3,944	46
Mexico .. .. ..	19° 04' N.	7,480	35
Kodaikanal .. .. ..	10° 14' N.	7,688	52

It will be seen that the amplitude decreases from Madras to Bangalore and from Bangalore to Mexico, corresponding to the increasing altitude. The values for Periyakulam at a small altitude and for Kimberley at an altitude approximately the same as that of Bangalore fit well into this scheme. Kodaikanal only seems to form a serious exception. According to

Pramanik, Chatterjee and Joshi the data for Kodaikanal and Periyakularam are not so reliable. Even if these two stations be omitted, it will be seen that the remaining figures indicate a decrease in the amplitude of the lunar tide with increasing altitude of the station. But on the dynamical theory of atmospheric oscillations as developed by Lamb, Chapman and others, in an atmosphere with a uniform vertical temperature-gradient (as is nearly the case for the first 10 km. of the actual atmosphere), the amplitude should be practically independent of the altitude.<sup>6</sup> It must however be borne in mind that while the theoretical result refers to the variation of the amplitude with altitude at a single station, the observational results given above refer to different stations and the latter may be affected to some extent by differences of local conditions. Whether the decrease in amplitude indicated by the data given above is merely an accidental one or whether it represents a systematic decrease with altitude can only be settled by the determination of the lunar atmospheric tide at a few more stations of high altitude.

#### 6. Summary

The lunar atmospheric tide at Bangalore has been determined, using the data for 1895-1904. The result is that the semi-diurnal component of the annual mean tide at Bangalore may be represented by  $46 \sin(2t + 84^\circ)$ . The seasonal variation of the tide is similar to that at most other stations in that the amplitude and phase are minimum in winter. The dependence on lunar distance is also well shown, the amplitude at apogee being much less than that at perigee. A comparison of the results for Bangalore and other stations at different altitudes suggests that the amplitude diminishes with increasing altitude.

#### REFERENCES

1. Chapman .. *Mem. Roy. Met. Soc.*, 1928, **2**, No. 19.
2. Pramanik .. *Mem. Ind. Met. Dept.*, 1931, **25**, Part VIII.
3. ———, Chatterjee and Joshi *Ind. Met. Dept. Sci. Notes*, 1931, **4**, No. 31.
4. Chapman .. *Mem. Roy. Met. Soc.*, 1932, **4**, No. 33.
5. ——— .. *Ibid.*, 1928, **19**, No. 19.
6. ——— .. *Quart. J. Roy. Met. Soc.*, 1924, **50**, No. 211, 191.

# FLUORESCENCE SPECTRUM OF URANYL FLUORIDE

BY D. D. PANT AND N. D. SAKHWALKAR

(*From the Department of Physics, Indian Institute of Science, Bangalore*)

Received January 30, 1944

(Communicated by Sir C. V. Raman, Kt., F.R.S., N.L.)

## 1. Introduction

THE green fluorescence of uranyl compounds originally discovered by Stokes in 1852 was later studied in detail by various workers namely, Becquerel (1872), Morton and Bolton (1873), Hagenbach (1872), Becquerel and Onnes (1909) and several others. Nichols and Howes (1919) in collaboration with Merrit, Wilber and Wick very extensively studied the fluorescence and absorption spectra of a large number of uranyl salts both at room and liquid-air temperatures. Their work shows that the fluorescence spectra at ordinary temperature consist of eight broad and diffuse bands. On reducing the temperature to that of liquid air, the first and the eighth bands disappear and the remaining six get resolved into several line-like components. The new spectrum which now consists of several sharp and discrete bands falls into six regularly spaced groups of bands. The components contained in a group are the members of different series of bands. The frequency interval between two successive members of the same series is nearly  $860 \text{ cm}^{-1}$ . In the corresponding absorption spectra this interval diminishes to  $700 \text{ cm}^{-1}$ ; both in fluorescence and absorption spectra it varies only slightly from compound to compound, and small variations are also sometimes noticed from series to series in the same spectrum.

This regularity in the spectra and the fact that only those compounds of uranium which possess the uranyl ( $\text{UO}_2$ ) group are fluorescent led Nichols and Howes to suggest that the constant frequency intervals are due to the uranium oxide. Dieke and Van Heel (1925) explained the constancy in the frequency intervals by attributing the observed bands to a simultaneous change of the electronic moment and of the oscillations of the nuclei of the  $\text{UO}_2$  molecule. Thus, by assuming the oscillation frequency to be  $860 \text{ cm}^{-1}$  the main frequency interval observed in the fluorescence spectra could easily be explained. But unfortunately, the appearance of the large number of

bands and the smaller frequency intervals cannot be understood on this simple idea. Van Heel (1925) assuming the existence of one more frequency which he attributed to the vibration of  $\text{UO}_2$  in the crystalline space-lattice attempted an interpretation of the bands. But as will be shown elsewhere, his explanation of the spectra is not satisfactory for various reasons. Furthermore, the subject requires to be revised in the light of the new information regarding the vibrations of the  $\text{UO}_2^{++}$  molecule which has been obtained quite recently from the studies of Raman and infra-red spectra of uranyl salts in solution and solid state respectively by Conn and Wu (1938) and by studies of Raman spectra in solution of uranyl chloride by Satyanarayana (1942).

In this connection it will be mentioned that till now the uranyl compounds studied were of complicated structure like nitrates, double nitrates, sulphates, double sulphates, double chlorides, acetates, and phosphates. The comparatively simpler substances such as the uranyl halides were left out, apparently because of their weak fluorescence. However, as these substances, on account of their simpler structure are more likely to reveal the mechanism of fluorescence in uranyl compounds, a study of fluorescence spectrum of uranyl fluoride was undertaken in the present investigation.

## 2. *Experimental Arrangement*

The salt was in the form of a greenish grey powder and contained water of crystallisation. But unlike many other uranyl salts it was not hygroscopic. The experimental arrangement for studying the fluorescence spectrum of the salt at liquid-air temperature was quite simple. It consisted of two rods—one of copper and the other of wood—joined together to form a longer rod. A rectangular slot with a hole in the middle (which was useful for experiments on absorption spectra only) was made in the copper portion of the rod. The latter was held vertically by clamping the wooden portion, while the copper portion was immersed in liquid air contained in a Dewar flask. A small rectangular glass cell which contained the salt was placed tightly in the slot. The cell was made of two rectangular glass plates of the dimensions of the slot which were sealed on the edges by beeswax. Light from an iron arc after having been filtered through a Wood's glass and a water cell was focussed on the salt. The fluorescence radiation which did not pass through liquid air, was condensed on the slit of a Fuess glass spectrograph and the spectrum was recorded on Ilford HP2 plates. However, the intensity of fluorescence was so weak that even after an exposure of nine hours, only a few bands have appeared on the plate.

### 3. Results

The wave-numbers of the observed bands have already been reported by one of us (Pant, 1943). However, the accompanying table gives the results of more accurate measurements.

TABLE I

Group Series	1	2	3	4	5	Average $\Delta\nu$
A	20234 (W)	19366 (d)	18504 (d)	17641 (W)		864
B	20082 (S)	19217 (S)	18353 (S)	17492 (m)	*16640 (W)	863
C		19150 (d)	18289 (d)	17427 (m)	*16577 (W)	862
D		19124 (d)	18263 (W)	*17404 (W)		861
E		18970 (W?)				

\* Visually estimated values

? Fe line

S = Strong

m = Medium

d = Dim

W = Weak

### 4. Interpretation of the Results

The fluorescence spectrum of uranyl fluoride is the simplest of all the observed spectra of uranyl salts. This is so because owing to weak fluorescence of the substance, only the stronger bands have been recorded. The interpretation of the spectrum becomes very simple when attempted on the basis of the data for the vibrational frequencies of the  $\text{UO}_2^{++}$  ion. Three frequencies are known from the studies of Raman and infra-red spectra namely  $\nu_1$  (valence frequency) =  $860 \text{ cm}^{-1}$ ,  $\nu_2$  (deformational frequency) =  $210 \text{ cm}^{-1}$  and  $\nu_3$  (anti-symmetric frequency) =  $930 \text{ cm}^{-1}$ . In the energy level diagram given below we have (i) the electronic frequency  $\epsilon = 200$   $82 \text{ cm}^{-1}$ , (ii)  $\nu_1 = 863 \text{ cm}^{-1}$ , (iii)  $\nu_2 = 242 \text{ cm}^{-1}$  and (iv)  $\nu_3 = 928 \text{ cm}^{-1}$ . Transitions are also involved from a level at  $150 \text{ cm}^{-1}$  higher than the excited electronic state. This represents the first quantum level of the deformational vibration ( $\nu_2'$ ) in the excited state. The vibrations are practically harmonic. The valence frequency is the predominating one and other frequencies combine with the integral multiples of  $\nu_1$ .

We shall denote the quantum numbers of the vibrational levels of the ground state by  $(n_1, n_2, n_3)$  where  $n_1, n_2$  and  $n_3$  are the numbers denoting the multiples of frequencies  $\nu_1, \nu_2$  and  $\nu_3$  respectively, and the corresponding energy levels in the excited state will be denoted by  $(n_1, n_2, n_3)'$ . The various bands can now be obtained as transitions from the two excited states  $(0, 0, 0)'$  and  $(0, 1, 0)'$  to the various levels of the ground state, all transitions being allowed.

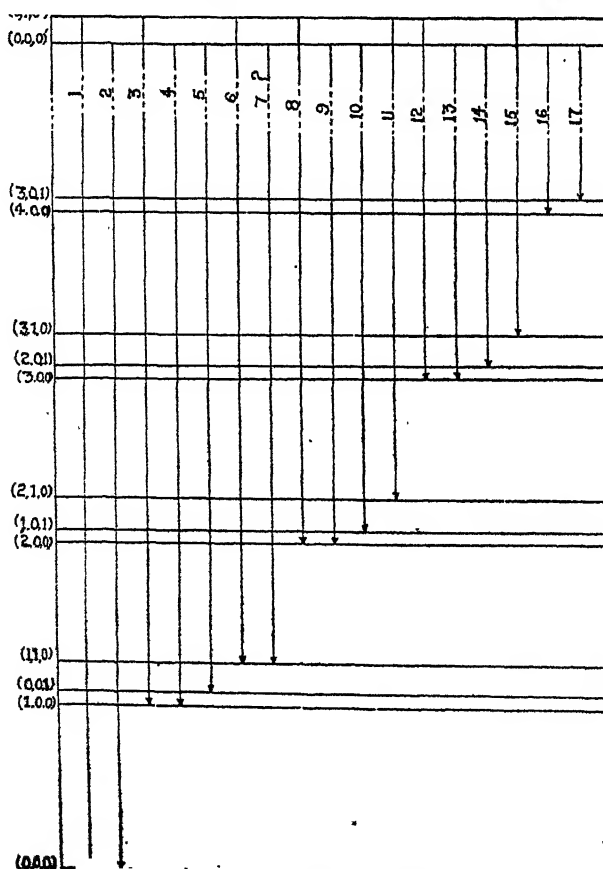
Table II which shows the transitions that give rise to the fluorescence bands in uranyl fluoride at  $-185^\circ$  is further illustrated with the following energy level diagram.

TABLE II

Serial No.	Transitions		Frequency in cm. <sup>-1</sup>			Remarks
	From	To	Calculated	Observed	$\Delta v$	
1	(0, 1, 0)'	(0, 0, 0)	20232	20234	- 2	
2	(0, 0, 0)'	(0, 0, 0)	20082	20082	0	
3	(0, 1, 0)'	(1, 0, 0)	19369	19369	+ 3	
4	(0, 0, 0)'	(1, 0, 0)	19219	19217	+ 2	
5	(0, 0, 0)'	(0, 0, 1)	19154	19150	+ 4	
6	(0, 1, 0)'	(1, 1, 0)	19127	19124	+ 3	
7	(0, 0, 0)'	(1, 1, 0)	18977	18970	+ 7	
8	(0, 1, 0)'	(2, 0, 0)	18306	18504	+ 2	
9	(0, 0, 0)'	(2, 0, 0)	18356	18353	+ 3	
10	(0, 0, 0)'	(1, 0, 1)	18291	18289	+ 2	
11	(0, 1, 0)'	(2, 1, 0)	18264	18263	+ 1	
12	(0, 1, 0)'	(3, 0, 0)	17644	17641	+ 3	
13	(0, 0, 0)'	(3, 0, 0)	17494	17492	+ 2	
14	(0, 0, 0)'	(2, 0, 1)	17429	17427	+ 2	
15	(0, 1, 0)'	(3, 1, 0)	17402	17404	- 2	
16	(0, 0, 0)'	(4, 0, 0)	16631	16640	- 9	
17	(0, 0, 0)'	(3, 0, 1)	16566	16577	- 11	

C coinides with iron line

Visually estimated values



Energy level diagram for the fluorescence spectrum of uranyl fluoride at liquid-air temperature

An objection that can be raised against the scheme of energy levels given above is that it takes all the three vibrational frequencies as allowed in transition while some of these, according to strict selection rules, are forbidden. However, these rules are never so strictly obeyed and even in the spectra of gaseous polyatomic molecules, departures have been observed. To apply the selection rules to the case of spectra of crystals where forbidden transitions are commonly met with, is not correct. We are therefore, justified in making use of all the three frequencies for explaining the observed spectrum. Further, it will be seen, that all the bands arise due to transitions from only two neighbouring levels  $(0, 0, 0)'$  and  $(0, 1, 0)'$  to the various levels of the ground state, in spite of the fact that the frequency of the exciting radiation (nearly  $27000 \text{ cm}^{-1}$ ) is much higher than the frequency of the electronic band  $(0, 0, 0)' - (0, 0, 0)$  ( $20082 \text{ cm}^{-1}$ ). This instead of being a defect, is a strong point in favour of the scheme of energy levels and is further supported by the fact that fluorescence spectra of uranyl salts are largely independent of the exciting wavelengths. Nichols and Howes for example, find that at room temperature the fluorescence spectra are independent of the mode of excitation. Further, the experiments of Van Heel (1925) on the monochromatic excitation of the fluorescence of uranyl potassium sulphate and autunite (calcium uranyl phosphate) at liquid air and liquid hydrogen temperatures clearly show that the fluorescence bands mainly arise from the excited electronic state. For, as soon as the frequency of the exciting radiation becomes equal to the frequency difference between the ground and excited electronic states, not only the strong lines but also the weak lines make their appearance in the fluorescence spectrum. However, it is not mentioned definitely whether the full spectrum appears at this stage. No definite mechanism for such a behaviour can be suggested at present, but it is obvious that following the excitation of the uranyl ion there must be a redistribution of vibrational energy in such a way that the electronic or the vibrational states important in the fluorescence emission are not very dependent on the wavelength of the exciting light. The loss of extra vibrational energy can be brought about either by collisions with the uranyl ions or by the removal of this energy to the entire crystal in form of lattice oscillations. In the case of uranyl fluoride, the energy after redistribution is concentrated partly in the electronic  $(0, 0, 0)'$  state and partly in the vibrational  $(0, 1, 0)'$  state. But the vibrational state is more thinly populated than the electronic state, because the bands arising from the former are weak in comparison to those arising from the electronic level.

In conclusion, the authors wish to express their indebtedness to Prof. Sir C. V. Raman for suggesting the problem and for guidance during the course of the work.

*Summary*

The fluorescence spectrum of solid uranyl fluoride has been studied at liquid-air temperature. The spectrum which consists of 17 sharp and discrete bands is classified into 5 groups and 5 series. The bands have been interpreted as being due to the transitions from  $(0, 0, 0)'$  and  $(0, 1, 0)'$  levels to the various vibrational levels of the ground state. All the three frequencies of the uranyl ion have been taken into account for the interpretation.

## REFERENCES

1. Nichols and Howes	.. <i>Fluorescence of Uranyl Salts</i> , Carnegie Institute Publications, No. 298, 1919.
2. Dieke and Van Heel	.. <i>Leiden Communications</i> , 1925, Suppl. No. 55 A.
3. Van Heel	.. <i>Ibid.</i> , 1925, Suppl. No. 55 B.
4. _____	.. <i>Ibid.</i> , 1925, Suppl. No. 187 A.
5. Conn and Wu	.. <i>Trans. Farad. Soc.</i> , 1938, <b>34</b> , 1483.
6. Satyanarayana	.. <i>Proc. Ind. Acad. Sci.</i> , 1942, <b>15</b> , 414.
7. Pant	.. <i>Ibid.</i> , 1943, <b>18</b> , 309.

## 5-HYDROXY AND METHOXY FLAVYLIUM SALTS

BY L. RAMACHANDRA ROW AND T. R. SESHADRI

(From the Department of Chemistry, Andhra University, Waltair, now at Madras)

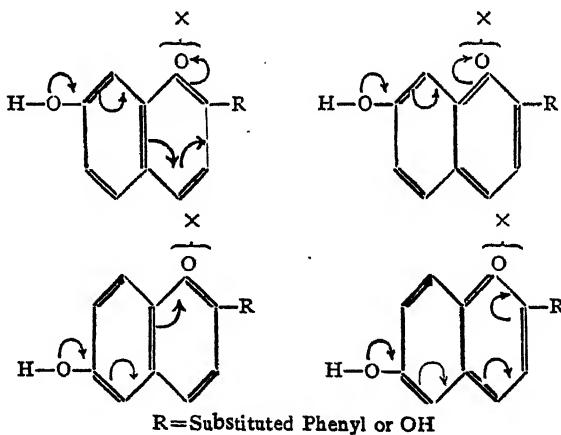
Received January 25, 1944

STARTING from  $\gamma$ -resorcyclic aldehyde<sup>1</sup> typical 5-hydroxy and-methoxy flavylium salts have now been prepared mainly with a view to study their fluorescence in solutions. Improved procedures for the preparation of the aldehyde and its methyl ether are described in the experimental part of this paper. By adopting them better yields are obtained and the operations are made easier. Attempts to condense the aldehyde with acetophenone itself have not been successful, but condensation has been effected with hydroxy substituted acetophenones and their acetates. In their colour reactions these new flavylium salts are less intense as compared with the 7-substituted isomers and their fluorescence in solutions is almost negligible.

Fluorescence emission of flavylium salts is maximum in concentrated sulphuric acid solutions, less intense in alcohol and minimum in aqueous medium. Only those that are very intense in sulphuric acid give detectable fluorescence in aqueous acid solutions. Ridgway and Robinson<sup>2</sup> reported that most simply constituted flavylium salts exhibit fluorescence in concentrated sulphuric acid though only a few having methoxyl or hydroxyl in the 7 or 6 positions retain it on dilution with water. The 7th position is the most favourable and the 6th comes next. They found that the 8th position is definitely inhibitive since 8-methoxy compounds had an almost negligible fluorescence even in sulphuric acid solution. From the results presented in this paper the 5th position seems to be similarly unfavourable. Further, Pelargonidin does not give fluorescence in alcoholic solutions though it contains a hydroxyl group in position 7; the 5-hydroxyl present in this molecule seems to have a definite inhibitory effect. If the 5-hydroxyl is modified by glucoside formation, is methylated or benzoylated or replaced altogether by a methyl group fluorescence reappears.<sup>3</sup> Flavylium salts with 7:8 combination of hydroxyl groups have been recently prepared by Robinson and Vasey.<sup>4</sup> They have not recorded any fluorescence; it is possible it was not noticeable in alcoholic or aqueous solutions. Detailed data do not seem to be available relating to the influence of the hydroxyl groups in the 3-position and in the side phenyl nucleus. In general as the number of these groups increases absorption colour is intensified. Visible

fluorescence also seems to increase up to a particular stage, but later on is lost either due to the shifting of the fluorescence band to the infra-red or due to degeneration of the energy into heat.

In some previous publications<sup>5</sup> the structural characters governing fluorescence in coumarins were discussed. With regard to the above-mentioned influence of the position of the hydroxy and methoxy groups on fluorescence emission, the similarity between flavylium salts and coumarins<sup>5</sup> is striking. It may be fortuitous or may be due to similar mechanisms functioning in both groups of compounds. The following suggestion may, however, be made. If we take into consideration only solutions in concentrated sulphuric acid in which the resemblance is closest, coumarins can form hydroxy pyrylium salts. For either of the structural formulæ that could be given for the pyrylium salts resonance originating from 7 and 6 positions may be represented as below. It is possible that the conditions represented by them are the optimum for producing visible fluorescence. The effect should be comparatively inferior from the 6th position since electromeric changes cannot be so facile as when the 7th position is involved.



### Experimental

$\gamma$ -Resorcylic aldehyde was prepared by the decarboxylation of 2:4-dihydroxy-3-formyl benzoic acid (Shah and Laiwalla<sup>1</sup>). Using a modified procedure for the decarboxylation and for the subsequent purification, the preparation was rendered more easy and the yield enhanced.

The aldehydo acid (6.5 g.) and water (100 c.c.) were taken in an open pyrex conical flask (250 c.c. capacity) which was placed in an autoclave containing about 200 c.c. of water. The autoclave was closed tight and heated at 108–10° for eight hours. The contents were allowed to cool,

pressure released, and the autoclave opened. The reddish-brown solid product found in the flask was extracted with ether repeatedly and the ethereal solution evaporated. A reddish oily residue (about 5 g.) was left behind which solidified in the course of a few hours. It was purified by dissolving in acetone and treating the solution with petroleum ether when an amorphous brown impurity was deposited. The liquid was filtered and the filtrate carefully concentrated when pale yellow needles of  $\gamma$ -resorcylic aldehyde (3.5 gm.) were obtained.

The monomethyl ether of the above aldehyde was originally prepared in an indirect way by Limaye.<sup>6</sup> Direct methylation using aqueous alkali and dimethyl sulphate or methyl iodide gave mainly the dimethyl ether. The mono-methyl ether could, however, be obtained directly from  $\gamma$ -resorcylic aldehyde by adopting the following procedure for the methylation.

$\gamma$ -Resorcylic aldehyde (0.1 g.) was dissolved in anhydrous benzene (20 c.c.) and treated with one molecular proportion of dimethyl sulphate in benzene solution and anhydrous potassium carbonate in excess (2.3 g.). After refluxing for 15 hours the mixture was treated with 10 c.c. of cold water in order to dissolve the potassium carbonate. The benzene layer was then separated and washed with a little water. It was then repeatedly extracted with aqueous sodium hydroxide (3%). The alkaline layer was acidified with hydrochloric acid, when the monomethyl ether of  $\gamma$ -resorcylic aldehyde separated out as a fine crystalline mass. It then crystallised from boiling water as clusters of long needles melting at 76-77° C.; yield 65%. (Limaye m.p. 75° C.)

*3:5:4'-Trihydroxy-flavylium chloride.*— $\gamma$ -Resorcylic aldehyde (0.2 g.) and  $\omega:p$ -dihydroxy acetophenone (0.2 g.) were dissolved in dry ethyl acetate, the solution saturated at 0° with dry hydrogen chloride and the gas passed slowly for a further period of 4 hours. The solution turned gradually red and after about an hour began to deposit bright red crystals of the flavylium chloride. It was kept overnight in a refrigerator and the crystals were filtered and washed with anhydrous ether. On recrystallisation from 2% aqueous methyl alcoholic hydrochloric acid, bright red needles with metallic lustre were obtained. Yield 63%. The product did not melt below 300° C. (Found: C, 61.4; H, 3.4;  $C_{15}H_{11}O_4$  Cl requires C, 62.0 and H, 3.8%).

*5-Methoxy-3:4'-dihydroxy-flavylium chloride* was prepared from the monomethyl ether of  $\gamma$ -resorcylic aldehyde adopting exactly the procedure given above. It was a dark red solid with a characteristic metallic sheen and appearing under the microscope as rhombic plates. It melted at 258-60°. (Found: C, 63.5; H, 4.0;  $C_{16}H_{13}O_4$  Cl requires C, 63.1 and H, 4.3%).

*3:5:3':4'-Tetrahydroxy-flavylium chloride.*—For preparing this substance  $\gamma$ -resorcylic aldehyde had to be condensed with  $\omega$ :3:4-triacetoxy acetophenone. On previous occasions when this ketone had to be used for flavylium salt synthesis a mixture of anhydrous ethyl acetate and anhydrous alcohol was used as solvent. Flavylium condensation and deacetylation took place simultaneously. In the present case, however, probably due to complex changes taking place with  $\gamma$ -resorcylic aldehyde (*cf.* phloroglucinaldehyde) in the presence of alcohol and hydrogen chloride, only brown amorphous substances insoluble in methyl alcoholic hydrogen chloride were obtained. Consequently the flavylium condensation and deacetylation had to be effected separately.

Through a solution of  $\gamma$ -resorcylic aldehyde (0.1 g.) and  $\omega$ :3:4-triacetoxy acetophenone (0.2 g.) in anhydrous ethyl acetate was passed a current of dry hydrogen chloride at ice temperature for about 3 to 4 hours. After keeping the contents in a refrigerator at 0° overnight they were filtered and the reddish brown solid washed with anhydrous ether. The product was dissolved in hot 2% aqueous alcoholic hydrochloric acid and treated with an equal volume of 20% sodium hydroxide. The resulting brown solution was raised to boiling and after a minute acidified with concentrated hydrochloric acid. The bright red solution of the flavylium chloride thus obtained was cooled and then treated with further quantities of hydrochloric acid so that the concentration of the acid in the mixture was finally about 10%. On leaving it in a refrigerator, a fine reddish brown solid was deposited. It was freely soluble in 1% alcoholic hydrogen chloride and 2% aqueous hydrochloric acid. It was crystallised by dissolving in the former solvent and adding concentrated hydrochloric acid. The pure substance appeared as bright red needles which did not melt below 300°C.; (Yield 50%). (Found: C, 58.1; H, 3.8;  $C_{15}H_{11}O_5Cl$  requires C, 58.7 and H, 3.6%).

*3:5:3':4':5'-Pentahydroxy-flavylium chloride* was prepared from  $\gamma$ -resorcylic aldehyde and  $\omega$ :3:4:5: tetra-acetoxy acetophenone adopting the above procedure. It was obtained as a reddish brown micro-crystalline solid which did not melt below 300°C. (Found: C, 55.3; H, 3.7;  $C_{15}H_{11}O_6Cl$  requires C, 55.8 and H, 3.4%).

The following table gives a summary of the colour reactions exhibited by the 5-hydroxy and 5-methoxy flavylium chlorides prepared above. A solution of each substance in 1% alcoholic hydrochloric acid was employed for all tests except 4 and 9 and the colour produced by the addition of various reagents recorded. For 4 the solid was used and for 9 an alcoholic solution without acid.

Reagent	3 : 5 : 4'-Trihydroxy	5-Methoxy-3 : 4'-dihydroxy	3 : 5 : 3': 4'-Tetrahydroxy	3 : 5 : 3': 4': 5'-Pentahydroxy
1. Colour of the solution	Red—no fluorescence	Orange red—no fluorescence	Deep red	Deep reddish purple
2. 1% HCl	Do.	Do.	Red	Red—precipitation
3. 20% HCl	Orange—precipitation—no fluorescence	Do.	Light red	Precipitation
4. Conc. $H_2SO_4$	Orange—very feeble green fluorescence ; lost on dilution with water	Orange—very feeble green fluorescence ; lost on dilution with water	Red—no fluorescence	Red—no fluorescence
5. Na Acetate	Pink—fades rapidly	Pink —fades rapidly	Bluish pink—fades rapidly	First violet changing to blue and fades rapidly
6. Na $HCO_3$	Purple—fades slowly	Pink—fades slowly	Blue—fades rapidly	Blue—fades rapidly
7. $Na_2CO_3$	Purple-dichroic blue—fades slowly	Violet-red—fades slowly	Deep blue—rapidly fades	Deep blue—rapidly fades
8. NaOH	Reddish-purple—rapidly fades to yellow	Violet-red—rapidly fades to very pale yellow	Blue-green—rapidly fades to yellowish brown	Blue-green and then quickly turns brown
9. $FeCl_3$	Nil	Nil	Blue	Blue

### Summary

Starting from  $\gamma$ -resorcylic aldehyde some typical 5-hydroxy and methoxy flavylium salts have been prepared and studied. They exhibit negligible fluorescence even in concentrated sulphuric acid. The structural factors that affect fluorescence in flavylium salts are discussed and comparison effected with coumarins.

### REFERENCES

- Shah and Laiwalla .. *J. C. S.*, 1938, 1828.
- Ridgway and Robinson .. *Ibid.*, 1924, 215.
- Leon, Robertson, Robinson and Seshadri *Ibid.*, 1931, 2675.
- Robinson and Vasey .. *Ibid.*, 1941, 660.
- Balaiah, Seshadri and Venkateswarlu *Proc. Ind. Acad. Sci.*, 1942, 16, 68.  
Rangaswami and Seshadri .. *Ibid.*, 1940, 12, 375.  
\_\_\_\_\_, \_\_\_\_ and Venkateswarlu *Ibid.*, 1941, 13, 316.
- Limaye *Rasayanam*, 1936, 1, 12.

# CONGRUENCE PROPERTIES OF RAMANUJAN'S FUNCTION $\tau(n)$

BY K. G. RAMANATHAN

(Research Scholar, University of Madras)

Received January 26, 1944

(Communicated by Dr. R. Vaidyanathaswamy, F.A.Sc.)

RAMANUJAN'S multiplicative arithmetic function  $\tau(n)^*$  is defined by

$$\sum_{n=1}^{\infty} \tau(n) x^n = x [(1-x)(1-x^2)\dots]^{24} \quad (1)$$

He stated, some congruence properties of  $\tau(n)$  for the moduli 5, 7 and 23. These were later proved by L. J. Mordell.<sup>1</sup> In this paper I prove congruences to moduli which are divisors of 24, viz.,

- (a)  $\tau(n)$  is odd if and only if  $n$  is the square of an odd number.
- (b)  $\tau(3n - 1) \equiv 0 \pmod{3}$ .
- (c)  $\tau(4n - 1) \equiv 0 \pmod{4}$
- (d)  $\tau(6n - 1) \equiv 0 \pmod{6}$
- (e)  $\tau(8n - 1) \equiv 0 \pmod{8}$ .

These imply in turn

- (f)  $\tau(12n - 1) \equiv 0 \pmod{12}$
- (g)  $\tau(24n - 1) \equiv 0 \pmod{24}$ .

I think, these congruences have not been stated before [except (a) and (e) proved by Mr. Hansraj Gupta]. These resemble the congruences to  $\sigma(n)$  proved by me namely,

If  $\sigma(n)$  is the sum of the divisors of the positive integer  $n$  then

$$\sigma(kn - 1) \equiv 0 \pmod{k}$$

for  $k = 3, 4, 6, 8, 12$  and  $24$  and  $n \geq 1$ .

2. We shall now prove the congruences of  $\tau(n)$ . It is well known<sup>1</sup> that

$$[(1-x)(1-x^2)\dots]^3 = 1 - 3x + 5x^3 - 7x^6 + \dots$$

$$= \sum_{n=1}^{\infty} (-1)^n (2n+1) x^{\frac{n(n+1)}{2}} \quad (2)$$

\* It might be pointed out that Hardy's statement that  $\tau(23n) \equiv 0 \pmod{23}$  given on p. 165 is false since  $\tau(23) = 18643272 \not\equiv 0 \pmod{23}$ .

so that  $\sum_{n=1}^{\infty} \tau(n) x^n = x [1 - 3x + 5x^3 - 7x^5 + \dots]^8$  (3)

But if  $f(x)$  is any rational integral function of  $x$  then

$$[f(x)]^8 \equiv f(x^8) \pmod{2}. \quad (4)$$

Therefore

$$\sum_{n=1}^{\infty} \tau(n) x^n \equiv x \sum_{n=0}^{\infty} (-1)^n (2n+1) x^{4n^2+4n} \pmod{2}.$$

$$\equiv \sum_{n=0}^{\infty} (-1)^n (2n+1) x^{(2n+1)^2} \pmod{2}$$

which shows that:  $\tau(n)$  is odd if and only if  $n$  is the square of an odd number. (5)

3. Differentiating logarithmically both sides of (1) we obtain

$$\sum_{n=1}^{\infty} n \tau(n) x^n = P(x) \sum_{n=1}^{\infty} \tau(n) x^n \quad (6)$$

$$\text{where } P(x) = 1 - 24 \left( \frac{x}{1-x} + \frac{2x^2}{1-x^2} + \dots \right)$$

$$= 1 - 24 \sum_{n=1}^{\infty} \sigma(n) x^n \quad (7)$$

where  $\sigma(n)$  is the sum of the divisors of  $n$ .

Equating coefficients of like powers of  $x$  we get

$$(1-m) \tau(m) = 24 \sum_{r=1}^{m-1} \sigma(r) \tau(m-r) \quad (8)$$

which shows that since  $\tau(n)$  and  $\sigma(n)$  are integers.

$$(m-1) \tau(m) \equiv 0 \pmod{24} \quad m \geq 1 \quad (9)$$

Putting in succession  $m = 2n, 3n, 3n-1, 4n, 4n-1$  we get

$$\tau(2n) \equiv 0 \pmod{8} \quad (10)$$

$$\tau(3n) \equiv \tau(3n-1) \equiv 0 \pmod{3} \quad (11)$$

$$\tau(4n) \equiv \tau(4n-1) \equiv \tau(4n-2) \equiv 0 \pmod{4} \quad (12)$$

As regards  $\tau(6n-1)$  we see that, since  $-1$  is a quadratic non-residue of 6,  $6n-1$  cannot be a square and by (5)  $\tau(6n-1)$  is even.

Also by (11)  $\tau(6n-1)$  is divisible by 3. Thus:

$$\tau(6n-1) \equiv 0 \pmod{6} \quad (13)$$

For  $1 < r \leq 8n-1$  we have

$$\tau(8n-r) \sigma(r-1) \equiv 0 \pmod{2}. \quad (14)$$

Because if  $r \equiv 7 \pmod{8}$  then  $r - 1 \equiv 6 \pmod{8}$ , i.e.,  $-1 \pmod{4}$  so that  $\sigma(r - 1) \equiv 0 \pmod{2}$ . For all other  $r$ 's we see that (14) holds in virtue of 10, (11) and (12) and the congruences of  $\sigma(n)$  stated by me.<sup>2</sup>

$$\begin{aligned} \therefore 2(1 - 4n)\tau(8n - 1) &= 24 \sum_{r=2}^{8n-1} \sigma(r - 1)\tau(8n - r) \\ &\equiv 48 \pmod{8} \\ \therefore \tau(8n - 1) &\equiv 0 \pmod{8} \end{aligned} \tag{15}$$

(11) and (12) imply  $\tau(12n - 1) \equiv 0 \pmod{12}$  and

(11) and (15) imply  $\tau(24n - 1) \equiv 0 \pmod{24}$ .

#### REFERENCES

1. Hardy, G. H. .. *Ramanujan*, Cambridge, 1940, Lecture X, pp. 165–69.
2. Hansraj Gupta .. *Abstracts of Papers presented to the Thirteenth Conference of Ind. Math. Soc.*, 1943, p. 6.
3. Ramanathan, K. G. .. *Ibid.*, 1943, p. 6.

# THE MEASUREMENT OF SURFACE TENSION BY MEANS OF SESSILE DROPS

BY H. J. TAYLOR AND J. ALEXANDER

(*From the Department of Physics, Wilson College, Bombay*)

Received January 24, 1944)

## 1. Introduction

THE main object of this paper is to describe a technique for the production and measurement of sessile drops, which offers a convenient and accurate method of measuring surface tension. Although the method has been known in principle for many years, its possibilities have not hitherto been fully exploited, for the following reasons:

(1) Drops have usually been formed on a flat plate, which limits the application of the method to cases where an angle of contact greater than  $90^\circ$  can be realized.

(2) It is difficult to form drops on a plate of reproducible size, and still more difficult to ensure freedom from contamination. The method has thus compared unfavourably with, e.g., the maximum bubble-pressure method, where a fresh surface is formed immediately before each observation.

(3) The elementary text-book theory applies only to a drop of infinite, or at least very large radius, and until recently there have been very few attempts to develop the theory of small drops. The theory available to the earlier workers was wholly inadequate.

For these reasons the sessile drop method, though familiar as a laboratory exercise, has seldom been used in exact work. Sieg, in 1887, obtained the value 74.3 dyn./cm. for the surface tension of pure water at  $20^\circ\text{ C}.$ , from the measurement of sessile drops. This value is now known to be in error by about  $1\frac{1}{2}$  units, which gives an idea of the magnitude of the uncertainties involved. In the present modification of the method we consider that the difficulties have been largely overcome.

## 2. Theory

The form of a liquid surface depends on the fundamental capillary equation

$$p_1 - p_2 = \alpha(1/R_1 + 1/R_2), \quad (1)$$

where  $p_1 - p_2$  is the pressure difference across the surface,  $\alpha$  the surface tension, and  $R_1, R_2$ , are the principal radii of curvature. For a sessile drop, formed in air saturated with the vapour of the liquid, this becomes

$$\alpha(1/R_1 + 1/R_2) = gz(d_1 - d_2) + A, \quad (2)$$

where  $z$  is the depth below the uppermost point,  $d_1$  the density of the liquid and  $d_2$  that of the saturated air, and  $A$  is a constant depending on the size of the drop and having the value zero for an infinitely large drop. Introducing  $x$  as a horizontal co-ordinate and taking the uppermost point as origin, the equation may be put in the form (*vide* Adam, 1941, p. 365):

$$\frac{1}{\rho/b} + \frac{\sin \phi}{x/b} = 2 + \beta \frac{z}{b}, \quad (3)$$

where  $\phi$  is the inclination of the surface at any point to the horizontal,  $\rho$  the radius of curvature in the vertical section at that point,  $b$  the radius of curvature at the origin, and  $\beta$  is the ratio  $2b^2/a^2$ ,  $a^2$  being the capillary constant defined by

$$a^2 = 2\alpha/g(d_1 - d_2). \quad (4)$$

Equation (3) cannot be integrated in finite terms, but a numerical solution was given by Bashforth and Adams (1883) for surfaces of revolution. Their tables give the values of  $x/b$ ,  $z/b$ , and  $V/b^3$  for given values of  $\phi$  and  $\beta$ ,  $V$  being the volume between the origin and a horizontal plane at the level  $z$ . Nearly all studies of the theory of surface tension measurements have been based on Bashforth and Adams' tables. Unfortunately the tables are out of print and very rare, and no copy has been available to us for the present work.

In experiments with sessile drops, the quantities which it is practicable to measure are  $h$ , the height of the drop measured from its equatorial plane, and  $r$ , its radius in that plane. For a very large drop we have the simple relation

$$a^2/r^2 = h^2/r^2 \quad (5)$$

from which  $a^2$  is at once found. A formula equivalent to this is used in the well-known experiment with mercury ("Quincke's method") usually to be found in laboratory courses. Even to secure 1% accuracy with this simple formula, it can be shown that  $h/r$  must not exceed 1/60, which means an impossibly large drop of at least 24 cm. radius for water, and 16 cm. for mercury. For smaller, but still approximately 'flat' drops, formulæ have been given by Worthington (1885), Fergusson (1913), and Rayleigh (1915). These formulæ enable  $a^2$  to be obtained with fair accuracy for values of  $h/r$  less than about 0.18. This means, for water, a radius greater than 2.2 cm. and for mercury, 1.5 cm.

Smaller drops have been considered by Porter (1933). He gives a table of corresponding values of  $a^2/r^2$  and  $h^2/r^2$  for values of  $h/r$  from 0.457 upwards. These are obtained directly from Bashforth and Adams' tables, and are therefore exact, at least to the fifth figure. The gap between Rayleigh's formula and the B. and A. values is then filled by an empirical equation, adjusted to fit the known points as closely as possible. His proposed equation (expressed in the notation of the present paper) is

$$a^2/r^2 - h^2/r^2 = -0.6094(1 - 4h^2/r^2)h^3/r^3. \quad (6)$$

Unfortunately this does not fit accurately the B. and A. values which Porter himself quotes. In a later paper (1938) while not admitting this explicitly, he gives a modified curve, which is equivalent to a formula with slightly changed values of the constants.

According to Porter's equation, the simple relation (5) holds exactly for  $h/r = 0.50$ . In the later paper, this is corrected to 0.498. Porter recommends that all measurements should be made on drops which have a value of  $h/r$  close to this. The correction to equation (5) is then small, and may be obtained from his table. The corresponding radii of the drop would be about 7.7 mm. for water, and 5.4 mm. for mercury.

In the present work we have thought it advisable to work with drops of a slightly larger radius, falling entirely within the range of the B. and A. values quoted by Porter. If this is to take its place as one of the standard methods, an accuracy approaching 1 in 1000 must be aimed at. There is no means of knowing whether Porter's curve is of this accuracy over the whole range.

We have therefore fitted an empirical equation, of the same form as Porter's, to the standard B. and A. values which he gives. The new equation is

$$a^2/r^2 = h^2/r^2 - 0.67338(h/r)^3 + 2.71434(h/r)^5. \quad (7)$$

The five standard values between  $h/r = 0.46$  and  $h/r = 0.56$  fit the new equation with residuals which in no case exceed 1 in 1,250. We believe, therefore, that the equation has the required accuracy over this range. It reduces to the simple equation (5) for the value  $h/r = 0.498$ , in agreement with Porter's revised value. Since the equation agrees in form with Porter's equation, which was designed for lower values of  $h/r$ , we consider that the new equation may be extrapolated to slightly smaller values with safety. On this basis we have calculated  $a^2/r^2$  for values of  $h/r$  from 0.446 to 0.558, at intervals of 0.002. Intermediate values may be read off by direct interpolation. The results are given in Table I, and all our observations have been reduced by the use of this table.

TABLE I

$h/r$	$a^2/r^2$	$h/r$	$a^2/r^2$	$h/r$	$a^2/r^2$
0.446	0.18708	0.484	0.23000	0.522	0.28190
0.448	0.18914	0.486	0.23249	0.524	0.28492
0.450	0.19123	0.488	0.23501	0.526	0.28797
0.452	0.19333	0.490	0.23755	0.528	0.29105
0.454	0.19546	0.492	0.24012	0.530	0.29416
0.456	0.19760	0.494	0.24271	0.532	0.29730
0.458	0.19977	0.496	0.24533	0.534	0.30048
0.460	0.20196	0.498	0.24798	0.536	0.30369
0.462	0.20417	0.500	0.25065	0.538	0.30693
0.464	0.20642	0.502	0.25335	0.540	0.31020
0.466	0.20866	0.504	0.25608	0.542	0.31351
0.468	0.21094	0.506	0.25883	0.544	0.31685
0.470	0.21324	0.508	0.26162	0.546	0.32022
0.472	0.21557	0.510	0.26443	0.548	0.32363
0.474	0.21792	0.512	0.26727	0.550	0.32707
0.476	0.22028	0.514	0.27014	0.552	0.33055
0.478	0.22268	0.516	0.27303	0.554	0.33407
0.480	0.22510	0.518	0.27596	0.556	0.33762
0.482	0.22754	0.520	0.27892	0.558	0.34121

### 3. Experimental Arrangements

Drops are formed conveniently by means of the apparatus shown in Fig. 1. The liquid is contained in a wide tube  $T$ , connected by a capillary  $A$  to a vertical tube  $V$ .  $B$  is a cylindrical brass ring cemented to the upper end of the tube  $V$ . When the clip  $C$  is opened liquid flows through the system under gravity, and a drop is formed on the ring  $B$ . The capillary serves to reduce the rate of flow, so that the drops form slowly. With water, the complete process takes 25 sec. or more, depending on the pressure, and it may be stopped at any stage by closing the clip.

The various stages of formation are shown in Fig. 2. A very remarkable 'overhang' can be attained before the drop runs over. During the early stages the contact angle is variable up to about  $90^\circ$ , but this has no special significance. When the drop reaches the edge of the ring it begins to bulge out, and the apparent contact angle increases to  $180^\circ$  before the drop collapses. This is due to the reluctance of the line of contact between the liquid and the brass to pass the sharp edge of the ring. This property of sharp edges has been discussed by Coghill and Anderson (1918) in connection with the stability of flotation of solid particles.

The tube is mounted on a substantial wooden holder fitted with levelling screws. The surface through which the tube  $V$  projects is plane, and on it rests the removable cylinder  $D$  enclosing the ring  $B$  in a small chamber. This maintains thermal equilibrium. The temperature is read by a thermometer graduated in tenths of a degree, with its bulb a few mm. above the

drop. The drops which now flow from *B* accumulate on the floor of the chamber, where filter-paper is placed. This ensures that the air in the chamber is saturated with vapour. The excess liquid can escape slowly through a small aperture, and drips into a beaker placed below the apparatus. The drop is illuminated and observed through windows *W*<sub>1</sub> and *W*<sub>2</sub>.

Recording is done photographically. An objective of 4" focus, provided with a sensitive focussing adjustment, throws an image of the drop on a photographic plate, with a magnification of about 2·7. An ordinary 40 W electric lamp, with a condenser, provides the illumination. A large glass tank filled with water is interposed in order to reduce the danger of temperature fluctuations when the lamp is switched on. These arrangements are not shown in the figure. A weighted thread hangs as a plumb line immediately in front of the plate, and its image defines the vertical. Ilford R plates are used, as the laboratory happens to have a considerable stock of these. They are slow, and require an exposure of some 12 seconds at *f*/6·5, but they are of fine grain and yield excellent images. We generally use a smaller aperture, but not smaller than *f*/11. It is evident from the geometry of the arrangement that a very small aperture could not form a sharp image of the profile of the drop in a plane passing exactly through its centre.

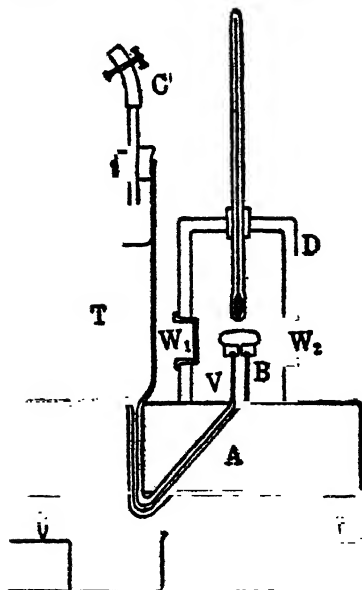


FIG. 1

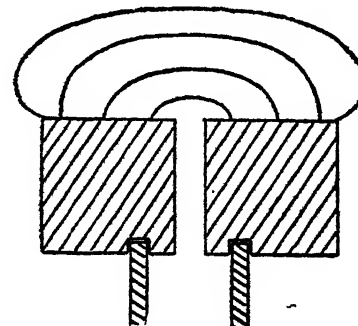


FIG. 2

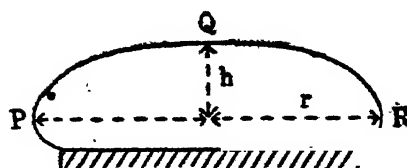


FIG. 3

After development the plates are measured on a Gaertner comparator reading to 1/1000 mm. The plate is placed on a holder mounted on a rack

and pinion, so that it may be displaced perpendicularly to the direction of traverse of the comparator. The vertical height  $h$  is measured (Fig. 3) by setting the vertical along the direction of traverse. By using the auxiliary motion at right angles, the cross hairs are set successively on  $P$ ,  $Q$ , and  $R$ . The mean reading at  $P$  and  $R$  is used, to eliminate any small error in the perpendicularity of the two motions. We find in practice that the estimate of the point of contact of the vertical tangent at  $P$  and  $R$  can be made with considerable precision, and the accuracy is much greater than can be attained by observing the original drop directly with a travelling microscope. A reproduction of one of the photographs is shown in Fig. 4.

In an actual experiment the procedure is as follows. After cleaning and mounting the tube on the holder, the levelling screws are adjusted until the upper surface of the ring  $B$  is horizontal. This is done by placing on it a small mirror, and observing the image of a plumb-line. When the surface is horizontal the plumb-line and its image are in one straight line. This gives quite a sensitive test. The cover is then placed in position, and the liquid introduced. A preliminary drop is formed, which is focussed accurately on the screen. A number of drops are then allowed to form and run over, in order to remove any residual trace of contamination. The final drop is then formed, and a photograph taken immediately. The plate is measured as already described. Since the diameter of the ring  $B$  is known accurately, the actual dimensions of the drop can be deduced immediately from the measurements.

#### 4. The Surface Tension of Distilled Water

To test the possibilities of the method, we have applied it to measure the surface tension of distilled water. Due precautions have been taken to secure purity and cleanliness. The following results are based on photographs of six different drops, and ten independent sets of measurements have been made on each plate. The measurements are very concordant, and are summarized in Table II.

TABLE II  
(Dimensions are given in mm.)

Plate	$H$	$R$	$H/R = h/r$	$r$	$a^2/r^2$	$\alpha$	Temp.
1	$10 \cdot 424 \pm 0 \cdot 008$	22.180	0.46997	8.3097	0.21321	$71 \cdot 687 \pm 0 \cdot 19$	27.6
2	$10 \cdot 634 \pm 0 \cdot 007$	22.490	0.47283	8.2344	0.21655	$71 \cdot 497 \pm 0 \cdot 19$	27.7
3	$10 \cdot 492 \pm 0 \cdot 005$	21.650	0.48462	7.9860	0.23077	$71 \cdot 665 \pm 0 \cdot 16$	27.7
4	$10 \cdot 538 \pm 0 \cdot 005$	22.025	0.47846	8.1062	0.22324	$71 \cdot 429 \pm 0 \cdot 16$	27.7
5	$10 \cdot 596 \pm 0 \cdot 004$	22.475	0.47146	8.2759	0.21493	$71 \cdot 680 \pm 0 \cdot 15$	27.7
6	$10 \cdot 652 \pm 0 \cdot 004$	22.905	0.46505	8.4071	0.20760	$71 \cdot 448 \pm 0 \cdot 15$	27.7

In this table,  $H$  and  $R$  refer to the photographs,  $h$  and  $r$  to the original drops. Equation (7) shows that  $a^2$  is relatively insensitive to small errors in  $r$ . The probable error of  $a^2$  thus depends chiefly on the uncertainty in the value of  $H$  and in the magnification. The result is also affected by uncertainties in the temperature. The latter has not been very rigorously controlled, but we are satisfied that the probable error in  $a$ , from this cause alone, would not exceed 0·01. The density of water and of saturated air have been taken from standard tables, and are not subject to any appreciable uncertainty.

We have analysed the influence of these various factors on the accuracy of the result, and have deduced the following weighted mean as a final value:

$$a = 71 \cdot 56 \pm 0 \cdot 07 \text{ dyn./cm. at } 27 \cdot 7^\circ \text{ C.}$$

In order to compare this result with others, it is convenient to reduce it to  $20^\circ \text{ C.}$  This can be done without appreciably increasing the probable error, since the temperature variation is known far more accurately than the absolute values. We use the formula of Richards, Speyers, and Carver (1924)

$$a_t = a_0 - 0 \cdot 1585 t + 0 \cdot 00023 t^2$$

which gives the result

$$a_{20^\circ} = 72 \cdot 70 \pm 0 \cdot 07 \text{ dyn./cm.}$$

In Table III we have collected a number of other published values for comparison. The list is representative, but by no means exhaustive. It is evident that the extreme uncertainty in this constant is still of the order of one-tenth of a unit. The present result agrees very well with other modern determinations.

TABLE III

Surface Tension of Water at  $20^\circ \text{ C.}$ 

1885	Volkmann	..	..	Capillary rise	72·53
1919	Harkins and Brown	..	..	do.	72·80
1921	Sugden	..	..	do.	72·70
1921	Richards and Carver	..	..	do.	72·73
1922	Sugden	..	..	Bubble pressure	72·91
1927	Moser	..	..	Ring detachment	72·58
1928	<i>International Critical Tables</i>	..	..	Adopted mean	72·75
1931	Schwenker	..	..	Ring detachment	72·55
1934	Achmatov	..	..	Differential Capillary	72·70
1939	Cockett and Ferguson	..	..	Plane meniscus method	72·80

### 5. Discussion

We believe this to be the first attempt to put the sessile drop method on a footing with the other standard methods. It bears some resemblance to the method of Andreas, Hauser and Tucker (1938), who photographed hanging drops and measured the dimensions. The hanging drop, however, has a very different shape, since its curvature is a maximum at the apex, while that of a sessile drop is a minimum. Further their reduction table is based on observations made with distilled water, of which the surface tension was taken as known. Our method has many of the advantages of theirs, and also yields absolute values. It may be useful to indicate the chief advantages as follows:

- (1) The observations, made on a free liquid surface, are entirely independent of contact angles.
- (2) The apparatus is simple to construct and operate, and the procedure involves no special technical skill.
- (3) It is a static method, and there are no viscosity effects.
- (4) The method, unlike those involving jets and capillary tubes, is relatively insensitive to small departures from perfection in the apparatus.
- (5) A fresh surface is formed for each observation, so that with reasonable care the risk of contamination is practically nil.
- (6) Successive observations can be made on the same surface, if it is desired to study the variation with time.
- (7) Permanent records are obtained.

The chief disadvantages are:

- (1) Relatively large quantities of liquid are required, since each filling of the tube takes some 25 c.cm.
- (2) In its present form the method is applicable to water and aqueous solutions only. (It is probable, however, that slight modifications would permit its extension to other liquids.)

The possible sources of systematic error in this method are not numerous. Imperfections in the optical system would be one possible source. In the present arrangement the rays forming the marginal parts of the image make an angle of less than  $2\frac{1}{2}^\circ$  with the axis. The lens is a standard photographic objective of excellent quality, and the effect of any residual astigmatism or other aberration in such a small angular field is almost certainly inappreciable. The window  $W_2$  is actually a piece of a microscope slide, selected for its optical quality from many pieces tested. It is placed as close as

*H. J. Taylor and  
J. Alexander*

*Proc. Ind. Acad. Sci., A, vol. XIX, Pl. II*

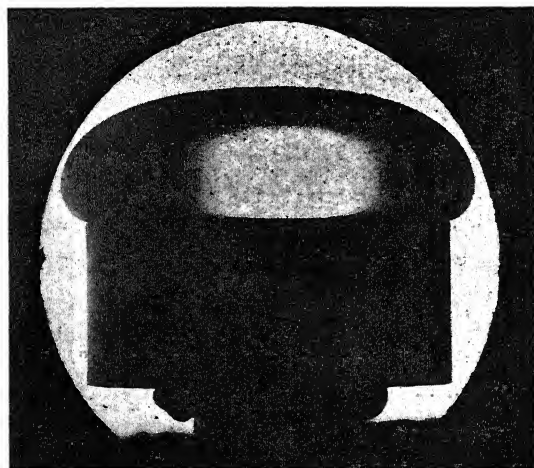


FIG. 4



possible to the drop. Systematic errors might also conceivably arise in the temperature readings, and in the measurement of the plates. On examining these possibilities we conclude that any such errors, if present, are very small.

We are of the opinion that the fluctuations in the results are almost entirely due to the random errors of observation. In further work it seems probable that an appreciably higher accuracy can be attained. To secure this, more rigorous temperature control will be needed, and closer attention to the details of photography and measurement. It will be necessary, moreover, to give further attention to the theory. We believe Table I, within its range, to be the most reliable reduction table for sessile drops yet available, but the probable errors of the measurements are already small enough to be comparable with the uncertainties in the tabulated values.

#### *Summary*

Apparatus is described by means of which sessile drops can be formed on the upper end of a vertical tube. The drops can be renewed as frequently as desired. Photographs of the drops are measured and from the dimensions the surface tension is calculated with the help of a new reduction table given in the paper. The method in this form is considered to be as reliable as any of the other standard methods. It has been applied to measure the surface tension of pure water against saturated air. The value at 20° C. is found to be  $72.70 \pm 0.07$  dyn./cm. in good agreement with other determinations.

#### REFERENCES

Adam	.. <i>The Physics and Chemistry of Surfaces</i> , 3rd edn., 1941.
Bashforth and Adams	.. <i>An Attempt to Test the Theories of Capillary Action</i> , Cambridge, 1883.
Worthington	.. <i>Phil. Mag.</i> , 1885, 20.
Ferguson	.. <i>Ibid.</i> , 1913, 25, 509.
Rayleigh	.. <i>Proc. Roy. Soc.</i> , A, 1915, 92, 184.
Porter	.. <i>Phil. Mag.</i> , 1933, 15, 163. .. <i>Ibid.</i> , 1938, 25, 752.
Coghill and Anderson	.. <i>J. Phys. Chem.</i> , 1918, 22, 245.
Richards, Speyers and Carver	.. <i>J. Am. Chem. Soc.</i> , 1924, 46, 1196.
Andreas, Hauser and Tucker	.. <i>J. Phys. Chem.</i> , 1938, 42, 1001.



# INFLUENCE OF TEMPERATURE ON THE QUENCHING OF ACTIVE NITROGEN AT VARIOUS PRESSURES

BY S. S. JOSHI AND A. PURUSHOTHAM

(*From the Department of Chemistry, Benares Hindu University*)

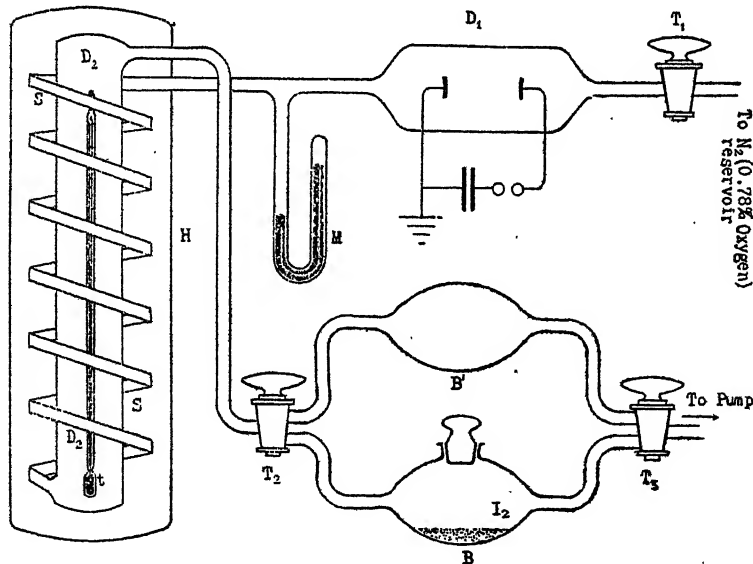
Received March 2, 1944

§1. THAT the after-glow due to active nitrogen is extinguished on streaming the gas through a heated tube was first observed by the present Lord Rayleigh.<sup>1</sup> Jones and Grubb<sup>2</sup> have reported that a greenish yellow glow which appeared intense at  $-20^{\circ}\text{C}.$ , disappeared on heating to  $30^{\circ}\text{C}$ . Rudy<sup>3</sup> studying the influence of temperature in the range  $20\text{--}120^{\circ}\text{C}.$ , observed that the corresponding coefficient was much smaller than in ordinary chemical reactions. Results of Cario and Kaplan,<sup>4</sup> Willey,<sup>5</sup> Okubo and Hamada<sup>6</sup> in this line, have raised the interesting question of the nature of the glowless state of active nitrogen obtained by its de-activation by heat or by a weak electrical discharge. A review of these and allied results has shown that the possible influence of the gas pressure in regard to its quenching by heat has been almost entirely ignored; the present work was undertaken to investigate the role of this factor.

§2. The general experimental procedure similar to that adopted in earlier work,<sup>7</sup> is shown in Fig. 1. The cylinder nitrogen containing 0.78% oxygen was activated in  $D_1$ , at a pressure shown by the manometer M. The activated gas was then allowed to flow through a long spiral S so as to attain the temperature of the air thermostat H, which was heated electrically from outside. The temperature of the glowing gas issuing from the spiral and entering the wider tube  $D_2$  at its bottom was shown by a thermometer t. The two bulbs B, B' were made as similar as possible; B contained a thin layer of very fine iodine crystals to serve as a sensitive detector of active nitrogen. The gas entering from  $D_2$  could be made to flow through either B or B' by an appropriate manipulation of the stop-cocks  $T_2$ ,  $T_3$ . Within the range of the flow-rates of the gas which were adjusted by means of  $T_2$ ,  $T_3$  and suction at  $T_1$ , the relative volumes of  $D_1$  and  $D_2$  were such that the after-glow was seen clearly in B or B'. The observation bulbs B and B' were carefully screened from any extraneous light, so as to enable the

detection of the faintest after-glow by either direct observation in  $B'$  or with the help of the very characteristic bluish white luminescence excited in iodine by making the gas flow *via*  $B$ .<sup>8,7</sup>

The quenching temperature at a given pressure was determined as follows:—At a conveniently low pressure (*cf.* Table I), the gas was allowed to stream through  $D_1SD_2B'$ . The discharge tube  $D_1$  was then excited and the heater for the thermostat  $H$  started. At a well-defined temperature shown by the thermometer  $t$  in  $D_2$ , it was found that the after-glow in  $B'$  ceases to be observable. The stop-cocks  $T_2$  and  $T_3$  are then quickly manipulated so that the gas flows *via*  $D_1S_1D_2B$ . It is found that the iodine in  $B$  now fails to show the characteristic luminescence. By reducing the heating current, the temperature is allowed to fall slowly. The glow due to the excitation of iodine then soon reappears in  $B$ ; the temperature and the pressure, when the iodine glow in  $B$  is just perceptible are observed. The heating is once again commenced until the iodine glow in  $B$  is undetectable. The mean of these two temperatures is taken as the quenching temperature. It is found that the temperature corresponding to the appearance of the glow on cooling and that for its obliteration on warming at a given streaming

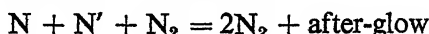


pressure, but seldom differed by more than 1–2° C. The pressure of the activated gas is then slightly raised and the corresponding quenching temperature determined, and so on. These results are shown in Table I.

TABLE I

Press mm. Hg. of streaming gas ..	15	17	20	24	33
Quenching temperature in °C. ..	215	223	236	255	330

§3. Despite investigations by numerous workers, the mechanism of the formation of active nitrogen in the electrical discharge and that of its de-activation is not understood in adequate detail. Evidence based chiefly on the spectroscopy of the after-glow would appear to indicate that besides normal atoms, metastable molecules of 8.2 volts are involved. The occurrence of 2.3 and 3.6 volt metastable atoms has also been postulated. Amongst the several theories for the production of the after-glow, a ternary collision of the following type would appear to summarise most of the facts and has also the advantage of simplicity.<sup>5,12</sup>



where  $N'$  denotes a 2.3 volt metastable atom.

The work of Rayleigh<sup>9</sup> as far back as 1912, Angerer,<sup>10</sup> Bonhoeffer and Kaminsky,<sup>11</sup> Rudy<sup>3</sup> and especially Willey<sup>5,12</sup> has established that kinetically the decay of the after-glow is a 'high order' re-action. The above type of mechanism is in agreement with this finding. It also explains the observed pronounced influence of the gas pressure on the reduction of the duration of the after-glow. The after-glow may be ascribed chiefly to de-activation due to collisions of the second type of the nitrogen atoms and molecules, with the rest of the molecules both in the gas space and on the walls of the containing vessel. The observed general suppressant effect of both heat and rise of the gas pressure may then be attributed to the corresponding increase in the collision frequency. These general considerations are, however, insufficient to explain our finding—which does not appear to have been recorded in the now considerable literature on active nitrogen, that its quenching at a given pressure is characterised by a definite temperature and that furthermore, this quenching temperature increases by increasing the gas pressure. In fact, on general grounds indicated above, it would appear that a rise in gas pressure should correspond to a *decrease* in the quenching temperature. Further work is necessary to elucidate this discrepancy. The quenching temperature being determined by the cessation of the after-glow and the sensibly simultaneous loss of capacity for exciting the iodine luminiscence as the streaming gas is progressively warmed, and by observation of their concomitant reappearance on cooling, suggest that

the above properties, *viz.*, the after-glow and capacity for exciting luminiscence are inseparable. We are of opinion therefore, that the evidence of our observation argues against the existence of a 'dark' but chemically active form of nitrogen.

### *Summary*

Effect of heating active nitrogen has been investigated at various streaming pressures in the range 15 to 33 mm. Hg by observation of its after-glow visually and excitation of the iodine luminiscence. It is found, it would appear for the first time in this field of research that the quenching of the after-glow is produced at a well-defined temperature, which increases with increase of the gas pressure. Existence of a glowless but chemically active form of nitrogen is considered improbable.

### REFERENCES

1. Rayleigh .. *Proc. Roy. Soc.*, 1911, A **85**, 219-29.
2. Jones and Grubb .. *Nature*, 1924, **134**, 140.
3. Rudy .. *J. Franklin Inst.*, 1926, **201**, 247 ; **202**, 376 ; *Phys. Rev.*, 1926, **27**, 110.
4. Cario and Kaplan .. *Zeit. f. Phys.*, 1929, **58**, 769.
5. Willey .. *J. Chem. Soc.*, 1927, 2831 : 1930, 336.
6. Okubo and Hamada .. *Phil. Mag.*, 1923, **15**, 103.
7. Joshi and Purushottam .. *Proc. Ind. Acad. Sci.*, 1943, A **18**, 218 ; *Nature*, 1942, **149**, 250.
8. Eason and Avman .. *Proc. Roy. Soc. Edin.*, 1928, **48**, 1-9.
9. Rayleigh .. *Ibid.*, 1912, A **86**, 263.
10. Angerer .. *Physikal Z.*, 1921, **22**, 97.
11. Bohmoeffer and Kamusky .. *Z. physik. Chem.*, 1927, **127**, 385.
12. Willey .. *Collisions of the Second Kind*, London, 1937.

# CHEMICAL EXAMINATION OF THE ROOTS OF *CENTAUREA BEHEN* LINN.

## Isolation of Behnin

BY PRITHVI NATH BHARGAVA AND SIKHIBHUSHAN DUTT

(*Chemistry Department, Allahabad University*)

Received October 25, 1943

*Centaurea Behen* or *Centaurea Behman*, commonly known in Hindustani as 'Lal Behman' and 'Rakta Barni' in Bengali, is an annual herb belonging to the Natural Order 'Compositæ'. It is cultivated throughout Northern India for the sake of its highly medicinal roots, which are used as remedial agents in various diseases.

Red Behman is a tuberous root consisting of a central part about 2" in diameter, from which spring 5 or 6 tapering tubes 1½" to 2" long and ½" to 1" in diameter. At the top of the central tuber the scaly crown is 2" in diameter. The external surface of the root is reddish brown and marked by numerous circular and longitudinal wrinkles, but internally there is a dull red woody central portion surrounded by a thick yellowish white horny layer. In the commercial article the root is sliced and the central woody part removed, but it is always associated with the white layer.

Red Behman, the drug of the ancient Persians, was introduced by the Arabs in the West. The drug is considered to be expelling flatulence and aphrodisiac by Dymock, Warden and Hooper.<sup>1</sup> Accordingly these are used in callous affections and jaundice as well as resolvents of phlegmatic humours.

In literature nothing has been mentioned regarding the chemical constituents of this plant. In view of its important medicinal properties however, the present authors have been tempted to put it to a thorough chemical examination in order to have an insight into the nature of its active principle. An account of the active principle of the root is given in this paper. It is indeed amazing that no alkaloid has been found in it as is mentioned by Kirtikar and Basu.<sup>2</sup> Instead, a resinous fatty matter, a saponin and a reddish white crystalline substance of the nature of a  $\Delta^{\alpha\beta}$ -unsaturated lactone have been isolated in small amounts and analysed. Most probably its medicinal property is due to the latter substance. It has been named 'Behnin', having a molecular formula  $C_{24}H_{48}O_3$ . Further it is

found to contain a methoxy group according to the determination made by micro-Zeissel's method.

### *Experimental*

For extraction with different solvents, the dry root was crushed to fine powder and extracted in a Soxhlet's extractor in lots of 25 gm. each in order to ascertain the best solvent. The solvent was recovered by distillation in each case and the residue brought to a constant weight by keeping in a steam oven with the following results:—

1. *Alcohol extract* (15.7%).—Brown resinous mass, soluble in benzene but insoluble in water, giving a yellow colour with caustic soda, an intense red colour with concentrated sulphuric acid no precipitate with lead acetate, thus showing the presence of a lactone.
2. *Benzene extract* (10.5%).—Brown waxy residue, soluble in chloroform, insoluble in water, giving a yellow colour with caustic soda and red with strong sulphuric acid.
3. *Ethyl acetate extract* (4.36%).—Red resinous product, soluble in hot alcohol, neutral to litmus, yellow with caustic soda, decolourising bromine water, reducing potassium permanganate and finally giving a dirty green precipitate with ferric chloride.
4. *Chloroform extract* (10.4%).—Brown fatty residue, giving a beautiful yellow colour with alcoholic caustic potash.
5. *Aqueous extract* (23.2%).—A red brittle solid giving froths on heating the aqueous solution, precipitating with lead acetate and reducing Fehling's solution, probably due to sugars and tannins.

The powdered root on complete incineration left 14.85% water-soluble and 85.15% water-insoluble ash. The following radicals were detected:—

- (a) In the water-soluble portion:  $\text{SO}_4\text{CO}_3$ , Cl, Na and K
- (b) In the water-insoluble portion:  $\text{CO}_3$ , Al, Ca and Mg.

For exhaustive extraction 8 kg. of the powdered roots were extracted with alcohol three times, in lots of 2 kg. each, in a 5 litre flask. The extract was filtered hot and allowed to stand overnight, when it gave a buff coloured precipitate. It was filtered and the filtrate was set aside for further examination. The precipitate was washed with alcohol in order to remove the tannin and the colouring matter. On keeping in air, it could not be obtained dry on account of the presence of fatty and resinous matter in it. Hence it was repeatedly washed with petroleum ether to remove the impurities. The product was then extracted with hot alcohol

and animal charcoal a number of times and the solution filtered through a hot water filter funnel. After keeping for some time, the precipitate was filtered through a Buchner funnel under suction, washed with petroleum ether and dried in air. On crystallisation from alcohol slightly red crystalline leaflets, melting at 79-80° C. were obtained.

The previous filtrate already mentioned was distilled to recover the solvent and the residue poured into water to remove the sugars and tannins which were soluble in water. It could not be filtered due to the formation of an emulsion. Hence it was allowed to stand for two days, treated with common salt and heated in a beaker. On cooling, a slightly red precipitate was formed. It was filtered, dissolved in alcoholic caustic soda and precipitated with dilute sulphuric acid. This precipitate was filtered, washed with alcohol and dried in air. The above filtrates were combined and examined later on. On crystallisation of the precipitate alternately from benzene and methyl alcohol with the addition of animal charcoal crystalline leaflets sintering at 72° C. and melting at 79-80° C. were obtained. The whole operation was tedious and involved tremendous difficulties.

From the combined filtrates mentioned above a saponin was isolated but it was insufficient for further examination.

*Properties.*—It is a light buff coloured crystalline substance. It is soluble in chloroform, sparingly soluble in ethyl alcohol, benzene and methyl alcohol and insoluble in water. On boiling with water for a long time, it melts to an oily liquid which on cooling becomes resinous and greasy probably due to decomposition. When heated quickly, it decomposes completely with the evolution of black fumes and a luminous flame. On exposure to ordinary sun light, behnin assumes a yellow colour, but in strong direct sun light it is converted into a sticky yellow resin. It is insoluble in 5% aqueous caustic soda solution but on heating it dissolves slowly with a yellow colour. It develops an intense beautiful yellow colour with alcoholic caustic potash as in the case of  $\Delta^{\alpha\beta}$ -unsaturated lactones studied first by Thiele<sup>3</sup> and subsequently by Jacobs and Hoffmann.<sup>4</sup>

In strong sulphuric acid, it produces a red colour. It decolourises a solution of bromine in chloroform and a dilute alkaline solution of potassium permanganate. It does not give any colour with ferric chloride, nor does it reduce Fehling's solution. It gives a positive Salkowski's reaction producing a red tinge. In Liebermann-Burchard reaction, behnin turns green. It becomes intense yellow in strong nitric acid and gives no precipitate with lead acetate. Behnin gives no colour with an alkaline solution of sodium nitroprusside. It has been found to contain a methoxy group and

forms tetrabromo derivative. It has got no alcoholic hydroxy group, as it does not form any acetyl or benzoyl derivative. Thus both the remaining oxygen atoms account for the lactonic grouping. Results of a series of analyses and molecular weight determinations point to a molecular formula  $C_{24}H_{48}O_3$ . (Found: C = 75·18, 74·79; H = 12·66, 12·72; M.W. by Rast's camphor method = 372, 378, 408;  $C_{24}H_{48}O_3$  requires C = 75·01; H = 12·5%; M.W. = 384.)

*Estimation of Methoxyl Group.*—The determination was conducted by the micro-Zeissel's method. (Found:  $OCH_3$  = 7·94;  $C_{23}H_{45}O_2$  ( $OCH_3$ ) requires  $OCH_3$  = 8·07%).

*Tetrabromo Derivative.*—Behnin (0·2 gm.) was dissolved in chloroform (15 c.c.) and treated with a solution of bromine in chloroform. It was allowed to stand in dark for 4 hours and heated on a water-bath under reflux for half an hour. On evaporating the solvent, a semi-solid pasty mass was obtained. It was crystallised from alcohol in yellow needles melting at 67° C. (Found: Br, 45·12;  $C_{24}H_{48}O_3Br_4$  requires Br, 45·45%).

#### Summary

From the roots of *Centaurea Behen* a crystalline unsaturated lactone having a molecular formula  $C_{24}H_{48}O_3$  has been obtained.

It has been found to contain a methoxy group and to yield a tetrabromo derivative.

#### REFERENCES

1. Dymock, Warden and Hooper *Pharmacographia Indica*.
2. Kiritkar and Basu .. *Indian Medical Plants*.
3. Thiele .. *Annalen*, 1901, **319**, 155.
4. Jacobs and Hoffmann .. *J. Biol. Chem.*, 1926, **67**, 333.

# ON THE EXISTENCE OF A METRIC FOR HIGHER PATH-SPACES\*

BY V. SEETHARAMAN

*(Annamalai University, Annamalainagar)*

Received February 10, 1944

(Communicated by Dr. A. Narasinga Rao)

THE geometry associated with the system of differential equations

$$\frac{d^{(\sigma+1)} x^i}{dt^{(\sigma+1)}} + \Gamma^i(t, x, x', \dots, x^{(\sigma)}) = 0 \\ i = 1, 2, \dots, n \quad \sigma \geq 2$$

has been studied by Kosambi. In this note we investigate the conditions under which the above system of differential equations may be identified with the extremals  $\delta \int f dt = 0$ . D. R. Davis<sup>1</sup> and D. D. Kosambi<sup>2</sup> for the case  $\sigma = 1$  and the present author<sup>3</sup> for  $\sigma = 2$  have already established the result that "The necessary and sufficient condition for the differential equations I to be the extremals of a regular problem of the calculus of variations is that the equations of variation of I be self-adjoint." In this note we establish the above result for the general  $\sigma$ .

1. We find that the self-adjointy conditions imply the existence of a tensor  $f_{ij}$  such that

$$f_{ij} = f_{(\lambda)i(\lambda)j}, \quad \lambda = \frac{\sigma+1}{2} \text{ when } (\sigma+1) \text{ is even,} \\ f_{ij} = \phi_{i(\lambda)j} - \phi_{j(\lambda)i}, \quad \lambda = \frac{\sigma}{2} \text{ when } (\sigma+1) \text{ is odd} \quad \left. \right\} \quad (1.1)$$

We shall consider for the present the even and odd order cases separately.

*Case i* ( $\sigma+1$ ) even.—In this case, the self-adjointy conditions are merely linear conditions on  $f_{(\lambda)i(\lambda)j}$ ; so that we can add to  $f$ , a function  $\phi$  such that

\* Read at the Thirteenth Conference of the Indian Mathematical Society held at Annamalai-nagar (December 1943).

I express my grateful thanks to Prof. D. D. Kosambi for his valuable suggestions.

<sup>1</sup> D. R. Davis, *Bull. Amer. Math. Soc.*, 1929, 371–80.

<sup>2</sup> D. D. Kosambi, *Quart. J. of Math.* (Oxford), 1935, 6, 9.

<sup>3</sup> V. Seetharaman, *Proc. Ind. Acad. Sci.*, 1940, 12, No. 4.

$\phi_{(\lambda)i(\lambda)j} = 0$ , i.e.,  $\phi = \phi_r x^{(\lambda)r} + \psi$ , where  $\phi_r$  and  $\psi$  are functions of  $(t, x, x^1, \dots, x^{(\sigma-1)})$  and

$$\delta_i(f + \phi_r x^{(\lambda)r} + \psi) = 0 \\ \text{or} \quad E_i = \delta_i f = -\delta_i(\phi_r x^{(\lambda)r} + \psi).$$

We can regard this as a differential system for the unknowns  $\phi_r$  and  $\psi$  in terms of the known  $f$ . The conditions of integrability of this system should be identically satisfied in virtue of the self-adjointness conditions. Or we can argue thus : The system  $E_i$  should be identified with  $-\delta_i(\phi_r x^{(\lambda)r} + \psi)$ . We assume that for this which is a differential system of order  $\sigma$ , the necessary and sufficient condition for the identity to hold good is that the equations of variation of  $E_i$  should be self-adjoint. That  $E_i$  satisfies this criterion is established in Art. 3. Since the result has been established for  $\sigma = 1$  and  $\sigma = 2$  it transpires that the theorem is true for the general  $\sigma$  by induction. That is, the existence Theorem is carried over automatically to one order lower at which stage the argument may be repeated.

*Case ii ( $\sigma + 1$ ) odd.*—In this case, the metric sought must be of the form  $f = \phi_r x^{(\lambda)r} + \psi$ . The Euler equations assume the form

$$[\phi_{i(\lambda)j} - \phi_{j(\lambda)i}] x^{(\sigma+1)j} + M_i = 0.$$

Since the self-adjointness conditions imply, in this case, the existence of an  $f_{ij} = \phi_{i(\lambda)j} - \phi_{j(\lambda)i}$  we can regard the function  $\phi_i$  in  $f$  as known and determined to within a function whose  $\lambda$ -curl vanishes. The addition of such a function to  $f$  merely amounts to adding a perfect differential and hence can be ignored. So we now regard  $\delta_i(\phi_r x^{(\lambda)r} + \psi) = 0$  as a differential system for the unknown  $\psi$  in terms of the known  $f$ , or we can argue as in case i.

In both cases we find that the discussion practically reduces to one of the lower order. The only point to be kept in mind is that even and odd orders which alternate in the reduction have a different structure.

## 2. Self-adjointness conditions:

It is known<sup>4</sup> that  $A_{ij} u^{(p)j} = 0$  will be self-adjoint if and only if

$$A_{ij} = \sum_{r=p}^{\sigma+1} (-1)^r \binom{r}{p} A_{ji}^{(r-p)}, \quad p = 0, 1, \dots, \sigma + 1.$$

Applying these conditions to the equations of variation of

$$H_i(t, x, x', \dots, x^{(\sigma+1)}) = 0 \text{ we get}$$

$$H_{i(p)j} = \sum_{r=p}^{\sigma+1} (-1)^r \binom{r}{p} H_{j(r)p}^{(r-p)} \quad (2.1)$$

<sup>4</sup> D. D. Kosambi, *Quart. J. of. Math.*, 1936, 7, 103.

For  $p = \sigma + 1$  we get  $H_{i(\sigma+1)j} = (-1)^{\sigma+1} H_{j(\sigma+1)i}$  (2.2)

For  $p = \sigma$   $H_{i(\sigma)j} = (-1)^\sigma H_{j(\sigma)i} + (-1)^{\sigma+1} (\sigma+1) H_{j(\sigma+1)i}^{(1)}$  (2.3)

Equating to zero the coefficient of  $x^{(\sigma+1)k}$  in the above, we get

$$H_{j(\sigma+1)i(\sigma+1)k} = 0$$

and hence

$$H_i = f_{ij} x^{(\sigma+1)j} + M_i \quad (2.4)$$

where  $f_{ij}$  and  $M_i$  contain  $(t, x, x' \dots x^{(\sigma)})$ .

It follows from (2.2) that  $f_{ij} = (-1)^{\sigma+1} f_{ji}$ , which shows that the tensor of association is symmetric if  $(\sigma+1)$  is even and anti-symmetric when  $(\sigma+1)$  is odd. The condition (2.3) applied to the form (2.4) gives

$$[f_{ik(\sigma)j} x^{(\sigma+1)k} + M_{i(\sigma)j}] \\ = (-1)^\sigma [f_{jk(\sigma)i} x^{(\sigma+1)k} + M_{j(\sigma)i}] + (-1)^{\sigma+1} (\sigma+1) f_{ji}^{(1)} \quad (2.5)$$

The co-efficient of  $x^{(\sigma+1)k}$  in (2.5) equated to zero gives

$$f_{ik(\sigma)j} + f_{jk(\sigma)i} - (\sigma+1) f_{ij(\sigma)k} = 0$$

Permuting  $i, j, k$  cyclically and adding, we get

$$f_{ik(\sigma)j} + f_{ji(\sigma)k} + f_{kj(\sigma)i} = 0$$

and hence

$$f_{ij(\sigma)k} = 0. \quad (2.6)$$

The residual terms in (2.5) give us  $Df_{ij} = 0$  (2.7)

For  $p = \sigma - 1$  we get

$$[f_{ik(\sigma-1)j} x^{(\sigma+1)k} + M_{i(\sigma-1)j}] \\ = (-1)^{\sigma-1} [f_{jk(\sigma-1)i} x^{(\sigma+1)k} + M_{j(\sigma-1)i}] + (-1)^\sigma \binom{\sigma}{\sigma-1} M_{j(\sigma)i}^{(1)} \\ + (-1)^{\sigma+1} \binom{\sigma+1}{\sigma-1} f_{ji}^{(2)}$$

Equating to zero, the coefficient of  $x^{(\sigma+1)k}$  in this we get

$$f_{ik(\sigma-1)j} - f_{kj(\sigma-1)i} + (-1)^{\sigma+1} \sigma M_{j(\sigma)i(\sigma)k} - \binom{\sigma+1}{2} f_{ij(\sigma-1)k} = 0.$$

Interchange  $i$  and  $k$  and subtract in the even case and add in the odd case. We get

$$\left. \begin{aligned} f_{jk(\sigma-1)i} - f_{ji(\sigma-1)k} &= 0 \quad (\text{even case}) \\ \left[ \binom{\sigma+1}{2} + 1 \right] (f_{kj(\sigma-1)i} + f_{ij(\sigma-1)k}) &= (-1)^\sigma \cdot 2\sigma \cdot M_{j(\sigma)i(\sigma)k} \end{aligned} \right\} \quad (2.8)$$

(odd case)

Similarly, equating to zero, the coefficient of the highest derivative of  $x^k$  that is present in the other conditions for  $p = \sigma - 2, \sigma - 3, \dots, 1, 0$  we get

$$\left. \begin{aligned} \binom{\sigma-1}{p} f_{j\bar{k}(\sigma-1)i} - \binom{\sigma}{p} M_{j(\sigma)i(\sigma)\bar{k}} + \binom{\sigma+1}{p} f_{j\bar{i}(\sigma-1)\bar{k}} &= 0 \\ p = \sigma - 2, \sigma - 3, \dots, 1, 0 \end{aligned} \right\} \quad (2.9)$$

In the even case (2.8) can be derived from (2.9). So that (2.9) constitute a set of  $(\sigma - 1)$  simultaneous homogeneous linear equations in the three unknowns  $f_{j\bar{k}(\sigma-1)i}$ ,  $M_{j(\sigma)i(\sigma)\bar{k}}$ ,  $f_{j\bar{i}(\sigma-1)\bar{k}}$  and hence they vanish if  $\sigma - 1 \geq 3$ , i.e.,  $\sigma + 1 \geq 6$ . In the odd case there are  $\sigma$  such equations and hence they vanish if  $\sigma \geq 3$ , i.e., if  $\sigma + 1 \geq 5$ . It is easily verified that the matrix of the coefficients is of the required rank 3. Hence we have,

$$f_{j\bar{i}(\sigma-1)\bar{k}} = 0, M_{j(\sigma)i(\sigma)\bar{k}} = 0 \quad (2.10)$$

Using the results (2.10) let us equate to zero, the coefficients of the next highest derivative of  $x^k$  that is present in these conditions. We get for  $p = \sigma - 2$ ,

$$f_{i\bar{k}(\sigma-2)\bar{j}} + (-1)^\sigma \left[ f_{j\bar{k}(\sigma-2)i} - \binom{\sigma-1}{\sigma-2} M_{j(\sigma-1)i(\sigma)\bar{k}} + \binom{\sigma}{\sigma-2} M_{j(\sigma)i(\sigma-1)\bar{k}} - \binom{\sigma+1}{\sigma-2} f_{j\bar{i}(\sigma-2)\bar{k}} \right] = 0.$$

Interchange  $i$  and  $k$  and subtract in the even case and add in the odd case. We have,

$$\left[ 1 \pm \binom{\sigma+1}{3} \left[ f_{i\bar{k}(\sigma-2)\bar{i}} \mp f_{j\bar{i}(\sigma-2)\bar{k}} \right] - \left[ \binom{\sigma}{2} \pm \binom{\sigma-1}{1} \left[ M_{j(\sigma-1)i(\sigma)\bar{k}} \mp M_{j(\sigma)i(\sigma-1)\bar{k}} \right] \right] = 0 \quad (2.11)$$

(Upper sign in the even case.)

The others give us the following equations:

$$\left. \begin{aligned} \binom{\sigma-2}{p} f_{j\bar{k}(\sigma-2)i} - \binom{\sigma-1}{p} M_{j(\sigma-1)i(\sigma)\bar{k}} + \binom{\sigma}{p} M_{j(\sigma)i(\sigma-1)\bar{k}} \\ - \binom{\sigma+1}{p} f_{j\bar{i}(\sigma-2)\bar{k}} &= 0 \\ p = 0, 1, \dots, \sigma-3 \end{aligned} \right\} \quad (2.12)$$

(2.11) and (2.12) are a set of  $(\sigma - 1)$  linear homogeneous equations in the 4 unknowns  $f_{j\bar{k}(\sigma-2)i}$ ,  $M_{j(\sigma-1)i(\sigma)\bar{k}}$ ,  $M_{j(\sigma)i(\sigma-1)\bar{k}}$ ,  $f_{j\bar{i}(\sigma-2)\bar{k}}$  and hence they vanish if  $\sigma - 1 \geq 4$  and the matrix of the coefficients is of rank 4. When  $\sigma - 1 = 4$ , we find that the corresponding determinant vanishes. Hence for  $\sigma + 1 \geq 7$  we have

$$f_{j\bar{i}(\sigma-2)\bar{k}} = 0, M_{j(\sigma)i(\sigma-1)\bar{k}} = 0 \quad (2.13)$$

Proceeding thus we arrive at the results :

$$\left. \begin{array}{ll} f_{ij(\mu)k} = 0 & \mu > \lambda \\ M_{i(\sigma)j(\mu)k} = 0 & \mu > \lambda + 1 \\ M_{i(\sigma-1)j(\mu)k} = 0 & \mu > \lambda + 2 \end{array} \right\} \quad (2.14)$$

and so on, where  $\lambda$  has the value given in (1.1).

When  $\sigma + 1 = 2\lambda$ , we arrive at the critical stage while considering the condition (2.1) for  $p = \lambda$ . We get

$$\begin{aligned} & \left[ f_{ik(\lambda)i} + (-1)^{\lambda+1} f_{jk(\lambda)i} - \binom{2\lambda}{\lambda} f_{ji(\lambda)k} \right] \\ &= (-1)^{\lambda+1} \binom{\lambda+1}{\lambda} M_{j(\lambda+1)i(\sigma)k} + (-1)^{\lambda+2} \binom{\lambda+2}{\lambda} M_{j(\lambda+2)i(\sigma-1)k} + \dots \\ & \quad \dots + (-1)^\sigma \binom{\sigma}{\lambda} M_{j(\sigma)i(\lambda+1)k}. \end{aligned}$$

Interchanging  $i$  and  $k$  and subtracting, we get

$$a_0 [f_{ik(\lambda)i} - f_{ji(\lambda)k}] + a_1 [M_{j(\lambda+1)i(\sigma)k} - M_{j(\lambda+1)k(\sigma)i}] + \dots = 0 \quad (2.15)$$

Similarly, from the remaining conditions we have

$$\begin{aligned} & \binom{\lambda}{p} f_{jk(\lambda)i} - \binom{\lambda+1}{p} M_{j(\lambda+1)i(\sigma)k} + \binom{\lambda+2}{p} M_{j(\lambda+2)i(\sigma-1)k} - \dots \\ & \quad \dots + (-1)^\lambda \binom{2\lambda}{p} f_{ji(\lambda)k} = 0 \quad (2.16) \\ & p = 0, 1, \dots, \lambda - 1. \end{aligned}$$

(2.15) and (2.16) together are a set of  $(\lambda + 1)$  equations in the  $(\lambda + 1)$  unknowns  $f_{ik(\lambda)i}$ ,  $f_{ji(\lambda)k}$ ,  $M_{j(\lambda+1)i(\sigma)k}$ ,  $M_{j(\lambda+2)i(\sigma-1)k}$ , ...,  $M_{j(\sigma)i(\lambda+1)k}$ .

But the determinant of the coefficients is of rank  $\lambda$ . Hence the quantities do not vanish and there is a unique solution for their ratios. The determinant in question is

$$\begin{vmatrix} a_0 & a_1 & a_2 & \cdot & \cdot & \cdot & \cdot & a_\lambda \\ \binom{\lambda}{0} & -\binom{\lambda+1}{0} & \binom{\lambda+2}{0} & \cdot & \cdot & \cdot & \cdot & (-1)^\lambda \binom{2\lambda}{0} \\ \binom{\lambda}{1} & -\binom{\lambda+1}{1} & \binom{\lambda+2}{1} & \cdot & \cdot & \cdot & \cdot & (-1)^\lambda \binom{2\lambda}{1} \\ \cdot & \cdot \\ \cdot & \cdot \\ \cdot & \cdot \\ \binom{\lambda}{\lambda-1} & -\binom{\lambda+1}{\lambda-1} & \binom{\lambda+2}{\lambda-1} & \cdot & \cdot & \cdot & \cdot & (-1)^\lambda \binom{2\lambda}{\lambda-1} \end{vmatrix}$$

where  $a_p + a_q = 0$  if  $p + q = \lambda$ .

For convenience let us consider the determinant

$$\begin{vmatrix} \beta_0 & \beta_1 & \cdot & \cdot & \cdot & \cdot & \cdot & \beta_\lambda \\ \binom{\lambda}{0} & \binom{\lambda+1}{0} & \cdot & \cdot & \cdot & \cdot & \cdot & \binom{2\lambda}{0} \\ \binom{\lambda}{1} & \binom{\lambda+1}{1} & \cdot & \cdot & \cdot & \cdot & \cdot & \binom{2\lambda}{1} \\ \cdot & \cdot \\ \cdot & \cdot \\ \cdot & \cdot \\ \binom{\lambda}{\lambda-1} \binom{\lambda+1}{\lambda-1} & \cdot & \cdot & \cdot & \cdot & \cdot & \cdot & \binom{2\lambda}{\lambda-1} \end{vmatrix}$$

so that  $\beta_r = (-1)^r a_r$ .

Let us keep the first column as it is, and subtract from each one of the remaining columns, the previous column and use the formula  $\binom{n}{r} - \binom{n-1}{r} = \binom{n-1}{r-1}$ . Repeat the process, stopping at the second row, then at the third row and so on. Finally after  $\lambda$  such operations, the matrix of the binomial coefficients alone will become

$$\begin{vmatrix} \binom{\lambda}{0} & 0 & 0 & \cdot & \cdot & \cdot & 0 & 0 \\ \binom{\lambda}{1} & \binom{\lambda}{0} & 0 & \cdot & \cdot & \cdot & 0 & 0 \\ \binom{\lambda}{2} & \binom{\lambda}{1} & \binom{\lambda}{0} & \cdot & \cdot & \cdot & 0 & 0 \\ \cdot & \cdot & \cdot & \cdot & \cdot & \cdot & 0 & 0 \\ \cdot & \cdot & \cdot & \cdot & \cdot & \cdot & 0 & 0 \\ \cdot & \cdot & \cdot & \cdot & \cdot & \cdot & 0 & 0 \\ \binom{\lambda}{\lambda-1} \binom{\lambda}{\lambda-2} \binom{\lambda}{\lambda-3} \cdots & \cdot & \cdot & \cdot & \cdot & \cdot & \binom{\lambda}{0} & 0 \end{vmatrix}$$

There are  $\lambda$  rows and  $(\lambda + 1)$  columns.

As a result of these operations which are merely taking the successive finite differences, the last element in the first row of the  $\beta$ 's will become

$$\beta_\lambda - \binom{\lambda}{1} \beta_{\lambda-1} + \binom{\lambda}{2} \beta_{\lambda-2} - \dots + (-1)^\lambda \binom{\lambda}{\lambda} \beta_0$$

and

$$\beta_r = (-1)^r a_r$$

∴ This is equal to

$$a_\lambda + \binom{\lambda}{1} a_{\lambda-1} + \binom{\lambda}{2} a_{\lambda-2} + \dots + \binom{\lambda}{\lambda} a_0$$

with the proper sign.

As  $a_p + a_q = 0$  when  $p + q = \lambda$ , this expression vanishes.

So all the elements of the last column in the determinant are zero and hence the determinant vanishes.\*

Also it is seen from the above that the determinant of order  $\lambda$  formed by the binomial coefficients is equal to 1.

The  $(\lambda + 1)$  quantities  $f_{j,k(\lambda),i}$ ,  $M_{j(\lambda+1)i(\sigma)k}$ , ...,  $M_{j(\sigma)i(\lambda+1)k}$ ,  $f_{j,i(\lambda)k}$  are hence proportional to  $A_0, A_1, \dots, A_\lambda$ , the co-factors of  $a_0, a_1, \dots, a_\lambda$  in the determinant. It is seen that  $A_r = \binom{\lambda}{r}$ .

This proves that

$$\left. \begin{aligned} f_{j,k(\lambda),i} &= f_{j,i(\lambda),k} \\ M_{j(\lambda+1)i(\sigma)k} &= M_{j(\sigma)i(\lambda+1)k} \end{aligned} \right\} \quad (2.17)$$

and so on.

Also

$$\frac{f_{j,i(\lambda),k}}{\binom{\lambda}{0}} = \frac{M_{j(\lambda+1)i(\sigma)k}}{\binom{\lambda}{1}} = \frac{M_{j(\lambda+2)i(\sigma-1)k}}{\binom{\lambda}{2}} = \dots$$

The symmetry of  $f_{ij}$  together with the first of conditions (2.17) ensures that

$$f_{ii} = f_{(i)(i)(i)} \quad (2.18)$$

When  $(\sigma + 1) = 2\lambda + 1$  we have the following equations corresponding to (2.15) and (2.16).

$$\begin{aligned} & \left[ f_{i,k(\lambda),i} + (-1)^{\lambda+1} f_{j,k(\lambda),i} + \binom{2\lambda+1}{\lambda} f_{j,i(\lambda),k} \right] \\ &= (-1)^{\lambda+1} \binom{\lambda+1}{\lambda} M_{j(\lambda+1)i(2\lambda)k} + (-1)^{\lambda+2} \binom{\lambda+2}{\lambda} M_{j(\lambda+2)i(2\lambda-1)k} + \\ & \dots + (-1)^\sigma \binom{2\lambda}{\lambda} M_{j(2\lambda)i(\lambda+1)k}. \end{aligned} \quad (2.19)$$

and

$$\binom{\lambda}{p} f_{j,k(\lambda),i} - \binom{\lambda+1}{p} M_{j(\lambda+1)i(\sigma)k} + \dots + (-1)^{\lambda+1} \binom{2\lambda+1}{p} f_{j,i(\lambda),k} = 0$$

$$p = 0, 1, \dots, \lambda - 1. \quad (2.20)$$

\* I am thankful to Mr. M. Venkatraman in helping me to evaluate this determinant.

These are  $(\lambda + 1)$  equations in  $(\lambda + 2)$  unknowns. Let us permute  $i, j, k$  cyclically twice and add. Let

$$A_{[ijk]} = (A_{ijk} + A_{jki} + A_{kij}).$$

We get, then  $(\lambda + 1)$  equations in the  $(\lambda + 1)$  unknowns

$$f_{[ij(\lambda)k]}, M_{[i(\lambda+1)j(2\lambda)k]}, \dots, M_{[i(2\lambda)j(\lambda+1)k]}$$

The determinant of the coefficients can by the methods followed in the symmetric case, be shown to be *not* equal to zero.

Hence

$$f_{ij(\lambda)k} + f_{jk(\lambda)i} + f_{ki(\lambda)j} = 0 \quad (2.21)$$

This, together with the anti-symmetry of  $f_{ij}$ , ensures that  $J_{ij}$  is a curl, i.e.,

$$J_{ij} = \phi_{i(\lambda)j} - \phi_{j(\lambda)i}. \quad (2.22)$$

By equating to zero, the residual terms in the above conditions for different values of  $p$  we get conditions on the various curvature tensors.

For  $p = \sigma$  we get  $D f_{ij} = 0$

For  $p = \sigma - 1$  we will have

$$f_{ir} P_j^r = (-1)^{\sigma-1} f_{jr} P_i^r$$

and so on, for the general  $p$ ,

$$f_{ir} P_j^r = f_{ir} \sum_{s=p}^{\sigma-1} (-1)^s \binom{s}{p} D^{s-p} P_j^r. \quad (2.23)$$

From (2.14) we infer that the Euler equations should be of the form

$$\begin{aligned} f_{ij} (x^{(\sigma+1)j} + a^j) &= f_{ij}(\lambda) x^{(\sigma+1)j} + a_{ij}(\lambda+1) x^{(\sigma)j} + \\ &\quad + b_{ij}(\lambda+2) x^{(\sigma-1)j} + \end{aligned} \quad (2.24)$$

where

$f_{ij}(\lambda)$  means that  $f_{ij}$  contains  $x, x', \dots, x^{(\lambda)}$ .

The terms are linear up to  $x^{(m)j}$  where  $m = I\left(\frac{3\lambda}{2} + 1\right)$ .

3. *Conditions of Integrability.*—The conditions of self-adjointness of the variation of  $H_i$ , we have seen are,

$$H_{i(p)j} = \sum_{r=p}^{\sigma+1} (-1)^r \binom{r}{p} H_{j(r-p)}^{(r-p)}.$$

The right-hand side resembles the E-vectors of Synge. Let us express this in invariant form making use of the identities in the present author's previous paper.<sup>5</sup> We get

$$\begin{aligned} \nabla_j H_i &= \sum_{\gamma=\nu+2}^{\sigma+1} \nabla_\gamma H_i \left[ \sum_{r=0}^{\nu-p-2} (-1)^{r+1} \binom{\sigma-\nu+r}{r} D_{\sigma-\gamma+\nu+r+1}^r P_j^r \right] \\ &= \sum_{\gamma=\nu}^{\sigma+1} (-1)^\nu \binom{\nu}{p} D^{\nu-p} \nabla_\gamma H_i \\ &+ \sum_{\gamma=1}^{\sigma-p} \left[ \left\{ \sum_{s=0}^{\nu-1} (-1)^s \binom{\sigma-\nu+s}{s} D^s P_j^s \right\} \times \right. \\ &\quad \left. \left\{ \sum_{r=0}^{\sigma-\nu} (-1)^r \binom{r}{p} D^{\nu-p} \nabla_r H_i \right\} \right] \end{aligned}$$

We can re-write this in the form

$$\begin{aligned} \nabla_j H_i &= \sum_{\nu=p+2}^{\sigma} \nabla_\nu H_i \left[ \sum_{r=0}^{\nu-p-2} (-1)^{r+1} \binom{\sigma-\nu+r}{r} D_{\sigma-\nu+p+r+1}^r P_j^r \right] \\ &- \sum_{\nu=p}^{\sigma} (-1)^\nu \binom{\nu}{p} D^{\nu-p} \nabla_\nu H_i \\ &- \sum_{\nu=1}^{\sigma-p} \left[ \left\{ \sum_{s=0}^{\nu-1} (-1)^s \binom{\sigma-\nu+s}{s} D^s P_j^s \right\} \right. \\ &\quad \left. \times \left\{ \sum_{r=0}^{\sigma-\nu-1} (-1)^r \binom{r}{p} D^{\nu-p} \nabla_r H_i \right\} \right] \\ &= - \nabla_{\sigma+1} H_i \left\{ P_j^{\sigma+1} \right\} + \nabla_{\sigma+1} H_i \left\{ \sum_{s=0}^{\sigma-p-1} (-1)^{\sigma+s} \binom{p+s}{s} D^s P_j^s \right\} \\ &+ (-1)^{\sigma+1} \binom{\sigma+1}{p} D^{\sigma+1-p} \nabla_{\sigma+1} H_i \\ &+ \sum_{\nu=1}^{\sigma-p-1} \left[ \left\{ \sum_{s=0}^{\nu-1} (-1)^s \binom{\sigma-\nu+s}{s} D^s P_j^s \right\} \times \right. \\ &\quad \left. \times \left\{ (-1)^{\sigma-\nu} \binom{\sigma-\nu}{p} D^{\sigma-\nu+p} \nabla_\nu H_i \right\} \right] \\ &\quad p = 0, 1, \dots, \sigma. \end{aligned} \tag{3.1}$$

The left side of (3.1) equated to zero give us the self-adjointcy conditions for equations of order  $\sigma$ . We have to show that they are satisfied by  $H_i \equiv \delta_i f$ .

Since  $f$  is known, we see that

$$\delta_i f = f_{ij} x^{(\sigma+1)j} + A_i(\sigma)$$

and hence

$$\nabla_j (\delta_i f) = f_{ij}.$$

<sup>5</sup> V. Seetharaman, Proc. Lond. Math. Soc., 1939, Series 2, 45, formula (3.7).

The right side of (3·1) consequently becomes

$$\begin{aligned}
 &= \left[ -f_{ir} P_j^r + f_{jr} \sum_{s=p}^{\sigma-1} (-1)^s \binom{s}{p} D^{s-p} P_i^r \right] \\
 &+ (-1)^{\sigma+1} \binom{\sigma+1}{p} D^{\sigma+1-p} f_{ji} \\
 &+ \sum_{\nu=1}^{\sigma-\sigma-1} \left[ \left\{ \sum_{s=0}^{\nu-1} (-1)^s \binom{\sigma-\nu+s}{s} D^s P_i^{\nu} \right\} \times \right. \\
 &\quad \left. \times \left\{ (-1)^{\sigma-\nu} \binom{\sigma-\nu}{p} D^{\sigma-\nu+p} f_{ij} \right\} \right] \quad (3·2)
 \end{aligned}$$

These equated to zero are the self-adjointy conditions for the equations of order  $(\sigma+1)$ .<sup>6</sup> Hence we have established the conditions of Integrability and hence the main theorem of this note.

---

<sup>6</sup> *Vide* formulæ (2·7) and (2·23). Also cf. D. D. Kosambi, *Quart. J. of Math.*, 1936, 7, 104.

# SEPARATION OF ELECTRONIC AND NON-ELECTRONIC COMPONENTS OF COSMIC RADIATION BY BHABHA'S METHOD

BY S. V. CHANDRASHEKHAR AIYA

(*Cosmic Ray Research Unit, Indian Institute of Science, Bangalore*)

Received April 4, 1944

(Communicated by H. J. Bhabha, F.R.S.)

## *Introduction*

WHENEVER the intensity of the hard component of cosmic radiation is measured, the soft component is usually cut out by the inclusion of an absorber like lead between the counters of a counter telescope. If small thicknesses of lead are used for the purpose, all the electrons cannot be absorbed. If large thicknesses of lead are used, there is always the possibility of cutting out low energy mesons. Schein, Jesse and Wollan<sup>1</sup> and Sarabhai<sup>2</sup> have made use of the fact that electrons produce showers to cut out electrons. Bhabha<sup>3</sup> has considered this problem in detail and has arrived at certain conclusions on the basis of the cascade theory. He has shown that any given thickness of lead can be made more effective in cutting out electrons by splitting it in the approximate ratio of 1:4. The smaller thickness is to be used for shower production and the high energy electrons get cut out by the showers tripping counters in anti-coincidence included in the counter telescope. A fraction of low energy electrons produce showers of very few particles, often of only one, in the shower producing lead. This fraction is quite large and can only be cut out by absorption in the larger block of lead. Experiments were carried out by the author to test these conclusions of Bhabha at Ootacamund (Geomagnetic latitude = 1.7° N. and altitude = 7,200 ft. above mean sea-level) and this paper is mainly a report of that work. In particular, the theoretical result is confirmed that shower production alone is not sufficient to cut out the whole electronic component, and the lower block of lead is essential for the purpose of cutting out the relatively lower energy electrons.

## *Experimental Arrangement*

In designing the apparatus, the choice of the total thickness of lead to be used was of primary importance. A total thickness of 5.25 cm. was used and the reason for choosing this thickness is as follows. Bhabha has shown that this thickness cuts out all but about 5% of the electrons and that splitting the lead would only assist in cutting out this last 5%. According to Rossi and Greisen,<sup>4</sup> mesons of energy above  $0.93 \times 10^8$  eV can penetrate 5.25 cm. of lead. From the curve given by Euler and Heisenberg<sup>5</sup> for the

energy spectrum of mesons, the fraction of mesons of energy below  $10^8$  eV is about 2% of the total meson intensity. It is clear therefore that very few mesons would be absorbed in this thickness of 5.25 cm. Of this, 1.25 cm. were used for shower production and 4.0 cm. for absorption only. The number of mesons cut out by shower production in 1.25 cm. of lead is quite negligible.

The counter telescope used for the experiments is shown in Fig. 1. Counters 1, 2 and 3 form the vertical telescope and they can all be connected in coincidence. Counters 4 and 5 are connected in parallel and can be set in anti-coincidence with counters 1, 2 and 3. The pulse was taken from the copper cylinders of the anti-counters and they were enclosed in an earthed shield of  $1/32$ " aluminium. All the counters used were of the same size, *viz.*, 6" long and  $1\frac{1}{4}$ " in diameter.

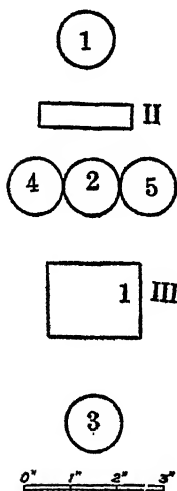


FIG. 1

Each of the counters, 1, 2 and 3, was fixed in two duraluminium rings  $1/16$ " thick and  $\frac{1}{4}$ " wide. These rings were riveted to a rectangular frame of the same thickness and width. This frame was fixed at the two ends to two L angles which acted as vertical supports. The frames in positions II and III for supporting lead consisted of a rectangular frame similar to the ones used for the counters but had cross strips instead of the rings. The shields of counters 4 and 5 were attached to the rectangular frame of counter 2. The complete structure weighed only 4 ozs. This gives an idea of the extent to which showers, etc., caused in the frame are reduced to a minimum. This kind of frame also enabled the alignment of counters to be done with a high degree of precision.

#### *Location of the Apparatus*

The counter telescope was first placed in open air with no lead in positions II and III. Counters 1, 2 and 3 were connected in coincidence and counts registered for 8 hours. The reading was 1531, giving an hourly average of  $191.4 \pm 3.3$ . Next the apparatus was shifted to a large room having a thin roof of tile and the experiment was repeated. 4579 counts were registered in 24 hours. This gives an hourly average of  $190.8 \pm 1.9$ . Since the two readings were substantially the same, all other measurements were carried out inside the room.

#### *Effect of Side Showers*

It has recently been pointed out<sup>6</sup> that errors due to chance coincidences, inefficiency of counters, etc., are negligible in coincidence counter work when

compared with the errors due to the effect of side showers. Consequently it was felt desirable to obtain some information on the effect of side showers before actually commencing measurements. The observations recorded for the purpose are given below in Table I.

TABLE I  
(No lead is placed in positions II or III)

No.	Counters in coincidence	Counters in anti-coincidence	Counts	Time	Counts/hour	% effect of showers
a	123	..	4579	24	190.8 ± 1.9	4.4
b	123	45	8768	48	182.7 ± 1.3	..
c	13	..	1688	7.5	225.1 ± 3.7	23.2
d	13	45	1940	9	215.6 ± 3.3	18.0

One method of estimating the effect of side showers on a counter telescope is to put one of the counters out of line. In (b), two counters 4 and 5 are out of line and in anti-coincidence with counters 1, 2 and 3. Therefore, the arrangement (b) can be considered to give the readings free from the effect of side showers. The only objection to this is the fact that it cuts out a certain number of Auger showers. But since the difference between (a) and (b) is only 4.4%, it is clear that the number of Auger showers ruled out by this method is certainly less than 4.4%.

The percentage effect of side showers calculated on the assumption that (b) gives the correct reading is shewn in the last column.

#### Results of Measurements

Counters 1, 2 and 3 were connected in coincidence. Counters 4 and 5 were connected in parallel and in anti-coincidence with counters 1, 2 and 3. The distance of the tray of counters 4, 2 and 5 from the shower producing lead in position II is rather *critical*. The position shown in the figure was best and has, therefore, been used. As it was found that there was a distinct diurnal variation of meson intensity, all measurements were taken for periods of 24 hours at a time. Owing to unavoidable reasons, the last measurement in Table II could only be taken for 10 hours. Each of the measure-

TABLE II

No.	Lead in position II	Lead in position III	Counts	Time	Counts/hour
A	cm.	cm.	4389 + 4379	24 + 24	182. ± 1.3
B	1.25	..	2889 + 2924 + 2902 + 2911	24 + 24 + 24 + 24	121.1 ± 0.75
C	..	5.25	3008 + 3010	24 + 24	125.4 ± 1.08
D	1.25	..	3336	24	139.0 ± 1.6
E	..	1.25	1485	10	148.5 ± 2.6

ments for 24 hours periods were taken at random and the consistency gave an independent check on the efficiency, etc., of the counters and circuits. The readings obtained for each period of 24 hours are shown separately in the table.

#### *Discussion of the Results*

(A) gives the total intensity and (B), on the basis of Bhabha's theory, the intensity of the hard component. (A-B) gives the total electron component. (C-B) represents the number of electrons which can penetrate 5.25 cm. of lead but which can be cut out by splitting the lead as suggested by Bhabha.  $(C-B)/(A-B) \times 100 = 7.0 \pm 2.9\%$ . According to Bhabha, about 5% of the total electron component can penetrate 5.25 cm. of lead and this can be cut out by splitting the lead. Therefore, the experimental result, *viz.*,  $7.0 \pm 2.9\%$  is in agreement with Bhabha's calculations.

(D) gives the result of using only the shower producing lead. It is clear that a considerable number of electrons get through. This number is obtained by subtracting (B) from (D). It is found to be 29.1% of the total electron component. The necessity for using the extra 4.0 cms. of lead for *absorption only*, therefore, becomes obvious and is in accordance with Bhabha's deductions.

(A-E) represents the electron component absorbed in 1.25 cm. of lead.

As it is possible to get some idea of the energy spectrum of electrons from these experiments, the results are tabulated below in a slightly different manner and are of some significance as the measurements were carried out very near the geomagnetic equator ( $1.7^\circ$  N.) and at a high altitude (7,200 ft.).

TABLE III

Component	How deduced	Intensity in counts/hour	% of total soft component
1. Very low energy electrons absorbed in 1.25 cm. of lead ..	(A-E)	34.2	55.5
2. Low energy electrons absorbed in 5.25 cm. of lead which penetrate 1.25 cm. but are incapable of producing showers in 1.25 cm. of lead to trip counters 4 or 5	(D-B)	17.9	29.1
3. High energy electrons absorbed in 5.25 cm. of lead but capable of producing showers in 1.25 cm. of lead to trip counters 4 or 5	{(E-D)-(C-B)}	5.2	8.4
4. Very high energy electrons capable of penetrating 5.25 cm. of lead	(C-B)	4.3	7.0
5. Electrons absorbed in 5.25 cm. of lead .. .. ..	(A-C)	57.3	93.0

The total intensity and the percentages of the soft and hard components are given below:—

TABLE IV

Component	How deduced		Intensity in counts/hour	% of total intensity
Total intensity ..	..	A	182·7	
Hard component ..	..	B	121·1	66·3
Soft component ..	..	A—B	61·6	33·7

*Acknowledgement*

The author desires to thank Prof. H. J. Bhabha, F.R.S., for his interest and encouragement and the Trustees of the Sir Dorabji Tata Trust who have financed this scheme of research.

The author's thanks are also due to Dr. K. R. Ramanathan of the India Meteorological Department for the loan of Prof. Millikan's counters which were tested and used in the experiments reported here.

*Summary*

The theoretical results of the method suggested by Bhabha for the separation of the electronic and non-electronic components of cosmic radiation are experimentally verified. The absorption spectrum of electrons has been investigated by this method. At 1·7° N. of the geomagnetic equator and an altitude of 7,200 ft., the hard component constitutes 66·3% of the total intensity.

## REFERENCES

1. Schein, Jesse and Wollan .. *Phy. Rev.*, 1941, **59**, 615.
2. Sarabhai .. *Proc. Ind. Acad. Sci. (A)*, 1944, **19**, 37.
3. Bhabha .. *Ibid.*, (A), 1944, **19**, 23.
4. Rossi and Greisen .. *Rev. Mod. Phys.*, 1941, **13**, 240.
5. Euler and Heisenberg .. *Ergebnisse der Exakten Naturwissenschaften*, 1938, 1-69.
6. Greisen and Nereson .. *Phy. Rev.*, 1942, **62**, 316.

# THE EVALUATION OF THE SPECIFIC HEAT OF ROCK-SALT BY THE NEW CRYSTAL DYNAMICS

BY BISHESHWAR DAYAL

(From the Department of Physics, Indian Institute of Science, Bangalore)

Received March 30, 1944

(Communicated by Sir C. V. Raman, Kt., F.R.S., N.L.)

## 1. Introduction

ROCK-SALT is a typical polar crystal and has therefore been a subject of close study by many theoretical physicists. Numerous attempts have been made to correlate its observed properties with the forces operative in its structure. A simplified method of treatment was first given by Madelung (1910) and later by Born and Karman (1912) in which the actual forces were replaced by quasi-elastic bindings between the neighbours and next nearest neighbours, and a determination of the infra-red frequencies was attempted from Voigt's elastic constants. The approximation used was obviously unsatisfactory because the forces between the ions are electrical in nature and are not confined to the neighbouring atoms alone but in consequence of Coulomb's Law, diminish very slowly with the distance. The ionic theory of crystals developed by Born and his school takes the electrical origin of the forces into consideration and has, at present, reached a finished state in which it has been possible to determine the various observed properties of polar crystals such as lattice energy, lattice constant, compressibility, etc., from the forces between the ions. Amongst the more recent workers who have made such calculations successfully are Huggins (1937) and Wasestjerna (1939). In their application to the problem of lattice vibrations and specific heats, it has been customary to proceed on the basis of the lattice theory of Born and Karman which gives a continuous spectrum of frequencies in the optical branch. A few typical frequencies corresponding to some important normal modes are usually evaluated and an estimate made of the approximate form of the Born and Karman frequency distribution curve. For NaCl, this has been partially done by Lyddane and Herzfeld (1938) who have given the numerical values of a few frequencies. Kellermann (1940) has determined a larger number (288) and has, in addition, used them for evaluation of the specific heats (1941).

Spectroscopic studies, however, show that the vibrations of crystal lattices exhibit numerous discrete frequencies, and do not support the theory

of Born and Karman which demands a continuous spectrum for them. In the case of diamond, for example, the experimental situation in this respect has been made perfectly clear by several independent methods of investigation, *viz.*, the study of the luminescence, absorption, and Raman spectra [Nayar, 1941-42; Miss Mani (under publication); R. S. Krishnan (under publication)]. That a similar situation arises also in the case of rock-salt is apparent from Rasetti's photographs of its Raman spectrum (Rasetti, 1931; Fermi, 1938), the interpretation of which on the basis of the selection rules has been discussed by R. S. Krishnan (1943). In order to explain these experimental facts, Sir C. V. Raman (1943) has recently made a new approach to the whole problem of lattice vibrations. According to his theory, the vibration pattern of the optical spectrum repeats itself exactly in a supercell consisting of eight simple cells. The normal modes of the lattice can then be described in terms of those of this supercell. For a face-centred cubic lattice the supercell has, besides the three translations, four modes of oscillation corresponding respectively to the cases when the atoms in successive octahedral or cubic planes move with opposite phases and either transversely or longitudinally to these planes. In rock-salt which consists of two interpenetrating face-centred lattices, we have double the number, namely eight modes, in addition to the fundamental vibration of the structure in which Cl and Na lattices vibrate against each other as a whole. There are thus nine optical modes which comprise 45 out of a total of 48 degrees of freedom, the remaining three degrees going over to the elastic spectrum. Chelam (1943) has given a description of the nine modes with the degeneracies attached to each of them. The numerical values of the corresponding frequencies can be easily obtained either from Lyddane and Herzfeld's work (*I.c.*) or Kellermann's (*I.c.*), and with the help of the known degeneracies it is possible to calculate the specific heats of the crystal and to compare them with the thermal data.

## 2. *Evaluation of the Frequencies*

(a) *Optical Frequencies*.—The nine possible modes of vibration of the lattice have been reproduced from Chelam's paper along with their degeneracies in Table I, which also contains the numerical values of corresponding frequencies as calculated by Lyddane and Herzfeld and by Kellermann. For comparison we have also given the frequencies derived by R. S. Krishnan from the observed lines in Rasetti's photographs of Raman effect on the basis (suggested by the selection rules) that they represent the octaves of the fundamental lattice oscillations. The values given in the last column are, therefore, half of the observed frequencies. It will be seen that seven of the calculated frequencies agree closely with the experimental values, the

TABLE I  
*Lattice Frequencies of Rock-salt*

Designation and Description of Mode	Degeneracy	Calculated Frequency I	Calculated Frequency II	Observed Frequency
$v_1$ : Oscillation of sodium and chlorine lattices against each other ..	3	Cm. <sup>-1</sup> 162	Cm. <sup>-1</sup> 152	Cm. <sup>-1</sup> 158
$v_2$ : Oscillation of sodium layers against each other normally to the octahedral planes ..	4	Cm. <sup>-1</sup> 244	Cm. <sup>-1</sup> 240	..
$v_3$ : Oscillation of chlorine layers against each other normally to the octahedral planes ..	4	Cm. <sup>-1</sup> 196	Cm. <sup>-1</sup> 193	Cm. <sup>-1</sup> 175
$v_4$ : Same as $v_1$ but transversely ..	8	Cm. <sup>-1</sup> 135	Cm. <sup>-1</sup> 127	Cm. <sup>-1</sup> 140
$v_5$ : Same as $v_3$ but transversely ..	8	Cm. <sup>-1</sup> 109	Cm. <sup>-1</sup> 102	Cm. <sup>-1</sup> 117
$v_6$ : Coupled oscillation of sodium and & chlorine ions normally to the cubic planes ..	3	Cm. <sup>-1</sup> 226	Cm. <sup>-1</sup> 223	..
$v_7$ : planes ..	3	Cm. <sup>-1</sup> 170	Cm. <sup>-1</sup> 165	Cm. <sup>-1</sup> 170
$v_8$ : Coupled oscillation of sodium and & chlorine ion tangentially to the cube ..	6	Cm. <sup>-1</sup> 173	Cm. <sup>-1</sup> 164	Cm. <sup>-1</sup> 170
$v_9$ : planes ..	6	Cm. <sup>-1</sup> 99	Cm. <sup>-1</sup> 94	Cm. <sup>-1</sup> 91

I from Lyddane and Herzfeld (*loc. cit.*, p. 858); II from Kellermann (*loc. cit.*, p. 543).

agreement with the results of Lyddane and Herzfeld being slightly better. The slight difference between the two calculated values arises from the fact that the authors have used slightly different constants for the repulsive forces (A and B of Kellermann's paper). For the infra-red proper frequency 162 cm.<sup>-1</sup> which corresponds to the vibration of the Na and Cl lattices against each other, Lyddane and Herzfeld have got the curious result that the frequencies of longitudinal and transverse oscillations are different from each other. Kellermann has questioned the validity of this result, and has obtained the same frequency for both the types, thus confirming the triple degeneracy assigned to this vibration by Chelam. Kellermann's expression for this frequency is the same as that of the transverse frequency of the former authors, the difference in numerical values again arising from the choice of slightly different constants. For this reason, we have only given the transverse frequency of Lyddane and Herzfeld in column III.

(b) *Elastic Spectrum.*—We have now to determine the frequency spectrum corresponding to the three degrees of freedom left over after the enumeration of the optical modes of vibration. We have no spectroscopic data which would enable us to do this. On the other hand, a theoretical calculation of the nature of this spectrum would involve much labour and would also raise difficult questions as to the possible influence of the external boundary of the crystal on the modes of vibration other than those

considered above. For these reasons, it is both convenient and probably also a fair approximation to the truth to identify the three omitted degrees of freedom with the elastic spectrum of the solid and to calculate its contribution to the thermal energy by means of a Debye function, the characteristic temperature  $\theta_D$  being obtained from the elastic data. It is usual to do this using the formula

$$\theta_D = \frac{h}{k} \left( \frac{3N}{4\pi V} \right)^{\frac{1}{3}} \bar{v}$$

where  $V$  is the atomic volume, and  $\bar{v}$  is obtained from

$$\frac{1}{\bar{v}^3} = \frac{1}{3} \sum_1^3 \frac{1}{4\pi} \int \int \frac{1}{v_i^3} d\omega$$

$v_i$  is the velocity of elastic waves in the direction  $i$  and the summation is over all the three waves for the whole solid angle. The integral (2) has been evaluated by Durand (1936) by Hopf and Lechner's interpolation method from the elastic constants at 80° K. The numerical value of  $\theta_D$  is 320° K. In Raman's theory, only 1/16 of the total degrees of freedom in the rock-salt structure are assignable to the elastic spectrum. The formula for the characteristic temperature has therefore to be modified by writing  $\frac{3N}{16}$  in place of  $3N$ . We thus obtain

$$\theta_D = \frac{320}{\sqrt[3]{16}} = 127^\circ \text{K.}$$

### 3. Evaluation of $C_v$

Unfortunately, the experimental data on the molar heats of rock-salt are very meagre. Nernst (1911) measured the specific heats at a few temperatures from 25° to 238° K, and these are practically the only data available to us. McGraw's (1931) measurements cover a large number of temperatures between 95 and 245° K, and show a maximum deviation of 5% from Nernst's results, but he himself considers Nernst's values as more reliable. As a matter of fact, his measurements were made to test the accuracy of his technique by comparing his results with those of Nernst. Clusius, Perlick and Goldmann's (Keesom, 1934) measurements extend only to a small range between 10 and 40° K. Their experimental results have not been reported, but a  $\theta_D/T$  curve has been given in the above-mentioned paper. This is rather unfortunate since a 1% deviation from  $\theta_D/T$  curve in this region corresponds to a 3% error in the specific heats. The experimental values between 10 and 40° K in the last column of Table II have been read from the above curve, at 25° and 28° K by us, and at other temperatures by Blackman (1942). Nernst's values wherever available have been shown in the last column but

one. They have been taken from *Handbuch der Experimental Physik*, vol. 8 page 256, which contains the values of  $C_v$ . It will be noticed that there is a large difference of the order of 10 to 15% between the two sets of observations.

For the purpose of evaluation of  $C_v$  we have preferred to use Lyddane and Herzfeld's values of the frequencies, as they seem to be nearer to the experimental values both in the infra-red and the Raman effect. That Kellermann's values are definitely lower is also seen from the fact that his elastic constants ( $c_{11}$  and  $c_{12}$ ) are slightly smaller than the observed ones. Of course, considering the nearness of the two sets of frequencies and the large uncertainty in the experimental values of  $C_v$ , this particular choice is not very material. The expression for  $C_v$  (Molar) is

$$C_v \text{ (molar)} = 3R \left[ \sum_1^9 \sigma_s E\left(\frac{hv_s}{kT}\right) + \frac{1}{8} D\left(\frac{127}{T}\right) \right],$$

where  $E$  and  $D$  stand for the Einstein and Debye functions respectively, and  $\sigma_s$  is the statistical weight of the frequency  $v_s$  and has the value  $\frac{1}{8}, \frac{1}{6}, \frac{1}{6}, \frac{1}{3}, \frac{1}{3}, \frac{1}{8}, \frac{1}{8}, \frac{1}{4}$  and  $\frac{1}{2}$  for each of the frequencies of Table I taken in order. The results of the calculations are shown in Table II. They exhibit a very close agreement with Perlick's observations wherever they are available.

TABLE II  
*Molecular Heats of NaCl*

Temperature °K	Optical frequencies	Elastic Spectrum	Total $C_v$	$C_v$ Experimental (Nernst)	$C_v$ Experimental C, P & G
10		.0282	.0282	..	.0326
20	.123	.176	.299	..	.310
25	.379	.268	.65	.58	.63
28	.602	.319	.92	.80	.93
30	.794	.350	1.14	..	1.150
40	1.911	.471	2.38	..	2.380
69	5.204	.633	5.84	6.24	..
81.4	6.26	.66	6.92	7.04	..
83.4	6.429	.666	7.10	7.44	..
110	7.964	.698	8.66	8.65*	..
138	8.940	.714	9.65	9.58	..
235	10.30	.73	11.03	11.10	..

\* Interpolated by Forsterling (1920) from Nernst's data.

The slight difference at 10° K is probably due to the Debye function not being a very good approximation to the true spectrum. Nernst's values in this region differ considerably from those of the other investigators, and at 83.4° show rather too large an increase for a rise of 2°. Considering

these facts, the agreement with Nernst's results at the higher temperatures seems to be quite satisfactory.

In conclusion, the author wishes to record his grateful thanks to Professor Sir C. V. Raman for the interest taken by him in this work.

#### 4. Summary

The new treatment of the dynamics of crystal lattices put forward by Sir C. V. Raman shows that the rock-salt structure has nine distinct frequencies of vibration in the optical branch which represent forty-five out of the forty-eight degrees of freedom of the group of 8 sodium and 8 chlorine ions present in a super-lattice cell. The theoretical calculations of Lyddane and Herzfeld as well as those of Kellermann have enabled these nine frequencies to be evaluated. They agree well with the experimental frequencies given by Rasetti's photographs of the Raman spectrum. The remaining three degrees of freedom represent the spectrum of the elastic vibrations of the lattice which may be evaluated from the known elastic constants. The thermal energy calculated on this basis shows a very satisfactory agreement with the experimental data.

#### REFERENCES

Blackman	.. <i>Proc. Phys. Soc.</i> , 1942, <b>54</b> , 377.
Born and Karman	.. <i>Phys. Zeits.</i> , 1912, <b>13</b> , 297.
Chelam	.. <i>Proc. Ind. Acad. Sci.</i> , (A), 1943, <b>18</b> , 261.
Durand	.. <i>Phys. Rev.</i> , 1936, <b>50</b> , 449.
Fermi	.. <i>Moleküle und Kristalle</i> , 1938.
Forsterling	.. <i>Ann. der phys.</i> , 1920, <b>61</b> , 558.
Huggins	.. <i>J. Chem. Phys.</i> , 1937, <b>5</b> , 143.
Keesom	.. <i>Phys. Zeits.</i> , 1934, <b>35</b> , 943.
Kellermann	.. <i>Phil. Trans. Roy. Soc.</i> , (A), 1940, <b>283</b> , 513. .. <i>Proc. Roy. Soc.</i> , (A), 1941, <b>178</b> , 16.
<hr/>	
Krishnan, R. S.	.. <i>Proc. Ind. Acad. Sci.</i> , (A), 1943, <b>18</b> , 298.
Lyddane and Herzfeld	.. <i>Phys. Rev.</i> , 1938, <b>54</b> , 846.
Madelung	.. <i>Phys. Zeits.</i> , 1910, <b>11</b> , 898.
McGraw, Jr.	.. <i>J. Am. Chem. Soc.</i> , 1931, <b>53</b> , 3683.
Nayar	.. <i>Proc. Ind. Acad. Sci.</i> , (A), 1941, <b>13</b> , 483, 534 ; 1941, <b>14</b> , 1 ; 1942, <b>15</b> , 293.
Nernst	.. <i>Ann. der Physik</i> , 1911, <b>36</b> , 395.
Raman	.. <i>Proc. Ind. Acad. Sci.</i> , (A), 1943, <b>18</b> , 237.
Rasetti	.. <i>Zeits. f. phys.</i> , 1930, <b>61</b> , 598.
Wasesjerna	.. <i>Phil. Trans. Roy. Soc.</i> , (A), 1939, <b>237</b> , 105.



# THE CRYSTAL SYMMETRY AND STRUCTURE OF DIAMOND

BY SIR C. V. RAMAN

(*From the Department of Physics, Indian Institute of Science, Bangalore*)

Received April 17, 1944

## CONTENTS

1. The Crystal Symmetry of Diamond; 2. The Four Possible Structures of Diamond; 3. Confirmation of the Theory by Infra-Red Spectroscopy; 4. Interpenetration of Positive and Negative Tetrahedral Structures; 5. Lamellar Twinning of Octahedral Structures; 6. Inter-Twinning of Tetrahedral and Octahedral Structures; 7. Summary.

### 1. *The Crystal Symmetry of Diamond*

DIAMOND was assigned by the earlier crystallographers (*vide* Groth, 1895; Liebisch, 1896; Hintze, 1904) to the ditesseral polar or tetrahedrite class of the cubic system. The assignment was based on the fact that though diamond commonly exhibits octahedral symmetry of form, specimens showing only the lower tetrahedral symmetry were forthcoming, and it was therefore natural to suppose that the higher symmetry when observed was the result of a supplementary twinning of the positive and negative tetrahedral forms. In particular, the appearance of octahedral forms with grooved or re-entrant edges could be explained in this way. We may here quote from the first edition of Miers' *Mineralogy* (1902) where the forms of diamond are discussed at considerable length: "Much controversy has taken place upon the question whether the diamond is really octahedral as it appears or tetrahedral as is suggested by the grooves; the problem may now be regarded as decided in favour of the tetrahedrite class by the following two facts: (1) several crystals have been found which are undoubtedly simple crystals of tetrahedral habit..... (2) the supplementary twinning of such crystals sufficiently explains all the other peculiarities of form." Sutton (1928) who has written a treatise on the South African diamonds gives illustrations of crystals having the forms of hexakis-tetrahedra, truncated tetrahedra, duplex-tetrahedra and others which are entirely typical of ditesseral polar symmetry.

Van der Veen (1908) noticed that diamond does not exhibit any pyroelectric properties and expressed the view that this is irreconcilable with the assignment of tetrahedral symmetry. The results of the X-ray analysis of the crystal structure of diamond by W. H. Bragg and W. L. Bragg (1913) have also usually been regarded as demonstrating that diamond possesses holohedral symmetry (Tutton, 1922; W. L. Bragg, 1937). These contentions are, however, open to question. It may, in the first place, be pointed out that the evidence of the crystal forms on which the earlier assignment was based cannot be lightly brushed aside. Secondly, it is very significant that the X-ray data show the structure of diamond to be analogous to that of zinc blende which is a typical crystal of the tetrahedrite class, and this is a hint that the crystal symmetry of diamond might also be of the same class. It is thus evident that the matter deserves more careful consideration than it appears to have received so far. It is the purpose of the present paper critically to examine the question whether the crystal symmetry of diamond is octahedral or only tetrahedral. The investigation reveals that there are several alternative possibilities and thereby furnishes the key to an understanding of many remarkable and hitherto imperfectly understood facts regarding the diamond and its physical properties.

## 2. *The Four Possible Structures of Diamond*

We shall accept the X-ray finding that the structure of diamond consists of two interpenetrating face-centred cubic lattices of carbon atoms which are displaced with respect to one another along a trigonal axis by one-fourth the length of the cube-diagonal. Each carbon atom in the structure has its nucleus located at a point at which four trigonal axes intersect. Hence, we are obliged to assume that the electronic configuration of the atoms possesses tetrahedral symmetry. It must also be such that the alternate layers of carbon atoms parallel to the cubic faces have the same electron density. This is shown by the X-ray finding that the crystal spacings parallel to the cubic planes are halved. Hence, the possibility that the two sets of carbon atoms carry different total charges is excluded. In other words, diamond is not an electrically polar crystal in the ordinary sense of the term. It is readily shown, however, that the charge distributions may satisfy both of these restrictions and yet not exhibit a centre of symmetry at the points midway between neighbouring carbon atoms. To show this, we remark that when two similar structures having tetrahedral symmetry interpenetrate, centres of symmetry would not be present at the midpoints between the representative atoms unless the tetrahedral axes of the two structures point in opposite directions. We may, in fact, have *four* possible kinds of arrangement as indicated in Fig. 1. Of these the arrangements

shown in Td I and Td II have tetrahedral symmetry, while Oh I and Oh II would be distinct forms, both having octahedral symmetry.

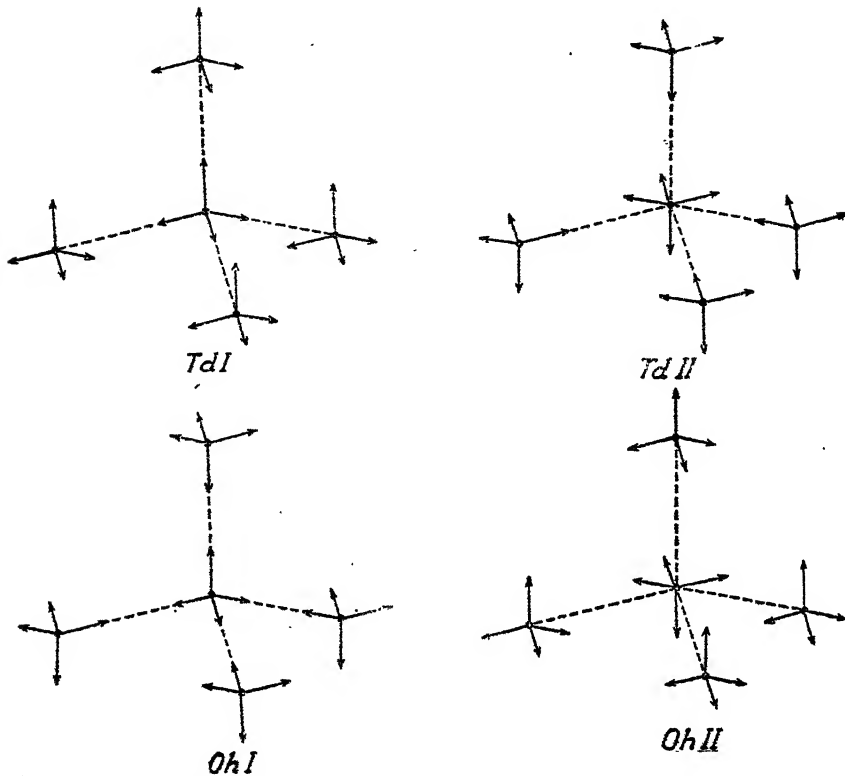


FIG. 1. The Four Possible Structures of Diamond

The tetrahedral symmetry of the atoms required by virtue of the special positions which they occupy in the crystal lattice must be satisfied both by the electrostatic distributions of charge and by the orientations of the orbital and spin moments of the electrons. When the structure as a whole is considered, the magnetic moments should be fully compensated, since the crystal is diamagnetic. But such compensation may be secured in several distinct ways which would endow the structure with different symmetry properties. On the one hand, four equal magnetic moments directed either all inwards or all outwards along the four tetrahedral axes of a cubic crystal would automatically cancel each other. On the other hand, if the pair of electrons which bind neighbouring atoms have opposite magnetic moments (directed inwards or outwards as the case may be), these would directly cancel each other. Considering these two pairs of possibilities, we have four different ways in which the extinction of the resultant magnetic moment

may be secured. It is seen that these correspond to the four possible structures of diamond indicated in Fig. 1.

It is readily shown that if the charge distributions which differ in their angular setting as shown in Fig. 1 are otherwise identical, the electron density in the alternate layers of atoms parallel to the cubic planes would be the same. This follows immediately from the fact that these planes are equally inclined to the tetrahedral axes. Hence, all the arrangements shown in Fig. 1 would be consistent with the observed halving of the spacing of these planes. Hence, the X-ray findings leave the question whether diamond possesses tetrahedral or octahedral symmetry entirely open.

The expectation that diamond would have pyro- or piezo-electric properties would only be justified if the neighbouring carbon atoms carry different electric charges. Since this is not the case, the absence of such properties cannot be regarded as a contradiction of the views of the earlier crystallographers regarding the symmetry class to which diamond belongs.

### *3. Confirmation of the Theory by Infra-Red Spectroscopy*

Placzek (1934) has discussed the relation between the symmetry class of crystallographic groups and their activity in infra-red absorption, as also in the scattering of light with change of frequency. He has shown that for the groups which contain a symmetry centre, the selection rules for infra-red absorption and for light-scattering are complementary, *viz.*, the modes of vibration which can appear in light-scattering are forbidden in infra-red absorption, and *vice versa*. For those groups which do *not* have a centre of symmetry, there is a possibility that the same vibrations may appear both in the scattering of light and in infra-red absorption. The simplest illustration of these principles is furnished by the case of a diatomic molecule, its vibrations being active in light-scattering and inactive for infra-red absorption provided the atoms are similar, and active in both if they are dissimilar. Placzek's rules successfully explain the experimentally observed behaviour of many crystals in light-scattering and in infra-red absorption. Taking, for instance, the case of rock-salt which has holohedral symmetry, its fundamental frequency is that of the triply degenerate oscillation of the sodium and chlorine lattices with respect to each other. This is observed to be active in infra-red absorption and inactive in light-scattering, in accordance with the behaviour indicated by the selection rules.

The infra-red absorption of diamond was studied by Angstrom (1892), Julius (1893) and by Reinkober (1911), and has been investigated with especial thoroughness by Robertson, Fox and Martin (1934). From these studies, and especially from the work of the last mentioned investigators,

the remarkable fact emerges that diamonds are not all identical in respect of their behaviour in infra-red absorption. In the majority of diamonds the infra-red absorption coefficient rises very steeply from a comparatively moderate value to a maximum of about 90% in the wave-number range 1350–1300 cm.<sup>-1</sup>. This steep rise in absorption as well as the entire band of which it is the head are, however, wholly absent in other diamonds which evidently form a second and rarer variety.

The significance of these facts becomes clearer when it is remarked that the fundamental frequency of the diamond structure is that of the triply-degenerate oscillation of the two lattices of carbon atoms with respect to each other, and that this falls precisely within the range of wave-numbers where the sudden rise of infra-red absorption occurs in the commoner variety of diamond. This is proved by the appearance of an intense line with a frequency-shift of 1332 cm.<sup>-1</sup> in the spectrum of the scattering of monochromatic light by diamond; the wave-number of the fundamental vibration of the diamond structure calculated from its specific heat data is also 1332 cm.<sup>-1</sup> (Ramaswamy, 1930). The investigations of Robertson and Fox (1930) have shown that both the commoner variety of diamond which exhibits the infra-red absorption in this region of frequency and the rarer variety in which it is missing, alike exhibit the strong line with a frequency shift of 1332 cm.<sup>-1</sup> in the spectra of the scattering of light.

Placzek's selection rules (*loc. cit.*) for the point-groups of the cubic system show that a triply-degenerate vibration in a crystal having octahedral symmetry can manifest itself *only* in infra-red absorption or in light-scattering *but not in both*. On the other hand, in a crystal with tetrahedral symmetry, such a vibration must appear *both* in absorption and light-scattering or else can appear in *neither*. Taking these selection rules in conjunction with the experimental facts, it follows at once that the commoner variety of diamond has only tetrahedral symmetry, while the rarer variety of diamond has octahedral symmetry. *The views of the earlier crystallographers assigning only the lower symmetry are thus completely vindicated by the infra-red absorption data and the selection rules so far as the commoner variety of diamond is concerned. The rarer variety of diamond must however be credited with the full or holohedral symmetry of the cubic system.*

Infra-red spectroscopy thus compels us to recognize the existence of two forms of diamond, a commoner form having only tetrahedral symmetry of structure, and a rarer form having octahedral symmetry. We have now to consider the further implications of the theory which indicates that each of these forms has two variants, namely those whose symmetry characters

are indicated in Fig. 1 as Td I and Td II respectively for the tetrahedral type of diamond, and as Oh I and Oh II respectively for the octahedral type. The question arises whether there is any physical evidence for the existence of these four types of diamond and in what manner, if any, it is possible to differentiate between them. In this connection, it is worthy of note that both the tetrahedral and octahedral types of diamond, as we may now designate them, exhibit the same frequency shift ( $1332 \text{ cm}^{-1}$ ) in the scattering of light within the limits of observational error. This indicates that the forces which hold the carbon atoms together in the two kinds of diamond do not differ sensibly, despite the difference in the symmetry of their<sup>1</sup> structures. Accepting this as an experimental fact, it follows that in respect of the energy of formation and the lattice spacings in the crystal, and therefore also all the commoner physical properties, such as density, elasticity, specific heat, refractivity, dielectric constant, diamagnetic susceptibility, etc., any differences which may exist between the four types of diamond must be small. It is very remarkable that though the symmetry of the electronic configuration is not the same in the two types of diamond, the strength of binding between the carbon atoms is not sensibly different. *Prima facie*, this result indicates that the electrostatic distributions of charge are the same. We are therefore led to assume that the differences which exist lie essentially in the orientations of the orbital and spin moments of the electrons, as already indicated.

#### 4. *Interpenetration of Positive and Negative Tetrahedral Structures*

As the commoner type of diamond has only tetrahedral symmetry, crystallographic considerations compel us to admit the existence of two variants of the tetrahedral type, namely the positive and negative structures indicated by Td I and Td II respectively in Fig. 1. It is evident that these two sub-classes would be completely identical in respect of energy of formation and lattice spacing, and consequently also in respect of density, refractive index and such other physical properties. The question then arises how we can distinguish between them.

It is possible, of course, for diamond having the positive or negative tetrahedral structure to have an external form with octahedral symmetry. For, both positive and negative tetrahedral faces may appear in the same diamond—as they actually do in zinc-blende—and it is quite possible that they are equally well developed with nothing whatever to distinguish one from the other. The comparative infrequency of crystals having a simple tetrahedral habit would, however, be easier to understand on the basis of the supplementary twinning of the positive and negative tetrahedral forms.

That such twinning is possible and indeed common finds support in the various peculiarities of form (e.g., the grooving of the octahedral edges) observed in actual specimens. Further, the identity of the physical properties of the positive and negative tetrahedral structures makes the assumed interpenetration highly probable on theoretical grounds. We are therefore justified in assuming that such interpenetration twinning is a phenomenon of very general occurrence.

It is well known that when interpenetrative twinning occurs, there is no "plane of composition", in other words, the interpenetrating forms are separated from each other in an irregular way. In the present case, the interpenetration is often complete and it is a reasonable assumption that it may occur on a microscopic or even ultra-microscopic scale. Whether this is so or not, the identity of density and refractive index would make the direct observation of such internal twinning impossible, and we would have to depend on the study of structure-sensitive properties to demonstrate its existence. Diamond is rightly regarded as one of the most perfect crystals, if not the most perfect of them all, as shown by the extreme sharpness of the setting for the reflection of monochromatic X-rays exhibited by well-chosen specimens. It is evident however, that unless a specimen consists *exclusively* of sub-type Td I or of sub-type Td II, we cannot consider it as ideally perfect and homogeneous. Hence, the existence of the interpenetrative twinning should be capable of detection by X-ray methods. The *smaller* the volume-elements inside the crystal which are exclusively of one or the other sub-type, the more numerous would be the elementary blocks of which the crystal is built up, and the easier, therefore, would it be to observe the resulting non-homogeneity of the crystal by its X-ray behaviour or by other delicate methods of study.

##### 5. *Lamellar Twinning of Octahedral Structures*

Fig. 1 indicates that the sub-types Oh I and Oh II cannot, unlike the sub-types Td I and Td II, be regarded as necessarily identical with each other in observable physical properties. They would nevertheless resemble each other sufficiently closely to make it highly probable that the Oh I and Oh II types would frequently appear together in the same specimens of diamond of the octahedral variety.

It is significant in this connection that a laminated structure in which layers parallel to one, two, three or even all the four faces of the octahedron appear simultaneously has been recognised as a characteristic phenomenon exhibited by some diamonds. Sutton (1928) describes and illustrates this kind of structure in diamond. He recognises that it is quite different from

the macking or twinning which has been often observed in diamond, since in the latter case, the components differ in orientation as shown by the difference in their planes of cleavage, and also, of course, by their X-ray patterns. Sutton therefore considers the lamellar structure to be an "illusory" type of twinning. Since, however, it is a real phenomenon it is no explanation of its existence to call it by such a name. Indeed, the appearance of a finely laminated structure is a well-known experience in crystallographic studies. It is observed for instance, in iridescent crystals of potassium chlorate and in various other substances. Hence, it is a reasonable assumption that when it is observed in diamond, it is also a specific form of twinning. We have already seen that an interpenetrative twinning of the Td I and Td II types would not exhibit any specific planes of composition. Hence, the presence of a lamellar structure in diamond parallel to the octahedral planes is a definite indication of the presence of the Oh types in the specimen and if, further, the specimen consists exclusively of these types, we may explain it on the basis that the Oh I and Oh II sub-types appear in alternate layers within the crystal. The simultaneous appearance of laminations parallel to more than one of the octahedral planes presents no difficulty of explanation on this view, since it would indicate merely that the two sub-types appear in the diamond as small blocks bounded by surfaces parallel to the laminations instead of as thin layers.

#### *6. Inter-Twinning of the Tetrahedral and Octahedral Structures*

Though diamonds having the lower and higher symmetry are physically different, yet they are so closely alike in their structure that the appearance of the two types simultaneously in the same individual crystal must be a not uncommon event. Indeed, since diamond has usually the lower symmetry, it may be expected that the higher symmetry would appear as an intrusion in diamond of the lower symmetry more frequently than as a type by itself. Since there are altogether four types of diamond, the number of possible modes of combination amongst them is fairly large, and we may have a wide range of possible space distributions of the different kinds of structure within the crystal.

Inter-twinning of the tetrahedral and octahedral forms of diamond may ordinarily be expected to exhibit a composition plane or planes parallel to each other within the crystal, thus dividing up the latter into layers which are physically different. The alternate layers may consist exclusively of the Td I or Td II types and of the Oh I or Oh II respectively. On the other hand, it is also possible that the Td I and Td II types may appear together in the layers having tetrahedral symmetry, while similarly, the Oh I and Oh II

types may appear as alternate finely-spaced laminae within the layers having octahedral symmetry. Besides such cases, others may conceivably arise in which diamond of the lower symmetry is dispersed in microscopically small volume elements or even ultra-microscopically in diamond of the higher symmetry, or *vice versa*. The possibility of such cases is distinctly suggested by the situation which exists in relation to the individual types of diamond.

### 7. Summary

By virtue of the special positions which they occupy in the crystal lattice, the carbon atoms in diamond must have a tetrahedrally symmetric configuration of the electron orbital movements and spins. A tetrahedral axis has both direction and sense, and the carbon atoms in the two Bravais lattices may therefore be orientated in space and with respect to each other in four distinct ways, each of which corresponds to a possible structure for diamond. In two of these structures, diamond has only tetrahedral symmetry and in the two others the full or octahedral symmetry of the cubic system. The selection rules require that the fundamental vibration of the diamond lattice having a frequency  $1332\text{ cm.}^{-1}$  should appear both in light-scattering and infra-red absorption if the crystal has tetrahedral symmetry, while it would appear only in light-scattering and not in the infra-red absorption spectrum if the symmetry is octahedral. These predictions are in accord with the observed spectroscopic behaviours respectively of the commoner and rarer types of diamond recognised as such by Robertson, Fox and Martin. Hence, the assignment of tetrahedral symmetry to diamond by the earlier crystallographers is confirmed for the commoner type of diamond, while on the other hand, the rarer type is shown to have the full symmetry of the cubic system. The crystallographic facts also support the theoretical result that there should be two sub-types of diamond for each kind of symmetry. The positive and negative structures having tetrahedral symmetry have identical physical properties and can therefore interpenetrate freely. The two sub-types having octahedral symmetry cannot be considered as physically identical and their inter-twinning would therefore have composition planes. The lamellar structure parallel to the octahedral planes observed in some diamonds thereby becomes explicable. The possibility that diamond having the higher and lower types of symmetry may appear inter-twinned in the same crystal has also to be recognised.

## REFERENCES

Angstrom, K. . . 1892 (quoted by Reinkober).

Bragg, W. H., and Bragg, W. L. *Proc. Roy. Soc.*, A, 1913, **89**, 277.

Bragg, W. L. . . *Atomic Structure of Minerals*, Oxford University Press, 1937, p. 52.

Groth, P. . . *Physikalische Kristallographie*, Engelmann, 1895, p. 515.

Hintze, C. . . *Handbuch der Mineralogie*, Veit, 1904, **Band 1**, Abt. I, p. 3.

Julius . . . 1893 (quoted by Reinkober).

Liebisch, T. . . *Physikalische Kristallographie*, Veit, 1896, p. 88.

Miers, H. E. . . *Mineralogy*, MacMillan, 1902, p. 291.

Placzek, G. . . "Rayleigh-Streuung und Raman-Effekt," *Handbuch der Radiologie*, 1934, **Band 6**, 2nd Auf., Teil. II, p. 231, Table 9 on p. 297 and p. 305.

Ramaswamy, C. . . *Nature*, 1930, **125**, 704; and *Ind. Jour. Phys.*, 1930, **5**, 97.

Reinkober . . . *Ann. der Phys.*, 1911, **34**, 343.

Robertson, R., Fox, J. J., and Martin, A. E. . . *Phil. Trans. Roy. Soc.*, A, 1934, **232**, 482.

Robertson, R., and Fox, J. J. . . *Nature*, 1930, **126**, 279.

Sutton, J. R. . . *Diamond*, Murby, 1928, Plates, II, IV, XVII, XVIII, XX and XXI. Also pp. 9 and 32-33.

Tutton, A. E. H. . . *Crystallography and Practical Crystal Measurement*, MacMillan, 1922, **1**, 502.

Van der Veen . . . *Proc. Acad. Sci.*, Amsterdam, 1908, **10**, 182.

# THE NATURE AND ORIGIN OF THE LUMINESCENCE OF DIAMOND

BY SIR C. V. RAMAN

(From the Department of Physics, Indian Institute of Science, Bangalore)

Received April 17, 1944

## CONTENTS

1. Introduction; 2. The Material for Study; 3. Intensity and Colour of Luminescence; 4. Luminescence Patterns in Diamond; 5. Luminescence and Ultra-Violet Transparency; 6. Luminescence and Structural Birefringence; 7. Interpretation of the Experimental Facts; 8. The Spectral Characters of Luminescence; 9. Luminescence and X-Ray Reflection Intensities; 10. Excitation of Luminescence by X-Rays; 11. Phosphorescence; 12. Summary.

### 1. *Introduction*

Nor the least interesting of the many remarkable properties of diamond is that it emits visible light on excitation by appropriate methods. Many investigators have studied the luminescence of diamond since Robert Boyle in 1663 published his observations of the phenomenon. To the methods of exciting luminescence described by him, *viz.*, light, heat and friction, the advance of knowledge has added others, *viz.*, cathode-ray bombardment and X-rays. It has also provided instruments, *viz.*, the phosphoroscope and the spectroscope for the critical study of the phenomenon and extended the range of temperatures over which it may be observed downwards to the lowest values. A full summary of the earlier investigations is given in the fourth volume of Kayser's *Handbuch* (1908). In view of the fact that diamond is an elementary solid and is the typical valence crystal, it might have been supposed that its behaviour would figure prominently in any account of the subject of luminescence. Far from this being the case, the luminescence of diamond does not even find a mention in the two bulky treatises written by Lenard for the *Handbuch der Experimental Physik*, or in Pringsheim's article of 1928 in the *Handbuch der Physik*. The reason for this lack of interest is clear from the brief reference made in Pringsheim's book (1928) and in his earlier *Handbuch* article (1926), namely the belief

that the centres of luminescence in diamond are not the atoms of carbon of which it is composed, but some foreign atoms of undetermined identity present in it as impurity. The basis for this belief has been the variability of the intensity and colour of the emitted light, and the fact that not all diamonds show the phenomenon. The impurities suggested in the literature as the origin of the luminescence make a lengthy list, viz., samarium, yttrium, sodium, aluminium, chromium, iron and titanium, and include even some hydrocarbons !

The considerations regarding the crystal symmetry and structure of diamond developed in the introductory paper of this Symposium (Raman, 1944) enable us to make a fresh approach to the problem of its luminescence. It is proposed to give a general outline of the experimental facts regarding the luminescence properties of diamond and to show that they fit naturally into the framework of the ideas developed in that paper, while, on the other hand, the facts remain wholly unintelligible on the impurity hypothesis. On the basis of the new ideas, it follows that the behaviour of diamond in respect of luminescence should stand in the closest relationship with its other properties, namely the absorption spectra in visible, ultra-violet and infra-red regions of the spectrum, the isotropy or birefringence observed in the polariscope, the X-ray reflection intensities, and so on. The evidence that such relationships actually exist, thereby placing the new ideas on a firm basis of experimental fact, is briefly set out in the present paper, and in fuller detail in others following it in the symposium.

## 2. *The Material for Study*

Opportunities for observing the luminescence of diamond in an impressive fashion first presented themselves to the writer in the year 1930 in connection with spectroscopic studies on the scattering of light in crystals. Several diamonds of exceptional size and quality (one of them as large as 143 carats) had been loaned by kind friends for use in those investigations. It was then found that the luminescence spectrum of diamond recorded itself on the spectrograms simultaneously with the scattering of light in the crystal, its leading feature being a band at 4155 A.U., and its intensity varying enormously from specimen to specimen (Bhagavantam, 1930). These observations on photo-luminescence suggested a comparison with the case of cathode-ray luminescence. A spectroscopic investigation of the latter phenomenon was then undertaken and showed very clearly the similarity between the results in the two cases (John, 1931). The very striking character of the photo-luminescence as observed visually with some of the diamonds indicated that its further study should prove a fascinating

line of research. The difficulty of obtaining suitable material, however, discouraged the pursuit of the subject.

About five years ago, the writer became aware that cleavage plates of diamond of good size and of excellent quality could be obtained at very modest prices. It was also recognized that diamond in this form is often more suitable for physical investigations than the high-priced brilliants of the jeweller's trade. The difficulty of obtaining material having thus disappeared, a sufficient number of specimens was acquired to make a start with the research, and a very fruitful series of investigations on the scattering and absorption of light in diamond and its photo-luminescence at various temperatures was carried out (Dr. P. G. N. Nayar, 1941, *a, b, c, d*; 1942 *a, b*).

In June 1942, the writer was enabled through the kindness of the Maharaja of Panna to visit his State in Central India where diamond-mining has been carried on since very early times. The necessary instruments were transported to Panna and set up in a room in the State Treasury, and with the assistance of Dr. Nayar, a physical examination was made of some hundreds of diamonds in their natural state. In particular, the valuable opportunity was afforded to us of observing the crystal form and luminescence properties of a unique set of 52 large diamonds of the finest quality belonging to the Maharaja. The writer was also enabled during this visit and also a subsequent one in December 1942 to purchase a representative collection of the diamonds mined in the State and of enlarging his collection of polished cleavage plates. Preliminary reports of the observations made on the Panna diamonds have already appeared (Raman, 1942, 1943).

The observations made at Panna and the more detailed systematic studies made at Bangalore with the diamonds in the writer's collection have furnished ample material on which to base trustworthy conclusions. The material available for the laboratory investigations includes 310 specimens which may be classified as under:

- (a) 29 Panna crystals in their natural condition, selected so as to be representative of the forms and qualities of diamond as found in the State.
- (b) 65 Polished cleavage plates, for the greater part of Indian origin.
- (c) 88 Brilliants, made from South African diamonds, and set together as a jewel.
- (d) 10 Diamonds of various origins specially chosen for their interesting behaviour in regard to luminescence or colour.
- (e) 118 Other diamonds, mostly of Indian origin.

### 3. Intensity and Colour of Luminescence

*The 88 South African Diamonds.*—These diamonds are in the form of brilliants of varying size. Set in gold surrounded by a circle of pearls and interspersed by lines of rubies and emeralds, the pattern formed by them represents the double-headed eagle which is the heraldic emblem of the Mysore State (Fig. 1 in Plate III). The brilliants are not quite large enough to exhibit the inherent colour, if any, of the diamonds. So far as can be seen, however, they appear to be clear and colourless.

The ensemble of diamonds, pearls, rubies and emeralds formed by the ornament makes a striking exhibit when irradiated by ultra-violet light in the wave-length range 3500–3900 A.U. obtained by filtering the rays of the sun or of an electric arc through a plate of Wood's glass. The circle of pearls shines brightly with a uniform bluish-white lustre, while the lines of rubies appear a brilliant red and the emeralds a very faint yellow. The diamonds on the other hand, vary enormously in their appearance. A few of them irregularly scattered over the set emit a bright blue light of great intensity, while others not so luminous are also to be seen here and there. A cursory inspection suggests that only some ten or twelve of the diamonds emit any visible light. On a closer examination, however, it becomes evident that this is not really the case and that *all the 88 diamonds excepting three or four are luminescent*, though with enormously different intensities. This fact becomes particularly clear when the ultra-violet rays are focussed on each individual diamond so that the intensity of the light emitted by it is as great as possible. It is then noticed that the great majority of the diamonds exhibit luminescence of various shades of blue, the fainter ones appearing an indigo-blue and the brighter ones purer blue. Half a dozen of the diamonds, however, exhibit other colours, *viz.*, greenish blue, greenish yellow, or pure yellow.

The range of variation of intensity between the different diamonds may be roughly estimated from the photographic exposures necessary to record them on a plate. The appearance of the ornament as seen by daylight is shown in Fig. 1 and photographed by (Miss) Mani with different exposures under ultra-violet light in Figs. 2 to 6 in Plate III. A cell containing a concentrated solution of sodium nitrite was placed in front of the camera lens as a complementary filter when obtaining the luminescence photographs. Its effectiveness is shown by the fact that the gold setting and all the gems with the exception of the diamonds and one of the emeralds remain completely invisible. An exposure of two seconds was found to be sufficient to record the three mostly strongly luminescent diamonds. Exposures of

5 seconds, 15 seconds and 30 seconds respectively resulted in substantial increases in the number of diamonds visible in the photograph (Figs. 2, 3 and 4 respectively). An exposure of two minutes (Fig. 5) was necessary before the pattern bore any recognizable resemblance to its appearance as seen by daylight, while an exposure of 30 minutes was necessary in order to record the most feebly luminescent diamonds (Fig. 6). The brightest diamonds are, of course, then heavily overexposed. A ratio of the order of 1000:1 or even more, between the strongest and the feeblest emission intensities, is thus indicated.

*The 52 Large Panna Diamonds.*—Crystals having smooth and lustrous faces and exquisitely beautiful geometric forms (rounded hexakis-octahedra or tetrakis-hexahedra) are to be found amongst those mined in the Panna State. Mr. Sinor's book (1930) on the diamond mines of Panna contains an illustration of a remarkable and probably unique set of 52 diamonds of this kind, all having the form of hexakis-octahedra, every one of them of the finest water, and their sizes forming a regular gradation from 24 carats for the largest to 1½ carats for the smallest. The diamonds are strung together as a garland in their natural state by thin girdles of gold which leave the crystal faces exposed. The luminescence properties of the entire set of diamonds could therefore be very conveniently examined one after another in succession. For this purpose, the light of a carbon-arc was filtered through a plate of Wood's glass and focussed by a lens on one of the faces of the crystal, and the track of the beam inside the diamond as made visible by the luminescence could be observed through another face. In this way, besides noting the colour of the luminescence, some idea of its relative intensity in the different diamonds could also be obtained.

Of the 52 diamonds in the set, the luminescence of 3 diamonds was visually classified as "intense", of 12 as "strong", of 21 as "weak", of 14 as "very weak" and of the remaining 2 diamonds as "unobservable". The luminescence as observed in all the 50 fluorescent diamonds was of a blue colour, though, as stated, its intensity varied enormously.

*The Writer's Collection of 29 Panna Diamonds.*—The specimens in this collection fall into two groups. Group A comprises 10 diamonds of the best quality, colourless and transparent, having well-developed crystal forms and smooth lustrous faces. Group B comprises 19 so-called "industrial" diamonds, mostly of irregular shape and having a noticeable colour, grey, brown, or yellow. From a scientific point of view, however, some of these diamonds are of great interest, thereby justifying their inclusion in the collection.

The diamonds were in the first instance tested in the usual manner under ultra-violet irradiation and all of them were found to be luminescent. At a later stage in the investigations, it was found useful to immerse the diamonds, while irradiated, in a cell containing a highly refractive liquid and thereby diminish the disturbing effect of reflections and refractions at their external surfaces. The behaviour of the diamonds in the two groups showed many notable differences. Those in Group A were all blue-luminescent. So far as could be made out, the intensity was uniform within the substance of each crystal, though it differed enormously as between the different diamonds. The diamonds in Group B showed a very varied behaviour. Some exhibited a blue luminescence very similar to that given by the diamonds in Group A, but its intensity varied greatly, not only as between the different specimens but also within the volume of each individual crystal. Others, again, of the diamonds in Group B showed a greenish-yellow luminescence of which the intensity varied from specimen to specimen. Careful examination showed that luminescence of this colour was, in general, not uniformly distributed within the specimen, but appeared in parallel bands or stripes running through the volume of the crystal. The remaining crystals in Group B showed a mixed type of luminescence in which yellow bands or stripes of varying width appeared crossing a background of blue colour. In some of them, the yellow luminescence was most pronounced near projecting tips or bosses on the surface of the crystal, while the blue luminescence appeared in the interior.

The observations made with the Panna diamonds are of particular value, as the specimens were studied individually in their natural state and were in some cases also of considerable size. The observations with the brilliants of South African origin were not made under such favourable conditions, and hence they are not scientifically so significant. Broadly speaking, however, the results obtained with the two sets of diamonds are in excellent accord. The experimental situation may be summarised as follows:

- (a) Luminescence under ultra-violet excitation is exhibited by the vast majority of diamonds, including especially those of the finest quality.
- (b) A blue luminescence is characteristic of nearly all diamonds which are colourless and crystallographically perfect, its intensity, however, varying enormously from specimen to specimen.
- (c) Imperfect diamonds show sometimes a blue luminescence, sometimes a greenish-yellow luminescence and sometimes a mixed

type of luminescence, the intensity of which varies not only from specimen to specimen but also within the volume of each specimen.

(d) A few diamonds are definitely non-luminescent.

#### *4. Luminescence Patterns in Diamond*

The difficulties which arise in working with the immersion method are altogether avoided by the use of polished cleavage-plates of diamond. 65 such plates are included in the writer's collection. Their thickness is generally small (from half a millimetre to one millimetre or more), but this is far from being a disadvantage in these investigations. The luminescence of the plates may be conveniently studied by placing them on a polished sheet of copper and irradiating them normally with ultra-violet light, a complementary filter of sodium nitrite solution being used when photographs are desired.

The enormous variations in the intensity of luminescence are best appreciated by viewing a group of diamonds at the same time (see Fig. 7, in Plate IV which includes 46 diamonds). Six plates in the collection exhibit no observable luminescence except very feebly at their edges, as shown by the bottom row in the figure. The luminescence of 34 plates is a blue, of 6 plates a yellowish-green, and of the remaining 19 plates a mixture of the two. The blue-luminescing plates may be divided into two groups of approximately equal number; in the first group, the luminosity is more or less uniform over the plate except at the unpolished edges which shine out brightly; in the second group, the luminosity is highly non-uniform over the area of the plate and exhibits a pattern of bright and dark regions, usually with geometric features related to the crystal structure, the lines of equal brightness running parallel to the inter-sections of one, two or three sets of octahedral planes with the surface of the plate. Most of the yellow-luminescent diamonds show a pattern of fine streaks running parallel to one another within the plate. In the plates showing the mixed type of luminescence, sets of yellow bands running parallel to one another in one or two or even three different directions within the crystal are a conspicuous feature. The appearance of these yellow bands is found to depend on the angle at which the plate is viewed; they appear as fine sharp lines at some angles of observation and as broad bands at others, thereby indicating that they represent thin luminescent layers within the substance of the crystal.

Many of the 46 cleavage plates appearing in Fig. 7 in Plate IV exhibit luminescence patterns, as may be seen in that figure. The scale of this photograph is however rather too small and the exposures in most cases either too great or too small to record the patterns satisfactorily. Six typical

patterns photographed on a larger scale are reproduced as Fig. 8 and Fig. 9 respectively in Plate V, appearing in the upper half of these pictures. The geometric character of the patterns shown by D38 in Fig. 8 and by D179 in Fig. 9 is particularly noteworthy. These, as well as D224 appearing in Fig. 8, are blue-luminescent diamonds. The non-uniform intensity and the appearance of dark streaks in the luminescence of D179 and D224 are also worthy of remark. D200 seen in Fig. 8 has a greenish-yellow luminescence in which the most prominent feature is a set of four parallel bands. D188 and D190 appearing in Fig. 9 are typical diamonds exhibiting the mixed variety of luminescence. The former shows an extremely interesting pattern consisting of an intense blue spot surrounded by a faint blue ground which is crossed by sets of parallel yellow bands running in different directions across the plate. D190 exhibits a pattern of parallel bands running in different directions, blue in one part of the diamond and yellow in other parts.

Many other examples of luminescence patterns and a detailed description of the same will be found in a paper by Mrs. K. Sunandabai (1944) appearing in this symposium.

##### 5. Luminescence and Ultra-Violet Transparency

It has long been known that while the majority of diamonds are opaque to ultra-violet radiation of wave-lengths smaller than about 3000 A.U., there are some diamonds which transmit the ultra-violet rays freely up to about 2250 A.U. The investigations of Roberston, Fox and Martin (1934) have shown that this difference in ultra-violet transparency goes hand in hand with other notable differences in behaviour, especially in respect of infra-red absorption and in respect of photo-conductivity. It is therefore of obvious importance to ascertain whether the luminescence properties are in any way correlated with the empirical classification of diamond into two types which has been suggested by these investigators.

The ultra-violet transparency of diamond may be studied with a suitable source of radiation and a quartz spectrograph, and if quantitative results are desired, also an ultra-violet spectro-photometer of some kind. When a cleavage plate is employed, it is also possible by traversing its area in successive steps to investigate whether its ultra-violet transparency varies over the surface. A much simpler and more satisfactory procedure adopted by the author and Mr. Rendall for this purpose is to place the plate in contact with a sheet of uranium glass and illuminate the latter *through* the diamond with the 2537 A.U. radiations of a water-cooled quartz mercury arc, its other radiations being deflected aside with a quartz prism and a couple of quartz lenses. The plates which are opaque to the 2537 rays

are then seen as dark areas in the surface of the uranium glass lit up by these radiations, while those which transmit them are seen as bright areas. On placing a group of cleavage plates together on the sheet of uranium glass, it may be seen at a glance that a few of them transmit while others are opaque to the 2537 A.U. radiations. Further, it is noticed that the plates which are not opaque to the 2537 radiations may differ greatly in their degree of transparency. The method of observation also reveals that the extent of transparency may vary greatly over the surface of a given plate. Indeed, a plate may be perfectly opaque to the 2537 radiation in certain areas, perfectly transparent to it in other areas, and exhibit an intermediate behaviour elsewhere. *The procedure thus enables as visually to observe and photograph the ultra-violet transparency patterns of the cleavage plates of diamond.* Using this method of study, the following relations between luminescence and ultra-violet transparency have been established:

- (a) A blue-luminescent diamond is invariably of the ultra-violet opaque type, but the opacity diminishes with increasing intensity of luminescence.
- (b) Non-luminescent diamonds are invariably of the ultra-violet transparent type.
- (c) The diamonds which exhibit an yellowish-green luminescence are of the intermediate type, in other words, are neither perfectly transparent nor perfectly opaque to the 2537 radiations.
- (d) These statements are also valid in respect of the individual areas in a cleavage plate which exhibits a luminescence pattern.

It follows that the luminescence pattern should show a close resemblance to the ultra-violet transparency pattern in those cases where part of the diamond is blue-luminescent and another part is non-luminescent, or when the plate exhibits a greenish-yellow banded luminescence. On the other hand, if a cleavage plate consists exclusively of blue-luminescent diamond, it is ultra-violet opaque and can therefore show no transparency pattern, even though it may exhibit local variations in the intensity of the luminescence.

To illustrate these remarks, the luminescence and ultra-violet transparency patterns of the diamonds numbered D48, D198 and D235 in the collection are reproduced side by side in Fig. 10. D48 exhibits three different types of behaviour simultaneously in different areas, *viz.*, non-luminescence, blue-luminescence and the greenish-yellow banded luminescence, as can be seen from the pattern reproduced in the upper part of Fig. 10, while the corresponding variations in ultra-violet transparency are noticeable in the

lower part of the same figure. D198 is non-luminescent at the centre and around it shows a geometric pattern of bands of greenish-yellow luminescence, changing to blue at the outer margin. It will be noticed that the resemblance between the luminescence and ultra-violet transparency patterns is extremely striking. D235 shows patches which are non-luminescent and ultra-violet transparent, while in the main it is blue-luminescent and ultra-violet opaque. Where the opaque and transparent diamonds mix, we have an imperfect transparency, and streaks of greenish-yellow luminescence are observed. It may be remarked that none of these three diamonds shows the least trace of non-uniformity when critically examined in ordinary daylight.

Illustrations of many more ultra-violet transparency patterns and a detailed discussion of the same will be found in a paper by Mr. G. R. Rendall (1944) appearing in this symposium.

#### *6. Luminescence and Structural Birefringence*

Diamond is a cubic crystal. Hence, if the structure is the same throughout the volume of a specimen, it should be optically uniform and isotropic. If, however, structures which differ from each other ever so little in their lattice spacings are incorporated in the same specimen, it is inevitable that stresses would be set up, with the result that a strain pattern indicating the inhomogeneity of the specimen would be visible between crossed nicols in the polariscope. Cleavage plates with polished faces are particularly well-suited for such studies, as disturbing effects due to oblique reflection or refraction at the surfaces do not arise. Further, the cleavage which enables the plate to be detached from the crystal automatically releases the stresses arising from flaws, cracks or inclusions located outside the plate, and hence eliminates the purely accidental birefringence due to such causes, thereby enabling the true structural birefringence, if it exists, to be perceived.

The examination of the 65 cleavage plates in the writer's collection has furnished much valuable information regarding the nature and origin of the birefringence sometimes observed in diamond. These results will be fully dealt with in another paper appearing in the symposium. It will be sufficient here to state the following relations which the observations show to exist between luminescence and the presence or absence of birefringence in diamond.

- (a) Diamond may be perfectly isotropic and strain-free; it is then invariably of the blue-luminescent type.
- (b) Non-luminescent diamond exhibits a characteristic and readily recognisable type of birefringence, consisting of closely-spaced parallel streaks running in several directions through the crystal.

- (c) Diamond exhibiting the greenish-yellow luminescence invariably shows a characteristic type of structural birefringence consisting of parallel dark and bright bands, usually rather wider apart than those shown by non-luminescent diamonds.
- (d) Diamond in which the blue-luminescent and non-luminescent types, or the blue-luminescent and the greenish-yellow luminescent types are simultaneously present invariably shows structural birefringence.

To illustrate the structural birefringence which appears associated with luminescence in the particular circumstances explained above, the patterns seen between crossed polaroids of the diamonds D38, D224, D200, D188 D179 and D190 are reproduced in Figs. 8 and 9 (Plate V), side by side with the corresponding luminescence patterns. In all these cases, the general resemblance between the two kinds of pattern can be made out easily. It is most obvious in the case of the three diamonds which exhibit a greenish yellow luminescence, *viz.*, D200, in Fig. 8, and D188 and D190 in Fig. 9. Diamonds D38 and D224 in Fig. 9 and D179 in Fig. 10 are blue-luminescent, the two former strongly, and the latter weakly. The dark streaks appearing in their luminescence-patterns correspond to bright streaks in the birefringence patterns and arise from the intrusion of non-luminescent diamond into the blue-luminescent kind.

#### *7. Interpretation of the Experimental Facts*

We are now in a position to consider the question of the origin of the luminescence. As we have seen, Indian and South African diamonds exhibit essentially similar phenomena. The fact that the effects observed do not depend on the locality of origin makes it highly improbable that impurity atoms are responsible for the luminescence. Then again, it is the clearest and most colourless, in other words, the chemically purest diamonds which exhibit the blue luminescence in the most striking fashion. The necessity for rejecting the impurity hypothesis becomes even clearer when we consider the luminescence patterns exhibited by individual diamonds. In numerous cases, as we have seen, particular regions with sharply defined boundaries show a vivid luminescence, while adjoining regions are non-luminescent. The patterns observed in many cases have geometric configurations clearly related to the symmetry of the crystal, indicating that the luminescence is fundamentally connected with the crystal structure.

Positive proof that the luminescence is an inherent property of the diamond itself is furnished by the relationships between the phenomenon and the other physical properties of diamond which are also dependent on

crystal structure. Particularly significant is the fact that non-luminescent diamonds are completely transparent to the 2537 radiations of the mercury arc. According to the investigations of Robertson, Fox and Martin (*loc. cit.*), such ultra-violet transparency goes hand in hand with the absence of a prominent infra-red absorption band which is markedly present in diamonds opaque to the 2537 radiations. This infra-red absorption band has its head at the characteristic frequency of the diamond lattice ( $1332\text{ cm.}^{-1}$ ), and its absence and presence respectively indicate, as shown in the preceding paper, that the diamond has full octahedral symmetry or only tetrahedral symmetry as the case may be.

In the light of the foregoing remarks, the experimental facts set out in the preceding sections may be re-stated in the following words:

- (a) Diamonds with tetrahedral symmetry of structure are, in general, blue-luminescent.
- (b) Diamonds with octahedral symmetry of structure are non-luminescent.
- (c) Diamonds in which the tetrahedral and octahedral types of structure are intimately mixed exhibit the greenish-yellow type of luminescence.

It remains to explain the enormous variations found in the intensity of the luminescence. In the case of the blue-luminescent diamonds, the most natural interpretation of the facts is that the luminescent property arises from the interpenetration of the positive and negative tetrahedral structures and consequent heterogeneity of the crystal. The intensity of the luminescence would then be determined by the nature and extent of such interpenetration. Similarly, in the case of the greenish-yellow luminescence, its intensity would be determined by the extent and distribution of the tetrahedral structure which is present as an admixture with the octahedral type. The features exhibited by the luminescence patterns and the analogies and differences noticed between them and the patterns of ultra-violet transparency and of structural birefringence give strong support to these ideas.

#### *8. The Spectral Characters of Luminescence*

The blue and greenish-yellow types of luminescence should evidently show different spectra. Since as we have seen, the greenish-yellow luminescence is exhibited by diamonds in which the non-luminescent and blue-luminescent varieties are mixed, it follows that the spectrum of the greenish-yellow type should always be accompanied, feebly or strongly, with that of the blue type. Non-luminescent diamond, on the other hand, should show neither type of spectrum; even under the most prolonged exposures.

A striking experimental confirmation of these conclusions is furnished by the investigations of the luminescence and absorption spectra in the visible region carried out by (Miss) Anna Mani with 32 representative diamonds and reported in this symposium (Mani, 1944). She has shown that the spectra are of two types which may be designated as the 4152 and 5032 systems, these being respectively characteristic of the blue and greenish-yellow luminescence. These always appear together, though with varying intensities whenever a diamond is luminescent, while neither appears when it is non-luminescent. Each system consists of a principal electronic line appearing at the wave-length stated in emission as well as absorption, and this is accompanied by weaker electronic lines at other wave-lengths and by a subsidiary lattice spectrum in which the principal electronic frequency combines with the various possible frequencies of vibration of the crystal lattice. The lattice spectrum appears with mirror-image symmetry about the principal electronic frequency, towards longer wave-lengths in emission and towards shorter wave-lengths in absorption.

The significant facts which emerge from the spectroscopic studies of Nayar (*loc. cit.*) and of Miss Mani (*loc. cit.*) are the following:

- (a) Given sufficient exposures, the type of diamond which is opaque to the 2537 A.U. radiations invariably records the 4152 system with an intensity which varies enormously as between different specimens.
- (b) No trace of either the 4152 or the 5032 systems is recorded, either in emission or in absorption, with diamonds which are perfectly transparent to the 2537 A.U. radiations. But diamonds which are imperfectly transparent to these radiations show both the 4152 and 5032 systems, with varying relative strengths.
- (c) Whenever the 5032 system is recorded with any specimen, the 4152 system is an invariable accompaniment, though its strength may be greater or smaller than that of the former system.

These facts fit naturally into the ideas regarding the structure of diamond and the origin of its luminescence developed in these pages. But it is not easy to reconcile them with the 'impurity' hypothesis.

#### 9. *Luminescence and X-Ray Reflection Intensities*

A further striking confirmation of the idea that the luminescence of diamond is associated with the interpenetration of different crystal structures and the inhomogeneity resulting therefrom is furnished by X-ray studies. Actually, we have four possible structures, two with tetrahedral symmetry

designated as Td I and Td II, and two with octahedral symmetry designated as Oh I and Oh II. The two tetrahedral structures are physically identical but geometrically different. Hence, they can interpenetrate freely without any composition planes and without setting up stresses in the crystal. The mixed structure is nevertheless not ideally homogeneous, and its lattice planes should therefore give X-ray reflections stronger than those given by either structure individually. The smaller the blocks in which the structure is homogeneous, the more intense would be the X-ray reflections, as also the luminescence. Hence, a close correlation must exist between luminescence and X-ray reflection intensity. The lowest reflection-intensities should be given by the most feebly blue-luminescent diamonds which accordingly are the nearest approach to the ideal crystal. *Per contra*, the strongest X-ray reflection intensities and the largest departures from crystal perfection would be provided by the intensely blue-luminescing diamonds.

The theoretical inferences stated above have been confirmed experimentally by Dr. R. S. Krishnan. The effect is conspicuously seen in the two Laue diagrams obtained by him and reproduced in an article by the present writer (Raman, 1943). One of the diamonds (D31) is weakly blue-luminescent, while the other (D224) shows an extremely strong luminescence of the same colour and gives a much more intense Laue pattern than the other. A similar effect has also been observed by Dr. R. S. Krishnan on comparing the intensities of the Bragg reflections by the oscillating crystal method.

If the Oh I or Oh II type of diamond structure exists by itself, it should give the weak X-ray reflections characteristic of an ideal crystal. Actually, when the two structures appear in the same diamond, they exhibit planes of composition and a characteristic streaky birefringence, indicating that they are physically different and that their juxtaposition sets up stresses in the solid. Hence the Oh I-Oh II mixed type should show much more intense X-ray reflections than the most intensely blue-luminescing diamond having the Td I-Td II structure. For the same reason also, diamonds having the Td-Oh mixed structures and exhibiting the yellow luminescence should stand half-way between these in respect of X-ray reflection intensities, just as they do in respect of ultra-violet transparency. That this is actually the case has been shown by Mr. P. S. Hariharan by photometric comparison of the intensity of the Bragg reflections by a series of cleavage plates of diamond having different luminescent properties. "A report of his work appears elsewhere in the symposium (Hariharan, 1944).

Luminescence patterns, ultra-violet transparency patterns and structural birefringence patterns are the various different ways in which the non-uniformity of structure of a plate of diamond may be made manifest to the

eye at a glance. Still another and quite different way of doing this is by the aid of X-rays, and the technique necessary for this purpose has been successfully worked out by Mr. G. N. Ramachandran. His results are reported in another paper in the symposium (Ramachandran, 1944). White X-radiation from a tungsten-target tube diverges from a pin-hole and falls upon the plate of diamond held at a sufficient distance from it. Each of the spots in the Laue pattern recorded on a photographic film is then seen as a topographic map of the diamond in which the variations of crystal structure are indicated by corresponding variations of X-ray reflection intensity. Very striking and interesting pictures are obtained in this way, the plate and the photographic film being so tilted that the Laue spot is recorded as an undistorted representation of the diamond.

#### 10. *Excitation of Luminescence by X-Rays*

The preceding discussion concerned itself with the effects observed under ultra-violet irradiation in the wave-length range 4000 A.U. to 3500 A.U. Luminescence is also excited by longer wave-lengths (5000 A.U. to 4000 A.U.) and by shorter waves (3500 to 2000 A.U.). This is readily demonstrated using the appropriate light-sources and a monochromator to isolate the desired exciting radiations. The intensity with which the 4152 and 5032 systems are excited would necessarily depend on the wave-length of the exciting radiation, being greatest when it coincides with the wave-length of the principal electronic radiation of the system concerned and becoming negligible when it is larger, while it would persist with appreciable but greatly diminished intensities for shorter wave-lengths. This has been shown to be the case for the 4152 system by Nayar (1941). In the ultra-violet beyond 3000 A.U., the imperfect transparency of the diamond also comes into play and causes the luminescence to be superficial and to be markedly enfeebled, these effects being the less conspicuous the more transparent the diamond under study is for the exciting radiations.

Diamonds also luminesce under the action of X-rays, unlike pearls and rubies which remain completely dark under such excitation. The intensity and also the colour of the luminescence varies as between different specimens, but the range of such variation is far less conspicuous than in the excitation by ultra-violet light. This is evident on a comparison of the series of Figs. 11 to 14 in Plate VI with the sequence of Figs. 2 to 6 in Plate III. Mr. G. N. Ramachandran who has made some observations on the subject has noticed a remarkable brightening up of the luminescence by increasing the voltage under which the X-ray tube is run, while the milliamperage seemed to have little or no obvious effect on the intensity. These effects obviously merit further investigation.

### 11. Phosphorescence

Diamonds which are strongly blue-luminescent emit a yellow phosphorescence when the exciting radiation is cut off. It follows that the spectrum of the emitted light should change rapidly with time when the incident radiation is cut off. Nayar (1941, b, c) has recorded some fluorescence and phosphorescence spectra showing this effect, as also the change in the spectrum of the emitted light when the wave-length of the incident light is altered by steps over the range 4000 A.U. to 6000 A.U. It is obviously desirable that the studies of the phosphorescence spectra should be extended to diamonds which show the 4152 and 5032 systems in fluorescence with comparable intensities. In this connection, it is noteworthy that strongly yellow-luminescent diamonds have a scarcely noticeable phosphorescence, thus markedly differing in their behaviour from blue-luminescing ones.

### 12. Summary

Luminescence is exhibited by nearly all diamonds, though with enormously varying intensities. Numerous specimens, both Indian and South African, in the form of natural crystals as also of cleavage plates, have been studied and the results are described and discussed. Observations with the cleavage plates are particularly significant, as many of them exhibit *luminescence patterns* having geometric characters obviously related to the structure of the crystal. The comparison of these luminescence patterns with the *patterns of transparency in the ultra-violet* beyond 3000 A.U. and with the *patterns of structural birefringence* observed between crossed polaroids is very instructive and shows that all these patterns have an essentially similar origin, viz., the interpenetrative or lamellar twinning of the different possible crystal structures in diamond. The interpenetration of the positive and negative tetrahedral structures gives rise to blue luminescence without any structural birefringence, the diamond remaining ultra-violet opaque. The interpenetration of the tetrahedral and octahedral structures gives rise to the yellow luminescence accompanied by a banded structural birefringence and an imperfect ultra-violet transparency. The lamellar twinning of the two possible octahedral structures gives diamond which is both non-luminescent and ultra-violet transparent but with a characteristic finely streaky birefringence. Spectroscopic study of the emission and absorption spectra of diamonds in the visible region, and a study of the variation of the reflecting power of the lattice planes for X-rays confirm these conclusions and show that the luminescence is essentially physical in origin and not due to foreign atoms present as impurities.

FIG. 1

FIG. 2

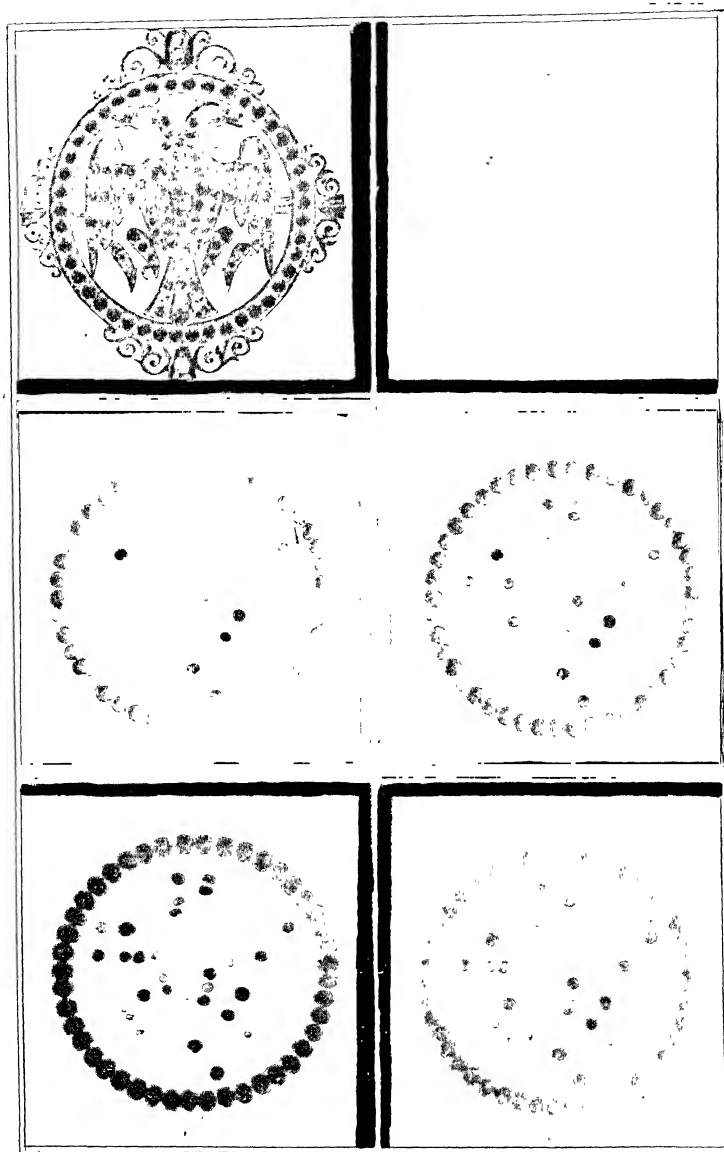


FIG. 5

FIG. 6

Luminescence of South African Diamonds

FIG. 1. Photograph in Daylight

Figs. 2 to 6. Luminescence in Ultra-Violet with Increasing Exposures

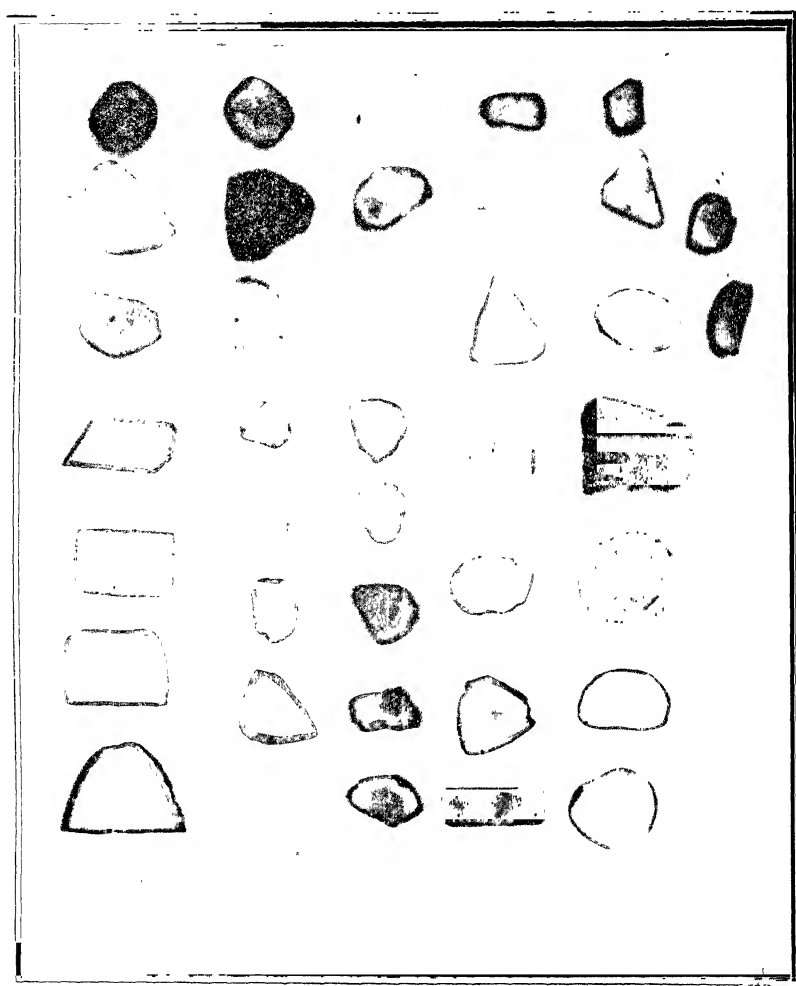


FIG. 7. Luminescence of Cleavage Plates of Diamond

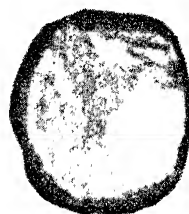
Catalogue Numbers					
D 188	200	199	196	193	191
175	190	192	198	48	194
185	210	211	195	177	202
31	231	182	178	34	
	176	183			
221	52	187	173	38	
36	174	189	180	181	
222	172	186	42	179	
57,208	209	206	39	207	
Non-Luminescent					

D200

D224

D38

Luminescence



Birefringence

D200

D224

D38

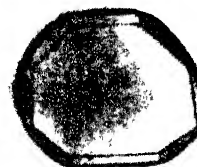
FIG. 8. Comparison of Luminescence and Birefringence Patterns

D190

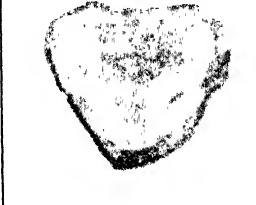
D179

D188

Luminescence



Birefringence



D190

D179

D188

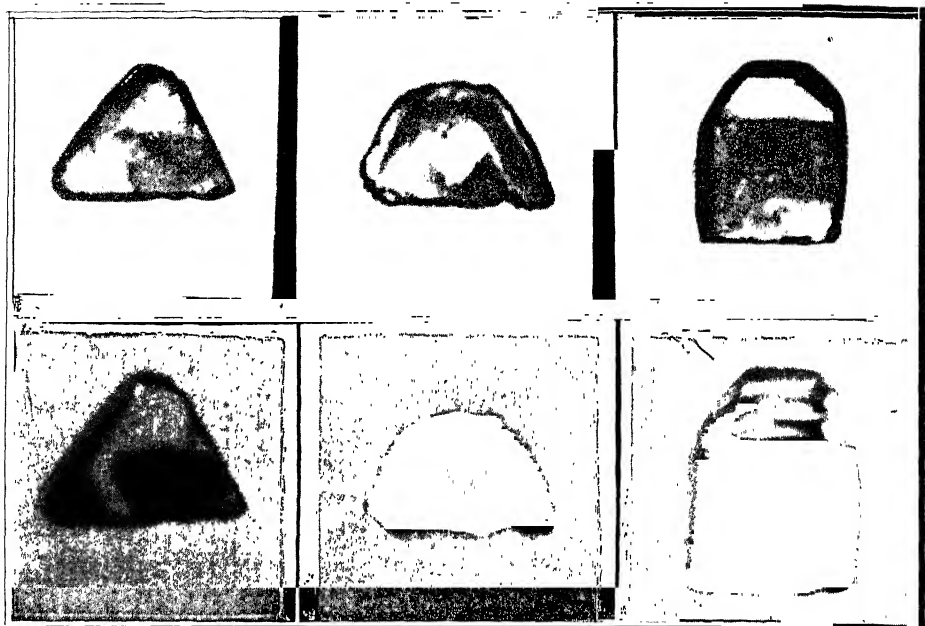
FIG. 9. Comparison of Luminescence and Birefringence Patterns

D48

D198

D235

Luminescence

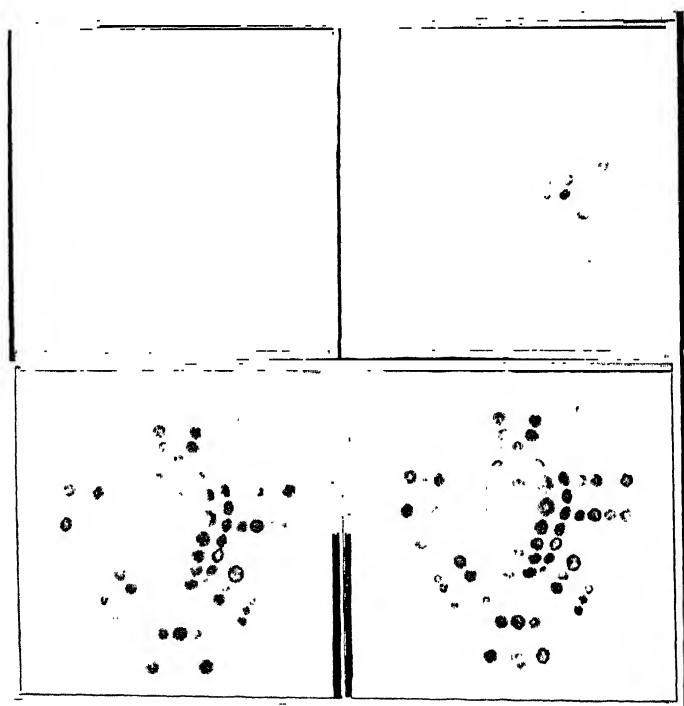
Ultra-Violet  
Transparency

D48

D198

D235

FIG. 10. Comparison of Luminescence and Ultra-Violet Transparency Patterns

FIG. 11  
50 K.V. 10 minutesFIG. 12  
56 K.V. 30 minutesFIG. 13  
50 K.V. 30 minutes  
FIG. 14  
70 K.V. 60 minutes  
Luminescence of Diamonds under X-Rays with Increasing Exposures

## REFERENCES

Bhagavantam, S.	.. <i>Ind. Jour. Phys.</i> , 1930, <b>5</b> , 169.
Hariharan, P. S.	.. <i>Proc. Ind. Acad. Sci.</i> , 1944, <b>19</b> .
John, M. V.	.. <i>Ind. Jour. Phys.</i> , 1931, <b>6</b> , 305.
Kayser	.. <i>Handbuch der Spectroscopie</i> , 1908, <b>4</b> , 830.
Mani, A.	.. <i>Proc. Ind. Acad. Sci.</i> , 1944, <b>19</b> .
Nayar, P. G. N.	.. <i>Ibid.</i> , 1941a, <b>13</b> , 284.
_____	.. <i>Ibid.</i> , 1941b, <b>13</b> , 483.
_____	.. <i>Ibid.</i> , 1941c, <b>13</b> , 534.
_____	.. <i>Ibid.</i> , 1941d, <b>14</b> , 1.
_____	.. <i>Ibid.</i> , 1942a, <b>15</b> , 293.
Pringsheim, P.	.. <i>Ibid.</i> , 1942b, <b>15</b> , 310.
_____	.. <i>Handbuch der Physik</i> , 1926, Band 23, Ziff. 60.
Ramachandran, G. N.	.. <i>Fluorescenz und Phosphorescenz</i> , 1928, 318.
Raman, C. V.	.. <i>Proc. Ind. Acad. Sci.</i> , 1944, <b>19</b> .
_____	.. <i>Current Science</i> , 1942, <b>11</b> , 261.
_____	.. <i>Ibid.</i> , 1943, <b>12</b> , 33.
Rendall, G. R.	.. <i>Proc. Ind. Acad. Sci.</i> , 1944, <b>19</b> , 189.
Roberston, Fox and Martin	.. <i>Ibid.</i> , 1944, <b>19</b> .
Sunandabai, K.	.. <i>Phil. Trans. Roy. Soc.</i> , A, 1934, <b>232</b> , 463.
	.. <i>Proc. Ind. Acad. Sci.</i> , 1944, <b>19</b> .

# THE RAMAN SPECTRUM OF DIAMOND

BY R. S. KRISHNAN

(*From the Department of Physics, Indian Institute of Science, Bangalore*)

Received April 17, 1944

## 1. Introduction

RAMASWAMY (1930), Robertson and Fox (1930) and Bhagavantam (1930) simultaneously and independently observed the Raman spectrum of diamond and found one sharp strong line with a frequency shift of  $1332 \text{ cm}^{-1}$ . As was pointed out by Ramaswamy and later fully confirmed by the theoretical investigations of Nagendra Nath (1934) and of Venkatarayudu (1938), this frequency represents the fundamental vibration of the diamond structure, *viz.*, the mode in which the two interpenetrating Bravais lattices of carbon atoms oscillate against each other. This mode, according to the usual selection rules (Placzek, 1934) should be active in the Raman effect. The researches of Nayar (1941, 1942) on the luminescence and absorption spectra of diamonds have, however, demonstrated the existence of many more vibrations of the diamond structure with discrete frequencies, besides the one found in the Raman effect. Nayar's results have been confirmed and extended by the investigations of (Miss) Mani of which a report appears elsewhere in this symposium. The appearance of several discrete monochromatic frequencies in the vibration spectrum of the diamond lattice is unintelligible on the basis of the older theories of the specific heat of solids. It, however, finds a natural explanation in the new theory of the dynamics of crystal lattices due to Sir C. V. Raman (1943). On the basis of the Raman dynamics, the possible modes of atomic vibration in diamond have been fully worked out and described by Chelam (1943) and by Bhagavantam (1943). They have both given explicit expressions for the frequencies in terms of the force constants. There are, on the whole, eight fundamental frequencies, of which only the one having the highest frequency is active in the Raman effect. Though the seven other vibrations are forbidden as fundamentals, they are allowed as octaves in light-scattering, according to the usual selection rules. Besides overtones, some of the combinations may also be Raman-active. There is thus a clear possibility that octaves and combinations of the eight frequencies of the diamond lattice might appear recorded in strongly exposed Raman spectra. The present research was undertaken to investigate this possibility. Its successful confirmation places the Raman dynamics of crystal lattices on a firm foundation of experimental reality.

## 2. Review of Previous Experimental Work

Besides the investigations already referred to in the Introduction, mention may be made here of others relevant to the subject of this paper.

During the course of their systematic investigations on the properties of diamond, Robertson, Fox and Martin (1934) examined the Raman spectra of a few samples of the two types of which the existence was recognized by them. They found that the principal Raman line had exactly the same frequency shift in both cases. With the diamonds which are more transparent in the ultra-violet, the Raman effect studies could be extended further into that region.

Bhagavantam (1930 a) studied the Raman spectra of numerous large diamonds of the ultra-violet opaque type, using the 4046 and 4358 radiations of the mercury arc as excitors, with a view to discover whether there are any observable frequency shifts besides the principal one of  $1332\text{ cm.}^{-1}$ . We shall consider his results on this point later in the present paper.

Contrary to a finding by Bhagavantam, Nayar (1941 a) reported that the intensity of the 1332 line did not vary with the specimen of diamond under study. He also made a careful study of the thermal behaviour of this line over a wide range of temperatures. He found the frequency shift to diminish from  $1333\cdot8\text{ cm.}^{-1}$  at  $-190^\circ$  to  $1316\cdot4\text{ cm.}^{-1}$  at  $860^\circ\text{C.}$ , in a manner evidently connected with the thermal expansion of the crystal. Continuing his earlier work, Nayar (1942 a) found that the line showed no measurable variation either in its frequency shift or in its intensity when the setting of the crystal or the angle of scattering was altered. He also drew attention to an interesting case in which the 1332 line appears distorted in an imperfect crystal.

## 3. Experimental Technique

In the present investigation the well-known Rasetti technique of using the 2536 radiation of a water-cooled quartz mercury arc has been adopted, and diamonds of the ultra-violet transparent type have been chosen for study. The ordinary type of diamonds are usually fluorescent to varying extents, the fluorescent bands falling in a region extending from 4000 A.U. to about 6000 A.U. Even the diamonds which are the least fluorescent give a weak continuous radiation in the visible region, and the faint Raman lines, if present, would be lost in the general background and remain unobserved. These difficulties are completely eliminated by working in the ultra-violet region and using the 2536 monochromatic radiations of mercury vapour for exciting the Raman lines. The enormously increased scattering power of the 2536 line arising from its exceptional intensity as compared

with the other mercury lines and from the  $\lambda^{-4}$  law, also makes it possible to record fainter Raman lines which would remain unobserved otherwise. The study of the Raman spectra using the Rasetti technique is, however, necessarily restricted to diamonds which are transparent to the 2536 radiation.

From Sir C. V. Raman's personal collection two diamonds were selected which were suitable for the present investigation. Their serial numbers are 206 and 227. Diamond No. 206 was colourless and in the form of a thin plate ( $10 \times 6 \times 0.6$  mm.) and its weight was 0.2 of a carat. The other diamond was cut in the form of a faceted prismatic rod with oblique ends and had a slight tinge of colour. It was a centimetre long and about 3 mm. thick, its weight being roughly 1.3 carats.

A vertical quartz mercury arc of a special design was constructed in the laboratory with mercury cathode and tungsten anode. The arc was kept immersed in running water to a depth of about one centimetre above the cathode bulb and was kept continuously evacuated by an efficient pumping system. The central vertical portion of the arc was inserted between the poles of a powerful electromagnet which caused the deflection of the discharge against the front wall of the tube. The water-cooling and the continuous evacuation prevented the mercury from acquiring any considerable density, and the magnet by squeezing the discharge against the wall still further prevented the reversal of the 2536 line. Under these conditions, this line was so intense that the main Raman lines of calcite could be recorded in a couple of minutes.

Diamond No. 206 being a flat plate was illuminated through one of its faces and the scattered light was observed through one of the edges in the end-on position. The maximum depth of illumination equal to the length of the plate was thus secured. By aluminising the opposite face of the diamond, the incident radiations were reflected back, thereby increasing the intensity of the scattered light. Diamond No. 227 was fixed inside a copper rod at the junction of two perpendicular holes cut through it. This diamond was irradiated through one of its long prismatic facets and the scattered light was taken out normally through one of the pyramidal end facets. In this arrangement, the parasitic illumination entering the spectrograph was negligible and the displaced lines could be photographed on a very clear background.

The diamond under investigation was held facing the most intense portion of the arc near the front wall of the quartz tube towards which the discharge was deflected. To prevent any appreciable rise in temperature of the diamond, a continuous stream of cold air was directed towards it. The

light scattered from the diamond was condensed on the slit of a Hilger Intermediate spectrograph. The 2536 radiation in the scattered light was suppressed before its entry into the spectrograph by absorption in a column of mercury vapour contained in a cell placed in front of the slit. With these arrangements, the 1332 line could be recorded in about ten minutes. Longer exposures of the order of 15 hours or more are required to record the fainter Raman lines. These were obtained also with the smaller diamond. The efficiency of the optical set-up could be judged from the fact that the anti-stokes of 1332 was recorded in about 24 hours with the smaller diamond. For obtaining strongly-exposed spectrograms, the larger diamond was used. Numerous photographs were taken varying the time of exposure up to a maximum period of 60 hours. On every negative, a series of photographs of the direct mercury spectrum with graded exposures was also recorded by the side of the spectrogram of the scattered light. The slit width employed was  $20\ \mu$ . The dispersion of the instrument was about 220 wave numbers per millimetre in the region of 2536. The plates were measured under a Hilger cross-slide micrometer. To measure the shift of very faint lines, an ordinary low-power microscope was used.

#### 4. Results

An intense Raman spectrum of diamond with 2536 excitation is reproduced in Plate VII along with a photograph of the direct arc. The microphotometric record of a less intense spectrogram is also reproduced. The displaced lines are clearly seen on the microphotometric record. Most of them can also be identified on the reproduced photograph. Their positions have been marked for clarity. The Raman spectra obtained with the two diamonds are exactly similar in nature. The recorded spectra show,

TABLE I

Ser. No.	Frequency shift in $\text{cm}^{-1}$	Intensity*	Nature	Assignment†
1	-1331.5	<1	Anti-stokes	$F_2$
2	1332.0	500	Fundamental	$F_2^2$
3	1925	<1	Combination	$H_1 + H_2$
4	2175.5	1	Octave	$K_3^2$
5	2245	1.5		
6	2267	2		
7	2300.5	4	Combination	$K_1 + M_1$
8	2467	10	Octave	$H_1^2$
9	2495	10	do.	$H_4^2$
10	2518	7		
11	2609.5	4.5	do.	$M_1^2$
12	2664.6	5	do.	$F_2^2$

Intensity values are only approximate.

† Notation taken from Bhagavantam's paper (1943).

besides the intense line with a frequency shift of  $1332 \text{ cm}^{-1}$ , a host of lines of comparatively feeble intensity. The frequency shifts of the two extreme lines are 1925 and  $2664\cdot6 \text{ cm}^{-1}$ . Of these, some are rather broad, while others are sharp. The shifts of these lines have been carefully measured and are given in Table I. Rough estimates of the relative intensities of these lines have also been made and the values entered in the table. There is a weak continuum starting from a point separated by about 2300 wave numbers from the 2536 line. This continuum is sharply cut off at  $2664 \text{ cm}^{-1}$  which corresponds to the octave of 1332. Even in the most heavily exposed photographs, no trace of any Raman line having a frequency shift less than  $1332 \text{ cm}^{-1}$  could be detected. In the direct picture of the mercury arc, one notices a faint mercury line at  $\lambda 2625\cdot2$ . The principal Raman line with the frequency shift of  $1332 \text{ cm}^{-1}$  falls on the top of this faint mercury line. The anti-stokes line corresponding to 1332 is also clearly recorded on the plate. The Raman line with a frequency shift of  $2467 \text{ cm}^{-1}$  unfortunately falls almost on the top of a faint mercury line in this region. This fact has been taken into account while estimating the intensity of this Raman line. The reproduced photograph shows the presence of a displaced line at 2749 A.U. which corresponds to the frequency shift of 1332 wave numbers excited by the strong mercury line  $\lambda 2652 \text{ A.U.}$ .

### 5. Discussion of Results

On the assumption that the diamond structure has octahedral ( $Oh$ ) symmetry, it is possible to calculate the Raman-active frequencies of diamond. The appropriate character table for a super-lattice based on the Raman theory of crystal dynamics has been given by Bhagavantam (1943). Of the eight fundamental frequencies of oscillation which have been designated by Bhagavantam as  $F_2$ ,  $H_1$ ,  $H_2$ ,  $H_4$ ,  $K_1$ ,  $K_3$ ,  $M_1$  and  $M_2$  with degeneracies 3, 6, 6, 6, 4, 4, 8 and 8 respectively, only  $F_2$  is active in the Raman effect, and it corresponds to the principal line of frequency shift 1332 wave numbers. The other seven modes which have frequency shifts less than  $1332 \text{ cm}^{-1}$  are inactive in light-scattering as fundamentals. This fact has been fully substantiated by the present experimental results. The use of the intense 2536 radiation and of exposures long enough to bring out the octaves, has failed to reveal the presence of any Raman line corresponding to a fundamental frequency of oscillation other than the principal one with the frequency shift of  $1332 \text{ cm}^{-1}$ . Bhagavantam (1930 a) had reported the existence of some feeble lines on either side of the 1332 line excited by 4046 in some diamonds and by 4358 in some others. The luminescence studies of Nayar and of (Miss) Mani have shown that many fluorescent lines (some of which are sharp) fall in the regions separated by about 1100 wave numbers.

from both the 4046 and 4358 mercury lines. These results together with the fact that no Raman line corresponding to a fundamental frequency of oscillation other than 1332 is excited by the 2536 radiation, suggest that the origin of the faint lines reported by Bhagavantam is in all probability fluorescence and not Raman effect.

The group characters for the various octaves and combinations have been determined and the selection rules applied for finding their activity in the Raman effect. The octaves of all the eight modes and four combinations, namely  $H_1 + H_2$ ,  $H_1 + H_4$ ,  $K_1 + M_1$  and  $K_3 + M_2$  should be Raman-active. The ten new Raman lines (see Table I) which are observed with intensities small compared with that of the principal 1332 line are therefore some of the allowed octaves and/or combinations. Of these, the line with the frequency shift of  $2664\cdot6 \text{ cm}^{-1}$  can be easily identified as the octave of 1332, i.e.,  $F_2^2$ . In order to give proper assignments for the remaining nine observed Raman lines, it is necessary to know the fundamental frequencies (in wave numbers) of the various modes. The lattice frequencies which appear very prominently in the absorption and luminescence spectra of diamonds are (in wave numbers) 1332, 1283, 1251, 1149, 1088, 1013, 785 and 544. These values have been taken from the recent and more accurate measurements of (Miss) Mani. On the assumption that these represent the eight fundamental frequencies of the diamond lattice, it is possible to assign them.  $F_2$  having the maximum and  $M_2$  the minimum frequency, should be identified with 1332 and  $544 \text{ cm}^{-1}$  respectively.  $M_1$  being the next highest, should correspond to  $1283 \text{ cm}^{-1}$ . As the frequency of  $H_2$  is  $\sqrt{2}$  times that of  $M_2$ ,  $785 \text{ cm}^{-1}$  should be assigned to  $H_2$ . Putting these values in the expressions for the frequencies given by Bhagavantam, one finds that 1251, 1149, 1088 and  $1013 \text{ cm}^{-1}$  represent the frequencies of  $H_4$ ,  $H_1$ ,  $K_3$  and  $K_1$  respectively. The Raman lines observed with frequency shifts of  $2175\cdot5$ ,  $2300\cdot5$ ,  $2495$ ,  $2609$  and  $2664\cdot6 \text{ cm}^{-1}$  are thus the octaves of  $K_3$  (1088),  $H_1$  (1149),  $H_4$  (1251),  $M_1$  (1283) and  $F_2$  (1332). The octave of  $K_1$  (1013), even if present, would not be detected as it would fall roughly on the mercury line at  $2675 \text{ A.U.}$  No Raman lines have been observed corresponding to the octaves of  $H_2$  and  $M_2$  which have the lowest frequencies.

Next to the Raman line of frequency shift  $2664\cdot6 \text{ cm}^{-1}$ , the line at  $2175\cdot5 \text{ cm}^{-1}$  is rather sharp and stands out clearly in the photograph. This is also true of the corresponding lattice frequency ( $1088 \text{ cm}^{-1}$ ) in the luminescence spectrum. The octave of 1251 appears to have been split into three components in the Raman effect, these having approximately the

same intensity. The frequency shifts of these components are 2467, 2495 and  $2518 \text{ cm}^{-1}$ .

The observed Raman lines with frequency shifts of 1925 and  $2267 \text{ cm}^{-1}$  can be considered as combinations of  $H_1$  and  $H_2$  ( $1149 + 785$ ) and of  $K_1$  and  $M_1$  ( $1013 + 1283$ ) which are allowed in light-scattering. The combinations of  $H_1$  and  $H_4$  ( $1149 + 1283$ ) and of  $K_3$  and  $M_2$  ( $1088 + 544$ ), though Raman-active, could unfortunately not be detected, as the former would fall on the top of the mercury line at  $2698\cdot9 \text{ A.U.}$ , while the latter would be masked by the halation due to the intense mercury line at  $2652 \text{ A.U.}$  The microphotometric record shows other kinks which remain unassigned. It is reasonable to suggest that these represent lines due to some of the so-called forbidden combinations. They are forbidden in the Raman effect on the basis of the ordinary selection rules which are valid provided the vibrations are harmonic. But the fact that combinations and overtones appear in Raman effect shows that the amplitudes of such oscillations need not necessarily be small. When once anharmonicity sets in, the ordinary selection rules cease to be valid and more combinations become Raman-active.

The appearance of several new Raman lines in diamond as overtones and combinations of modes of oscillation of the diamond structure which are inactive as fundamentals is a direct experimental verification of the predictions of the Raman theory of crystal dynamics. These results cannot be explained satisfactorily on the basis of the Born dynamics.

In conclusion the author takes this opportunity to express his grateful thanks to Professor Sir C. V. Raman at whose suggestion the present investigation was carried out.

### *Summary*

The Raman spectra of diamonds of the ultra-violet transparent type have been investigated using the 2536 resonance line of mercury as exciter. Besides the well-known 1332 Raman line, ten others with frequency shifts 1925,  $2175\cdot5$ , 2245, 2267,  $2300\cdot5$ , 2467, 2495, 2518,  $2609\cdot5$  and  $2664\cdot6 \text{ cm}^{-1}$  have been recorded. These new lines have been identified as the octaves and allowed combinations of some of the eight fundamental frequencies of oscillation of the diamond structure of which the existence is indicated by the Raman theory of crystal dynamics, but which are not themselves permitted to appear in light-scattering by reason of the selection rules.

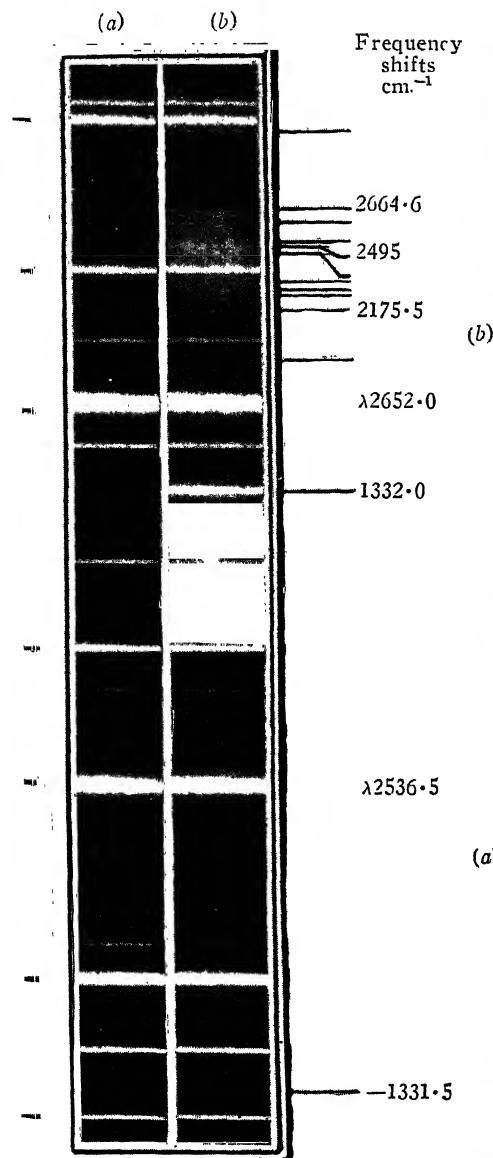


FIG. 1

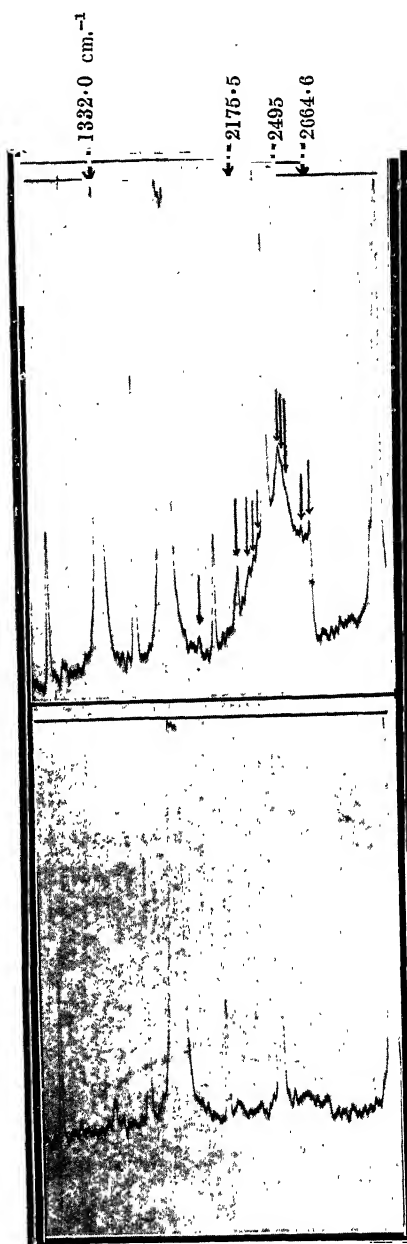


FIG. 2



## REFERENCES

Bhagavantam, S. .... *Ind. Journ. Phys.*, 1930, **5**, 169 ; 1930 *a*, **5**, 573.  
\_\_\_\_\_  
Chelam, E. V. .... *Proc. Ind. Acad. Sci.*, A, 1943, **18**, 251.  
Nagendra Nath .... *Ibid.*, 1943, **18**, 257, 327 and 334.  
Nayar, P. G. N. .... *Ibid.*, 1934, **1**, 333.  
Placzek, C. .... *Ibid.*, 1941, **13**, 483 ; **14**, 1 ; 1941 *a*, **13**, 284 ; 1942, **15**, 293 ;  
1942 *a*, **15**, 310.  
Raman, C. V. .... Marx—*Handbuch der Radiologie*, 1934, Vol. VI, Part 2.  
Ramaswamy, C. .... *Proc. Ind. Acad. Sci.*, A, 1943, **18**, 237.  
Robertson and Fox .... *Nature* (London), 1930, **125**, 704; *Ind. Journ., Phys.*, 1930, **5**, 97.  
\_\_\_\_\_, \_\_\_\_\_ and Martin .... *Ibid.*, 1930, **125**, 704.  
Venkatarayudu, T. .... *Phil. Trans. Roy. Soc.*, A, 1934, **232**, 482.  
\_\_\_\_\_. .... *Proc. Ind. Acad. Sci.*, A, 1938, **8**, 349.

# THE LATTICE SPECTRUM AND SPECIFIC HEAT OF DIAMOND

BY BISHESHWAR DAYAL

(From the Department of Physics, Indian Institute of Science, Bangalore)

Received April 17, 1944

(Communicated by Sir C. V. Raman, Kt., F.R.S., N.L.)

## 1. Introduction

THE mathematical problem of finding the vibration spectrum of the atoms in a crystal about their positions of equilibrium has been solved by Sir C. V. Raman (1943) in a recent memoir, it being assumed that the external boundaries of the crystal have no sensible influence on the vibrations of high frequency under consideration. The treatment leads to the result that there are  $(24p - 3)$  normal modes and frequencies of atomic vibration,  $p$  being the number of non-equivalent atoms in the crystal and  $24p$  being, therefore, the total number of degrees of freedom of the atoms contained in the cell of a super-lattice which has twice the linear dimension of the cells of the crystal structure. The number of distinct frequencies is reduced by degeneracy in the case of crystals possessing symmetry elements. The particular case of the diamond lattice has been fully worked out on the basis of this theory by Bhagavantam (1943) and by Chelam (1943) by different methods which yield the same results. It is found that the diamond structure has eight distinct frequencies of atomic vibration which between them embrace 45 out of the 48 degrees of freedom of movement of the 16 atoms of carbon contained in the cell of the super-lattice.

A remarkable confirmation of the correctness of this new approach to crystal dynamics is furnished by some recent experimental work by Dr. R. S. Krishnan which is reported in another paper in this symposium. If, as is indicated by the theory, the diamond lattice has eight discrete frequencies of vibration, it should be possible to demonstrate their existence by means of the Raman effect under appropriate experimental conditions, whereas hitherto only the so-called fundamental vibration has been recorded as a frequency-shift in the Raman spectrum. Using the well-known Rasetti technique and a diamond having the requisite transparency in the ultra-violet, Raman spectra have been successfully recorded by Dr. R. S. Krishnan in which several of the additional frequencies appear as octaves as permitted

by the selection rules, though their fundamentals are not allowed. It is gratifying that the nature of the lattice spectrum as thus deduced from Raman effect data agrees with that deduced from other entirely independent methods of spectroscopic study, *viz.*, the investigation of the luminescence spectra and the absorption spectra of the diamond made by Dr. Nayar (1942) and recently in a more exhaustive way by (Miss) Anna Mani, a report of whose work appears as another paper in this symposium.

It is the purpose of the present writer to correlate the theoretical results of Bhagavantam and of Chelam with the experimental results of R. S. Krishnan, Nayar, and of (Miss) Mani, in other words, to identify the particular modes of vibration indicated by theory with the frequencies as spectroscopically observed. This enables us to ascertain the degeneracy attached to each particular observed frequency and hence to evaluate the specific heat of diamond in a manner fully justified by both theory and experiment.

## 2. *Identification of the Optical Frequencies*

The formulæ for the optical frequencies as given by Bhagavantam and Chelam have been reproduced in Table I where we have followed the group-theoretical designation of the former author and the force-constant notation of the latter. The force constants  $K$  and  $K''$  arise from the mutual displacements of the neighbours and next nearest neighbours respectively, and  $K_a$  from the changes in the angle between the various valence bonds.

The most intense line at  $1332 \text{ cm}^{-1}$  in the Raman spectrum was interpreted by Ramaswamy (1930) as the fundamental lattice oscillation. The theoretical investigations of Nagendra Nath (1934), Venkatrayudu (1939) and Bhagavantam and Venkatrayudu (1939) have proved conclusively that the mode  $F_2$  which is an oscillation of the two interpenetrating lattices of carbon atoms with respect to each other has this value. It follows from the formulæ of Table I that this is the highest lattice frequency. The two next highest frequencies taken in order evidently belong to the modes  $M_1$  and  $H_4$  and should satisfy the relation  $\nu_{F_2}^2 - \nu_{M_1}^2 = \nu_{M_1}^2 - \nu_{H_4}^2$ . A line with a frequency shift of nearly twice 1284 has been observed by Krishnan in the Raman spectrum, while there is an indication of a line at twice 1248 also in his photographs. Both these lines have been observed by Nayar (*loc. cit.*) and (Miss) Mani (this symposium) in fluorescence and absorption. They approximately satisfy the above-mentioned difference relationship for these frequencies and there seems little doubt that they belong to the modes  $M_1$  and  $H_4$  respectively. The modes  $M_2$  and  $H_2$  should have low frequencies since they do not involve the largest force constant  $K$ , while the numerical

values of their frequencies are in the ratio  $1 : \frac{1}{\sqrt{2}}$ . No low frequency lines have been observed in light-scattering, but two lines at 565 and 784 satisfying the above relationship have been observed both by Nayar and (Miss) Mani, and have been assigned by us to the above two modes. The other three lines can also be assigned by inspection and have been given in Table I. In order to show that the assignment is correct, we have also given the calculated values of the frequencies in the same table. The force-constants have been calculated by approximately solving the equations for the frequencies belonging to the modes  $F_2$ ,  $H_2$  and  $M_2$ . It is seen that there is a good agreement between the theoretical and observed values. The values of the force-constants are

$$K = \cdot314 \times 10^6 \text{ dynes/cm.}$$

$$K'' = \cdot039 \times 10^6 \text{ "}$$

$$K_a = \cdot0197 \times 10^6 \text{ "}$$

TABLE I  
*Lattice Frequencies of Diamond*

Mode	Degeneracy	$4 \pi^2 v^2$	Calculated $v$ cm. <sup>-1</sup>	Observed $v$ cm. <sup>-1</sup>	Evidence
$F_2$	3	$\frac{8 K + 64 K_a}{3 m}$	1332	1332	Fundamental Raman and infra-red active, observed in luminescence and absorption.
$H_1$	6	$\frac{4 K + 40 K_a}{3 m} + \frac{8 K''}{m}$	1185	1149	Octave at 2245 in Raman spectrum. Fundamental in fluorescence and absorption.
$H_2$	6	$\frac{12 K_a + 4 K''}{m}$	745	784	Fluorescence and absorption.
$H_4$	6	$\frac{8 K + 4 K_a}{3 m} + \frac{4 K''}{m}$	1200	1248	Fluorescence and absorption. Octave in Raman effect.
$K_3$	4	$\frac{2 K + 8 K''}{m}$	1153	1088	do.
$K_1$	4	$\frac{2 (K + 32 K_a + 12 K'')}{3 m}$	1153	1013	Fluorescence and absorption.
$M_1$	8	$\frac{8 K + 34 K_a}{3 m} + \frac{2 K''}{m}$	1269	1284	Fluorescence and absorption. Octave in Raman effect.
$M_2$	8	$\frac{6 K_a + 2 K''}{m}$	527	565	Fluorescence and absorption.

### 3. Elastic Constants of Diamond

Nagendra Nath (1935) has investigated the relation between the elastic data and the force-constants of diamond. If we neglect the intravalence force-constant  $K'''$ , his expressions are

$$c_{11} = \frac{1}{3d} [K + 12K'' + 12K_a]$$

$$c_{12} = \frac{1}{3d} [K + 6K'' - 6K_a]$$

$$c_{44} = \frac{2}{d} [K'' + 3K_a]$$

where  $d$  is the lattice constant of diamond  $= 3.552 \times 10^{-8}$  cm. Substituting the values of the force-constants given earlier, we have

$$c_{11} = 9.6 \times 10^{12} \text{ dyne/cm.}^2$$

$$c_{12} = 4.0 \times 10^{12} \text{ "}$$

$$c_{44} = 5.6 \times 10^{12} \text{ "}$$

The calculated value of the bulk modulus  $\frac{1}{\kappa}$  is  $\frac{1}{3} (c_{11} + 2c_{12}) = 5.9 \times 10^{12}$  dyne/cm.<sup>2</sup> This agrees well with the experimental values  $6.25 \times 10^{12}$  and  $5.56 \times 10^{12}$  determined by Adams (1921) and Williamson (1922) respectively, and is a fair check on the values of the force-constants and the assignment of frequencies.

### 4. Evaluation of the Specific Heat

We have now to ascertain the modes and the frequencies of the vibration which represent the three degrees of freedom of movement of the 16 atoms contained in the super-lattice cell which are left over after considering the optical modes of vibration. The exact knowledge of these modes and frequencies is of importance for the specific heat evaluation only in the lower ranges of temperature. Lacking such knowledge and in view of the fact that they represent only  $\frac{1}{16}$  of the total number of degrees of atomic freedom, we may evaluate their contribution to the thermal energy by using the Debye approximation and assuming that they represent the elastic spectrum of the crystal lattice. The characteristic temperature  $\theta_D$ , however, has to be altered by putting  $\frac{3N}{16}$  in place of  $3N$  in the usual Debye formula.

The modified expression for it is

$$\theta_D = \frac{h}{k} \left( \frac{3N}{64\pi V} \right)^{\frac{1}{3}} v$$

where  $V$  is the atomic volume and  $\bar{v}$  the average velocity obtained from

$$\frac{1}{\bar{v}^3} = \frac{1}{3} \sum_i \frac{1}{4\pi} \int \int \frac{1}{v_i^3} d\omega$$

$v_i$  is the velocity corresponding to the direction  $i$  and the summation is to be made over the whole solid angle for all the three waves. The integral has been evaluated by Hopf and Lechner's interpolation method (1914) from the above-mentioned theoretical elastic constants. The numerical value of  $\theta_D$  thus obtained is 820 which has been used for the evaluation of the specific heat. This is accordingly given by the formula

$$C_v = 3R \left[ \sum_s \sigma_s E\left(\frac{hv_s}{kT}\right) + \frac{1}{16} D\left(\frac{820}{T}\right) \right],$$

where  $E$  and  $D$  stand for Einstein and Debye functions respectively.  $\sigma_s$  is the statistical weight of frequency  $v_s$  and can be obtained from the degeneracies given in Table I.

The calculated values of  $C_v$  are given in Table II. The experimental data below 273° K. have been taken from Pitzer (1938) and above that temperature from Magnus and Hodler (1926). Near the room temperature—the region common to both sets of observations—Pitzer's determinations of  $C_v$  are systematically lower than those of the other authors. The order of difference can be judged from the fact that the  $C_v$  measured by him at 276.6° K. coincides with that given by Magnus and Hodler for 273° K. If we accept the latter's result as standard, the experimental values of Pitzer given in Table II are about 5% lower near about 252° K.

Considering these facts, we find that the theoretical values follow the course of experimental data fairly closely above 200° K. It is, however, precisely this region of high temperatures where no arbitrary constants are involved in the calculation and where, therefore, the present theory is rigorously valid. The contribution of the elastic spectrum to the thermal energy reaches its limiting value at about 300° K., so that its value above this temperature is entirely determined by the optical frequencies and their degeneracies. Below 200° K., there is a small systematic deviation between the theoretical and calculated results, but owing to the increasing importance here of the contribution of the elastic branch, there are two uncertain factors involved in the calculations. In the first place, the elastic constants used in the calculation of the Debye characteristic temperature have been derived on certain simplifying assumptions about the nature of the forces between the atoms, and, secondly, the Debye function itself is only used as an approximation to represent the elastic spectrum. Further, the atomic

heats are particularly sensitive to changes of frequencies in the low-temperature region, so that small errors either in measurements of frequencies or estimation of the characteristic temperature can cause rather large deviations in the atomic heats.

TABLE II  
*Atomic Heats of Diamond*

Temp. 0° K.	Optical frequencies	Elastic spectrum	Total $C_v$	Observed $C_v$
70·16	.0013	.0180	.0193	.022
81·59	.0046	.0280	.033	.036
105·1	.0284	.0547	.083	.079
125·3	.072	.082	.154	.138
162·8	.222	.135	.357	.318
200·9	.445	.183	.628	.595
252·4	.839	.231	1.070	1.032
273	1.014	.247	1.261	1.252
300	1.253	.263	1.516	1.520
400	2.122	.305	2.427	2.411
500	2.873	.326	3.199	3.149
600	3.442	.340	3.782	3.749
700	3.851	.348	4.199	4.222
800	4.200	.354	4.554	4.580
1000	4.630	.357	4.987	4.992
1100	4.780	.362	5.142	5.060

In the end the author wishes to express his indebtedness to Professor Sir C. V. Raman, Kt., F.R.S., N.L., for his kind suggestions and guidance in the course of the work.

#### Summary

The new view of crystal dynamics developed by Sir C. V. Raman indicates that the diamond lattice has eight distinct normal frequencies of vibration which comprise forty-five out of the forty-eight degrees of freedom of the atoms present in a group of eight lattice cells, while the remaining three degrees of freedom represent the elastic vibrations of lower frequency. These eight frequencies of atomic vibrations are actually observed in the Raman spectrum recorded by Dr. R. S. Krishnan and in the luminescence and the absorption spectra in the visible region investigated by Dr. P. G. N. Nayar and (Miss) Anna Mani. The modes corresponding to the observed frequencies and their respective degeneracies have been ascertained from the theoretical formulæ given by Bhagavantam and Chelam. The elastic constants have been calculated from the spectroscopic data with the aid of the same formulæ. The calculated and experimental values of the bulk modulus agree well. The thermal energy of diamond has been evaluated from the spectroscopically observed frequencies and the known degeneracies, the three degrees of

freedom not covered by these frequencies being considered as an elastic spectrum for which a formula of the Debye type with greatly reduced characteristic temperature is an approximate representation. The theoretical and experimental results agree throughout the whole range of temperature and particularly well in the temperature range between 200 and 1100° K. where the thermal energy content is principally determined by the optical frequencies of vibration.

#### REFERENCES

Adams	.. <i>Journ. Wash. Acad. Sc.</i> , 1921, <b>11</b> , 45.
Bhagavantam	.. <i>Proc. Ind. Acad. Sci.</i> , 1943, <b>18</b> , 251.
____ and Venkatrayudu	.. <i>Ibid.</i> , 1939, <b>9</b> , 224.
Chelam	.. <i>Proc. Ind. Acad. Sci.</i> , 1943, <b>18</b> , 237.
Hopf and Lechner	.. <i>Ber. Deutsch. Phys. Ges.</i> , 1914, 643.
Magnus and Hodler	.. <i>Ann. der Physik</i> , 1926, <b>80</b> , 808.
Nagendra Nath	.. <i>Proc. Ind. Acad. Sci.</i> 1934, <b>1</b> , 333 ; 1935, <b>1</b> , 841.
Nayar	.. <i>Ibid.</i> , 1942, <b>15</b> , 293.
Pitzer	.. <i>J. Chem. Phys.</i> , 1938, <b>6</b> , 68.
Raman	.. <i>Proc. Ind. Acad. Sci.</i> , 1943, <b>18</b> , 334.
Ramaswamy	.. <i>Ind. Jour. Phys.</i> , 1930, <b>5</b> , 97.
Venkatrayudu	.. <i>Proc. Ind. Acad. Sci.</i> , 1939, <b>8</b> , 349.
Williamson	.. <i>J. Franklin Inst.</i> , 1922, <b>193</b> , 491.

# THE FLUORESCENCE AND ABSORPTION SPECTRA OF DIAMOND IN THE VISIBLE REGION

BY ANNA MANI

(*From the Department of Physics, Indian Institute of Science, Bangalore*)

Received April 26, 1944

(Communicated by Sir C. V. Raman, Kt., F.R.S., N.L.)

## 1. Introduction

THE luminescence of diamond has long been familiar knowledge, but spectroscopic studies of it have not been very numerous. E. Becquerel (1859) and W. Crookes (1879) were amongst the earlier observers. The latter noticed some bright lines in the spectrum of the cathode luminescence of diamond and ascribed them to the presence of foreign atoms. Walter (1891) who studied the absorption of light by diamond and noticed a dark band at 4155 A.U., also ascribed it to the presence of impurities. The luminescence of diamond appears in the spectrum along with the scattering of light when the Raman effect is studied, thus directing attention to itself [Ramaswamy (1930), Bhagavantam (1930), Robertson and Fox (1930), and Robertson, Fox and Martin (1934)]. The important observation was made by these authors that a bright line appears in luminescence which coincides with the dark line at the same wave-length noticed in absorption by Walter. John (1931) observed the cathode luminescence spectrum of diamond and found it to be very similar to that excited by ultra-violet irradiation.

Dr. P. G. N. Nayar (1941 *a, b, c, d*; 1942 *a, b*) made a notable advance by his comparative studies of the luminescence and absorption spectra of diamond over a wide range of temperatures. His investigations at liquid air temperatures, in particular, yielded highly interesting and valuable results. His most important findings were, however, made with one single strongly blue-luminescent diamond. It is well-known that diamond may also emit luminescence of other colours and that the intensity of such luminescence may vary over a wide range of values. It is therefore of importance that the investigation of the luminescence and absorption spectra should be extended to specimens showing the widest range of behaviour. Such studies may be expected to throw light on the question of the reason for such difference of behaviour and ultimately also on the general question of the nature and origin of the luminescence of diamond.

The present paper describes a detailed investigation of the fluorescence and absorption spectra of 32 diamonds from Sir C. V. Raman's collection, so selected to be as widely representative as possible of the behaviour of this substance. To enable this wide range of specimens to be successfully studied, a spectrograph of high light-gathering power combined with good resolution was found to be necessary. A two-prism Hilger glass spectrograph (E 328) was used which gave a dispersion of 28 A.U./mm. in the 4358 A.U. region and 63 A.U./mm. in the 5500 A.U. region. To study the absorption spectra under high dispersion in a few cases, a spectrograph of three-metre focal length (Hilger E 185) having a dispersion of 2 A.U./mm. in the 4200 A.U. region and 6 A.U./mm. in the 5200 A.U. region was employed.

Except with regard to the spectrographs employed, the technique of the investigation was generally similar to that followed by Nayar. A specially designed demountable Dewar flask was used to hold liquid air, and the diamonds were mounted in copper blocks screwed on to the bottom of its inner metal tube. This ensured the specimen reaching and remaining at the liquid air temperature. The source of ultra-violet light was a small carbon arc run at 5 amperes, the light from it being filtered through a plate of Wood's glass. The fluorescent light was focussed on the slit of the spectrograph by a short-focus cylindrical lens. The light-source for the absorption studies was a gas-filled incandescent lamp with a straight filament run at 30% more than the usual voltage. In every case, the diamonds were set so that the maximum thickness was employed. The spectra were photographed on Ilford selochrome plates in the blue region of the spectrum, on Ilford HP<sub>2</sub> plates in the green, and on Kodak extra-rapid infra-red plates in the red.

The fluorescence spectrum of each diamond was recorded both at room and at liquid air temperature, while the absorption spectrum was similarly recorded in each case with a graded series of exposures. In all, some 67 fluorescence spectra and 590 absorption spectra were obtained. Except where specifically mentioned, however, the data given in the paper always refer to the measurements of the plates taken at liquid air temperature.

## 2. Description of the Diamonds

As mentioned above, the 32 specimens chosen for examination covered a wide range of behaviour. Four of them were totally non-fluorescent; sixteen showed a blue luminescence with intensities ranging from extreme brilliance to almost complete invisibility; seven showed a greenish-blue and five a greenish-yellow fluorescence, in each case with widely different

intensities. By placing all the diamonds together under the ultra-violet lamp they could be sorted out, and those in each class of luminescence arranged in order of their apparent brightness. Table I shows the catalogue numbers of the 32 diamonds arranged in the order of decreasing intensity of luminescence as visually observed. The twelve diamonds with catalogue numbers between D1 and D30 were crystals from Panna in their natural state. Ten of the other diamonds were cleavage plates with their faces polished flat, while the rest had been fashioned into different shapes for use as jewellery.

TABLE I  
*List of Diamonds Studied*

*Diamonds which were non-fluorescent : (4)*

D39	D206	D207	D227	
6·6	7·2	6·8	11·2	millimetres

*Diamonds showing a blue fluorescence : (16)*

D223	D224	D40	D226	D34	D27	D32	D3	
4·4	8·7	4·6	3·8	9·2	7·0	11·5	7·0	millimetres
D8	D38	D33	D43	D42	D36	D221	D31	

6·0 7·6 7·6 7·8 7·7 8·4 8·2 10·0 millimetres

*Diamonds showing a greenish-blue fluorescence : (7)*

D225	D4	D15	D10	D11	D7	D47	
10·3	7·9	6·7	8·9	6·2	6·7	4·4	millimetres

*Diamonds showing a greenish-yellow fluorescence : (5)*

D13	D12	D19	D1	D197	
6·5	5·0	5·0	9·8	9·4	millimetres

The great majority of the non-fluorescent and blue-fluorescent stones were colourless as seen in daylight. The exceptions were the following: in the non-fluorescent class, D227, a rod-shaped diamond with a slight brownish tinge; in the blue-fluorescent class, D226, a small brilliant with a lively pink colour; D27, a grey hexakis-octahedron from Panna; D32, a heart-shaped diamond with a distinct yellow tinge.

On the other hand, the majority of the diamonds with a greenish-blue or greenish-yellow fluorescence showed various shades of brown or yellow or yellowish brown difficult to describe exactly. The exceptions were D47, a small colourless octahedron with an extremely feeble bluish-green fluorescence, and the two diamonds D225 and D13 which exhibited a greenish tint by daylight, possibly due to their fluorescing with that colour.

The maximum linear dimension (in millimetres) of each diamond has been entered under it. This is of importance, as it influences the observed results, especially in the case of the absorption spectra.

### 3. General Results of the Investigation

Nayar's published studies (*loc. cit.*) relate to the class of diamonds which exhibit a blue fluorescence of greater or less intensity. Such diamonds show a bright band in luminescence at 4156 Å.U. and a dark band in absorption at the same wave-length. A summary of the results obtained by him with regard to the fluorescence and absorption spectra of such diamonds appears in the preface to his doctorate thesis. It is useful to quote the same here *in extenso*, in view of its bearing on the present investigations and to enable it to be better appreciated how the latter have advanced our knowledge of the subject.

\* \* \* \* \*

" The fluorescent band at 4156 Å varies enormously in intensity between different diamonds, but is nevertheless found to be present with every one of the specimens examined, and is thus evidently characteristic of diamond. The 4156 band occurs also in absorption, the peak of intensity coinciding exactly with that observed in fluorescence, and the intensity varying with the specimen studied in precisely the same fashion. Both in absorption and fluorescence, the 4156 band sharpens at liquid air temperature, shifting to 4152 Å and appears resolved into a close doublet. On the other hand, at higher temperatures, there is a shift to greater wave-lengths, the band becomes progressively more diffuse, and fades off to invisibility above 600°K.

" The 4156 Å band in the spectrum is accompanied by subsidiary bands between 4156 Å and 4900 Å in fluorescence, and between 4156 Å and 3600 Å in absorption. These are present strongly in crystals in which the 4156 band is intense. The bands in absorption exhibit a perfect mirror image symmetry about the 4156 frequency with respect to the bands observed in fluorescence. When the diamond is cooled to liquid air temperature, and the bands are examined under high dispersion, they appear resolved into a spectrum of discrete frequencies. The frequency shifts from the principal band at 4152 Å in fluorescence and in absorption are found to be exactly equal but of opposite sign. They lie in the infra-red range, indicating that the subsidiary bands arise from a combination of certain infra-red or atomic vibrations with the electronic frequency manifesting itself both in emission and absorption at 4152 Å.

" The 18 discrete infra-red frequencies ranging from  $137 \text{ cm}^{-1}$  to  $1332 \text{ cm}^{-1}$  deduced as explained above from the fluorescence and absorption spectra of diamond at low temperature, are interpreted as the characteristic

vibration frequencies of the diamond lattice. This interpretation is confirmed by the agreement of the frequency shifts with the Raman effect data reported by Bhagavantam, and with the infra-red absorption frequencies reported by Julius, Reinkober and by Robertson *et al.* The fact that the lattice spectrum of diamond consists of 18 discrete frequencies covering such a wide range, is evidently irreconcilable with the assumptions on which the Debye theory of specific heats is based."

\* \* \* \* \*

The present investigation shows the appearance of a *second system of subsidiary bands which may be designated as the 5032 system* to distinguish it from the 4152 system described in Nayar's thesis. As will be set out later in the paper, this 5032 system is related to a line observed at 5032 Å, appearing at longer wave-lengths in emission and at shorter wave-lengths in absorption in a manner generally analogous to, but differing in important details from the relation between the 4152 system and the 4152 Å line. The important point is that both the 4152 and 5032 systems appear in the fluorescence and absorption spectra, but that their relative as well as their absolute intensities vary enormously from diamond to diamond. The great differences in the intensity and colour of the light emitted by different stones as perceived by the unaided eye arise from these variations. These points are illustrated by the five fluorescence spectra reproduced as Fig. 8 in Plate X appearing at the end of the paper. The spectra were those obtained with two diamonds of the blue-fluorescing type, two of the greenish-blue and one of the yellowish-green fluorescing type.

Another important result of the present investigation has been to show that besides the 4152 and 5032 lines and the bands which accompany them in luminescence and in absorption, there are numerous other lines which are quite sharply defined at liquid air temperature and of which the positions as observed in emission and in absorption coincide. These are interpreted as electronic frequencies. No fewer than 36 such lines have been recorded in the present investigation, their wave-lengths ranging between 3934 and 6358 Å. They may roughly be divided into two groups, the behaviour of which in respect of intensity is similar to that of the 4152 and 5032 systems respectively in the spectra.

The present investigation also shows that the relations between emission and absorption observed by Nayar in respect of the 4152 line and its associated bands are much more general, and extend also to the lines and bands of the 5032 system and to the numerous other electronic frequencies mentioned above. A particular case of this correlation which is of great importance is that of the non-fluorescent diamonds. It has been found that

these show no trace of any absorption lines in the visible spectrum even under the most favourable conditions, namely with the longest possible absorption paths and the exposures most suitable for their detection. No trace of any emission lines, either, appears with such diamonds even after prolonged exposures.

Still another interesting result of the present investigation is that the doublet structure of the 4152 line detected in *absorption* by Nayar in a particular diamond is observable also in the *emission spectra* of numerous diamonds. Further, it has been found that the width and separation of the components of the doublet varies from diamond to diamond in a manner generally related to the intensity of the luminescence of the specimen.

#### *4. The Colour of Fluorescence and its Spectrum*

The 22 diamonds whose fluorescence spectra have been studied may be arranged in the order of the *relative intensities* of the band systems accompanying the 4152 and 5032 lines, beginning with those in which the former is the principal feature while the latter is barely recorded, and ending with those in which the 5032 system is much more prominent than the 4152 system. It should be mentioned that in no case does the 5032 system appear in the spectrum without the 4152 system being also recorded.

TABLE II

*Order of Relative Intensities of the 4152 and 5032 Systems in Emission*

D33, D8, D27, D36, D38, D34, D40, D42, D223, D224, D32,  
D12, D226, D3, D225, D7, D4, D47, D15, D1, D13, D19

Examining this list and comparing it with Table I, it will be noticed that all the diamonds which appear earliest in Table II are those classified as blue-luminescent in Table I, while those which appear last are mostly those shown in it as having a greenish-yellow luminescence. The diamonds shown in Table I as giving a greenish-blue fluorescence appear somewhere midway between the beginning and the end of the list in Table II. There are a few anomalies, e.g., D12 appears high up in the list instead of towards the end. The order in which the blue-fluorescent diamonds appear in Table II is also not the same as that in which they are shown in Table I. It is quite clear, however, on a comparison of the two tables that the difference in the relative intensities of the 4152 and 5032 band systems in the spectrum is the origin of the differences in the colour of the fluorescence as visually observed.

#### *5. Relation between Fluorescence and Absorption*

The intensity of the luminescence of diamond varies enormously. An idea of the range of this variation may be obtained by photographing a

group of stones with a series of graded exposures and counting the number rendered visible by their luminescence. Such photographs also enable a large group of diamonds to be sorted to small groups of approximately equal brightness and their relative intensities to be estimated microphotometrically. The figures obtained in this way for a group of 88 South African diamonds are:—

5(0), 2(1), 4(3), 9(10), 16(20), 4(30), 14(50), 7(100), 6(200), 4(400),  
3(700), 2(1,000), 6(1,800), 3(3,000), 1(5,000), 1(10,000), 1(12,000).

It will be seen that the majority of the diamonds have small intensities of fluorescence, while a few exhibit intense luminescence or else are entirely non-fluorescent.

The diamonds whose emission and absorption spectra have been studied in the present investigation exhibit similar variations in their intensities of luminescence. While the spectra of the most intensely fluorescent diamonds were recorded in a few minutes, to photograph the emission spectrum of the weakly fluorescent diamonds, long exposures of the order 15 to 20 hours were found to be necessary even when thinner plates of Wood's glass and broader slits were used, and the source of light was brought much nearer the diamond.

Accompanying these large differences in the intensities of luminescence, we have corresponding differences in the intensity of absorption of the electronic lines, especially those at the wave-lengths 4152 and 5032. There is also a corresponding increase in the intensity of the subsidiary absorption bands associated with these two electronic lines and appearing towards shorter wave-lengths. It should be mentioned that if the diamonds are arranged in the order of the relative intensities of the two systems of bands as they appear in absorption, the list would be the same as Table II. The absolute intensities of absorption would, however, depend on the length of the absorbing column and cannot therefore be directly compared unless the latter is equal.

Figs. 9 and 10 in Plate XI illustrate the 4152 and 5032 systems respectively, as seen in absorption in a sequence of seven diamonds in one case, and a sequence of five in the other. We have only to compare the spectra of D36 and D224 in Fig. 9 or those of D1 and D197 in Fig. 10 to realise that great differences in the strength of absorption go hand in hand with the differences in the intensity of luminescence. It is not unlikely that the absorption coefficients for the electronic lines are proportional to the intensity of their emission and that the subsidiary band-systems also vary proportionately in intensity. No quantitative measurements have, however, been made to test these points.

It is important to remark that the intensity with which *the 4152 and 5032 electronic lines* are actually recorded in emission would be affected by the absorption of these same radiations before they emerge from the diamond. Hence, the apparent intensities of these lines as recorded in the spectra would not be proportional to the intensity of the luminescence as visually observed, especially when considerable thicknesses are involved. The subsidiary bands accompanying the electronic lines are a better criterion for the visually observed intensity of luminescence. The effect of self-reversal in reducing the intensity of the 4152 and 5032 lines compared with that of the band systems accompanying them is clear on an inspection of several of the spectrograms reproduced in Figs. 1, 7 and 8 in Plates VIII and X. This is also startlingly evident in the emission spectrum of D32 reproduced in Fig. 7, where the 4152 line has completely disappeared due to self-reversal in passing through a thickness of over one centimeter of diamond.

#### 6. *The Electronic Frequencies*

In the fluorescence spectra taken at liquid air temperature, the presence is noticed of several sharply defined lines, besides those at 4152 and 5032 Å and the emission band-systems associated with these which appear at longer wave-lengths. The absorption spectra of luminescent diamonds similarly show several sharply defined dark lines other than 4152 and 5032 and the absorption band-systems associated with these toward shorter wave-lengths. When the absorption and emission spectra are compared, the positions of the bright and dark lines respectively noticed in them are found to coincide, and their identification as distinct electronic frequencies is thereby confirmed.

It must not be supposed, however, that an electronic absorption line would necessarily be observable in the same position in the spectrum as every electronic emission line. The effective absorption depends on the luminescent intensity of the diamond, the intrinsic strength of the electronic absorption and the length of the path available, and when these factors (or all of them working together) make the effective absorption very small, the absorption line in the spectrum would be overpowered by the transmission on either side of it and become unobservable. In general, therefore, a weak electronic line would be more easily observed in emission than in absorption, and only the strongest electronic lines could be expected to be recorded with very weakly luminescent diamonds, unless very long absorption paths are available. Another inherent difficulty in observing weak electronic lines arises when the region in which they appear coincides with the regions in which the subsidiary bands associated with the 4152 and 5032 lines appear.

The latter regions are fortunately different in emission and in absorption, and the relative intensity with which the two systems appear differs greatly with different diamonds. These facts and the sharpness and intensity of the electronic lines are an aid to their discrimination from the background of the band-system on which they may appear superposed.

The foregoing remarks will enable the results shown in Appendices I and II at the end of the paper to be better understood. These appendices give a list of the electronic lines observed in the emission and absorption spectra of the 28 diamonds investigated. Where a column has been left blank under either emission or absorption, it is to be understood that the same has not been studied. The figures recorded in these tables reveal the following features:—

- (a) The most strongly luminescent diamonds show the largest number of electronic lines, and the number of such recorded in emission is generally greater than in absorption, for the reasons already explained.
- (b) The blue-fluorescing diamonds show characteristic electronic lines at the wave-lengths 4090, 4109, **4152**, 4189, 4197, 4206, 4959 and **5032** Å.
- (c) The yellow-fluorescing diamonds show characteristic electronic lines at the wave-lengths 4060, 4123, **4152**, **4194**, 4222, 4232, 4277, **4907**, 5014, **5032**, **5359**, 5658, 5695, **5758**, 6177, 6265 and 6358 A.U.

The more intense lines are printed in heavy type. They may be recognised in the spectrograms reproduced in the Plates. Fig. 11(a), (b) and (c) indicate diagrammatically the changes of the electronic spectrum occurring in the transition from yellow to blue fluorescence. While the diagram represents the facts generally both as regards the positions of the lines and (qualitatively) also their relative intensities, individual diamonds show peculiarities of behaviour, as will be seen from the data given in Appendices I and II. For instance, D42 shows 4907, 6177, 6265 and 6358 but not 4959, 5359 or 5758. Then again, D13 shows strong lines at 4388 and 4833, D32 a strong line at 5895, and D47 strong lines at 4175 and 6043 which are not usually observed in other diamonds. A remarkable observation worthy of special mention is the appearance of an extremely sharp and intense absorption line at 3934 Å with D225 and D36.

#### 7. *Structure of the 4152 and 5032 Lines*

In one particular diamond, the 4152 line in absorption was observed by Nayar to exhibit a doublet structure. In the present investigation it is

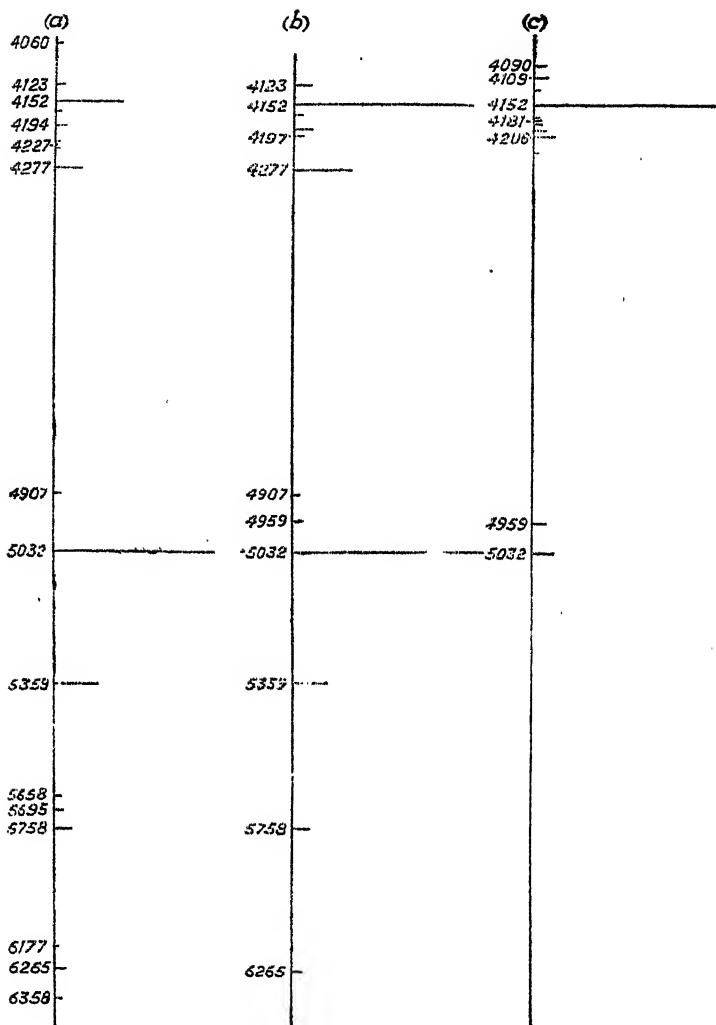


Fig. 11

FIG. 11. Electronic Spectrum of Diamond for (a) yellow, (b) green and (c) blue fluorescence. found that in most diamonds the 4152 line appears as a doublet with widely separated components in both emission and absorption. The width and separation of the components generally increases with the intensity of luminescence. In very weakly fluorescent diamonds, the doublet is so close as to be scarcely resolved. With increasing intensities of luminescence, the separation as well as the width of each component increases, so that in the most intensely fluorescent diamonds the 4152 line is the most diffuse and the separation of the components the largest. This is strikingly illustrated in Fig. 13, Plate XII, where the microphotometer tracings of the 4152

line for 6 diamonds of increasing intensities of blue luminescence are reproduced. Table III gives the wave-lengths, width and separation of the two components of the 4152 line for 13 diamonds. It will be noticed that the two components always appear centred about the mean wave-length at 4152 A.U. and that the line is thus symmetrically split with regard to the positions of the two components. The intensity and the width of the component of longer wave-length are, however, larger than those of the component of shorter wave-length.

TABLE III  
*Structure of the 4152 Line*

Number of Diamond	Component I		Component II		Separation in A.U.
	Wave-length in A.U.	Width in A.U.	Wave-length in A.U.	Width in A.U.	
D223	4155	3	4149	3	6
D224	4156	3	4150	2	6
D27	4155-	3	4149	2	6
D40	4155	2	4149	2	6
D226	4155	5	4150	4	5
D42	4154	3	4149	2	5
D225	4154	3	4150	2	4
D34	4154	3	4151	3	3
D3	4153	2	4151	2	2
D38	4153	2	4151	2	2
D15	4153	2	4151	2	2
D13	4153	2	4151	1	2
D4	4153	2	4151	1	2

The four diamonds D3, D33, D34 and D226 appear to be exceptions to the general rule stated above as existing between the intensity of luminescence and the structure of the 4152 line. In D3, D33 and D34, the separation of the components is not as high as we might expect from their luminescence intensity. In D226 the two components of the 4152 doublet are extremely broad and more diffuse than in D223 or D224. It is likely that D226 owes its pink colour to some extraneous impurities and that these are responsible for the observed diffuseness of the line. It should be remarked however,

that in the case of diamonds showing a tinge of yellow or brown colour, impurities if present, appear to have no effect on the sharpness of the electronic lines.

In the case of two diamonds D223 and D225, it was observed that different portions of the same diamond give the 4152 line respectively as a well-separated doublet and as a single line. In D223, where the 4152 appears as a line, it is accompanied by two wings of high intensity extending to 4 A.U. on either side. D225 showed in the same spectrogram the upper portions of the doublet clearly split, while in the lower portion the two components were very close to each other. These observations become intelligible when it is remembered that in many cases diamonds show definite regions of both high and low luminosity and patterns of blue and green fluorescence. The weakly blue-fluorescent portions of the same diamond will show 4152 as a close doublet or a single line, while with the strongly fluorescent parts it will appear as a well-separated doublet.

Under the high dispersion of the three-metre spectrograph and at liquid air temperature the 4152 line in D42 appears as a triplet, the central line at 4152.2 A.U. being very much sharper and fainter than the two outer components. Absorption photographs of the 4152 line taken at room temperature and at liquid air temperature respectively on the three metre spectrograph are reproduced in Fig. 3(a) and (b) Plate VIII.

The principal electronic line appearing in fluorescence and absorption at 5032 A.U., on the other hand, does not alter in its width and structure with variations in the intensity of luminescence. As will be noticed in the photographs of the 5032 system for different diamonds reproduced in Fig. 8 (emission) and Fig. 10 (absorption), there is no marked broadening of the line as the intensity of yellow luminescence increases, the width of the line in the strongest and weakest fluorescing diamonds being approximately the same, *viz.*, 7 to 8 A.U. In all yellow-fluorescing diamonds, with the exception of D1, D13 and D15 where it appears as a very close doublet, 5032 is present as a single line. Absorption spectra taken on the three-metre spectrograph also failed to reveal any clear splitting of the 5032 line. No definite relationship thus seems to exist between the intensity of yellow luminescence and the structure of the 5032 line. In D226, the 5032 line as well as the other electronic frequencies at 4206, 4388 and 4959 are broader than in other diamonds. This, as mentioned before, is to be ascribed to probable impurities in this diamond.

#### *8. The Lattice Spectrum of Diamond*

(a) *The 4152 System.*—The wave-lengths, intensities and frequencies of the principal electronic line at 4152 and the associated subsidiary bands

in both fluorescence and absorption are given in Table IV. Column 6 gives the descriptions of the lines and bands, and columns 5 and 9 the frequency differences of the subsidiary bands from 4152 in fluorescence and absorption respectively. The microphotometer tracing of the 4152 system in emission for D4 is reproduced in Fig. 14, Plate XIII, and the prominent lattice frequencies indicated by their frequency shifts. The bands are numbered from II to XI, extending to 4825 A.U. in fluorescence and to 3730 A.U. in absorption. The continuous spectrum in fluorescence lies between 4110 and 6500 A.U. A number of new lines have been observed in the present investigation, *viz.*, 4158, 4164, 4169, 4189, 4215, 4248, 4279, 4373, 4386 and 4401 in fluorescence and 4140, 4135, 4123, 4116, 4109, 4092, 4060, 3952 and 3930 in absorption. The bands X and XI in fluorescence could not be obtained in absorption, owing to the lack of sensitiveness of the selochrome plates in the 3500–3700 Å region.

An examination of the 4152 system, in both emission and absorption reveals that though the intensity of the subsidiary bands relative to that of 4152 varies from diamond to diamond, the relative intensities of the lattice bands among themselves are constant. The only exception to this rule is the first subsidiary band II which generally consists of two faint lines at 4164 and 4169 in fluorescence and at 4140 and 4135 in absorption. In D47 this appears as a fairly intense band with limits at 4158 and 4169 and is observed in D3, D4, D19, D40 and D225 but weakly. This band is however present in fluorescence and absorption with identical frequency shifts in both the 4152 and 5032 systems and hence 34, 70 and 98 cm.<sup>-1</sup> are classed as genuine lattice frequencies.

The lattice lines at 4060, 4109, 4175, 4189, 4197 and 4304 coincide with electronic lines present at the same wave-lengths and this is evidently responsible for the observed small variations in the relative intensities of these lines.

A number of lines which could not be classified with any certainty as either lattice or electronic lines are listed separately in Table V.

D32 exhibits the lattice spectrum in absorption also at wave-lengths greater than 4152. The bands in absorption at longer wave-lengths disappear at low temperatures and are therefore probably thermally excited. D32 also exhibits three broad bands in absorption with approximate limits at 4494 and 4538, 4602 and 4701 and 4758 and 4794 A.U., which are apparently unrelated to either the 4152 or 5032 systems. The last one at 4776 A.U. is the most intense of the three and appears in the fluorescence spectrum as a dark band.

TABLE IV  
*Lattice Spectrum in the 4152 System*

No.	FLUORESCENCE				Description of the Bands	ABSORPTION		
	Wave-length in A.U.	Intensity	Frequency in cm. <sup>-1</sup>	Frequency differences from 4152 in cm. <sup>-1</sup>		Wave-length in A.U.	Frequency in cm. <sup>-1</sup>	Frequency differences from 4152 in cm. <sup>-1</sup>
I	4152	20	24077	..	Intense line	4152	24077	..
II	4158	$\frac{1}{2}$	24043	34	Sharp edge			
	4164	$\frac{1}{2}$	24009	68	Discrete line	(4140)	24148	(71)
	4169	$\frac{1}{2}$	23980	97	Discrete line	(4135)	24177	100
III	4175	$\frac{1}{2}$	23945	132	Sharp limit	4130	24206	131
	4183	$\frac{1}{2}$	23900	177	Discrete line	(4123)	24247	(170)
	4189	$\frac{1}{2}$	23865	212	Discrete line	(4116)	24288	(211)
	4197	$\frac{1}{2}$	23820	257	Discrete line	(4191)	24330	(253)
	4215	1	23718	359	Discrete line	(4092)	24431	(354)
	4230	1	23634	443	Sharp limit	4077	24521	444
IV	4246	3	23545	532	Very sharp edge	4062	24611	533
	4248	4	23534	543	Discrete line	4060	24624	544
	4273	5	23396	681	Discrete line	4057	24642	565
	4279	5	23363	714	High int. edge	4038	24758	681
	4292	6	23293	784	Discrete line	4032	24795	717
					Sharp edge	4021	24862	785
V	4304	$\frac{1}{2}$	23228	849	Discrete line	4011	24924	847
	4322	1	23131	946	Discrete line	3995	25024	947
	4334	3	23067	1010	Discrete line	3984	25093	1016
	4349	4	22987	1090	Discrete line	3973	25163	1086
VI	4357	3	22945	1132	Sharp edge	3966	25207	1130
	4360	4	22929	1148	Discrete line	3963	25226	1149
	4373	4	22861	1216	Discrete line	(3952)	25296	1219
	4380	5	22825	1252	Discrete line	3947	25328	1251
	4386	5	22793	1284	Discrete line	3942	25360	1283
	4395	6	22747	1330	Discrete line	3935	25406	1329
	4397	5	22736	1341	Sharp edge	3933	25419	1342
VII	4401	2	22716	1361	Sharp line	3930	25438	1361
	4406	2	22690	1387	Sharp limit	3927	25457	1380
(4461)	1	22410	(1667)		Limit approx.	(3890)	25700	(1623)
VIII	(4490)	2	22265	(1812)	Limit approx.	(3865)	25865	(1788)
(4511)	3	22162	(1915)		Peak approx.	(3850)	25967	(1890)
(4547)	3	21986	(2091)		Limit approx.	(3827)	26123	(2046)
IX	(4611)	2	21681	(2396)	Limit approx.	(3782)	26434	(2357)
(4635)	2	21569	(2508)		Peak approx.	(3758)	26602	(2525)
(4667)	2	21421	(2656)		Limit approx.	(3742)	26716	(2639)
X	(4678)	1	21370	(2707)	Limit approx.	..	..	..
(4700)	1	21271	(2806)		Peak approx.	..	..	..
(4710)	1	21225	(2852)		Limit approx.	..	..	..
XI	(4760)	1	21002	(3075)	Limit approx.	..	..	..
(4795)	1	20849	(3228)		Peak approx.	..	..	..
(4825)	1	20719	(3358)		Limit approx.	..	..	..

N.B.—The figures within brackets refer to lines which are doubtful or to those whose frequencies could not be measured accurately.

The sharpness of the lattice lines in the 4152 system is closely associated with the structure of the 4152 line. In strongly fluorescing diamonds where the 4152 is broad and diffuse, the lattice lines are broad and the edges of the bands slightly diffuse, while in weakly fluorescent diamonds, where the 4152 is sharp, the lattice lines and edges are correspondingly sharp. This is clearly seen in the spectra of D3, D1, D42 and D225 in the Plates and may more readily be noticed in the case of the lines at 4334 and 4349 which are a prominent feature of every spectrum. In D226, these two lines are scarcely observable owing to their diffuseness. In D3 and D1 they are seen to be very sharp. The variations in the breadth of the lattice lines with the broadening and splitting of the 4152 line suggest that both components of the doublet are capable of exciting the lattice frequencies. Therefore the procedure adopted in Table IV of considering neither of the components but the central wave-length at 4152 as responsible for exciting the lattice spectrum appears justified.

TABLE V  
*Unassigned Frequencies*

No.	Wave-length of lines in		Diamonds in which present	Frequency in cm. <sup>-1</sup>
	Emission	Absorption		
1	5128	..	D225	19495
2	4200	..	D3	23803
3	4310	..	D223	23195

(b) *The 5032 System.*—Preliminary investigations by Nayar on the yellow luminescence and absorption of diamond had shown that the fluorescence spectrum is similar to that in the blue and consists of a principal band accompanied by subsidiary bands at longer wave-lengths in fluorescence and at diminished wave-lengths in absorption. A photograph of the 5032 system in emission and absorption taken by Nayar is reproduced in an article by Sir C. V. Raman in *Current Science* for January 1943.

At room temperature the principal electronic line lies at 5038 A.U. and is about 15 A.U. broad. The subsidiary bands, as will be seen in Fig. 5(a), are correspondingly broad and diffuse. As the temperature is lowered, both the main and subsidiary bands become more intense and sharper and shift towards shorter wave-lengths. The peak of the band at liquid air temperature as determined by a microphotometer curve was found to be at 5032·0 A.U. Descriptions of the bands, their wave-lengths, intensities

and frequencies are given in Table VI for both emission and absorption. Columns 5 and 9 give the frequency shifts of the subsidiary bands from 5032 in fluorescence and absorption respectively. A microphotometer tracing of the 5032 system in emission is reproduced in Fig. 15, Plate XIII.

TABLE VI  
*Lattice Spectrum in the 5032 System*

No.	FLUORESCENCE				Description of the Bands	ABSORPTION		
	Wave-length in A.U.	Intensity	Frequency in cm. <sup>-1</sup>	Frequency Shifts from 5032 in cm. <sup>-1</sup>		Wave-length in A.U.	Frequency in cm. <sup>-1</sup>	Frequency Shifts from 5032 in cm. <sup>-1</sup>
I	5032	20	19867	..	Intense line	5032	19867	..
II	5040 (5049) (5056)	4 4 2	19836 19800 19773	31 (67) 94	Sharp limit Fall in intensity Diffuse limit	(5015) (5009)	19934 19958	(67) (91)
III	(5062) (5080) (5100)  (5130) (5144)	2 4 7  7 3	19750 19680 19602  19488 19435	(117) (187) (265)  (379) (432)	Diffuse limit Rise in intensity Further rise in intensity Fall in intensity Diffuse limit	(5002) (4985) (4966) (4930) (4920)	19986 20054 20131 20278 20320	(119) (187) (264) (411) (453)
IV	(5170) (5180)  (5216) (5230)	3 5  5 3	19337 19300  19166 19115	(530) (567)  (701) (752)	Diffuse limit Rise in intensity  Fall in intensity Diffuse limit	(4900) (4890)  (4840)	20402 20444  20655	(535) (577)  (788)
V	(5260) (5284) (5304) (5320)	2 3 3 2	19006 18920 18848 18792	(861) (947) (1019) (1075)	Diffuse limit Rise in intensity Fall in intensity Diffuse limit	(4825) (4788) (4768)	20720 20880 20967	(853) (1013) (1100)
VI	(5335) 5341 5372 5381 5393 (5397)	1 2 3 2 2 1	18739 18718 18610 18579 18537 18524	(1128) 1149 1257 1288 1330 (1343)	Fairly sharp limit Sharp line Sharp limit Sharp limit Sharp limit Fairly sharp limit	(4762) 4757 4733 4727 4716 (4713)	20994 21016 21122 21149 21198 21212	(1127) 1149 1255 1282 1331 (1345)
VII	(5420) (5455) (5492)	2 2 2	18445 18327 18203	(1422) (1540) (1664)	Limit approx. Peak approx. Limit approx.	(4692) (4673) (4645)	21307 21394 21522	(1440) (1527) (1655)
VIII	(5520) (5560) (5602)	1 1 1	18110 17980 17846	(1757) (1887) (2021)	Limit approx. Peak approx. Limit approx.	(4611) (4588) (4566)	21681 21790 21895	(1814) (1923) (2028)
IX	(5639) .. ..	1 .. ..	17729 .. ..	(2138) .. ..	Limit approx. Peak approx. ..	(4468) .. ..	22375 .. ..	(2508) .. ..

The bands are numbered from II to IX and extend to 5700 A.U. in fluorescence and to 4400 in absorption. The continuous spectrum in this system extends to 6500 A.U., and beyond 5600 A.U. is as intense as the subsidiary bands whose limits could not therefore be located with any certainty. The relative intensities of the subsidiary bands as in the 4152 system are always constant with the exception of the band II which is generally weak, but appears with fairly high intensity in D225 (see Fig. 7c and Fig. 8c).

(c) *Lattice Frequencies.*—An examination of Tables IV and VI shows that the frequency shifts of the subsidiary bands in both the 4152 and 5032 systems are identical within the limits of accuracy of measurement and that these bands arise from a combination of the lattice frequencies of the diamond lattice with the electronic frequencies at 4152 and 5032 respectively. The intensity and structure of the bands in the two systems are, however, very different. In the 4152 system, the bands II to VI consist of sharp lines or bands with extremely sharp edges, while in the 5032 system all the bands with the exception of VI are broad and diffuse. The lattice bands in the 4152 system alternate in intensity, II, V, VII, IX and XI being weaker than IV, VI and VIII. In the 4152 system VI is the most intense band and III one of the weakest. On the other hand in the 5032 system, the bands progressively decreasing in intensity as we proceed away from 5032, III is the most intense band of the group and VI one of the weakest.

The lattice frequencies derived from fluorescence and absorption measurements may be classified into ten groups: 34-98, 132-443, 532-784, 848-1088, 1131-1341, 1361-1667, 1800-2090, 2400-2660, 2700-2850 and 3100-3350 cm.<sup>-1</sup> The principal discrete frequencies are listed below:—

34, 70, 98, 132, 178, 212; 258, 359, 443, 533, 543, 565, 681, 716, 784, 848, 946, 1013, 1088, 1131, 1149, 1218, 1252, 1284, 1330.

#### 9. Effect of Temperature Variation on the 5032 System

The general effect of cooling the crystal from room temperature to liquid air temperature is to increase the intensity of fluorescence and absorption in the whole region of the 5032 system. The bands become considerably sharper and shift towards the blue, the general behaviour being analogous to that of the 4152 system. The changes in absorption in every case are parallel to those in fluorescence. In Table VII are given the wave-lengths and frequencies of the principal electronic line and the lattice bands of the 5032 system at room temperature and at liquid air temperature respectively. In column (3) are shown the shifts of the bands in cm.<sup>-1</sup> as the temperature is lowered from 25° C. to -189° C. In column (6) the changes in

TABLE VII

*Effect of Temperature Variation on Electronic and Lattice Lines*

No.	25° C.		-189° C.		Wave-numbers shift	Shift per 1000 cm. <sup>-1</sup>
	Wave-length in A.U.	Frequency in cm. <sup>-1</sup>	Wave-length in A.U.	Frequency in cm. <sup>-1</sup>		
I	5038	19844	5032	19868	24	1.2
III	5123	19514	5115	19545	31	1.6
IV	5204	19210	5198	19233	23	1.2
V	5292	18891	5286	18912	21	1.1
VI	5367	18627	5359	18655	28	1.5
VII	5455	18327	5451	18340	13	0.71
XI	5701 5768	17536 17332	5695 5758	17554 17362	18 30	1.0 1.7
1	4156	24057	4152	24077	20	0.83
2	3450	28975	3447	28999	24	0.83
3	3304	30257	3299	30303	46	1.5
4	3159	31648	3154	31699	51	1.6
5	Raman line	1332.1	Raman line	1333.8	1.7	1.3

frequencies in each case are shown as a shift per 1000 cm.<sup>-1</sup>. In the lower half of the table are given similar data for the prominent electronic lines in the 4152 system and in ultra-violet absorption along with those of the 1332 line in Raman effect (taken from Nayar's tables). An examination of the last column shows that the shifts per 1000 cm.<sup>-1</sup> are more or less of the same order and about the same as that of the 1332 line in Raman effect.

In conclusion, the author wishes to express her respectful thanks to Professor Sir. C. V. Raman for his constant guidance and encouragement during the course of this work.

#### 10. Summary

A detailed study of the fluorescence and absorption spectra of 32 diamonds of widely different intensities and colours of luminescence has been made at room temperature and at liquid air temperature, using a two-prism spectrograph of good resolution and large light-gathering power. A clear relation is observed to exist between the fluorescence and absorption spectra in the visible region and this is shown to extend both to the

general character of the spectra and to their intensities. In spite of the enormous variations in the intensity and colour of luminescence, the spectra in all diamonds consist mainly of the 4152 and 5032 systems which consist of (*a*) a set of lines appearing as bright and dark at the same wave-lengths respectively in fluorescence and absorption, (*b*) subsidiary or lattice lines appearing at greater wave-lengths in fluorescence and at diminished wave-lengths in absorption, associated with the principal electronic lines at 4152 and 5032 Å respectively. In blue-fluorescing diamonds the 4152 system is more prominent than the 5032 system. In yellow-fluorescent diamonds the reverse is the case. More generally, the two systems appear with comparable intensities. The intensity and colour of luminescence is thus determined by the absolute and relative intensities of the two systems.

Thirty-six electronic lines other than 4152 and 5032 are found to be present in the visible region. Of these the lines at 4060, 4123, 4194, 4222, 4232, 4277, 4907, 5359, 5695, 5758, 6177, 6265 and 6358 are characteristic of yellow fluorescence while those at 4090, 4109, 4189, 4197, 4206 and 4959 are characteristic of blue fluorescence.

The 4152 line appears in most diamonds as a doublet in both emission and absorption, the width and separation of the components increasing with the intensity of blue luminescence. The 5032 line shows no such variation with changes in the intensity of yellow fluorescence.

The frequency differences between the principal electronic lines at 4152 and 5032 and the lattice lines associated with them are the same in fluorescence and absorption, and lie in the infra-red range; they thus represent the vibration frequencies of the diamond lattice. Their values as derived from the 4152 and 5032 systems are identical, but the degree of sharpness and the intensity distributions are different in the two systems. From the observed frequency differences 25 monochromatic frequencies, *viz.*, 34, 70, 98, 132, 178, 212, 258, 359, 443, 533, 543, 565, 681, 716, 784, 848, 946, 1013, 1088, 1131, 1149, 1218, 1252, 1284 and 1330 have been obtained as constituting the lattice spectrum of diamond.

**APPENDIX I**  
***List of Electronic Lines***

Observed in Diamond	Wave-lengths in A.U. and intensities (on a scale of 20) of the lines present in	
	Fluorescence	Absorption
D3	4152 (20), 4189 (0), 4197 (1), 4206 (2), 4959 (5), 5032 (6)	4152 (20), 5032 (4), 4959 (2)
D7	4152 (20), 5032 (3)	
D8	4152 (20)	
D12	4152 (20), 4206 (2), 5032 (1)	
D27	4152 (20), 4206 (4), 4222 (2)	
D31		4152 (20)
D32	4152 (-), 4197 (6), 4206 (6), 4227 (15), 5895 (20)	4152 (20), 4189 (1), 4197 (1), 4206 (2), 4304 (1), 4380 (1), 4252 (1), 4959 (1), 5032 (1)
D33	4152 (20), 4197 (3), 4206 (2)	4152 (20)
D34	4152 (20), 4189 (1), 4197 (1), 4206 (2), 4959 (2), 5032 (1)	
D36	4152 (20), 4197 (1), 4206 (3), 4227 (1), 5032 (0)	4152 (20), 3934 (5),
D38	4152 (20), 4206 (2), 4227 (2), 5032 (4)	
D40	4152 (20), 4189 (0), 4197 (0), 4206 (1), 4227 (1), 4959 (2), 5032 (6), 5233 (1)	
D42	4152 (20), 4189 (1), 4197 (2), 4206 (4), 4907 (2), 5032 (8), 6177 (1), 6265 (2), 6358 (1)	4152 (20), 5032 (4)
D42+D43		4152 (20), 4206 (1), 5014 (1), 5032 (3)
D221		4152 (20)
D223	4090 (1), 4109 (1), 4152 (20), 4175 (2), 4189 (1), 4197 (2), 4206 (3), 5233 (2)	
D224	4090 (2), 4109 (1), 4152 (20), 4189 (2), 4197 (3), 4206 (4)	4152 (20)
D226	4152 (20), 4206 (2), 4388 (5), 4959 (2), 5032 (7)	4152 (20), 5032 (5)

**APPENDIX II**  
**List of Electronic Lines**

Observed in Diamond	Wave-lengths in A.U. and intensities (on a scale of 20) of the lines present in	
	Fluorescence	Absorption
D1	4060 (1), 4123 (1), 4152 (20), 4194 (2), 4222 (1), 4227 (0), 4232 (1), 4277 (3), 4907 (2), 5014 (0), 5032 (20), 5359 (4), 5658 (1), 5695 (1), 5758 (2), 6177 (0), 6265 (0), 6358 (0)	4152 (20), 4907 (2), 5014 (1) 5032 (20), 5359 (4)
D4	4152 (20), 4175 (1), 4206 (2), 4907 (3), 4959 (1), 5032 (7), 5359 (1)	4152 (20), 5032 (6)
D10		4152 (15), 4907 (2), 5032 (20), 5359 (3)
D11		4152 (5), 4907 (1), 5032 (20), 5359 (4)
D13	4123 (1), 4152 (20), 4175 (1), 4194 (3), 4222 (1), 4227 (0), 4232 (1), 4277 (5), 4388 (6), 4590 (1), 4606 (2), 4833 (4), 5014 (0), 5032 (20), 5359 (3), 5658 (0), 5695 (0), 5758 (2), 6177 (0), 6265 (0), 6358 (0)	
D15	4123 (1), 4152 (20), 4194 (3), 4222 (1), 4227 (0), 4232 (1), 4277 (6), 4907 (2), 4959 (1), 5032 (15), 5359 (6), 5658 (0), 5695 (0), 5758 (1), 6177 (0), 6265 (0), 6358 (0)	4152 (15), 4907 (2), 5032 (20), 5359 (5)
D19	4152 (10), 5032 (20), 5359 (3)	
D47	4152 (20), 4175 (4), 4959 (1), 5032 (12), 5233 (2), 5359 (2), 5758 (2), 5895 (1), 6043 (4)	
D197		4060 (1), 4152 (6), 5014 (1), 5032 (20)
D225	4152 (20), 4189 (2), 4197 (3), 4206 (4), 4959 (18), 5032 (12)	3934 (10), 4152 (20), 4245 (1), 4295 (2), 4304 (1), 4959 (6), 5032 (10)

REFERENCES

Becquerel, E. . . *Ann. Chem. Phys.*, 1859, 55, 89 ; 57, 62.  
 Bhagavantam, S. . . *Ind. Journ. Phys.*, 1930, 5, 35, 169, 573.  
 Crookes, W. . . *Phil. Trans.*, 1879, 170, 135, 641.  
 John, M. V. . . *Ind. Journ. Phys.*, 1931, 6, 305.  
 Nayar, P. G. N. . . *Proc. Ind. Acad. Sci.*, 1941a, 13, 284 ; 1941b,  
                           13, 483 ; 1941c, 13, 534 ; 1941d, 14, 1 ;  
                           1942a, 15, 293 ; 1942b, 15, 310.  
 Raman, C. V. . . *Curr. Sci.*, 1943, 12, 33.  
 Ramaswamy, C. . . *Ind. Journ. Phys.*, 1930, 5, 97.  
 Robertson and Fox . . . *Nature*, 1930, 125, 704.  
 Robertson, Fox and Martin . . . *Phil. Trans.*, 1934, 232, 494.  
 Walter . . . *Wied. Ann.*, 1891, 42, 505.

## DESCRIPTION OF PLATES VIII TO XIII

FIG. 1. Fluorescence spectra, (a) at room temperature, and (b), (c), (d) at liquid air temperature. In these, 4152 appears at the extreme left and 5032 at the extreme right. The latter is much brighter than the former for D1 which is a yellow-luminescing diamond, while the reverse is the case for D3 and D42 which are blue-luminescing diamonds. 4152 is clearly seen as a doublet in Fig. 1 (d). The electronic frequency at 4959 is seen with D3 but not with D1. Note other electronic frequencies at 4194, 4222, 4232, 4277 in (c) and 4189, 4197 and 4206 in (b).

FIG. 2. Fluorescence and absorption spectra juxtaposed after inverting the latter to exhibit the mirror-image symmetry of the lattice lines about the electronic frequency at 4152.

FIG. 3. The 4152 line of D42 in absorption at room temperature and at liquid temperature with the three-meter spectrograph.

FIG. 4. The 5032 system of D1 in emission and absorption at liquid air temperature, showing mirror-image symmetry. Note the two prominent electronic lines at 5359 and 5758 A.U.

FIG. 5. (a) The 5032 system in emission at room temperature; (b) and (c), the same in emission and absorption at liquid air temperature, with the latter inverted.

FIG. 6. (a) and (b). The 4152 and 5032 systems in emission for diamonds D1 and D3 respectively.

FIG. 7. (a), (b), (c) and (d). Emission spectra of four diamonds, showing variations in the appearance of the 4152 line, and its effect on the associated lattice spectrum. In Fig. 7 (a) the 4152 has disappeared by self-reversal, while in Fig. 7 (c), it has been much weakened.

FIG. 8. (a), (b), (c), (d) and (e). Sequence showing progressive change in the relative intensities of the 4152 and 5032 systems. Notice also the changes in the appearance of the 4152 line.

FIG. 9. Sequence showing the appearance of the 4152 system in absorption and its increased intensity with increasing intensity of luminescence. Note also the increased width of the 4152 line in the sequence. D227 is non-fluorescent and shows no lines.

FIG. 10. Sequence showing the 5032 system in absorption and its increasing intensity with intensity of luminescence.

FIG. 12. The complete fluorescence and absorption spectra of diamond in the visible with wave-length scale, to illustrate the general relationship between fluorescence and absorption.

FIG. 13. Microphotometer tracings of the 4152 line for six diamonds of increasing intensities of luminescence, illustrating the corresponding variations in the structure of the line.

FIG. 14. Microphotometer tracing of the 4152 system of D4 in fluorescence at liquid air temperature. The prominent electronic frequencies are indicated by their wave-lengths in A.U. and the lattice lines by their frequency shifts in cm.<sup>-1</sup> from the 4152 line.

FIG. 15. Microphotometer tracing of the 5032 system of D15 in fluorescence at liquid air temperature. The electronic and lattice lines are indicated as in Fig. 14.

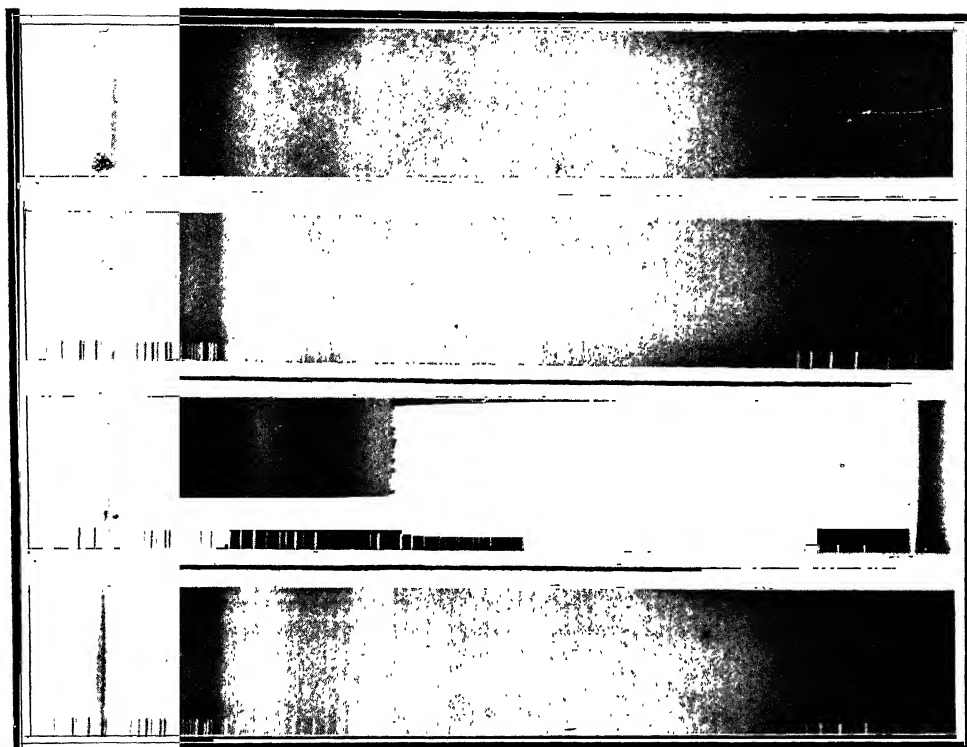


FIG. 1

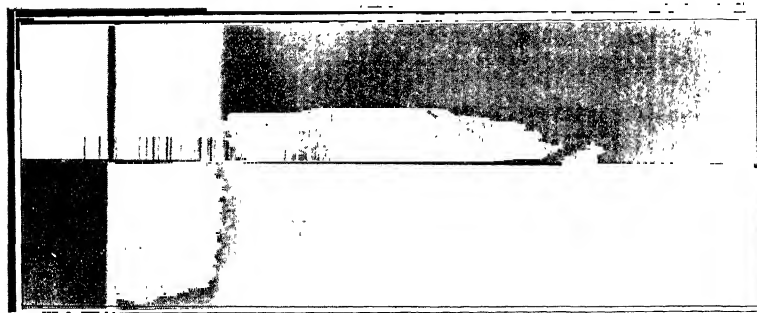
 $\lambda \rightarrow$  $\leftarrow \lambda$ 

FIG. 2

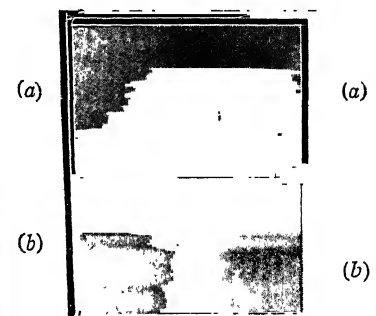


FIG. 3

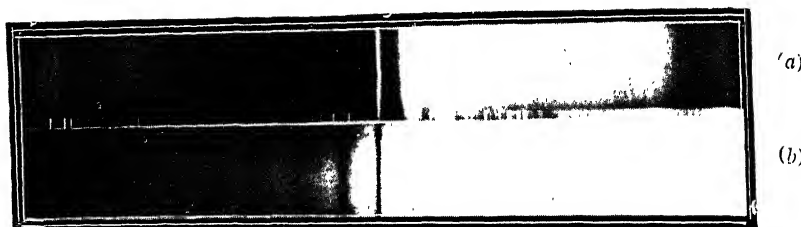


FIG. 4

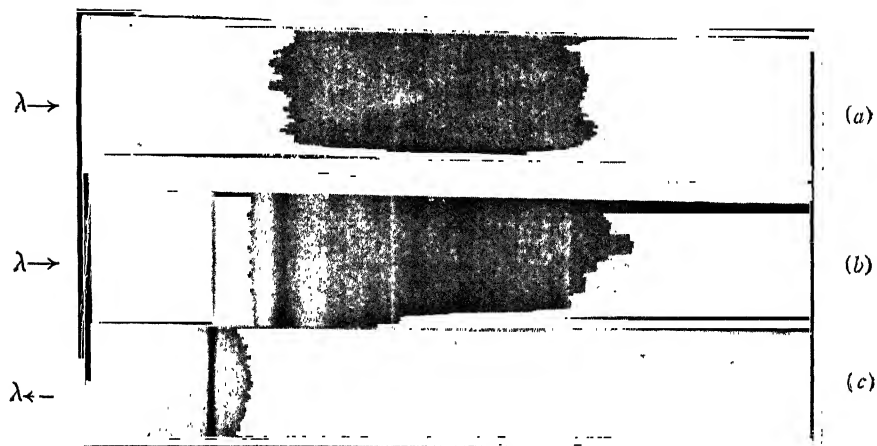


FIG. 5

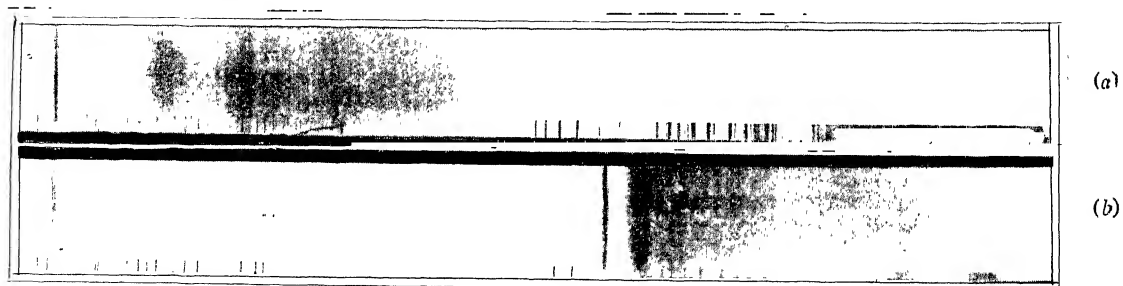


FIG. 6

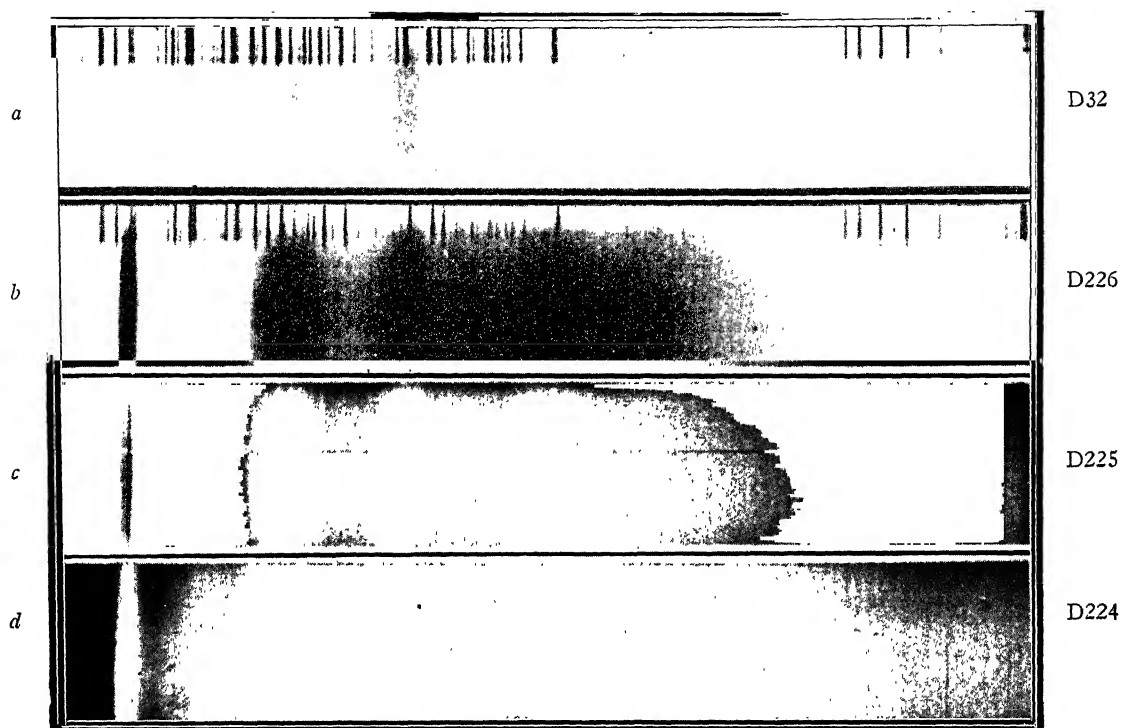


FIG. 7

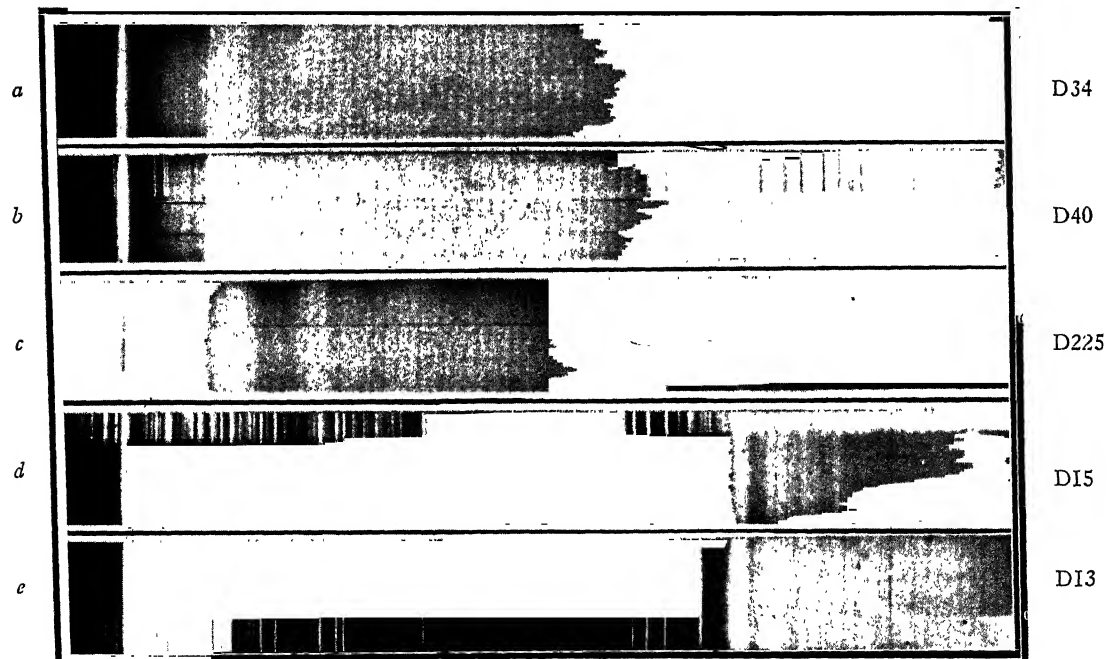


FIG. 8

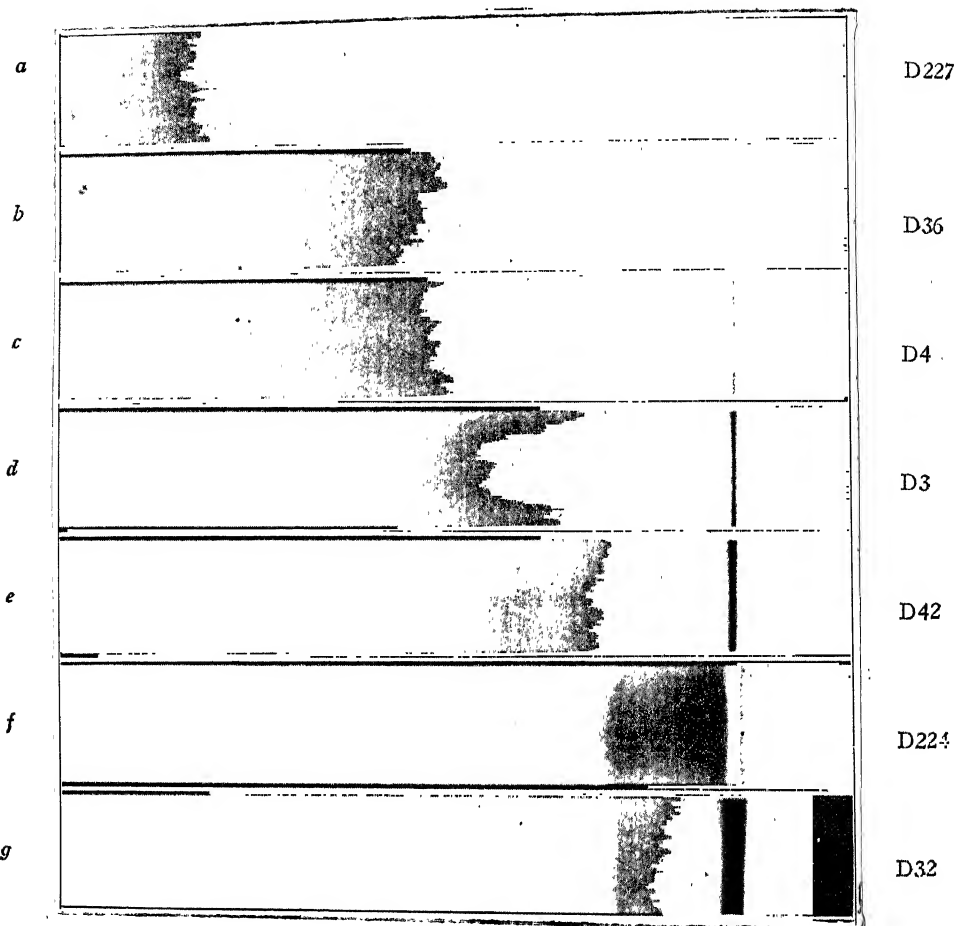
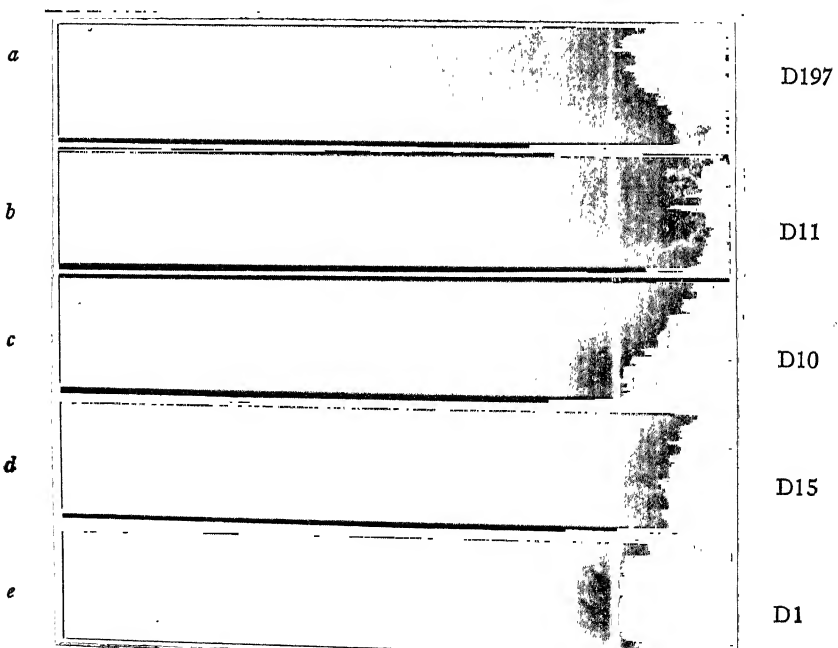


FIG. 9



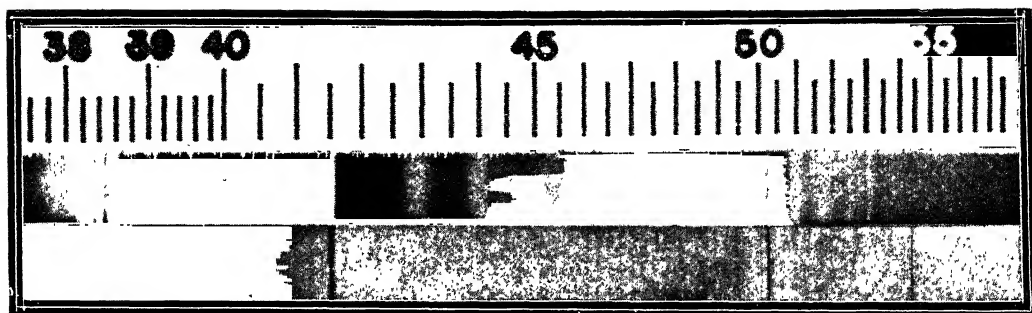
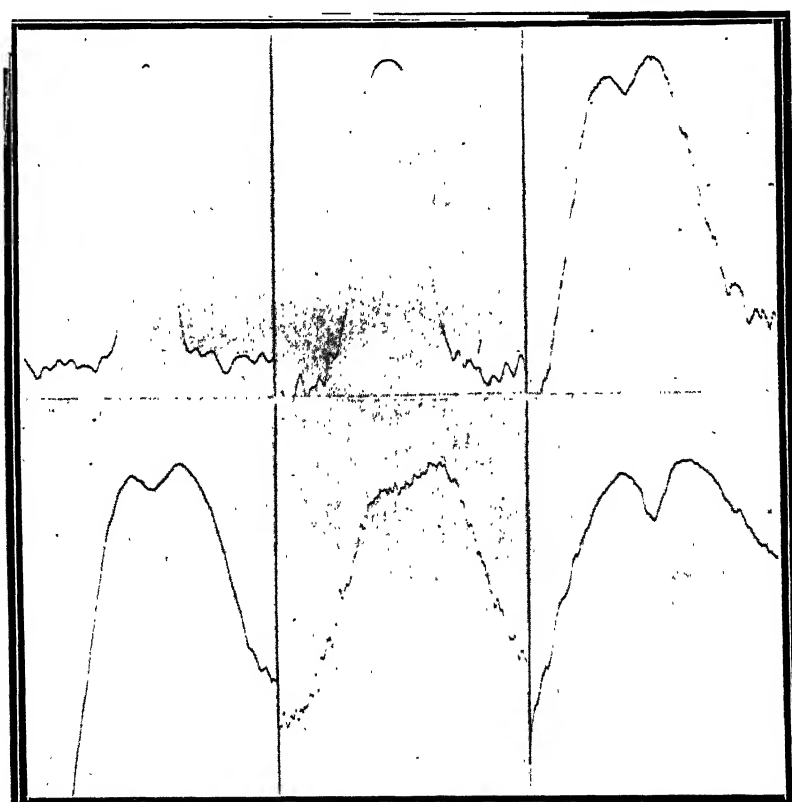


FIG. 12

D47

D4

D225



D42

D27

D224

FIG. 13

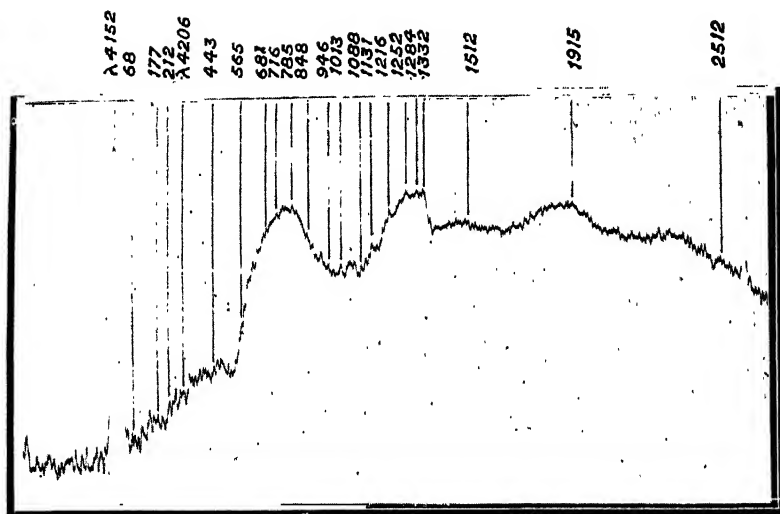


FIG. 14

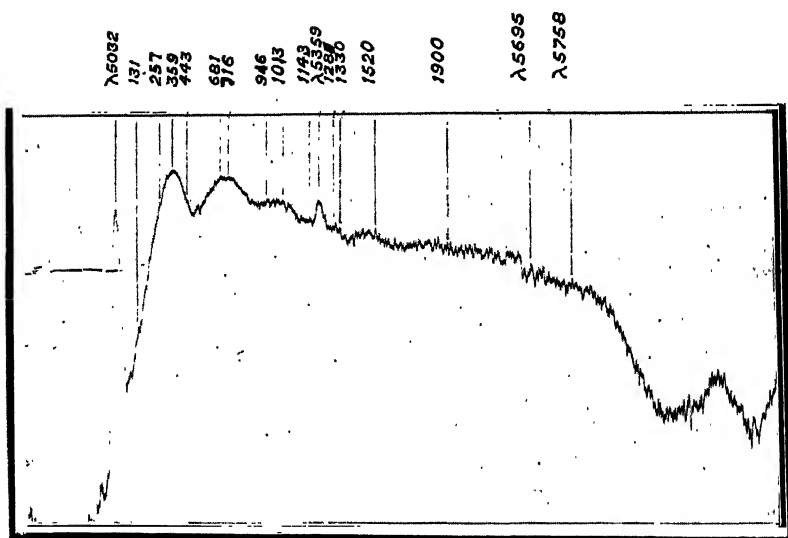


FIG. 15

# THE ULTRA-VIOLET ABSORPTION SPECTRUM OF DIAMOND

BY K. SUNANDA BAI

(*From the Department of Physics, Indian Institute of Science, Bangalore*)

Received May 8, 1944

(Communicated by Sir C. V. Raman, Kt., F.R.S., N.L.)

## 1. Introduction

It has long been known that the transparency of diamond in the ultra-violet region of the spectrum is variable, some specimens allowing transmission only a little farther into the ultra-violet than ordinary window glass, while others transmit the major part of the spectrum to which quartz is transparent. It was also recognized (Gudden and Pohl, 1920, Pringsheim, 1928) that these differences in ultra-violet transparency go hand in hand with striking variations of the behaviour of diamond in other respects, *viz.*, in the excitation of luminescence and of photo-conductivity by the incident radiation. More recently, Robertson, Fox and Martin (1934) noticed that these variations in ultra-violet transparency are accompanied by significant differences in the infra-red absorption spectrum of diamond of the kind to which attention had been drawn earlier by Reinkober (1911). They accordingly suggested that there are two distinct types of diamond, one giving a complete cut-off of the ultra-violet spectrum beyond about 3000 Å while the other shows a similar cut-off at 2250 Å.

The studies made at this Institute during recent years have however shown that neither the description given of the behaviour of diamond nor the interpretation of the same suggested by Robertson, Fox and Martin is adequate. Dr. P. G. N. Nayar (1941, 1942) found that there is no complete cut-off at 3000 Å in the spectrum transmitted by the commoner varieties of diamond and that the limit could be extended progressively into the ultra-violet up to about 2700 Å by reducing the thickness of the specimen and by suitably increasing the photographic exposures. It was observed that a system of five absorption bands at 2715, 2770, 2845, 2950 and 2975 Å appeared in this extended region of transmission. Nayar also found that all such diamonds are blue-luminescent in greater or less degree and that their behaviour in the region of wave-lengths greater than 3000 Å depended greatly on the intensity of such luminescence. Working at liquid air temperatures with diamonds which fluoresced only feebly, he observed a

set of 25 sharply defined absorption lines in the region of wave-lengths between 3000 Å and 3500 Å, eight of the strongest of which had been recorded earlier by Robertson, Fox and Martin. The width and intensity of these lines, however, showed a striking dependence on the luminescence properties of the diamond; the strongest of them lying in the region between 3000 Å and 3300 Å were practically unobservable in his most intensely luminescent specimen. Later, Nayar also found that while some diamonds transmitted freely up to 2250 Å, there are others in which the absorption progressively increases as this limit is approached, and in which also a clearly marked absorption band appears in the vicinity of 2370 Å. Pictures of the different types of absorption spectra in the ultra-violet region exhibited by diamond are reproduced in an article by Sir C. V. Raman in *Current Science* for July 1942. They clearly show a much wider range of behaviour than can be described in terms of two alternatives only.

It is thus evident that the absorption spectrum of diamond and its luminescence properties are intimately connected with each other. This relationship also manifests itself, though in a different way, in the visible region of the spectrum. This has been clearly shown by Nayar (*loc. cit.*) in the case of blue-luminescent diamonds and by (Miss) Mani (1944) in a paper appearing in this symposium in respect of other varieties of luminescence. It is obviously important, therefore, that study of the absorption spectrum of diamond in the ultra-violet region should be extended to specimens showing the widest range of behaviour in respect of the intensity and spectral character of their luminescence and that the results should be correlated with the variations of the latter properties. The present investigation was undertaken with the object stated, and the results obtained will now be described.

## 2. Materials and Methods

The diamonds used in the present investigation were chosen from the personal collection of Sir C. V. Raman. 45 of them were polished cleavage plates, while two were crystals in their natural condition. Most of the cleavage plates were the same as those of which photographs are reproduced in another paper by the author on the luminescence patterns in diamond appearing in this symposium. As will be noticed from those photographs, several of the plates show a uniform or practically uniform luminescence, while others exhibit striking variations of its intensity over their area. The very great differences in the intensity of luminescence with which we are concerned will be appreciated on a reference to the group picture of 46 cleavage plates reproduced with Sir C. V. Raman's paper on the nature and origin of the luminescence of diamond. For our present purpose, the

diamonds may be grouped into four classes: (a) non-fluorescent diamonds; (b) diamonds exhibiting a yellowish-green fluorescence; (c) diamonds showing a blue fluorescence and (d) diamonds showing a mixture of the two types of fluorescence. Enormous variations in the intensity of luminescence in each of the three groups (b), (c) and (d) appear, both in respect of different specimens and also over the area of an individual specimen in the case of those diamonds which show a luminescence pattern.

The source of ultra-violet light used for recording the absorption spectra was a water-cooled hydrogen lamp with an exit-window of quartz made by the firm of Hilger. It was run with 200 to 300 milliamperes current at 3000 volts, and produced an intense continuous spectrum extending up to 1800 Å. The diamonds to be studied were set in small apertures made in a sheet of lead so as to completely cover the same except for the exposed area of the plate. The procedure for recording the spectra was slightly different according as it was desired to study the transmission by the whole area of the specimen, or the local variations of the transmission spectrum over the different parts of the area. In the former case, an image of the quartz window of the lamp was thrown on the slit of the spectrograph by a short-focus quartz lens. In the latter case, an image of the cleavage plate was carefully focussed on the slit of the spectrograph by a quartz lens, and by moving the specimen, different parts of the image were made to pass over the slit. In this way, a series of spectra with equal exposures could be obtained exhibiting the local variations of the absorption in the case of diamonds showing luminescence patterns.

When it was desired to record the absorption spectrum of the specimen at liquid air temperature, the diamond was embedded in a cylindrical copper rod with two circular apertures for the entrance and exit of light. This rod was fixed at the bottom of a long-thin-walled brass cylinder in which liquid air is kept. In order to ensure good thermal contact, Wood's metal was used to fix the diamond in the copper rod. Another jacket of pyrex glass with putty seal between the metal and the glass formed a vacuum jacket round the metal cylinder. The system was kept continuously evacuated by a Cenco pump. With this arrangement, the crystal attained the temperature of liquid air within a few minutes.

As already remarked, the thickness of the specimen and the photographic exposures employed are factors of very considerable importance in determining the nature of the recorded spectra. In the case of all the cleavage plates used, the light passed normally through the specimens. The slit width of the spectrograph and the exposures employed were varied according to the nature of the investigation. A few minutes usually sufficed for

recording the region of free transmission by the specimen, while exposures up to one hour had to be employed fully to record the regions of partial transparency.

A Spekker ultra-violet photometer by Hilger was also used to investigate the transmission spectra of two diamonds D221 and D39 by comparison with that of the tungsten-iron spark used as the source in this instrument, their intensity-ratio being altered step by step over a wide range of values.

### 3. Non-Fluorescent Diamonds

The absorption spectra of seven non-fluorescent diamonds, *viz.*, D39, D57, D206, D207, D208, D209 and D227 have been recorded and the effect of cooling them to liquid air temperature has also been studied with D39. These diamonds were found to be all of the ultra-violet transparent type. At room temperature, the intensity of the transmitted radiation falls off rapidly beyond 2350 Å, a cut-off being observed at about 2255 Å. At liquid air temperature, the absorption beyond 2350 Å disappears, and the cut-off shifts to 2251 Å. These results completely confirm similar observations reported by Robertson, Fox and Martin. A new result obtained in the present investigation is the appearance of a region of feeble transparency extending beyond the edge at 2255 Å up to about 2242 Å at room temperature. This effect becomes more pronounced at liquid air temperature. Fig. 5 reproduces two spectra taken at room temperature and at liquid air temperature respectively, using a Hartmann diaphragm and the same time of exposure. The region of feeble transmission and the shift of the edge at liquid air temperature towards the ultra-violet are both clearly seen. A careful examination of the spectra of D39 and D57 revealed no local variations in transparency over the area of these plates. The Spekker-photometer records of D39 show that at room temperatures, there is a fairly strong absorption commencing at 2350 Å which increases up to the absorption edge at 2255 Å, there becoming very large.

In all the four diamonds studied which fluoresce with a greenish-yellow colour, *viz.*, D199, D200, D201, D202, the recorded spectra for shorter exposure times showed a progressive increase in absorption beyond 2750 Å. When the exposure time was increased, the recorded spectra extended clearly up to 2250 Å and rather weakly beyond to about 2242 Å, as in the case of the non-fluorescent diamonds. No local variations in their transparency were noticed in these diamonds as well.

### 4. Blue-Fluorescent Diamonds

Nayar's observation that the absorption bands at 3030, 3060, 3075 and 3157 Å which are exhibited by weakly blue-fluorescing diamonds tend to

disappear in strongly fluorescent specimens has been completely confirmed in the present investigation. It is noticed that whether these bands are recorded or not depends both on the thickness employed as well as on the fluorescence intensity of the specimen. Thus, in the case of diamonds D31 (thickness 0.97 mm.) and D36 (thickness 0.80 mm.) which are only feebly blue-fluorescent, no trace of these bands could be observed. On the other hand, the crystal D234 of which the fluorescence was much weaker and indeed scarcely observable showed the absorption bands very clearly, though its thickness was only 1.4 millimeters. Then again, with D34 (thickness 1.22 mm.) and D224 (thickness 1.5 mm.) in which the fluorescence was strong and very intense respectively, the bands were wholly unobservable. They were, however, feebly recorded with the crystal D3 which had a moderate intensity of fluorescence, evidently because an absorption thickness of 4 millimeters was employed in this case.

*A new and remarkable result noticed in the present investigation is that the ultra-violet transparency of diamonds increases with their intensity of fluorescence.* This effect appears to be closely related to the one mentioned above. The extension of the spectrum transmitted in the ultra-violet depends on the thickness of the specimen, its luminescence intensity, and to some extent, also the photographic exposures employed. We may illustrate this by the behaviour of the same specimens as those mentioned above.

The crystal D234 which shows the absorption bands at 3060, 3075 and 3157 Å very clearly exhibits a practically complete cut-off at 3050 Å, even the most prolonged exposures failing to record an extension beyond that wave-length. On the other hand D31, D36 and D34 which do not show these bands show a transmission into the ultra-violet far beyond 3000 Å, increasing in the order stated which is also the order of their luminescence intensities. Even with moderate exposures, D31 goes up to 2850 Å and D36 to 2750 Å, while the transmission of D34 goes up to 2550 Å with sufficient exposures, an absorption band being clearly visible at 2845 Å. On the other hand, the crystal D3 with an absorption thickness of 4 millimeters which shows the bands at 3060, 3075 and 3157 Å (though very feebly) shows a practically complete cut-off at about 3000 Å.

The highly blue-luminescent diamond D224 of which the ultra-violet transmission spectra are reproduced as Fig. 3 in Plate XV affords a very striking illustration of the new effect now under consideration. It will be noticed that its transmission extends up to 2450 Å, a series of step-like falls in intensity occurring at 2845, 2715 and 2570 Å. The first two edges coincide with the positions of absorption bands reported previously by

Nayar. It should not be supposed, however, that only highly luminescent diamonds have a transmission extending so far into the ultra-violet. Actually, the feebly luminescent diamond D221 which is a plate 0.68 millimeters thick of which two Spekker-photometer records are reproduced as Fig. 4 in Plate XV, shows a transmission extending up to 2570 Å. The smaller thickness and the much greater exposures employed (about 6 hours) have contributed to enable the very feeble transmissions of this diamond extending so far into the ultra-violet to be successfully recorded.

### 5. Diamonds showing the Mixed Fluorescence

For short exposure times, the recorded absorption spectra of the diamonds which exhibit both the blue and yellowish-green types of fluorescence showed a gradual fall of intensity beyond 2700 Å. As the photographic exposures are increased, the spectra recorded approach the transmission limit at 2250, however still exhibiting a region of absorption beyond 2500 Å. 19 diamonds belonging to this class, *viz.*, D48, D53, D56, D175, D180, D185, D186, D188, D189, D190, D191, D192, D193, D194, D195, D196, D197, D210, D235, exhibit an absorption band with a clearly resolved doublet structure at about 2360 Å accompanied by a group of absorption bands on either side of it. The strength of these absorption bands varies enormously with the specimen under examination and is found to depend on its luminescence properties. D190 which is the most intensely luminescent diamond in the whole group shows them with the greatest strength, D189 less strongly, while in D210 and D191 which are only weakly fluorescent, they are very feeble (Fig. 1 in Plate XIV). These differences are most clearly seen in the doublet 2360–2357 Å and also in the bands at longer wave-lengths, but not so clearly in those nearer the absorption edge. Table I shows their positions both at room and at liquid air temperature.

The effect of cooling the diamond is to increase the transmission in the whole region between 3000 and 2250 Å. The diamonds D190 and D195 have been investigated at liquid air temperature as well as room temperature, their spectra being recorded side by side with identical exposures, using a Hartmann diaphragm. These are reproduced in Fig. 2 (Plate XIV). It is noticed that at liquid air temperature, the bands became sharper and shift towards the ultra-violet. The extent of this shift could be accurately determined only in the case of the principal doublet, and the extent of the shift is shown in Table I. The change of frequency between 29° C. and –180° C. is found to be 1.6 per 1,000 wave numbers.

TABLE I  
*Ultra-Violet Absorption Bands*

Robertsan <i>et al.</i>		Author	
$\lambda$ in A.U.	29° C. $\lambda$ in A.U.	—180° C. $\lambda$ in A.U.	—180° C. $\nu$ in cm. <sup>-1</sup>
2363 to 2359	2364.5	2405 (weak) 2399 (strong) 2396 (weak) 2395 (weak) 2388 (weak) 2359.9 (very strong) 2356.5 (very strong) 2314 (weak)	41567 41671 41723 41740 41863 42361 42423 43202
2312 to 2300	2359.5	2309 to 2306 (strong band) 2300 to 2296 (strong band)	43295 to 43352 43464 to 43540

As will be noticed from Fig. 2, the components of the principal doublet in the highly fluorescent diamond D190 have considerable breadth, while they are much sharper in the weakly fluorescent D195. This is also observed in the case of some of the subsidiary bands, especially those at shorter wave lengths.

In conclusion, the author wishes to record her grateful thanks to Prof. Sir C. V. Raman, Kt., F.R.S., N.L., for the suggestion of the problem and for helpful advice during the course of the investigation.

#### 6. Summary

The ultra-violet absorption spectra of 47 diamonds in the region between 3300 and 2200 Å have been investigated. A striking correlation between the nature of these spectra and the intensity and spectral character of their fluorescence has been noticed. In non-fluorescing diamonds and those showing yellowish-green fluorescence, the recorded absorption spectra extend up to 2250 Å and even a little beyond, though long exposures were necessary for this purpose in the case of the latter. In the case of weakly blue-fluorescent diamonds, the spectrum shows a cut-off at 3050 Å preceded by a group of three sharp and intense bands at 3060, 3075 and 3157 Å. In strongly blue-fluorescent diamonds these bands disappear, but the region of transmission is enlarged, extending up to 2450 Å with three steep step-like falls in intensity at 2845, 2715 and 2570 Å.

In diamonds showing both the blue and greenish-yellow types of fluorescence, the spectrum recorded with long exposures shows a transmission extending up to 2250 Å. Absorption lines appear in these

diamonds at 2359·0 and 2356·5 Å with five bands on one side and three on the other, viz., 2405, 2399, 2396, 2395, 2388 and 2314, 2309 to 2306, 2300 to 2296. The intensity and breadth of these absorption lines and bands are directly correlated with the intensity of luminescence, being great in highly fluorescent diamonds and small in weakly fluorescent ones. The bands sharpen and shift towards shorter wave-lengths at liquid air temperature.

## REFERENCES

1. Anna Mani .. *Proc. Ind. Acad. Sci.*, 1944, **19**, 231.
2. Gudden and Pohl .. *Z. Physik*, 1920, **3**, 127.
3. Nayar, P. G. N. .. *Proc. Ind. Acad. Sci.*, 1941, **14**, 1.
4. \_\_\_\_\_ .. *Ibid.*, 1942, **15**, 293.
5. Pringsheim .. *Fluorescenz u. phosphorescenz*, Julius Springer, Berlin, 1928, 183, 313.
6. Raman, C. V. .. *Current Science*, 1942, **7**, 261.
7. Reinkober .. *Ann. d. Physik*, 1911, **34**, 343.
8. Robertson, Fox and Martin *Phil. Trans.*, 1934, **232**, 463.

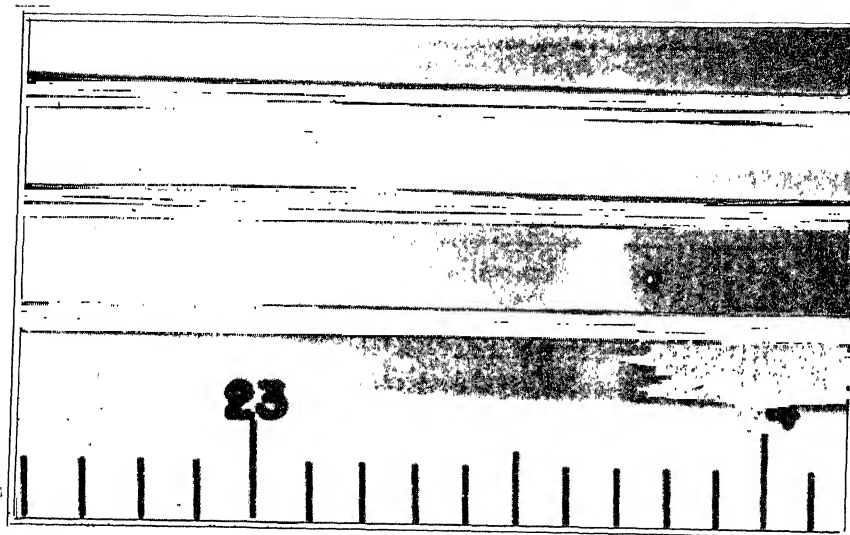


FIG. 1. Absorption in relation to Intensity of Fluorescence

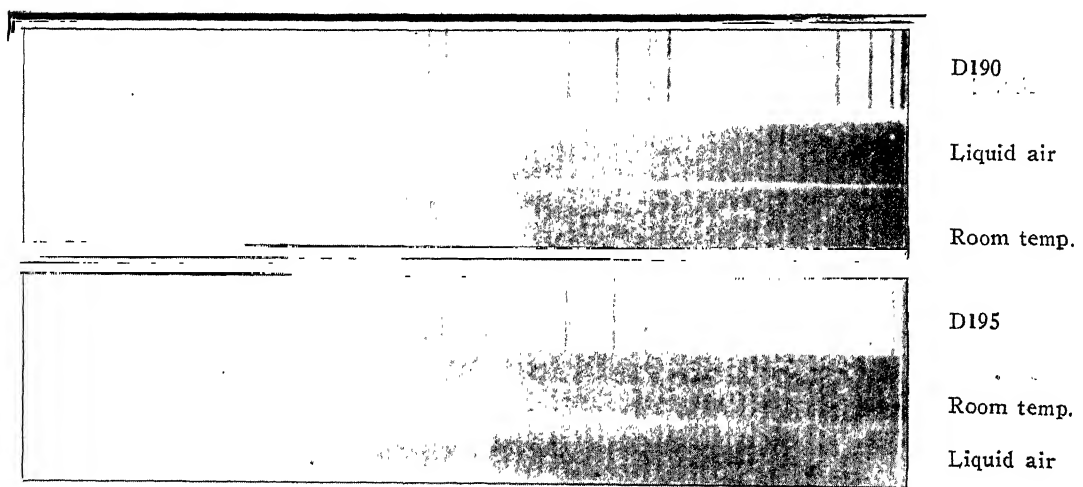
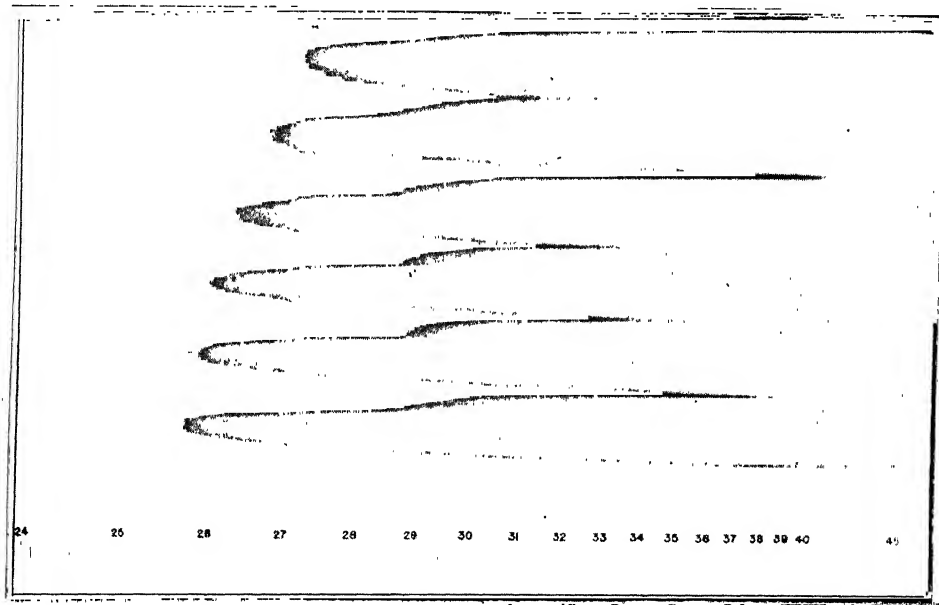


FIG. 2. Sharpening and Shift of Absorption Bands at Low Temperatures

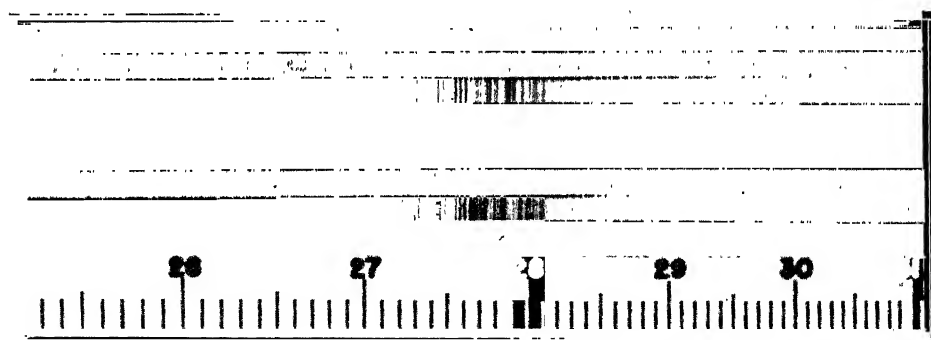
FIG. 3



D224

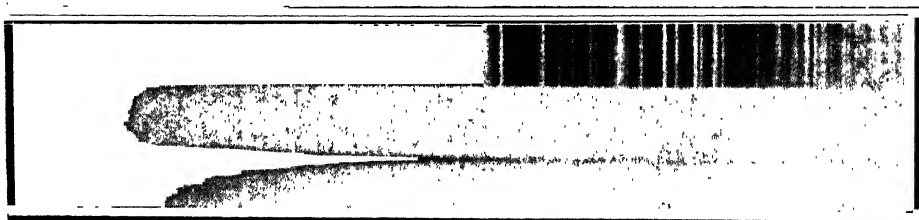
Ultra-Violet Transmission by Strongly Blue-Luminescent Diamond

FIG. 4



D221

FIG. 5



D39

Liquid air

Room temp.

Transmission Spectra in Ultra-Violet

# INTENSITY OF X-RAY REFLECTION BY DIAMOND

BY P. S. HARIHARAN

(*From the Department of Physics, Indian Institute of Science, Bangalore*)

Received April 17, 1944

(Communicated by Sir C. V. Raman, Kt., F.R.S., N.L.)

## 1. Introduction

It is a well-known fact that X-ray reflections from crystals are affected by the imperfections of the crystal lattice. The subject has been investigated by many authors, and it has been shown that the defects in the lattice structure have a tendency to increase the intensity of X-ray reflections. Ehrenberg, Ewald and Mark (1928) have studied the case of diamond, and found that some specimens give extraordinarily sharp geometric reflections, indicating a high degree of crystal perfection, while other specimens gave decidedly less satisfactory results. More recently, Lonsdale (1941) showed that diamonds which belong to the ultra-violet-transparent type give a very intense (111) reflection compared with diamonds of the other type. These observations indicated the desirability of a more complete study of the subject.

Such a study is particularly interesting in view of the new theory of the structure of diamond put forward by Sir C. V. Raman (1944). According to him, diamonds which are opaque to the ultra-violet consist exclusively of the tetrahedral varieties (Td I and Td II), and the interpenetration of these gives rise to the blue fluorescence. So also, the ultra-violet transparent and non-fluorescent type of diamonds consists solely of the octahedral structures, while the yellow fluorescent diamonds contain both the tetrahedral and octahedral structures intermixed. Obviously, such an interpenetration of different structures would give rise to discontinuities in the crystal, so that one should expect the intensity of X-ray reflection to vary with the nature and intensity of its fluorescence.

This paper sets out the results of the investigations carried out by the author on the intensity of the (111) Bragg reflection given by a large number of diamonds in the collection of Prof. Sir C. V. Raman. The problem has specially been taken up with a view to correlate the intensity of X-ray reflection with the intensity of fluorescence. The fluorescence of diamonds has been studied by Nayar (1941), and his results made it very improbable that fluorescence is due to the presence of chemical impurities, and that, on the other hand, it has a physical origin. Fresh light has been thrown on the question by the work of Dr. R. S. Krishnan (Raman, 1943) who obtained

the Laue patterns of a couple of diamonds, and also the Bragg reflections from the (111) planes by the oscillation method. He found that in the case of two diamonds exhibiting blue fluorescence with widely different intensities, the whole Laue patterns as well as the (111) Bragg reflections were much more intense in the case of the intensely fluorescing crystal. The present investigation was taken up with a view to study this effect in greater detail, and in particular to extend the investigation to a variety of diamonds.

## 2. Experimental Arrangement

A metal Shearer tube with a copper anti-cathode was the source of X-rays. The tube was excited by a transformer, the voltage applied being in the neighbourhood of 50 K.V., and the current, 9 milliamperes. The X-ray beam was collimated through a slit 0·2 mm. wide, 6 mm. high and 130 mm. deep.

The diamond was mounted on a goniometer kept at a distance of about 2 cm. from the exit end of the slit. The goniometer was provided with an oscillating device, and the patterns were photographed on a plane X-ray film kept normal to the incident X-rays at a distance of about 4 cm. from the crystal.

The diamonds used were all cleavage plates with their plane faces parallel to the octahedral plane. One could therefore get the (111) Bragg reflection either by reflection from the (111) planes parallel to the surface, or by internal reflections from any one of the other three sets of (111) planes. As the diamonds examined were of varying thickness, surface reflections only were studied in the present investigation.

The crystal was set on the goniometer with the surface (111) planes vertical and the glancing angle approximately equal to the Bragg angle for the CuK<sub>α</sub> radiation. The crystal was then oscillated over an angle of 4° through the Bragg position with uniform angular velocity. The exposures varied from 1 to 10 minutes.

The absolute intensity of the incident X-ray beam was not measured directly in every case. The voltage applied and the current passing through the X-ray tube were maintained at specific values during each exposure and also for different exposures. The distance of the photographic film was also kept constant. Identical exposures were given, and the films which were taken from the same packet were developed in the same stock developer under identical conditions of time and temperature.

The integrated intensity of the Bragg spot was determined using a Moll microphotometer. The density-log intensity curve for the grade of X-ray film used was drawn employing the step-wedge method. The microphoto-

metric curve for the Bragg spot was converted into a curve of intensity *versus* distance, and the area of this was taken to be proportional to the intensity of the Bragg reflection.

### 3. Results and Interpretation

The table below gives the relative values of the integrated intensities of reflection of the Cu K<sub>α</sub> radiation from the (111) planes for the samples studied. The type, and a qualitative estimate of the intensity of fluorescence are also included in the table.

TABLE I

Blue-fluorescing diamonds			Non-fluorescing and yellow-fluorescing diamonds		
Diamond	Integrated intensity	Colour of fluorescence	Diamond	Integrated intensity	Colour of fluorescence
36	1.0	Very faint blue	48	5.6	Blue and green
45	1.1	do.	56	6.2	Green
31	1.3	Faint blue	53	7.1	do.
52	2.1	Moderate blue	51	10.1	do.
44	2.2	do.	39	11.8	Non-fluorescent
33	2.6	Bright blue	57	14.0	do.
54	3.4	Very bright blue			
41	3.5	do.			
34	4.5	Intense blue			

The following facts emerge out of a study of the table:—

- (1) In the case of the blue-fluorescing diamonds, the intensity of X-ray reflection increases steadily with intensity of fluorescence. This confirms Dr. Krishnan's observation.
- (2) The green-fluorescing diamonds, in general, give greater intensities of X-ray reflection than the blue-fluorescing ones.
- (3) The non-fluorescing diamonds give the greatest intensity of X-ray reflection. These, together with the green-fluorescent diamonds, belong to the ultra-violet transparent type of diamonds. Thus, it appears, that in this type, there is an inverse correlation between the intensity of yellow fluorescence and that of X-ray reflection.

These results form a good confirmation of Sir C. V. Raman's theory of the structure of diamonds. In the blue-fluorescing diamonds, the tetrahedral structures Td I and Td II intermix, and the extent of the interpenetration decides the intensity of fluorescence. Obviously, a greater interpenetration produces a greater "mosaic structure" in the crystal, so that it should give more intense X-ray reflections.

The high intensity of X-ray reflection given by the non-fluorescent diamonds is also to be expected on this theory, for these diamonds consist of the Oh I and the Oh II structures. The two are physically different, so that their intermixing sets up strains, and a consequent high mosaicity. The evidence of the polarising microscope also points to such a possibility, for the non-fluorescent diamonds exhibit a fine criss-cross pattern when viewed through it.

The yellow-fluorescent diamonds fall midway between the other two types, since they contain both Td and Oh types of structures. Consequently, they should exhibit properties intermediate between the blue and non-fluorescent varieties. In fact, their ultra-violet absorption shows such an intermediate behaviour, and their X-ray behaviour also thus fits in with Sir C. V. Raman's theory.

It is with great pleasure that I take this opportunity of expressing my grateful thanks to Prof. Sir C. V. Raman for suggesting the problem, for the loan of the diamonds used for the investigation and for the kind interest he has taken in the investigation. My thanks are also due to Dr. R. S. Krishnan for helpful suggestions in the course of the experiment.

### *Summary*

The paper deals with the study of the intensity of the Bragg reflections from the (111) planes of diamond, and its variation from specimen to specimen. The diamonds were chosen so as to include a variety exhibiting different types and intensity of fluorescence. The study brings out the following facts :

- (1) In blue-fluorescing diamonds, the intensity of X-ray reflection increases with intensity of fluorescence.
- (2) Yellow-fluorescent diamonds give greater intensity than the blue ones.
- (3) Among these, the intensity decreases with increasing intensity of yellow-fluorescence, and is largest for non-fluorescent diamonds. A discussion is given regarding these phenomena, and it is shown that they fit in with Sir C. V. Raman's new theory of the structure of diamond.

### REFERENCES

1. Ehrenberg, Ewald and Mark *Zeits. f. Krist.*, 1928, **66**, 547.
2. Lonsdale, K. .. *Nature*, 1942, **148**, 112.
3. Nayar, P. G. N. .. *Proc. Ind. Acad. Sci., A*, 1941, **13**, 483.
4. Raman, Sir C. V. .. *Curr. Sci.*, 1943, **12**, 35.
5. \_\_\_\_\_ .. *Proc. Ind. Acad. Sci., A*, 1944, **19**, 189.

# BIREFRINGENCE PATTERNS IN DIAMOND

BY SIR C. V. RAMAN AND G. R. RENDALL

(*From the Department of Physics, Indian Institute of Science, Bangalore*)

Received May 11, 1944

## 1. Introduction

MINERALOGISTS have long been familiar with the fact that diamonds exhibit a very varied behaviour when examined under the polarising microscope. Sinor (1930) made extensive observations on the diamonds mined in the Panna State and found that very clear crystals in which all the faces were symmetrically developed showed very little or no double refraction. On the other hand, crystals containing flaws and inclusions, distorted crystals, and brownish tinted crystals showed bands and stripes of colour between crossed nicols. Since perfection of external form and of optical quality are both indicative of a homogeneity of structure, the specimens exhibiting them should naturally also show the optical isotropy characteristic of a cubic crystal. *Per contra*, it is not surprising that diamonds having an irregular form or visible internal flaws or inclusions should exhibit birefringence. Even a small difference in crystal orientation in the different parts of a diamond which has solidified under unsatisfactory conditions would result in enormous stresses and strains being set up which would reveal themselves in the polariscope. Such birefringence would necessarily be irregular. The variations of crystal orientation within the diamond giving rise to it should be evident on an X-ray examination, e.g., in a Laue photograph, the spots in the pattern being distorted or drawn out into streaks or even appearing multiplied in number.

Birefringence of a wholly different kind which may be described as *structural* and not as accidental, is also exhibited by many specimens of diamond. Such birefringence is distinguished by the geometric character of the figures observed in the polariscope, as also by the relationship of the figures to the crystal architecture and symmetry. Birefringence of this kind in diamond and its interpretation forms the subject of the present paper. Somewhat analogous patterns are exhibited by crystal plates of isomorphous mixtures of substances crystallising in the cubic system, e.g., the nitrates of barium, strontium and solids, and especially by crystal plates of the mixed alums when examined between crossed nicols (Liebisch, 1896). As is shown in the introductory paper of this symposium, crystallographic considerations as well as spectroscopic evidence compel us to admit

the possibility of four different structures for diamond, two with tetrahedral and two others with octahedral symmetry, which may coexist in one and the same specimen. This fact opens the way to an understanding of the geometric birefringence patterns observed in diamond, as also of other properties which vary with its structure, e.g., its luminescence, its transparency in the visible, ultra-violet and infra-red regions of the spectrum, its reflecting power for X-rays and its photoconductivity, all of which stand in close relation to each other.

## 2. Crystals in their Natural Form

Observations with diamonds in their natural state placed between crossed nicols are of interest in view of the fact that the absence of birefringence is a very delicate test of crystal perfection. Consider for instance, an octahedral diamond of 20 carats which would be about a centimeter thick and the optical path through which would be some 50,000 wave-lengths of visible light. A difference of one part in a million in the refractive indices for vibrations in different directions would produce an easily observable restoration of light between crossed nicols, while a difference of one part in a hundred thousand would give polarisation colours. It will be evident that the test is an extraordinarily sensitive one for crystal perfection, especially where large diamonds are concerned.

Owing to the high refractivity of diamond, such observations are necessarily be confined in any one setting of the crystal to small portions of it bounded by parallel faces. These regions would be further restricted if, as is often the case, the surfaces of the crystal are curved. The difficulties mentioned are least serious in the case of large regular crystals with nearly plane faces and most serious for small crystals having highly curved surfaces and with irregular diamonds. They may, however, be minimised by immersing the crystal in a cell containing a transparent liquid of sufficiently high refractive index.

The optical behaviour of numerous diamonds, including some of large size and in particular, the Maharajah's necklace of 52 octahedral crystals was studied by Sir C. V. Raman and Dr. P. G. N. Nayar during their visit to Panna State in July 1942. More recently at Bangalore, 42 Panna crystals of various sizes and qualities have been critically examined for birefringence when immersed in liquid monobromnaphthalene. The conclusions indicated by these studies are as follows:—

- (a) Diamonds which are of the blue luminescent and ultra-violet opaque type are optically isotropic, their birefringence, if any, being less than 1 part in 100,000. This is subject to the proviso that the

crystal is of perfect form, free from flaws and inclusions, and colourless.

- (b) Small diamonds of the kind stated above may be optically isotropic even if the crystal form is not absolutely regular.
- (c) Other diamonds usually exhibit marked birefringence of which there are two kinds, appearing each by itself or together, *viz.*, birefringence which is wholly irregular, and birefringence which is related to the crystal architecture and exhibits a geometric character.
- (d) While birefringence of the latter kind may appear in blue-luminescent diamonds, it is an invariable feature in the yellow-luminescing ones.

### 3. *Observations with Polished Cleavage Plates*

There are notable advantages in the study of the birefringence patterns in diamond gained by the use of polished cleavage plates, such as are readily obtainable. As these plates are parallel to the octahedral planes (more rarely to the dodecahedral planes) in the crystal, the relationship of the pattern seen in the polariscope to the crystal architecture is immediately apparent. Moreover, the pattern over the whole area of the plate is visible and can be photographed at the same time, while the disturbing effects due to oblique reflection and refraction which are so troublesome in working with crystals in their natural form do not arise at all. There is also another notable gain in the use of cleavage plates. The act of cleavage releases the material in the plate from stresses having their origin in faults or irregularities elsewhere in the original crystal from which it is split off. The accidental or irregular birefringence due to those stresses is thereby eliminated and the real optical character of the material in the plate made accessible to observation.

A beautiful illustration of the foregoing remarks is furnished by the case of the cleavage plates D36 and D45, the birefringence patterns of which are reproduced in juxtaposition in Fig. 4 of Plate XIX. These two diamonds originally formed a single plate, the whole area of which exhibited a strong restoration of light between crossed nicols. This had its origin in certain irregularities located in the lower part included in D36 and which are clearly seen in the pattern of the latter. When D45 broke off, the stresses in it were released with the result that the birefringence in it has disappeared, while that in D36 remains undiminished (possibly even a little enhanced)

The birefringence patterns as seen between crossed polaroids of several cleavage plates are reproduced as Figs. 1, 2, 3 and 4 in Plates XVI to XIX accompanying this paper. These were chosen from amongst a large number so as to be generally representative of the whole and at the same time to illustrate points of special interest. The significance of these patterns becomes evident when they are carefully compared with the luminescence patterns, the ultra-violet transparency patterns and X-ray topographs of the same diamonds appearing with the papers immediately following the present one in the symposium.

#### 4. *Description of the Patterns*

The diamonds D221 (Fig. 1) and D45 (Fig. 4) are opaque to the 2536 Å radiations of the quartz mercury arc lamp and are both feebly blue-luminescent. It will be noticed from the figures that they give no sensible restoration of light between the crossed polaroids, thereby confirming the essentially isotropic character of diamonds of this class already made evident from the study of the best Panna crystals. The statement made by Robertson, Fox and Martin (1934) that Type I or ultra-violet opaque diamonds are optically anisotropic is thus clearly not justified.

D174, D178 and D179 (Fig. 1) are three diamonds which exhibit rather striking patterns of geometric type. These diamonds are, over the greater part of their area, of the blue-fluorescent and ultra-violet opaque type. That they are optically isotropic in the same regions is evident from the fact that nearly the whole area of D178, the central region of D174 and the major part of the area of D179 remain quite dark as seen at all settings between crossed polaroids. The symmetric patterns shown rather feebly in D178 and more strongly in D174 and D179 consist of bands running parallel to the octahedral planes in the crystal. The region of the diamond which appears as a particularly bright line in the birefringence pattern of D179 appears as a dark line in its luminescence pattern and as a line of diminished opacity in its ultra-violet transparency pattern, thereby clearly showing that it is an intrusive layer of diamond having different properties from the rest of the material in the plate. The same result is indicated by the X-ray topographs of D174 and D179 obtained by Mr. G. N. Ramachandran (1944), where the intruding layers reveal themselves by the increased intensity of X-ray reflection at precisely the same regions in the plates. D181 and D38 illustrated in Fig. 1 are also blue-luminescent diamonds. The strong birefringence which they exhibit has essentially the same explanation, *viz.*, the intrusion into the blue-luminescent diamond of thick layers of non-luminescent diamond. This is clearly

shown by the X-ray topographs which exhibit a perfect correspondence with the birefringence patterns.

The appearance between crossed polaroids of D206, D207, D208, D209 and of D39 and D57 is illustrated in Figs. 2, 3 and 4. All these six diamonds are of the ultra-violet transparent and non-fluorescent class, and it will be seen that the birefringence which they exhibit is of a highly characteristic type, *viz.*, sets of parallel dark and bright streaks running through the crystal in various directions. The spacing of these streaks is extremely variable, and indeed, both coarsely and finely-spaced streaks may often be seen at the same time in any particular specimen. A special remark is necessary regarding D39, which at first sight seems different in its behaviour from the others. In this diamond, an irregular birefringence is present, due to some obvious imperfections in the crystal which are also revealed by X-ray examination. This obscures the characteristic streaky birefringence of diamonds of this class over a greater part of its area. Careful examination under higher magnification, however, reveals the presence of the latter, and especially clearly when the irregular birefringence is eliminated in a particular area by an appropriate setting of the plate between the crossed polaroids. The patterns of D57 appearing in Fig. 4 have been reproduced under rather high magnification in order to exhibit the characteristic criss-cross streakiness of the field more clearly.

The case of D39 (and also of some other diamonds in the collection) shows clearly that diamonds of the ultra-violet transparent class *may* exhibit irregular birefringence. The statement made by Robertson, Fox and Martin in their paper that diamonds of this class are optically isotropic is therefore not justified. While all diamonds may exhibit irregular birefringence if they have imperfections, perfect crystals of the blue-fluorescent ultra-violet opaque type are, as we have seen, essentially isotropic and free from birefringence, while diamonds of the non-fluorescent ultra-violet transparent type have a characteristic structural birefringence of the kind illustrated in Figs. 2, 3 and 4 in the Plates. The situation is thus actually the reverse of that stated to exist by Robertson, Fox and Martin.

The remaining patterns illustrated in the Plates accompanying the paper fall into two groups. Some of them are essentially of the same nature as the patterns of the six ultra-violet transparent diamonds considered above. The diamonds D199 and D202 are of this kind. They exhibit a yellow fluorescence. They are not fully ultra-violet transparent, but as has been shown in the paper by Sunanda Bai (1944), if adequate exposures are given, the recorded absorption spectra of these diamonds extend to the same

limit as that of the fully ultra-violet transparent diamonds. It is therefore scarcely surprising that the birefringence patterns are also of the same nature for the two sets of diamonds. The other two plates whose patterns have been reproduced, *viz.*, D48 and D235, are typical *mixed* diamonds, showing in different parts of their area all the three kinds of behaviour in respect of luminescence, *viz.*, blue-luminescence, non-luminescence and yellow-luminescence, and the corresponding three different behaviours in their ultra-violet absorption, *viz.*, opacity, perfect transparency and partial transparency. The respective regions in the areas of the plate can be distinguished in the luminescence and ultra-violet transparency patterns, while the X-ray topographs show clearly the intrusion into each other of the different types of diamond. The corresponding variations in the nature of the birefringence in different areas of the plate can also be readily made out in Figs. 2 and 4.

##### 5. The Origin of Structural Birefringence

The origin of *irregular* birefringence has already been considered and pointed out earlier in the paper, *viz.*, accidental imperfections of the crystal structure. The appearance of such imperfections is scarcely surprising when the structure of diamond and the nature of the atomic forces in it are considered. The binding forces acting directly between neighbouring atoms of carbon are the strongest of these and are sufficient to secure the coherence of all the atoms in a specimen even when the circumstances of formation of the crystal are such that complete uniformity of the inter-atomic distances and especially of the valence angles throughout its volume is not possible. Atomic equilibrium can then only be secured by the existence of a system of macroscopic stresses and strains in the solid.

The origin of the kind of birefringence with which we are principally concerned in this paper is, however, of an altogether different nature. As we have seen, it arises from the co-existence in the same specimen and inter-penetrating into each other of kinds of diamond having different physical properties. Considering, first, the diamonds of the blue-luminescent ultra-violet opaque class, these have tetrahedral symmetry, the two variants Td I and Td II having this symmetry being co-existent and interpenetrating to varying extents. The absence of birefringence in such diamonds indicates that the crystal spacings of these two structures are perfectly identical and that they can therefore fit into each other without any stresses or strains arising. Indeed, the relationship between neighbouring carbon atoms in Td I and Td II is physically the same, but geometrically different. Hence, the identity of crystal spacing and the absence of any birefringence in

diamonds of this class is fully to be expected. *Per contra*, the appearance of a characteristic streaky or lamellar birefringence in the non-luminescent ultra-violet transparent diamonds indicates that the Oh I and Oh II structures of which these diamonds consist, and the co-existence and interpenetration of which gives rise to their lamellar structure, are not physically identical. It is evident that even a small difference in the crystal spacing of the two interpenetrating forms would give rise to a streaky or lamellar birefringence, and that it would also give rise to marked inhomogeneities giving a greatly increased intensity of X-ray reflection.

The explanation of structural birefringence in diamond indicated above is confirmed in a striking manner by the existence of observable variations of crystal spacing in diamonds of the ultra-violet transparent class. This is shown in another paper by Dr. R. S. Krishnan (1944) appearing in this symposium. His experiments were made with the diamond D209 whose birefringence pattern is reproduced in Fig. 2 of the Plates accompanying this paper. The variations in crystal spacing in alternate layers of the diamond were revealed by X-ray methods and found to be accompanied by periodic variations in the intensity of the X-ray reflections from these layers, indicating the existence of a close physical relationship between the two effects. The periodic variations in crystal spacing found were of the order of 5 parts per 10,000. Small though these are, they are clearly sufficient to explain the observed birefringence which is itself small and is so readily noticed only because of the delicacy of the method of observation.

X-ray observations with specimens, such as D48 and D235, in which the tetrahedral and octahedral varieties of diamond appear juxtaposed in adjacent areas should similarly be capable of ascertaining the differences in crystal spacing of the Td structures from those of the Oh I and Oh II types. A knowledge of these differences would assist in a fuller elucidation of the birefringence patterns observed in such cases. In some of these patterns, e.g., those of D174 and D178 appearing in Fig. 1, only the intruding layers of octahedral diamond show an appreciable restoration of light, while in others e.g., the patterns of D181 and D38, the entire diamond shows a restoration though of varying intensity, though the intrusions extend over only part of its area. It would seem that in cases of the latter kind, the stresses set up by the presence of the intruding layers extend over the entire diamond and are of sufficient magnitude to cause an appreciable birefringence to be exhibited by it.

#### 6. *Nature and Magnitude of the Stresses*

Since the birefringence patterns are photoelastic effects due to the variations of the crystal spacing in diamond, it follows that the axes of

birefringence should be related to the orientation of the layers in the crystal in a determinate way. In particular, when there is only one set of laminations in the crystal, the axes of birefringence should be parallel and perpendicular respectively to the laminations. This is readily tested by placing the diamond between crossed polaroids and observing the changes in the pattern as the diamond is rotated in its own plane. As is to be expected, it is found that the bands in the pattern appear most intense when they run at an angle of  $45^\circ$  with the axes of the polaroids and vanish when they are set parallel or perpendicular to them.

In more complicated cases when there are two or more sets of parallel laminations running in different directions and intersecting each other, both the nature of the pattern and the axes of birefringence would be determined by their joint effect, and not by any one of them separately. A striking illustration of this is furnished by D209, the birefringence patterns of which taken at two different settings of the diamonds are reproduced in Fig. 2. It will be noticed that in one setting, the pattern is very bright and shows a rectangular patchwork of dark and bright lines, while in the other setting, it is of much smaller intensity and of irregular character. It is found that the pattern is most intense when the bands in the birefringence pattern are inclined at  $45^\circ$  to the axes of the crossed polaroids, and least intense when they are parallel and perpendicular respectively to these axes. It may be remarked that the X-ray topograph of D209 shows the presence of two sets of strongly reflecting layers of diamond which are inclined to each other at an angle of  $60^\circ$ , while the birefringence pattern, on the other hand, shows a rectangular pattern of bright and dark bands. This difference is, however, entirely to be expected in view of the remarks made above. Indeed, the resemblances as well as the differences noticed between the birefringence pattern of this diamond and its X-ray topograph form a striking confirmation of the explanations put forward of the origin of the former pattern.

Quantitative measures of the birefringence are obviously desirable to enable a more complete account of the subject to be given. A knowledge of the elastic-optic constants of diamond, the orientation and thickness of the intruding layers, and of their crystal spacings, should enable the expected birefringence to be computed and compared with the observed values. Such an investigation should be well worth undertaking. It should be remarked also that the birefringence patterns reveal only the *differences* in the refractive index for vibrations along the principal axes of stress. Observations of interference patterns may conceivably reveal the *absolute* variations of the refractive index, though these would naturally be very small. A knowledge of them would be necessary for a complete evaluation of the stress system of pressures and shears present in the diamond.

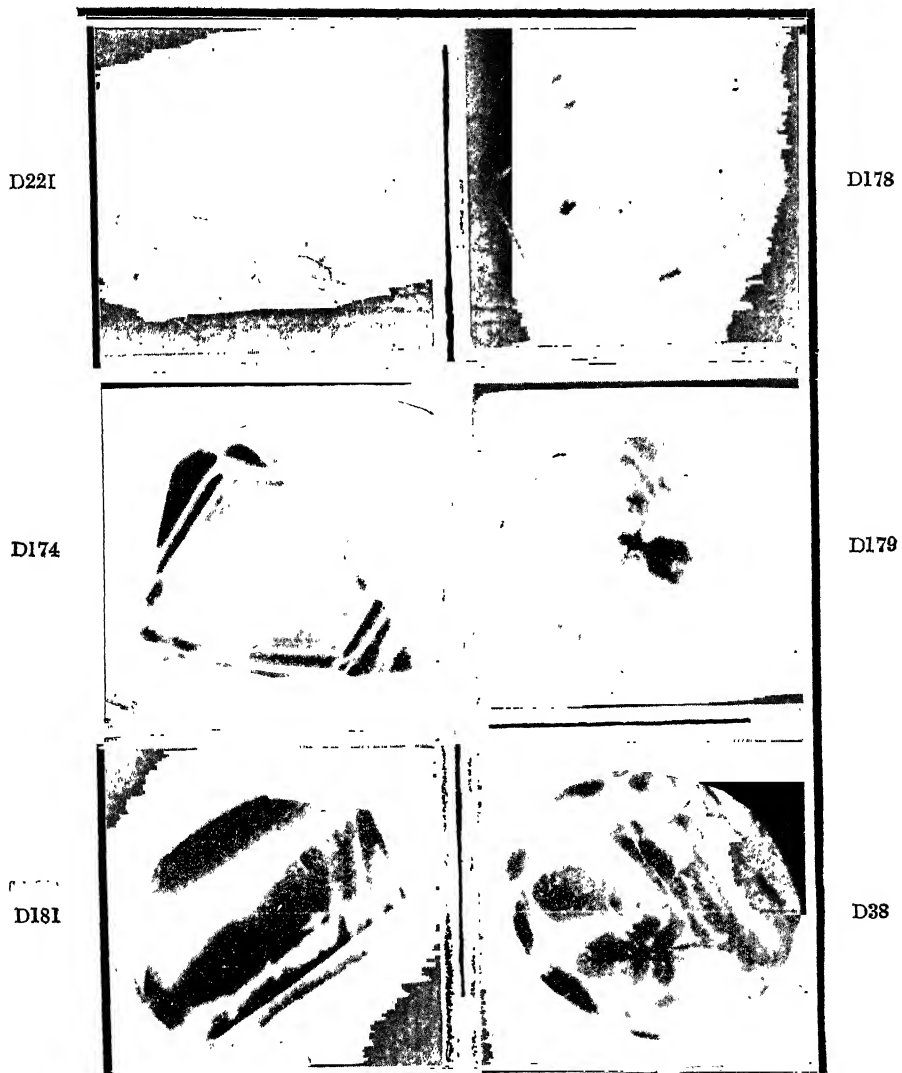


FIG. 1. Birefringence Patterns in Blue-Luminescent Diamonds

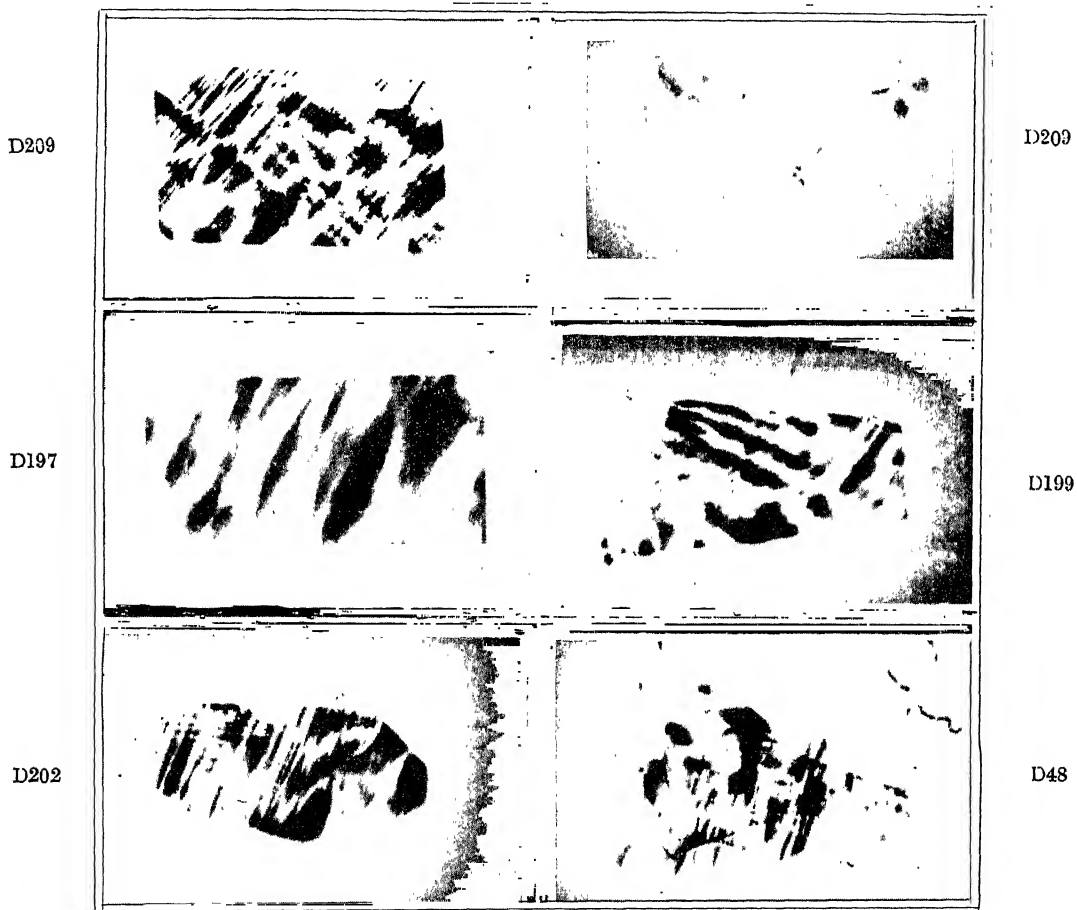
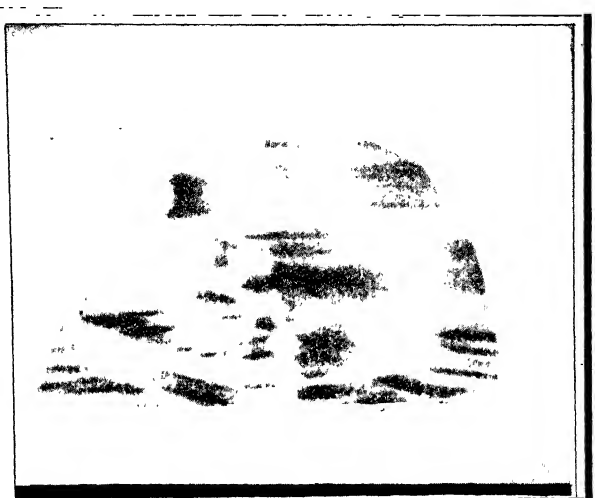


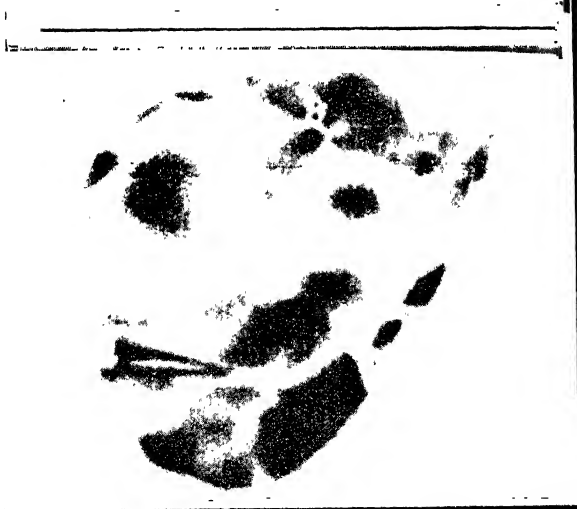
FIG. 2. Streaky Birefringence in Diamonds



D206



D208



D39

FIG. 3. Birefringence in Non-Luminescent Diamonds

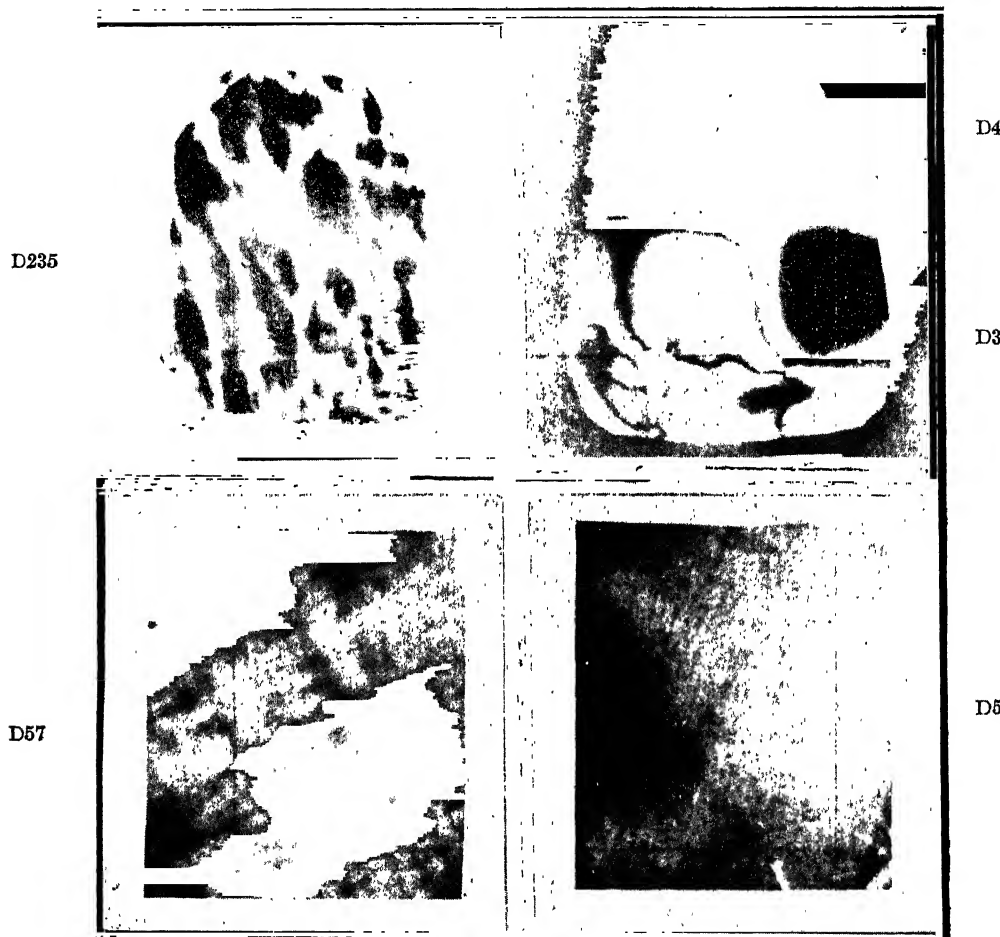


FIG. 4. Birefringence in Diamonds

### 7. Summary

Birefringence in diamond may be either *irregular* or of *geometric* character. In the former case, it is due to structural imperfections, but its magnitude is negligible in well-formed perfect crystals. *Geometric* or *structural* birefringence manifests itself in regular patterns related to the symmetry of the crystal. It arises from the co-existence in the crystal of structures with different properties and crystal spacings. Extensive studies prove that diamond of the blue-luminescent ultra-violet opaque type is isotropic, while diamond of the non-luminescent ultra-violet transparent type invariably shows a structural birefringence. These facts find a natural explanation when the relationships existing between the four possible structure-types in diamond namely Td I, Td II, Oh I and Oh II are considered. A difference in the crystal spacings of the Oh I and Oh II structures present in the ultra-violet transparent diamonds is proved by X-ray studies and is the origin of the streaky or laminar birefringence exhibited by such diamonds. Birefringence patterns may also arise from the intrusion of the Oh structure into Td diamonds. This is fully confirmed by the variations of luminescence, ultra-violet transparency, and of X-ray reflection intensities over the area of the specimen exhibited by such diamonds.

### REFERENCES

Krishnan, R. S.	.. <i>Proc. Ind. Acad. Sci.</i> , 1944, <b>19</b> .
Liebisch, T.	.. <i>Physikalische Krystallographie</i> , Veit, Leipzig, 1896, 325.
Ramachandran, G. N.	.. <i>Proc. Ind. Acad. Sci.</i> , A, 1944, <b>19</b> .
Robertson, Fox and Martin	.. <i>Phil. Trans. Roy. Soc.</i> , A, 1934, <b>232</b> , 463.
Sinor	.. <i>The Diamond Mines of Panna</i> , 1930.
Sunanda Bai, K.	.. <i>Proc. Ind. Acad. Sci.</i> , A, 1944, <b>19</b> , 253.

# LUMINESCENCE PATTERNS IN DIAMOND

BY K. SUNANDA BAI

(From the Department of Physics, Indian Institute of Science, Bangalore)

Received May 17, 1944

(Communicated by Sir C. V. Raman, Kt., F.R.S., N.L.)

## 1. Introduction

THE luminescence of diamond can be readily observed with sunlight and a simple fluoroscope, *viz.*, a piece of Wood's glass and a condensing lens at one end of a tube, a holder for the diamond inside it and a transversely-mounted eyepiece. Examining the specimens in his personal collection with this simple instrument, Sir C. V. Raman made the interesting observation that polished cleavage plates of diamond not infrequently exhibit patterns of luminescence, *viz.*, striking variations of its intensity and colour over the area of the plates. He noticed also that the luminescence pattern often bears a surprising resemblance to the birefringence pattern shown by the same specimen when viewed between a pair of crossed polaroids. Photographs exhibiting such resemblance have been secured by the author for some selected specimens and are reproduced with the paper appearing in the symposium in which Sir C. V. Raman (1944) has discussed the nature and origin of the luminescence of diamond.

To elucidate the nature of the structures which give rise to luminescence, the author undertook a systematic study of the ultra-violet absorption spectra of the diamonds in the collection. The results of the investigation are described in another paper appearing in the symposium. They show clearly that there is an intimate relationship between the ultra-violet absorption spectrum of diamond on the one hand and the colour and intensity of its luminescence on the other. Hence, it follows that a diamond which exhibits a luminescence pattern should also exhibit notable variations in its ultra-violet absorption spectrum over its area. This has also been shown to be actually the case, using the technique which has been described in the paper referred to. Typical absorption spectra illustrating such variations obtained with the diamonds D38 and D235 are reproduced as Fig. 8 in the Plates accompanying this paper.

In view of the great experimental and theoretical interest of the luminescence patterns shown by diamond, it appeared desirable to classify and describe the patterns of all the cleavage plates in the collection and also

to record them, thereby facilitating comparison with other effects exhibited by the same diamonds. Photographs in black and white convey but a faint reflection of the beauty and interest of these patterns with their varied colours. Nevertheless, they are not without value, since they can be studied at leisure, and in the case of the faintly luminescent specimens exhibit features which are not easy to observe visually.

## 2. *Photographing the Luminescence Patterns*

It has been shown by Miss Anna Mani (1944) in another paper appearing in the symposium, that the variations in the intensity and of the colour of the luminescence of diamond arise from variations in the absolute and relative intensities of two distinct sets of radiations which appear respectively in the regions of shorter and longer wave-lengths of the visible spectrum. For brevity, these will be referred to respectively as the "blue" and "yellow" luminescence spectra. The luminescence patterns may therefore also be ascribed to the local variations of the absolute and relative intensities of these spectra in the emitted light. The rendering of the patterns given by a photographic plate naturally depends on its sensitivity to the two spectral regions under consideration. The most satisfactory arrangement would evidently be to use appropriate filters and obtain two photographs in which the "blue" and the "yellow" luminescence are separately recorded. On setting these side by side, we should obtain an accurate idea of the distribution in the diamond of the structures responsible for their emission. In the present investigation, for the sake of simplicity, no such special arrangements were made, and only one photograph was obtained in each case. It should be mentioned that the patterns of "yellow" luminescence exhibit some fine detail which is not recorded except when high magnifications and plates specially sensitive to the yellow were employed, and long exposures given.

The source of light employed in securing the photographs reproduced was a carbon arc run at 220 volts with 6 to 8 amperes current. A box lined inside with black velvet served as an enclosure for the diamond during the exposure. The light of the arc, after passage through a water-cell and an aperture covered by a plate of Wood's glass, was focussed by a quartz lens on the plate of diamond. The latter was stuck on a polished sheet of copper, and its inclination to the incident beam was so adjusted as to secure a uniform irradiation. Occasionally, some trouble was encountered from the reflections at the bevelled edges of the plate which resulted in bright streaks appearing which ran across the area of the plate. By suitably varying the setting of the diamond, however, these streaks could usually be eliminated.

A rectangular glass cell containing a concentrated solution of sodium nitrite placed in front of the camera lens served as a complementary filter. A camera with a 5-inches focus lens was employed and set so that the image of the diamond appeared suitably enlarged on the plate. The Ilford selochrome plates used for the photographs gave a satisfactory rendering of the "blue" luminescence, but only weakly recorded the "yellow" luminescence even in the areas where actually it was strong. This fact has to be remembered in examining the figures reproduced in the paper. The advantage of using plates sensitive to the yellow region in some cases is illustrated by the striking photograph obtained with D198 (Fig. 5) for which a HP2 plate was employed. It should be mentioned that both the degree of enlargement employed and the photographic exposures were such as to secure the most satisfactory picture in each case. Neither the relative sizes of the diamonds nor their relative intensities of luminescence can therefore be judged from the reproductions.

### *3. Description of the Patterns*

Photographs of 42 diamonds (mostly flat cleavage plates) are reproduced as Fig. 1 to 7 in Plates XX to XXIII. They have been grouped in these figures according to the nature of the effects exhibited by them. Fig. 1 shows the diamonds having a more or less perfectly uniform blue luminescence. (The streaks in D178 are spurious.) Fig. 2 and Fig. 3 also represent diamonds of this kind, the latter of those which exhibit striking patterns. Figs. 4, 5, 6 and 7 represent (with a few exceptions) diamonds showing a mixed blue and yellow luminescence. The exceptions are D200 and D202 in Fig. 7 which exhibit a yellow luminescence, and D182 and D236 in Fig. 7 which are blue-luminescent.

Striking examples of geometric patterns of luminescence are D38, D179 and D180 in Fig. 3, D191 and D194 in Fig. 4, D195, D198 and D235 in Fig. 5, D48 and D56 in Fig. 6, and D186 in Fig. 7. A common feature in many of the patterns is that the lines tend to run parallel to the edges of the plate; these, it may be recalled, represent its intersections with the faces of the crystal from which it was cleaved off. This feature is particularly well shown by D180 in Fig. 3, D191 in Fig. 4, D195 and D198 in Fig. 5, and indeed also by several others. It is a general feature in diamonds showing a yellow luminescence that numerous bright streaks appear running parallel to each other, sometimes in several directions simultaneously. Indications of this feature appear in some of the photographs, viz., D194 in Fig. 4, D196 and D198 in Fig. 5, D48 in Fig. 6, D200 and D202 in Fig. 7. Only traces of the numerous parallel bands seen visually in D193 can be made out in its reproduced photograph (Fig. 4). D188

shows visually numerous yellow bands traversing a blue field in several directions simultaneously, but only with difficulty can this feature be noticed in the photograph (Fig. 6).

The lack of sensitiveness of the selochrome plates has resulted in the areas showing a greenish-yellow luminescence appearing as darker in the photographs than the blue-luminescent ones. The dark areas in the photographs of D191, D192, D193 and D194 in Fig. 4 and of D210 in Fig. 5 are actually areas of greenish-yellow luminescence, while the bright areas in these figures represent a blue luminescence. In D195 (Fig. 5), a band of bright yellow luminescence running parallel to one of the sides of the triangle of blue luminescence is recorded as a dark strip. Many other examples of this kind can be quoted.

#### 4. Origin of the Patterns

The first and most important point to be borne in mind in considering the origin of the luminescence in diamond is that the behaviour of different specimens is very varied. Some are non-luminescent, some are blue-luminescent, some are yellow-luminescent, while others again show both types of luminescence. Further, the intensity of each kind of luminescence may also show enormous variations. The natural interpretation of these facts and of the existence of the patterns is that any given specimen may be a mixture of different species of diamond intertwined with or inter-penetrating each other. As the different species are isomorphous, the geometric character of the patterns immediately becomes intelligible.

Accompanying the differences in the luminescence of diamond, we have also differences in other properties of which the ultra-violet absorption spectrum of diamond is one which is readily accessible to observation. The variation in ultra-violet absorption and its correlations with luminescence have been described in detail in another paper, and it is not necessary to set them out again here. It is sufficient to remark that using the knowledge gained by that investigation, it is possible from a study of the ultra-violet absorption over the different areas of a given specimen to infer the nature of the variations in the diamond which give rise to the luminescence pattern. *Vice versa*, the existence of such correlations between the local variations of luminescence and ultra-violet absorption spectra is evidence for the existence of a relationship between the crystal structure of diamond and its luminescence properties.

A striking example of the presence of material having very different properties in the same specimen of diamond is the dodecahedral cleavage plate D235 whose luminescence pattern appears in Fig. 5. As visually

observed, the central area of this plate shows a fairly bright blue luminescence, while dark patches appear towards both of the extremities as seen in the figure. Visually, some faint bands of yellow luminescence can be seen traversing the plate obliquely from end to end. The ultra-violet absorption spectrum shows corresponding variations over the area of the plate. The non-luminescent areas exhibit a free transmission up to 2250 Å, while the blue-luminescent area shows a transmission extending up to about 2700 Å with moderate exposures, but with prolonged exposures right up to 2250 Å crossed by an absorption doublet at 2360 Å. The latter feature is characteristic of the diamonds which show both the blue and yellow types of luminescence.

Another example illustrating the correlation between luminescence and ultra-violet absorption is D210 (Fig. 5). The central dark region showing a yellow fluorescence gives an ultra-violet transmission spectrum which extends with sufficiently long exposures to 2250 Å traversed, however, by a set of absorption bands in the region between 2500 Å and 2250 Å. On the other hand, the blue-fluorescent marginal region of the diamond shows a transmission only up to 2500 Å even with long exposures. Another interesting case is D180. The brightly blue-luminescent part in the centre of its area shows an ultra-violet transmission up to 2600 Å only, while the marginal non-luminescent areas show a transmission extending to 2250° (with absorption bands between) when sufficiently long exposures are given. The blue-luminescent diamond D38 which shows a very striking pattern (Fig. 3) has a free transmission up to 2900 Å followed by a weak transmission up to 2600 Å in the luminescent areas. On the other hand, the non-luminescent strips give bands of free transmission up to about 2400 Å, showing clearly that they represent the intrusion of a more transparent variety of diamond into a less transparent one.

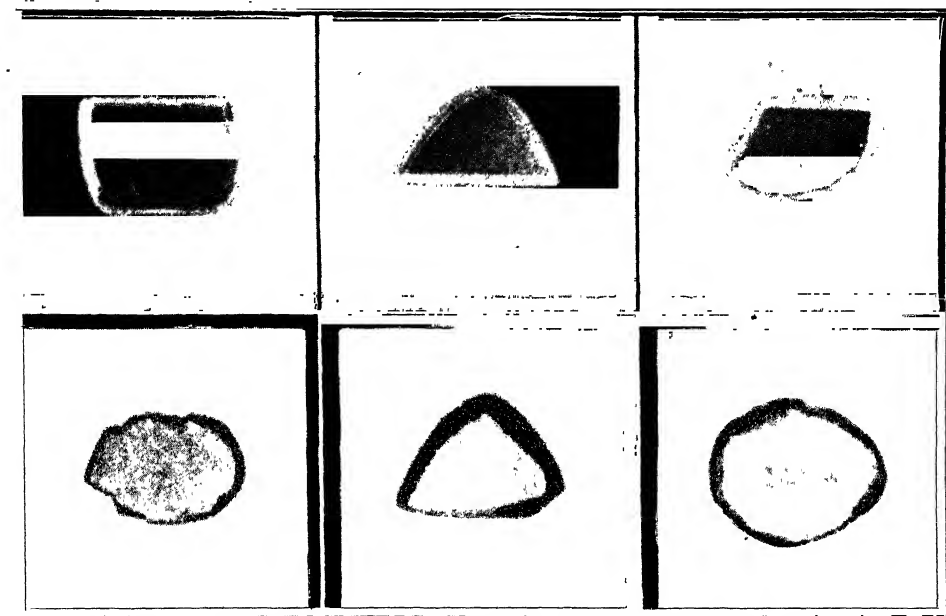
Considering the whole complex of facts, *viz.*, the existence of two distinct varieties of luminescence, the enormous variations possible in their intensities, and the appearance of patterns of blue and yellow luminescence with distinctive features in each case, it appears scarcely possible to reconcile it with the idea that there are only two alternatives possible for the crystal structure of diamond. The wider range of possibilities indicated in the papers by Sir C. V. Raman in the symposium appears easier to reconcile with the observed facts.

In conclusion, the author desires to record her grateful thanks to Prof. Sir C. V. Raman, Kt., F.R.S., N.L., for his valuable help and inspiring guidance throughout the course of this investigation.

D36

D45

D172



D173

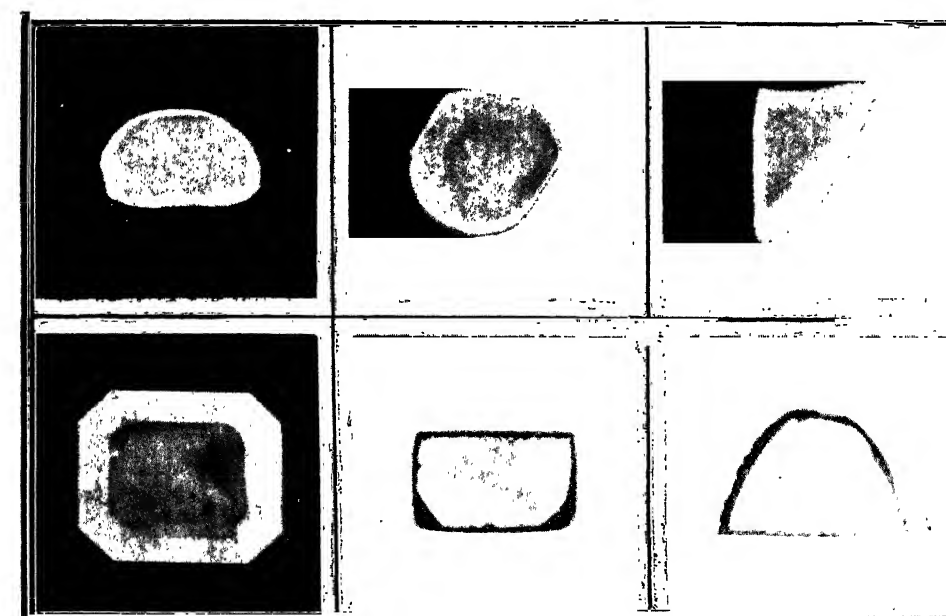
D174

D178

D181

D211

D184



D224

D221

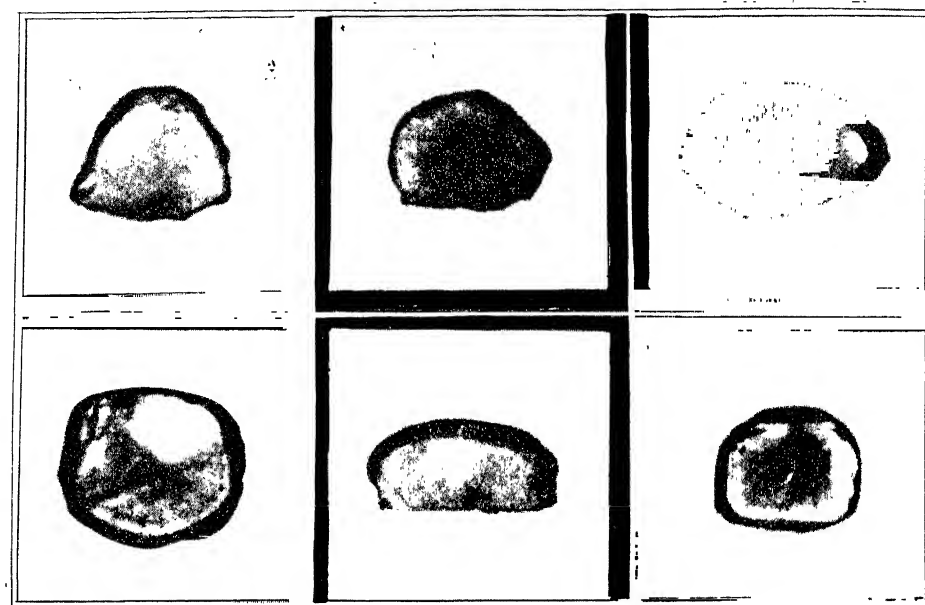
D222

FIG. 2

D182

D185

D186

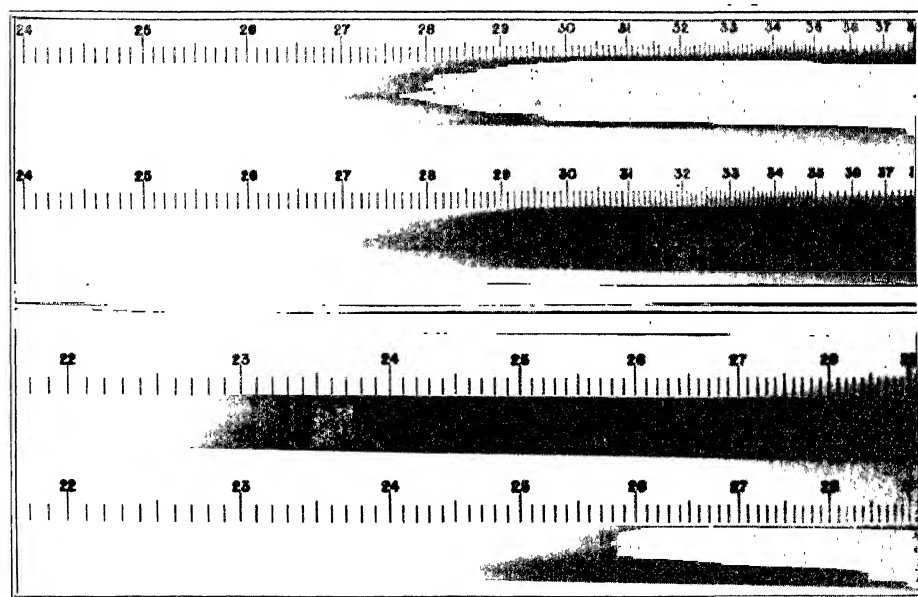


D200

D202  
FIG. 7

D236

D38



D235  
FIG. 8

### 5. Summary

*Geometric* patterns showing variations of intensity or colour or of both are often observed in the luminescence of cleavage plates of diamond excited by long-wave ultra-violet irradiation. The lines in the pattern not infrequently also run parallel to the natural faces of the crystal from which the plate was cleaved. Such patterns may be altogether lacking in some cases where the diamond shows a uniform blue luminescence. On the other hand, such patterns are always present when the diamond shows both blue and yellow luminescence. The appearance of numerous bright streaks running parallel to each other, sometimes in several directions simultaneously, is characteristic of yellow luminescence. A study of the local variations of the ultra-violet absorption spectrum of the diamond is usually successful in revealing that the luminescence patterns, when observed, arise from intrusion into the crystal of diamond having properties different from the rest of the material.

42 luminescence photographs are reproduced with the paper.

### REFERENCES

Anna Mani	.. <i>Proc. Ind. Acad. Sci.</i> , 1944, <b>19</b> , 231.
Raman, C. V.	.. <i>Ibid.</i> , 1944, <b>19</b> , 199.
Sunanda Bai, K.	.. <i>Ibid.</i> , 1944, <b>19</b> , 253.

# X-RAY TOPOGRAPHS OF DIAMOND

BY G. N. RAMACHANDRAN

(From the Department of Physics, Indian Institute of Science, Bangalore)

Received May 3, 1944

(Communicated by Sir C. V. Raman, Kt., F.R.S., N.L.)

## 1. Introduction

As is well known, the spots in the Laue pattern of a crystal arise from the reflection of X-rays by particular sets of lattice planes. The size of each spot in the pattern increases with the extension of the area of the crystal traversed by the X-ray beam, and reaches its maximum when the crystal is completely bathed in the latter. In the particular case when the crystal is in the form of a thin plate, its form and size would determine those of the Laue spot, and each spot in the X-ray pattern becomes, in effect, a geometric representation of the crystal plate. The representation would be perfect if there is no blurring and no distortion. The former condition may be secured by arranging that the beam emerging from the target of the X-ray tube is limited by a fine pinhole, and that the crystal plate is placed at a sufficient distance from the latter to ensure that it is completely bathed by the beam diverging from the pinhole. The fact that the spots in Laue patterns as usually recorded with an X-ray beam of circular cross-section are elliptical shows that, in general, distortion will occur in the present arrangement. It is possible, however, to secure that it is practically eliminated in respect of a chosen Laue spot by suitably inclining the photographic film, or the crystal plate, or both, to the beam of X-rays incident on the latter. The particular spot whose definition and freedom from distortion are thus secured, thereby making it an exact representation of the crystal plate, would evidently be formed by the reflection of white X-radiation by the chosen set of lattice planes over a small range of angles of incidence. Each point in the area of the particular Laue reflection would correspond to a particular point in the crystal plate, and if the strength of the incident beam and the reflecting power of the lattice planes are uniform over its area, the reflection would also appear of uniform intensity. The proviso must however be made that the range of angles of incidence employed does *not* include the Bragg angle for any of the monochromatic components present in the incident X-ray beam.

The considerations set out above become of practical interest, if, for any reason, the reflecting power for X-rays is *not constant* over the area of the

crystal plate under study. The geometric representation of the plate obtained by the method explained would then exhibit corresponding variations in intensity over its area, thereby revealing the local variations in the structure of the crystal which are responsible for the variations of reflecting power. The Laue spot becomes, in effect, a topographic map (or for brevity, a *topograph*) of the crystal plate exhibiting these variations of structure.

Topographs of 18 polished cleavage plates of diamond selected from Sir C. V. Raman's personal collection with their catalogue numbers entered against them, obtained in the manner briefly explained above, are reproduced in Figs. 4 to 6 in Plates XXIV and XXV, accompanying the present paper. Their significance will be discussed later in the course of the paper. To appreciate the X-ray topographs fully, they must be compared with the luminescence patterns (Sunanda Bai, 1944), the ultra-violet transparency patterns (Rendall, 1944), and the birefringence patterns (Raman and Rendall, 1944) of the same diamonds reproduced in the plates accompanying other papers published in this symposium.

## *2. Practical Details and Theory for Obtaining the Topographs*

The experimental arrangement used is as follows, and is represented diagrammatically in Fig. 1. A fine pinhole P of diameter 0·3 mm. made in a sheet of lead, and placed in front of the window of a tungsten target X-ray tube, forms a point-source of diverging white X-radiation. The diverging cone of X-rays is limited by an aperture  $A_1$ , placed at a suitable distance (20 cm.) from the pinhole. The crystal plate CD is mounted on a two-circle X-ray goniometer, kept at a distance of 30 cm. from the pinhole, which is adjusted so that one of its axes of rotation is vertical, and the other coincides with the axis of the cone of X-rays. Just in front of the crystal, a second aperture  $A_2$  is placed. This aperture is of such a size that the direct X-ray beam just passes through it, without striking its boundary. In this way, it effectively prevents the X-rays scattered by  $A_1$  from striking the photographic film F. The apertures are of such a size that the crystal is completely bathed in the X-rays. The film holder of the X-ray camera is capable of rotation about a vertical axis. It is also capable of longitudinal motion along the line joining the pinhole and the crystal. The film holder was always set such that the film was tangential to the circular head of the goniometer and the normal distance of the film from the crystal was a constant (2·5 cm. in the present case).

The diamond plates that were employed were usually octahedral cleavage plates with their surface parallel to one set of (111) planes, or slightly

inclined to it at angles of  $1^\circ$  or  $2^\circ$  owing to errors in polishing. A few specimens were however found which were dodecahedral cleavage plates. The setting required for getting the topograph was different in the two cases. Although any one of the Laue spots can be used for the purpose, it is an

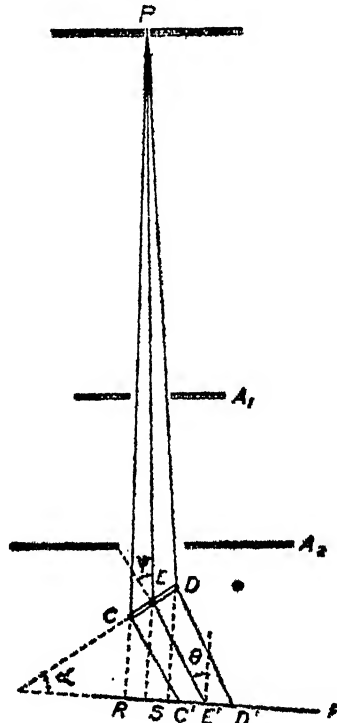


Fig. 1. Arrangement for obtaining topographs

advantage to use a strongly reflecting plane in order to minimise the exposure. For the octahedral cleavage plates, any one of the three sets of internal octahedral planes, *viz.*,  $(1\bar{1}\bar{1})$ ,  $(1\bar{1}1)$  or  $(\bar{1}11)$  can be used. For dodecahedral cleavage plates with their surface parallel to the  $(110)$  planes, any one of the reflections  $(\bar{3}13)$ ,  $(\bar{3}\bar{1}3)$ ,  $(1\bar{3}3)$ ,  $(1\bar{3}\bar{3})$  can be employed.

The crystal plate (whether of octahedral or dodecahedral cleavage) is first mounted so that its surface is normal to the incident X-ray beam. A photograph is taken with this arrangement, and with its help, the requisite reflection, the  $(111)$  or the  $(331)$  as the case may be, is brought so as to be in the same horizontal line as the central spot, by rotating the crystal about the axis of the cone of X-rays. Next, the crystal is rotated about the vertical axis through an angle of  $33\frac{1}{2}^\circ$  for the octahedral plate and  $38^\circ$  for the dodecahedral plate, so that the same reflection occurs on the opposite side at an

angle of  $14^\circ$  and  $19^\circ$  respectively. The film holder is then rotated in a direction opposite to that of the crystal through an angle of  $14^\circ$  and  $3^\circ$  respectively. An exposure is then taken with this arrangement when an undistorted X-ray topograph is obtained. It may be pointed out that in these settings, the angles of incidence were beyond the Bragg angle for any of the characteristic lines of tungsten, and that the topograph was produced by white radiation alone.

We shall now develop the theory of the method for eliminating distortion, and show how the elimination is secured in the settings described above. Let  $CD$  be the crystal, and  $C'D'$  the image of it produced on the film  $F$ ,  $E$  and  $E'$  being the middle points of these (Fig. 1). Let  $\alpha$  be the angle between the plane of the crystal and of the film,  $\theta$  the angle made by the X-ray reflected by  $E$  with the normal to the film,  $\psi$  the angle between the axis of the X-ray beam and the normal to the crystal, and  $\phi$  the divergence of the incident X-ray beam, *i.e.*, the angle subtended by  $CD$  at the source  $P$ . The rest of the symbols are clear from the figure.

$$\begin{aligned} \text{Now, } C'D' &= RD' - RC' = SD' - RC' + RS \\ &= SD \tan(\theta - \phi) - RC \tan(\theta + \phi) + CD \cos \alpha. \end{aligned}$$

This must be equal to  $CD$  if there is to be no distortion.

$$\text{Now, } SD = r + \frac{CD}{2} \sin \alpha, \quad RC = r - \frac{CD}{2} \sin \alpha.$$

Also, since  $\phi$  is a small quantity, putting  $\tan \phi = \phi$ , and writing  $t$  for  $\tan \theta$ ,  $\tan(\theta + \phi) = t + \phi + \phi t^2$ ,  $\tan(\theta - \phi) = t - \phi - \phi t^2$ .

Substituting these, the condition for no distortion comes out as

$$2r\phi(1 + t^2) - (CD \sin \alpha)t + CD(1 - \cos \alpha) = 0.$$

Divide this equation by  $R$ , the distance  $PE$  of the crystal from the pinhole. Then, since  $CD \cos \psi / R = \phi$ , one obtains

$$\frac{2r}{R} \phi(1 + t^2) - \frac{\phi}{\cos \psi} t \sin \alpha + \frac{\phi(1 - \cos \alpha)}{\cos \psi} = 0.$$

Putting  $R/r = K'$ , this can be written in the form

$$t^2 - \frac{K'}{2 \cos \psi} t \sin \alpha + \left[ 1 + \frac{K'}{2 \cos \psi} (1 - \cos \alpha) \right] = 0.$$

or, if  $K'/\cos \psi = K$ ,  $t^2 - \frac{K}{2} t \sin \alpha + \left[ 1 + \frac{K}{2} (1 - \cos \alpha) \right] = 0$ .

If this equation is satisfied, then there will be no distortion laterally.

Before proceeding further, it is interesting to notice that when  $\theta$  and  $\alpha$  satisfy the above equation, the image is a normal representation of the crystal. In other words, if  $F$  is any point on the crystal, and  $F'$  is the corresponding one in the reflected image, then  $CF = C'F'$ , and this is true for all points  $F$  in the cross-section  $CD$ . This is easily seen to be so, for the final equation is independent of  $\phi$ , which alone depends on the dimensions of the crystal. Of course, the above theory rests on the assumption that  $\phi$  is a small quantity, but this is true in the present experiment where the dimensions of the crystal never exceeded 10 mm., for which  $\phi$  is less than  $1/30$ . For these, the image will be a true reproduction of the object.

In order to make the theory capable of practical application, curves have been drawn for different values of  $K$ , connecting the values of  $\theta$  and  $\alpha$  which satisfy the equation for no distortion. These are reproduced in Fig. 2. It will be noticed that all the curves are closed. Only for conditions corresponding to points on the curves will there be no lateral distortion;

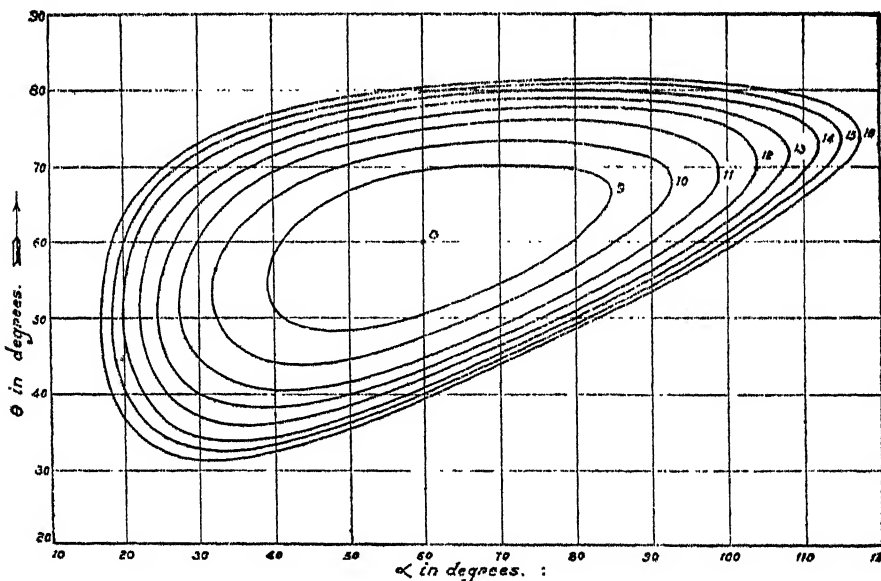


FIG. 2. Curves showing relation between  $\theta$  and  $\alpha$

if the point is outside, the lateral dimensions of the image will be smaller than that of the object, while if it is inside, the reverse will be the case. It is also found that there is a limiting value of  $K$ , ( $K = 8$ ), below which there can be no undistorted position for any values of  $\theta$  or  $\alpha$ . For this particular value of  $K$ , the curve reduces to a point ( $\theta = 60^\circ$   $\alpha = 60^\circ$ ), which is the only position of no distortion.

Taking now the particular case of an octahedral cleavage plate of diamond, it is clear that when it is mounted with the surface normal to the X-rays, the internal (111) planes reflect at an angle of  $19\frac{1}{2}^\circ$ . As already said, the crystal is rotated through  $33\frac{1}{2}^\circ$ , so that the same planes reflect at an angle of  $14^\circ$  in the opposite direction (which may be denoted by  $-14^\circ$ ). In this case,  $\psi = 33\frac{1}{2}^\circ$ , and with the present arrangement for which  $R'r = 12$ , the value of  $K = 14.4$ . If the film is rotated through  $5^\circ$  in a direction opposite to that of the crystal, then it is easily seen that  $\alpha$  and  $\theta$  have the values  $38\frac{1}{2}^\circ$  and  $33^\circ$ , which thus satisfy the condition for no lateral distortion.

It must be mentioned that even with this arrangement, the image will not be a perfect reproduction of the crystal, for there is a small divergence in the vertical direction. The arrangement only secures that the horizontal dimensions are unaltered, but does not compensate for the vertical divergence. However, even this small distortion can be eliminated by further increasing the tilt of the film, so that the working point moves inside the curve of no lateral distortion, and the horizontal dimensions of the image become actually greater than that of the object. The additional tilt can be adjusted so that the lateral dimensions are also increased in the same ratio as the vertical ones. This quantity was not calculated, but was determined by trial to be nearly  $9^\circ$ . Thus the total tilt necessary is  $14^\circ$ , which is the one used. With this arrangement, the distortion, if any, would be less than 2%. It might be pointed out that even if the vertical divergence were not corrected for, the consequent increase in the vertical dimensions would only be about 8%.

In the case of the dodecahedral plates, the method employed is to rotate the crystal through  $38^\circ$ , so that  $\psi = 38^\circ$  and  $K = 15.2$  for this setting. From the curves in Fig. 2 it is seen that there is no distortion if  $\theta = 32^\circ$  and  $\alpha = 32^\circ$ . Here also, the additional tilt necessary to compensate for the vertical divergence is  $9^\circ$ , and the final setting is  $\theta = 41^\circ$ ,  $\alpha = 41^\circ$ , which can be realised by rotating the film in a direction opposite to that of the crystal through  $3^\circ$ . This justifies the arrangement used.

It will not be out of place here if it is pointed out that this method of obtaining X-ray topographs is quite general, and can be used for any crystal, provided it is available in the form of a plate. Even the indices of the spot need not be known; what is needed is only the angle which the corresponding plane makes with the surface of the plate, which can easily be determined by taking a picture with the plate normal to the X-ray beam. If we call this angle by  $\beta$ , the author found that it is most convenient to make the planes reflect at  $-\beta$ , rotating the crystal through an angle  $\psi = 2\beta$ .

Then, the reflected beam is normal to the surface of the plate. In fact, this was the procedure adopted for obtaining the topographs of dodecahedral cleavage plates. For octahedral plates, the method is not feasible on account of the fact that the angle  $\beta$  ( $19\frac{1}{2}^\circ$ ) is in the neighbourhood of the Bragg angle for the characteristic lines of tungsten, so that the angle  $-14^\circ$  had to be employed.

If, however, it is required to obtain the X-ray topograph by surface reflection, an exactly similar method can be used. It may be remarked that, in this case, the condition for no distortion is extremely simple, namely that the film must be parallel to the crystal. This is because the reflected beam is divergent both in the horizontal and the vertical directions, so that if the photographic film is parallel to the crystal plate, the impression on it is merely an enlarged picture of the crystal, and will in fact be a true reproduction of the object.

### *3. Intensity of X-Ray Reflection in Diamond*

As a preliminary to an examination of the individual topographs and of their significance, we may briefly consider here the problem of the structure of diamond in relation to the intensity of X-ray reflections given by it. Many of the physical properties of diamonds are highly variable, *viz.*, the colour and intensity of the visible luminescence exhibited by it under ultra-violet irradiation, as also its transparency to the visible, ultra-violet and infra-red radiations and the corresponding absorption spectra. The question arises as to what the origin of these variations is. An answer to this has been given by Prof. Sir C. V. Raman in two papers appearing earlier in this symposium. According to his theory, diamond can exist in four allotropic modifications. Two of these modifications have tetrahedral symmetry and the other two octahedral. In any actual crystal, these structures may appear either alone, or intermingled with one another and the properties of the specimen are determined by the nature and the extent of interpenetration of the structures that are present in it. Such an interpenetration may be on a macroscopic, microscopic or sub-microscopic scale. Now, any variations from perfect regularity in a crystal will give rise to an enhanced intensity of X-ray reflection as is well-known. But the scale in which these variations occur is an important fact to be considered. If the interpenetration of the different structures is on a macroscopic scale, then what one expects is not an increased reflection, but only what is to be expected for a perfect crystal, except that different parts of the crystal may conceivably behave differently, giving slightly varying intensities of X-ray reflection. On the other hand, if the interpenetration and the consequent

inhomogeneity of the structure is on a microscopic or sub-microscopic scale, the crystal can be considered to possess a mosaic structure, which at once leads to an increased intensity of X-ray reflection.

Striking support is given to these considerations by the fact that the crystallographically most perfect diamonds, which exhibit a blue luminescence, show variations in the X-ray reflection intensity, which is clearly correlated to their luminescence intensity. Diamonds of this class show a strong absorption in the ultra-violet at wave-lengths below 3000 Å.U., and the best specimens appear perfectly isotropic and free from birefringence. According to Sir C. V. Raman, diamonds of this class have an inherently tetrahedral symmetry of structure, but this is, in general, disguised by an intimate inter-penetration of the positive and negative tetrahedral forms with the result that the higher octahedral symmetry of form is simulated. The resulting heterogeneity, however, reveals itself in the capacity of the diamond to luminesce. In agreement with this view, it is found that specimens of this class of diamond which exhibit the feeblest blue luminescence show the lowest X-ray reflection intensities, while those showing an intense blue luminescence give enhanced reflection intensities. This is beautifully shown by the Laue patterns of two diamonds, one feebly and the other strongly blue luminescent, obtained by Dr. R. S. Krishnan, and reproduced in Sir C. V. Raman's article in *Current Science* for January 1943. A similar pair of photographs obtained by the author under strictly comparable conditions for diamonds D31 and D41 are reproduced in Fig. 3, Plate XXIV of the present paper. These two diamonds are of equal thickness, but differ enormously in the intensity of blue luminescence, D31 being very weak and D41 very strong. It will be seen that the Laue pattern of the former is much the weaker. A quantitative study of the patterns, and a theoretical discussion of the same appears as another paper of the symposium.

It has long been known that some diamonds are completely non-luminescent and that these exhibit a higher degree of transparency to the ultra-violet, transmitting freely upto 2300 Å.U., or even shorter wave-lengths. According to Sir C. V. Raman, these belong to the class of diamonds having octahedral symmetry, there being two variants of this class (Oh I and Oh II), which are physically different. In general, both the variants are present in specimens of diamond belonging to this class, exhibiting a lamellar twinning parallel to one, two, three or even all the four sets of octahedral planes in the crystal. The existence of such lamellar twinning is proved by the external striations visible on the surface of the crystals, and by the finely spaced streaky birefringence patterns, running parallel to the planes of lamination, which are seen when plates of such diamonds are

examined between crossed nicols. The multiple lamellar twinning, in effect, divides the crystal into a great number of very small, and slightly disoriented crystal blocks, with the result that the X-ray reflection intensities of this type of diamond is much greater than even for the most intensely blue-luminescent diamond (Lonsdale, 1942; Hariharan, 1944).

Finally, we have to consider the kind of diamond in which the tetrahedral and the octahedral structures are more or less closely intermingled, and which exhibits a partial transparency in the spectral region between 2300 and 3000 Å.U. These diamonds show a mixed type of luminescence. They also exhibit an X-ray reflecting power intermediate between the two extremes, represented by the feebly luminescent tetrahedral and the non-luminescent octahedral types (Hariharan, *loc. cit.*).

A natural consequence of the possibility of interpenetration or intertwining of the four possible structures of diamond is that the structure of any particular specimen may vary from part to part within its volume. Hence, it follows that a cleavage plate of diamond may exhibit variations of its various properties over its area, such as the colour and intensity of its luminescence, its transparency to the ultra-violet, and its absorption spectra in the visible, the ultra-violet and the infra-red. It also follows that diamonds in which the tetrahedral and octahedral forms of diamond intrude into each other should exhibit a birefringence pattern related to the nature and extent of such intrusions. These conclusions are strikingly supported by a comparison between the luminescence, ultra-violet transparency and the birefringence patterns of the same diamond placed side by side. The existence of such variations of structure should also reveal itself as corresponding variations of X-ray reflection intensity, the nature of which would depend upon the precise details of the case.

#### 4. *Description of the Topographs*

The 18 topographs reproduced as Figs. 4, 5 and 6 in Plates XXIV and XXV show great differences amongst themselves. The cleavage plates of diamond with which they were recorded were, in fact, selected so as to be representative of a wide range of variation of the behaviour of diamond as exhibited in other physical properties, *viz.*, colour and intensity of luminescence, ultra-violet transparency and the absence or presence of birefringence as seen between crossed nicols. The interpretation of the topographs is greatly facilitated by a knowledge of the behaviour of the specimens under study in these respects. While each diamond shows individual peculiarities, the topographs may be broadly classified into three groups:

(A) Those in which the reflecting power of the crystal plate is more or less uniform over its surface, so that but little detail is visible in the topographs, *e.g.*, D36, D45, D221. It should be mentioned that in these cases the intensity of the X-ray reflection is so weak that exposures of from two to three hours were found necessary to get a satisfactory picture.

(B) Those in which the topograph exhibits a great general intensity of X-ray reflection, so that from ten to twenty minutes of exposure was found to be sufficient. D206, D207, D208, D209 are examples of this class. It will be noticed that in all of them, sets of parallel streaks running in different directions through the plate are a characteristic feature. This is seen in a particularly striking manner in D208 and D209.

(C) Those diamonds in which the features described in classes (A) and (B) appear to coexist, so that while the crystal as a whole exhibits comparatively weak X-ray reflection, overlying this some intense regions also appear. These intense regions may be of several kinds. They may consist of:

- (i) small areas of comparatively intense, but fairly uniform reflection, or
- (ii) a few fine streaks running through the crystal in different directions, or
- (iii) a combination of both these features. D180 shows both these features in a very striking way, *viz.*, a central bright patch with fine streaks running out in different directions. D181 is a fine example of a diamond showing a fairly uniform weak X-ray reflection, which is overlaid by a set of intensely reflecting parallel streaks. All the diamonds not mentioned under class (A) or (B) may be included in this class.

##### *5. Interpretation of the Topographs*

The interpretation is somewhat simplified on account of the fact that the classification in the preceding section also follows the classification that one would make considering the other properties of diamond. Thus, the diamonds in class (A) are weakly blue-luminescent, are opaque to the ultra-violet, and show no noticeable birefringence. They must therefore belong to the tetrahedral variety, and the extent of interpenetration of the two types Td I and Td II must be uniform throughout these specimens, as is shown by the uniform intensity of their luminescence. The mosaic structure in these diamonds must be on an extremely fine scale, showing no gross variations in the structure.

Diamonds belonging to the class (B) are transparent to the ultra-violet upto 2250 Å.U., are non-luminescent and show an intense birefringence, the

restoration under crossed nicols consisting of a large number of parallel streaks, related to, but not necessarily identical with, those in the topograph. It is clear, therefore, that they are purely of the octahedral type, in which the intense reflection arises from the fact that the two modifications Oh I and Oh II interpenetrate. The fact that the intensity is not uniform, but that the topograph exhibits parallel bands of intense reflection shows that the extent of interpenetration of the two structures is variable.

Diamonds belong to class (C) exhibit the properties of both the above classes. In fact, they are mixtures of the two structures, part of them being of the octahedral type, and the remainder of the tetrahedral. The mixing of the two types may occur in different ways. The whole diamond may consist of the tetrahedral type, and a few streaks of the other type may intrude into it. In this case, the intrusions alone will give a strong X-ray reflection, while the rest of it will be very weak. On the other hand, there may be an intimate mixture of the two types on a rather fine scale. It is not then possible to detect it by X-ray methods alone. Here, it may be pointed out that an intense X-ray reflection given by a portion of a diamond may mean one of two things—either it may be due to an increased interpenetration of the Td I and Td II structures, or it may be due to the presence of the octahedral structure.

The results obtained from the X-ray topographs confirm, and are confirmed by, those from the other patterns. First, we shall take up the evidence of the luminescence patterns. As already said, D36, D45 and D221 exhibit practically uniform fluorescence over their body, as is to be expected from their X-ray behaviour. D180 shows an intense central triangular region in the X-ray topograph, and this beautifully corresponds with a similar bright region in the luminescence photograph. A few bright streaks running in various directions are also seen in the topograph in addition. These are presumably due to the intrusion of the octahedral diamond, and are not shown by the luminescence pattern, although they are revealed by a spectroscopic study of the light transmitted by the various parts of the diamond. The topograph of D38 shows a few streaks brighter than the surrounding, but these correspond to dark regions in luminescence, showing that they are streaks of the octahedral diamond. A similar relation exists between the two patterns of D188. This diamond exhibits an intensely blue-fluorescing region at its centre, which is surrounded by a feebly blue-fluorescing background traversed by yellow bands running in various directions, and forming a figure similar to that of a spider web. In the X-ray topograph, the central portion shows itself as an intensely reflecting region.

The portions corresponding to the yellow bands also come out as bright streaks, showing that they arise from the intrusion of the octahedral structure.

In the ultra-violet transparency patterns, the transparent and consequently bright portions in the pattern are of the octahedral type, while the opaque portions must contain the tetrahedral structure. D235 is a fine example of a mixed type, in which the top semi-circular portion, and one of the bottom corners show transparent patches, while the rest is mostly opaque to the ultra-violet. The X-ray picture confirms this, since the same two portions give more intense reflections than the rest of the diamond. The other parts of the picture are however crossed by a few bright bands, showing that these portions are not purely of the tetrahedral structure. Another interesting example of the correlation between the ultra-violet and the X-ray patterns is that of D188, already described, whose ultra-violet pattern also shows transparent bands surrounding the centre of the diamond.

Intrusions of the octahedral variety in the other type will clearly set up strains, and give rise to birefringence. Hence, the X-ray topographs of the mixed type of diamonds must show some similarities to the birefringence pattern. One of the finest examples is that of D181, which shows practically uniform blue fluorescence, but in which a few faint yellow bands could be seen only with difficulty. The presence of these streaks of octahedral diamond is, however, clearly demonstrated by the X-ray topograph in which they reveal themselves as a set of bright parallel streaks. The birefringence pattern of this diamond shows features remarkably corresponding to those in the X-ray patterns, and thus confirms the finding of the latter. So also, the two patterns of D179 show a very close similarity. In the topograph of D174, there is a bright central region, surrounded by a bright boundary in the form of an irregular pentagon. In the birefringence pattern of the diamond, the same figure is visible, and outside it, there are a number of bands parallel to the sides of the figure.

The X-ray patterns of other mixed diamonds are too complicated to be resolved and interpreted. But the case of D195 is interesting. Here, there is a central triangular portion which luminesces strong blue, and corresponding to this, there is also a bright triangular patch in the X-ray pattern. Round this triangle, and parallel to its sides, there are a few bands in the topograph, showing that the octahedral structure is present in these portions. These regions either luminesce green or are non-luminescent.

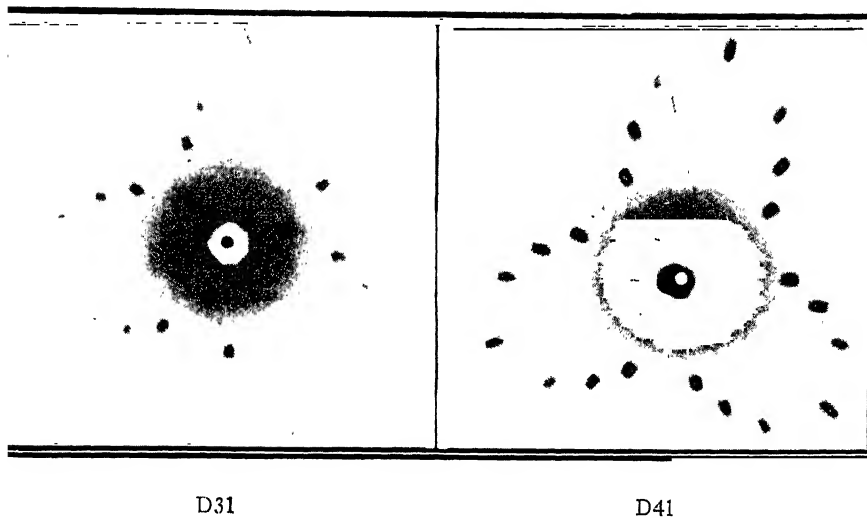
I wish to record my heartfelt gratitude to Prof. Sir C. V. Raman for the suggestion of the problem, and for the many helpful hints which he gave me during the course of the experiment.

### 6. Summary

The paper reports a method by which it is possible to obtain topographic maps representing the variations in the reflecting power for X-rays over the area of a plate of any crystal. The method consists in using white X-radiation diverging from a pinhole, and photographing the Laue reflection from any set of crystallographic planes within the crystal. The distortion, which is inevitable in such an arrangement, can be eliminated by suitably tilting the crystal and the photographic plate. Eighteen such "topographs" of cleavage plates of diamond in the collection of Sir C. V. Raman are reproduced in the plates accompanying the paper. A discussion is given of the relation of these to other patterns, such as the luminescence, ultra-violet transparency and birefringence patterns of the same diamonds. It is shown that the evidence of these corroborates and supports that of the X-ray topographs, and that the increased intensity of X-ray reflection arises out of the mosaic structure produced by the interpenetration of the various possible structures of diamond.

### REFERENCES

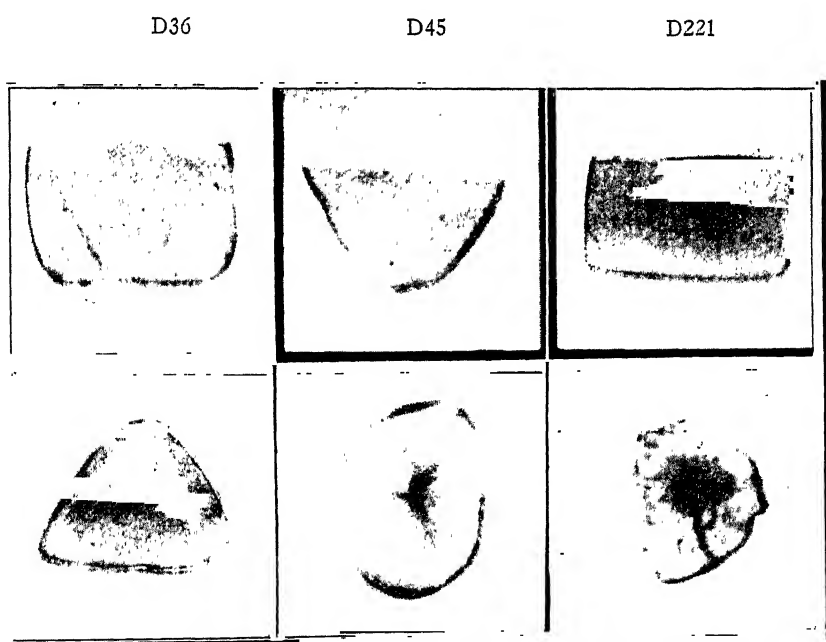
1. Hariharan, P. S. . . *Proc. Ind. Acad. Sci. (A)*, 1944, **19**, 261.
2. Lonsdale, K. . . *Nature*, 1942, **148**, 112.
3. Raman, Sir C. V. . . *Curr. Sci.*, 1943, **12**, 35.
4. ————— . . . *Proc. Ind. Acad. Sci. (A)*, 1944, **19**, 189.
5. ————— . . . *Ibid.*, 1944, **19**, 199.
6. ————— and Rendall, G. R. . . *Ibid.*, 1944, **19**, 205.
7. Rendall, G. R. . . *Ibid.*, 1944, **19**, 293.
8. Sunanda Bai, K. . . *Ibid.*, 1944, **19**, 274.



D31

D41

FIG. 3. Laue Photographs of two Blue-Fluorescent Diamonds



D174

D179

D180

FIG. 4. X-Ray Topographs of Blue-Luminescent Diamonds

D38

D181

D48



D195

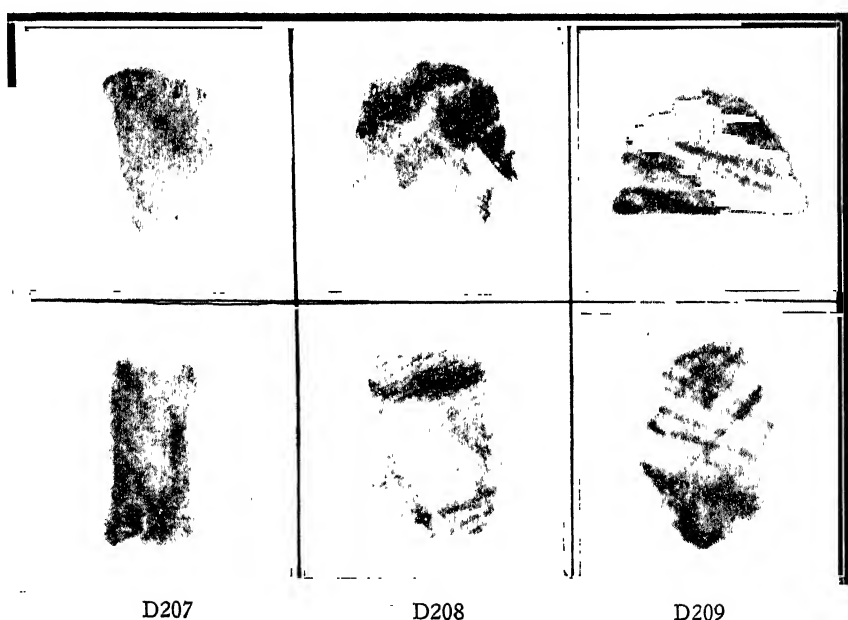
D188

D235

D199

D200

D206



D207

D208

D209

FIG. 6. X-Ray Topographs of Yellow-Luminescent and Non-Luminescent Diamonds

# ULTRA-VIOLET TRANSPARENCY PATTERNS IN DIAMOND

BY G. R. RENDALL

(*From the Department of Physics, Indian Institute of Science, Bangalore*)

Received May 18, 1944

(Communicated by Sir C. V. Raman, Kt., F.R.S., N.L.)

## 1. Introduction

THE observation by Sir C. V. Raman (1943) that luminescence patterns are shown by some of the cleavage plates of diamond in his collection pointed the way to further researches in various other directions. Working with one such diamond which showed a pattern prominently, Mrs. K. Sunanda Bai (1944) noticed that the extent of the ultra-violet spectrum which it transmits is highly variable over its area. This observation indicated the desirability of developing a method by which such variations of ultra-violet transparency could be more conveniently observed and exhibited. The present paper describes the successful realisation of this idea. The method developed renders evident to the eye at a glance both the degree of transparency of the diamond as a whole and also its local variations for the chosen wave-length in the ultra-violet region. The current belief that a diamond is either opaque or transparent—oftener opaque—to the ultra-violet spectrum beyond 3000 A.U. is shown to be incorrect. Actually, every behaviour ranging between the extremes of transparency and opacity is observed—even inside a single individual piece of diamond.

## 2. Experimental Technique

The familiar way of examining whether an object is transparent is to hold it up against an extended source of light, e.g., a window lit by the sky. An imperfect transparency of the object or of any portion of it then immediately reveals itself. In endeavouring to apply this simple technique to the study of the transparency of diamond in the ultra-violet, the principal difficulty is that of isolating the desired region of the spectrum and eliminating the rest. If the unwanted radiations are not completely excluded, wholly erroneous conclusions would be arrived at from the observations. The use of filters and of monochromators or of a combination of them were amongst the devices thought of and rejected after trial as unsuitable for the present purpose.

A procedure which has been found to be both simple and successful in practice is the use of an ultra-violet light-source in which the radiations of a chosen suitable wave-length are of such preponderating intensity that the other radiations can be easily and effectively eliminated without prejudice to the main purpose of the arrangement. Such a source is furnished by a water-cooled magnet-deflected mercury arc in quartz which emits an extremely intense radiation of wave-length 2536 A.U. The highly monochromatic image of the arc formed by this radiation and a suitable optical system is thrown on a plate of uranium glass and made visible by the resulting intense fluorescence of the latter. If a piece of diamond is stuck on to the front surface of the uranium glass, its behaviour in respect of the transmission through it of the 2536 radiations is immediately rendered evident by its screening effect on the fluorescence of the uranium glass.

Some experimental details may be worth recording. A small horizontal Heraus quartz mercury arc 5 cms. long and 1·5 cms. diameter was employed. It was held dipped in a trough containing flowing water so that the electrodes were completely immersed and remained cool when the arc was running. The discharge was deflected to the upper wall of the quartz tube by a small electromagnet, and the light emerging from it upwards was reflected horizontally forwards by a small stainless steel mirror. A quartz lens of 50 cms. focus, a constant-deviation quartz prism 5 cms. high (which could be adjusted) and a second quartz lens of 60 cms. focus were the successive items in the optical train which formed monochromatic images of the light source on a plate of uranium glass. The image formed by the 2536 radiations and made visible by the fluorescence of the plate could be readily picked out by its great intensity. By enclosing the lenses and prism in a wooden box with darkened sides and suitable apertures, extraneous light was avoided. Even so, there was some parasitic illumination due to the scattering of light at the surfaces of the lenses and prism, but this gave no trouble whatever, *provided the uranium glass plate was viewed by the fluorescent light alone in a slightly oblique direction and not by the parasitic light which came directly through it.* The appearance of the diamond as seen on the fluorescent screen could be readily photographed with the same precautions as those noted above. A camera with 5 cms. focus lens and Ilford selochrome plates gave good pictures, the exposures being regulated according to the nature of the case.

### 3. Some General Observation

The method of observation described above is so quick and convenient that a great many specimens can be rapidly examined by its use. It is not even necessary that they should be flat cleavage plates. For, if a specimen

of diamond were opaque to the 2536 radiations, it would appear opaque and throw a black shadow on the fluorescent screen having the shape of its external boundary irrespective of its shape, while if it were wholly or partially transparent, some evidence of this would appear on the screen when the specimen is suitably orientated.

On examining the transparency to the 2536 radiations of a batch of diamonds whose behaviour in respect of luminescence under long-wave ultra-violet irradiation (4000–3000 A.U.) is known, it becomes immediately evident that there is a very intimate relationship between these two characters of diamond. At one extreme, we have the diamonds which exhibit a blue luminescence of feeble or moderate intensity. These appear *perfectly opaque* to the 2536 radiations. Remarkably enough however, the diamonds that show an *intense blue luminescence* are *not* opaque to the 2536 radiations nor are they fully transparent to them. The partial transparency to the ultra-violet of highly luminescent diamonds was earlier and independently noticed by Sunanda Bai in spectroscopic tests. It is very readily exhibited by the present method of observation with all the diamonds in the collection which luminesce at all strongly with a blue colour.

At the other extreme, we have the diamonds which do not luminesce at all. With regards to these, we have the opposite situation, *viz.*, the more perfectly non-luminescent they are, the more perfect is their transparency. The merest trace of yellow luminescence results in a detectable deviation from complete ultra-violet transparency, while the more strongly yellow-luminescing diamonds approach nearer and nearer to complete opacity.

The situation as described above is, however, complicated by the fact, that in numerous cases, the ultra-violet transmission by the diamond is not uniform but patchy, often showing patterns of various kinds, and a comparison of these with the luminescence patterns shown by the same specimens indicates an intimate relationship between the two. The present paper is, in fact, principally concerned with these patterns, 24 of which have been photographed and are reproduced in Plates XXVI and XXVII. The catalogue numbers of the diamonds have been entered against them. With one or two exceptions, the luminescence patterns of all these diamonds have been reproduced with the paper by Sunanda Bai (1944) preceding the present one in the symposium. It is thus readily possible to compare them critically and determine the nature of the relationship between them.

#### 4. The Patterns and Their Origin

Some of the most striking patterns have been grouped together as Fig. 1 in Plate XXVI. Though those reproduced in Figs. 2, 3 and 4 do not all

exhibit such vivid detail, nevertheless there is much in them worthy of careful examination, especially in relation to the corresponding luminescence patterns.

A very striking feature of the ultra-violet transparency patterns is that several of them bear nearly the same relation to the corresponding luminescence patterns as a lantern-slide does to the photographic negative from which it is prepared. Comparing for instance, the patterns of D48, D198, D235, D56, D189, D210, D194, D192, and D177, one finds an almost perfect correspondence of the kind indicated. This feature becomes intelligible in the light of the general observations made earlier regarding the relationships between luminescence and ultra-violet transparency, when we remember that the patterns have the same origin, *viz.*, the intrusion of one type of diamond into another. If one kind of diamond is luminescent and ultra-violet opaque, and the other kind is non-luminescent and ultra-violet transparent, we would have an explanation of the kind of relationship between the patterns which we have noted.

The matter is, however, not quite so simple as might appear from what has been said. There are cases where the relationships are quite different. Taking the instance, D180 which shows a bright blue patch surrounded by a dark area in its luminescence, its ultra-violet transparency shows no indication of this. The outline of the patch however appears as a faint line on a dark field. Take again the case of D179 which shows a striking luminescence pattern. But little of this can be made out in the ultra-violet transparency pattern except for a bright streak which appears where a dark streak appears in the luminescence pattern. These and other examples could be quoted to show that variations in the intensity of blue luminescence do not necessarily show up prominently in the ultra-violet transparency pattern.

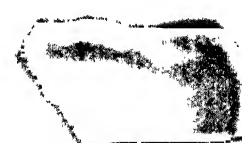
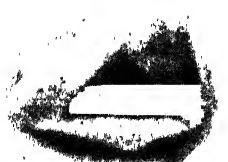
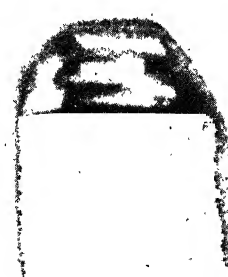
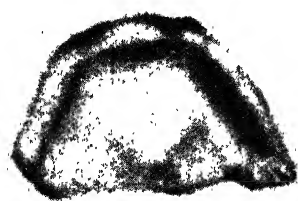
A striking characteristic of yellow luminescence is the appearance of numerous bright streaks running parallel to one another, sometimes in several directions simultaneously. Such an effect, for example, is exhibited very prominently in the luminescence of D188, D193, D199, D200 and D202. Their ultra-violet transparency patterns do also give indications of the presence of parallel streaks, but nothing at all comparable in fulness of detail with what is seen in luminescence. This is a point worthy of closer investigation.

It must of course, be admitted that many blue-luminescing diamonds which show a vivid pattern, *e.g.*, D38, and others which show by their birefringence, *e.g.*, D181 that they include non-luminescent diamond, are completely opaque to the 2536 radiations and therefore yield no result

D48

D198

D235



D56

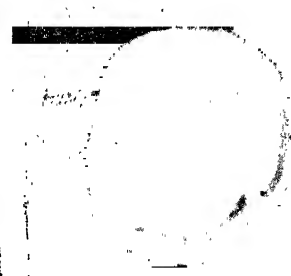
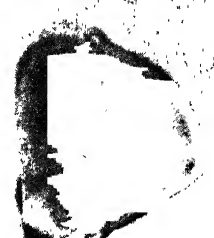
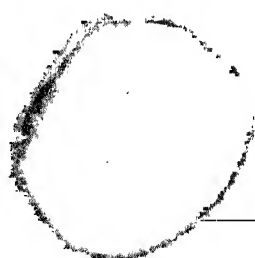
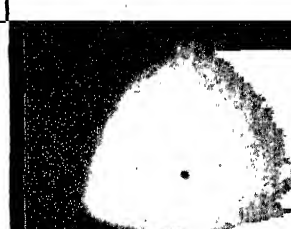
D195

D189

D179

D180

D188



D180

D200

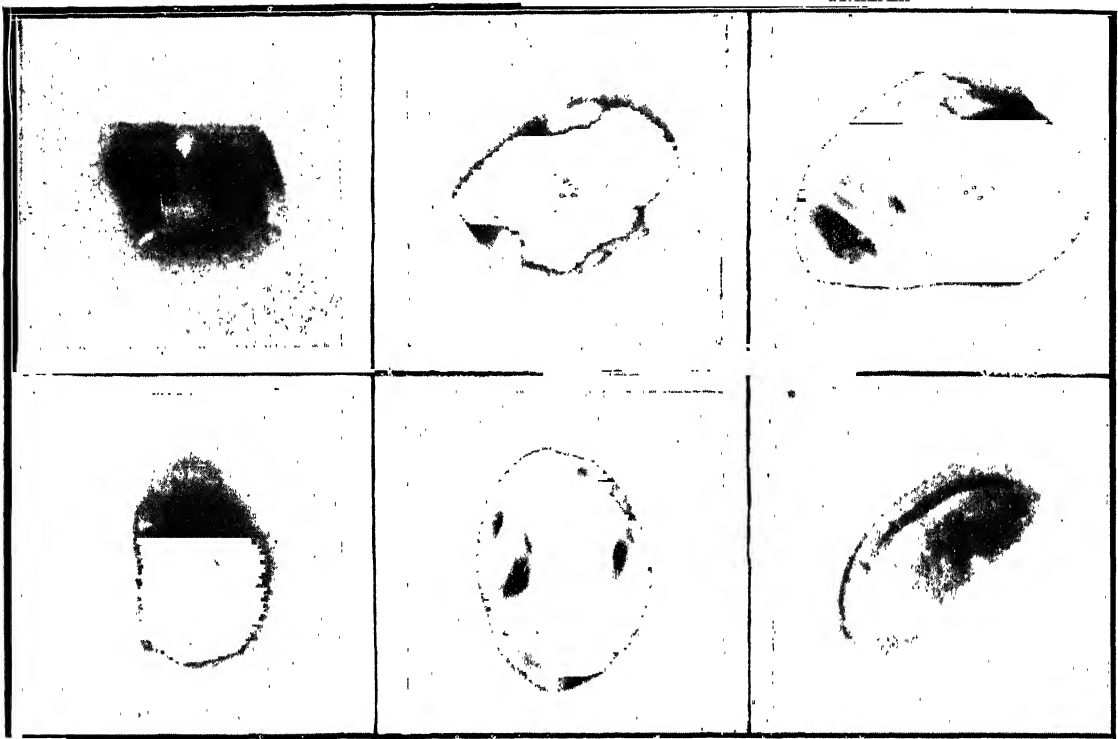
D210

FIG. I. Ultra-Violet Transparency Patterns

D193

D194

D192



D185

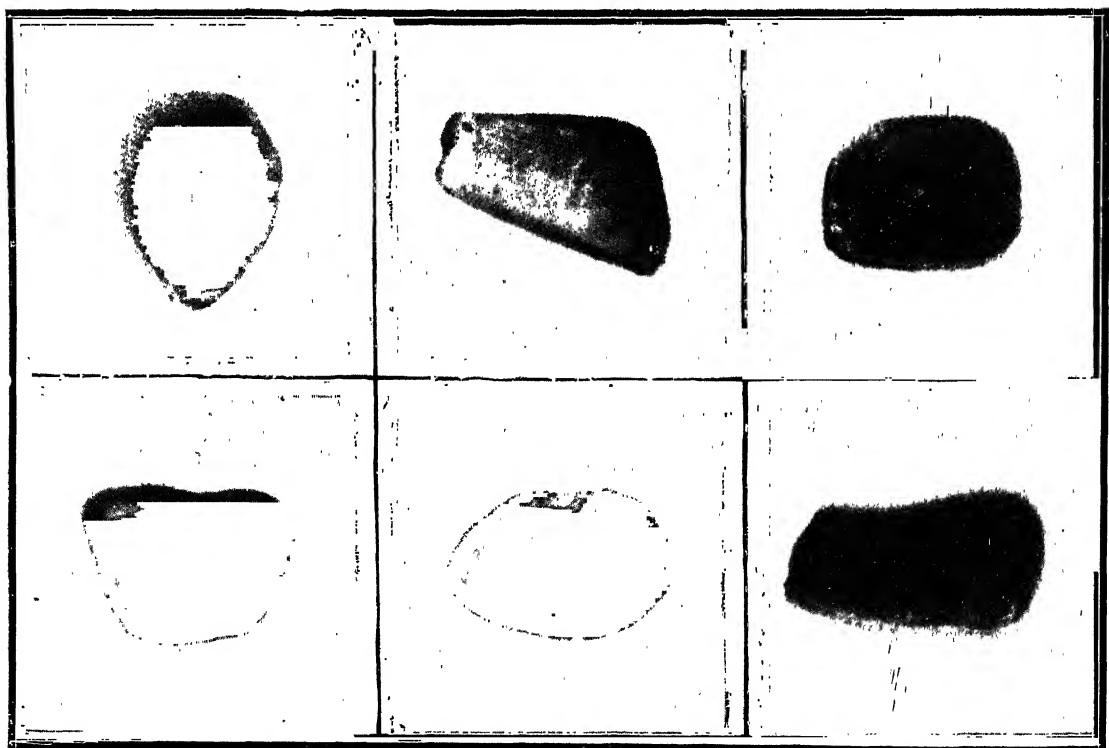
D177

D202

D178

D199

D236



D191

D201

D106

FIG. 3. Ultra-Violet Transparency Patterns

under the present technique. It is possible that if a suitable light source of a somewhat longer wave-length could be developed, it would extend the range of investigation.

In conclusion, the author wishes to place on record his deep gratitude to Prof. Sir C. V. Raman, Kt., F.R.S., N.L., for suggesting the problem and for his inspiring guidance.

### 5. Summary

Using the 2536 A.U. radiations of a water-cooled magnet-deflected mercury arc in quartz, and an optical system which forms an intense monochromatic image of it on a plate of uranium glass, it is possible to examine the ultra-violet transparency of diamond very conveniently and thoroughly. The investigation reveals that the current idea that diamonds are either opaque or transparent in this region is incorrect. A wide range of behaviour ranging between complete opacity and complete transparency is possible, and it stands in the closest relationship to the luminescence properties of the diamond. The same method enables the ultra-violet transparency patterns of cleavage plates of diamond to be photographed. In not a few cases, these patterns are very similar to the luminescence patterns but reversed. In other cases, again, such a similarity is not observed. The origin of these resemblances and differences is discussed.

24 photographs are reproduced with the paper.

### REFERENCES

Raman, Sir C. V.	... <i>Current Science</i> , 1943, <b>12</b> , 42.
Sunanda Bai, K.	... <i>Proc. Ind. Acad. Sci., A</i> , 1944, <b>19</b> , 274.

# EXPERIMENTAL EVIDENCE FOR THE EXISTENCE OF THE FOUR POSSIBLE STRUCTURES OF DIAMOND

BY R. S. KRISHNAN

(*From the Department of Physics, Indian Institute of Science, Bangalore*)

Received May 10, 1944

## 1. *Introduction*

IN the introductory paper of this symposium, Sir C. V. Raman has set out the theoretical considerations which indicate that the crystal structure of diamond has four possible forms. Two of these ( $Td\text{ I}$  and  $Td\text{ II}$ ) have only tetrahedral symmetry, while the other two ( $Oh\text{ I}$  and  $Oh\text{ II}$ ) have the full symmetry of the cubic system. These considerations receive support from the known spectroscopic behaviour of diamond, as also from the observed crystallographic facts. The fundamental oscillation of the two interpenetrating lattices of carbon atoms with respect to each other should be active in the infra-red absorption in the tetrahedral varieties of diamond, since these do not possess a centre of symmetry. On the other hand, this vibration should be infra-red inactive in the octahedral types of diamond, since these possess a centre of symmetry. The well-known fact that an intense infra-red absorption in the neighbourhood of  $7.5 \mu$  (corresponding to the lattice frequency of 1332 wavenumbers) is exhibited by some diamonds, while such absorption is absent in others, thus receives a natural explanation.

Accepting the conclusion indicated by the infra-red absorption data and the observed crystal forms that diamond may have either tetrahedral or octahedral symmetry, it is difficult to resist the further implication of the theory that there are two variants under each class. It is obviously of great importance to obtain convincing experimental evidence for the physical existence of all the four forms postulated. Since *prima facie*, all the four types should have closely similar properties, such evidence must be sought in measurements where the highest degree of precision is possible, *viz.*, in X-ray and in spectroscopic data. It is the object of this paper to present such evidence.

## 2. *The Two Tetrahedral Structures*

It is obvious that the two tetrahedral types of diamond, namely, the positive and the negative forms, are physically identical and only geometrically

different. Hence, they should possess precisely the same crystal spacing and lattice vibration frequency, and therefore apparently be indistinguishable from each other. If, however, both forms co-exist in one and the same specimen of diamond, this would give rise to a heterogeneity, and variations in the physical properties should arise depending upon the extent of their interpenetration. The spectroscopic studies of Nayar (1941), (Miss) Mani (1944) and Mrs. Sunanda Bai (1944) on the absorption and the luminescence spectra of diamonds show clearly the existence of such large variations. These may be regarded as fairly convincing evidence for the existence of the interpenetration and consequent variations in structure.

A clearer and more direct proof is, however, forthcoming from X-ray studies. The interpenetration of the positive and negative tetrahedral structures and consequent heterogeneity should evidently manifest itself in increased intensity of X-ray reflections from the lattice planes of the crystal. This conclusion was experimentally tested out by the author as early as May 1942. The diffraction of X-rays in a few typical diamonds of the tetrahedral variety exhibiting luminescence in varying degrees, was studied both by the Laue and by the Bragg methods, in the latter case with oscillating crystals. It was found that there was a direct correlation between the intensities of X-ray reflections and of luminescence of the diamond. The diamond exhibiting the blue luminescence with the least observable intensity were also the diamonds which gave the least intensities of X-ray reflections, showing thereby that these diamonds approached more closely to the ideal homogeneous structure. The strongly blue fluorescent diamonds gave rise to intense Laue and Bragg reflections, suggesting thereby that these specimens had a heterogeneous or mosaic structure arising from the interpenetration of the two tetrahedral types. These observations of the author have later been confirmed and extended by Hariharan (1944) and Ramachandran (1944).

### *3. The Two Octahedral Structures*

Unlike the two forms of the tetrahedral type, the possible forms of the octahedral type, namely, Oh I and Oh II should be physically different from one another. Consequently, whenever interpenetration of the two octahedral forms occurs, the specimen exhibits a lamellar structure parallel to one or more of the cleavage planes of the crystal. Such specimens of diamond often show a streaky birefringence. Because of their physical difference, it is reasonable to expect the two octahedral forms of diamond structure to show a small but measurable difference in crystal spacing. The direct way of testing out the above conclusion would consist in an accurate determination of the lattice spacing in two perfectly homogeneous specimens

belonging to the Oh I and Oh II types respectively and comparing the values thus obtained. There is, however, ample evidence to show that the two structures do not ordinarily occur apart from each other, but that they co-exist in the same specimen, endowing it with a finely laminated structure. Such a structure may be expected to show periodic variations in crystal spacing detectable by appropriate methods. Indeed, the fact that diamonds of this type show characteristic birefringence patterns exhibiting their laminated structure may itself be regarded as a proof that the alternate layers in it do not have an identical crystal spacing. For, if the lattice spacings were the same throughout, there is no *prima facie* reason why any birefringence should arise.

From the large collection of diamonds of this kind in the possession of Sir C. V. Raman, diamond D209 which showed a well-defined streaky birefringence between crossed polaroids was selected for the present investigation. The geometric character of the birefringence pattern and its periodic disappearance as the crystal is rotated between the crossed polaroids, indicated that this sample would be an ideal one for the purpose of the present test. The diamond (an octahedral cleavage plate) was mounted on a goniometer with its faces vertical. The X-rays from a copper target after passing through an extremely fine vertical slit (5 mm.  $\times$  0.4 mm.) were allowed to fall on the crystal nearly at the Bragg angle for the surface reflection. The crystal was oscillated through a small angle about this position and the resulting Bragg reflection from the front surface of the crystal was recorded on a photographic film. The film was kept normal to the diffracted beam at a distance of about 40 cm. from the crystal. A typical oscillation photograph obtained is reproduced in Fig. 1 (b) in the accompanying plate. The reflections due to the Cu  $K\alpha_1$ , and Cu  $K\alpha_2$  radiations are seen well resolved in the photograph; the intense one corresponds to Cu  $K\alpha_1$ . It will be noticed that these Bragg reflections instead of being linear in shape and of uniform intensity are wavy in nature and also show a periodic variation of intensity. The most intense portions are bent towards the direct beam and hence correspond to smaller values of  $\theta$ , while the less intense portions are bent away from the direct beam. If the crystal were perfectly homogeneous through the section where the X-rays were incident, the Bragg reflections would give rise to a linear and true image of the slit. As the crystal used was heterogeneous with periodic variation in crystal spacing, the Bragg reflections would show a corresponding waviness. From a measurement of the amplitudes of the waviness and the average separation of the  $K\alpha_1$  and  $K\alpha_2$  reflections, the difference in crystal spacing has been estimated. It is found that the difference is of the order of 5 parts in 10,000. The inter-

penetration of one octahedral form into the other has not only caused a periodic variation in the crystal spacing, but also given rise to a mosaicity, as is evident from the increase in intensity of Bragg reflections from these layers.

Oscillation photographs were also taken for various settings of the same crystal and the Bragg reflection in every case showed the wavy character. The distribution of the intense and weak spots was different in each case. A typical oscillation photograph for a different setting of the crystal is reproduced in Fig. 1 (c) in Plate. XXVIII. The experiment was repeated with a second diamond (D45 in Sir C. V. Raman's collection) which was only very feebly fluorescent and belonged to the tetrahedral type. The oscillation photograph is reproduced in Fig. 1 (d). As is to be expected, the Bragg reflection from D45 does not exhibit any wavy character. The reflected image is quite linear and of uniform intensity.

Very recently, Mrs. Lonsdale (1944) has carried out measurements of the crystal spacing in a large number of diamonds. She found no variation in the spacing greater than 2 parts in 10,000 in the various specimens examined by her. Very few diamonds which were transparent to the ultra-violet were included in her list. As already mentioned, however, the transparent variety of diamond usually occurs as a mixture of the two octahedral structures. Hence what Mrs. Lonsdale measured was the mean of the spacings of the two octahedral structures and her observations leave the question of the difference between the Oh I and Oh II spacings with which we are here concerned entirely untouched. It should be remarked that the success attained in the present investigation is largely due to the choice of the specimen in which the spacings of the laminations were sufficiently great to exhibit the waviness of the Bragg reflections. Specimens in which the laminations are very fine would obviously fail to show the effect.

#### 4. *The Spectroscopic Evidence*

As has already been pointed out earlier in the paper, the two octahedral structures are physically different. It is therefore reasonable to suppose that the frequency of the fundamental lattice oscillation would be different for the two structures. The expected variation in lattice frequency would probably be of the same order of magnitude as the variation in the crystal spacing, namely, about 5 parts in 10,000. Even such a small difference in lattice frequency should, however, be sufficient to give rise to an observable broadening of the fundamental Raman line in the case of a diamond containing a mixture of the two forms. The experiment was carried out as follows :—

The Raman spectrum of diamond D227 (which belonged to the octahedral variety) was photographed through a Hilger E<sub>1</sub> quartz spectrograph using as fine a slit as possible. The 2536 resonance radiations of a water-cooled quartz mercury arc were used for exciting the Raman line. Visual observation of the recorded spectrum showed that the 1332 line had a finite breadth greater than that of any of the mercury lines of comparable intensity. This was confirmed by taking a microphotometric record of the spectrum. The microphotometric records of the mercury triplet at 2655·1, 2653·7 and 2652·0 A.U. and that of the Raman line are reproduced in Figs. 2 *a*, *b* *c*, and *d* respectively in the accompanying Plate. The mercury line at 2655·1 A.U. has nearly the same intensity as the 1332 Raman line, whereas the width of the Raman line is a little more than one and a half times that of the mercury line. The difference in width between the two is approximately one wavenumber. This is of the same order of magnitude in relation to 1332 as the observed difference in lattice spacings. Thus, the spectroscopic data also lend support to the view that there are two different structures in the octahedral type of diamond, though, no doubt, the observed width of the Raman line is, in part, due to the finite width of the 2536 line itself.

As the two tetrahedral forms of diamond are physically identical, their lattice vibrations should have identical frequencies but different from that of either of the octahedral forms. It is conceivable, however, that the *mean* lattice frequency of the octahedral types might be the same as that of the tetrahedral variety. In order to test these points, the Raman spectra of two diamonds D36 and D227 (the former of the tetrahedral type, while the latter of the octahedral type) were photographed side by side through a Fuess spectrograph using a Hartmann diaphragm. The spectrogram is reproduced in Fig. 1*a* in Plate XXVIII. The top picture represents the Raman spectrum of D227, while the bottom picture represents the Raman spectrum of D36. As far as can be made out, there is no difference in the frequency shifts and the Raman line appears in exactly the same position for the two diamonds. An enlarged picture of the 1332 Raman line excited by the 4046 radiation with suitable adjustment of the background intensity is reproduced in Fig. 1*e*. The upper portion of the figure represents the spectrum in D36, while the lower portion represents the spectrum in D227. The Raman line in D227 appears to be definitely broader than the corresponding line in D36, in agreement with the general considerations indicated above.

In conclusion, the author wishes to express his grateful thanks to Prof. Sir C. V. Raman for suggesting the problem and for valuable discussions during the progress of the investigation.

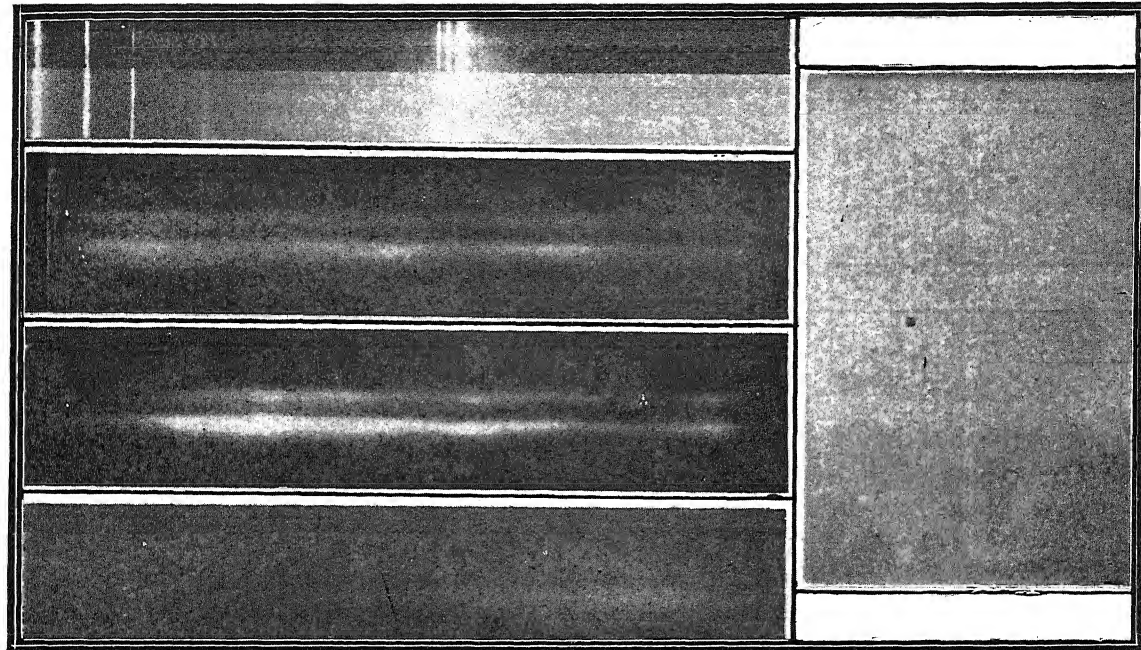


FIG. 1

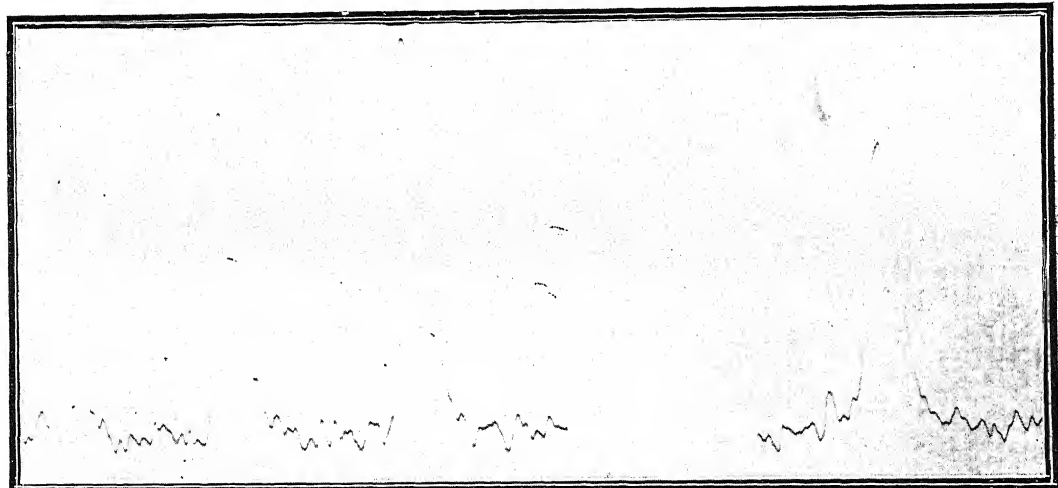


FIG. 2



### 5. Summary

Experimental evidence has been obtained for the existence of the four possible structures of diamond from X-ray and spectroscopic studies. The co-existence of the two variants of the tetrahedral structure in one and the same specimen and the heterogeneity arising therefrom have been confirmed from the observed increased intensities of X-ray reflections in such diamonds. Using the oscillating crystal method and a diamond in which the two structures of the octahedral type co-exist in adjacent layers of the crystal, it is observed that the Bragg reflections exhibit a waviness such as should be observed if there be a difference in the crystal spacings of the alternate layers. The observed difference in crystal spacings thus deduced is of the order of 5 parts in 10,000. The Raman line corresponding to the fundamental lattice vibration shows a definite width in the case of the octahedral type of diamond which agrees at least, in the order of magnitude, with the expected difference in the vibration frequencies of the two octahedral structures.

### REFERENCES

Hariharan, P. S.	.. <i>Proc. Ind. Acad. Sci.</i> , 1944, A., <b>19</b> , 261.
Lonsdale, K.	.. <i>Nature</i> , 1944, <b>153</b> , 22.
Mani, A.	.. <i>Proc. Ind. Acad. Sci.</i> , 1944, A., <b>19</b> , 231.
Nayar, P. G. N.	.. <i>Ibid.</i> , 1941, <b>13</b> , 483 and <b>14</b> , 1.
Ramachandran, G. N.	.. <i>Ibid.</i> , 1944, <b>19</b> , 280.
Raman, C. V.	.. <i>Ibid.</i> , 1944, <b>19</b> , 189.
Sunanda Bai, K.	.. <i>Ibid.</i> , 1944, <b>19</b> , 253.

# X-RAY REFLECTION AND THE STRUCTURE OF DIAMOND

BY G. N. RAMACHANDRAN

(From the Department of Physics, Indian Institute of Science, Bangalore)

Received May 9, 1944

(Communicated by Sir C. V. Raman, Kt., F.R.S., N.L.)

## 1. Introduction

ACCORDING to the well-known Ewald-Darwin theory of the reflection of X-rays by perfect crystals, the integrated reflection, or the total intensity reflected as the crystal is swung through the Bragg angle, is proportional to the structure factor of the particular set of planes concerned. On the other hand, if the crystal were ideally imperfect, so that one can neglect the effect of both primary and secondary extinction, then the integrated reflection becomes proportional to the square of the structure factor (Darwin, 1914 *a*, 1922). In general, therefore, the intensity of reflection is much greater for an imperfect crystal than for a perfect one. Crystals have generally been classified as either perfect or ideally imperfect, according as the integrated reflection approximates to the theoretical value calculated for the one or the other. To the latter class are assigned most of the crystals like rocksalt, fluorspar and barytes (Bragg, Darwin and James, 1926). Calcite is the only example for which values of the integrated intensity approaching that for a perfect crystal have been obtained (for references see Compton and Allison, 1935, pp. 399 to 405). Although the integrated reflection has not been measured for diamonds, measurements of the width of reflection have been made by Ehrenberg, Ewald and Mark (1928), who found values remarkably close to that for a perfect crystal with some specimens.

As already said, ordinary crystals either belong to the perfect or to the imperfect variety. It is not easy to get samples of the same crystal possessing varying degree of mosaic structure. However, in the case of diamond, such a procedure is possible. For, diamond can exist in four allotropic modifications, and, in an actual crystal, these can appear either alone, or two or more structures can appear intermingled (Raman, 1944 *a* and *b*). The extent of interpenetration of the different structures may also vary from sample to sample. Thus, one can obtain various types and degrees of mosaic structure by having crystals of diamond which exhibit different

colour and intensity of fluorescence. *Vice versa*, by studying the reflection of X-rays by different crystals of diamond, one can obtain some knowledge of the nature of the mosaic structure in diamond.

That such a mosaic structure exists in blue-fluorescent diamonds was first shown by R. S. Krishnan (Sir C. V. Raman, 1942), who obtained the Laue photographs of two such diamonds, one of which D31 was feebly blue-fluorescent and the other D224 was strongly fluorescent, also blue. He found that all the spots in the Laue pattern of the latter were more intense than the corresponding ones of the former. Following this discovery, P. S. Hariharan (1944) studied the intensity of the (111) Bragg reflection given by a number of diamonds, and found that there is a direct correlation between the intensity of X-ray reflection and of blue-fluorescence. It was therefore thought worthwhile to extend the investigation to some of the other important reflections given by diamond. This was done by taking the Laue patterns of two typical blue-fluorescent diamonds, which differ widely in their intensity of fluorescence.

## 2. Experimental Details and Results

The specimens used were carefully selected out of the collection of Sir C. V. Raman so as to have as nearly as possible the same thickness, and to be as perfectly isotropic as could be obtained. The diamonds used were D31 and D41, both octahedral cleavage plates of very nearly the same thickness, about 1 mm. The actual thicknesses were 0.96 mm. and 1.0 mm. D31 was feebly blue-fluorescent, while the other one was intensely fluorescent, also blue.

The source of X-rays consisted of a self-rectifying Shearer tube, excited by a transformer, and worked at 50 K.V. and 9.5 milliamperes. This was kept steady by continuous adjustment of the air-leak and the resistance in the primary circuit of the transformer. The X-ray beam was collimated through a pinhole 1 mm. in diameter and 10 cm. long.

The diamond plate could not be mounted on a goniometer since this prevented the photographic film from being brought close to the crystal so as to record the complete pattern. Consequently, the goniometer was dispensed with, and the diamond was placed straight against the exit end of the slit and stuck to it by means of wax. As already said, the surface of the diamond was parallel to the (111) plane, so that it was most convenient to mount the plate with the surface (111) planes normal to the X-ray beam. This was done by hand, the normality being judged by taking a picture of the (111), ( $\bar{1}\bar{1}1$ ), and ( $\bar{1}11$ ) Laue spots and verifying

that they are at equal distances from the central spot. After this adjustment was made, the complete pattern was photographed by placing the film quite close to the crystal (at a distance of 9.5 mm.) and normal to the X-ray beam. An exposure of 3 hours was required to obtain a clear picture. Throughout the exposure, both the voltage applied and the current through the tube were maintained rigorously constant by continuous manipulation.

With diamond 31, standard pictures with exposures of 5, 90 and 180 minutes were taken. Then, using diamond 41, a series of pictures were taken with exposures varying from 2 to 180 minutes (for reasons to be explained shortly) under the same conditions as for D31. All the films were developed under standard conditions in the same stock developer.

The photographs obtained with an exposure of three hours in the two cases are reproduced in Fig. 3, Plate XXIV in a previous paper by the author appearing in this symposium. The Laue pattern consists of spots lying in the three zones, the  $(1\bar{1}0)$ ,  $(10\bar{1})$  and  $(01\bar{1})$ , and the indices of the spots in any zone belong to the forms  $\{111\}$ ,  $\{211\}$ ,  $\{311\}$ ,  $\{511\}$ ,  $\{711\}$  and  $\{100\}$ . It will be seen from the figure the intensities of the spots are greater in the pattern of D41 than of D31.

A detailed microphotometry of the peak intensities of the various spots was then undertaken. In this connection, it must be noted that the wave-lengths of the X-rays giving rise to the different Laue spots are different. Consequently, the calibration curve for the determination of the intensity had to be plotted for each wave-length required. It was for this purpose that a number of photographs were taken with a wide range of exposures, with the diamond giving stronger reflections. Using these photographs, and assuming the well-known result that the Schwarzschild's constant for X-rays does not differ appreciably from unity, the density-log intensity curve was drawn for each of the wave-lengths. From this curve, the intensity of the corresponding spots in the pattern of D31 were evaluated. It may be remarked in this connection that the Laue photographs obtained are not absolutely symmetrical, but that there is a small asymmetry. In order to avoid the errors arising from this, the intensity of all the six or three (as the case may be) spots having the same indices were measured, and the average was taken as the correct value.

The ratios of the intensities obtained in this way are shown in the second row in Table I.

TABLE I

Indices of the reflection ..	111	422	311	511	711	400
$I_{41}/I_{31}$ .. ..	3.36	2.24	2.31	1.93	1.49	2.72
$I_{224}/I_{31}$ .. ..	..	3.20	3.61	2.55	1.81	4.61
$I_{224}/I_{41}$ .. ..	..	1.54	1.56	1.32	1.21	1.69

It will be seen from the table that the ratio of the intensities given by the two diamonds is not a constant for all the planes, but that it varies from one to another. In order to confirm this fact, the photographs taken by Dr. R. S. Krishnan with diamonds 31 and 224, which were reproduced in *Current Science* (Sir C. V. Raman, 1943) were subjected to microphotometry. The original negatives of these were kindly lent to the author by Dr. Krishnan. Although the thicknesses of these two diamonds were not the same, still the photographs could be used for the purpose of a check. The values obtained for the ratio  $I_{224}/I_{31}$  are shown in the third row in Table I. The ratios deduced for  $I_{224}/I_{41}$  from the above are tabulated in the fourth row. Although no claim is made as to the accuracy of the values of  $I_{224}/I_{31}$  and of  $I_{224}/I_{41}$ , it is clear that the ratio of the intensities of reflection given by two blue-fluorescent diamonds is not the same for all the planes, but that it varies. Further, the plane whose intensity is affected most is the same for all diamonds, and the order in which the intensities are enhanced is also the same.

### 3. Interpretation of the Results

From the experimental results described in the preceding section, it is clear that the enhancement in intensity produced by the mosaic structure which is present in blue-fluorescent diamonds is not the same for the various planes. A clue to the understanding of the cause for this comes out of a study of the intensity of X-ray reflection by perfect and by ideally imperfect crystals. According to Darwin (*loc. cit.*), the expressions for the integrated intensity reflected out of a crystal plate are, for a perfect one,

$$I_p = \frac{8}{3\pi} N\lambda^2 F \frac{e^2}{mc^2} \cdot \frac{1 + |\cos 2\theta_0|}{2 \sin 2\theta_0},$$

and for an ideally imperfect one,

$$I_i = \frac{N^2 \lambda^3}{2\mu} \cdot \left( F \frac{e^2}{mc^2} \right)^2 \cdot \frac{1 + \cos^2 2\theta_0}{2 \sin 2\theta_0},$$

where  $N$  is the number of unit cells per c.c.,  $F$  is the crystal structure factor for the unit cell,  $\lambda$  is the wave-length reflected, and  $\theta_0$  is the angle of

incidence for the particular reflection,  $\mu$  is the linear absorption coefficient, and  $e$ ,  $m$  and  $c$  have their usual significance. The perfect crystal formula is true only for a non-absorbing crystal, and for one which is not so  $I_p$  would obviously be less. Consequently, while comparing the two quantities  $I_p$  and  $I_i$ , we need not consider the factor  $1/\mu$  in the expression for  $I_i$ , and the ratio of the two may be written as

$$\frac{I_i}{I_p} \propto N\lambda F \frac{e^2}{mc^2} \cdot \frac{1 + \cos^2 2\theta_0}{1 + |\cos 2\theta_0|}$$

Here,  $e^2/mc^2$  is a universal constant, and  $N$  is a constant for a particular crystal, so that one may write

$$I_i/I_p \propto k\lambda F,$$

where  $k$  stands for the ratio  $(1 + \cos^2 2\theta_0)/(1 + |\cos 2\theta_0|)$ .

The above expression relates to the increase in intensity when a perfect crystal is completely broken up. However, in the case of diamond, with which we are concerned, the crystal approaches perfectness, but possesses a slight mosaic structure, which increases with increase in the intensity of blue-fluorescence. Therefore, we may expect the ratio of the intensities for two blue-fluorescent diamonds to be some function of  $(k\lambda F)$ . In Fig. 1, the quantities  $I_{41}/I_{31}$ ,  $I_{224}/I_{31}$  and  $I_{224}/I_{41}$  (which may be denoted by  $r_1$ ,  $r_2$  and  $r_3$  respectively) are plotted as ordinates against  $(k\lambda F)$  as abscissæ.

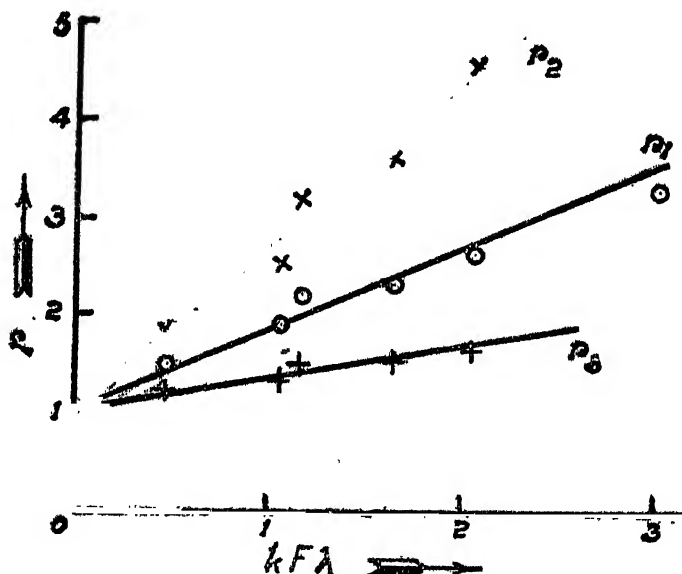


FIG. 1. X-Ray Reflection and the Structure of Diamond

The plotted points are found to lie approximately on straight lines, the equations to which are:

$$(r_1 - 1) = c_1(k\lambda F); (r_2 - 1) = c_2(k\lambda F); (r_3 - 1) = c_3(k\lambda F),$$

where the  $c$ 's are constants. Thus the ratio  $r$  depends linearly on the product  $(k\lambda F)$ , having a value unity when the structure factor  $F$  is zero.

The author is not in a position at present to give a theoretical explanation for this empirical relation connecting  $r$  and  $(k\lambda F)$ . It may be remarked that even if  $r$  is plotted against  $(\lambda F)$ , then also the points lie on straight lines intersecting the  $r$  axis at  $r = 1$ .

In conclusion, I wish to express my deep sense of gratitude to Prof. Sir C. V. Raman for the suggestion of the problem and for the encouraging guidance which he gave me during the investigation. My thanks are also due to Dr. R. S. Krishnan for the loan of the two negatives taken by him.

### Summary

Laue photographs with the X-ray beam normal to the surface (111) planes have been taken for two typical blue-fluorescent diamonds exhibiting widely different intensities of fluorescence, but similar in other respects. Microphotometry of the peak intensity of the various spots shows that although the intensity of all the spots is greater with the more fluorescent diamond, the ratio ( $r$ ) of the intensities of the corresponding spots varies. Empirically, it is found that  $(r - 1)$  is proportional to the product of the structure factor, the wave-length reflected and a function of the angle of incidence.

### REFERENCES

1. Bragg, Darwin and James .. *Phil. Mag.*, 1926, **1**, 897.
2. Compton and Allison .. *X-Rays in Theory and Experiment*, 1935, p. 399.
3. Darwin, C. G. .. *Phil. Mag.*, 1914a, **27**, 315.
4. — .. *Ibid.*, 1914b, **27**, 675.
5. Ehrenberg, Ewald and Mark .. *Zeits. f. Krist.*, 1928, **66**, 547.
6. Ewald, P. P. .. *Ann. der. Phys.*, 1918, **54**, 519, 577.
7. Hariharan, P. S. .. *Proc. Ind. Acad. Sci., A*, 1944, **19**, 261.
8. Raman, Sir C. V. .. *Ibid.*, 1944a, **19**, 189.
9. — .. *Ibid.*, 1944b, **19**, 199.
10. — .. *Curr. Sci.*, 1943, **12**, 35.

# MAGNETIC SUSCEPTIBILITY OF DIAMOND

By A. SIGAMONY

(*From the Department of Physics, Indian Institute of Science, Bangalore*)

Received April 17, 1944

(Communicated by Sir C. V. Raman, Kt., F.R.S., N.L.)

## 1. Introduction

DIAMOND is a solid of which several of the physical characters show remarkable variations. While the finest specimens are perfectly colourless and transparent, this is far from being generally the case. The majority of the so-called "industrial" diamonds have noticeable tints such as gray, brown or yellow, while some highly prized specimens exhibit quite definite colours such as pink or blue. Under long-wave ultra-violet irradiation many diamonds luminesce, the intensity and colour of the emitted light varying enormously from specimen to specimen, while some diamonds remain completely dark. It is a statement often made in the literature that the colours of diamond and its luminescent properties owe their origin to the presence of impurities. One method of testing these suppositions which does not involve the destruction of the diamond by chemical analysis is the accurate measurement of its magnetic susceptibility. As is well known, diamond is diamagnetic and it is therefore a possibility that such measurements may indicate the presence of para-magnetic or ferromagnetic impurities even in small amounts. The present investigation was undertaken to find whether there are any observable variations in the susceptibility of diamond, and if so, whether they show a correlation with the colour of the specimen, its luminescence and also with such other properties as have been known to vary, *viz.*, the transparency in the ultra-violet region of the spectrum and the photo-conductivity.

The 40 specimens examined were chosen from the personal collection of Sir C. V. Raman. Many of them were crystals in their natural form from the Panna diamond mines in Central India. Some of the others were cleavage plates, mostly of Indian origin, while the rest were diamonds of South African origin which had been faceted and polished for use as jewellery.

## 2. Experimental Arrangements

The susceptibility measurements were made by a Curie balance constructed by the author. An electromagnet with arrangement to clamp the coils at any suitable angle was used. A light aluminium beam was suspended by a torsion wire from a drum-head capable of rotation. The specimen was placed in a container made of thin silver foil and suspended in the field by a thin fibre from one end of the beam. The deflections of the beam were measured by the lamp and scale method. The non-homogeneous field was produced by pole pieces 5 cm. in diameter which were fixed at a suitable inclination so as to give a flat maximum for the factor  $H.dH/dx$ . Its variation in this region was investigated by finding the force on water enclosed in small glass bulbs of different sizes. The force was found to be proportional to the mass of water taken within the experimental error, showing that the "nonhomogeneity" was uniform. Further, for plates of diamond, closely fitting containers were made to hold the diamond as well as the standard substance, and they were suspended so as to have the broader side parallel to the field. The specimen was always brought to this region of the field by rotating the drum-head. This was accurately done by using a plane mirror placed below the specimen with its plane at an angle of  $45^\circ$  to the vertical, a tele-microscope being arranged to view the reflected image.

The diamonds were cleaned thoroughly in alcohol before taking measurements with them. Double distilled water was used as the standard substance and its susceptibility taken as  $-0.72$ . The deflections were measured with the container alone, then with the diamond inside the container, and finally with the standard substance. The mass susceptibility was calculated by the relation

$$\frac{D_d}{D_\omega} = \frac{\chi_d M_d - K_a V_d}{\chi_\omega M_\omega - K_a V_\omega},$$

where  $D_d$  and  $D_\omega$  are the deflections due to the diamond and water;  $\chi_d$ ,  $M_d$  and  $V_d$  are the mass susceptibility, mass and volume respectively of the diamond,  $\chi_\omega$ ,  $M_\omega$  and  $V_\omega$  are those for water and  $K_a$  the volume susceptibility of air at room temperature. The volume of diamond was calculated from its mass, assuming its density to be  $3.5$ . The volume susceptibility of air was taken as  $0.0296$ . The working of the apparatus was tested by determining the susceptibility of pure samples of  $KCl$ ,  $NaCl$ , etc., and the standard values were obtained within an error of  $1\%$ . For each specimen, independent repetitions were made and values differing by about  $\frac{1}{2}\%$  were obtained.

*3. Results*

The values obtained for the susceptibility of diamond and the description of the shape and colour of the specimen are tabulated below.

Catalogue No.	Mass in mgm.	Shape	Colour	$-X \times 10^6$
14	177.0	Irregular crystal	Light brown	.456
8	278.0	Regular crystal	Colourless	.455
224	195.5	Faceted tablet	do.	.452
27	343.8	Regular crystal	do.	.451
12	183.5	Irregular crystal	Pale yellow	.450
9	222.5	Regular crystal	Colourless	.450
47	46.6	do.	do.	.449
19	56.3	Irregular crystal	Yellow	.448
199	24.2	Cleavage plate	Colourless	.447
226	39.0	Faceted tablet	Pink	.447
48	42.0	Cleavage plate	Colourless	.446
16	173.6	Irregular crystal	Light yellow	.446
22	41.1	Regular crystal	Colourless	.445
24	31.8	do.	do.	.445
209	49.5	Cleavage plate	do.	.444
206	38.6	do.	do.	.444
207	65.8	do.	Light brown	.443
179	56.8	do.	Colourless	.443
6	341.1	Irregular crystal	Light yellow	.442
197	88.0	Cleavage plate	Light brown	.441
23	37.7	Irregular crystal	Colourless	.440
20	54.3	Regular crystal	do.	.438
18	61.3	do.	do.	.438
21	50.2	do.	do.	.437
200	49.1	Cleavage plate	do.	.437
201	23.4	do.	do.	.437
223	54.7	Faceted brilliant	do.	.435
181	43.2	Cleavage plate	do.	.434
178	32.6	do.	do.	.433
210	47.1	do.	do.	.428
198	35.7	do.	do.	.428
13	182.4	Irregular crystal	do.	.426
5	342.6	do.	Brown	.421
39	75.7	Cleavage plate	Colourless	.418
29	29.9	Twin crystal	do.	.416
28	214.3	do.	do.	.411
*227	270.6	Faceted rod	Pale brown	.398
*30	93.6	Irregular crystal	Light brown	.372
*15	174.8	do.	do.	.326
*2	790.6	do.	Dark brown	.29

\* See Text.

*4. Discussion*

The above results show that the susceptibility of most of the specimens lie between  $-0.456$  and  $-0.411$ . The few specimens which give still lower values were examined for ferromagnetic impurities. No. 227 (pale yellow in colour) showed a definite fall of the numerical value of the susceptibility as the magnetising field was diminished (the values being  $-0.398$ ,  $-0.386$  and  $-0.366$  for magnet currents 4.5 amp., 3.5 amp. and 2.6 amp. respectively), thereby indicating the presence of ferromagnetic impurities in it.

These values of susceptibility were plotted against the corresponding values of  $1/H$  and the value at infinite field was obtained by extrapolation to be  $-0.448$ . Nos. 30 and 15 (susceptibility  $-0.372$  and  $-0.326$  respectively) both light brown in colour and both having very small quantities of inclusions showed no variation of susceptibility with field strength. No. 2 a dark brown crystal having visible inclusions gave a very low value  $-0.29$ . In these cases the low value of susceptibility has to be attributed to the inclusions. It is a surprising and remarkable fact that some of the coloured diamonds gave the normal values. No. 226 is pink; No. 19 is yellow, Nos. 14, 12, 6 and 16 are light yellow or brown and these specimens gave values ranging from  $-0.456$  to  $-0.442$ . In these cases, if impurities are present, their effect on the susceptibility is unobservable. A comparative study of the values with the other properties shows that there is no systematic variation of susceptibility with the difference in shape or colour. There is also no correlation between the susceptibility and fluorescence. For example, 224 is a colourless diamond with an intense blue fluorescence, 47 is faintly luminous, 48 has a strong green fluorescence and 206 is non-fluorescent and they gave very nearly the same values ( $-0.452$ ,  $-0.449$ ,  $-0.446$  and  $-0.444$  respectively). Similarly, there is no correlation between the susceptibility and the differences in ultra-violet absorption or photo-conductivity.

The susceptibilities found by the author are slightly lower than the values obtained by the previous authors. Honda (1910) obtained the value  $-0.49$ , Paramasivan (1929) obtained the value  $-0.47$  while P. Pascal\* (1923) and S. Meyer\* (1899) gave values  $-0.52$  and  $-0.33$  respectively.

The effect of illuminating the diamond on its susceptibility was investigated with two crystals, No. 224 and No. 48, the former being intensely blue fluorescent and the latter strongly green fluorescent. The sensitiveness of the apparatus was increased considerably by using a fine quartz fibre for the suspension of the beam, which gave large angles of torsion for the force acting on the diamonds and by detecting the deflection of the beam by the lamp and scale. The deflection due to the diamond was compensated by suspending in the magnetic field a container slightly above the diamond and adding bits of aluminium wire to it. When an intense beam of light from a carbon arc was focussed on the diamond by a condensing lens, after cutting off the infra-red, no change in the reading of the scale was detected.

---

\* Quoted by J. W. Mellor.

In conclusion the author wishes to record his deep sense of gratitude to Professor Sir C. V. Raman, for his helpful interest and encouragement in this work.

### 5. Summary

The magnetic susceptibilities of 40 specimens of diamond were measured with a Curie balance. The specimens employed were very varied in their physical properties, *viz.*, colour, absorption, luminescence and photoconductivity. No systematic changes in the susceptibility with the differences in these properties were found. The values obtained ranged between  $-0.456$  to  $-0.411 \times 10^{-6}$ . They are slightly lower than those found by earlier workers.

Observations on two specimens of highly fluorescent diamond showed that there was no change of the magnetic susceptibility, when they were exposed to an intense beam of light.

### REFERENCES

Honda, K.	.. <i>Ann. d. Phys.</i> , 1919, <b>32</b> , 1027.
Paramasivan, S.	.. <i>Ind. J. Phys.</i> , 1929, <b>4</b> , 139.

# THE PHOTO-CONDUCTIVITY OF DIAMOND

## Part I. Experimental Results

BY DEVI DATT PANT

(From the Department of Physics, Indian Institute of Science, Bangalore)

Received April 26, 1944

(Communicated by Sir C. V. Raman, Kt., F.R.S., N.L.)

### 1. Introduction

AMONGST the many remarkable properties of diamond is that when illuminated by visible or ultra-violet radiation, it has a detectable electrical conductivity, while ordinarily it is an excellent insulator. This property of diamond which it shares with certain other highly refractive solids was discovered by Gudden and Pohl (1920) and was the subject of extended researches by them designed to elucidate the nature of the phenomenon. Under controlled conditions of illumination and applied voltages, Gudden and Pohl observed what they describe as the primary photo-electric current, which under appropriate conditions satisfied the quantum equivalence law, namely the release of one electron per absorbed quantum of radiation. With stronger or more prolonged illumination and larger applied voltages, what is known as a secondary current is produced. The action of red light in producing an extra current in previously illuminated diamond is another remarkable phenomenon studied by Gudden and Pohl.

Even in these earliest researches, it was clear that not all diamonds behaved alike. Gudden and Pohl found that the photo-conductivity was much more conspicuous with one specimen which was transparent to ultra-violet radiation upto  $\lambda$  2300 A.U. than with two others which were opaque to wavelengths smaller than  $\lambda$  3000 A.U. The spectral distribution of photo-conductivity was also different. In the former case the curve had a pronounced tail, the photo-current continuously rising with shorter wavelengths, while in the latter there was a maximum at approximately  $\lambda$  3400 A.U. and a minimum at  $\lambda$  3000 A.U. followed again by a rise in the photo-current for still smaller wavelengths. In their later work, Gudden and Pohl (1922) found a marked selective effect for incident light at  $\lambda$  2260 A.U. Generally similar results have been observed by other workers, notably Robertson, Fox and Martin (1934). These authors found that the differences in ultra-violet transparency and photo-conductivity were accompanied

by differences in the infra-red absorption spectrum, and they therefore suggested a formal recognition of the existence of two distinct types of diamond. But that such a classification is inadequate to explain the facts is evident even from their own observations. The spectral distribution curves of photo-conductivity reproduced in Fig. 13 on page 505 of their memoir for four ultra-violet transparent diamonds differ widely amongst themselves, indeed nearly as much as any one of them differs from the spectral distribution curves for the two ultra-violet opaque diamonds given in Fig. 12 on page 503 of the same paper. Both in respect of the actual magnitude of the photo-current and the shape of the spectral distribution curve, their six diamonds,  $D_{24}$ ,  $D_{16}$ ,  $D_{22}$ ,  $D_2$ ,  $D_1$  and  $D_{10}$  evidently form a continuous sequence. The suggested classification of diamonds into two distinct types is therefore incapable of describing the facts in respect of photoconductivity in a satisfactory manner.

It is evident from what has been said that we cannot hope to understand the true nature and origin of photoconductivity in diamond unless we start with correct ideas regarding the crystal structure of the substance and its possible variations in different specimens. The introductory paper by Sir C. V. Raman of the present symposium (1944) deals with just these questions, and the results of that paper afford a fresh starting point for a consideration of the phenomena of photoconductivity and enable us to present an intelligible picture of the facts. In Part I of this paper, some observations by the author will be described which exhibit the wide range of variation of the phenomena amongst different specimens of diamond. The theoretical interpretation of the results will be considered in Part II.

## 2. *Experimental Arrangements*

The apparatus employed was a D.C. valve-bridge amplifier, the detailed working of which, with a circuit diagram, was described by Ananthakrishnan (1934). However, in the present case, the photo-electric cell of the set-up was replaced by a diamond holder. The latter was made of two brass rods which passed through two small ebonite pillars fixed on an ebonite base. The tips of the brass rods were made of lead which for its softness and stability was found to be more suitable than any other metal or graphite. The diamond could be tightly screwed between the two electrodes and good contact could be secured. The source of light was a quartz mercury arc of moderate intensity; the light from it was focussed on the diamond with a quartz lens. When required, the diamond could be illuminated simultaneously with red light from the opposite side, *viz.*, the white light from a 500-watt tungsten lamp filtered through a red glass. The high tension

source was a set of dry batteries giving up to 250 volts. The same high tension set was used for the plate voltage of the amplifier as well as for applying a voltage to the diamond. The linearity of amplification was tested by measuring the photoconductivity of a specimen of diamond at different voltages (small compared to the saturation potential of the photo-current in diamond). The strict proportionality found between the applied voltage and the corresponding observed current showed the correct working of the amplifier.

It was found necessary, at least in some cases, that the diamond should be heated to a temperature of nearly 100° C. to remove any dark current due to moisture or previous excitation of the crystal. Since the applied voltage was small and the intensity of the mercury arc not very great, troubles due to secondary currents were mostly absent. An ordinary needle-galvanometer, therefore, served the purpose of measuring the photo-currents. However, a few diamonds which showed secondary effects on being illuminated for too long a time were examined by applying a smaller voltage to them. In each case, therefore, only the primary photo-electric current was measured.

The photo-conductivity of numerous diamonds from the personal collection of Sir C. V. Raman was measured, as far as possible under identical conditions. The crystals were either sandwiched between the electrodes so that the light entered through the edges of the plate (position A), or they were screwed tightly between them such that one of the broad faces alone could be illuminated (position B). Most of the diamonds studied were cleavage plates having a thickness of between half a millimetre and one millimetre, their linear dimensions varying between a few millimetres and one centimetre. Owing to the varying thickness and area of the plates, any comparison of the photo-currents obtained with them is necessarily only qualitative. Nevertheless, the variation in the magnitudes of the primary photo-currents observed in position A with different diamonds was so marked, that it could easily be recognised as due to an inherent property of the diamond and not to its varying dimensions. This becomes clearer on correlating the variations in photo-conductivity with the variations in other properties of the diamond.

### 3. *Photo-Currents under Ultra-Violet Irradiation*

Tables I, II and III give the values of the photo-currents of 36 diamonds arranged in the decreasing order of magnitude of the photo-currents observed in the position A. For all these measurements, the illumination was the total light of the quartz mercury arc and the applied voltage was

150 volts. The 36 diamonds have been grouped in three tables according to the magnitude of the photo-currents given by them in the position A. Table I refers to five diamonds giving high photo-currents of the order of  $10^{-8}$  ampere; Table II to eleven diamonds which give moderate photo-currents of the order of  $10^{-9}$  ampere and Table III to twenty diamonds giving small photo-currents of the order of  $10^{-10}$  ampere. It will be noticed that the diamonds listed in the first two tables show higher photo-conductivity in the position A than in the position B, while under similar conditions, the diamonds appearing in the third table usually show slightly higher photo-conductivity in the position B than in position A.

TABLE I  
*Five diamonds exhibiting large photo-currents*

Unit =  $10^{-8}$  ampere

Diamond No.	Distance between electrodes in millimetres		Photo-current in the unit stated	
	Position A	Position B	Position A	Position B
208	0.62	3.4	7.0	1.0
227	2.10	3.1	3.0	1.5
39	1.12	4.9	2.5	0.5
57	0.75	..	2.0	..
206	0.63	3.9	..	0.5

TABLE II  
*Eleven diamonds exhibiting moderate photo-currents*

Unit =  $10^{-9}$  ampere

Diamond No.	Distance between electrodes in millimetres		Photo-current in the unit stated	
	Position A	Position B	Position A	Position B
201	0.53	3.5	5.2	0.9
207	0.94	3.8	5.0	2.0
48	0.82	5.4	5.0	0.8
209	0.71	4.3	4.0	1.8
200	0.74	4.7	4.8	0.6
47	2.50	2.5	1.8	1.8
199	0.68	3.6	1.6	1.3
202	0.72	2.7	1.5	1.8
198	0.59	4.2	1.4	1.0
195	0.60	5.9	1.4	0.7
49	2.40	2.4	1.1	1.1

TABLE III  
*Twenty diamonds exhibiting small photo-currents*  
 Unit =  $10^{-10}$  ampere

Diamond No.	Distance between electrodes in millimetres		Photo-current in the unit stated	
	Position A	Position B	Position A	Position B
31	0.96	4.2	9.6	8.8
36	0.76	5.8	8.7	12.0
210	0.64	4.7	8.0	0.8
180	0.48	5.5	7.6	3.2
45	0.68	4.7	7.6	9.6
197	0.88	3.1	5.6	8.8
53	0.78	4.0	5.2	2.5
196	0.62	2.6	4.8	2.4
188	0.71	4.7	4.8	2.4
221	0.68	5.1	4.0	11.0
211	0.55	4.3	4.0	4.0
187	0.52	5.4	4.0	4.4
171	0.67	3.5	4.0	1.2
224	1.52	7.4	4.0	2.8
41	1.10	4.7	3.6	1.8
34	1.20	7.2	3.2	1.8
40	2.70	..	3.2	..
181	0.60	4.6	2.0	4.0
184	0.81	3.1	2.8	0.8
38	0.85	7.0	1.6	4.0

#### 4. Photo-Conductivity in the Visible Spectrum

Table IV gives the spectral sensitivity data of a few selected diamonds showing high or moderate photoconductivity for wavelengths lying in the visible region. The source of light was a 500-watt pointolite lamp and the various regions of the visible spectrum were isolated by means of suitable light filters. The observations were made only in the position A.

TABLE IV  
*Five diamonds with large or moderate photo-conductivity*

Diamond No.	Applied voltage	Photo-current in amperes					
		White light	Red	Yellow	Yellow-green	Blue	Blue-violet
57	Volts 120	$4.0 \times 10^{-8}$	$2.7 \times 10^{-9}$	$1.5 \times 10^{-9}$	$9.0 \times 10^{-9}$	$1.2 \times 10^{-9}$	$1.0 \times 10^{-9}$
39	120	$7.6 \times 10^{-9}$	$2.0 \times 10^{-10}$	$1.4 \times 10^{-10}$	$1.5 \times 10^{-9}$	$1.0 \times 10^{-9}$	$6.0 \times 10^{-10}$
206	220	$4.2 \times 10^{-9}$	$8.0 \times 10^{-11}$	$4.0 \times 10^{-11}$	$3.2 \times 10^{-10}$	$7.6 \times 10^{-10}$	$4.4 \times 10^{-10}$
48	220	$1.6 \times 10^{-9}$	..	..	$1.2 \times 10^{-10}$	$2.8 \times 10^{-10}$	$1.6 \times 10^{-10}$
56	220	$8.4 \times 10^{-10}$	..	..	$1.6 \times 10^{-10}$	$8.0 \times 10^{-11}$	$6.0 \times 10^{-11}$

Table V gives the data for four weakly photo-conducting diamonds. The readings were taken both for the positions A and B, the source of light being the 500-watt pointolite lamp without any filters.

TABLE V  
*Four diamonds with small photoconductivity*

Diamond No.	Applied voltage	Photo-current in amperes	
		Position A	Position B
36	Volts 150	$4 \cdot 4 \times 10^{-10}$	$1 \cdot 2 \times 10^{-10}$
31	150	$4 \cdot 0 \times 10^{-10}$	$1 \cdot 2 \times 10^{-10}$
224	150	$3 \cdot 2 \times 10^{-10}$	$4 \cdot 0 \times 10^{-10}$
221	150	$1 \cdot 6 \times 10^{-10}$	..

It will be noticed that with these diamonds, white light gives a higher photo-current in the position A.

### 5. The Effect of Red Light

Ordinarily, no photo-conductivity is produced even with strong illumination by red or infra-red light. A very interesting phenomenon, however, arises when the diamond is illuminated simultaneously by strong red or infra-red light and by light of a shorter wave-length which excites photo-conductivity. It is then noticed that the photo-current given by the shorter wave-length light is greatly enhanced by the presence of the red light, increasing under suitable conditions to double its original value. The extra current produced by red light in the manner stated above is known as the positive primary, ersatz or substitution current. This effect was demonstrated by Gudden and Pohl as early as 1924 and it is of interest to study its variation in different diamonds. Table VI gives the data for the red light effect with some eighteen diamonds. It will be seen that it is conspicuously shown by the strongly and moderately photo-conducting diamonds, but is scarcely noticeable or altogether absent in the weakly photoconducting ones.

### 6. Secondary Current Phenomena

The primary photo-electric current which is observed when the crystal is illuminated for a short time starts or falls down to zero instantaneously with the imposition or cutting off of the irradiating light. But if the crystal is illuminated for too long a time, the current begins to increase and finally reaches a steady maximum value which is often several times the initial value.

TABLE VI  
*Effect of red light*

Diamond No.	Photo-current in amperes			
	Hg. Arc	Hg. Arc + Red light	Red light alone	Extra current due to red light
208	$7.0 \times 10^{-8}$	$10.0 \times 10^{-8}$	$2.4 \times 10^{-10}$	$3.0 \times 10^{-8}$
39	$2.5 \times 10^{-8}$	$4.2 \times 10^{-8}$	$2.0 \times 10^{-10}$	$1.7 \times 10^{-8}$
206	$2.0 \times 10^{-8}$	$2.8 \times 10^{-8}$	$8.0 \times 10^{-11}$	$8.0 \times 10^{-9}$
207	$5.0 \times 10^{-9}$	$7.4 \times 10^{-9}$	nil	$2.4 \times 10^{-9}$
201	$5.2 \times 10^{-9}$	$7.8 \times 10^{-9}$	nil	$2.6 \times 10^{-9}$
200	$4.8 \times 10^{-9}$	$6.8 \times 10^{-9}$	nil	$2.0 \times 10^{-9}$
209	$4.0 \times 10^{-9}$	$4.4 \times 10^{-9}$	nil	$4.0 \times 10^{-10}$
199	$1.6 \times 10^{-9}$	$2.0 \times 10^{-9}$	nil	$4.0 \times 10^{-10}$
195	$1.4 \times 10^{-9}$	$2.2 \times 10^{-9}$	nil	$8.0 \times 10^{-10}$
198	$1.4 \times 10^{-9}$	$1.9 \times 10^{-9}$	nil	$5.0 \times 10^{-10}$
210	$8.0 \times 10^{-10}$	$9.6 \times 10^{-10}$	nil	$1.6 \times 10^{-10}$
180	$7.6 \times 10^{-10}$	$8.0 \times 10^{-10}$	nil	$4.0 \times 10^{-11}$
86	$8.7 \times 10^{-10}$	$8.7 \times 10^{-10}$	nil	nil
221	$4.0 \times 10^{-10}$	$4.0 \times 10^{-10}$	nil	nil
31	$9.6 \times 10^{-10}$	$9.6 \times 10^{-10}$	nil	nil
45	$7.6 \times 10^{-10}$	$7.6 \times 10^{-10}$	nil	nil
224	$4.0 \times 10^{-10}$	$4.0 \times 10^{-10}$	nil	nil
184	$2.8 \times 10^{-10}$	$2.8 \times 10^{-10}$	nil	nil

of the primary photo-electric current. If the light is now cut off, this increased current, unlike the primary photo-electric current, does not fall down instantaneously but decays with a considerable time-lag. This current which starts as well as decays with a time-lag is known as the secondary current. High applied voltages and strong intensity of light help the production of the secondary current.

In the present case although high voltages were not applied, yet on continued illumination for a long time some diamonds did show secondary currents, the magnitudes of which were in some cases 3 to 5 times the initial or primary photo-electric current. On sufficiently lowering the applied voltage, no diamond showed the secondary current. The diamonds which gave the secondary currents are those listed in Table I and a few others, namely D202, D199, and D195, appearing in Table II. None of the diamonds appearing in Table III gives any secondary current. It should also be remarked that secondary currents developed much more promptly in the position A than in B. In fact D202, D199, D195 did not show any secondary currents in the position B.

As mentioned above, the secondary current persisted even after the illumination was cut off and as a result of this a "dark current" in other

words, a current without illumination was observed. A diamond in this state when exposed to light of a longer wave-length gave a current which was much larger than that obtained when this radiation was imposed on the normal diamond. With red light, this increased current showed a close relationship with the dark current and decayed in a manner similar to the latter, finally coming to a constant value which was still higher than that produced by red light in the normal diamond (Fig. 1, curves I and II). A somewhat similar effect has been described by Robertson, Fox and Martin (*loc. cit.*)

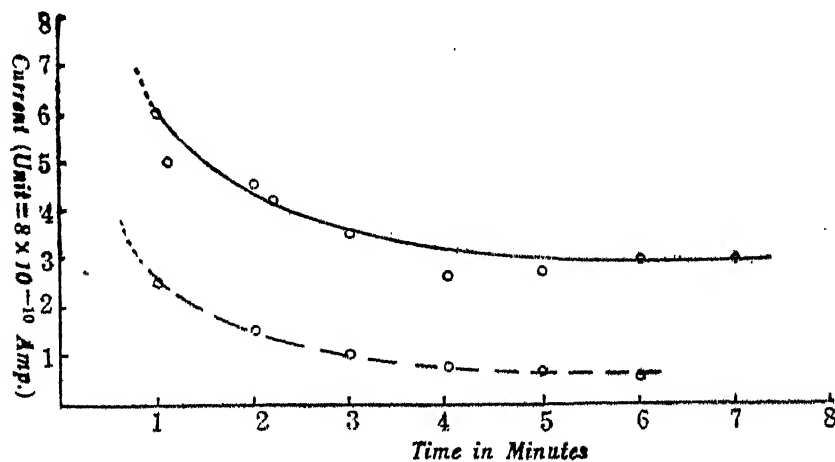


FIG. 1. Relation between  $I_r$  and  $I_d$

----- Curve showing the decay of  $I_d$  with time  
— Curve showing the decay of  $I_r$  with time

### 7. Relation to Other Optical Properties

The remarkable variations in photo-conductivity described above admit of being correlated with other properties of the specimens, namely (a) their transparency to the radiations exciting photoconductivity, (b) their absorption spectra, and (c) their luminescence. These latter properties have been studied extensively and are being reported on in other papers appearing in the symposium (Sunanda Bai, 1944; Rendall, 1944; Mani, 1944). It has accordingly been easy to establish the relationships between them and photoconductivity.

The division of the 36 diamonds into three groups (Tables I, II and III) according to the magnitude of the photo-currents developed under ultra-violet irradiation, also practically represents their classification according to their degree of transparency to the 2537 radiation of the quartz mercury

arc. The diamonds appearing in Table I are transparent to those radiations, those in Table II are partially transparent in greater or less degree, while those in Table III are practically opaque to those radiations. The absorption spectra of the diamonds appearing in the three Tables also differ widely. The diamonds in Table I have a transmission extending up to  $\lambda$  2250 A.U. in the ultra-violet and even beyond. Nearly all the diamonds in Table II show a similar transmission, but this is much weaker and there are several absorption bands in the region of wave-lengths greater than  $\lambda$  2250. The diamonds in Table III show strong absorption bands in the region between  $\lambda$  3000 and  $\lambda$  2800 A.U. and a practically complete extinction at shorter wavelengths. The diamonds in Table III may also be subdivided into two classes, those nearer the top of the table which are more or less completely transparent in the visible spectrum, and those nearer the bottom which show strong absorption bands in that region. A classification is also possible on the basis of the luminescence properties. The five diamonds listed in Table I are non-luminescent. Of the eleven diamonds in Table II D207 is non-luminescent, while the luminescence of all the others is very weak with the exception of the three yellow diamonds D200, D201 and D202. The twenty diamonds appearing in Table III are moderately or strongly luminescent. Those nearer the top of the table have relatively small intensities, while those near the bottom, especially D187, D224, D41, D34, D40 and D38 exhibit very intense luminescence. There is, thus, a clear inverse correlation between photoconductivity and luminescence in the diamonds studied.

In conclusion, the author wishes to express his indebtedness to Prof. Sir C. V. Raman for suggesting the problem and for guidance during the course of the work.

#### 8. Summary

The photo-conductivity of 36 diamonds, mostly in the form of polished cleavage plates, has been studied. They may be roughly classified into three groups showing respectively high, moderate or weak photo-conductivity. But there is no sharply defined demarcation between these groups and it is therefore not possible to make a clear-cut division of diamonds into two distinct types on the basis of their photoconductivity as proposed by Robertson, Fox and Martin.

The diamonds which are highly photo-conducting under ultra-violet irradiation are also those which give high photo-conductivity with visible light. They also exhibit the well-known red light effect and give rise on continued illumination to a secondary current which persists when such

illumination is cut off. A diamond in this state gives a larger current when illuminated by red light, and the magnitude of this is quantitatively related to that part of the secondary current which persists even without illumination. The weakly photo-conducting diamonds do not give these effects. The correlations which exist between photo-conductivity, ultra-violet transparency, spectral transmission curves and the intensity of luminescence of the diamond are pointed out.

## REFERENCES

Ananthakrishnan	.. <i>Proc. Ind. Acad. Sci.</i> , 1934, <b>1</b> , 205.
Gudden and Pohl	.. <i>Zeit. f. Phys.</i> , 1920, <b>3</b> , 123.
<hr/>	
Mani	.. <i>Zeit. f. Tech. Phys.</i> , 1922, <b>3</b> , 199.
Raman	.. <i>Proc. Ind. Acad. Sci.</i> , 1944, <b>19</b> , 231.
Rendall	.. <i>Ibid.</i> , 1944, <b>19</b> , 189.
Robertson, Fox and Martin	.. <i>Ibid.</i> , 1944, <b>19</b> , 293.
Sunanda Bai	.. <i>Phil. Trans. Roy. Soc.</i> , 1934, <b>232</b> , 463.
	.. <i>Proc. Ind. Acad. Sci.</i> , 1944, <b>19</b> , 253.

# THE PHOTO-CONDUCTIVITY OF DIAMOND

## Part II. Theoretical Considerations

BY DEVI DATT PANT

(From the Department of Physics, Indian Institute of Science, Bangalore)

Received May 19, 1944

(Communicated by Sir C. V. Raman, Kt., F.R.S., N.L.)

### 1. The Structure of Diamond

ACCORDING to the theory put forward by Sir C. V. Raman (1944), the crystal structure of diamond has four possible variants; two of these, namely, Td I and Td II, have tetrahedral symmetry and the remaining two, namely, Oh I and Oh II, have the full or octahedral symmetry of the cubic system. The structure of any actual specimen of diamond is, in general, composite and includes more than one of the possible variants. Thus, in the non-fluorescent and ultra-violet transparent variety of diamonds, the Oh I and Oh II sub-types interpenetrate giving rise to lamellar twinning; the two sub-types are separated in the crystal by extended surfaces of discontinuity or laminations and the diamond is highly non-homogeneous. In the blue-fluorescent and ultra-violet opaque variety of diamond, the Td I and Td II sub-types are present, interpenetrating each other. As these two sub-types are not physically but only geometrically different, such interpenetration is irregular and occurs without any composition planes. Hence, diamonds of this class have a much higher degree of crystal perfection than those in which the Oh I and Oh II are mingled. Nevertheless, the interpenetration of the Td I and Td II does give rise to a non-homogeneity of the crystal which shows itself in the development of luminescence in diamonds of this class. The irregularities of crystal structure are of an entirely different type from those observed in the non-fluorescent diamonds, being in the present case closely connected with the intensity of the luminescence exhibited. The theory indicates further the possibility of the mixing up of the tetrahedral and octahedral types of structure in various ways. When there is an intimate mixing of tetrahedral and octahedral structures, the diamond gives a yellow luminescence and is of an intermediate type; the diamond in parts may exclusively be of the transparent type and in others it may be of the other variety; finally, in some cases a small quantity of a particular variety may be embedded in the bulk of the other variety. On account of these different

possibilities, the properties of diamond vary greatly from specimen to specimen.

These conclusions find unmistakable support in the experimental results contained in the various papers appearing in the present symposium. However, from our point of view we wish to draw attention to the results regarding the imperfection or mosaicity of structure of diamond obtained from the X-ray studies made at this Institute by R. S. Krishnan (1944), P. S. Hariharan (1944) and G. N. Ramachandran (1944). These studies show clearly that the mosaicity of the ultra-violet transparent variety of diamond is of a very high degree and varies not only from diamond to diamond but also from place to place in the same specimen. On the other hand, the mosaicity of structure of the blue fluorescent diamonds is comparatively low and increases with the intensity of blue fluorescence. The yellow fluorescent diamonds in this respect also are intermediate between these types.

## 2. *The Photo-Electrically Active Centres*

In view of the extremely small magnitude of the primary photo-electric current and the absence of any definite threshold frequency for its generation, it is hard to believe that the normal atoms of the crystal form the photo-electrons. Gudden and Pohl expressed the opinion that only a few "privileged atoms" are responsible for photo-conductivity. These atoms, which are probably those situated at slight irregularities, form the photo-electrically active centres, while the normal atoms of the lattice remain photo-electrically inactive. If these conceptions are correct, the greater the mosaicity of structure, the greater should be the photo-conductivity of the diamond. The high photo-conductivity of the highly imperfect ultra-violet transparent variety of diamond and the low photo-conductivity of the more perfect ultra-violet opaque variety thus becomes intelligible. A slight anomaly is presented by the weakly photo-conducting, strongly blue-fluorescent diamonds, namely, that in such diamonds higher mosaicity gives lower photo-conductivity. But this is not surprising in view of the fact that the mosaic structure revealed by the intensity of X-ray reflections being closely connected with the intensity of luminescence, it produces the luminescent centres and not the photo-electrically active centres. That the two are quite distinct in the present case is obvious from the fact that while a photo-electrically active centre is ionised by the absorption of a suitable quantum and the liberated electron is raised to the condition level, the luminescence centre absorbs a quantum of radiation only to raise its electron to an intermediate level below the conduction band (production of an exciton). The dependence of the intensity of the 4152 absorption band on the intensity of

blue-fluorescence is a proof of this statement. Incidentally, since the absorbed energy is radiated again as luminescence energy, it is obvious that high intensity of fluorescence will only diminish the photo-conductivity. A close relationship between photo-conductivity and luminescence should be expected only in those solids where the mechanism of luminescence is analogous to that operating in the Lenard phosphors, *viz.*, when by the absorption of light energy, the electron is completely separated from the parent centre and is trapped at a distance from it, the luminescence occurring when the trapped electron comes back to the ionised centre.

### *3. The Spectral Distribution Curves of Photo-Conductivity*

An atom situated at a lattice defect will have one or more of its bonds ruptured due to the presence of the discontinuity, the electron or electrons of which the valence bonds are broken being attached to the atom only loosely. This atom, which for all practical purposes, may be taken as a combined electron-positive charge system, will be ionised by absorption of a lower energy quantum than is necessary for a normal atom of the lattice and will constitute a photo-electrically active centre. The energy of the quantum necessary to ionise the centre will depend on the strength of the binding of the electron to the positive charge. This in turn will depend on the degree of the rupture of the bond and the environment of the centre. The discontinuity will not equally affect all the atoms situated at it ; some will have their electrons more loosely bound than the others and so on. The centres would, therefore, not have a definite threshold frequency, and a long-wave-length tail in the spectral sensitivity curve would be an invariable accompaniment, the magnitude and the length of the tail depending on the mosaicity of the diamond. At the characteristic edge however, where the normal atoms of the lattice get ionised, the coefficient of absorption is so high that the whole phenomenon is confined to an extremely thin layer of the crystal. A high rate of absorption, therefore, naturally leads to a high rate of recombination and the two are probably so adjusted that before a liberated electron can move appreciably under an applied field, it recombines with the positive charge. The photo-conductivity, therefore, vanishes in the characteristic absorption region (Gurney and Mott, 1940). The spectral distribution curve of the transparent variety of diamond which has a pronounced long-wave-length tail, the photo-current dropping down at  $\lambda$  2250 A.U., is thus clearly understood. The selective excitation of photo-conductivity for  $\lambda$  2300 A.U. merely shows that the absorption of light is photo-electrically active in the volume of the crystal.

Sometimes, the normal atoms of the lattice absorb energy even in the region far removed from the characteristic absorption region and here also the

absorption is photo-electrically inactive. An interesting fact is then observed, namely, that though the quantity of absorbed energy is large, the observed photo-conductivity becomes less. The spectral distribution curve for photo-conductivity of the opaque variety of diamond shows a continuous rise in photo-conductivity upto  $\lambda$  3400 A.U. but for wave-lengths between 3400–3000 A.U., the photo-current falls down in magnitude, showing a minimum at  $\lambda$  3000. In the absorption spectra (Nayar, 1942), several absorption bands are observed in this region, clearly indicating that most of the energy absorbed is photo-electrically inactive and is spent only in raising the atoms to some higher levels. Even more interesting than this is the photo-conductivity of this variety of diamond in the region between  $\lambda\lambda$  3000–2250 A.U. Although the diamond is practically opaque to these wave-lengths, the photo-conductivity does not fall down to zero but rises, showing a broad maximum and falling down to zero only at  $\lambda$  2250 A.U. But the curious fact is that although the energy absorbed by this variety of diamond is far greater than absorbed by the transparent variety, the observed photo-conductivity is far smaller in the former case. The absorption is not photo-electrically inactive, since a considerable rise in the photo-conductivity is observed for these wave-lengths. The answer to this anomaly lies in the peculiar absorption characteristic of these diamonds. It is most probable that the characteristic absorption edge for these diamonds is also at  $\lambda$  2250 A.U. and that absorption of the type where simultaneous ionisation and recombination occur as described previously, takes place only at this edge. For other wave-lengths in the region between  $\lambda$  2250 A.U. and  $\lambda$  3000 A.U., the absorption coefficient may not be very high and the absorbed energy is then confined to a thin though not to an extremely thin layer of the diamond. The recombination between the positively charged ion and the electron produced by absorption of light does take place but only after the electron has moved a short distance (short compared to the mean free path). The photo-current will be smaller than expected on the quantum equivalence law, yet it will always be observed, the magnitude depending on the distance the electrons travel before recombination.

In the intermediate type of diamonds where the octahedral and the tetrahedral types of structures get mixed up, the spectral distribution curve of photo-conductivity also takes an intermediate shape depending upon the extent to which the diamond approaches more closely the opaque or the transparent variety. The diamonds D2 and D22, whose special sensitive curves are figured by Robertson, Fox and Martin (1934), appear to be of this intermediate type, D2 approaching rather closely to the opaque variety in its behaviour both in the magnitude of the photo-current given by it and in

the presence of a subsidiary maximum at  $\lambda$  3400 A.U. in the spectral sensitivity curve, which is quite analogous to that shown by their ultra-violet opaque diamonds D1 and D10.

#### 4. *The Secondary Current*

The quantity of electricity that flows in the secondary current is so large that it is impossible to interpret it as a simple photo-electric effect. It is generally believed that this current is generated in the crystal on account of the reduction in the resistance of the crystal brought about by the flow of the primary photo-electric current. In ionic crystals, Tubandt (1920-21), Joffe (1928) and Gudden and Pohl (1926) maintain that the secondary currents are due to the conductivity being ionic, but as Hughes and Du Bridge (1932) remark, an alternative explanation is necessary in the case of crystals like diamond.

We may expect that the same irregularities in the crystal structure which give rise to the production of the photo-electrically active centres also serve as good trapping centres for the liberated electrons. In crystals with repeated twinnings, tablets of compressed powders and some glasses, which may be regarded as the collection of tiny crystals welded together, the primary photo-electric current is largely suppressed and only a high secondary current is observed, except when the intensity of light is low and the applied voltage is small. The facts that even when the primary photo-electric current is large, time is required for the development of the secondary current, and that flaws and irregularities of structure help its production show that the trapping of electrons along the surfaces of discontinuity is responsible for the secondary current. If the discontinuity is such that it extends from one end of the crystal to the other even along irregular paths, in due course of time, due to the trapping of the electrons, a sort of "conducting channel" will be formed from one electrode to the other. The trapped electrons can deliver the charge from one place to the next close by, even if they are not free in the same sense as in the metallic conductors. All the trapped electrons are not equally free to move in the channel; those trapped in the vacant lattice points or at other obstacles are held more firmly than those which are in the middle of the channel. The electrons are attracted to the anode and at the same time they enter the crystal from the cathode, delivering charge from one place to the other in the manner stated above. The net result is a flow of electrons belonging to the metallic electrodes. Also, it is easy to see that due to the surplus of the electrons, all the positive ions left in the crystal would be neutralised in due course of time. Further, it is also clear that time would always be required for establishing and destroying

the "conducting channels" in the crystal and that the secondary current would always develop or decay with a time lag. It would develop more promptly if the primary photo-electric current be large and also if the thickness of the crystal between the electrodes be small. In the latter case, many more channels bridging over the electrodes can be formed, and it is due to these reasons that the secondary current is produced more easily in the diamond in the position A. It will also be seen that when all the conducting channels are established, the secondary current would reach a steady maximum value.

The absence of the secondary current in the opaque variety of diamond is due to the absence of the extended surfaces of discontinuity and the small magnitude of the primary photo-electric current.

### 5. Relation between $I_r$ and $I_d$

It is well known that when electrical charges are left behind in the crystal (the activated crystal), the absorption curve broadens towards the longer wave-lengths (Gudden and Pohl, 1925) and consequently the photo-electric effect for longer wave-lengths increases. From the picture given already for the production of the secondary current, it can be visualised that the trapped electrons will produce a similar effect on the atoms situated in the neighbourhood. This happens because the active centre which is more of a combined electron-positive charge system than an actual atom, is further influenced by the presence of the charge in its vicinity. If the trapped charge is an electron, it will attract the positive charge and repel the electron of the centre, producing a further instability in the centre. Again, if the trapped electron comes quite close to an active centre, the instability produced in the latter may be so great that it can now lose its electron even by the absorption of a quantum of red light. Any other active centre which is not close to the electron or which itself is not much affected by the discontinuity would not so much be influenced; only by absorption of a higher energy quantum than that of red light could such a centre be deprived of its electron. In short, the photo-conductivity of the crystal for longer wave-lengths would increase and on illumination by a long-wave-length light say, red light, it would give an increased current  $I_r$ . Since this increase is due to the presence of the trapped electrons,  $I_r$  must have a close dependence on their number. Again, as the dark current  $I_d$  (*i.e.*, decaying secondary current) depends on the number of the conducting channels and the latter on the number of the trapped electrons, a linear relation  $I_r - KI_d$  obviously follows. But not all the trapped electrons are capable of contributing to the dark current, for unless they are so arranged that a chain of them along the

channels from one end of the crystal to the other is created, their irregular distribution would not be of any help. But such electrons influence their neighbours as well as the electrons taking part in the production of the secondary current. Clearly, therefore,  $I_r$  is due to the sum of two currents, one produced by the presence of the electrons for the dark current and the other by the rest of the trapped electrons.

If, at any instant,  $N$  be the number of trapped electrons of which  $n_1$  are responsible for the dark current and  $n_2$  are irregularly distributed, we must have

$$I_d = xn, \text{ where } x \text{ is a constant.}$$

But  $I_r = K'y(n_1 + n_2)$  where  $K'$  depends on the intensity of red light and  $y$  depends on the number of centres per trapped electron which will be ionised by absorption of red light. Therefore,

$$\begin{aligned} I_r &= K'y\left(\frac{I_d}{x} + n_2\right) = K'\frac{y}{x}(I_d + n_2x) \\ &= K(I_d + n_2x) = K(I_d + a), \end{aligned}$$

where  $a$  depends on the degree of activation. It will be seen that this relation is the same as that obtained by Robertson, Fox and Martin (*loc. cit.*).

Now, when the trapped electrons are ejected out of the channels by an absorption of energy (or by thermal agitation) sufficiently large to overcome the potential barrier presented by the boundaries of the channel, the diamond would come back to its normal state. Not all but a great majority of these electrons would have the same potential barrier to overcome and, hence, although there would be no definite frequency necessary for bringing back the diamond to its original state, there would be an optimum frequency required for this purpose. Probably this corresponds to  $\lambda 2800$  A.U. Red light being unable to eject the electrons from their trapped position would continue to excite a constant current.

#### 6. *The Effect of Red Light*

This phenomenon has been explained by Gudden and Pohl by suggesting that the positive charges left behind in the crystal as a result of the removal of the electrons by the primary photo-electric current are released by the absorption of red light. A more specific theory of the effect of red light again has been put forward by Gudden and Pohl (1926) which suggests that due to the presence of the positive charges, a temporary photo-electric effect by longer wave-lengths becomes possible. Electrons are separated from the active centres until the accumulated charge builds up to a maximum value. At this stage, a sort of rearrangement (or local recrystallisation) takes place, whereby the location of the positive charges slips

towards the space element adjacent on the side next to the cathode. The commonly accepted view to-day is that not the positive charges but their locations slip towards the cathode (Hughes, 1936).

The principal effect of red light in producing the positive primary current should be the same as for the production of  $I_p$ , already discussed, the difference arising only due to the fact that the charges left behind in the crystals are positive charges, and not electrons. A particular space-element of the surface of discontinuity, after the separation of the primary photo-electric current, will have accumulated a large positive charge and will have formed what is called an excitation centre. Now, the total effect of the excitation centre will be so great on the neighbouring active centres that they can be ionised by the absorption of red light even if they are not quite close to it. The liberated electrons will travel to the anode under the external applied field and will be caught by the excitation centre, turning the latter into neutral centres. The location of the excitation centre will thus slip continuously towards the cathode by a repetition of this process (Fig. 1).

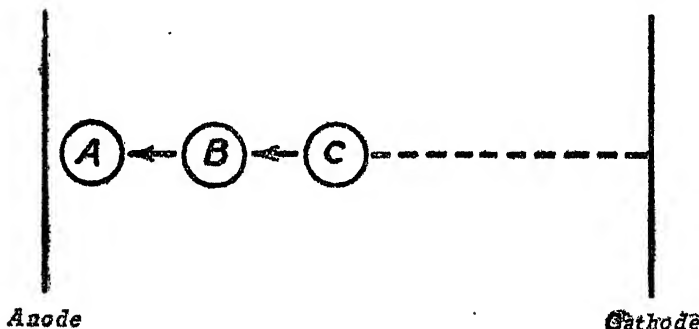


FIG. 1

It is easy to see that no electrons on the side towards the anode of the excitation centre can be released by red light after the excitation centre has begun to travel. For, as soon as the photo-electric effect in the centres (B) adjacent to the excitation centre (A) take place, A shifts to B. The liberated electrons have not time enough to reach the previous excitation centre A which still remains positively charged. The excitation centre at B, therefore, cannot release any positive charges from A and by continuation of the above process travels to C and so on.

It is easy to see now that as long as the active centres lie in the neighbourhood of the excitation centre so that by the presence of the latter a temporary photo-electric effect by red light is possible in them, the effect of red light will be observed. But as soon as this condition breaks down, the excitation centre can no longer slip towards the cathode, for the influence of

the positive charges on the normal atoms will be negligible. In the opaque variety of diamonds where there are only a very few centres and these are distributed in an irregular way, no positive primary current will be observed.

In conclusion, the author wishes to express his grateful thanks to Sir C. V. Raman, Kt., F.R.S., N.L., with whom he has had many useful discussions on the topics dealt with in this paper.

### 7. Summary

The variations in the photo-conductivity of diamond have been explained in this paper on the basis of the variations in the structure of the crystal, evidence for the existence of which is forthcoming from other directions, especially the study of the X-ray reflection intensities. Assuming that the non-homogeneities and irregularities in the crystal produce the photo-electrically active centres, the differences in the magnitudes of the photo-currents given by the different types of diamonds are explained. Various other observed facts regarding photo-conductivity also become intelligible, *viz.*, the spectral distribution curves of photo-conductivity, the absence of a definite threshold frequency, the effect of red light, and the production of a secondary current. The differences between the spectral distribution curves for the ultra-violet opaque and transparent types of diamond, and in particular the rising of the curve for wavelengths below 3000 A.U. are explained. A theoretical relation is also derived connecting the magnitude of the dark current and that of the current produced on excitation by red light.

### REFERENCES

1. Gudden, B., and Pohl, R. .. *Zeits. f. Phys.*, 1921, **8**, 248.
2. \_\_\_\_\_ .. *Ibid.* 1925, **35**, 243.
3. \_\_\_\_\_ .. *Ibid.* 1926, **37**, 881.
4. Gurney and Mott .. "Luminescence," *Trans. Farad. Soc.* 1938, **69**.
5. Hariharan, P. S. .. *Proc. Ind. Acad. Sci., A.*, 1944, **19**, 261.
6. Hughes, A. L. .. *Rev. Mod. Phys.*, 1936, **8**, 294.
7. Hughes, A. L. and Du Bridge, L. A. .. *Photo-Electric Phenomena*, 1932, Ch. VIII.
8. Joffe, A. F. .. *The Physics of Crystals*, 1928, Ch. XIII.
9. Nayar, P. G. N. .. *Proc. Ind. Acad. Sci., A.*, 1942, **15**, 293.
10. Ramachandran, G. N. .. *Ibid.* 1944, **19**, 280.
11. Raman, Sir C. V. .. *Ibid.* 1944, **19**, 189.
12. Robertson, Fox and Martin .. *Phil. Trans. Roy. Soc., A.*, 1934, **232**, 463.
13. Tubandt, C. .. *Zeits. f. Anorg. Chem.*, 1920, **110**, 196; **115**, 105.
14. \_\_\_\_\_ .. *Ibid.*, 1921, **117**, 48.

# THE CRYSTAL FORMS OF THE PANNA DIAMONDS

BY S. RAMASESHAN

(From the Department of Physics, Indian Institute of Science, Bangalore)

Received May 19, 1944

(Communicated by Sir C. V. Raman, Kt., F.R.S., N.L.)

## 1. Introduction

THE opportunity for the present study arose from the visits made by Sir C. V. Raman two years ago to the State of Panna in Central India where diamonds have been mined since very ancient times. One result of these visits was the acquisition by him of 29 diamonds in their natural state as crystals. This material has been placed at the disposal of the author for a report on the crystal form of these specimens. Not one of them exhibits the plane faces and straight edges demanded by the ordinary rules of crystallography. Nevertheless, several of them show a high degree of geometric symmetry, as also smooth lustrous faces and rounded contours which endow them with a distinctive beauty. They also show various other characteristic features which appear to merit careful study and description. It has been found convenient to adopt the usual crystallographic nomenclature in classifying the specimens, though this procedure has no strict scientific justification, even in the case of the more regularly shaped diamonds.

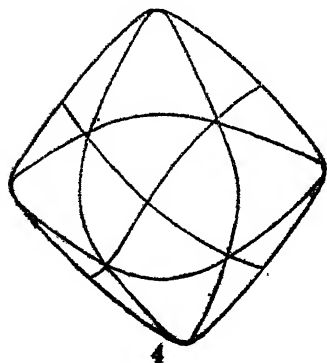


FIG. 4. Form of D9

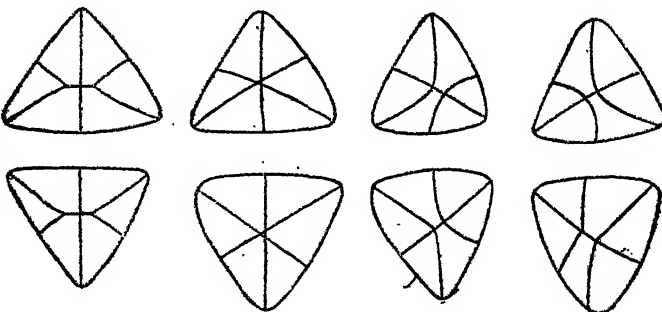


FIG. 5. The Eight Faces of D9

## 2. The Hexakis-Octahedral Forms

Three of the diamonds in the collection, namely D8, D9 and D27, approach sufficiently to the general form of the cubic system with 48 faces

to justify their being compared with it. Fig. 4 represents D9 which is the most perfect of this group. The resemblance, it will be noticed, is far from being exact. The six vertices or protuberances are, no doubt, present and convey to the eye the suggestion that the crystal has an octahedral form. The edges separating the octahedral faces are however missing, these regions being smoothly rounded off. The transverse curvature along them is sufficiently great, however, especially in D8 and D9, to suggest a resemblance to the octahedral form. Sharp edges cutting across the octahedral faces and dividing them into segments are observed. Four such edges meet at each vertex of the octahedron and run across to the opposite vertex, intersecting at or near the centre of the faces. Since, however, the octahedral edges are absent, the curved surface of the crystal appears actually divided up into 24 clearly defined and approximately equilateral triangles and not into the 48 faces required for the hexakis-octahedron. It should be remarked also that the angle between the curved surfaces meeting along these edges is highly variable. It is greatest near the vertices of the octahedron and diminishes to a relatively small value midway between them. This circumstance makes the observed form tend somewhat towards the triakis-octahedron.

There are, however, certain minor irregularities. Instead of the edges meeting exactly at the centre of the octahedral faces, they may deviate slightly, or even meander, with the result that their meeting point is on one side or another of the centre. The edges in such cases do not run a continuous course from each vertex to the opposite one. It is an interesting point that in D9 even these irregularities appear symmetrically. Fig. 5 shows its eight octahedral faces, their features being qualitatively indicated and parallel faces being drawn one above the other.

D27 is the largest of the three diamonds and weighs 341 milligrams. It has a grey tinge which is probably superficial. D8, which is the next in size and weighs 279 milligrams, has a delicate greenish tinge which is particularly evident at the octahedral tips. This is a superficial tint characteristic of many of the best Panna diamonds which disappears when they are cut and polished (Sinor, 1930). D9 which weighs 226 milligrams is perfectly colourless. Both D8 and D9 have lustrous surfaces, while D27 has rather a dull appearance.

### 3. *The Tetrakis-Hexahedral Forms*

The six diamonds D18, D20, D21, D22, D24 and D25 may reasonably be compared with this ideal form. They are relatively small diamonds weighing 61, 56, 51, 41, 32 and 22 milligrams respectively. All of them

have the common feature that the surface of the crystal appears divided up into 24 distinct areas bounded by sharply defined edges. These are, however, not plane figures but are curved surfaces, with the result that all these diamonds, at a first glance, appear like small transparent globules. These features will be evident from the photographs of D18 and D20 in Plate XXIX which are the two largest diamonds in the group. It is evident that the three diamonds described in the preceding section, and the six now under consideration, have in reality the same basic form, a solid having 24 curved faces bounded by sharply defined edges. These edges meet on the surface quite exactly at six vertices in groups of four each and more or less exactly at eight points in groups of six each. In the ideal case, therefore, the surface appears divided up into 24 triangles. The general shape of the crystal is determined by the size and shape of these triangles, as well as by the angles which they make with each other along the lines where they meet:

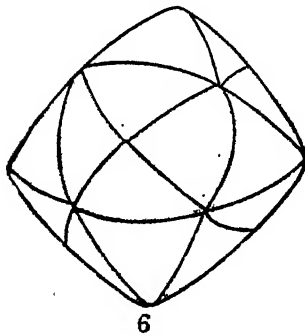


FIG. 6. Form of D18

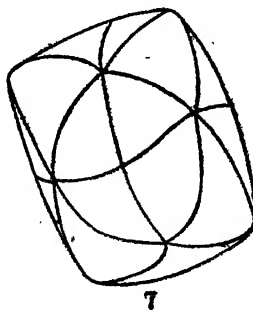


FIG. 7. Form of D20

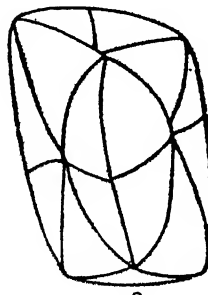


FIG. 8. Form of D21

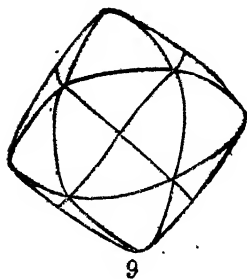


FIG. 9. Form of D22

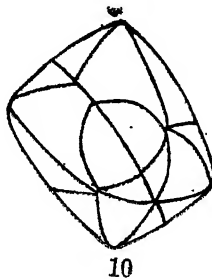


FIG. 10. Form of D24

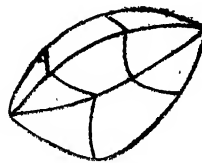


FIG. 11. Form of D25

Each of the six diamonds has 6 protuberances like those of the octahedron or the tetrakis-hexahedron, but they are not equally prominent in all the crystals. They are particularly conspicuous in D18 and D22 which most nearly resemble the ideal form and less conspicuous in the other four

iamonds. The angle between the faces meeting along the shorter diagonal of the rhombus (Fig. 6) is much less than that between the faces which meet along one of its sides, thereby suggesting an approach to the dodecahedral form. This is a common feature in the Panna diamonds. D20 (Fig. 7) is a beautiful crystal which shows some resemblance to the octahedral form. Here again, the edges are sharp and clear. D21, D24 and D25 (Figs. 8, 10 and 11) are ellipsoidal crystals which are comparatively irregular. The faces are unequal and the edges meander so much that it would not be correct to call some of the faces triangular in shape. These irregularities are evident from the figures. D25 in some positions, presents a very flat surface which is divided into 6 faces. Such a view is portrayed in Fig. 11.

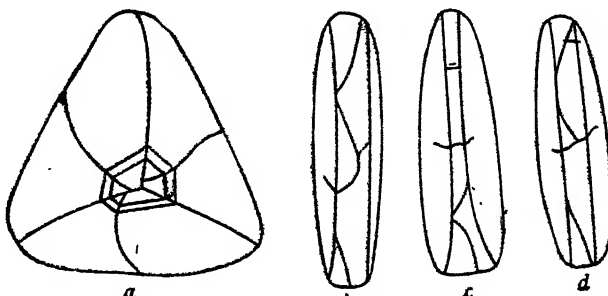


FIG. 12. Front and Edge Views of D28

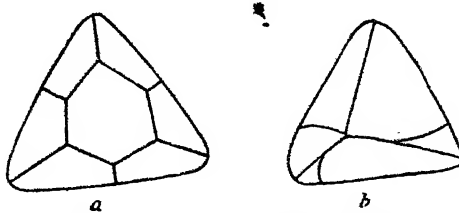


FIG. 13. Front and Rear of D29

The remaining crystals can only be classed as irregular and most of them are heavy distortions of the tetrakis-hexahedron. These diamonds can be divided into two groups, those which are colourless and transparent and those which are coloured yellow or grey. Some irregular crystals are illustrated in Fig. 2, Plate XXIX. As examples, a few of them are described below.

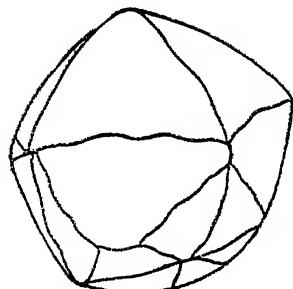
D3 is a colourless transparent crystal which appears highly distorted, but a close examination shows that it resembles a hexakis-octahedron whose growth has been restricted in one particular direction. The crystal can be described as a hexakis-octahedron cut by a plane which is approximately parallel to one of the octahedral faces. This intersecting plane is

a natural face and it has six well-marked lines on it which divide it into six segments. The crystal exhibits practically all the characteristics of the hexakis-octahedron which have already been described. It weighs 405 mgm.

D1 and D12 (Figs. 14 and 15) are both yellow crystals which are heavy distortions of the tetrakis-hexahedral form, but nevertheless display its characteristics. The most striking feature about these diamonds is the enormous variation in the area of the faces. The crystals are flattened and the flat portions are those where six faces meet. These faces are much larger in area than the others. The edges are sharp but wavy and are distinctly seen on the surface. The faces are curved but the variation in curvature is not always continuous as in the other diamonds. Sometimes on a convex surface, a small concave depression is present.

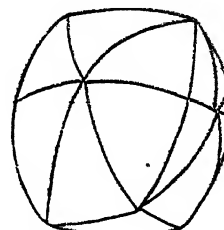
#### 4. Twinned Crystals

There are two flat triangular crystals in the collection which closely resemble the macked diamonds of the Kimberley mines and have been found by X-ray examination to be actually twins. D28 (Fig. 12) weighs 214 milligrams and D29 (Fig. 13) weighs 29.9 milligrams. The crystals appear to have 24 faces, 6 faces being found on either of the flat sides and the remaining 12 being distributed on the thin girdle which connects the two components. The line of demarcation or seam between the two components (which is a common feature of the Kimberley twins) is absent. The edge view presents distinct faces (Fig. 12 b, c, d). The edges on the flat side are fairly sharp ; but those on the thin sides are faint and wavy.



14

FIG. 14. Form of D1



15

FIG. 15. Form of D12

The two sides of D29 do not appear alike (Figs. 13 a and b). On one side there is a flat area which is full of rugged triangular pits. The faces are, as usual, curved and the curvature increases as one moves from the centre to the edge of the triangle.

*5. Surface Characters.*

The surface markings of the Panna diamonds show great variety and beauty. All the diamonds examined have striations on the surface, but their nature varies from crystal to crystal. The striae on the clear colourless diamonds are very close together and they have a kind of satiny sheen to the surface. They are so disposed on the octahedral face as to give the appearance of a spider's web. A microphotograph of such striations on D3 is given in Fig. 3 *a* in Plate XXX. The lines found on the yellowish diamonds are quite different. The surfaces reveal somewhat rough and bold striae, each face having two or three sets of such parallel lines. The criss-crossing of these lines gives a drusy appearance to the surface. Sometimes, but not often, tiny tetrahedral pits are found at the intersections of these lines. Under fairly high magnification the lines, although absolutely straight, are found to be discontinuous (Fig. 3 *c*) in Plate XXX. Most of the striations are parallel to the intersection of the octahedral planes with the surface.

The faint milky white appearance of D20 and D3 is due to the scattering of light by the large number of pits which abound on their surface. These pits are rather peculiar in nature, being circles with the circumference sunk into the diamond, the central area being shiny. Some of the pits are incomplete circles and occasionally only semi-circular. A few such pits are also seen in Fig. 3 *a*. D29 has triangular pits on its surface, all the triangles pointing in the same direction. Microscopic examination of these pits shows that they are really tetrahedral cavities with flat sides. Some of these sides are striated. The angle between two faces of a "trigon" was measured and was found to be near about the angle between the octahedral planes. A microphotograph of the pits on D29 is given in Fig. 3 *b* in Plate XXX.

*6. Photographic Study of the Diamonds*

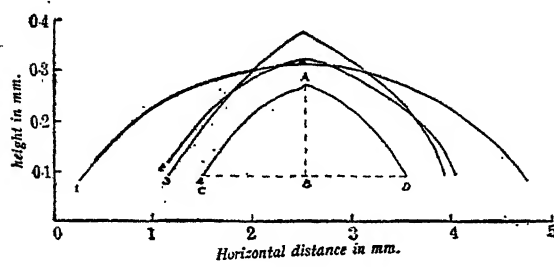
It is difficult to obtain a satisfactory photograph of a crystal of diamond showing the detail on its faces. The strong internal and surface reflections conspire to defeat any attempt to bring out the outlines and natural beauty of crystal form. However, in the case of small crystals, these difficulties are not insuperable. Seven out of the twelve photographs reproduced in Plate XXIX; viz., the representations of D20, D18, D9, D3, D12, D4 and D10, were obtained by illuminating the diamond obliquely and avoiding any direct reflection from its surfaces entering the camera. The remaining five pictures, viz., those of D27, D28, D9, D8 and D1 were obtained by photographing the diamond by its luminescence under ultra-violet irradiation. This was done by passing sunlight through a plate of Wood's

glass, a cell of sodium nitrite solution being used as a complementary filter. The bright patch at the centre of the green fluorescent D1 represents an intensely blue fluorescent region.

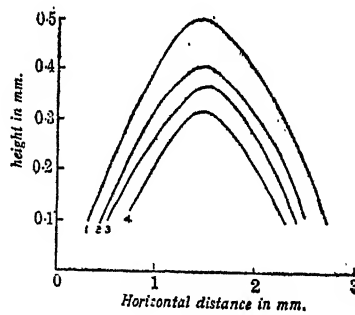
### 7. Measurements of Curvature

It appeared to be of interest to study the curvature of the surface in some of the more regular diamonds, and to find in what respects they differed from each other. As already stated, the surface of every such diamond consists of 24 similar triangles, and it is sufficient therefore to determine the configuration of the area included within a rhombus formed by a pair of adjacent triangles of this kind. The two vertices at the ends of the longer diagonal of the rhombus are points where four edges meet, and the two other vertices are points where six edges meet on the surface of the crystal. The measurements could be made by setting the crystal on the movable stage of a microscope and focussing the latter on a series of points on the area of the rhombus and reading off the vertical and horizontal displacements.

Figs. 16 and 17 represent the results of such a study for the four diamonds D9, D20, D18 and D22, the graphs for which are numbered serially in that order.



16



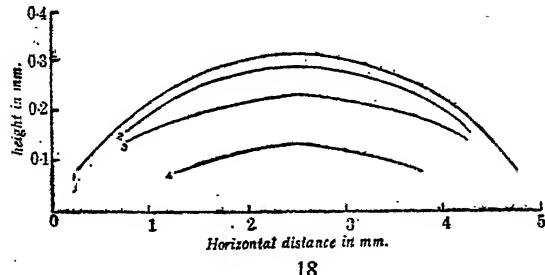
17

FIG. 16. Sections through the longer diagonal for D9, D20, D18 and D22

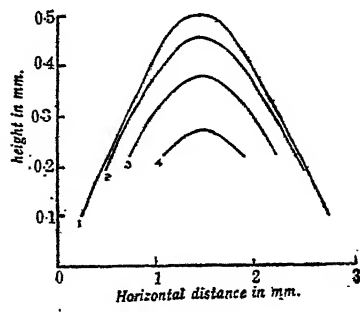
FIG. 17. Sections through the shorter diagonal for D9, D20, D18 and D22

It will be seen from the figures that the general shape of the section along the shorter diagonal is very similar for these four diamonds. On the other hand, the sections along the longer diagonal show conspicuous differences, the curve being very open in the case of the approximately octahedral diamond D9. A further idea of the configuration of the surface of this particular diamond is conveyed by Figs. 18 and 19 respectively, in which its sections by a series of planes 0.25 millimetre apart are shown. The

graphs are numbered in serial order moving away from the diagonal referred to in the caption of the figures.



18



19

FIG. 18. Sections of D9 by a series of planes parallel to the longer diagonal

FIG. 19. Sections of D9 by a series of planes parallel to the shorter diagonal

As we pass along the longer diagonal of the rhombus, we meet an edge or discontinuity of direction when crossing the shorter diagonal of the rhombus. This discontinuity is small, but it becomes more pronounced when we move to one side or another of the longer diagonal. This is shown by the series of graphs in Fig. 18. No such discontinuity is encountered as we move along the shorter diagonal or parallel to it, but the curvature becomes distinctly more marked as we approach the vertices of the rhombus (Fig. 19).

The angles between the tangents to the surface of the four diamonds at the ends of the longer and shorter diagonals were carefully measured. They are given in Table I together with the theoretical angles for the ideal geometric forms with which the crystals have been compared. It is clear from these figures that the crystals cannot in strictness be assigned to any particular form of the kind usually considered in geometric crystallography.

TABLE I

Crystal		Angle between ends of longer diagonals	Angle between ends of shorter diagonals
D9	..	152°	124° 30'
D20	..	144°	130°
D18	..	140° 30'	137° 30'
D22	..	140°	138° 30'
Tetrakis-hexahedron	..	143° 8'	180°
Octahedron	..	180°	109° 30'
Triakis-octahedron	..	180°	141°
Hexakis-octahedron	..	157° 30'	158° 30'
Dodecahedron	..	180°	180°

In conclusion, the author wishes to thank Prof. Sir C. V. Raman for his guidance throughout the course of this investigation.

### 8. Summary

The external forms and surface characters of 29 diamonds from the Panna mines in the personal collection of Sir C. V. Raman have been studied. Drawings and photographs of a selection from amongst them have been reproduced with the paper. In all the specimens examined, the surface of the crystal exhibits a set of sharply defined edges dividing up the area into 24 segments. In the best specimens, these segments have the shape of triangles, and the edges bounding them meet at points or vertices on the surface of the crystal respectively in groups of four and six. Measurements have been made of the curvatures of the surface in four of the best specimens. They show that these curvatures are highly variable both in an individual diamond and also as between different specimens.

### REFERENCE

Sinor, K. P.

.. *Diamond Mines of the Panna State*, 1930.

D27

D8

D9

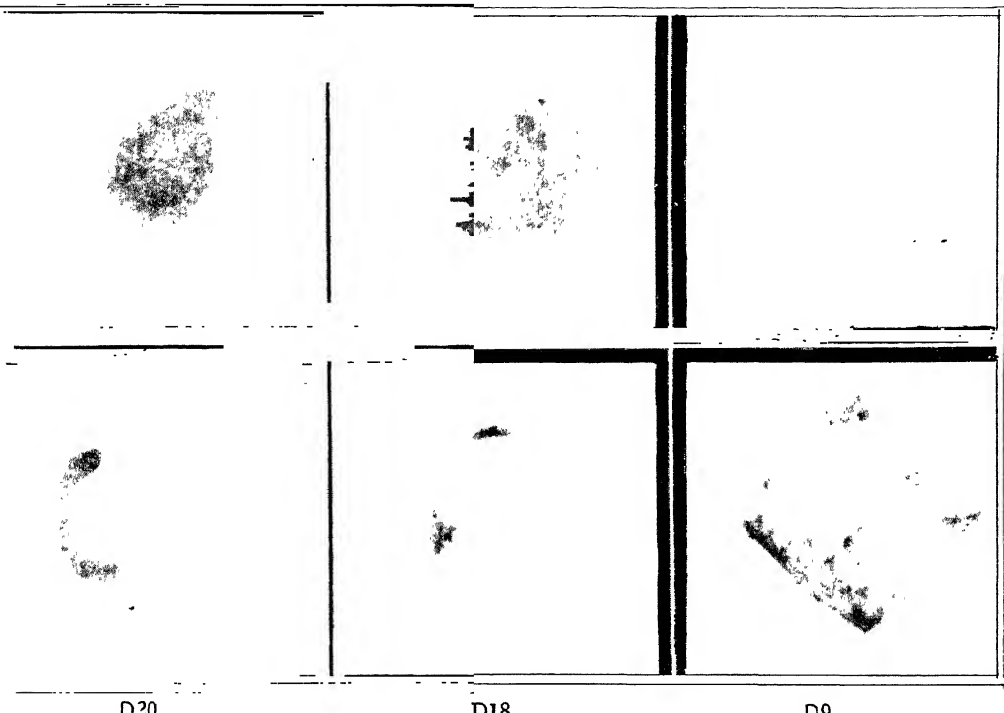


FIG. 1 Crystal Forms of Panna Diamonds

D3

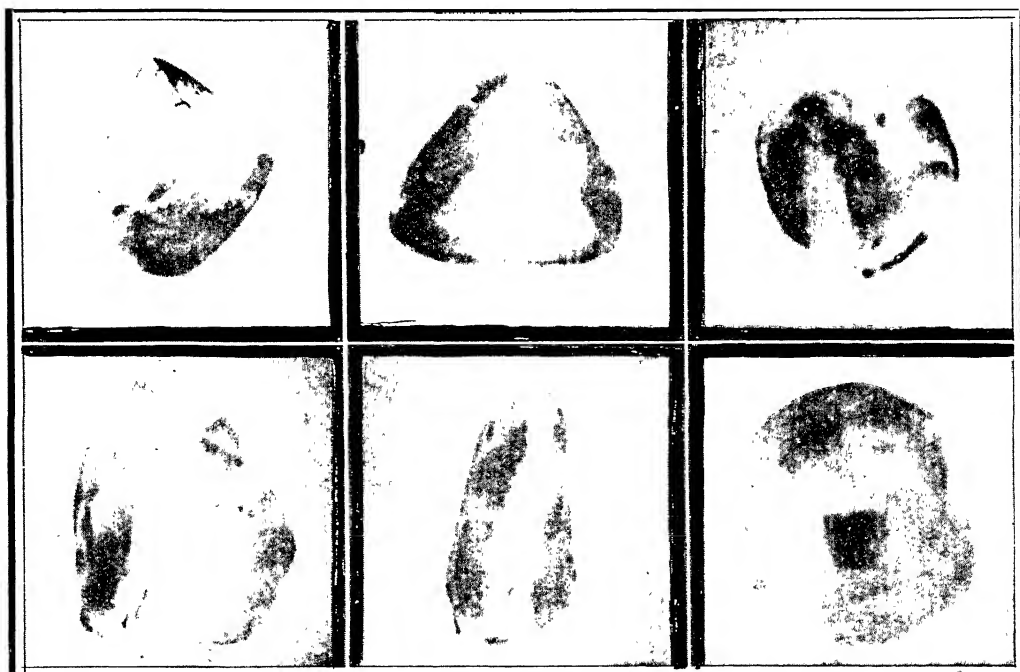
D28

D9

D20

D18

D12



D4

D10

D1

FIG. 2 Crystal Forms of Panna Diamonds

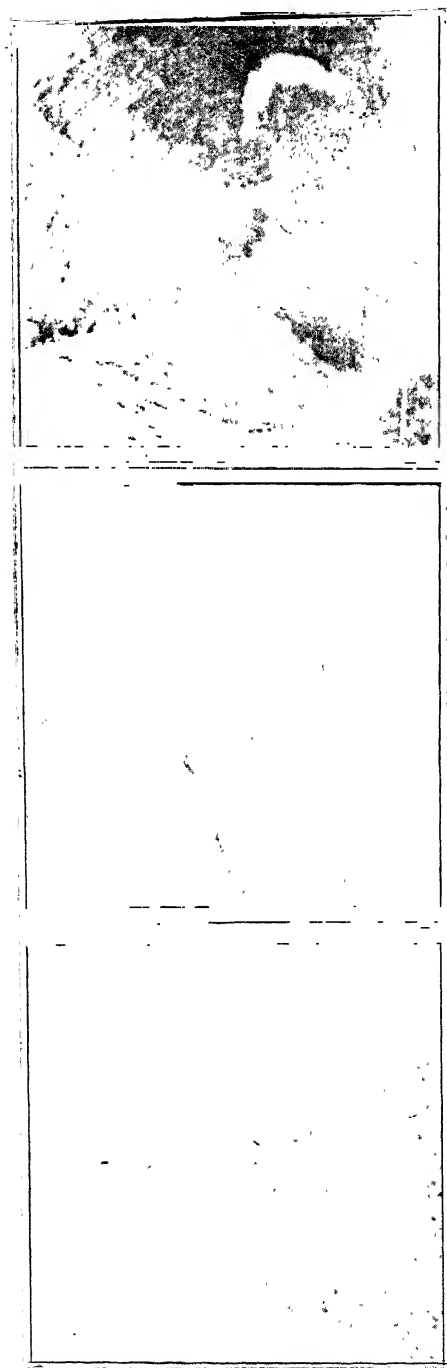


FIG. 3  
Surface Markings on Panna Diamonds

## BACTERIAL CHEMOTHERAPY

### IV. Synthesis of N<sup>4</sup>, N<sup>1</sup>-Diacyl Sulphanilamides\*

BY S. RAJAGOPALAN

(From the Haffkine Institute, Bombay)

Received January 3, 1944

(Communicated by Lt.-Col. S. S. Sokhey, M.A., M.D., I.M.S., F.A.Sc.)

THAT sulphanilamide acts by blocking the enzyme concerned in the utilisation of *para*-aminobenzoic acid (PAB), an "essential metabolite" in the bacterial cells of the susceptible organisms, by virtue of its structural resemblance to PAB, was first postulated by Fildes and Woods.<sup>2,3</sup> This concept has been extended,<sup>4</sup> in recent times, to cover the other well-known sulphonamides also: the varying potencies of the latter have been explained by the additional effect of the heterocyclic halves of their molecules on other metabolic processes peculiar to or more important to the particular bacterium under consideration.<sup>5,6</sup> In addition the hypothesis of Fildes and Woods receives its strongest support from the work of McIlwain and his collaborators, who by a study of the nutritional requirements of bacteria both in the presence and absence of antibacterial agents, were able to lay down successfully rules regarding structural specifications required for drug action in possible chemotherapeutics.<sup>7,8,9</sup>

Despite the proved adequacy of the Fildes-Woods theory of the mechanism of action of the sulphonamides, yet another theory, namely, the Acidic Dissociation Theory has been recently formulated by Schmelkes<sup>10</sup> and Fox and Rose.<sup>11</sup> According to these authors, considering the present theory as only a slight elaboration of the original concept of Fildes and Woods and the non-specificity of sulphonamide action observed by other workers,<sup>12</sup> the sulphonamides act by virtue of the similarities of their ions

$\text{R} \cdot \text{S} \begin{array}{c} \diagup \\ \text{O} \end{array} - \text{NH} -$  to the  $\text{R} \cdot \text{C} \begin{array}{c} \diagdown \\ \text{O} \end{array}^-$  of PAB. They also state that the anions of the sulphonamide acids, rather than the cations or the undissociated acids, exert the bactericidal action. In support, they adduce evidence to show that the minimal amount of each drug (ionised drug) needed for bacteriostasis is approximately the same, irrespective of the test organisms used.

\* A preliminary note on a few compounds reported in this communication appeared in *Current Science*.<sup>1</sup>

Although the acidic dissociation theory appears to open up new aspects of chemotherapeutical possibilities, exceptions can be taken to the theory in its present form. For instance, the hypothesis is founded on the classical conception of acids and consequently lays emphasis on acidic dissociation of the sulphonamides as an essential prerequisite for the antibacterial activity of the latter. On this basis it is difficult to explain the activity of the sulphonamides in which both the hydrogen atoms at the  $-\text{SO}_2\text{NH}_2$  have been substituted and which in all probability are unlikely to give rise *in vivo* to ionisable derivatives: examples of this class of compounds are the sulphanilyl derivatives of dimethyl amine,<sup>13,14</sup> diethylamine,<sup>13</sup> diethanolamine<sup>15,16</sup> and, of the  $\alpha$ -pyridyl,  $\alpha$ -thiazolyl and  $\alpha$ -thiazolinyl methylamines.<sup>17</sup> In contrast to the Fildes-Woods theory which is based on the structural specificity of the sulphonamide types, the acidic dissociation theory maintains that the heterocyclic halves of the sulphonamides contribute only to a greater capacity of the molecules for acidic dissociation. However, conception of the sulphonamides as acids in the more comprehensive, modern sense, postulated by Brönsted<sup>18</sup> and Lowry,<sup>19</sup> helps to remove the above and other apparent anomalies in the acidic dissociation theory which, it will be remembered, arise from the interpretation of acids in the classical restricted sense by the sponsors of the theory.

The acidic dissociation theory suggests the possibility that if sulphonamides could be rendered more "acidic" by suitable means more potent chemotherapeutics than those hitherto available could be obtained. It also raises the question whether by transformation of the sulphanilamide molecule itself compounds of the same acidity and the same degree of activity as the most powerful sulphonamides now known cannot be prepared. It appeared that these objects could be achieved by the incorporation of acyl radicals at the sulphonamide part of the molecule instead of the more difficult task of introducing heterocyclic ring systems at the N<sup>1</sup>-position of sulphanilamide. A search of the literature reveals that many compounds of the N<sup>1</sup>-acyl sulphanilamide type have already been disclosed.<sup>16,28</sup> Although they have not been investigated at length with the exception of "albucid", many of the straight chain derivatives and the N<sup>1</sup>-isocyclicacyl sulphanilamides are stated to be, weight for weight, as good as sulphanilamide in experimental streptococcal infections. On an equimolecular basis, these derivatives—some contain less than fifty per cent. of sulphanilamide—were definitely superior to sulphanilamide. These results are parallel to those obtained with some the higher straight chain N<sup>4</sup>-acyl sulphonamides,<sup>20</sup> which include a few therapeutically valuable members.<sup>21</sup> The case of albucid is remarkable: recent studies<sup>22</sup> have revealed it to possess not only a low order of toxicity

but also effectiveness, at least in some infections, in even sulphathiazole-resistant cases. Interesting data of a far-reaching nature may therefore be expected to accrue by a detailed study of members of the N<sup>1</sup>-acyl sulphamides group and by attempting correlation of the degree of dissociation of the N<sup>1</sup>-acyl sulphanilamides with their activity in experimental infections.

The author's interest in the N<sup>4</sup>-, N<sup>1</sup>-diacyl sulphanilamides was stimulated by the earlier attempt<sup>23</sup> to render the sulphonamides mycobactericidal by the further introduction of fatty acid groupings in their molecules. The present communication deals with the synthesis of a series of N<sup>4</sup>, N<sup>1</sup>-diacyl derivatives of sulphanilamide which are listed in the table.

Serial No.	Name	M.P./°C.	Nitrogen percentage	
			Found	Required
42	N <sup>4</sup> -n, Caproyl, N <sup>1</sup> -acetyl sulphanilamide	.. 166-69 dec.	8.8	9.0
43	N <sup>4</sup> -n, Caproyl, N <sup>1</sup> -n, butyryl sulphanilamide	.. 164-68	8.2	8.2
44	N <sup>4</sup> , N <sup>1</sup> -Di (n, caproyl) sulphanilamide	.. 164-72	7.9	7.6
45	N <sup>4</sup> -n, Caproyl, N <sup>1</sup> -n, heptyoyl sulphanilamide	.. 148-52	7.7	7.3
46	N <sup>4</sup> -n, Caproyl, N <sup>1</sup> -palmitoyl sulphanilamide	.. 123-26	5.6	5.5
47	N <sup>4</sup> -n, Caproyl, N <sup>1</sup> -stearyl sulphanilamide	.. 127-30	5.0	5.2
48	N <sup>4</sup> , N <sup>1</sup> -Di (n, butyryl-) sulphanilamide	.. 217-20	8.7	9.0
49	N <sup>4</sup> , N <sup>1</sup> -Di (n, heptyoyl-) sulphanilamide	.. 131-34	7.6	7.1
50	N <sup>4</sup> -n, Caproyl, N <sup>1</sup> -benzoylsulphanilamide	.. 180-83	8.0	7.5
51	N <sup>4</sup> -n, Caproyl, N <sup>1</sup> -cyclohexoxysulphanilamide	.. 185-87	7.3	7.3
52	N <sup>4</sup> -n, Caproyl, N <sup>1</sup> -cinnamoyl sulphanilamide	.. 228-31	7.1	7.0
53	N <sup>4</sup> -n, Caproyl, N <sup>1</sup> -(a, naphthoyl-) sulphanilamide	.. 154-57	6.8	6.5
54	N <sup>4</sup> -n, Caproyl, N <sup>1</sup> -(m, nitrobenzoyl-) sulphanilamide	.. 173-78	10.1	10.4
55	N <sup>4</sup> -n, Caproyl, N <sup>1</sup> -(p, nitrobenzoyl-) sulphanilamide	.. 222-30	10.0	10.4
56	N <sup>4</sup> , N <sup>1</sup> -Dibenzoyl sulphanilamide	.. 239-40	..	..
57	N <sup>4</sup> , N <sup>1</sup> -Dicyclohexoxyl sulphanilamide	.. 248-50	7.0	7.1
58	N <sup>4</sup> , N <sup>1</sup> -Dicinnamoyl sulphanilamide	.. 216-18	6.8	6.5
59	N <sup>4</sup> , N <sup>1</sup> -Di (p-nitrobenzoyl-) sulphanilamide	.. 251 dec.	11.7	11.9
60	N <sup>4</sup> , N <sup>1</sup> -Difuroyl sulphanilamide	.. 255 dec.	7.8	7.7
72	N <sup>4</sup> , N <sup>1</sup> -Di (p-nitrobenzoyl-) sulphapyridine	.. 232-34 dec.	13.0	12.9

From the standpoint of both the acidic dissociation and the Fildes-Woods theories, the presence of the grouping H<sub>2</sub>N-SO<sub>2</sub>·NH in the sulphonamide molecules is considered to be of fundamental physiological significance.<sup>3,5,1,24,25</sup> A stable structural alteration in this unit has been observed to be accompanied by a destruction of therapeutic activity and is comprehensible in the light of the finding that similar permanent alterations in the molecule of PAB depress or nullify<sup>3,2</sup> the growth-promoting action of PAB.<sup>37</sup> The synthesis of N<sup>4</sup>, N<sup>1</sup>-diacyl sulphanilamides may, perhaps, be considered as unproductive of interesting results on the ground that the significant, free amino group is not present in their molecules.

It may, therefore, be well, at this stage, to state the theoretical considerations for undertaking the synthesis of  $N^4$ ,  $N^1$ -diacyl sulphanilamides. In the synthesis of this type of compounds, in addition to the possibility of their proving mycobactericidal, a primary consideration was the relative ease with which they could be prepared as compared to the strictly  $N^1$ -acyl derivatives of sulphanilamide. Considering the smoothness with which some of the  $N^4$ -acyclic acyl sulphanilamides are cleaved to sulphanilamide<sup>24,27</sup> and the facility with which the  $N^4$ -acyl group is split off from  $N^4$ ,  $N^1$ -diacyl sulphanilamides,<sup>28</sup> the  $N^4$ -acyclic acyl,  $N^1$ -substituted sulphanilamides (Nos. 42-55) will, in all probability, give rise *in vivo* to the respective  $N^1$ -acyl sulphanilamides. It was, therefore, of particular interest to ascertain whether or not the observed therapeutic effect of this class of compounds may not after all be that of the  $N^1$ -acyl sulphanilamides themselves, modified or otherwise by the presence of the fatty acids simultaneously liberated. Such an enquiry was expected to lead to a study of the detoxication mechanisms involved in the passage of the active members through the animal body both in a state of health and disease. Again, the synthesis of the  $N^4$ ,  $N^1$ -isocyclic acyl sulphanilamides (Nos. 56-72) needs explanation. It is true that the lack of activity of the  $N^4$ -isocyclic or heterocyclic acyl sulphonamides, hitherto reported, is generally understood to bedue to the inability of experimental animals to hydrolyse aroyl or heteroöyl amide linkages.<sup>16</sup> Nevertheless, there are a few instances of this kind of  $N^4$ -substituted sulphanilamides, for example,  $N^4$ -furoyl sulphapyridine<sup>29</sup> and the  $N^4$ -nicotinyl,<sup>16,29,30</sup>  $N^4$ -quinolinyl,<sup>31</sup> and  $N^4$ -(5, pyrrolidone-2, carbonyl-<sup>32</sup>) and the  $N^1$ , 4'-(*p*-anisylidene-) or the  $N^1$ , 4'-(*p*-dimethylaminobenzylidene-) aminophenyl,  $N^4$ - acetyl sulphanilamides,<sup>16</sup> whose activity is consequently surprising and has not yet been plausibly explained. In the contemplation of the synthesis of the  $N^4$ ,  $N^1$ -diisocyclic acyl sulphanilamides, it was encouraging to find that a further substitution of the acyl group at the sulphonamide portion, even though exemplified so far in the isolated case of  $N^4$ ,  $N^1$ -dibenzoyl sulphanilamide,<sup>33</sup> is sufficient to render active an otherwise inert  $N^4$ -acyl sulphanilamide.<sup>34</sup> Unfortunately, an explanation for the activity of dibenzoyl sulphanilamide founded on experimental data has not yet been offered by the original investigators. Such an explanation would no doubt have a important bearing on the Fildes-Woods theory of sulphonamide action which lays emphasis on the role of a free or potential amino group in conditioning the physiological action of the sulphonamides. A study of the compounds, Nos. 56-72 was, for obvious reasons, expected to answer ultimately the question of whether or not the activity of  $N^4$ ,  $N^1$ -dibenzoyl sulphanilamide is the consequence of an inherent characteristic of this type

of compounds. The case of the *p*-nitrobenzoyl derivatives (Nos. 55, 59, 72) deserves mention. Judging from analogy,<sup>35</sup> they are to be expected to be reduced *in vivo* to the corresponding amino bodies; these latter, besides probably fulfilling the requisites for high anionic dissociation, would then represent compounds bearing a structural resemblance to the bacterial "essential metabolite". PAB different from the type obtaining in other sulphonamides.

Whether any or all of the expectations of this study will be realised can be settled only by actual biological trials. It is however reasonable to hope that even if no highly antibacterial agents are encountered in the group of compounds now synthesised, the present study would be atleast instrumental in shedding additional and useful light on the existing theories\* of the mechanism of action of the sulphonamides.

### Experimental

For the N<sup>4</sup>-*n*, caproyl, N<sup>1</sup>-substituted derivatives (Nos. 42, 43, 45, 46, 47, 50-55) of sulphanilamide, N<sup>4</sup>-*n*, caproyl sulphanilamide—reported<sup>34</sup> to be as antistreptococcal as sulphanilamide itself, but much less toxic—constituted the starting material: the condensations with the desired acid chlorides were carried out in pyridine medium. The remaining N<sup>4</sup>, N<sup>1</sup>-diacyl sulphanilamides (Nos. 44, 48, 49, 56-60) resulted directly by the operation of slightly more than 2 mols. of the appropriate acid chlorides on sulphanilamide itself in pyridine solution.

The condensation products, obtained by dilution of the reaction mixtures with excess of water, were severally purified usually through precipitation from their dilute sodium hydroxide solutions (charcoal) by acidification. They were mostly recrystallised from alcohol, the exceptions being Nos. 53, 56, 57 and 60 which were crystallised from acetone and No. 59 which was obtained from nitrobenzene. All these compounds (Nos. 42-60) were obtained as colourless needles.

The disubstituted pyridine derivative (No. 72) was prepared by similar action of 2 mols. of *p*-nitrobenzoyl chloride on sulphapyridine in the presence of pyridine. It separated from acetone as colourless plates.

The yields of the compounds reported in this paper were, in all instances, good.

\* While this MS. was under preparation, there has appeared an interesting paper by Bell and Roblin,<sup>36</sup> admirably correlating ionic dissociation with activities of the sulphonamide types.

The melting points of many of the compounds listed are not at all sharp in spite of their many recrystallisations and homogeneous crystalline structure: this appears to be an inherent characteristic, as has previously been observed<sup>28</sup> in the case of the N<sup>1</sup>-acyl sulphanilamide derivatives.

I desire to take this opportunity of expressing my indebtedness to Col. S. S. Sokhey but for whose kind interest and encouragement this investigation would not have been possible. I am also thankful to the Lady Tata Memorial Trust for the award of a Scholarship.

### Summary

With the object of exploring the group of N<sup>4</sup>, N<sup>1</sup>-diacyl sulphanilamides for practicable antibacterial agents and in view of the possibility of shedding further light on the existing theories of the mode of sulphonamide action by a study of the N<sup>4</sup>, N<sup>1</sup>-diacyl sulphanilamide type of compounds, a number of N<sup>4</sup>, N<sup>1</sup>-diacyl sulphanilamides, twenty in all, have so far been synthesised.

### REFERENCES

1. Rajagopalan .. *Curr. Sci.*, 1942, 11, 394.
2. Fildes .. *Lancet*, 1940, 1, 955.
3. Woods .. *Brit. J. Exp. Path.*, 1940, 21, 74.
4. Landy and Wyeno .. *Proc. Soc. Exp. Biol., Med.* 1941, 46, 59.
5. Straus *et al.* .. *J. Clin. Invest.*, 1941, 20, 189.
6. Green and Bielschowsky .. *Brit. J. Exp. Path.*, 1942, 23, 13.
7. Dorfman *et al.* .. *J. Bact.*, 1942, 43, 69.
8. McIlwain .. *Biochem. J.*, 1941, 35, 1311.
9. \_\_\_\_\_ .. *Lancet*, 1942, 1, 412.
10. \_\_\_\_\_ .. *Brit. J. Exp. Path.*, 1940, 21, 136; 1941, 22, 148; 1942, 23, 95.
11. \_\_\_\_\_ .. *Biochem. J.*, 1942, 36, 417.
12. \_\_\_\_\_ and Hawking .. *Lancet*, 1943, 1, 449.
13. Robinson .. *J. Chem. Soc.*, 1940, 505.
14. Barnet and Robinson .. *Biochem. J.*, 1942, 36, 364.
15. Harris and Kohn .. *J. Pharm. Exp. Therap.*, 1941, 73, 383.
16. Snell *et al.* .. *J. Amer. Chem. Soc.*, 1940, 62, 1776, 1791.
17. \_\_\_\_\_ .. *J. Biol. Chem.*, 1941, 139, 975; 141, 121.
18. Wyss .. *Proc. Soc. Exp. Biol. Med.*, 1941, 48, 122.
19. Fildes .. *Brit. J. Exp. Path.*, 1941, 22, 293.
20. Woods .. *J. Exp. Med.*, 1942, 75, 369.
21. Schmelkes *et al.* .. *Proc. Soc. Exp. Biol. Med.*, 1942, 50, 145.
22. \_\_\_\_\_ .. *J. Bact.*, 1942, 43, 71.
23. Fox and Rose .. *Proc. Soc. Exp. Biol. Med.*, 1942, 50, 142.

12. Schmidt and Hilles .. *J. Infect. Dis.*, 1939, **65**, 273.  
 Wyss *et al.* .. *Proc. Soc. Exp. Biol. Med.*, 1942, **49**, 618.  
 Green and Parkin .. *Lancet*, 1942, **1**, 205.

13. Fourneau *et al.* .. *Compt. rend. soc. biol.*, 1936, **122**, 258, 652.  
 Tréfouël *et al.* .. *Ann. inst. Pasteur*, 1937, **58**, 30.

14. Sakai and Yamamoto .. *J. Pharm. Soc. Japan*, 1938, **58**, 683.

15. Kolloff .. *J. Amer. Chem. Soc.*, 1938, **60**, 950.  
 Adams *et al.* .. *Ibid.*, 1939, **61**, 2342.

16. Northey .. *Chem. Revs.*, 1940, **27**, 85.

17. Rajagopalan, Ganapathi and others .. *Unpublished work.*

18. Brönsted .. *Rec. trav. chim.*, 1923, **42**, 718; *J. Phys. Chem.*, 1926, **30**, 777.

19. Lowry .. *Chem. and Ind.*, 1923, **42**, 43.

20. Miller *et al.* .. *J. Amer. Chem. Soc.*, 1939, **61**, 1198.  
 Moore *et al.* .. *Ibid.*, 1940, **62**, 2097.

Bergmann and Haskelberg .. *J. Amer. Chem. Soc.*, 1941, **63**, 2243.

21. Cooper *et al.* .. *Proc. Soc. Exp. Biol. Med.*, 1940, **43**, 491.  
 Hampil *et al.* .. *J. Pharm. Exp. Therap.*, 1941, **71**, 52.  
 Maxwell and Bazalis .. *J. Amer. Med. Assoc.*, 1941, **117**, 2238.  
 Hansen and Kreidler .. *J. Infect. Dis.*, 1942, **70**, 208.

22. Richard and Henderson .. *J. Pharm. Exp. Therap.*, 1941, **73**, 170.  
 Welebir and Barnes .. *J. Amer. Med. Assoc.*, 1941, **117**, 2132.  
 Robson and co-workers .. *Nature*, 1942, **149**, 581.  
 \_\_\_\_\_ .. *Brit. Med. J.*, 1942, **1**, 687.

Young *et al.* .. *J. Urol.*, 1941, **45**, 903.  
 Parentis and Kanealy .. *Ibid.*, 1942, **47**, 11.

23. Rajagopalan .. *Proc. Ind. Acad. Sci.*, 1943, **18**, 108.

24. Kohl and Flynn .. *Proc. Soc. Exp. Biol. Med.*, 1940, **44**, 445.  
 Bradbury and Jordan .. *Biochem. J.*, 1942, **36**, 287.

25. Tréfouël *et al.* .. *Compt. rend. soc. biol.*, 1935, **120**, 756.  
 Fourneau *et al.* .. *Bull. acad. Med.*, 1937, **118**, 210.  
 \_\_\_\_\_ .. *Compt. rend. soc. biol.*, 1938, **127**, 397.  
 Fuller .. *Lancet*, 1937, **1**, 194.

Molitor and Robinson .. *J. Pharm. Exp. Therap.*, 1939, **65**, 405.  
 Fuller and James .. *Biochem. J.*, 1940, **34**, 648.  
 Lewis and Tager .. *Yale J. Biol. Med.*, 1940, **13**, 111.

26. Kuhn *et al.* .. *Ber.*, 1942, **75**, 711.

27. Hansen and Kreidler .. *Loc. cit.*

28. Crossley *et al.* .. *J. Amer. Chem. Soc.*, 1939, **61**, 2950.

29. Kolloff and Hunter .. *Ibid.*, 1940, **62**, 1646.

30. Daniels and Iwamoto .. *Ibid.*, 1940, **62**, 741.

31. Hykes *et al.* .. *Compt. rend. soc. biol.*, 1937, **126**, 635.  
 Schering-Kahlbaum, A.-G. *Br.*, 1939, **502**, 558.

- 32. Gray *et al.* .. *Biochem. J.*, 1937, **31**, 724.
- 33. Dewing *et al.* .. *J. Chem. Soc.*, 1942, 239.
- 34. Miller *et al.* .. *Loc. cit.*
- 35. Kohl and Flynn .. *Proc. Soc. Exp. Biol. Med.*, 1941, **47**, 466, 470.
- 36. Bell and Roblin .. *J. Amer. Chem. Soc.*, 1942, **64**, 2905.
- 37. Rubbo and Gillespie .. *Nature*, 1940, **146**, 838.  
Lampen and Peterson .. *J. Amer. Chem. Soc.*, 1941, **63**, 2283.  
Moller and Schwartz .. *Ber.*, 1941, **74**, 1612.  
Kuhn and Schwartz .. *Ibid.*, 1941, **74**, 1617.  
Park and Wood .. *Bull. Johns Hopkins Hosp.*, 1942, **70**, 19.

## BACTERIAL CHEMOTHERAPY

### V. Synthesis of Phenolic Azo-dyes derived from the Sulphonamides

BY S. RAJAGOPALAN

(From the Haffkine Institute, Bombay)

Received January 3, 1944

(Communicated by Lt.-Col. S. S. Sokhey, M.A., M.D., I.M.S., F.A.S.C.)

THE effective chemotherapy of many bacterial infections with the sulphonamide group of drugs which has been possible in recent times owes its origin to the introduction of an azo-dye, *prontosil* in clinical practice by Domagk.<sup>1</sup> While very different explanations for the ways in which the various azo-dyes in therapeutic use<sup>2,3</sup> exert their antiseptic action have been advanced, opinion<sup>4</sup> concerning the mode of action of the azo-dyes derived from the sulphonamides, of which *prontosil* is one, is at the present time almost unanimous. Although by no means fully proved, it is generally believed that the therapeutic properties of the sulphonamido azo-dyes are primarily the therapeutic properties of the sulphamamide itself, which has resulted from reductive cleavage of the azo-linkage *in vivo* and this explains, to a great extent, the increasing disuse of the *prontosil* types in the treatment of acute bacterial infections.

It should be remembered that in addition to the sulphonamides resulting from these azo-dyes, amino phenols or aromatic polyamines are also at the same time liberated by the *in vivo* cleavage at the azo double bonds. It is, therefore, of interest to enquire whether or not the latter contribute in any manner to the observed final physiological effect. Previous knowledge of biological oxidations and the detoxication mechanisms of amino phenols, aromatic polyamines and the anti-hæmorhagic compounds<sup>5</sup> would suggest the possibility of production *in vivo* of quinonoid bodies from the "second ring" not bearing the sulphonamido group. This assumes great interest because many natural and synthetic quinones have recently come to be recognised as powerful antibacterial agents<sup>6</sup> and many quinones, in addition to their occurrence<sup>7</sup> in some bacteria, are known to constitute essential growth factors<sup>8</sup> for many types of bacteria. Furthermore, the observed influence of other compounds on the detoxication of the sulphonamides themselves<sup>9,10,11,12</sup> and the phenomenon of synergism of action of the sulphonamides

and azochloramide,<sup>13</sup> urea<sup>14</sup> or some purines,<sup>15</sup> which is finding increasing application in actual practice, would appear to have a bearing on enquiries directed towards the mode of action of the sulphonamido azo-dyes. Such enquiries would appear to be somewhat justified in view of past literature on the sulphonamido Schiff's bases; the Schiff's bases derived from the sulphonamides are hydrolysed, after oral administration, into the component parts; the possibility of the "aldehyde half" of the molecule or its derivative elaborated *in vivo* exerting a modifying influence on the chemotherapeutic efficacy of the active half has already been indicated in an earlier paper.<sup>16</sup> That the second ring in azo-dyes may well be of significance was indicated by Gley and Girard's finding<sup>17</sup> that whereas molecular equivalents of prontosil and sulphanilamide were of equal therapeutic value in experimental streptococcal infections, the carboxy derivative of prontosil, which could liberate no more sulphanilamide than prontosil, was twice as effective, therapeutically, as prontosil. The possibility envisaged by Gley and Girard may be construed to receive support from the activities reported for the azo-dyes derived from sulphanilamide and resorcinol,<sup>18</sup> 3:5-diamino-benzoic acid,<sup>19</sup> *p*-hydroxy phenyl glycine and histidine,<sup>20</sup> pyrrole and indole<sup>21</sup> and some purines<sup>22</sup>; prontosil and neoprontosil may also probably be included in this group.

A scrutiny of the existing literature on the sulphonamido azo-dyes brings to light many curious generalities. For instance, while quite a considerable number of dyes derived from sulphanilamide itself is known, a comparatively smaller number of their heterocyclic analogues has been disclosed. Again, as against the basic dyes, very few phenolic dyes have, so far, been revealed. Furthermore, only a small proportion of either the basic or acidic dyes have been studied in detail in respect of their activity and their detoxication mechanisms. That a study of the sulphonamido azo-dyes need not be considered entirely fruitless is supported by the use of other dyes still in medicine and the notable success achieved recently<sup>23</sup> by Congo red in even the sulphonamide-resistant bacterial infections.

For the reasons stated above, it was therefore, considered worthwhile to synthesise a series of azo-dyes derived on the one hand, from sulphonamides which have already earned a definite place in chemotherapy and on the other, from mono- and poly-hydric phenolic compounds. In the hope that useful information likely to lead to a better understanding of the evolution of future chemotherapeutics could be gained, it was further planned to investigate first their usefulness in experimental bacterial infections and later, the mechanism of action of the active members. The phenolic dyes which were prepared in this connection are represented in the table.

Serial No.	Name	Nitrogen percentage		
		Found	Required	
99	2 : 4-Dihydroxy, ( <i>p</i> -sulphamyl phenyl azo) benzene	H OH OH	H H H	13.8 17.4 17.7
100	2 : 4-Dihydroxy, 1 : 5-bis ( <i>p</i> -sulphamyl phenyl azo) benzene	H OH N:N-C <sub>6</sub> H <sub>4</sub> .SO <sub>2</sub> NH <sub>2</sub>	H H H	12.3 12.8 11.1
101	4-Hydroxy, ( <i>p</i> -sulphamyl phenyl azo) naphthalene	H HO	H H	11.3 11.1
102	3-Hydroxy, 4 ( <i>p</i> -sulphamyl phenyl azo) phenanthrene		H H	12.6 13.1
103	2-Methyl, 4-hydroxy, 5-isopropyl, ( <i>p</i> -sulphamyl phenyl azo) benzene	CH <sub>3</sub> HO CH (CH <sub>3</sub> ) <sub>2</sub>	H H H	11.9 13.1 20.9
104	2 : 3 : 4-Trihydroxy, ( <i>p</i> -sulphamyl phenyl azo) benzene	HO OH OH	H H H	21.0 14.6 14.8
105	2 : 4-dihydroxy, ( <i>p</i> -sulphonguanidyl phenyl azo) benzene	OH OH	$\text{--C}(\text{NH}_2)\text{NH}_2$ H	14.8 14.3 16.4
106	2 : 4-Dihydroxy, ( <i>p</i> -N <sup>1</sup> , 2'-pyridyl sulphamyl phenyl azo) benzene	HO OH	H H	15.1 14.8
107	2 : 4-Dihydroxy, ( <i>p</i> -N <sup>1</sup> , 2'-thiazolyl phenyl azo) benzene	HO OH	H H	14.6 17.0
108	2 : 4-Dihydroxy, ( <i>p</i> -N <sup>1</sup> , 2'-thiazolyl sulphamyl phenyl azo) benzene		H H	14.3 17.0
109	2 : 4-Dihydroxy, 5 ( <i>p</i> -N <sup>1</sup> , 2'-thiazolyl sulphamyl phenyl azo) quinoline		H	14.8

Two compounds listed in the table have previously been reported but in insufficient detail and were therefore included with the object of a comparative and detailed study in animal experiments: the compounds are No. 99<sup>18</sup> and No. 103.<sup>24</sup> Four of the dyes (Nos. 106-109) have, so far, been subjected by Dr. B. B. Dikshit to preliminary tests in experimental *Pasteurella pestis* infections in mice. Although the results obtained were somewhat interesting, none of them exhibited an activity greater than that of sulpha-thiazole, the control used in comparative bio-assays of the efficacies of new sulphanilamide derivatives in this Institute.

### *Experimental*

The dyes, Nos. 99-104, 106-109 were all prepared by the following general procedure which is illustrated by the preparation of the compound, No. 99. A solution of sulphanilamide (17.2 g., 1 mol.) in sodium hydroxide (4 g. in 100 c.c. of water), cooled to 15°, was treated with a solution of sodium nitrite (7.4 g. in 20 c.c. of water; 1.08 mol.) and the resulting solution poured with stirring on to a mixture of concentrated hydrochloric acid (21.2 c.c. of D, 1.18; 2.5 mols.) and crushed ice (120 g.). The diazonium salt mixture, after standing 15-20 minutes, was then added with good stirring to a solution of resorcinol (11 g., 1 mol.) in sodium hydroxide (20 g. in 80 c.c. of water; 5 mols.) which had previously been cooled to about 0-5° C. by addition of ice (80 g.). The resulting solution was allowed to stand at ordinary temperature for one half hour, filtered and acidified with hydrochloric acid when the dye separated out as a voluminous precipitate.

For the compound, No. 105, a slightly different process was adopted. This consisted in the direct diazotisation of a dilute hydrochloric acid solution of sulphaguanidine itself by means of sodium nitrite followed by coupling with resorcinol in alkaline medium on the same lines as has been worked out for the other azo-dyes.

The attempts to crystallise the dyes from the usual organic solvents or mixtures of them did not meet with success. Resort was therefore had, for purposes of purification, to repeated fractional precipitation of the dyes from their aqueous alkaline solutions (Norite) by acetic acid, the first and final fractions being rejected. The dyes after washing with water and drying in an air-oven, were then obtained as powders without any definite melting points or crystalline natures but possessing one or other grades of redness.

The yields of the pure dye-stuffs should, in all the instances, be considered good since they average from 75-90 per cent. of the theoretical.

The author wishes to express his gratefulness to Col. S. S. Sokhey for his kind interest in this investigation and to the Lady Tata Memorial Trust for the award of a Research Scholarship.

### Summary

The synthesis of a series of phenolic azo-dyes derived from the sulphonamides with the object of exploring their therapeutic potentialities and of gaining an insight into their mode of action, has been effected and reported.

### REFERENCES

1. Domagk .. *Deut. Med. Wochschr.*, 1935, **61**, 250, 929.
2. Churchman .. *The Newer Knowledge of Bacteriology and Immunology*, 1928, Chap. 3.
3. McCulla and others .. *Stain Tech.*, 1941, **65**, 27, 95.  
Doladilbe and Guy .. *Compt. rend.*, 1941, **211**, 675.  
Albert and co-workers .. *Nature*, 1941, **147**, 332, 709.  
\_\_\_\_\_ .. *Brit. J. Exp. Path.*, 1942, **23**, 69.  
\_\_\_\_\_ .. *Lancet*, 1942, **2**, 633.
4. Trefquel *et al.* .. *Compt. rend. soc. biol.*, 1935, **120**, 756.  
Fourneau *et al.* .. *Ibid.*, 1936, **122**, 156.  
Buttle *et al.* .. *Lancet*, 1936, **2**, 1323.  
Fuller .. *Ibid.*, 1937, **1**, 194.  
Bliss and Long .. *Bull. Johns Hopkins Hosp.*, 1937, **60**, 149.
5. Tischler *et al.* .. *J. Amer. Chem. Soc.*, 1940, **62**, 1881.  
Butt and Snell .. *Vitamin K*, 1941.  
Doisy *et al.* .. *Chem. Revs.*, 1941, **28**, 477.  
Almquist .. *Physiol. Revs.*, 1941, **21**, 194.
6. Raistrick and co-workers .. *Chem. and Ind.*, 1941, **60**, 828 ; 1942, **61**, 22, 48, 128, 485.  
Waksman and Tischler .. *J. Biol. Chem.*, 1942, **142**, 519.  
\_\_\_\_\_ and Woodruff .. *J. Bact.*, 1942, **44**, 373.
7. Anderson and Newman .. *J. Biol. Chem.*, 1933, **101**, 773 ; **103**, 197.  
Almquist *et al.* .. *Proc. Soc. Exp. Biol. Med.*, 1938, **38**, 336.  
Butt and Osterburg .. *J. Nutrition (Suppl.)*, 1938, **15**, 11.  
Snell and co-workers .. *J. Amer. Med. Assoc.*, 1939, **112**, 1457 ; **113**, 2056.
8. Woolley and McCarter .. *Proc. Soc. Exp. Biol. Med.*, 1940, **45**, 357.
9. Martin *et al.* .. *J. Biol. Chem.*, 1941, **139**, 871.  
\_\_\_\_\_ .. *Arch. Int. Med.*, 1942, **69**, 662.
10. Dainow .. *Biol. Abst.*, 1940, **14**, 654.  
\_\_\_\_\_ .. *Dermatologia*, 1941, **83**, 43.  
Tarentelli .. *Athena*, 1941, **10**, 80.
11. Findlay .. *Recent Advances in Chemotherapy*, 1939.
12. McGinty *et al.* .. *J. Med. Assoc. Georgia*, 1939, **28**, 54.  
Cottini .. *Dermatologia*, 1940, **81**, 83.  
Roy .. *Ind. Med. Gaz.*, 1942, **77**, 729.

13. Neter .. *Proc. Soc. Exp. Biol. Med.*, 1941, **47**, 303.  
Schmelkes and Wyss  
et al. .. *J. Pharm. Exp. Therap.*, 1942, **74**, 52.  
Tsuchiya et al. .. *Proc. Soc. Exp. Biol. Med.*, 1942, **49**, 263.  
Sobin and co-workers .. *J. Bact.*, 1942, **43**, 71.  
Wallersteiner .. *Proc. Soc. Exp. Biol. Med.*, 1942, **50**, 262.  
15. Harris and Kohn .. *J. Amer. Med. Assoc.*, 1942, **118**, 1324.  
16. Rajagopalan .. *J. Lab. Clin. Med.*, 1942, **27**, 1567.  
17. Gley and Girard .. *Nature*, 1943, **151**, 586.  
18. Goissedet et al. .. *J. Biol. Chem.*, 1941, **141**, 981.  
Trefouel et al. .. *Proc. Ind. Acad. Sci.*, 1943, **18**, 100.  
Northey .. *Presse. med.*, 1936, **42**, 1775.  
19. Levaditi and Vaisman .. *Compt. rend. soc. biol.*, 1936, **121**, 1082.  
20. Passedouet and Vaisman .. *Ann. inst. Pasteur*, 1937, **58**, 30.  
21. Northey .. *Chem. Revs.*, 1940, **27**, 85.  
22. Mazza and Migliardi .. *Presse. med.*, 1935, **103**, 2097.  
23. Green .. *Compt. rend. soc. biol.*, 1939, **130**, 130.  
24. Buttle et al. .. *Loc. cit.*  
.. *Brit. Chem. Abstr.*, 1939, **2A**, 346.  
.. *J. Indiana State Med. Assoc.*, 1941, **34**, 306.  
.. *Lancet*, 1936, **230**, 1286.

# CALCULATION OF THE ELASTIC CONSTANTS OF QUARTZ AT ROOM TEMPERATURE FROM THE RAMAN EFFECT DATA

BY BISHAMBHAR DAYAL SAKSENA

(*Lecturer, Department of Physics, University of Allahabad*)

Received March 23, 1944

(Communicated by Sir C. V. Raman, Kt., F.R.S., N.L.)

## 1. Introduction

THE elastic constants of a crystal can be calculated if the various force-constants in the crystal are known. When a crystal is subjected to a homogeneous strain, the various bond distances and the bond angles in the unit cell of the crystal get altered, and these can be calculated on the basis of the known crystal structure. By assuming the force-constants for the changes along valence bonds and angular deformations, the energy per unit volume due to the strain can be calculated. As this energy is known in terms of the elastic constants, the latter can be expressed in terms of the force-constants. These force-constants can be calculated from the Raman and infra-red data, and thus we get a method of calculating the elastic constants of the crystal directly from the spectroscopic observations. Both the elastic deformations and infra-red vibrations take place sufficiently slowly for the electronic cloud of atoms to adjust themselves to altered conditions. Whatever changes may take place are therefore fully taken care of in any scheme of force-constants which fits the infra-red data, and same scheme should therefore also fit the elastic constants.

In the present paper the elastic constants of  $\alpha$ -quartz have been calculated on the basis of the ideas set forth above. The crystal structure of  $\alpha$ -quartz is known from the X-ray studies of Gibbs<sup>1</sup> (1925), and the force constants in the crystal can be calculated on the basis of the group theoretical analysis of the Raman and infra-red spectra of  $\alpha$ -quartz made by the author<sup>2</sup> (1940). The four force-constants which have been calculated from the

Raman effect data are those of Si—O valence,  $\text{Si}\diagup\text{O}\diagdown\text{Si}$  and  $\text{O}\diagup\text{Si}\diagdown\text{O}$

deformation, and O—O repulsion, and these explain the elastic constants as well.

## 2. Calculation of the Variations of the Bond Distances and Bond Angles due to Strain

When a crystal is subjected to homogeneous strain we may assume the strain to consist of two parts—the one involving displacements of partial lattices relative to each other and a second part in which the distance from basis to basis is altered as if the basis were rigid and attached at one point in the continuum subjected to strain. The high frequencies of vibration observed spectroscopically and also the structure of the crystal shows that quartz is not an ionic crystal. The silicon-oxygen bonds are largely covalent in nature. For this reason the piezo-electric forces produced by the strain are not likely to effect the elastic constants to any marked extent, and we may therefore treat the strain from the continuum stand point alone. But in the covalent binding between dissimilar atoms there would be a certain displacement of electric charges which would explain the piezo-electric behaviour of the crystal.

In any homogeneous pure strain, if  $x, y, z$  be the co-ordinates of a point in a body before it is strained and if  $x + u, y + v, z + w$  be the co-ordinates of the same point after the body has been strained then we have (Love, *vide* ref. 3).

$$u = u_{xx} \cdot x + \frac{1}{2} u_{xy} \cdot y + \frac{1}{2} u_{xz} \cdot z$$

$$v = \frac{1}{2} u_{yx} \cdot x + u_{yy} \cdot y + \frac{1}{2} u_{yz} \cdot z$$

$$w = \frac{1}{2} u_{zx} \cdot x + \frac{1}{2} u_{zy} \cdot y + u_{zz} \cdot z$$

where  $u_{xx}, u_{yy}, u_{zz}$  represent the strain components parallel to  $x, y, z$  axes and  $u_{yx}, u_{xz}, u_{zy}$  represent components of shear in the  $yz, xz$  and  $xy$  planes. The strain may be regarded as a symmetrical tensor so that  $u_{sr} = u_{rs}$ . If P and Q be two points  $x_1, y_1, z_1$  and  $x_2, y_2, z_2$  and if  $r$  be the distance between them and  $l, m, n$  the direction cosines of the line PQ then the change in the length of PQ after deformation is given by

$$\begin{aligned} r(u_{xx} \cdot l^2 + u_{yy} \cdot m^2 + u_{zz} \cdot n^2 + u_{xy} l \cdot m + u_{yz} m \cdot n + u_{zx} n \cdot l) \\ = \frac{1}{r} [\sum u_{xx} (x_1 - x_2)^2 + \sum (v_1 - v_2)(x_1 - x_2) u_{xy}] \end{aligned}$$

The unit cell of  $\alpha$ -quartz is shown in Fig. 1. Atoms 1 to 6 are silicon atoms and atoms 7 to 12 are oxygen atoms contained in the unit cell while the remaining marked ones are oxygen atoms not contained in the unit cell but linked to silicon atoms 1 to 6 of the unit cell. The co-ordinates of the atoms in the unit cell were given by the author<sup>4</sup> (1942) while the co-ordinates

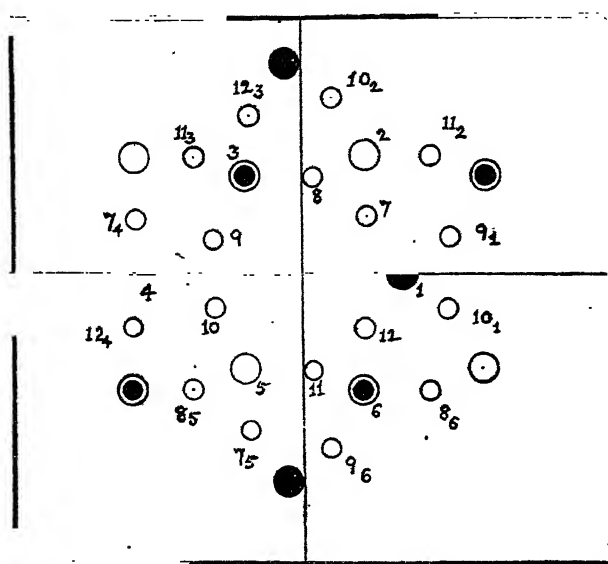


FIG. 1. Projection of Si & O atoms on the basal plane

of the remaining oxygen atoms such as 9<sub>1</sub> and 9<sub>6</sub> linked to silicon atoms 1 and 6 respectively can be obtained from those of oxygen atom 9 by moving this atom through a distance equal to 4.879 parallel to the lines joining Si atoms (1 and 4) and (3 and 6) respectively. The co-ordinates are given in Table I.

TABLE I

Atoms contained in the unit cell				Atoms not contained in the unit cell			
Atom number	x	y	z	Atom number	x	y	z
8—O	.3322	1.853	-2.966	9 <sub>1</sub> —O	3.1082	.6389	1.168
2—Si	1.318	2.282	-1.798	10 <sub>1</sub> —O	3.1082	-.6389	-1.168
7—O	1.4386	1.214	-.63	8 <sub>6</sub> —O	2.7717	-2.3722	2.428
1—Si	2.244	0	0	9 <sub>6</sub> —O	.6687	-3.5863	1.168
12—O	1.4386	-1.214	.63	7 <sub>5</sub> —O	-1.0009	-3.0112	-.63
6—Si	1.318	-2.282	1.798	8 <sub>5</sub> —O	-2.1073	-2.3722	-2.966
11—O	.3322	-1.853	-2.428	12 <sub>4</sub> —O	-3.4404	-1.214	.63
5—Si	-1.122	-1.944	-1.798	7 <sub>4</sub> —O	-3.4404	1.214	-.63
10—O	-1.7708	-.6389	-1.168	11 <sub>8</sub> —O	-2.1073	2.3722	2.966
4—Si	-2.635	0	0	12 <sub>3</sub> —O	-1.0009	3.0112	-.63
9—O	-1.7708	.6389	1.168	10 <sub>2</sub> —O	.6687	3.5863	-1.168
3—Si	-1.122	1.944	1.798	11 <sub>2</sub> —O	2.7717	2.3722	-2.428

The variations ( $\Delta r_i$ ) of the Si — O distances are given by

$$\Delta r_{1,7} = \frac{1}{1.588} [ \cdot 6486 u_{xx} + 1.474 u_{yy} + \cdot 397 u_{zz} - \cdot 9777 u_{xy} - \cdot 7647 u_{yz} + \cdot 5074 u_{xz} ]$$

$$\Delta r_{1,12} = \frac{1}{1.588} [ \cdot 6486 u_{xx} + 1.474 u_{yy} + \cdot 397 u_{zz} + \cdot 9777 u_{xy} - \cdot 7647 u_{yz} - \cdot 5074 u_{xz} ]$$

$$\Delta r_{2,7} = \frac{1}{1.588} [ \cdot 0155 u_{xx} + 1.141 u_{yy} + 1.364 u_{zz} - \cdot 1288 u_{xy} - 1.248 u_{yz} + \cdot 1408 u_{xz} ]$$

$$\Delta r_{6,12} = \frac{1}{1.588} [ \cdot 0155 u_{xx} + 1.141 u_{yy} + 1.364 u_{zz} + \cdot 1288 u_{xy} - 1.248 u_{yz} - \cdot 1408 u_{xz} ]$$

$$\Delta r_{2,8} = \frac{1}{1.588} [ \cdot 972 u_{xx} + \cdot 1840 u_{yy} + 1.364 u_{zz} + \cdot 4239 u_{xy} + \cdot 5010 u_{yz} + 1.152 u_{xz} ]$$

$$\Delta r_{6,11} = \frac{1}{1.588} [ \cdot 972 u_{xx} + \cdot 1840 u_{yy} + 1.364 u_{zz} - \cdot 4239 u_{xy} + \cdot 5010 u_{yz} - 1.152 u_{xz} ]$$

$$\Delta r_{4,9} = \frac{1}{1.588} [ \cdot 7468 u_{xx} + \cdot 4081 u_{yy} + 1.364 u_{zz} + \cdot 5521 u_{xy} + \cdot 7461 u_{yz} + 1.009 u_{xz} ]$$

$$\Delta r_{4,10} = \frac{1}{1.588} [ \cdot 7468 u_{xx} + \cdot 4081 u_{yy} + 1.364 u_{zz} - \cdot 5521 u_{xy} + \cdot 7461 u_{yz} - 1.009 u_{xz} ]$$

$$\Delta r_{3,9} = \frac{1}{1.588} [ \cdot 4209 u_{xx} + 1.703 u_{yy} + \cdot 397 u_{zz} + \cdot 8465 u_{xy} + \cdot 8219 u_{yz} + \cdot 4087 u_{xz} ]$$

$$\Delta r_{5,10} = \frac{1}{1.588} [ \cdot 4209 u_{xx} + 1.703 u_{yy} + \cdot 397 u_{zz} - \cdot 8465 u_{xy} + \cdot 8219 u_{yz} - \cdot 4087 u_{xz} ]$$

$$\Delta r_{3,8} = \frac{1}{1.588} [ \cdot 115 u_{xx} + \cdot 00686 u_{yy} + \cdot 397 u_{zz} - \cdot 1323 u_{xy} - \cdot 0573 u_{yz} + \cdot 9160 u_{xz} ]$$

$$\Delta r_{5,11} = \frac{1}{1.588} [ \cdot 115 u_{xx} + \cdot 00686 u_{yy} + \cdot 397 u_{zz} + \cdot 1323 u_{xy} - \cdot 0573 u_{yz} - \cdot 9160 u_{xz} ]$$

The variations ( $\Delta \Phi_i$ ) of  $\text{Si}-\text{O}-\text{Si}$  angles are given by

$$1.355 \Delta \Phi_{1,7,2} = -\cdot 3645 u_{xx} + \cdot 389 u_{yy} - \cdot 013 u_{zz} - \cdot 074 u_{xy} - \cdot 394 u_{yz} + \cdot 47 u_{xz}$$

$$1.355 \Delta \Phi_{1,12,6} = -\cdot 3645 u_{xx} + \cdot 389 u_{yy} - \cdot 013 u_{zz} + \cdot 074 u_{xy} - \cdot 394 u_{yz} - \cdot 47 u_{xz}$$

$$1.355 \Delta \Phi_{3,9,4} = \cdot 137 u_{xx} - \cdot 11 u_{yy} - \cdot 013 u_{zz} + \cdot 365 u_{xy} + \cdot 607 u_{yz} + \cdot 108 u_{xz}$$

$$1.355 \Delta \Phi_{4,10,5} = \cdot 137 u_{xx} - \cdot 11 u_{yy} - \cdot 013 u_{zz} - \cdot 365 u_{xy} + \cdot 607 u_{yz} - \cdot 108 u_{xz}$$

$$1.355 \Delta \Phi_{3,8,2} = \cdot 2644 u_{xx} - \cdot 241 u_{yy} - \cdot 013 u_{zz} + \cdot 2558 u_{xy} - \cdot 2297 u_{yz} + \cdot 576 u_{xz}$$

$$1.355 \Delta \Phi_{5,11,6} = \cdot 2644 u_{xx} - \cdot 241 u_{yy} - \cdot 013 u_{zz} - \cdot 2558 u_{xy} - \cdot 2297 u_{yz} - \cdot 576 u_{xz}$$

Each silicon atom is joined to four oxygen atoms so that at each Si atom there are six  $\text{O}-\text{Si}-\text{O}$  angles and also six O—O distances. As each Si atom is shared by two unit cells, the contribution of the six angles and the six O—O distances will be equally shared by the two unit cells. As there are six silicon atoms to a unit cell there are 36  $\text{O}-\text{Si}-\text{O}$  angles and 36 O—O distances to be considered. The variations of 18 of these  $\text{O}-\text{Si}-\text{O}$  angles and O—O distances are given below and the variations of the remaining 18 are also the same. These latter are the 18  $\text{O}-\text{Si}-\text{O}$  angles and

the 18 O—O distances at silicon atoms 3, 4, 5 whose variations are the same as those of the  $\text{Si}=\text{O}$  angles and O—O distances at silicon atoms 6, 1, 2 respectively.

The variations ( $\Delta\phi_i$ ) of the various  $\text{Si}=\text{O}$  angles are given by

$$\begin{aligned}
 2 \cdot 436 \Delta\phi_{7,1,9_1} &= 1 \cdot 031 u_{xx} - 2 \cdot 038 u_{yy} + 1 \cdot 015 u_{zz} - 4245 u_{xy} - 1 \cdot 012 u_{yz} + 1 \cdot 093 u_{xz} \\
 2 \cdot 436 \Delta\phi_{12,1,10_1} &= 1 \cdot 031 u_{xx} - 2 \cdot 038 u_{yy} + 1 \cdot 015 u_{zz} + 4245 u_{xy} - 1 \cdot 012 u_{yz} - 1 \cdot 093 u_{xz} \\
 2 \cdot 414 \Delta\phi_{12,1,9_1} &= .989 u_{xx} + 1 \cdot 008 u_{yy} - 1 \cdot 982 u_{zz} + 1 \cdot 124 u_{xy} + 1 \cdot 022 u_{yz} + 2516 u_{xz} \\
 2 \cdot 414 \Delta\phi_{7,1,10_1} &= .989 u_{xx} + 1 \cdot 008 u_{yy} - 1 \cdot 982 u_{zz} - 1 \cdot 124 u_{xy} + 1 \cdot 022 u_{yz} - 2516 u_{xz} \\
 2 \cdot 305 \Delta\phi_{8,1,1,10_1} &= -2 \cdot 102 u_{xx} + 4841 u_{yy} + 1 \cdot 619 u_{zz} + .886 u_{yz} \\
 2 \cdot 207 \Delta\phi_{7,1,12} &= -1 \cdot 928 u_{xx} + 1 \cdot 519 u_{yy} + .409 u_{zz} - .7868 u_{yz} \\
 2 \cdot 436 \Delta\phi_{8,2,10_2} &= -1 \cdot 6404 u_{xx} + .626 u_{yy} + 1 \cdot 015 u_{zz} + 1 \cdot 1146 u_{xy} + 1 \cdot 451 u_{yz} - 3294 u_{xz} \\
 2 \cdot 414 \Delta\phi_{7,2,10_2} &= -.0294 u_{xx} + 1 \cdot 96 u_{yy} - 1 \cdot 982 u_{zz} - .568 u_{xy} - .728 u_{yz} + .7592 u_{xz} \\
 2 \cdot 414 \Delta\phi_{8,2,11_2} &= 1 \cdot 974 u_{xx} + .0221 u_{yy} - 1 \cdot 982 u_{zz} + .572 u_{xy} - .294 u_{yz} + 1 \cdot 009 u_{xz} \\
 2 \cdot 436 \Delta\phi_{7,2,11_2} &= -.905 u_{xx} - 104 u_{yy} + 1 \cdot 015 u_{zz} + 1 \cdot 561 u_{xy} - .439 u_{yz} - 1 \cdot 421 u_{xz} \\
 2 \cdot 305 \Delta\phi_{7,2,8} &= -.163 u_{xx} - 1 \cdot 457 u_{yy} + 1 \cdot 619 u_{zz} - 1 \cdot 122 u_{xy} - .443 u_{yz} + .767 u_{xz} \\
 2 \cdot 207 \Delta\phi_{10_2,2,11_2} &= .658 u_{xx} - 1 \cdot 067 u_{yy} + .409 u_{zz} - 1 \cdot 467 u_{xy} + .395 u_{yz} - .683 u_{xz} \\
 2 \cdot 436 \Delta\phi_{8_6,6,11} &= -1 \cdot 6404 u_{xx} + .626 u_{yy} + 1 \cdot 015 u_{zz} - 1 \cdot 1146 u_{xy} + 1 \cdot 451 u_{yz} + 3294 u_{xz} \\
 2 \cdot 436 \Delta\phi_{8_6,6,12} &= -.905 u_{xx} - 104 u_{yy} + 1 \cdot 015 u_{zz} - 1 \cdot 561 u_{xy} - .439 u_{yz} + 1 \cdot 421 u_{xz} \\
 2 \cdot 414 \Delta\phi_{9_6,6,12} &= -.0294 u_{xx} + 1 \cdot 96 u_{yy} - 1 \cdot 982 u_{zz} + .568 u_{xy} - .728 u_{yz} - .7592 u_{xz} \\
 2 \cdot 414 \Delta\phi_{8_6,6,11} &= 1 \cdot 974 u_{xx} + .0221 u_{yy} - 1 \cdot 982 u_{zz} - .572 u_{xy} - .294 u_{yz} - 1 \cdot 009 u_{xz} \\
 2 \cdot 305 \Delta\phi_{11,6,12} &= -.163 u_{xx} - 1 \cdot 457 u_{yy} + 1 \cdot 619 u_{zz} + 1 \cdot 122 u_{xy} - .443 u_{yz} - .767 u_{xz} \\
 2 \cdot 207 \Delta\phi_{8_6,6,9_6} &= .658 u_{xx} - 1 \cdot 067 u_{yy} + .409 u_{zz} + 1 \cdot 467 u_{xy} + .395 u_{yz} + .683 u_{xz}
 \end{aligned}$$

The variations ( $\Delta R_i$ ) of the O—O distances are given by

$$\begin{aligned}
 2 \cdot 52 \Delta R_{7,9_1} &= 2 \cdot 788 u_{xx} + .3307 u_{yy} + 3 \cdot 232 u_{zz} - 9603 u_{xy} - 1 \cdot 035 u_{yz} + 3 \cdot 002 u_{xz} \\
 2 \cdot 52 \Delta R_{12,10_1} &= 2 \cdot 788 u_{xx} + .3307 u_{yy} + 3 \cdot 232 u_{zz} + 9603 u_{xy} - 1 \cdot 035 u_{yz} - 3 \cdot 002 u_{xz} \\
 2 \cdot 52 \Delta R_{7,11_2} &= 1 \cdot 777 u_{xx} + 1 \cdot 341 u_{yy} + 3 \cdot 232 u_{zz} + 1 \cdot 544 u_{xy} - 2 \cdot 082 u_{yz} - 2 \cdot 397 u_{xz} \\
 2 \cdot 52 \Delta R_{12,8_6} &= 1 \cdot 777 u_{xx} + 1 \cdot 341 u_{yy} + 3 \cdot 232 u_{zz} - 1 \cdot 544 u_{xy} - 2 \cdot 082 u_{yz} + 2 \cdot 397 u_{xz} \\
 2 \cdot 551 \Delta R_{12,9_1} &= 2 \cdot 788 u_{xx} + 3 \cdot 434 u_{yy} + .2894 u_{zz} + 3 \cdot 096 u_{xy} + .9979 u_{yz} + .8982 u_{xz} \\
 2 \cdot 551 \Delta R_{7,10_1} &= 2 \cdot 788 u_{xx} + 3 \cdot 434 u_{yy} + .2894 u_{zz} - 3 \cdot 096 u_{xy} + .9979 u_{yz} - .8982 u_{xz} \\
 2 \cdot 52 \Delta R_{8,10_2} &= .1136 u_{xx} + 3 \cdot 003 u_{yy} + 3 \cdot 232 u_{zz} + .5826 u_{xy} + 3 \cdot 117 u_{yz} + .606 u_{xz} \\
 2 \cdot 52 \Delta R_{11,9_6} &= .1136 u_{xx} + 3 \cdot 003 u_{yy} + 3 \cdot 232 u_{zz} - .5826 u_{xy} + 3 \cdot 117 u_{yz} - .606 u_{xz} \\
 2 \cdot 551 \Delta R_{8,11_2} &= 5 \cdot 954 u_{xx} + .2694 u_{yy} + .2894 u_{zz} + 1 \cdot 267 u_{xy} + .2793 u_{yz} + 1 \cdot 313 u_{xz} \\
 2 \cdot 551 \Delta R_{11,8_6} &= 5 \cdot 954 u_{xx} + .2694 u_{yy} + .2894 u_{zz} - 1 \cdot 267 u_{xy} + .2793 u_{yz} - 1 \cdot 313 u_{xz} \\
 2 \cdot 551 \Delta R_{7,10_2} &= .592 u_{xx} + 5 \cdot 626 u_{yy} + .2894 u_{zz} - 1 \cdot 825 u_{xy} - 1 \cdot 277 u_{yz} + .4139 u_{xz} \\
 2 \cdot 551 \Delta R_{12,9_6} &= .592 u_{xx} + 5 \cdot 626 u_{yy} + .2894 u_{zz} + 1 \cdot 825 u_{xy} - 1 \cdot 277 u_{yz} - .4139 u_{xz} \\
 2 \cdot 734 \Delta R_{7,12} &= 5 \cdot 896 u_{yy} + 1 \cdot 588 u_{zz} - 3 \cdot 0586 u_{yz} \\
 2 \cdot 663 \Delta R_{9,10} &= 1 \cdot 632 u_{yy} + 5 \cdot 456 u_{zz} + 2 \cdot 9844 u_{yz} \\
 2 \cdot 663 \Delta R_{7,8} &= 1 \cdot 226 u_{xx} + .4083 u_{yy} + 5 \cdot 456 u_{zz} - 7068 u_{xy} - 1 \cdot 493 u_{yz} + 2 \cdot 584 u_{xz} \\
 2 \cdot 663 \Delta R_{11,12} &= 1 \cdot 226 u_{xx} + .4083 u_{yy} + 5 \cdot 456 u_{zz} + 7068 u_{xy} - 1 \cdot 493 u_{yz} - 2 \cdot 584 u_{xz} \\
 2 \cdot 734 \Delta R_{9,8} &= 4 \cdot 423 u_{xx} + 1 \cdot 474 u_{yy} + 1 \cdot 588 u_{zz} + 2 \cdot 553 u_{xy} + 1 \cdot 53 u_{yz} + 2 \cdot 65 u_{xz} \\
 2 \cdot 734 \Delta R_{10,11} &= 4 \cdot 423 u_{xx} + 1 \cdot 474 u_{yy} + 1 \cdot 588 u_{zz} - 2 \cdot 553 u_{xy} + 1 \cdot 53 u_{yz} - 2 \cdot 65 u_{xz}
 \end{aligned}$$

### 3. Calculation of the Energy due to Strain

If  $K$  be the force-constant of Si - O valence,  $K_1$  and  $K_2$  the force-constants of angular deformations of  $\text{Si}-\text{O}-\text{Si}$  and  $\text{O}-\text{Si}-\text{O}$  angles respectively and  $K_3$  the force-constant O - O repulsion, then the energy  $U$  per unit cell is given by

$$2U = \sum_{i=12}^{i=1} K (\Delta r_i)^2 + \sum_{i=6}^{i=1} K_1 (\Delta \Phi_i)^2 + \frac{1}{2} \sum_{i=36}^{i=1} K_2 (\Delta \phi_i)^2 + \frac{1}{2} \sum_{i=36}^{i=1} K_3 (\Delta R_i)^2.$$

The energy of the strain per unit volume is then  $U/V$  where  $V$  is the volume of the unit cell. A unit cell of  $\alpha$ -quartz contains three molecules of  $\text{SiO}_2$ . The volume of the unit cell obtained from the relation  $V = 3m/\rho N$  where  $m$  is the molecular weight,  $\rho$  the density,  $N$  the Avagadro's number ( $6.06 \times 10^{23}$ ), is  $111.2 \times 10^{-24}$  c.c. The same volume is obtained from the geometry of the figure. The area included within the irregular hexagon formed by joining the silicon atoms of the unit cell is  $15.365 \times 10^{-16}$  sq. cm. Three such hexagons enclose a triangle of Si atoms of area  $2.62 \times 10^{-16}$  sq. cm. There are six such triangles, one corresponding to each side of the irregular hexagon, of total area  $15.72$  sq. cm. which have not been included in the hexagons. Hence in averaging over the whole space the volume of the unit cell  $= (15.365 + \frac{1}{3} \times 15.72) \times 5.394 \times 10^{-24}$  c.c.  $= 111.2 \times 10^{-24}$  c.c. (the length of the  $c$ -axis for  $\alpha$ -quartz is  $5.394 \times 10^{-8}$  cm.). The energy of the strain per unit volume is therefore

$$\frac{1}{2 \times 111.2} \left[ \sum_{12}^1 K (\Delta r_i)^2 + \sum_6^1 K_1 (\Delta \Phi_i)^2 + \frac{1}{2} \sum_{36}^1 K_2 (\Delta \phi_i)^2 + \frac{1}{2} \sum_{36}^1 K_3 (\Delta R_i)^2 \right] \times 10^{24}.$$

On substituting the values of  $\Delta r_i$ ,  $\Delta \Phi_i$ ,  $\Delta \phi_i$ ,  $\Delta R_i$  the above expression becomes

$$\begin{aligned} & \frac{1}{222.4} [(5.20 K^1 + 2415 K_1 + 4.997 K_2 + 22.5 K_3^1) (u_{xx}^2 + u_{yy}^2) + (4.797 K^1 + 6.668 K_2 \\ & + 23.5 K_3^1) u_{zz}^2 + 2(1.729 K^1 - 2403 K_1 - 1.638 K_2 + 7.49 K_3^1) u_{xx} u_{yy} + 2(2.87 K^1 \\ & - 3.344 K_2 + 9.35 K_3^1) u_{zz} (u_{xx} + u_{yy}) + (1.729 K^1 + 241 K_1 + 3.314 K_2 + 7.5 K_3^1) u_{xy}^2 \\ & + (2.87 K^1 + 627 K_1 + 2.094 K_2 + 9.35 K_3^1) (u_{yy}^2 + u_{xz}^2) + 2(6.026 K^1 + 181 K_1 - 781 K_2 \\ & + 465 K_3^1) (u_{xz} u_{yz} - u_{yy} u_{yz} + u_{xz} u_{xy})] \times 10^{24} \text{ where } K^1 = K \times 10^{-16}, K_3^1 = K_3 \times 10^{-16}. \end{aligned}$$

### 4. Expressions for Elastic Constants

$\alpha$ -Quartz belongs to the point-group  $D_3$ , and according to the figure it has an axis of twofold symmetry in the  $x$ -axis. The energy of the strain

per unit volume in terms of the elastic constants for a crystal belonging to this point-group is given by (Love, *vide* ref. 5).

$$\frac{1}{2} [c_{11} (u_{xx}^2 + u_{yy}^2) + c_{33} u_{zz}^2 + 2 c_{12} u_{xx} u_{yy} + 2 c_{13} u_{zz} (u_{xx} + u_{yy}) + c_{66} u_{xy}^2 + c_{44} (u_{xz}^2 + u_{yz}^2) \\ + 2 c_{14} (u_{xx} u_{yz} - u_{yy} u_{xz} + u_{xz} u_{xy})]$$

The expression given by Love relates to the axis of symmetry being the  $y$ -axis. It becomes identical with our expression if we put  $x = -y$  and  $y = x$  in it thereby changing  $e_{xy}$ ,  $e_{xz}$ ,  $e_{yz}$  in the expression given by Love into  $-u_{xy}$ ,  $-u_{yz}$ ,  $-u_{xz}$  respectively of our expression.  $c_{11}$ ,  $c_{12}$ ,  $c_{13}$ ,  $c_{14}$ ,  $c_{66}$ ,  $c_{33}$ ,  $c_{44}$  are the seven elastic constants of  $\alpha$ -quartz. They can now be expressed in terms of the force-constants  $K$ ,  $K_1$ ,  $K_2$ ,  $K_3$ . We have

$$c_{11} = \frac{1}{111 \cdot 2} [5 \cdot 2 K \times 10^{-16} + 2415 K_1 + 4 \cdot 997 K_2 + 22 \cdot 5 K_3 \times 10^{-16}] \times 10^{24}$$

$$c_{12} = \frac{1}{111 \cdot 2} [1 \cdot 729 K \times 10^{-16} - 2403 K_1 - 1 \cdot 638 K_2 + 7 \cdot 49 K_3 \times 10^{-16}] \times 10^{24}$$

$$c_{33} = \frac{1}{111 \cdot 2} [4 \cdot 797 K \times 10^{-16} + 6 \cdot 668 K_2 + 23 \cdot 5 K_3 \times 10^{-16}] \times 10^{24}$$

$$c_{13} = \frac{1}{111 \cdot 2} [2 \cdot 87 K \times 10^{-16} - 3 \cdot 344 K_2 + 9 \cdot 35 K_3 \times 10^{-16}] \times 10^{24}$$

$$c_{44} = \frac{1}{111 \cdot 2} [2 \cdot 87 K \times 10^{-16} + 627 K_1 + 2 \cdot 094 K_2 + 9 \cdot 35 K_3 \times 10^{-16}] \times 10^{24}$$

$$c_{14} = \frac{1}{111 \cdot 2} [-6026 K \times 10^{-16} + 181 K_1 - 781 K_2 + 465 K_3 \times 10^{-16}] \times 10^{24}$$

$$c_{66} = \frac{1}{111 \cdot 2} [1 \cdot 729 K \times 10^{-16} + 241 K_1 + 3 \cdot 314 K_2 + 7 \cdot 5 K_3 \times 10^{-16}] \times 10^{24}$$

We find from these relations that  $c_{11} - c_{12} = 2c_{66}$ .

### 5. Expressions for Force-Constants from Raman Effect Data

In an earlier paper the author had calculated the three force-constants of Si—O valence ( $K$ ), of  $\text{Si}\backslash\text{O}—\text{Si}$  and  $\text{O}\backslash\text{Si}—\text{O}$  deformation ( $K_1$ ,  $K_2$ ) from the Raman effect data. For the calculation of the elastic constants we have used a fourth constant  $K_3$  that of O—O repulsion. It is therefore necessary to calculate the four constants again. In order to calculate the force-constants we use the four frequencies in the Raman spectrum of  $\alpha$ -quartz which belong to the totally symmetric class. They are 207, 356, 466, 1082 cm.<sup>-1</sup>. The potential energy and the kinetic energy of the vibration can be written down by the use of symmetry co-ordinates and the frequencies calculated.

If  $\Delta r$ ,  $\Delta R$  represent the variations of Si—O and O—O distances, and  $\Delta\Phi$  and  $\Delta\phi$  the variations of  $\text{Si}\backslash\text{O}—\text{Si}$  and  $\text{O}\backslash\text{Si}—\text{O}$  angles respectively and if  $K$ ,  $K_1$ ,  $K_2$ ,  $K_3$  represent the force-constants of Si—O valence,

$\text{Si}-\text{O}-\text{Si}$  and  $\text{O}-\text{Si}-\text{O}$  deformation, and  $\text{O}-\text{O}$  repulsion respectively the potential energy of each unit cell is given by

$$2V = K \sum_{12} (\Delta r)^2 + K_1 \sum_6 (\Delta \Phi)^2 + \frac{1}{2} K_2 \sum_{36} (\Delta \phi)^2 + \frac{1}{2} K_3 \sum_{36} (\Delta R)^2.$$

There are twelve  $\text{Si}-\text{O}$  bonds and six  $\text{Si}-\text{O}-\text{Si}$  angles in each unit cell. Further four oxygen atoms are bound to each silicon atom and so we have to consider six  $\text{O}-\text{Si}-\text{O}$  angles and six  $\text{O}-\text{O}$  distances at each silicon atom or thirty-six  $\text{O}-\text{Si}-\text{O}$  angles and thirty-six  $\text{O}-\text{O}$  distances for the whole cell. As each silicon atom is common to two cells, the contributions to the potential energy due to these  $\text{O}-\text{Si}-\text{O}$  angles and  $\text{O}-\text{O}$  distances will be equally shared by the two cells. For finding the variations of  $\text{O}-\text{Si}-\text{O}$  angles we have to consider the oxygen atoms like  $9_1, 10_1$  in the adjacent cells.

The symmetry co-ordinates corresponding to the four totally symmetric frequencies are

- (i)  $x_7+x_8+x_9+x_{10}+x_{11}+x_{12}$
- (ii)  $x_2+x_4+x_6-x_1-x_3-x_5$
- (iii)  $y_7+y_9+y_{11}-y_8-y_{10}-y_{12}$
- (iv)  $z_8+z_{10}+z_{12}-z_7-z_9-z_{11}$ ,

where  $x_i, y_i, z_i$  represent the motion of  $i$ th atom with respect to its position of rest as origin. Each  $x_i$  is directed towards a point in the basal plane containing the given atom where the threefold axis meets it,  $z_i$  is perpendicular to the basal plane and positive upwards and  $y_i$  is at right angles to both and positive in a direction making the motion right-handed. Let  $\beta, \gamma, \delta, \epsilon$  be the displacement of atoms in the four modes. The variations of  $\text{Si}-\text{O}$  distances are given by

$$\begin{aligned}\Delta r_{2,8} &= \Delta r_{2,7} = \Delta r_{6,12} = \Delta r_{6,1} = \Delta r_{4,10} = \Delta r_{4,9} \\ &= \frac{-5974 \beta - 8644 \gamma + 8946 \delta - 1 \cdot 168 \epsilon}{1 \cdot 588} = \Delta p_1\end{aligned}$$

$$\begin{aligned}\Delta r_{7,11} &= \Delta r_{1,12} = \Delta r_{5,11} = \Delta r_{5,10} = \Delta r_{3,9} = \Delta r_{3,8} \\ &= \frac{-1676 \beta + 8054 \gamma - 1 \cdot 147 \delta + 63 \epsilon}{1 \cdot 588} = \Delta p_2\end{aligned}$$

The variations of  $\text{Si}-\text{O}-\text{Si}$  angles are given by

$$\begin{aligned}\Delta \Phi_{2,7,1} &= \Delta \Phi_{1,12,6} = \Delta \Phi_{5,11,6} = \Delta \Phi_{5,10,4} = \Delta \Phi_{4,9,3} = \Delta \Phi_{3,8,2} \\ &= \frac{-7914 \beta - 4783 \gamma + 1 \cdot 018 \delta + 9915 \epsilon}{1 \cdot 355} = \Delta \Phi\end{aligned}$$

The variations of  $\text{O}_\text{Si}-\text{O}$  angles at silicon atom (1) are

$$\Delta \phi_{7,1_1,12} = \frac{-2 \cdot 634 \beta - 2 \cdot 391 \gamma + 0.585 \delta + 0.651 \epsilon}{2 \cdot 207} = \Delta \phi_1$$

$$\Delta \phi_{9,1_1,10_1} = \frac{-2 \cdot 546 \beta + 2 \cdot 431 \gamma - 11.138 \delta - 1 \cdot 387 \epsilon}{2 \cdot 305} = \Delta \phi_2$$

$$\Delta \phi_{9,1_1,7} = \Delta \phi_{12,1_1,10_1} = \frac{2 \cdot 131 \beta + 0.0743 \gamma - 7.96 \delta + 6.774 \epsilon}{2 \cdot 436} = \Delta \phi_3$$

$$\Delta \phi_{7,1_1,10_1} = \Delta \phi_{12,1_1,10_1} = \frac{4.688 \beta + 0.07607 \gamma + 5.286 \delta - 3.824 \epsilon}{2 \cdot 414} = \Delta \phi_4$$

The variations of O—O distances at silicon atom (1) are

$$\Delta R_{7,1_1,12} = \frac{-3 \cdot 132 \beta - 3 \cdot 712 \delta + 2 \cdot 52 \epsilon}{2 \cdot 734} = \Delta R_1$$

$$\Delta R_{9,1_1,10_1} = \frac{-8.676 \beta + 2 \cdot 405 \delta - 4 \cdot 672 \epsilon}{2 \cdot 662} = \Delta R_2$$

$$\Delta R_{9,1_1,7} = \Delta R_{12,1_1,10_1} = \frac{2 \cdot 672 \beta - 1 \cdot 491 \delta}{2 \cdot 52} = \Delta R_3$$

$$\Delta R_{7,1_1,10_1} = \Delta R_{12,1_1,9_1} = \frac{1 \cdot 023 \beta - 18.34 \delta - 1 \cdot 076 \epsilon}{2 \cdot 551} = \Delta R_4$$

The variations of O—O distances and  $\text{O}_\text{Si}-\text{O}$  angles at all other silicon atoms are the same as these. Hence the potential energy becomes

$$2V = 6K \{(\Delta p_1)^2 + (\Delta p_2)^2\} + 6K_1(\Delta \bar{\Phi})^2 + \frac{1}{2}6K_2\{(\Delta \phi_1)^2 + (\Delta \phi_2)^2 + 2(\Delta \phi_3)^2 + 2(\Delta \phi_4)^2\} \\ + \frac{1}{2}6K_3\{(\Delta R_1)^2 + (\Delta R_2)^2 + 2(\Delta R_3)^2 + 2(\Delta R_4)^2\}$$

On expanding it becomes

$$2V = 6 [a\beta^2 + b\gamma^2 + c\delta^2 + d\epsilon^2 - 2e\beta\gamma + 2f\beta\delta - 2g\beta\epsilon - 2h\gamma\delta + 2i\gamma\epsilon - 2j\delta\epsilon]$$

where

$$a = 0.1525 K + 0.3412 K_1 + 2.124 K_2 + 1.993 K_3$$

$$b = 0.5535 K + 0.1264 K_1 + 0.144 K_2$$

$$c = 0.1476 K + 0.5641 K_1 + 0.1911 K_2 + 0.685 K_3$$

$$d = 0.6984 K + 0.5356 K_1 + 0.3271 K_2 + 0.141 K_3$$

$$e = 0.2581 K - 0.2061 K_1 - 0.0973 K_2$$

$$f = 0.3080 K - 0.4388 K_1 - 0.3744 K_2 - 0.027 K_3$$

$$g = 0.3184 K + 0.4274 K_1 - 0.3688 K_2 + 0.4091 K_3$$

$$h = 0.7687 K + 0.2652 K_1 + 0.1725 K_2$$

$$i = 0.6015 K - 0.2583 K_1 - 0.4734 K_2$$

$$j = 0.7757 K - 0.5495 K_1 + 0.071 K_2 + 0.386 K_3$$

Since each silicon atom is linked to two cells, the kinetic energy due to these will be equally shared by the two cells. The kinetic energy is given by  $2T = 6m_1 \dot{\beta}^2 + 3m_2 \dot{\gamma}^2 + 6m_1 \dot{\delta}^2 + 6m_1 \dot{\epsilon}^2$  where  $m_1 = 16$  and  $m_2 = 28 \cdot 3$ .

The frequencies in  $\text{cm.}^{-1}$  are given by the determinant

$$\begin{vmatrix} (a - 16 \lambda^2) & -e & f & -g \\ -e & (b - 14 \cdot 15 \lambda^2) & -h & i \\ f & -h & (c - 16 \lambda^2) & -j \\ -g & i & -j & (d - 16 \lambda^2) \end{vmatrix} = 0 \quad (5 \cdot 1)$$

where the frequency  $\omega$  (in  $\text{cm.}^{-1}$ ) =  $\frac{\lambda}{2\pi c} \times \sqrt{\frac{10^{21}}{1.65}} = 1307\lambda$

### 6. Calculation of Force-Constants, Raman Frequencies and Elastic Constants

On expanding the determinant we get

$$\begin{aligned} & 57958 \cdot 4 \lambda^8 - [9506 K + 5730 \cdot 4 K_1 + 14255 \cdot 6 K_2 + 21078 \cdot 7 K_3] \lambda^6 \\ & + [86 \cdot 83 K^2 + 905 \cdot 8 K_1^2 + 2069 \cdot 8 K_2^2 + 871 \cdot 6 K K_1 + 2151 \cdot 5 K K_2 + 2070 \cdot 1 K K_3 \\ & + 1058 \cdot 7 K_1 K_2 + 1715 \cdot 6 K_1 K_3 + 4014 K_2 K_3] \lambda^4 - [7 \cdot 04 K_2^3 + 43 \cdot 1 K_3^3 \\ & + 115 \cdot 5 K K_2^2 + 126 \cdot 8 K K_3^2 + 848 K^2 K_1 + 16 \cdot 46 K^2 K_2 + 12 \cdot 54 K^2 K_3 + 240 \cdot 0 K_2 K_3^2 \\ & + 190 \cdot 9 K_2^2 K_3 + 44 \cdot 89 K_1 K_2^2 + 111 \cdot 7 K_1 K_3^2 + 63 K_1^2 K_3 + 148 \cdot 4 K K_1 K_2 \\ & + 124 \cdot 6 K K_1 K_3 + 253 \cdot 4 K K_2 K_3 + 238 \cdot 8 K_1 K_2 K_3] \lambda^2 + [-1063 K K_2^3 \\ & + 7430 K^2 K_2^2 + 4121 K^2 K_3^2 + 5 \cdot 433 K K_2 K_3^2 + 4 \cdot 243 K K_2^2 K_3 \\ & + 5 \cdot 032 K K_1 K_2^2 + 3 \cdot 193 K K_1 K_3^2 + 0 \cdot 0467 K K_1^2 K_3 + 0 \cdot 0959 K^2 K_1 K_2 \\ & + 0 \cdot 0798 K^2 K_1 K_3 + 1 \cdot 111 K^2 K_2 K_3 + 8 \cdot 035 K K_1 K_2 K_3 + 3150 K_2^3 K_1 \\ & + 6 \cdot 264 K_1 K_2 K_3^2 + 7 \cdot 431 K_1 K_2^2 K_3 + 0 \cdot 0052 K_1^2 K_3^2 + 0 \cdot 0356 K_1^2 K_2 K_3 \\ & + 4 \cdot 624 K_2^2 K_3^2 + 2759 K_2^3 K_3 + 1 \cdot 687 K K_3^3 + 3 \cdot 794 K_3^3 K_2 + 3796 K_1 K_3^3] = 0 \end{aligned} \quad (6 \cdot 1)$$

If the observed frequencies are the roots of the given equation, it should be given by

$$\lambda^8 - 9122 \lambda^6 + 1698 \lambda^4 - 01017 \lambda^2 + 0001625 = 0 \quad (6 \cdot 2)$$

These two equations (6.1) and (6.2) give four expressions for the determination of the four force-constants  $K$ ,  $K_1$ ,  $K_2$ ,  $K_3$ , but it is extremely difficult to determine the constants in this way. It was therefore thought that if the same force-constants hold for the elastic constants as well as the Raman frequencies, the expressions for the elastic constants may be utilised to determine these constants. These expressions are much more convenient to work with as the force-constants occur with power-index one in them. The expressions for  $c_{13}$  and  $c_{33}$  were chosen for this purpose, and two equations obtained from the expanded determinant were used. If  $K$  and  $K_3$  are expressed in terms of  $10^5$  dynes and  $K_1$  and  $K_2$  in terms of  $10^{-11}$  dynes/radian, and using  $c_{33} = 10 \cdot 5 \times 10^{11}$  dynes,  $c_{13} = 1 \cdot 41 \times 10^{11}$  dynes we get from the expressions of elastic constants for  $c_{33}$  and  $c_{13}$

$$4 \cdot 797 K + 6 \cdot 668 K_2 + 23 \cdot 5 K_3 = 11 \cdot 68 \quad (6 \cdot 3)$$

$$2 \cdot 87 K - 3 \cdot 344 K_1 + 9 \cdot 35 K_3 = 1 \cdot 58 \quad (6 \cdot 4)$$

The expanded determinant (6.1) gives the two relations

$$\cdot 1640 K + \cdot 09887 K_1 + \cdot 246 K_2 + \cdot 3475 K_3 = \cdot 9122 \quad (6.5)$$

$$\text{and } [\cdot 001498 K^2 + \cdot 01567 K_1^2 + \cdot 03571 K_2^2 + \cdot 01504 KK_1 + \cdot 03712 KK_2 + \cdot 03572 KK_3$$

$$+ \cdot 01827 K_1 K_2 + \cdot 0296 K_1 K_3 + \cdot 06926 K_2 K_3] = \cdot 1698 \quad (6.6)$$

From equations (6.3), (6.4), (6.5) we get

$$K_1 = 6.621 - 1.111 K; K_2 = \cdot 5121 + \cdot 1603 K; K_3 = \cdot 3518 - \cdot 2498 K.$$

On substituting these values in (6.6) and solving the quadratic for K we get  $K = 5.01 \times 10^5$  dynes which gives

$$K_1 = 1.056 \times 10^{-11} \text{ dynes/radian}; K_2 = 1.315 \times 10^{-11}, K_3 = -\cdot 8992 \times 10^5 \text{ dynes}.$$

Substituting these values in the original determinant (5.1) we get the equation

$$57958 \cdot 4 \lambda^8 - 53463 \cdot 6 \lambda^6 + 9970 \cdot 5 \lambda^4 - 536 \cdot 3 \lambda^2 + 7 \cdot 55 = 0 \quad (6.7)$$

which gives the following values of frequencies in  $\text{cm.}^{-1}$

$$\bar{\omega} (\text{calc.}) \quad 1087, \quad 508, \quad 310, \quad 195$$

$$\bar{\omega} (\text{obs.}) \quad 1082, \quad 466, \quad 366, \quad 207$$

Using another set of force-constants (by slightly altering  $K_1$  and  $K_3$ ) namely  $K = 4.98 \times 10^5$ ,  $K_1 = \cdot 454 \times 10^{-11}$ ,  $K_2 = 1.565 \times 10^{-11}$ ,  $K_3 = -\cdot 892$  we get from (5.1) the equation

$$57958 \cdot 4 \lambda^8 - 53448 \cdot 2 \lambda^6 + 10012 \cdot 2 \lambda^4 - 570 \cdot 4 \lambda^2 + 8 \cdot 426 = 0 \quad (6.8)$$

which gives the frequencies 1087, 491, 333, 198.

Table II gives the force-constants, Raman frequencies and the calculated values of elastic constants. The observed values of the latter are due to Voigt.<sup>6</sup>

TABLE II

Force-constants				Calculated values of Raman frequencies		Calculated values of elastic constants										
$K \times 10^{-5}$	$K_1 \times 10^{11}$	$K_2 \times 10^{11}$	$K_3 \times 10^{-5}$			$C_{11} \times 10^{-11}$	$C_{12} \times 10^{-11}$	$C_{13} \times 10^{-11}$	$C_{23} \times 10^{-11}$	$C_{44} \times 10^{-11}$	$C_{14} \times 10^{-11}$	$C_{66} \times 10^{-11}$	$\eta \times 10^{-11}$			
4.98	.454	1.565	-.892	1087	491	333	198	12.3	-.64	.65	12.0	8.5	1.30	6.4	4.47	
5.01	1.056	1.315	-.8992	1087	508	310	195	11.3	-.44	1.40	10.5	8.4	1.59	5.87	4.38	
	Observed values			→	1082	466	356	207	8.68	.73	1.41	10.5	5.82	1.73	3.98	3.85

The compressibility  $\eta$  has been calculated from the relation  

$$\eta = \frac{(c_{11} + c_{12}) c_{33} - 2 c_{13}^2}{c_{11} + c_{12} + 2c_{33} - 4c_{13}}$$
. This expression can be readily obtained from the fundamental relations

$$-K_{xx} = c_{11}u_{xx} + c_{12}u_{yy} + c_{13}u_{zz} + c_{14}u_{yz}$$

$$-K_{yy} = c_{12}u_{xx} + c_{11}u_{yy} + c_{13}u_{zz} - c_{14}u_{yz}$$

$$-K_{zz} = c_{13}u_{xx} + c_{13}u_{yy} + c_{33}u_{zz}$$

when  $K_{xx} = K_{yy} = K_{zz}$ .

### 7. Discussion of Results

In the earlier paper the author had calculated the following values of force-constants

$$K = 5.065 \times 10^5, K_1 = 5.116 \times 10^{-11}, K_2 = 9.491 \times 10^{-11} \text{ dynes.}$$

We find from this investigation that value of  $K$  the force-constant of Si—O valence is very nearly the same although  $K_1$  and  $K_2$  are altered. An important result of the investigation is that  $K_3$  is negative and equal to about -89. With only three force-constants  $K$ ,  $K_1$ ,  $K_2$  the elastic constants show very considerable deviations from observed values, and it is only by using  $K_3$  that we get any approximation to the observed values.

The calculated and the observed values of elastic constants are in fair agreement for both the schemes of force-constants given in Table II, although in the second case there is slightly better agreement. A closer agreement between the observed and calculated values can hardly be expected unless all the force-constants and interaction terms are known. The investigation shows that the same scheme of force-constants holds for the elastic constants as well as for the infra-red frequencies.

### 8. Summary

The high frequencies of vibration in  $\alpha$ -quartz and the structure of the crystal show that the silicon-oxygen bonds are largely covalent in nature. We therefore assume that in a homogeneous strain the distance from the basis to basis is altered as if the basis were rigid and attached at one point in the continuum subjected to strain. It then becomes possible to find the change in the bond distances and bond angles on the basis of the known crystal structure. Assuming the four force-constants of Si—O valence, O—O repulsion and  $\overset{\text{Si}}{\text{O}}\text{—}\overset{\text{O}}{\text{Si}}$  and  $\overset{\text{O}}{\text{Si}}\text{—}\overset{\text{O}}{\text{O}}$  deformations the potential energy per unit volume can be calculated, and comparing this with the strain energy of the crystal, the elastic constants can be calculated in terms of the force-constants.

The four force-constants have been calculated from the Raman effect data. Taking the four frequencies 207, 356, 466, 1082 belonging to the totally symmetric class, the variations of the bond distances and bond angles have been worked out by the use of symmetry co-ordinates. Using the four force-constants, the potential as well as kinetic energy of the unit cell has been obtained and the force-constants calculated by obtaining the best agreement between the calculated and observed values of Raman frequencies. The elastic constants are then calculated. The observed and calculated values of elastic constants show good agreement to a first approximation. The investigation shows that the same force-constants hold for the elastic constants and the infra-red frequencies.

In conclusion, the author thanks Sir C. V. Raman, Kt., F.R.S., N.L., for his kind interest in the work and for several valuable suggestions.

#### REFERENCES

1. Bragg and Gibbs	.. <i>Proc. Roy. Soc. Lond.</i> , 1925, <b>109</b> , 425.
2. Saksena, B. D.	.. <i>Proc. Ind. Acad. Sci.</i> , A, 1940, <b>12</b> , 93.
3. Love	.. <i>Mathematical Theory of Elasticity</i> , pp. 38, 39.
4. Saksena, B. D.	.. <i>Proc. Ind. Acad. Sci.</i> , A, 1942, <b>16</b> , 270.
5. Love	.. <i>Mathematical Theory of Elasticity</i> , p. 160.
6. Voigt, W.	.. <i>Lehrbuch der Kristallphysik</i> , 1910 ; <i>Ann. Physik. u. Chem.</i> , 1887, <b>31</b> , 474, 401.

*Note added in proof.*—If from Section 4 we substitute the expressions for  $c_{11}$ ,  $c_{12}$ , etc., in the expression for the compressibility  $\eta$  given at the end of Section 6 we find that  $\eta = [3 \cdot 33 K + 13 \cdot 4 K_3] \times \frac{10^8}{111 \cdot 2}$ . The expression for compressibility thus comes out independent of the force-constants ( $K_1$  and  $K_2$ ) of angular deformation. This is to be expected since in a uniform dilatation or compression the angles do not alter and so the force-constants of angular deformation should not enter in the calculation of compressibility.

## CHEMISTRY OF GOSSYPOL

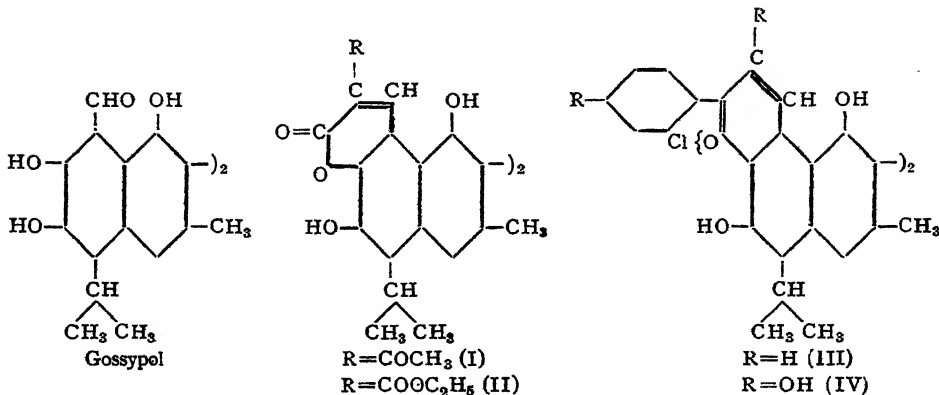
### Part IV. Behaviour of Gossypol as an Ortho-Hydroxy Aldehyde: Formation of $\alpha$ -Pyrones and Flavylium Salts

By B. KRISHNASWAMY, K. SATYANARAYANA MURTY AND T. R. SESHADRI  
(*From the Department of Chemistry, Andhra University*)

Received May 9, 1944

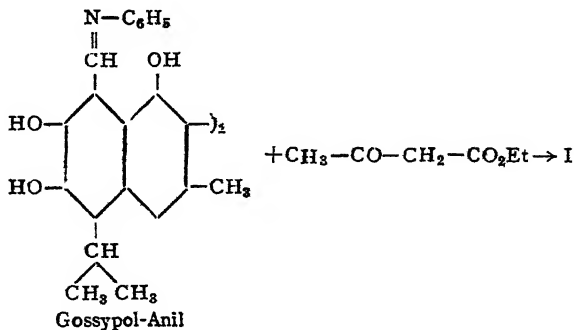
It has been established that gossypol contains six hydroxyl and two aldehyde groups in its molecule through the preparation of the hexa-acetate, the hexamethyl ether and the dianil. But there has been no direct and conclusive evidence about the positions which these groups occupy with reference to one another. Adams and co-workers<sup>1</sup> observed that gossypol gave a deep red colour with pyroboroacetate and a purple red colour with stannic chloride and inferred that ortho-hydroxycarbonyl groups existed. They have used the idea to explain the properties and certain of the unusual reactions of gossypol and its derivatives. The formation of apogossypol<sup>2</sup> by the loss of aldehyde groups when alkali acts upon gossypol may also be adduced in favour of it. But so far the existence of this structural feature has not been definitely proved by the formation of appropriate derivatives. The work described in this memoir has been done with a view to supply this proof.

Two reactions are very characteristic of ortho-hydroxy aldehydes; one of these leads to the formation of  $\alpha$ -pyrones by condensation with ethyl-acetoacetate and with diethylmalonate and the other to the formation of flavylium salts by condensation with acetophenone and with its derivatives in the presence of suitable condensing agents. Gossypol condenses with the above-mentioned esters with the aid of piperidine to form 3-acetyl and 3-carbethoxy- $\alpha$ -pyrones (I and II). These are definite crystalline compounds showing sharp difference in colour between alkaline and acid solutions. Their structures are based on Adams' formula of gossypol. They are sparingly soluble in ordinary solvents and possess high melting points. The condensation of gossypol with acetophenone and  $\omega:4$ -dihydroxy acetophenone takes place readily in ether or ethylacetate solution when saturated with dry hydrogen chloride. The characteristic deeply-coloured flavylium salts (III and IV) are formed and their reactions are described in the experimental part.



Having established as given above the existence of orthohydroxy aldehyde groups in gossypol it becomes necessary to explain the total absence of difficulty in completely methylating it to hexamethyl gossypol. It has been reported already<sup>3</sup> that even diazomethane methylates all the hydroxyl groups of gossypol readily whereas in other cases of ortho-hydroxy carbonyl compounds difficulty has been experienced. An explanation may probably be found in the weakness of the chelation involving the hydroxyl and aldehyde groups in gossypol. That the presence of substituents in neighbouring positions can weaken chelation has been indicated by the work of Chaplin and Hunter<sup>4</sup> and Saunders *et al.*<sup>4a</sup> in other cases. Such substituents are present in the gossypol molecule.

It is interesting to record here that the above-mentioned  $\alpha$ -pyrones and flavylium salts can also be obtained pure when gossypol-dianil is used in the place of gossypol for the condensations. The anil seems to undergo decomposition even under the mild conditions of these reactions, liberating gossypol for condensation with the ketonic esters or the ketones. In some of our previous publications<sup>5</sup> it has been recorded that the anil is easily decomposed by short treatment with hot acetic anhydride to yield gossypol-acetic acid



and that under the ordinary conditions of methylation and acetylation it yields gossypol derivatives and not substitution products of the anil. The experiments recorded here show that even under milder conditions, e.g., mixing with ethyl acetoacetate and piperidine in the cold, the decomposition liberating gossypol takes place.

In the course of the above-mentioned experiments we had occasion to examine the action of aniline on gossypol carefully. It has not been possible to obtain the tetra-anilino compound pure. Though excess of aniline is held rather tenaciously and gives the impression that a tetra-anil is formed (high values for N), the excess of aniline can be removed by careful grinding and boiling of the substance with ether or chloroform (benzene is not quite suitable for the purpose) and only the dianil is left behind. Consequently this alone should be taken as a definite anilino derivative.

### *Experimental*

*Condensation of gossypol with acetoacetic ester (I).*—A mixture of gossypol (0.5 g.) and acetoacetic ester (2 c.c.) was dissolved in the requisite quantity of absolute ethyl alcohol (10 c.c.) to get a clear solution. A few drops of piperidine were added and the contents allowed to stand overnight after shaking for some time. An orange coloured precipitate slowly separated out; it was filtered and washed successively with alcohol and water.

The substance was insoluble in alcohol and other common organic solvents. It crystallised from hot pyridine as yellow thin rectangular plates, which did not melt below 330°. It dissolved in concentrated sulphuric acid giving a bright pink colour which was quite characteristic and stable. It was easily soluble in aqueous sodium hydroxide, forming again a bright pink solution which changed gradually to brown. The pink colour of a freshly made alkaline solution is changed to yellow by acid; the transition from pink to yellow and the reverse is very sharp and is a definite indication of the change from alkali to acid and *vice versa*. In this respect it compares favourably with ordinary indicators used in acidimetry-alkalimetry. The only difficulty in using this substance as an indicator is its insolubility in alcohol.

[Found in air-dried sample: C, 68.4; H, 5.4; loss on drying *in vacuo* at 120°, 2.6%;  $C_{38}H_{34}O_{10}$ ,  $H_2O$  requires C, 68.3, H, 5.4;  $H_2O$  (loss) 2.7%. Found in the vacuum dried sample: C, 69.9; H, 5.3;  $C_{38}H_{34}O_{10}$  requires C, 70.2; H, 5.2%.] Yield of the pure compound 0.3 g.

The same product was obtained even when concentrated sulphuric acid was used instead of alcohol and piperidine.

*Condensation of gossypol-anil with acetoacetic ester (I).*—Gossypol anil (0.5 g.) was dissolved in warm pyridine (15 c.c.), acetoacetic ester (2 c.c.) and a few drops of piperidine were added and the clear solution thus obtained was left over at room temperature for two days. There was only a very small quantity of precipitate which was removed by filtration. The clear filtrate on dilution with methyl alcohol (50 c.c.) gave an orange-yellow solid (0.2 g.). It did not melt below 330° and it was identical with the condensation product of acetoacetic ester and pure gossypol itself in all its properties.

This compound could be prepared in a much shorter time by heating the components in the given proportions on a boiling water-bath for two hours and working up the product as above.

[Found: C, 68.5; H, 5.6;  $C_{38}H_{34}O_{10}$ ,  $H_2O$  requires: C, 68.3; H, 5.4%.]

*Condensation of gossypol with diethyl malonate (II).*—A mixture of gossypol (0.5 g.) and malonic ester (2 c.c.) was dissolved in the requisite quantity of absolute ethyl alcohol to get a clear solution, a few drops of piperidine were added and the contents were allowed to stand for two days. No solid had precipitated at the end of this period. The solution was then poured into about 100 c.c. of water. The precipitate thus produced was filtered and recrystallised from acetic acid and methyl alcohol, when it was obtained as yellow tiny rectangular plates, melting at 248–50°; yield (0.2 g.). With concentrated sulphuric acid it gave a red solution and its solution in sodium hydroxide had a deep red colour which changed to yellow on acidifying; the transition was quite sharp. The number of carbethoxy groups in the molecule was found by estimating the ethoxyl content by the micro-zeisel method.

[Found in the air-dried sample: C, 66.1; H, 5.6;  $OC_2H_5$ , 12.4 and loss on drying *in vacuo* at 120°, 2.6%.  $C_{34}H_{28}O_8(COOC_2H_5)_2$ ,  $H_2O$  requires C, 66.0; H, 5.5,  $OC_2H_5$ , 12.4;  $H_2O$  (loss) 2.5%. Found in the vacuum dried sample: C, 67.5; H, 5.4;  $C_{34}H_{28}O_8(COOC_2H_5)_2$  requires C, 67.6; H, 5.3%.]

*Condensation of gossypol-anil with diethyl malonate (II).*—Gossypol-anil (0.5 g.) was dissolved in warm pyridine (15 c.c.), diethyl malonate (2 c.c.) and a few drops of piperidine were added and the solution was heated on a water-bath for about two hours. The solution was filtered to remove any suspended impurities. A small quantity of the filtrate was diluted with methyl alcohol, but no precipitate was obtained. So the remaining solution was poured into water (100 c.c.) and the precipitate thus obtained (0.2 g.) was filtered and recrystallised from acetic acid. In all respects this

product was found to be identical with the condensation product obtained straight from pure gossypol itself.

[Found: C, 66.4; H, 5.5;  $C_{34}H_{28}O_8$  ( $COOC_2H_5)_2$ ,  $H_2O$  requires: C, 66.0; H, 5.5%.]

*Condensation of gossypol with acetophenone (III).*—A solution of gossypol (0.5 g.) in sodium-dried ether (20 c.c.) was prepared, pure dry acetophenone (2 c.c.) was added and the container was cooled in ice. Dry hydrogen chloride gas was passed into the solution till it was saturated (one and half hours). The initial yellow solution slowly became intense pink. The flask was stoppered well and left in the ice-chest overnight. Only a small quantity of a crystalline solid was deposited on the sides of the container; however, on adding a large amount of ether, a considerable quantity of the pyrylium salt was obtained. It was filtered and recrystallised from methyl alcohol-hydrochloric acid mixture. It was thus obtained as pink-coloured thin rectangular plates and flat needles, melting at 295–97°. Like the salts of anthocyanidins, this flavylium salt was soluble in acidulated hydroxylic solvents like alcohol to give a deep reddish-violet colour. It was insoluble in non-hydroxylic solvents like benzene, ether, etc.

[Found in air-dried sample: C, 67.7; H, 5.9; Cl, 9.0;  $C_{46}H_{40}O_6Cl_2$ ,  $3H_2O$  requires C, 67.9; H, 5.7, and Cl, 8.7%.]

*Decomposition of gossypol-anil with hydrogen chloride.*—To a suspension of gossypol-anil (0.5 g.) in dry ether (20 c.c.), a current of dry hydrogen chloride gas was passed. As the ether absorbed the acid fumes, the original pale yellow solution turned first to orange and finally deep brown and all the suspension went into solution. The ether solution was shaken up with water to remove aniline hydrochloride formed in the reaction and then evaporated to dryness. The brown solid thus obtained was recrystallised from methyl alcohol. A pure sample of this product melted at 184–85° and was found to be identical with gossypol.

*Condensation of gossypol-anil with acetophenone (III).*—To a suspension of gossypol-anil (0.8 g.) in sodium-dried ether (20 c.c.), dry acetophenone (2 c.c.) was added and the container cooled in ice. A current of dry hydrogen chloride gas was passed till saturation (one and half hours). The initial pale yellow solution changed first to orange and finally to deep pink as the gossypol-anil went into solution and the condensation took place. The container was stoppered well and left in the ice-chest overnight. More ether was added to it the next day and the precipitate (0.25 g.) thus obtained was filtered and recrystallised from methyl alcohol-hydrochloric acid mixture. As regards melting point, crystal structure, colour reactions and other

properties, the pyrilium salt obtained by this method was quite identical with the one prepared starting with pure gossypol itself.

[Found: C, 67.9; H, 6.0;  $C_{46}H_{40}O_6Cl_2$ ,  $3H_2O$  requires: C, 67.9; H, 5.7%.]

*Condensation of gossypol with  $\omega$ :4-dihydroxy acetophenone (IV).*—Gossypol (30 mg.) and  $\omega$ :4-dihydroxy acetophenone (20 mg.) were dissolved in sodium-dried ether (20 c.c.), the ice-cooled solution was saturated with dry hydrogen chloride gas and the contents left in the ice-chest overnight. Since the quantities of the starting materials were small, ether and hydrogen chloride were evaporated at the laboratory temperature and the residue taken up in 1% methyl alcoholic hydrogen chlroide. The pyrylium salt was precipitated from this solvent by adding concentrated hydrochloric acid. The solid thus obtained was filtered and recrystallised from the same solvent, when it was obtained as tiny rectangular plates, having a deep pink colour. It did not melt below 320°.

[Found: C, 65.1; H, 5.6;  $C_{46}H_{40}O_8Cl_2$ ,  $3H_2O$  requires: C, 65.3; H, 5.4%.]

The above-mentioned two flavylium salts gave the following colour reactions with the reagents listed below. Solutions of the salts in methyl alcohol containing 1% hydrochloric acid were used for the purpose.

Reagents	Flavylium salt obtained from gossypol and	
	(i) Acetophenone (III)	(ii) $\omega$ :4-Dihydroxy acetophenone (IV)
1. Original colour of solution ..	Deep red-violet	Deep red ; in thin layers pink
2. Dilution with concentrated HCl	No change	No change
3. Sodium acetate solution ..	Blue	Only a small change to reddish-pink ; no change further
4. Sodium bicarbonate ..	Blue with a slight green tinge	Bluish-pink ; changes to violet-blue and fades slowly to violet-brown
5. Sodium carbonate ..	Greenish-blue	Same as bicarbonate colour but changes are more rapid
6. Sodium hydroxide ..	Sudden change to brown	Deep blue ; fades fast and becomes pale yellowish-brown

The flavylium salts undergo decomposition slowly on storage and the products become deficient in halogen. This behaviour has been found in the case of many other complex flavylium salts prepared in these laboratories.<sup>6</sup> Due to the presence of water of crystallisation, elimination of halogen acid

seems to take place leading to the formation of colour base or of the chalkone.<sup>7</sup>

### Summary

Gossypol condenses with ethylacetoacetate and diethyl malonate in the presence of piperidine to form pyrones and with acetophenone and dihydroxy acetophenone in the presence of hydrogen chloride to form flavylium salts. They are definite crystalline substances with characteristic properties. Thus the presence of two ortho-hydroxyaldehyde groups in the gossypol molecule is established. The dianilino-compound of gossypol also undergoes the above condensations smoothly indicating that it is easily split up into gossypol and aniline under the conditions of the reactions.

### REFERENCES

1. Adams *et al.* .. *J.A.C.S.*, 1937, **59**, 1723 ; 1938, **60**, 2193.
2. Clark .. *J. Biol. Chem.*, 1928, **78**, 159.
3. Murty and Seshadri .. *Proc. Ind. Acad. Sci., A*, 1942, **16**, 146.
4. Chaplin and Hunter .. *J.C.S.*, 1938, 375 and 1034.
- 4a. Sauunders *et al.* .. *J.A.C.S.*, 1941, **63**, 3121.
5. Murty, Murty and Seshadri *Proc. Ind. Acad. Sci., A*, 1942, **16**, 54.  
Murty and Seshadri .. *Ibid., A*, 1942, **16**, 141.
6. Row and Seshadri .. *Ibid., A*, 1942, **15**, 118.
7. \_\_\_\_\_ .. *Ibid., A*, 1941, **13**, 512.

# THE MAGNETIC SUSCEPTIBILITY AND ANISOTROPY OF CARBORUNDUM

BY A. SIGAMONY

(*From the Department of Physics, Indian Institute of Science, Bangalore*)

Received April 25, 1944

(Communicated by Sir C. V. Raman, Kt., F.R.S., N.L.)

## 1. Introduction

THE study of the magne-crystallic behaviour of carborundum should be of considerable interest in view of the fact that the crystal is a valence structure in which the atoms of carbon are bound tetrahedrally to the atoms of silicon and *vice-versa*. Remarkably enough, five crystalline modifications of the substance have been reported, two of which are of the rhombohedral class, two hexagonal and one cubic. According to Moissan, carborundum may be transparent and colourless or vary in tint from emerald green to brown or black. It is not improbable that these variations of colour arise from the presence of impurities in the crystal. If this be the case, they might be expected to affect its magnetic behaviour.

Carborundum was available in Sir C. V. Raman's crystallographic collection in the form of an aggregate in which large crystalline plates had formed out of a matrix. It was possible to break off the crystals and each specimen thus obtained from the matrix was about 5 mm. square in area and a couple of millimeters thick. These crystals were perfectly black, but had smooth and lustrous surfaces. Another sample was also available in the form of a crystalline plate which was translucent and green in colour. This sample had been examined by Dr. C. S. Venkateswaran who found that the Laue pattern given by it with the X-ray beam normal to the plate had hexagonal symmetry. This sample as well as three samples detached from the aggregate were examined for their magnetic behaviour.

The magnetic susceptibility was measured in a Curie balance. A large electromagnet, the coils of which could be clamped at a suitable angle was employed for this purpose. The plates were suspended with the plane parallel to the magnetic field and the susceptibility perpendicular to the hexagonal axis ( $\chi_{\perp}$ ) was measured by comparison with double distilled water.

The measurements of magnetic anisotropy were made by the torsional method of K. S. Krishnan (1933). A Cook electromagnet with large pole-pieces having an area of 8 cm.  $\times$  8 cm. was used and with a pole-gap of  $1\frac{1}{4}$ ", field strengths of the order of 4000 to 6000 oersted were obtained for moderate currents. A quartz fibre was drawn out in the blast of an oxy-gas flame and used as the suspension. Its torsional constant was determined by the oscillation method with glass cylinders of known moments of inertia and then used for the measurement of the angle of critical torsion. The orientation of the crystal in the magnetic field was determined by the usual method with the help of a telemicroscope mounted on a circular scale and a plane mirror. The non-homogeneity of the field was tested and its effect was found to be negligible. The field was measured with a search-coil and a calibrated fluxmeter.

## 2. Results

The magnetic characteristics of the green plate conformed strictly to the known hexagonal symmetry of the crystal. There was no anisotropy in the plane perpendicular to the hexagonal axis and when suspended with the axis horizontal the orientation of the axis was parallel to the field, showing that  $\chi_{||}$  was greater than  $\chi_{\perp}$  algebraically. Table I gives the experimental data.

TABLE I  
*Green Hexagonal Plate of Carborundum*

Mass of the crystal = 35.0 mgm.

Torsional constant of the fibre =  $1.429 \times 10^{-3}$

Field strength oersted	Critical angle of torsion $a_c$	$(\chi_{  } - \chi_{\perp})$ per gm. mol.
4640	357°	$0.82_5 \times 10^{-6}$
5270	446°	$0.82_1 \times 10^{-6}$
5760	526°	$0.82_5 \times 10^{-6}$
6160	597°	$0.83_0 \times 10^{-6}$

$$\text{Mean} = 0.82 \times 10^{-6}$$

Since the critical angle of torsion was small, the accurate formula

$$\chi_{||} - \chi_{\perp} = \frac{2 c}{m H^2} \left( a_c - \frac{\pi}{4} - \delta \right) \cdot M., \text{ was used where}$$

$$\tan 2\delta = \frac{1}{2 \left( a_c - \frac{\pi}{4} - \delta \right)}$$

The susceptibility was found to be independent of the field strength within the limits of experimental accuracy and a value  $-13.1 \times 10^{-6}$  per gm. mol. was obtained for  $\chi_{\perp}$ .

The deportment of the black crystals in the magnetic field was found to be irregular. All the specimens examined had appreciable anisotropy in the plane perpendicular to the axis. When suspended with the axis horizontal the plates set themselves with their axes at an angle to the field which was different for the different specimens and decreased slowly as the field strength increased. They were found to be diamagnetic but the numerical value of the susceptibility diminished at a rapid rate with the decrease of the magnetic field. Table II gives some experimental data.

TABLE II  
*Black Crystals of Carborundum*

Field strength oersted	$\chi_{\perp}$ per gm. mol.		
	Crystal I	Crystal II	Crystal III
3560	$-5.7 \times 10^{-6}$	$-7.5 \times 10^{-6}$	$-5.4 \times 10^{-6}$
3890	$-6.8 \times 10^{-6}$	$-7.9 \times 10^{-6}$	$-6.0 \times 10^{-6}$
4250	$-7.1 \times 10^{-6}$	$-8.2 \times 10^{-6}$	$-6.6 \times 10^{-6}$

### 3. Discussion

The gm. mol. anisotropy ( $\chi_{\parallel} - \chi_{\perp}$ ) obtained for the hexagonal green crystal of carborundum is  $0.82 \times 10^{-6}$  which is of the same order of magnitude as that for the sulphates and the selenates and much lower than that for the carbonates and the nitrates. In the latter crystals the complexes responsible for their anisotropy retain their characteristics practically unaltered in different compounds and hence the observed susceptibilities can be correlated with the magnetic constants of these complexes. The theory for the interpretation of the feeble diamagnetic anisotropy of crystals having isosthenic lattices is not developed. One example of this type of lattice is quartz which has a gm. mol. anisotropy ( $\chi_{\perp} - \chi_{\parallel}$ ) of  $0.12 \times 10^{-6}$ . The explanation for the anisotropy of such crystals has to be sought for in the deformation of the electron density distribution of the constituent atoms due to the interaction of their immediate neighbours. The anisotropy of carborundum is greater than that of quartz and this fact is intelligible in view of the fact that its bonds are much stronger and can produce a greater modification of the electron density distribution of the atoms.

The mean of the three principal susceptibilities of the green specimen is  $-12.8 \times 10^{-6}$  per gm. mol. Only a rough theoretical estimate of its susceptibility is possible. From Slater's expression for the mean square radius of the electron orbits, the susceptibilities of the free carbon and silicon atoms are calculated to be  $-9.1 \times 10^{-6}$  and  $-25.1 \times 10^{-6}$  respectively. The experimental value obtained by the author (1944, only the highest value obtained is used) for carbon in the form of diamond is  $-0.456 \times 10^{-6}$  per gm. which gives a gm. atomic susceptibility of  $-5.5 \times 10^{-6}$ . The value obtained by Honda (1910) for silicon is  $-3.5 \times 10^{-6}$  and by Owen (1912) is  $-3.6 \times 10^{-6}$  and these values are much lower than the theoretical value. Assuming an additive law, from the experimental values given above for diamond and carborundum, the susceptibility of silicon is found to be  $-7.3 \times 10^{-6}$  which is also lower than the theoretical value. Pascal however gets the value  $-20 \times 10^{-6}$  for the silicon atom in combination with organic compounds.

In conclusion the author wishes to express his gratitude to Professor Sir C. V. Raman for his keen interest and encouragement in this work.

#### 4. Summary

The magnetic susceptibility and anisotropy of carborundum have been measured. The crystals of the black variety examined are found to be diamagnetic but irregular in their behaviour. A green hexagonal plate of carborundum was however found to behave in a regular way. It had a mean gm. mol. susceptibility of  $-12.8 \times 10^{-6}$  and anisotropy of  $0.82 \times 10^{-6}$ , the susceptibility perpendicular to the hexagonal axis being numerically higher.

#### REFERENCES

Venkateswaran	.. <i>Proc. Ind. Acad. Sci.</i> , 1941, A <b>14</b> , 387.
Krishnan, Guha and Banerjee	.. <i>Phil. Trans. Roy. Soc. Lond.</i> , 1933, A <b>231</b> , 235.

## SYNTHESIS OF COMPOUNDS RELATED TO SANTONIN

By (Miss) K. D. PARANJAPE, N. L. PHALNIKAR, B. V. BHIDE  
AND K. S. NARGUND

(*Maharaja Pratapsinh Chemical Laboratory, S. P. College, Poona, 2*)

Received February 29, 1944

(Communicated by M. Sreenivasaya, F.A.Sc.)

SANTONIN, the lactone of 1-hydroxy-7-keto-8-10-dimethyl  $\Delta^{5:8}$ -hexahydro-naphthyl-2-propionic acid (A), the well-known naturally occurring anthelmintic, has been recently synthesised by us.<sup>1</sup> The anthelmintic action of santonin is generally attributed to the lactonic and ketonic groups in it. It will be interesting to see whether the methyl groups in 8 and 10 positions in santonin have any marked effect on the anthelmintic action. We have, therefore, synthesised the following compounds related to santonin by the series of reactions given below :—

- (1) Lactone of 1-hydroxy-7-keto- $\Delta^{5:8}$  hexahydro naphthyl 2-propionic acid (B).
- (2) Lactone of 1-hydroxy-7-keto-8-methyl  $\Delta^{5:8}$ -hexahydro-naphthyl-2-propionic acid (C).
- (3) Lactone of 1-hydroxy-7-keto-10-methyl  $\Delta^{5:8}$ -hexahydro-naphthyl-2-propionic acid (D).

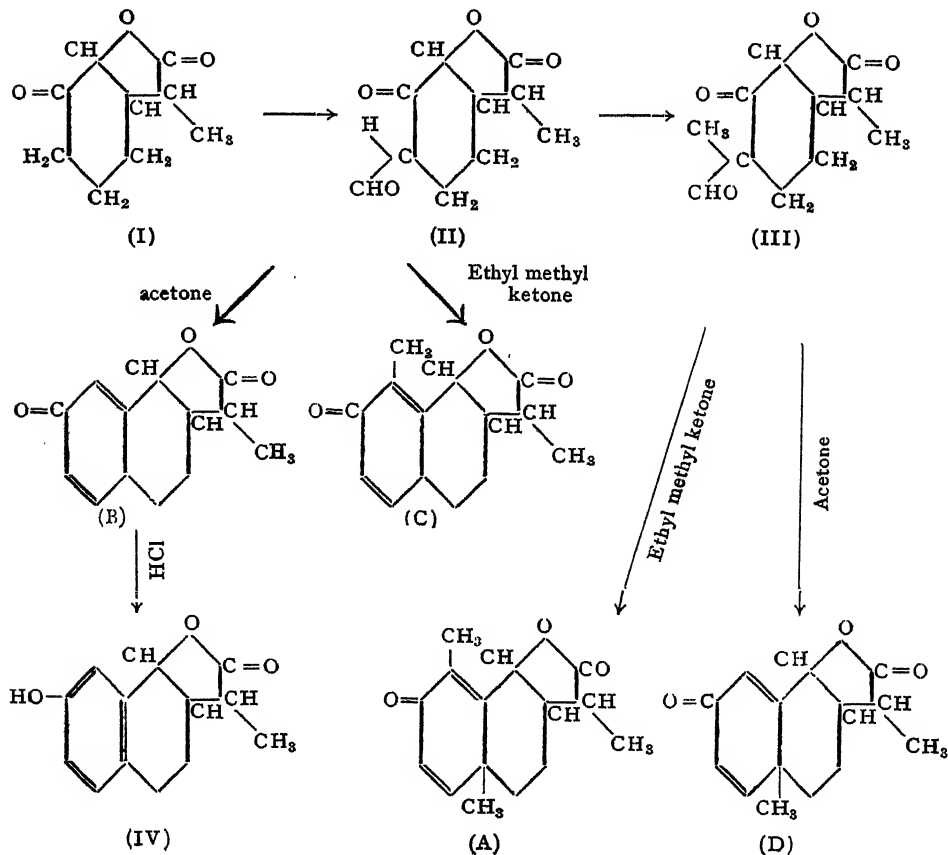
Condensation of 6-keto-2-chloro- $\Delta^1$ -cyclohexene<sup>3</sup> with diethyl sodio-mono-methyl-malonate, followed by hydrolysis gives the lactone of  $\alpha$ -(2-hydroxy-3-keto-cyclohexyl) propionic acid (I). This keto lactone (I) on condensation with ethyl formate in the presence of sodium gives the lactone of  $\alpha$ -(2-hydroxy-3-keto-4-formyl-cyclohexyl) propionic acid (II). Condensation of this keto-formyl lactone (II) with acetone and ethyl methyl ketone furnished the lactones (B) and (C) respectively.

The lactone (B) on treatment with fuming hydrochloric acid was converted into the lactone of 1,7-dihydroxy-tetrahydro-naphthyl propionic acid IV, identical with the lactone obtained from 7-methoxy tetralone by Paranjape, Phalnikar and Nargund.<sup>4</sup> It may be noted that the transformation of (B) into (IV) is a reaction analogous to the conversion of santonin into desmotroposantonin.

Condensation of this keto-formyl-lactone (II) with ethyl methyl ketone gave (C). Ethyl methyl ketone may condense with the lactone (II) in two different ways and may give either 8-methyl or 6-methyl lactone. It has been shown by us<sup>1</sup> that ethyl methyl ketone condenses with 2-formyl-cyclohexanone to give 7-keto-8-methyl-hexahydro-naphthalene. On similar lines it is assumed that ethyl methyl ketone will condense with the lactone (II) and give a 8-methyl compound (C) and not the 6-methyl one.

The sodio salt of the lactone (II) when treated with methyl iodide under pressure undergoes methylation and the methylated product (III) when condensed with acetone in the presence of sodium ethoxide gives the lactone (D).

It will be noted that these lactones (B), (C) and (D) differ from santonin in the fact that they contain two or one methyl group less than in santonin. The pharmacological actions of these lactones has been studied and will be reported later.



These compounds contain asymmetric carbon atoms. Details regarding their optical properties will be reported in another communication. A preliminary account of these properties however has been recently published.<sup>2</sup>

### Experimental

The preparation of the lactone of  $\alpha$ -(2-hydroxy-3-keto-cyclohexyl) propionic acid (I), the lactone of  $\alpha$ -(2-hydroxy-3-keto-4-formyl-cyclohexyl) propionic acid (II) and the lactone of  $\alpha$ -(2-hydroxy-3-keto-4-formyl-4-methyl cyclohexyl) propionic acid (III) has been described by us.<sup>1</sup>

*Lactone of 1-hydroxy-7-keto- $\Delta^{5:8}$ -hexahydro-naphthyl-2-propionic acid (B).*—The lactone of  $\alpha$ -(2-hydroxy-3-keto-4-formyl-cyclohexyl) propionic acid (II) (8 gm.) was mixed with acetone (2 gm.) and the mixture was added to sodium ethoxide prepared from sodium (3.2 gm.) and absolute alcohol (40 c.c.) and was allowed to stand overnight. Alcohol was then removed on a water-bath and the reaction mixture was acidified with dilute hydrochloric acid and extracted with ether. The ether layer was washed with water, dried over calcium chloride (anhydrous) and ether removed. The residue containing the lactone of 1-hydroxy-7-keto- $\Delta^{5:8}$ -hexahydro-naphthyl-propionic acid (B) was a semisolid, which on crystallisation from benzene was obtained as fine needles and melted at 91°.

[Found: C, 71.7; H, 6.5 per cent. Equi. wt. (by back titration), 217.7;  $C_{13}H_{14}O_3$  requires C, 71.6; H, 6.4 per cent. and Equi. wt. 218.0.] It gives a semicarbazone, m.p. 145°.

On keeping this lactone with fuming hydrochloric acid in a sealed tube for 21 days, it was transformed into the lactone of 1,7-dihydroxy-tetrahydro-naphthyl propionic acid (IV), m.p. 111° C. identical with the lactone prepared by Paranjape, Phalnikar and Nargund<sup>4</sup> from -7-methoxy-tetralone.

*Lactone of 1-hydroxy-7-keto-8-methyl- $\Delta^{5:8}$ -hexahydro-naphthyl-2-propionic acid (C):*—The lactone (II) was similarly condensed with ethyl methyl ketone in the presence of sodium ethoxide and was worked up as in the above case. The lactone of 1-hydroxy-7-keto-8-methyl- $\Delta^{5:8}$ -hexahydro-naphthyl-2-propionic acid (C) thus obtained, crystallised from alcohol and had m.p. 111°.

[Found: C, 72.7; H, 6.9 per cent. Equi. wt. (by back titration), 232.1;  $C_{14}H_{16}O_3$  requires C, 72.4; H, 6.9 per cent. and Equi. wt. 232.0.]

*Lactone of 1-hydroxy-7-keto-10-methyl- $\Delta^{5:8}$ -hexahydro-naphthyl-2-propionic acid (D).*—Condensation of the lactone of  $\alpha$ -(2-hydroxy-3-keto-4-formyl-4-methyl cyclohexyl)-propionic acid (III) with acetone was carried out as

in the above case. The lactone of 1-hydroxy-7-keto-10-methyl- $\Delta^5$ : $\delta$ -hexahydro-naphthyl-2-propionic acid (D) was first obtained as a syrupy liquid but on purification and crystallisation from alcohol it was obtained as a solid, m.p. 141°. It gave a semicarbazone, m.p. 201° C.

[Found: C, 72.8; H, 6.9 per cent. and Equi. wt. (by back titration), 231.8;  $C_{14}H_{16}O_3$  requires C, 72.4; H, 6.9 per cent. and Equi. wt. 232.0.]

### Summary

Following the methods used in the synthesis of santonin the synthesis of compounds related to santonin has been described.

### REFERENCES

1. Paranjape, Phalnikar, Bhide and Nargund *Rasayanam*, 1943, **1**, No. 8, 233 ; *Current Science*, 1943, **12**, 153.
2. \_\_\_\_\_ .. *Current Science*, 1943, **12**, 307.
3. Crossley .. *J.C.S.*, 1903, **83**, 494.
4. Paranjape, Phalnikar and Nargund *J. Univ. Bom.*, 1943, **12**, Part 3, 63.

## SYNTHESIS OF CANTHARIDINE AND DESOXYCANTHARIDINE

BY (MISS) K. D. PARANJAPE, N. L. PHALNIKAR, B. V. BHIDE  
AND K. S. NARGUND

(*Maharaja Pratapsinh Chemical Laboratory, S. P. College, Poona, 2*)

Received February 29, 1944

(Communicated by M. Sreenivasaya, F.A.Sc.)

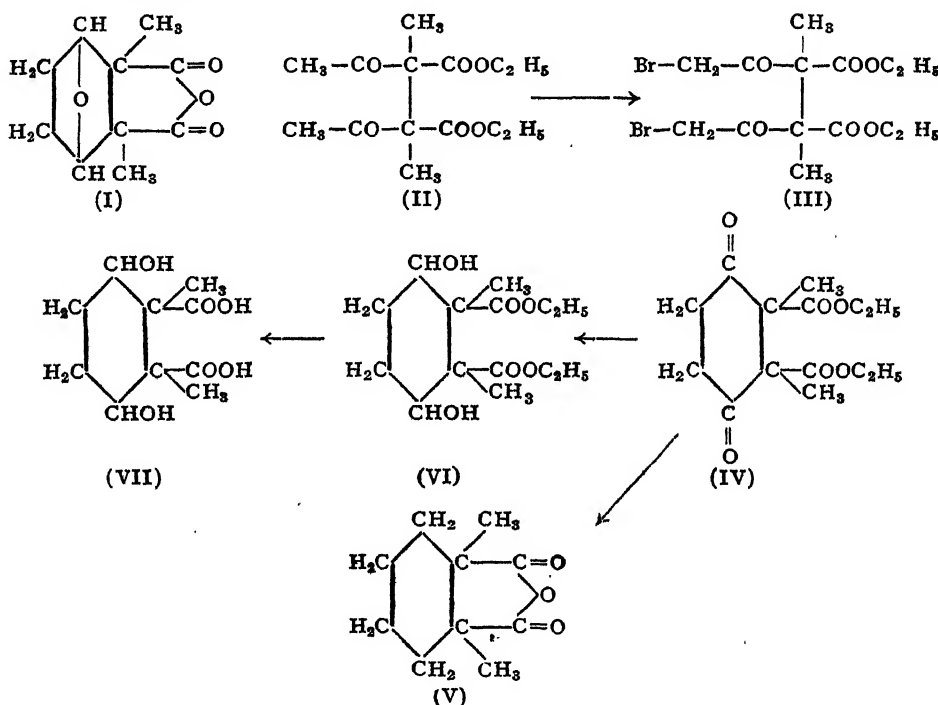
CANTHARIDINE, the active principle of *Cantharis vesicatoria*<sup>1</sup> and of *Mylabris pustulata* Fb. India<sup>2</sup>, has been assigned the structure (I) mainly on the basis of analytical evidence by Gadamer and others.<sup>3</sup> This structure has received further support by the observation of Bruchhausen and Bersch<sup>4</sup> that maleic anhydride is formed in the pyrolysis of cantharidine.

Various unsuccessful attempts at the synthesis of cantharidine have been made. Steele<sup>5</sup> attempted to prepare desoxycantharidine by debrominating  $\alpha\alpha'$ -dibromo- $\alpha\alpha'$ -dimethyl suberic acid but the debromination could not be effected. Guha and Iyer<sup>2</sup> unsuccessfully attempted to replace bromine by cyanogen in 1-2-dibromo-1-2-dimethyl-cyclohexane. Pai and Guha<sup>6</sup> attempted to methylate 3-6-diketo-cyclohexane-1-2-dicarboxylate but no C methylation took place. The condensation of ethyl  $\beta:\beta'$ -diketo-tetrahydrofuran- $\alpha\alpha'$ -dicarboxylate either with ethyl- $\alpha$ -bromo propionate or with alkylene bromides proved unsuccessful.<sup>7</sup> Diels and Alder<sup>8</sup> failed to add dimethyl maleic anhydride to furan although nor-cantharidine and iso-cantharidine were prepared by similar methods.

Recently Woodward and Loftfield<sup>9</sup> have reported the synthesis of desoxycantharidine by the reduction of the addition product obtained from butadiene and dimethyl maleic anhydride. Ziegler, Schenck, Krockow, Siebert, Wenz and Weber<sup>10</sup> have reported the synthesis of cantharidine and desoxycantharidine by a series of long and difficult reactions. The present paper describes the synthesis of these substances by a simpler method.

Sodio derivative of ethyl- $\alpha$ -methyl-acetoacetate when treated with iodine gave diethyl- $\alpha\alpha'$ -diacetyl- $\alpha\alpha'$ -dimethyl succinate (II). Bromination of (II) gave the dibromo-compound (III), which on treatment with finely divided silver was debrominated and cyclised to diethyl-3-6-diketo-1-2-dimethyl cyclohexane-1-2-dicarboxylate (IV). Clemmenson reduction of (IV) followed by hydrolysis and steam distillation gave desoxycantharidine (V). Reduction

of (IV) by aluminium isopropoxide gave (VI) which on hydrolysis gave the corresponding dihydroxy acid (VII). Treatment of crude (VI) with concentrated sulphuric acid at room temperature for 100 hours gave a black mass from which cantharidine was obtained by sublimation. The synthetic sample of cantharidine had m.p. 217° C. and did not depress the m.p. of an authentic sample kindly supplied by Dr. P. C. Guha, Indian Institute of Science, Bangalore, to whom our thanks are due.



### Experimental

*Diethyl-aa'-diacetyl-aa'-dimethyl succinate (II).*—To finely pulverised sodium (4.6 gm.) suspended in dry benzene (50 c.c.) was added ethyl-*a*-methyl-acetoacetate (28.8 gm.). It was then refluxed for three hours and iodine (25.4 gm.) was then added and refluxing continued till the colour of iodine disappeared. It was then treated with ice and dilute sulphuric acid. The benzene layer was separated, washed with water and dried and benzene was removed. The residue could not be purified by distillation under reduced pressure and was therefore used to prepare the bromo-compound as described below.

*Diethyl-aa'-di-(ω-bromoacetyl)-aa'-dimethyl succinate (III).*—To a solution of the above ester (II) (28.6 gm.) in carbon disulphide (50 c.c.) was

added bromine (32 gm.) dissolved in the same solvent (50 c.c.), a trace of anhydrous aluminium chloride being used as a catalyst. Vigorous evolution of hydrobromic acid took place. The residue after removal of carbon disulphide was crystallised from benzene and had m.p. 55° C.

[Found: Br, 36·4; C<sub>14</sub>H<sub>20</sub>O<sub>6</sub>Br<sub>2</sub> requires Br, 36·0%.]

*Diethyl-3-6-diketo-1-2-dimethyl-cyclohexane-1-2-dicarboxylate (IV).*—Diethyl-*αα'-di-(ω-bromoacetyl)-αα'-dimethyl succinate* (III) (22 gm.) and molecular silver (10·8 gm.) were heated together on an oil-bath at 120° C. for three hours and then at 150° C. for half an hour. The product recovered by ether extraction was a viscous liquid which could not be distilled without decomposition. It was characterised by its di-*p*-nitrophenyl hydrazone, m.p. 143° C.

[Found: C, 56·2; H, 5·4; N, 15·6. C<sub>26</sub>H<sub>30</sub>N<sub>6</sub>O<sub>8</sub> requires C, 56·3; H, 5·4; N, 15·2%.]

*1-2-Dimethylcyclohexane-1-2-dicarboxylic anhydride (V).*—Diethyl-3-6-diketo-1-2-dimethylcyclohexane-1-2-dicarboxylate (IV) (5 gm.) was reduced by zinc amalgam by Clemmenson's method. The product recovered by ether extraction was hydrolysed by alkali and the product obtained after acidification was steam-distilled. The steam volatile product was identified as desoxycantharidine, m.p. 128°. The steam-non-volatile product crystallised from alcohol when it had m.p. 165°. It was therefore 1-2-dimethyl cyclohexane dicarboxylic acid.

[Found: C, 60·3%; H, 8·0% and Eq. wt. 100·4. C<sub>10</sub>H<sub>16</sub>O<sub>4</sub> requires C, 60·0%; H, 8·0%; Eq. wt. 100.] Woodward and Loftfield<sup>9</sup> give m.p. 129° for desoxycantharidine and m.p. 166° for desoxycantharic acid.

*3-6-Dihydroxy-1-2-dimethylcyclohexane-1-2-dicarboxylic acid (VII).*—Diethyl 3-6-diketo-1-2-dimethylcyclohexane 1-2-dicarboxylate (IV) (15·2 gm.) was reduced by aluminium isopropoxide (from aluminium 0·8 gm. and isopropyl alcohol 34 c.c.) following the method of Lund.<sup>11</sup> The recovered product (VI) was directly hydrolysed by alkali and the acid obtained when crystallised from petrol, had m.p. 99°.

[Found: C, 51·92%; H, 7% and Eq. wt. 116·2. C<sub>10</sub>H<sub>16</sub>O<sub>6</sub> requires C, 51·72%; H, 6·89% and Eq. wt. 116.] It was soluble in all organic solvents except chloroform.

*3-6-Oxido-1-2-dimethyl-cyclohexane-1-2-dicarboxylic anhydride (Cantharidine) (I).*—Crude diethyl-1-3-6-dihydroxy-1-2-dimethyl-cyclohexane 1-2-dicarboxylate (VI) (10 gm.) obtained in the above experiment, was mixed with concentrated sulphuric acid (100 gm.) and the mixture was kept at room

temperature for 100 hours. It was then poured into water and the product recovered by ether extraction was hydrolysed by alkali. It was then acidified and extracted with chloroform. The product obtained after removal of chloroform was sublimed preferably with a drop of concentrated sulphuric acid when cantharidine was obtained in colourless needles, m.p. 217° and did not depress the m.p. of an authentic specimen. It gave all the colour reactions of cantharidine (yield 10% calculated on ethyl acetoacetate used).

[Found : C, 61.3%; H, 6.1%.  $C_{10}H_{12}O_4$  requires C, 61.2%; H, 6.1%.] It formed a mono-phenyl-hydrazone, m.p. 193 (*cf.* Spiegel<sup>12</sup>).

### Summary

A new and simple method for the synthesis of cantharidine and desoxy-cantharidine has been described.

### REFERENCES

1. Robiquet .. *Ann. Chim.*, 1810 (1), **76**, 307.
2. Guha and Iyer .. *J. Ind. Inst. Sc.*, 1931, **14 A**, 31.
3. Gadamer .. *Arch. Pharm.*, 1914, **252**, 609, 636, 662; 1917, **255**, 290, 315; 1920, **258**, 171.  
Rudolph .. *Ibid.*, 1916, **254**, 423.  
Dankworth .. *Ibid.*, 1914, **252**, 632.  
Coffey .. *Rec. Trav. Chim.*, 1923, **42**, 387, 1026.
4. Bruchhausen and Bersch .. *Arch. Pharm.*, 1929, **266**, 697.
5. Steele .. *J. A. C. S.*, 1931, **53**, 283.
6. Pai and Guha .. *J. Ind. Chem. Soc.*, 1934, **11**, 283.
7. Guha and Iyer .. *J. Ind. Inst. Sc.*, 1938, **21 A**, 115; 1940, **23 A**, 159.
8. Diels and Alder .. *Ber.*, 1929, **62**, 554.
9. Woodward and Loftfield .. *J. A. C. S.*, 1941, **63**, 3167.
10. Ziegler, Schenck, Krockow,  
Siebert, Wenz and Weber .. *Ann.*, 1942, **551**, 1 (*cf.* *B. C. A.*, 1943, **A 2**, 43).
11. Lund .. *Ber.*, 1937, **70**, 1520.
12. Spiegel .. *Ibid.*, 1892, **25**, 1469.

# OPACITY CHANGES DURING THE COAGULATION OF SOLS BY ELECTROLYTES

BY MATA PRASAD, S. GURUSWAMY\* AND N. A. PADWAL

(From the Chemical Laboratories, Royal Institute of Science, Bombay)

Received May 24, 1944

THE opacity method of following the coagulation of a sol was first developed by Mukherjee and Mujumdar<sup>1</sup> by allowing the light transmitted through the coagulating system to fall on a thermopile connected to a galvanometer. Desai<sup>2</sup> modified this method by using a photo-cell in place of thermopile. Prasad and Modak<sup>3</sup> modified Desai's method by amplifying the current from the photo-cell. Recently, Prasad and Gogate<sup>4</sup> have designed an apparatus for the measurement of opacity of gel-forming systems and they find that results of fairly high repeatability can be obtained by the use of this apparatus. This was therefore used to study the kinetics of coagulation of sols by electrolytes, and the effects of temperature and the addition of non-electrolytes on the coagulation were also examined. The sols employed were those of thorium, stannic, and zirconium hydroxides; the coagulation of some of these has been studied previously by some workers. The results obtained are discussed in the following pages.

## 1. Results and Discussion

(a) *Thorium hydroxide sol.*—The sol was prepared by the method adopted by Desai (*loc. cit.*), and was dialysed for 7 days. The concentration of the sol was found to be 4·1 g. of  $\text{ThO}_2$  per litre.

Equal volumes of the sol and electrolytes ( $\text{K}_2\text{SO}_4$ ,  $\text{KCl}$ ,  $\text{KNO}_3$ ,  $\text{BaCl}_2$ ,  $\text{NaCl}$ ) of different concentrations were mixed and the opacity of the coagulating mixture was measured at different intervals of time commencing from the time of mixing. The time-deflection curves obtained during the coagulation of the sol by the highest and lowest concentrations employed are shown graphically in Figs. 1 and 2. The concentrations of the electrolytes mentioned refer to the amounts of electrolytes present in the total volume (9 c.c.) of the coagulating mixture.

\* Springer Research Scholar of the Bombay University.

<sup>1</sup> *J. C. S.*, 1924, 125, 785.

<sup>2</sup> *Trans. Farad. Soc.*, 1928, 24, 181.

<sup>3</sup> *Proc. Ind. Acad. Sci.*, 1940, 12, 235.

<sup>4</sup> *Ibid.*, 1943, 17, 163.

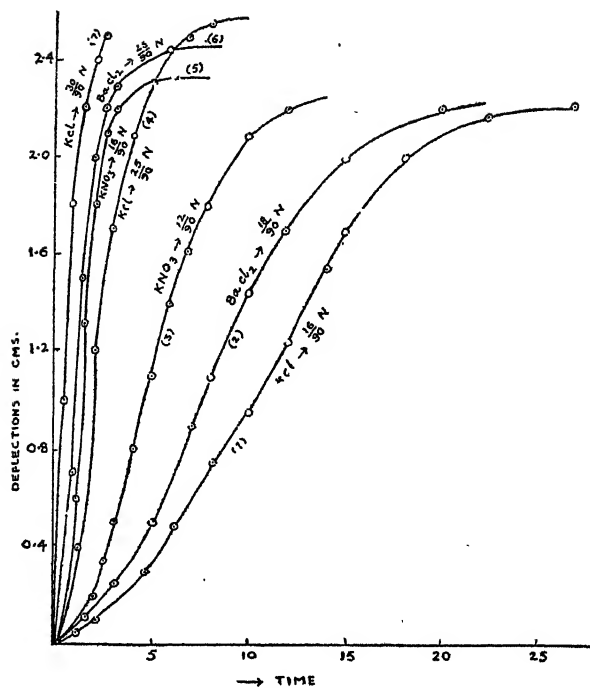


FIG. 1. Coagulation of Thorium Hydroxide Sol.

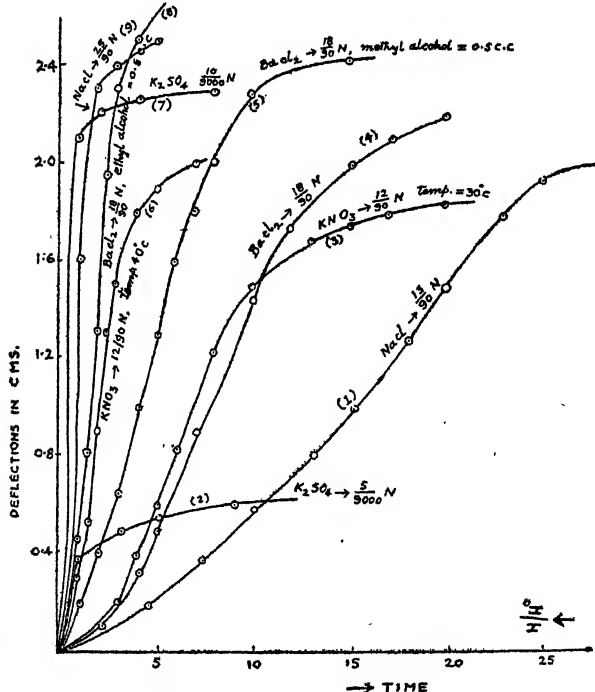


FIG. 2. Coagulation of Thorium Hydroxide Sol.

All the curves in Figs. 1 and 2 are continuous showing thereby that coagulation is a continuous phenomenon. Potassium sulphate is a good coagulator (*cf.* curves 2 and 7, Fig. 2) since its concentration required for coagulation is relatively smaller than those of other electrolytes. This may be due to the bivalent nature of the coagulating ion. Moreover, the coagulation in the presence of potassium sulphate is rapid, it being nearly completed in about 2 minutes in the presence of 1/900 N  $\text{K}_2\text{SO}_4$ ; if its concentration is less than this only partial coagulation takes place.

The behaviour of the other electrolytes is very similar to each other but different from that of potassium sulphate. The coagulation of the sol by barium chloride in the presence of ethyl and methyl alcohols shows that the rate of coagulation is greatly increased by such an addition (*cf.* curves 4, 5 and 8, Fig. 2), the increase being greater in the presence of ethyl than methyl alcohol.

Temperature has a great effect on the coagulation velocity (*cf.* curves 3 and 6, Fig. 2). The rate of coagulation is accelerated by the increase in temperature, but the nature of the curves remains the same.

The observations for the same sol taken at 30° with 12/90 N potassium nitrate given in Fig. 2 (curve 3) differ from those given in Fig. 1 (curve 3); the former were taken about a month after the latter. The observed differences are apparently due to the ageing of the sol during this period.

An examination of the various curves in Figs. 1 and 2 shows that the final value of opacity in the presence of different amounts of the same electrolyte is not the same. Usually it increases, though slightly, when increasing amounts of the electrolytes are added. This increase is also noticeable when the sol is coagulated at different temperatures and in the presence of ethyl and methyl alcohols. These changes are predominant in the coagulation of the sol by potassium sulphate. A comparison of the curves obtained with a freshly prepared sol and the one which has aged for a month shows that the final value of opacity in the case of the aged sol is less than that in the fresh one. The above-mentioned differences may have been caused by a number of factors which come into play during and immediately after the process of coagulation.

The coagulating power of an electrolyte is the reciprocal of the minimum concentration of the electrolyte required to effect a definite stage of coalescence (from the first appearance of turbidity to complete separation of the coagulum) in a given time. The results obtained in this investigation can be used to compare accurately the coagulating powers of the electrolytes employed for the coagulation of the sol since the measurements of

opacity give fairly high reproducible and accurate results. For this purpose curves were drawn between the time required for the coagulating mixture to attain a certain value of opacity (deflection of 1 cm.) against concentrations of several electrolytes used for coagulation. It is found from these curves that the concentrations of the different electrolytes necessary to cause coagulation in a given time follow the following descending order  $\text{KNO}_3 > \text{NaCl} > \text{KCl} > \text{BaCl}_2$ . Hence the descending order of coagulating power of these electrolytes is  $\text{KNO}_3 > \text{NaCl} > \text{KCl} > \text{BaCl}_2$ . For a time equal to 2 minutes the coagulating powers are  $\text{KNO}_3 : \text{NaCl} : \text{KCl} : \text{BaCl}_2 = 1.76 : 1.17 : 1.07 : 1.00$ .

(b) *Stannic hydroxide sol.*—This sol was prepared by the same method as adopted by Dhar and Vardhanam.<sup>5</sup> Three samples of the sol were employed for coagulation experiments: (A) undialysed sol, (B) sol dialysed for 8 days and (C) sol dialysed for 15 days. The colloidal contents of the three samples of the sol were 33.1, 17.4 and 13.9 g. of  $\text{SnO}_2$  per litre.

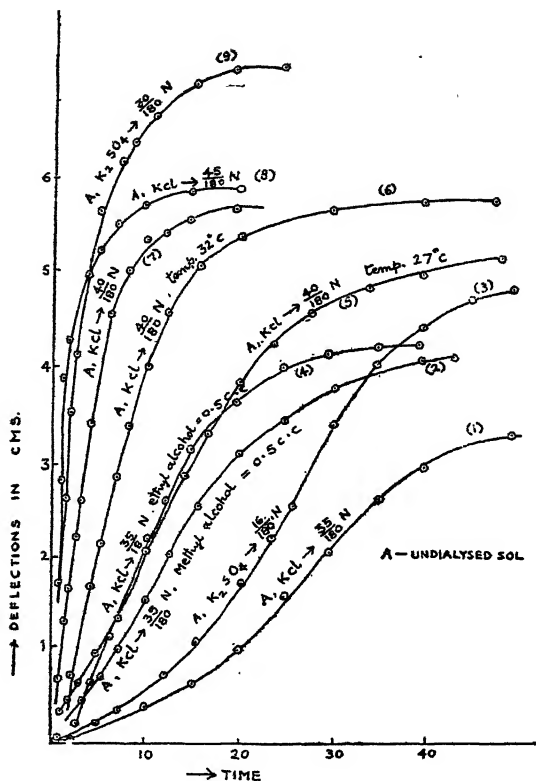
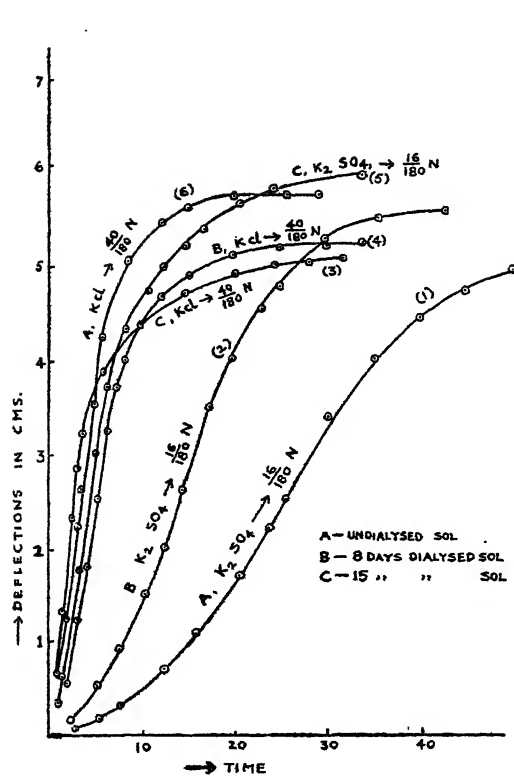
The experimental procedure followed was exactly the same as that adopted in the case of thorium hydroxide sol.

Some of the results obtained are graphically shown in Figs. 3 and 4. It will be seen in this case also that all the curves are continuous thereby showing that coagulation is a continuous phenomenon. Most of the curves are 'S' shaped while some of them are steep rising ones.

The coagulating power of the electrolytes employed for coagulation of this sol was compared by the same method as used in the case of thorium hydroxide sol and it was found that the coagulating power of potassium sulphate is greater than that of potassium chloride for all the three samples. This may be due to the bivalent nature of the coagulating ion in potassium sulphate. Moreover it appears from the large differences in opacity that the coagulation in the presence of potassium sulphate is more complete than that by potassium chloride. Further, it will be observed that the rate of change and the final values of opacity increase as the amount of the coagulating electrolyte increases. The coagulating powers of the two electrolytes for deflection equal to 2 cm. and time 10 minutes is  $\text{K}_2\text{SO}_4 : \text{KCl} = 1.88 : 1.00$ .

The coagulation by potassium chloride of the three samples of the sol in the presence of ethyl and methyl alcohols has been investigated. A comparison of the curves 1 and 4, 1 and 2, Fig. 3, for undialysed sample shows that the rate of coagulation is accelerated by the presence of alcohols

<sup>5</sup> J. Indian Chem. Soc., 1936, 13, 602.



FIGS. 3 and 4. Coagulation of Stannic Hydroxide Sol.

and that the effect of ethyl (curves 1 and 4) is greater than that of methyl (curves 1 and 2) alcohol. The effect of these alcohols on the other two samples is also of the same nature as on the undialysed sol.

Temperature increases the rate of coagulation (curves 5 and 6, Fig. 3). This observation is similar to that for thorium hydroxide sol (curves 3 and 6, Fig. 2).

The coagulation by the same concentration of KCl and K<sub>2</sub>SO<sub>4</sub> of sols (A), (B) and (C) is graphically shown in Fig. 4. The effect of dialysis on the coagulation of the sol by the same concentration of electrolytes cannot be well compared because the amount of colloidal matter in the three samples is not the same; it has been found to decrease as dialysis is continued. The curves in Fig. 4 show that the rate of change of opacity and the final values of opacity increase on dialysis when the sol is coagulated by potassium sulphate (curves 1, 2 and 5) and decrease when potassium chloride (curves 6, 4 and 3) is used as the coagulator; they thus point out the specific nature of the action of the coagulating electrolyte.

(c) *Zirconium hydroxide sol.*—The method employed for the preparation of this sol was the same as that used by Sharma and Dhar.<sup>6</sup> Two samples of the sol were employed for coagulation experiments: sol dialysed for 20 days (A) and 30 days (B). The concentrations of the two samples were 6.5 and 5.0 g. ZrO<sub>2</sub> per litre, respectively.

The results obtained are shown graphically in Fig. 5. The continuous nature of the curves points to the continuous nature of the coagulating process. It will be seen from the various curves in Fig. 5, that the rate of coagulation, as indicated by the rate of change of opacity, and the final values of opacity increase as larger amounts of electrolytes are used for coagulation.

The effect of dialysis on the coagulation of this sol also cannot be well compared as the concentrations of the differently dialysed sol are not the same. However, it can be said that the amount of electrolyte necessary for coagulation decreases as the sol is further dialysed (*cf.* curves 1 and 6, Fig. 5).

The effect of temperature is brought out by curves 3 and 5, Fig. 5. Temperature accelerates coagulation. The effect of alcohols on coagulation by electrolytes of this sol is the same as that for other sols investigated, namely, it increases the rate of coagulation (*cf.* curves 4 and 8, Fig. 5).

## 2. *Explanation of the Observed Results on Smoluchowski's Theory*

Smoluchowski has developed a theory of rapid coagulation velocity on the assumptions that (1) round each discharged particle there exists a sphere of attraction of radius  $r$  and (2) if two particles approach during molecular motion so closely that the centre of one enters the sphere of attraction of the other they would remain adherent. According to this theory the total number of particles  $\Sigma v$  at any time  $t$  is given by  $v_0(1+t/\theta)$ , where  $v_0$  is the number of single particles originally present in the sol and  $\theta = Kv_0$ , the specific coagulation time, is a constant. The number of single, double, triple, etc., particles at any time is given by the following relations:

$$v_1 = \frac{v_0}{\left(1 + \frac{t}{\theta}\right)^2}; \quad v_2 = \frac{v_0 \cdot \frac{t}{\theta}}{\left(1 + \frac{t}{\theta}\right)^3}; \quad v_3 = \frac{v_0 \left(\frac{t}{\theta}\right)^2}{\left(1 + \frac{t}{\theta}\right)^4} \dots$$

$$v_n = \frac{v_0 \left(\frac{t}{\theta}\right)^{n-1}}{\left(1 + \frac{t}{\theta}\right)^{n+1}}$$

<sup>6</sup> *Ibid.*, 1932, 9, 455.

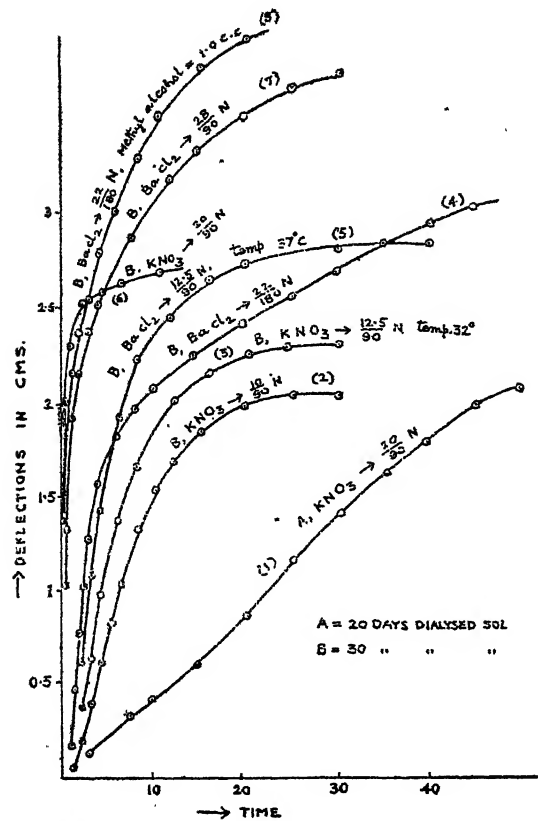


FIG. 5. Coagulation of Zirconium Hydroxide Sol

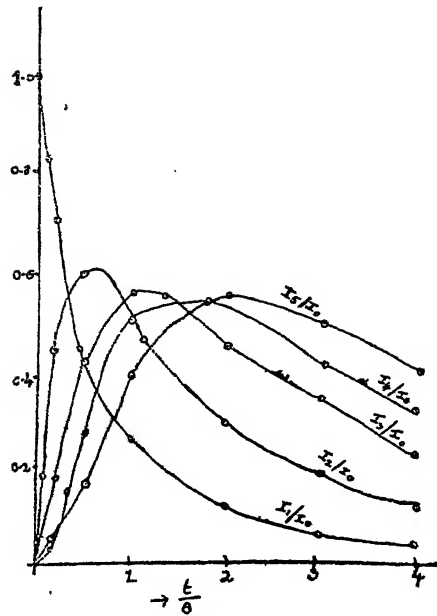


FIG. 6

The intensity of light scattered transversely by a colloidal system consisting of  $N$  particles of size  $V$  is proportional to  $NV^2$  provided the diameter of the particles is less than the wavelength of light. The diameter of the colloidal particles varies from  $1-100 \mu\mu$ ; taking the upper limit for the particle size, it is apparent that the law (Rayleigh) will hold true for the coalescence of a large number of particles. The intensity of light transversely scattered ( $I_1, I_2, I_3$ , etc.) by single, double, triple, etc., particles of twice, thrice, etc., the volume of the single particles, will be given by the following relations:

$$I_1 = \frac{I_0}{\left(1 + \frac{t}{\theta}\right)^2}; \quad I_2 = \frac{4 I_0 \frac{t}{\theta}}{\left(1 + \frac{t}{\theta}\right)^3}; \quad I_3 = \frac{9 I_0 \left(\frac{t}{\theta}\right)^2}{\left(1 + \frac{t}{\theta}\right)^4}$$

and so on

where  $I_0 = k\nu_0 V^2$ ,  $V$  being the volume of the single particles,

The variation of  $I_1/I_0$ ,  $I_2/I_0$ ,  $I_3/I_0$ , etc., with different intervals of  $t/\theta$  is shown in Fig. 6. It will be seen that the scattering due to single particles steadily decreases whereas that due to double and multiple particles at first increases, reaches a maximum value, and then falls off. At any instant, the total scattering will be the sum of  $I_1/I_0$ ,  $I_2/I_0$ ,  $I_3/I_0$ , etc. The variation of  $\Sigma I/I_0$

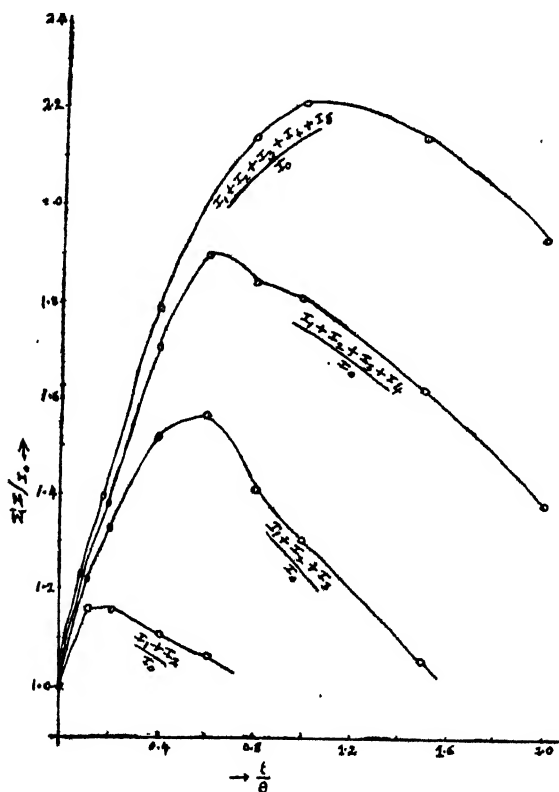


FIG. 7.

with  $t/\theta$  is given in Fig. 7. It will be seen that  $\Sigma I/I_0$  increases with time, reaches a maximum value and then begins to decrease. The time taken to reach the maximum value increases as the particles of greater multiplicity are formed when the intensity of scattered light also increases more rapidly with time.

According to Smoluchowski the kinetics of slow coagulation is the same as that for rapid; only in the case of slow coagulation the "adherence factor" is less than one. Hence  $\Sigma I/I_0 - t$  curves for slow coagulation must be the same as that for rapid.

The opacity-time curves during the coagulation of sols represent roughly the variation of the intensity of scattered light with time. The similarity of the curves in Fig. 7 with those rapidly rising curves in Figs. 1 to 5 explains the results in this investigation. The "S" shaped opacity-time curves obtained for slow coagulation show that the assumption of Smoluchowski, namely, that the kinetics of slow coagulation is the same as that for rapid coagulation may not be true.

### *3. Verification of Smoluchowski's Equation from Opacity Data*

The opacity data obtained can be employed to examine the applicability of Smoluchowski's equation to the coagulation of the sols studied in this investigation.

According to Smoluchowski  $\Sigma v$ , the total number of particles (single, double, triple, etc.) at a time  $t$  is given by  $v_0/(1 + t/\theta)$  as stated before and the stages of coalescence are independent of the external conditions which can change only the rapidity of succession of these stages. According to Mukherjee and Papaconstantinou<sup>7</sup> any property that varies continuously with the progress of coalescence without having a maxima or minima can be utilised to characterise the stages of coalescence, for each value of this property is characteristic of the time that has elapsed since the mixing of the electrolyte and the sol. Hence the coagulation velocity curves with the same electrolyte of different concentrations must be related to each other; that is, the values of the ratios of  $T_1/T$ ,  $T_2/T$ ,  $T_3/T$ , etc., must be the same for all concentrations of the same electrolyte ( $T$ ,  $T_1$ ,  $T_2$ ,  $T_3$ , etc., being the respective times taken to reach the same stage of coalescence with an electrolyte of concentrations  $C$ ,  $C_1$ ,  $C_2$ , etc.).

Assuming that the opacity measurements correctly represent the different stages of coalescence, the values of  $T$ ,  $T_1$ ,  $T_2$ ,  $T_3$ , etc., were read from the opacity-time curves obtained with different electrolytes of several concentrations in the case of sols studied in this investigation and the results obtained are given in Tables I to III, in which the different stages of coalescence are represented by opacity ( $d$ ) of the coagulating mixture.

It will be seen from the results that the values of  $T_n/T$  are fairly constant at higher concentrations and as the concentrations of the electrolytes are reduced, there are variations in the value of  $T_n/T$ , which shows definitely that the equation is applicable only upto a certain stage of coagulating

<sup>7</sup> *Phil. Mag.*, 1922, 44, 305.

TABLE I

*Thorium hydroxide sol*Values of  $T_n/T$  for various electrolytes(a) *Barium chloride*

d.	25/90 N	22/90 N	20/90 N	18/90 N
cm. 0.7	1	2.5	3.3	6.0
1.5	1	2.5	4.0	7.2
2.0	1	2.5	4.3	7.5
2.2	1	2.5	4.0	8.0

(b) *Potassium chloride*

d.	30/90 N	25/90 N	22/90 N	20/90 N	18/90 N	16/90 N
cm. 1.0	1	3.5	4.2	8.0	16.0	20.8
1.8	1	3.3	4.6	7.0	11.8	16.0
2.2	1	3.1	4.6	6.6	10.0	13.3

(c) *Potassium nitrate*

d.	16/90 N	15/90 N	14/90 N	13/90 N	12/90 N
cm. 0.6	1	1.2	1.7	2.3	3.4
1.3	1	1.1	1.8	3.0	3.6
1.8	1	1.2	2.0	3.2	4.0
2.1	1	1.6	2.4	3.6	4.0

(d) *Sodium chloride*

d.	25/90 N	20/90 N	17/90 N	15/90 N	13/90 N
cm. 1.6	1	4.3	9.0	10.3	21.0
1.9	1	4.4	8.8	11.2	19.2
2.1	1	4.3	8.7	11.3	..

TABLE II

*Stannic hydroxide sol*Values of  $T_n/T$  for different electrolytes(a) *Potassium chloride*

d.	45/180 N	40/180 N	37.5/180 N	35/180 N
cm. 1.7	1	2.7	10.0	34.8
2.8	1	3.0	10.0	37.0
3.5	1	2.9	9.5	..

(b) *Potassium sulphate*

d.	30/180 N	26/180 N	20/180 N	16/180 N
cm. 1.6	1	4.0	10.5	18.5
3.5	1	3.3	9.5	15.5
4.6	1	3.0	9.0	14.3
5.2	1	2.6	8.0	..

TABLE III

*Zirconium hydroxide sol*(a) *Barium chloride*

d.	28/180 N	25/180 N	22/180 N
cm. 1.3	1	2.0	3.0
1.9	1	2.0	4.0
2.1	1	2.0	5.0
2.5	1	1.5	6.2
3.0	1	1.1	4.0

(b) *Potassium nitrate*

d.	40/180 N	30/180 N	20/180 N
cm. 1.6	1	3.0	20.0
2.1	1	3.3	33.0

concentrations. This conclusion is in good agreement with those obtained by previous workers.

#### *Summary*

The changes in opacity during the coagulation of (a) thorium hydroxide, (b) stannic hydroxide and (c) zirconium hydroxide sols have been investigated. The results have been used to compare the coagulating power of electrolytes and also to study the applicability of Smoluchowski's equation to the coagulation of these sols. It has been found that Smoluchowski's equation is applicable upto a certain stage of coagulator concentrations only (corresponding to rapid coagulation). The effect of temperature and the influence of alcohols have also been studied. Both these factors accelerate the rate of coagulation in the case of all the sols investigated.

Basing on the theory of Smoluchowski for rapid coagulation an attempt has been made to follow theoretically the changes in the intensity of light scattered transversely ( $I$ ) by a system undergoing coagulation. The opacity-time curves obtained during the coagulation of sols have been compared with  $I-T$  curves obtained theoretically. The curves experimentally obtained for rapid coagulation are similar to those theoretically deduced. However the  $I-t$  curves for slow coagulation are "S" shaped and it has been inferred that Smoluchowski's equation is not applicable in the region of slow coagulation. This conclusion is the same as that obtained from the direct verification of Smoluchowski's equation from the opacity data.

# FLUORESCENCE REACTIONS WITH BORIC ACID AND O-HYDROXY-CARBONYL COMPOUNDS, AND THEIR APPLICATION IN ANALYTICAL CHEMISTRY

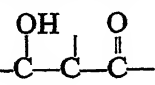
Part III. Effect of Bromination of the O-Hydroxy-Carbonyl Molecule  
on the Appearance of Fluorescence Effects with Boric Acid

BY K. NEELAKANTAM AND V. VENKATESWARLU

(From the Department of Chemistry, Andhra University, now at Madras)

Received March 28, 1944

IN a previous communication<sup>1</sup> Neelakantam, Row and Venkateswarlu

suggested a new fluorescence reaction for the detection of the 

group in aromatic compounds containing C, H and O only. This test is carried out by dissolving the substance in concentrated sulphuric acid, diluting with more acid if the solution is coloured and then adding boric acid to one half of the solution, leaving the other half for blank test. The solutions placed in quartz test-tubes are examined for fluorescence effects produced on adding boric acid, *viz.*, (a) appearance of fluorescence if the blank is non-fluorescent, and (b) an increase in intensity or (c) a change in colour of the fluorescence when the blank is itself fluorescent. Observations are made both in daylight and under ultra-violet light using the Cenco Black Light Source described as argon-filled gas glow lamp fitted with U.V. Filter.<sup>2</sup> If the results are positive, except in the case of the simple 3 hydroxy-flavones (*loc. cit.*), it could be deduced that the molecule contained the *O*-hydroxy-carbonyl group while negative results using this lamp, which is a very poor source of ultra-violet light, though cheap and readily handled, did not necessarily indicate the absence of this group. This reaction has been shown to be more general and of greater applicability, not being confined to any one type of compounds, than any other reaction previously reported in the literature. It is, therefore, of considerable interest to investigate the effect of introducing groups and atoms such as the sulphonate, nitro, amino and halogens into the molecule of the *O*-hydroxy-carbonyl compound on the applicability of this reaction.

Neelakantam and Row<sup>3</sup> pointed out that sulphonation of the *O*-hydroxy-carbonyl compound generally produced a marked increase in the intensity

of fluorescence while nitration and bromination damped the fluorescence considerably and in the cases examined the latter two caused the disappearance of fluorescence. Thus 5-nitrosalicylic acid and nitro-sulphosalicylic acid did not exhibit any fluorescence effects with or without boric acid in daylight or under the lamp while salicylic acid gave prominent effects with boric acid under the lamp, and with sulphosalicylic acid the effects were relatively more prominent. 5-Bromosalicylaldehyde, the only bromo com-

Compound	Under U.-V. Lamp		Remarks
	Without boric acid	With boric acid	
1. 3 : 5-Dibromo-resacetophenone	Nil	Greenish yellow	Resacetophenone—bright blue with boric acid under lamp ; blank nil
2. 2-Hydroxy-4-methoxy-5-bromo-benzaldehyde	Nil	do.	2-Hydroxy-4-methoxy-benzaldehyde—greenish yellow with boric acid under lamp ; blank nil
3. 2-Hydroxy-4-methoxy-3 : 5-dibromo-benzaldehyde	Nil	Nil	
4. 2 : 4-Dihydroxy-3 : 5-dibromobenzaldehyde	Nil	Nil	$\beta$ -Resorcylic aldehyde—green with boric acid under lamp ; blank nil
5. 3 : 5-Dibromo-resorcylic acid	Nil	Pale blue	$\beta$ -Resorcylic acid—bright violet with boric acid under lamp ; blank nil
6. Do. Methyl ester ..	Nil	do.	
7. 3 : 5-Dibromo-orsellinic acid-ethyl ester	Nil	do.	
*8. Do. Methyl ester ..	Nil	do.	Orsellinic acid and ethyl orsellinate—deep violet with boric acid under lamp ; blank nil
9. 3 : 5-Dibromo-orsellinic acid	Nil	do.	
10. 3 : 5-Dibromo-orc-acetophenone	Nil	Pale yellow	
11. 3 : 5-Dibromo-orcylic aldehyde	Nil	Nil	Orcyclic aldehyde—bright greenish yellow with boric acid under the lamp ; blank nil
12. 3 : 5-Dibromo-2 : 4 : 4'-trihydroxy-3'-methoxy-chalkone	Nil	Pale yellow	2 : 4 : 4'-trihydroxy-3'-methoxy-chalkone—yellow with boric acid under lamp ; blank nil
13. 3 : 5-Dibromo-6-methyl-2 : 4 : 4'-trihydroxy-3'-methoxy-chalkone	Nil	Nil	
14. 3 : 5-Dibromo-2 : 4-dihydroxy-chalkone	Pale yellow	Deeper yellow	2 : 4-Dihydroxy-chalkone—pale greenish yellow in blank and deeper greenish yellow under the lamp
15. 3 : 5-Dibromo-2 : 4-dihydroxy-4'-methoxy-chalkone	do.	do.	

\*Compounds 8 to 15 were recently synthesised by Seshadri and Venkateswarlu—unpublished work.

pound then examined, showed that introduction of bromine into salicylaldehyde led to complete disappearance of fluorescence effects with boric acid while salicylaldehyde itself gave a positive reaction. Further it was found that bromide interfered with the resacetophenone—boric acid reaction using concentrated sulphuric acid and the explanation was offered that this was due to the production of bromine and bromination of resacetophenone.<sup>4</sup>

The bathofloric effect of halogens on fluorescence of organic compounds is well known.<sup>5</sup> Thus fluorescein is much more fluorescent than eosin, erythrosin and Rose-Bengal which are its brominated, iodinated and chlorinated derivatives. The ability of free halogens to inhibit (or quench) the fluorescence of fluorescein is a well-known reaction for the detection of the halogen, especially bromide in presence of large amounts of chloride<sup>6</sup> and also iodide. The object of the present investigation, however, is to find out the effect of introducing one or more halogen atoms, e.g., bromine, into the molecule of an *O*-hydroxy-carbonyl compound on the "boric acid reaction". It may be pointed out that this investigation is not concerned with the differences in fluorescence of the parent compound and its halogen derivative but with the effect of adding boric acid to the latter.

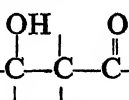
### Experimental

The solutions were prepared and the tests carried out exactly as described in the previous communications. With none of the compounds examined was any fluorescence observed with or without boric acid in daylight. In the following table, therefore, the results obtained under the lamp and the colour of the fluorescence are reported. For comparison the results previously reported with the bromine-free compounds are given under remarks.

### Discussion

It may be stated in general that the fluorescence effects obtained were much less marked in the case of the bromo-compounds than with the corresponding halogen-free compounds. Consequently care must be exercised in the interpretation of the results obtained. It must be emphasised in this connection that the lamp used is a very weak source of U.-V. light and the filter provided with the lamp transmits a little in the violet-blue region. Further it was observed that some samples of boric acid dissolved in concentrated sulphuric acid showed a very faint blue fluorescence. These, however, were of little significance when the bromine-free compounds were examined as the effects were prominent but could not be disregarded in the present investigation. Careful testing with the aid of blanks showed that there was an increase in intensity of fluorescence on the addition of boric acid

in several cases given in the table. From the results now reported taken in conjunction with those previously published it could be deduced that the introduction of bromine atoms into the molecule of an *O*-hydroxy-carbonyl compound does not invariably lead to complete disappearance of fluorescence effects with boric acid and though there is a marked diminution of intensity. The results depend on the nature of the compound and the number of bromine atoms introduced. From this it is clear that the boric

acid reaction serves for the detection of the  group in compounds containing bromine in addition to C, H and O. However it must be pointed out that negative results with boric acid are obtained more often when bromine is present than in its absence. Attention may be drawn in this connection to the fact recorded in the previous paper that a negative fluorescence reaction with boric acid using the Cenco lamp as the source of U.-V. light does not necessarily indicate the absence of the *O*-hydroxy-carbonyl group.

#### Conclusion

The introduction of bromine atoms into the molecule of an *O*-hydroxy-carbonyl compound does not invariably result in absence of fluorescence effects on the addition of boric acid.

The fluorescence test for the *O*-hydroxy-carbonyl group is also applicable in the case of brominated compounds but as with the bromine-free compounds a negative result does not necessarily mean absence of *O*-hydroxy-carbonyl group. Negative results are obtained more often when bromine is present than in its absence.

The authors wish to express their thanks to Professor T. R. Seshadri for valuable help rendered in the course of this investigation.

#### REFERENCES

1. Neelakantam *et al.* .. *Proc. Ind. Acad. Sci.*, 1943, **18A**, 364.
2. \_\_\_\_\_ .. *Ibid.*, 1941, **14A**, 307.
3. \_\_\_\_\_ .. *Ibid.*, 1942, **15A**, 81.
4. \_\_\_\_\_ .. *Ibid.*, 1942, **16A**, 349.
5. Pringsheim .. *Trans. Faraday Soc.*, 1939, **35**, 29.
6. Radley and Grant .. *Fluorescence Analysis in Ultra-Violet Light*, 1939, p. 195.

# EFFECT OF ELECTRIC FIELD ON TYNDALL SCATTERING

BY R. S. SUBRAHMANYA, K. S. GURURAJA DOSS AND  
BASRUR SANJIVA RAO

(From the Department of Chemistry, Mysore University, Central College, Bangalore)

Received November 18, 1943

## *Introduction*

AMONGST the agencies which can bring about a preferential orientation of particles in a mobile colloidal system having anisotropic particles are (*a*) its flow, (*b*) the magnetic field, and (*c*) the electric field. The existence of such orientation has been proved by the work of earlier investigators on double refraction, induced by these agencies.<sup>1</sup> The effect of the preferential orientation on the intensity of Tyndall scattering is of great interest. The only investigations which have been carried out in this field are by (*a*) Freundlich<sup>2</sup> on the changes in Tyndall intensity, induced by flow and (*b*) R. S. Krishnan<sup>3</sup> on the effect of magnetic field on the Tyndall intensity. The effect of the electric field however, has so far received little attention. Mueller<sup>4</sup> attempted to study this effect with bentonite sols, but did not get any positive results. This is probably due to the fact that the particles in the sols used by Mueller were very fine and the orientation was not sufficiently intense to show the effect, owing to the lively Brownian movement of the fine particles. The small intensity of the scattered light might have added to the difficulty in observing the effect. The present investigation was undertaken with a view to study the effect of the electric field on a few typical sols.

## *Experimental*

1. *Preparation of silver iodide sol.*—Silver iodide sol was prepared by the method of Kruyt and Verwey.<sup>5</sup> Silver nitrate was run dropwise into a solution of potassium iodide containing a 10% excess of the latter. The concentrations of potassium iodide solution and silver nitrate solution were so adjusted that the resulting sol contained about 40 millimols of AgI/litre. The sol was then subjected to hot dialysis, until the dialysate gave no test for iodide (14 hrs.). By this method a highly purified sol stabilised by iodide ions and having H<sup>+</sup> as gegen ions was got. It was found advantageous to further stabilize the sol by addition of potassium iodide to give a concentration of 0·001 N iodide ion. The sol was then centrifuged (1800 r.p.m.) for one and a half hours to remove the bigger particles. The clear sol was decanted out. The sol prepared in this way was stable for many months.

2. *Preparation of stearic acid sol.*—Stearic acid sol was prepared by Mukherjee's method.<sup>6</sup> 2.5 gm. of "extra pure" stearic acid was dissolved in 200 c.c. of methyl alcohol. The alcoholic solution was poured dropwise into 700 c.c. of boiling distilled water. Then the excess of methyl alcohol was boiled off. The sol was then filtered through Whatman No. 3 filter-paper, in order to free it from the larger particles. It was then protected by using 0.0003 N sodium hydroxide. The sol prepared by this method was stable for many months.

3. *Sol of Benzopurpurine 6 B.*—A five-year old sol of benzopurpurine (0.002 M) prepared by Doss<sup>7</sup> was used.

4. *Determination of size of the particles.*—The size of the particles in these sols was determined with the aid of the slit-ultramicroscope (Bausch and Lomb). The field of view in the ultramicroscope was limited by using an Ehrlich stop. The dimensions of the Ehrlich stop were determined by means of an eye-piece micrometer, previously calibrated using a stage micrometer. A concentrated sol was put into the cell, provided for the purpose. The slit was turned to the vertical position and the width of the beam as seen in the ultramicroscope was suitably adjusted, by rotating the screw head. This gave the depth of illumination, for the horizontal position of the slit. Then the slit was rotated to the horizontal direction. The volume of the illuminated portion of the sol = Length of the Ehrlich stop × Breadth of the Ehrlich stop × depth of illumination.

The illuminated zone was 0.1 cm. below the surface of the liquid in the cell. The Perrin distribution of micelles did not therefore interfere with the measurements.

The sol was diluted sufficiently so as to give an easily countable number of particles in the small illuminated element of volume. The number of particles N, in the element of volume, was counted every two seconds. About three hundred readings for N were taken. One of the typical sets obtained is given in Table I.

TABLE I

2	2	2	2	2	2	2	2	2	2	2	0	0	0	0	2	2	1	2	2	2	3	3	3
2	3	1	2	3	4	4	2	3	3	4	1	3	4	3	3	2	1	2	0	1	2	2	
0	0	0	0	0	0	0	0	0	0	0	0	0	0	0	2	0	0	1	2	4	3	4	5
2	2	1	4	1	2	3	3	3	4	4	3	1	2	3	2	1	1	1	1	0	0	0	
0	1	1	2	1	1	1	0	0	0	0	1	2	2	1	3	2	3	1	1	2	2		
2	2	1	1	2	1	1	1	2	1	1	1	1	1	1	0	2	1	2	1	0	2	1	
2	2	3	3	3	2	4	1	1	1	2	3	3	4	4	5	0	0	1	3	3	0	1	2

The average of the values was 1.66.

With a view to find out whether the values really correspond to the spontaneous concentration fluctuations, V. Smoluchowski's relations<sup>8</sup> for (a) the mean relative fluctuation  $\bar{\delta}$ , (b) the mean square relative fluctuation  $\bar{\delta}^2$  and (c) the probability  $P(n)$  for the occurrence of any particular  $N$  were verified. Results are given in Tables II and III.

TABLE II

$\bar{\delta}_{\text{obs.}}$	$\bar{\delta}_{\text{calc.}} = 2e^{-\nu} \nu k/k!$	$\bar{\delta}^2_{\text{obs.}}$	$\bar{\delta}^2_{\text{calc.}} = \frac{1}{\nu}$
0.66	0.63	0.56	0.60

TABLE III

	$n = 0$	$n = 1$	$n = 2$	$n = 3$	$n = 4$	$n = 5$
$P(n)_{\text{calc.}} = \frac{e^{-\nu} \cdot \nu^n}{n!}$	31.2	51.77	42.95	23.75	9.85	3.27
$P(n)_{\text{obs.}}$	35.0	41.00	46.00	25.00	12.00	2.0

These results (Tables II and III) show that the values for the spontaneous concentration fluctuations obey the Smoluchowski's equations.

The results obtained for the concentration and particle size are given below [Table III (a)]:—

TABLE III (a)

Sol.	Conc. of sol.	Dilution (to give a countable no. of particles)	No. of particles per c.c. of conc. sol.	Equivalent spherical diameter
Silver iodide sol. .. ..	0.25%	1 : 200,000	$7.32 \times 10^{11}$	104.8 $m\mu$
Stearic acid sol. .. ..	0.085%	1 : 10,000	$3.2 \times 10^{10}$	390.8 $m\mu$

Size of the particles in benzopurpurine 6 B sols however, could not be determined, since (a) the sols had, as was to be expected, particles of largely varying sizes and (b) the bigger particles broke down on dilution into particles of smaller size.

5. *Shape of the particles.*—Stearic acid sol at temperatures below the melting point has been shown to consist of anisotropic particles by Schlierung experiments.<sup>9</sup> The particles also exhibit in a striking manner the twinkling effect under the ultramicroscope. The sol also exhibits electric double refraction. The quantitative measurement of the double

refraction is difficult since the large scattering in the forward direction interferes with the measurement. These effects disappear when the sol is heated to about 70° C. (a temperature which is higher than the melting point of stearic acid), showing thereby that the observed effects are connected with the anisotropic shape of the particles. In order to find out if the particles are to be considered as rods or discs, the elegant new technique of Langmuir<sup>10</sup> was adopted. In this technique the sol is allowed to flow through a pipette. The stem of the pipette is illuminated by a beam of light polarised at 45° to the direction of flow. The light transmitted by the stem (in which the flow is occurring) is viewed through another polaroid which is crossed with reference to the former polaroid. If the sol consists of rods, the flow of the sol produces a uniform brightening throughout the thickness of the stem of the pipette. If the sol contains discs, a flowing sol shows a central dark band. We have confirmed the observation of Langmuir that vanadium pentoxide shows a uniform brightening. With stearic acid sols a clear dark band is noticed, showing that it contains disc-shaped particles.

Silver iodide sol did not show any schlierung. Under the ultramicroscope, the twinkling was not marked. The Langmuir technique showed that the particles were not appreciably anisometric.

The aged benzopurpurine sol showed marked schlierung. The Langmuir technique with a concentrated sol indicated that the particles were rod-shaped.

6. *Technique for investigating the effect of electric field on Tyndall scattering.*—The electric field was applied by employing platinum or carbon sheet electrodes having apertures in them so as to allow the incident or scattered beam to pass. The light was incident on the sol horizontally. The scattered light was viewed transversely in the vertical and in the horizontal directions. It can be shown that one of the directions of observation can be dispensed with since each of the cases in the vertical direction of observation has a completely corresponding position in the horizontal direction of observation. This fact was also confirmed experimentally. Only the results got with the horizontal direction of observation have been given in Table IV. The field could be applied (*a*) longitudinally parallel to the beam ( $E_l$ ) or transversely in the vertical ( $E_v$ ) or horizontal ( $E_h$ ) directions. These gave six modes of observation. The incident light was polarised horizontally or vertically by using a polaroid. The scattered light was viewed through a polaroid so as to enable us to notice the changes in the intensity of the scattered component, parallel or perpendicular to the direction of the incident

beam. The results are represented in Table IV. The fields used were of the order of 100 volts/cm. D.C. or 220 volts/cm. A.C. Both the types of fields gave identical results. With direct current, however, electrolysis often interfered with the work.

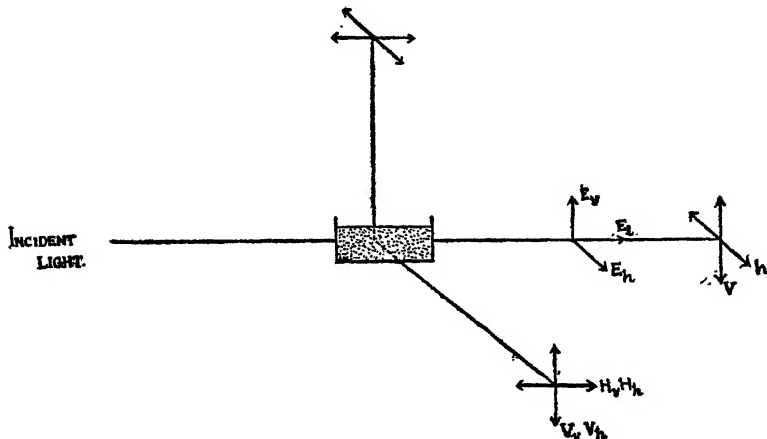


FIG. 1

The various symbols used in Table IV are illustrated in Fig. 1.

TABLE IV

*Effect of electric field on Tyndall scattering by stearic acid sol*

- ++ indicates strong brightening on applying the field
- + indicates moderate brightening on applying the field
- indicates darkening on applying the field

Field	Corresponding Orientation	Effect of the field			
		$v_v$	$H_v$	$v_h$	$H_h$
$E_v$	(O)	++	+	+	++
$E_l$	(E)	-	-	-	-
$E_h$	(H)	-	-	-	-

The results obtained with benzopurpurine sol were identical with those got with the stearic acid sol. With silver iodide sol, the effects were not observable at the low fields used.

### *Discussion*

Freundlich<sup>11</sup> has proposed a theory to account for the effect of flow on Tyndall scattering which can be applied *mutatis mutandis* to the action of the electric field. He assumes that the scattered intensity is determined by the orientation of the particle in relation to the direction of the incident electric vector. His predictions, no doubt, apply only to positively double refracting rod-shaped particles. This theory however can be extended to apply even to negatively double refracting disc-shaped particles and leads to the result that the scattering intensity will similarly be affected by the electric field in any of the transverse directions. But this conclusion is not at all in accord with our observations. Furthermore, since the scattering intensity is assumed to be dependent on the direction of the incident vector, the effect of field should differ according as the incident vector is horizontal or vertical. This too is not supported by our experimental results. The Freundlich theory therefore breaks down completely.

The applicability of the Rayleigh theory of scattering to the present case may now be considered. The electric field itself tends to orient the particles so as to make their longest axis parallel to the field. We shall discuss how this orientation affects the various scattered components. (In the present discussion we shall assume that the particles are discs.)

*The component  $V_v$ .*—The change in the intensity of  $V_v$  can be calculated by finding out the change in the average polarisability of the particle in the vertical direction brought about by the orientating influence of the field. Let the three principal polarisabilities of the disc-shaped particle be  $a$ ,  $a$  and  $b$  ( $b \ll a$ ). The average polarisability for the present purposes can be calculated by taking the mean of the values for the extreme orientations of the particle. This comes out to be:

$$\frac{a + \frac{a+b}{2} + \frac{a+b}{2}}{3} = \frac{2a+b}{3}$$

Particles oriented by  $E_v$  would have the various orientations given in Table IV. The average polarisability in the vertical direction corresponding to this orientation would be  $a$ . Since  $a$  is greater than  $\frac{2a+b}{3}$ , one should get a brightening in this case. For particles oriented by  $E_z$  and  $E_h$ , the average polarisability would be  $\frac{a+b}{2}$ . Since  $\frac{a+b}{2}$  is smaller than  $\frac{2a+b}{3}$ , there would be a darkening in these cases.

*The component  $H_v$ .*—Let the incident light be parallel to the X-axis, the horizontal direction of observation be along Y-axis and let the third axis be the Z-axis. In predicting the action of the electric field we shall consider the three main types of orientation:—

- (a) The plane of the discs  $\parallel$  to the X-axis.
- (b) The plane of the discs  $\parallel$  to the Y-axis.
- (c) The plane of the discs  $\parallel$  to the Z-axis.

In the absence of the field all the three orientations are equally probable. Of these, the orientations corresponding to (b) are the only ones which give rise to the component  $H_v$ . This type of orientation is favoured by  $E_h$  and disfavoured by  $E_v$  and  $E_l$ . Thus there should be a brightening produced by  $E_h$  and darkening by  $E_v$  and  $E_l$ .

*The component  $V_h$ .*—This component is got only by the orientation (a). Since  $E_l$  favours this orientation and the other two fields disfavour it, we should expect a brightening with  $E_l$  and darkening with  $E_v$  and  $E_h$ .

*The component  $H_h$ .*—This component is got only by the orientation (c). Since  $E_v$  favours this orientation and the other two disfavour it, we should expect a brightening with  $E_v$  and darkening with  $E_h$  and  $E_l$ .

The above predictions are summarised in Table V.

TABLE V  
*Predictions on the basis of the Rayleigh Theory*

Field	$V_v$	$H_v$	$V_h$	$H_h$
$E_v$	+	—	—	+
$E_l$	—	—	+	—
$E_h$	—	+	—	—

A comparison of Tables IV and V shows that the Rayleigh theory is not applicable to the present case.\* This is not very surprising. For, the stearic acid sol used in the present work consists of particles which are too large for the Rayleigh theory to hold good. This is supported by the fact that this sol shows a marked Krishnan effect, the  $\rho_h$  deviating appreciably from 100%.<sup>12</sup> Moreover, the scattering is highly asymmetric there being a large scattering in the forward direction and the Tyndall light has hardly any preponderance of the blue tint. A rigorous theoretical treatment of

\* We have assumed that the particles are disc-shaped. Assuming any other shape does not remove the difficulty.

systems such as this, composed of large and anisotropic particles is beset with many difficulties. Under these circumstances, we would formulate an empirical generalisation, which we would refer to as "The Reflection Rule", which summarises all the facts observed in such systems:—

"Large disc-shaped or rod-like particles oriented by a linear field, show enhanced scattering when the field is put on, if the plane of incidence and observation is perpendicular to the field; in other orientations the scattering is decreased by the field."

We may also add that the brightening when it occurs, is more marked with  $V_v$  and  $H_h$  than  $H_v$  and  $V_h$ .

It was also found that in the brightening positions the  $H_v$  or  $V_h$  had a distinct red tinge whereas the  $V_v$  and  $H_h$  had a distinct blue colour. This interesting observation remains to be elucidated.

It is interesting to note that benzopurpurine sol gave the same general results as given in Table I, though this sol consists of rod-shaped particles as shown by the Langmuir technique. We would also like to record the observation that the benzopurpurine sol treated with small amounts of sodium hexa-metaphosphate showed (a) diminished scattering and (b) no schlierung, and did not show any change in Tyndall scattering when an electric field was applied. This was presumably due to the dispersion caused by sodium hexa-metaphosphate. The exact mechanism of the action of the latter is not clear.

An attempt was made to make similar observations on the effect of flow on Tyndall scattering. Stearic acid sol was allowed to flow in a tube of circular cross-section. The observations were confined to the middle of the tube. A comparison of these observations with those obtained with the electric field, showed that an electric field is equivalent to a flow in a tube (of circular section) in the direction of the field. This is in agreement with the orientation of particles postulated by Langmuir.<sup>10</sup>

It is to be noted that the observations made by R. S. Krishnan<sup>3</sup> on graphite sols, using magnetic fields can mostly be interpreted in terms of the Reflection rules formulated in the present paper.

#### *Conclusion*

The study of the action of an electric field on the scattering intensity of sols has thus led to interesting results. The study is useful in determining the shape of the particles. The present technique would be supplementary to the studies of double refraction, in that the latter cannot be conveniently

investigated in a highly scattering system. With slightly conducting sols, large fields can be used so as to produce saturation effects. Under such conditions, the use of rotating fields would bring about a unique orientation of the discs. A superposition of two A.C. fields of different cycles at right angles to each other would have the same effect as the circular field. The use of elliptical fields would reveal any want of equality of the two axes in the plane of discs of flat particles. The technique itself is simpler than the flow technique. Since there is often a large difference in the dielectric constant between the particles and the medium, the orientation is marked even with small fields, and the electric field is thus more powerful than the magnetic field in bringing about orientation.

#### Acknowledgement

The authors are deeply grateful to Sir C. V. Raman for his kind and instructive discussions.

#### REFERENCES

1. Taylor .. *Treatise on Physical Chemistry*, Second Edition, Vol. II, 1608.
2. Freundlich .. *Colloid and Capillary Chemistry*, 1926, 407.
3. R. S. Krishnan .. *Proc. Ind. Acad. Sci.*, 1938, 7 A, 91-7.
4. Mueller .. *Phys. Rev.*, 1939, 55, 508.
5. Kruyt and Verwey .. *Inor. Colloid Chem. Weiser*, Vol. III, 115.
6. .. *Jour. Mys. Univ.*, 1935, 49, 84.
7. Doss .. *Kolloid-z.*, 1938, 84, 138.
8. Taylor .. *Treatise on Physical Chemistry*, Vol. II, 1577-8.
9. Subbaramiah, Iyer and Doss *Current Science*, 1939, 8, 360.
10. Langmuir .. *J. Chem. Phys.*, 1938, 6, 873.
11. Freundlich .. *Colloid and Capillary Chemistry*, 1926, 403 411.
12. Subrahmanyam, Doss and Rao (Unpublished).

## KOMBUR SESHA IYENGAR KUPPUSWAMY IYENGAR IN MEMORIAM

THE sudden death due to pneumonia of Kombur Sesha Iyengar Kuppuswami Iyengar—better known as K. S. K. Iyengar—at Mysore, on 23rd June 1944, marks the loss of one of our distinguished Fellows, and one who was well known in mathematical circles in India. The loss is all the more poignant because his death at the age of 45 is so premature.

Born on 29th August 1899, K. S. K. Iyengar finished his early education in the Government High School, and the Central College, Bangalore, and later went to Madras and joined the Presidency College to study for the Honours Degree Examination. He passed the Honours Examination with distinction in 1920, and noticing his pronounced ability in Mathematics his parents decided to send him to Cambridge to study for the Mathematical Tripos.

But for a short spell of a few months at London where he came in contact with Karl Pearson, K. S. K. Iyengar spent the good part of his stay of nearly five years in Europe in Cambridge itself. He took courses in several branches of pure and applied mathematics but his favourite subject was Analysis, and contact with Littlewood had a profound influence on him. He too was one of the many students who went to Cambridge, and came under the spell of the Hardy-Littlewood tradition. The pioneering work of W. H. Young on sets of points made a great appeal to him, and was responsible for the keen interest he always evinced in point set topology, Continental mathematical work of the time on the theory of functions of a complex variable, especially the work of the German school attracted him so much that he once made a trip to Germany and met Koebe who had by then perfected his uniformisation theory.

After taking a star wranglership at Cambridge he returned to India in 1925, and was soon appointed to the position of the Head of the Department of Mathematics in the University of Mysore, at the Central College, Bangalore, in January 1926. It was largely due to his high standards, energy, and vision that the department was adequately equipped with library and other facilities to keep pace with modern developments. He was largely instrumental in introducing rigour in mathematical teaching in the University, in making provision for teaching several advanced branches, specially theory of functions of a complex variable and real variables and

theories of integration, and in introducing methods of mathematical physics as a compulsory subject for the Honours Courses. In 1930 he was elected a Fellow of the Cambridge Philosophical Society from Trinity Hall. He was also a member of the London, American and Indian Mathematical Societies. He was elected a Fellow of the Academy in 1934. He served on the Boards of Studies, Boards of Examiners, Faculties and Academic Council of his University and several others in India. He was also in charge of the teaching of German in the Science Faculty.

It was only in 1938 that K. S. K. Iyengar started publishing his papers regularly and the bibliography of his published papers contains 20 titles and is appended at the end of this note. The important of these can be classified as follows:—four papers on sequences and series, four on summability and Tauberian theorems, three on normal orthogonal sets, two on derivatives of a function, one on integral functions, three on a geometrical problem, and one on the mathematical aspect of the Bhabha-Heitler cascade theory of cosmic rays. One of the papers on derivatives which consists of generalisations of the theorems of Khintchine and Mazurkiewicz were noticed by Saks and published in the *Proceedings of the Warsaw Scientific Society*. The papers dealing with summability are characteristic of his zeal for generalisation and contain many well-known theorems of Hardy and Littlewood as particular cases. The three connected papers on linear transformations of bounded sequences offer a penetrating study of this topic. I shall however give it as my personal opinion that K. S. K.'s paper dealing with the exact solution of the equations of the general cascade theory is his best. This paper, which arose out of discussions with Bhabha on the subject, consists of rigorous proofs for the existence of solutions of a type of differential equations, and the sharp and manifold analytical tools employed serve to show that their author is an analyst of high calibre.

He married in 1926, but had no children. A tall and arresting personality, a good sportsman, a charming conversationalist, full of foibles and lovable just because of them, K. S. K. Iyengar made a deep impression on all who came in contact with him. He was recently getting himself interested in point set topology which he had been studying deeply, but deeper still was his interest in Indian Philosophy, the Bhagavad Gita, Buddhism, religious mysticism, and systems of Yoga. His sudden death removes from our midst a good teacher, and a great friend of all who teach or learn mathematics.

K. S. K. IYENGAR

1. ON NARASINGA RAO'S PROBLEM AND ITS RECIPROCAL. *Mat. Student*, 5, 1938.
2. A NOTE ON NARASINGA RAO'S PROBLEM RELATING TO TETRAHEDRA, *Proc. Ind. Acad. Sci.*, 7, 1938, 269.
3. ON A PROBLEM RELATING TO TETRAHEDRA, *Ibid.*, p. 305.
4. THEOREMS ON THE FUNCTIONAL LIMITS OF DERIVATIVES OF A FUNCTION AT INFINITY, *ibid.*, p. 343.
- 5, 6, 7. ON LINEAR TRANSFORMATIONS OF BOUNDED SEQUENCES—I, II, III, *ibid.*, 7, p. 399 ; 8, p. 20, p. 135.
8. NOTE ON AN INEQUALITY, AND A NOTE ON THE ZEROS OF  $\sum_{n=0}^{\infty} z^n/r^n$ , *Math. Student*, 6, 1938.
9. ON A PROBLEM RELATED TO THE CAUCHY-MACLAURIN INTEGRAL TEST, *Proc. Ind. Acad. Sci.*, 9, 1939, 139.
10. A NEW PROOF OF MEHLER'S FORMULA AND OTHER THEOREMS ON HERMITIAN POLYNOMIALS, *ibid.*, 10, 1939, 211.
11. ON A NEW PROOF OF THE FORMULA FOR THE GENERATING FUNCTION OF LAGUERRE POLYNOMIALS AND OTHER RELATED FORMULAE, *ibid.*, p. 181.
12. ON A TEST FOR THE COMPLETENESS ( $L^2$ ) OF A NORMAL ORTHOGONAL SET AND ITS APPLICATIONS, *J. I. M. S.*, 4 (new series), 1939.
13. A NOTE ON THE SYMMETRIC FIRST AND SECOND MEAN DERIVATIVES OF A CONTINUOUS FUNCTION, *Comptes. Rendus d. Soc. Sc. Varsovie*, 31, 1938-39; 108.
14. A PROPERTY OF INTEGRAL FUNCTIONS WITH REAL ROOTS AND OF ORDER LESS THAN TWO, *Annals of Mathematics*, 42, 1941, 823.
15. ON FRULLANI INTEGRALS, *Proc. Camb. Phil. Soc.*, 37, 1941, 9.
16. NOTES ON SUMMABILITY, I, *J. Mys. Univ.*, 3, Pt. 17, 1942, 123.
17. EXACT SOLUTIONS OF THE EQUATIONS OF THE GENERAL CASCADE THEORY WITH COLLISION LOSS, *Proc. Ind. Acad. Sci.*, 15, 1942, 195-229.
18. NOTES ON SUMMABILITY, II, *J. Mys. Univ.*, 4, Pt. 9, 161.
19. A TAUBERIAN THEOREM AND ITS APPLICATION TO CONVERGENCE OF FOURIER SERIES, *Proc. Ind. Acad. Sci.*, 18, 1943, 81.
20. NEW CONVERGENCE AND SUMMABILITY TESTS FOR FOURIER SERIES, *ibid.*, p. 113.

B. S. MADHAVA RAO.

## INDEX TO VOL. XIX (A)

### AUTHORS' INDEX

Alexander, .. *See* Taylor and Alexander.

Bhabha, H. J. .. Note on the separation of the electronic and non-electronic components of cosmic radiation, 23.

Bhagavantam, S., and Venkateswarlu, K. Scattering of light in single crystals : intensity measurements, 108.

Bhargava, P. N. and Dutt, S. Chemical examination of the roots of *centaurea Behen* Linn., 163.

Bhide, B. V. .. *See* Paranjape and others.

Chandrasekhar Aiya, S. V. Separation of electronic and non-electronic components of cosmic radiation by Bhabha's method, 177.

Dayal, Bisheshwar .. The evaluation of the specific heat of rock-salt by the new crystal dynamics, 182.

Deo, P. G. .. The lattice spectrum and specific heat of diamond, 224.

Doss, K. S. Gururaja .. The *New light-effect* in chlorine under electrical discharge, I, 117.

Dutt, S. .. *See* Subrahmanya and others.

Guruswamy, S. .. *See* Bhargava and Dutt.

Hariharan, P. S. .. *See* Prasad and others.

Joshi, S. S. and Purushotham, A. Intensity of X-ray reflection by diamond, 261.

Kartha, A. R. S., and Menon, K. N. Influence of temperature on the quenching of active nitrogen at various pressures, 159.

Krishnan, R. S. The oil of *Mimusops elangi* (Linn.), 1.

Krishnaswamy, B., Murty, K. Satyanarayana and Seshadri, T. R. The Raman spectrum of diamond, 216.

Krishnaswamy, B., Rao, K. Ranganadha and Seshadri, T. R. Experimental evidence for the existence of the four possible structures of diamond, 298.

Mani, Anna .. Chemistry of gossypol, IV, 370.

Menon, K. N. .. Synthetic experiments in the benzo-pyrone series, VIII, 5.

.. The fluorescence and absorption spectra of diamond in the visible region, 231.

.. Alkaloids, I, 21.

Menon, K. N. . . . . See Kartha and Menon.

Momin, A. U. . . . . An electrical method of studying the movement of water and salts in soils, I, 100.

Murty, G. V. L. N. and Seshadri, T. R. . . . . Raman effect and hydrogen bonds, IX, 17.

Murty, K. Satyanarayana . . . . . See Krishnaswamy and others.

Nargund, K. S. . . . . See Paranjape and others.

Neelakantam, K. and Venkateswarlu, V. . . . . Fluorescence reactions with boric acid and *O*-hydroxy-carbonyl compounds, and their application in analytical chemistry, III, 401.

Padwal, N. A. . . . . See Prasad and others.

Pant, D. D. . . . . The photo-conductivity of diamond, I, II, 315, 325.

Pant, D. D. and Sakhwalkar, N. D. . . . . Fluorescence spectrum of uranyl fluoride, 135.

Paranjape, (Miss) K. D., Phalnikar, N. L., Bhide, B. V. and Nargund, K. S. . . . . Synthesis of compounds related to santonin, 381.

---

Phalnikar, N. L. . . . . Synthesis of cantharidine and desoxycantharidine, 385.

Prasad, Mata and Guruswamy, S. . . . . See Paranjape and others.

Prasad, Mata, Guruswamy, S. and Padwal, N. A. . . . . Study of the optical properties of gels, I, II, III, 47, 66, 77.

Prasad, Mata, Guruswamy, S. and Padwal, N. A. . . . . Opacity changes during the coagulation of sols by electrolytes, 389.

Purushotham, A. . . . . See Joshi and Purushotham.

Rajagopalan, S. . . . . Bacterial chemotherapy, IV, V, 343, 351.

Ramachandran, G. N. . . . . Diffraction corona due to non-spherical particles, 123.

---

Raman, C. V. . . . . X-ray topographs of diamond, 280.

---

Raman, C. V. . . . . X-ray reflection and the structure of diamond, 304.

---

Raman, C. V. . . . . The crystal symmetry and structure of diamond, 189.

---

Raman, C. V. and Rendall, G. R. . . . . The nature and origin of the luminescence of diamond, 199.

Raman, C. V. and Rendall, G. R. . . . . Birefringence patterns in diamond, 265.

---

Ramanathan, K. G. . . . . Congruence properties of Ramanujan's function  $\tau(n)$ , 146.

---

Ramaseshan, S. . . . . The crystal forms of the Panna diamonds, 334.

Rangaswami, S. and Azo dye formation in 5-hydroxycoumarins, 14.  
 Rao, K. Ranganadha.

Rao, Basrur Sanjiva .. See Subrahmanya and others.

Rao, B. S. Madhava .. Kombur Sesha Iyengar Kuppuswamy Iyengar—In memoriam, 414.

Rao, B. Sundara Rama .. Raman effect in relation to crystal structure : sodium nitrate, 93.

Rao, K. Ranganadha .. See Krishnaswamy and others.  
 .. See Rangaswami and Rao.

---

Rao, P. Suryaprakasa .. See Rao and others.  
 Rao, P. Ramachandra, Synthesis of Hibiscetin, 88.  
 Rao, P. Suryaprakasa and Seshadri, T. R.

Rendall, G. R. .. See Raman and Rendall.

---

Row, L. Ramachandra .. Ultra-violet transparency patterns in diamond, 293.  
 and Seshadri, T. R. 5-hydroxy and methoxy flavylum salts, 141.

Sakhwalkar, N. D. .. See Pant and Sakhwalkar.

Saksena, B. D. .. Calculation of the elastic constants of quartz at room temperature from the Raman effect data, 357.

Sarabhai, V. .. The method of shower anti-coincidences for measuring the meson component of cosmic radiation, 37.

Seetharaman, V. .. On the existence of a metric for higher path-spaces, 167.

Seshachar, C. and Thiruvenkatachar, V. R. The lunar atmospheric tide at Bangalore (1895–1904), 131.

Seshadri, T. R. .. See Krishnaswamy and others.  
 .. See Murty and Seshadri.  
 .. See Rao and others.  
 .. See Row and Seshadri.  
 .. See Krishnaswamy and others.

---

Sigamony, A. .. Magnetic susceptibility of diamond, 310.  
 .. The magnetic susceptibility and anisotropy of carborundum, 377.

Subrahmanya, R. S., Doss, K. S. Gururaja and Rao, Basrur Sanjiva Effect of electric field on Tyndall scattering, 405.

---

Sunanda Bai, K. .. The ultra-violet absorption spectrum of diamond, 253.  
 .. Luminescence patterns in diamond, 274.

Taylor, H. J. and Alexander, J. The measurement of surface tension by means of sessile drops, 149.

Thiruvenkatachar, V. R. See Seshachar and Thiruvenkatachar.

Venkateswarlu, K. .. See Bhagavantam and Venkateswarlu.

---

.. Effect of temperature on the intensities of Raman lines, III, 111.

Venkateswarlu, V. .. See Neelakantam and Venkateswarlu.

#### TITLE INDEX

Alkaloids, I (Menon), 21.

Azo dye formation in 5-hydroxycoumarins (Rangaswami and Rao), 14.

Bacterial chemotherapy, IV, V (Rajagopalan), 343, 351.

Benzo-pyrone series, synthetic experiments, VIII (Krishnaswamy and others), 5.

Cantharidine and desoxycantharidine, synthesis (Miss Paranjape and others), 385.

Carborundum, the magnetic susceptibility and anisotropy (Sigamony), 377.

*Centaurea Behen* Linn, roots, chemical examination (Bhargava and Dutt), 163.

Coagulation of sols by electrolytes, opacity changes (Prasad and others), 389.

Cosmic radiation, electronic and non-electronic components, note on the separation (Bhabha), 23.

Cosmic radiation, separation of electronic and non-electronic components by Bhabha's method (Chandrasekhar Aiya), 177.

Cosmic radiation, the meson component, the method of shower anti-coincidences for measuring (Sarabhai), 37.

Diamond, birefringence patterns (Raman and Rendall), 265.

Diamond, crystal symmetry and structure (Raman), 189.

Diamond, experimental evidence for the existence of the four possible structures (Krishnan), 298.

Diamond, intensity of X-ray reflection (Hariharan), 261.

Diamond, magnetic susceptibility (Sigamony), 310.

Diamonds, Panna, the crystal forms (Ramaseshan), 334.

Diamond, luminescence patterns (Sunanda Bai), 274.

Diamond, the fluorescence and absorption spectra, in the visible region (Mani), 231.

Diamond, the lattice spectrum and specific heat (Dayal), 224.

Diamond, the nature and origin of the luminescence (Raman), 199.

Diamond, the photoconductivity, I, II (Pant), 315, 325.

Diamond, the Raman spectrum (Krishnan), 216.

Diamond, the ultra-violet absorption spectrum (Sunanda Bai), 253.

Diamond, ultra-violet transparency patterns (Rendall), 293.

Diamond, X-ray topographs (Ramaiahchandran), 280.

Diamond, X-ray reflection and the structure (Ramachandran), 304.

Diffraction corona due to non-spherical particles (Ramachandran), 123.

Flavylium salts, 5-hydroxy and methoxy (Row and Seshadri), 141.

Fluorescence reactions with boric acid and *O*-hydroxy-carbonyl compounds, and their application in analytical chemistry, III (Neelakantam and Venkateswarlu), 401.

Fluorescence spectrum of uranyl fluoride (Pant and Sakhwarkar), 135.

Gels, study of the optical properties, I, II, III (Prasad and Guruswamy), 47, 66, 77.

Gossypol, chemistry, IV (Krishnaswamy and others), 370.

Hibiscetin, synthesis (Rao and others), 88.

Iyengar, Kombur Sesha Iyengar Kuppuswamy—In memoriam I (Rao), 414.

*Light-effect, new*, in chlorine under electrical discharge, I (Deo), 117.

Light, scattering, in single crystals : intensity measurements (Bhagavantam and Venkateswarlu), 108.

Lunar atmospheric tide at Bangalore (1895–1904) (Seshachar and Thiruvenkatachar), 131.

*Mimusops elangi* (Linn), oil (Kartha and Menon), 1.

Nitrogen, active, quenching, at various pressures, influence of temperature (Joshi and Purushotham), 159.

Path-spaces, higher, on the existence of a metric (Seetharaman), 167.

Quartz, elastic constants, calculation, at room temperature from the Raman effect data (Saksena), 357.

Raman effect and hydrogen bonds, IX (Murty and Seshadri), 17.

Raman effect in relation to crystal structure : sodium nitrate (Rao), 93.

Raman lines, intensities, effect of temperature, III (Venkateswarlu), 111.

Ramanujan's function  $\tau(n)$ , congruence properties (Ramanathan), 146.

Santonin, compounds related, synthesis (Miss Paranjape and others), 381.

Soil, movement of water and salts, an electrical method of studying (Momin), 100.

Specific heat of rock-salt, evaluation of, by the new crystal dynamics (Dayal), 182.

Surface tension, measurement, by means of sessile drops (Taylor and Alexander), 149.

Tyndall scattering, effect of electric field (Subrahmanya and others), 405.